Egon Krause

# Fluid Mechanics

Egon Krause

# Fluid Mechanics

## With Problems and Solutions, and an Aerodynamic Laboratory

With 607 Figures

Springer

Prof. Dr. Egon Krause
RWTH Aachen
Aerodynamisches Institut
Wüllnerstr.5-7
52062 Aachen
Germany

ISBN 3-540-22981-7 **Springer Berlin Heidelberg New York**

Library of Congress Control Number: 2004117071



**Springer is a part of Springer Science+Business Media**

springeronline.com


Printed in Germany



Typesetting: Data conversion by the authors.
Final processing by PTP-Berlin Protago-TEX-Production GmbH, Germany
Cover-Design: design & production GmbH, Heidelberg
Printed on acid-free paper 62/3020Yu - 5 4 3 2 1 0

# Preface

During the past 40 years numerical and experimental methods of fluid mechanics were substantially improved. Nowadays time-dependent three-dimensional flows can be simulated on high-performance computers, and velocity and pressure distributions and aerodynamic forces and moments can be measured in modern wind tunnels for flight regimes, until recently not accessible for research investigations. Despite of this impressive development during the recent past and even 100 years after Prandtl introduced the boundary-layer theory, the fundamentals are still the starting point for the solution of flow problems. In the present book the important branches of fluid mechanics of incompressible and compressible media and the basic laws describing their characteristic flow behavior will be introduced. Applications of these laws will be discussed in a way suitable for engineering requirements.

The book is divided into the six chapters: Fluid mechanics I and II, exercises in fluid mechanics, gas dynamics, exercises in gasdynamics, and aerodynamics laboratory. This arrangement follows the structure of the teaching material in the field, generally accepted and approved for a long time at German and foreign universities. In fluid mechanics I, after some introductory statements, incompressible fluid flow is described essentially with the aid of the momentum and the moment of momentum theorem. In fluid mechanics II the equations of motion of fluid mechanics, the Navier-Stokes equations, with some of their important asymptotic solutions are introduced. It is demonstrated, how flows can be classified with the aid of similarity parameters, and how specific problems can be identified, formulated and solved. In the chapter on gasdynamics the influence of variable density on the behavior of subsonic and supersonic flows is described.

In the exercises on fluid mechanics I and II and on gasdynamics the material described in the previous chapters is elaborated in over 200 problems, with the solutions presented separately. It is demonstrated how the fundamental equations of fluid mechanics and gasdynamics can be simplified for the various problem formulations and how solutions can be constructed. Numerical methods are not employed. It is intended here, to describe the fundamental relationships in closed form as far as possible, in order to elucidate the intimate connection between the engineering formulation of fluid-mechanical problems and their solution with the methods of applied mathematics. In the selection of the problems it was also intended, to exhibit the many different forms of flows, observed in nature and technical applications.

Because of the special importance of experiments in fluid mechanics, in the last chapter, aerodynamics laboratory, experimental techniques are introduced. It is not intended to give a comprehensive and complete description of experimental methods, but rather to explain with the description of experiments, how in wind tunnels and other test facilities experimental data can be obtained.

A course under the same title has been taught for a long time at the Aerodymisches Institut of the RWTH Aachen. In the various lectures and exercises the functioning of low-speed and supersonic wind tunnels and the measuring techniques are explained in experiments, carried out in the facilities of the laboratory. The experiments comprise measurements of pressure distributions on a half body and a wing section, of the drag of a sphere in incompressible and compressible flow, of the aerodynmic forces and their moments acting on a wing section, of velocity profiles in a flat-plate boundary layer, and of losses in compressible pipe flow. Another important aspect of the laboratory course is to explain flow analogies, as for example the

so-called water analogy, according to which a pressure disturbance in a pipe, filled with a compressible gas, propagates analogously to the pressure disturbance in supercritical shallow water flow.

This book was stimulated by the friendly encouragement of Dr. M. Feuchte of B.G. Teubner-Verlag. My thanks go also to Dr. D. Merkle of the Springer-Verlag, who agreed to publish the English translation of the German text. Grateful acknowledgement is due to my successor Professor Dr.-Ing. W. Schröder, who provided personal and material support by the Aerodynamisches Institut in the preparation of the manuscript. I am indebted to Dr.-Ing. O. Thomer who was responsible for the preparatory work during the initial phase of the project until he left the institute. The final manuscript was prepared by cand.-Ing. O. Yilmaz, whom I gratefully acknowledge. Dr.-Ing. M. Meinke offered valuable advice in the preparation of some of the diagrams.

Aachen, July 2004 E. Krause

# Table of Contents

# 1. Fluid Mechanics I

## 1.1 Introduction

Fluid mechanics, a special branch of general mechanics, describes the laws of liquid and gas motion. Flows of liquids and gases play an important role in nature and in technical applications, as, for example, flows in living organisms, atmospheric circulation, oceanic currents, tidal flows in rivers, wind- and water loads on buildings and structures, gas motion in flames and explosions, aero- and hydrodynamic forces acting on airplanes and ships, flows in water and gas turbines, pumps, engines, pipes, valves, bearings, hydraulic systems, and others.
Liquids and gases, often termed fluids, in contrast to rigid bodies cause only little resistance when they are slowly deformed, as long as their volume does not change. The resistance is so much less the slower the deformation is. It can therefore be concluded, that the arising tangential stresses are small when the deformations are slow and vanish in the state of rest. Hence, liquids and gases can be defined as bodies, which do not build up tangential stresses in the state of rest. If the deformations are fast, there results a resistance proportional to the friction forces in the fluid. The ratio of the inertia to the friction forces is therefore of great importance for characterizing fluid flows. This ratio is called Reynolds number.
In contrast to gases, liquids can only little be compressed. For example, the relative change in volume of water is $5 \cdot 10^{-5}$ when the pressure is increased by 1 bar, while air changes by a factor of $5 \cdot 10^{-1}$ under normal conditions in an isothermal compression. If liquid and gas motion is to be described, in general, not the motion of single atoms or molecules is described, neither is their microscopic behavior taken into account; the flowing medium is considered as a continuum. It is assumed to consist out of very small volume elements, the overall dimensions of which, however, being much larger than the intermolecular distances. In a continuum the mean free path between the collisions of two molecules is small compared to the characteristic length of the changes of the flow quantities. Velocity, pressure and temperature, density, viscosity, thermal conductivity, and specific heats are described as mean values, only depending on position and time. In order to be able to define the mean values, it is necessary, that the volume element is small compared to the total volume of the continuum. This is illustrated in the following example for the density of air flowing in a channel with a cross-sectional area of $1\,\mathrm{cm}^2$. At room temperature and atmospheric pressure one cubic centimeter of air contains $2.7 \cdot 10^{19}$ molecules with a mean free path of about $10^{-4}$ mm. A cube with length of side of $10^{-3}$ mm, – the $10^{12}th$ part of a cubic centimeter – still contains $2.7 \cdot 10^{7}$ molecules. This number is sufficiently large such that a mean value of the density can be defined for every point in the flow field.
The basis for the description of flow processes is given by the conservation laws of mass, momentum, and energy. After the presentation of simplified integral relations in the first chapter in Fluid Mechanics I these laws will be derived in Fluid Mechanics II for three-dimensional flows with the aid of balance equations in integral and differential form. Closed-form solutions of these equations are not available for the majority of flow problems. However, in many instances, approximate solutions can be constructed with the aid of simplifications and idealizations. It will be shown, how the magnitude of the various forces per unit volume and of the energy contributions, appearing in the conservation equations, can be compared with each other by introducing similarity parameters. The small terms can then be identified and dropped, and only the important, the largest terms are retained, often leading to simplified, solvable conservation equations, as is true for very slow fluid motion, at times referred to as creeping motion. In this

case the inertia forces can be neglected in comparison to the friction forces. As an example the solution of the simplified conservation equations for very slow motion will be derived for the flow in a friction bearing. If the inertia and pressure forces are dominant, the terms describing the friction forces per unit volume can be dropped. Inviscid flows can be shown to possess a potential, and with the aid of the potential theory the surface pressure distribution of external flows about rigid bodies can be determined. The potential flow theory forms the basis for determining the lift of aerodynamically shaped bodies. Several applications will be discussed with the aid of analytic functions. In the vicinity of rigid walls, in general, the friction forces cannot be neglected. It will be shown how their influence on the flow can be determined with Prandtl's boundary-layer theory, as long as the region, in which the viscous forces act, is thin compared to length of the body. The similar solution of the boundary-layer equations will be derived for the case of the flat plate. The importance of a non-vanishing pressure gradient will be elucidated for the case of separating flows.
In flows of gases at high speeds marked changes of the density occur. They have to be taken into account in the description of flow fields. The laws governing compressible flows will be described in the chapter Gasdynamics.

## 1.2 Hydrostatics

### 1.2.1 Surface and Volume Forces

A continuum is said to be in equilibrium, if the resultant of the forces, acting on every arbitrary part of the volume vanishes. The forces are called surface, volume, and inertia forces, as their magnitude is proportional to the surface, volume, or mass of the part of the continuum considered. The surface forces act normal to the surface, as long as the fluid is at rest. The corresponding stresses (normal force per surface element) are – after Euler (1755) – called fluid pressure or abbreviated pressure. The equilibrium condition is derived for an arbitrarily chosen triangular prismatic volume element. For the surface forces to be in equilibium, the sum of the vertical and horizontal components must be equal to zero. If the forces per unit area, the pressures on the surface, are denoted by $p_1$, $p_2$, and $p_3$, then the forces can be written as products of the pressures and the areas, on which they act.The following sketch shows the prismatic element with the surface forces indicated. If another geometric shape of the volume element would have been chosen, the equilibrium condition would always require the vanishing of the sum of the vertical and horizontal components of the surface forces.

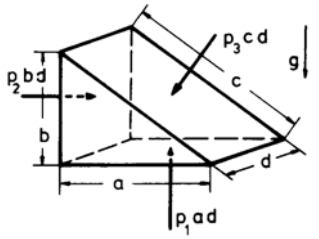


$$
\begin{aligned}
p_1\, a\, d \;&-\; p_3\, c\, d\, \cos(a,c) - \rho\, g\, \frac{a\, b\, d}{2} = 0 \\
p_2\, b\, d \;&-\; p_3\, c\, d\, \cos(b,c) = 0 \\
a \;&=\; c\, \cos(a,c) \\
b \;&=\; c\, \cos(b,c) \\
p_1 \;&=\; p_2 = p_3 = p \quad .
\end{aligned}
\tag{1.1}
$$

For $c \to 0$ the volume forces vanish. It follows for every point in a fluid which is in equilibrium, that the pressure $p$ does not depend on the direction of the surface element on which it acts.

The equilibrium condition for a cylinder with infinitesimally small cross-sectional area $A$, and with its axis normal to the positive direction of the gravitational force, yields the following relation

$$
p_1\, A = p_2\, A \quad \Rightarrow \quad p_1 = p_2 = p \quad . \tag{1.2}
$$

The axis of the cylinder represents a line of constant pressure. If the cylinder is turned by 90 degrees, such that its axis is parallel to the direction of the gravitational force, then the equilibrium of forces gives for the $z$-direction

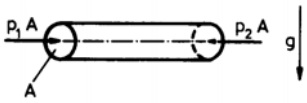


$$-\rho\, g\, A\, dz - (p + dp)\, A + p\, A = 0 \quad . \tag{1.3}$$

It follows from this relation, that in a fluid in the state of rest, the pressure changes in the direction of the acting volume force according to the differential equation

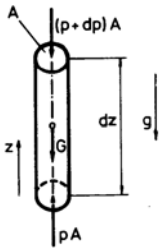


$$\frac{dp}{dz} = -\rho\, g \quad . \tag{1.4}$$

After integration the fundamental hydrostatic equation for an incompressible fluid ($\rho = const.$) and with $g = const.$ is obtained to

$$p + \rho\, g\, z = \text{const.} \quad . \tag{1.5}$$

If $\rho$ is determined from the thermal equation of state

$$\rho = \frac{p}{R\, T} \quad , \tag{1.6}$$

for a constant temperature $T = T_0$ (isothermal atmosphere) the so-called barometric height formula is obtained

$$p = p_0\, e^{-\frac{g\, z}{R\, T_0}} \quad . \tag{1.7}$$

The differential form of the fundamental hydrostatic equation is valid for arbitrary force fields. With $\boldsymbol{b}$ designating the acceleration vector, it reads

$$\text{grad}(p) = \rho\, \boldsymbol{b} \quad . \tag{1.8}$$

### 1.2.2 Applications of the Hydrostatic Equation

Assume, as shown in the sketch, that in a fluid-filled vessel the hatched parts are solidified without any change of density. The equilibrium of the fluid remains unchanged (Principle of solidification, Stevin 1586). By the process of solidification communicating vessels are generated. This principle is, for example, applied in liquid manometers and hydraulic presses.

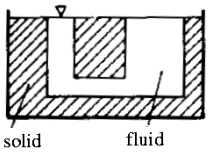


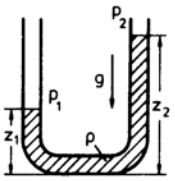


U-tube manometer

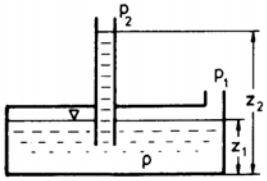


Single-stem manometer

The fundamental hydrostatic equation yields

$$p_1 - p_2 = \rho\, g\, (z_2 - z_1) \quad . \tag{1.9}$$

The pressure difference to be measured is proportional to the difference of the heights of the liquid levels.

*Barometer*

One stem of the U-tube manometer is closed and evacuated ($p_2 = 0$). The atmospheric pressure is

$$p_a = p_1 = \rho\, g\, (z_2 - z_1) \quad . \tag{1.10}$$

*Hydraulic Press*

For equal pressure on the lower sides of the pistons the force $F_2$ is

$$F_2 = F_1 \frac{A_2}{A_1} \quad . \tag{1.11}$$

Communicating vessels can be used for generating large forces, if $A_2 >> A_1$.

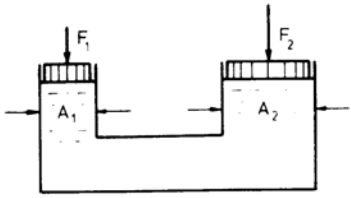


*Hydrostatic Paradox (Pascal 1647)*

The force acting on the bottom of all vessels is independent of the shape of the vessels and of the weight of the fluid, as long as the surface area of the bottom $A$ and the height $h$ of the vessels are constant.

$$F_B = (p_B - p_A)\, A = \rho\, g\, h\, A \tag{1.12}$$

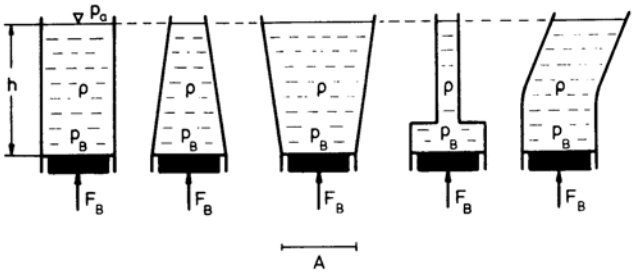


*Force on a Plane Side Wall*

The fluid pressure results in a force acting on the side wall of the vessel:

$$\begin{aligned} F_s &= \int_A (p - p_a)\, dA \\ F_s &= \int_0^h B\, \rho\, g\, z\, dz = \rho\, g\, \frac{B\, h^2}{2} \\ &= \rho\, g\, A\, \frac{h}{2} \end{aligned} \tag{1.13}$$

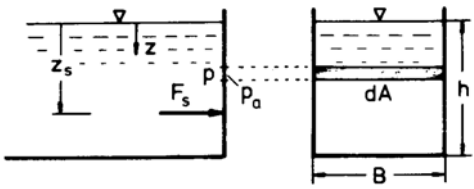

The location of the point of application of force follows from the balance of moments

$$z_s = \frac{2}{3}\, h \quad . \tag{1.14}$$

### 1.2.3 Hydrostatic Lift

A body immerged in a fluid of density $\rho_F$ experiences a lift or an apparent loss of weight, being equal to the weight of the fluid displaced by the body (Archimedes' principle 250 b. C.)

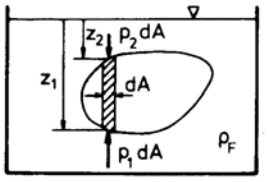


$$F_s = \rho_F\, g \int_A (z_1 - z_2)\, dA = \rho_F\, g\, \tau \quad . \tag{1.15}$$

$\tau$ is the volume of the fluid displaced by the body. Hence the weight of a body – either immersed in or floating on a fluid – is equal to the weight of the fluid displaced by the body. Balloons and ships are examples for the application of Archimendes' principle.

## 1.3 Hydrodynamics

### 1.3.1 Kinematics of Fluid Flows

Two methods are commonly used for the description of fluid motion, the Lagrangian method and the Eulerian method.

*Lagrangian Method (Fluid Coordinates)*

The motion of the fluid particles is described by specifying their coordinates as a function of time. The line connecting all points a particle is passing through in the course of time is called path line or Lagrangian particle path.

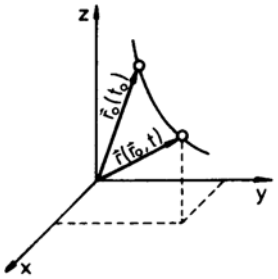


The path line begins at time $t = t_0$ at a point defined by the position vector

$$\boldsymbol{r}_0 = \boldsymbol{i}\, x_0 + \boldsymbol{j}\, y_0 + \boldsymbol{k}\, z_0 \quad . \tag{1.16}$$

The motion of the fluid is completely described, if the position vector $\boldsymbol{r}$ is known as a function of time:

$$\boldsymbol{r} = \boldsymbol{F}(\boldsymbol{r}_0, t) \tag{1.17}$$

or in components

$$\begin{aligned} x &= f_1(x_0, y_0, z_0, t) \quad ; \\ y &= f_2(x_0, y_0, z_0, t) \quad ; \\ z &= f_3(x_0, y_0, z_0, t) \quad . \end{aligned} \tag{1.18}$$

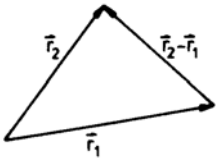


The velocity is obtained by differentiating the position vector with respect to time

$$\boldsymbol{v} = \lim_{\Delta t \to 0} \left( \frac{\boldsymbol{r}_2 - \boldsymbol{r}_1}{\Delta t} \right) = \frac{d\boldsymbol{r}}{dt} \tag{1.19}$$

where

$$\frac{d\boldsymbol{r}}{dt} = \boldsymbol{i}\,\frac{dx}{dt} + \boldsymbol{j}\,\frac{dy}{dt} + \boldsymbol{k}\,\frac{dz}{dt} = \boldsymbol{i}\,u + \boldsymbol{j}\,v + \boldsymbol{k}\,w \quad . \tag{1.20}$$

In the last equation $u$, $v$, and $w$ are the components of the velocity vector. The components of the acceleration vector are

$$b_x = \frac{d^2x}{dt^2} \quad ; \quad b_y = \frac{d^2y}{dt^2} \quad ; \quad b_z = \frac{d^2z}{dt^2} \quad . \tag{1.21}$$

For most flow problems the Langrangian method proves to be too laborious. Aside from a few exceptions, not the path-time dependence of a single particle is of interest, but rather the flow condition at a certain point at different times.

*Eulerian Method (Space Coordinates)*

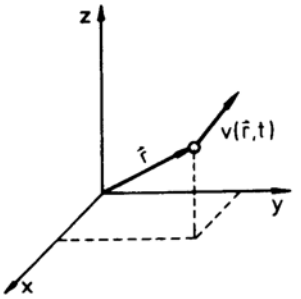


The motion of the fluid is completely determined, if the velocity $\boldsymbol{v}$ is known as a function of time everywhere in the flow field

$$\boldsymbol{v} = \boldsymbol{g}(\boldsymbol{r},t) \quad , \tag{1.22}$$

or written in components

$$\begin{aligned} u &= g_1(x,y,z,t) \quad ; \\ v &= g_2(x,y,z,t) \quad ; \\ w &= g_3(x,y,z,t) \quad . \end{aligned} \tag{1.23}$$

If the velocity $\boldsymbol{v}$ is independent of time, the flow is called steady. The Eulerian method offers a better perspicuity than the Lagrangian method and allows a simpler mathematical treatment.

*Particle Path and Streamline*

Particle paths designate the ways, the single fluid particles follow in the course of time. They can be determined by integrating the differential equations:

$$\frac{dx}{dt} = u \qquad ; \qquad \frac{dy}{dt} = v \qquad ; \qquad \frac{dz}{dt} = w \tag{1.24}$$

The integrals are identical with the functions $f_1$, $f_2$, and $f_3$, given previously in (1.18).

$$\begin{aligned} x &= \int u\,dt = f_1(x_0,y_0,z_0,t) \quad , \\ y &= \int v\,dt = f_2(x_0,y_0,z_0,t) \quad , \\ z &= \int w\,dt = f_3(x_0,y_0,z_0,t) \end{aligned} \tag{1.25}$$

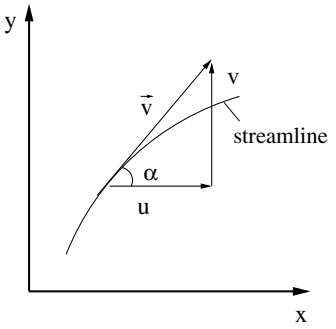


Streamlines give an instantaneous picture of the flow at a certain time.
Streamlines are defined by the requirement that in every point of the flow field their slope is given by the direction of the velocity vector. For plane flows there results

$$\tan(\alpha) = \frac{dy}{dx} = \frac{v}{u} \quad . \tag{1.26}$$

In a steady flow particle paths are identical with streamlines.

*Reference Frame and Form of Motion*

Certain unsteady motions can be viewed as steady motions with the aid of a coordinate transformation. For example, the flow about the bow of a ship appears to be unsteady to an observer standing on land, while the ship is passing by. The observer sees the single particle paths of the flow. The picture of the streamlines is different for every instant of time. However, for an observer on board of the ship the flow about the bow appears to be steady. Streamlines and particle paths are now identical, and the picture of the streamlines does not change in the course of time.

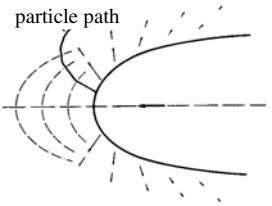


Observer at rest
(Unsteady motion)

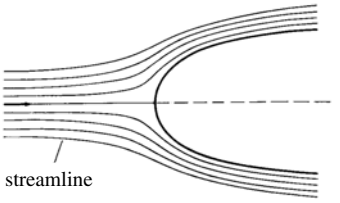


Observer aboard of the ship
(Steady motion)

### 1.3.2 Stream Tube and Filament

*Continuity Equation*

Streamlines passing through a closed curve form a stream tube, in which the fluid flows. Since the velocity vectors are tangent to the superficies, the fluid cannot leave the tube through the superficies; the same mass is flowing through every cross section.

$$\dot{m} = \rho\, v\, A \quad ; \quad \rho\, v_1\, A_1 = \rho\, v_2\, A_2 \qquad (1.27)$$

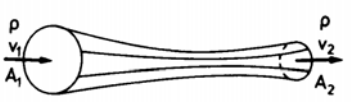


The product $v\ A$ is the volume rate of flow. A stream tube with an infinitesimal cross section is called stream filament.

*Bernoulli's Equation (Daniel Bernoulli 1738)*

It follows from Newton's law

$$m\,\frac{d\boldsymbol{v}}{dt} = \sum \boldsymbol{F_a} \qquad (1.28)$$

that, if pressure, volume, and friction forces act on a element of a stream filament, the equilibrium of forces is

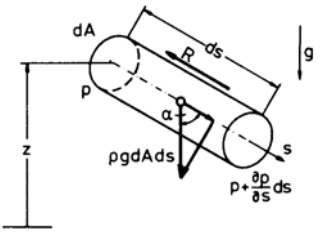


$$\rho\, dA\, ds\, \frac{dv}{dt} = -\frac{\partial p}{\partial s}\, ds\, dA + \rho\, g\, \cos\alpha\, ds\, dA - R \qquad (1.29)$$

with

$$ds\ \cos\alpha = -dz \tag{1.30}$$

and

$$R' = \frac{R}{dA\,ds} \tag{1.31}$$

there results

$$\rho\,\frac{dv}{dt} = -\frac{\partial p}{\partial s} - \rho\,g\,\frac{dz}{ds} - R' \quad . \tag{1.32}$$

If the velocity depends on the path $s$ and on the time $t$, then the total differential is

$$dv = \frac{\partial v}{\partial t}dt + \frac{\partial v}{\partial s}ds \quad . \tag{1.33}$$

With $v = ds/dt$ the substantial acceleration is

$$\frac{dv}{dt} = \frac{\partial v}{\partial t} + v\,\frac{\partial v}{\partial s} = \frac{\partial v}{\partial t} + \frac{1}{2}\,\frac{\partial(v^2)}{\partial s} \quad , \tag{1.34}$$

Therein $\partial v/\partial t$ is the local and $v(\partial v/\partial s)$ the convective acceleration and the differential equation becomes

$$\rho\,\frac{\partial v}{\partial t} + \frac{\rho}{2}\,\frac{\partial v^2}{\partial s} + \frac{\partial p}{\partial s} + \rho\,g\,\frac{dz}{ds} = -R' \quad . \tag{1.35}$$

With the assumption of inviscid ($R' = 0$), steady ($v = v(s)$), and incompressible fluid flow, the last equation can be integrated to yield the energy equation for the stream filament (Bernoulli's equation 1738).

$$p + \frac{\rho}{2}\,v^2 + \rho\,g\,z = \text{const.} \quad . \tag{1.36}$$

According to this equation the sum of the mechanical energies remains constant along a stream filament. The equilibrium of forces can be formulated for arbitrary force fields, if the acceleration vector $\boldsymbol{b}$ is known:

$$\rho\,\frac{\partial v}{\partial t} + \frac{\rho}{2}\,\frac{\partial v^2}{\partial s} + \frac{\partial p}{\partial s} - \rho\,b\,\cos(\boldsymbol{b},\boldsymbol{s}) = -R' \tag{1.37}$$

### 1.3.3 Applications of Bernoulli's Equation

*Measurement of the Total Pressure (Pitot Tube)*

If in an inviscid flow the velocity vanishes in a point, then this point is called stagnation point.

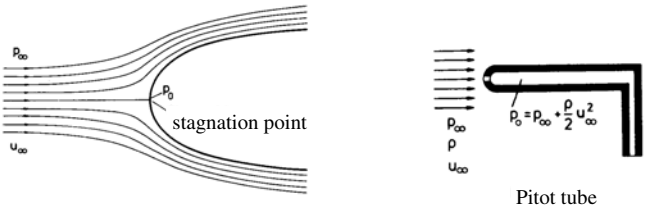


It follows from Bernoulli's equation that the pressure in the stagnation point (total pressure $p_0$) is equal to the sum of the static pressure $p_\infty$ and of the dynamic pressure $\rho\,u_\infty^2/2$ of the oncoming flow. The total pressure can be determined with the Pitot tube, the opening of which is positioned in the opposite direction of the flow.

*Measurement of the Static Pressure*

The so-called Ser's disc and a static pressure probe are used to measure the static pressure in a flow field. In contrast to the Pitot tube relatively large measuring errors result from small angles of attack.


*Measurement of the Dynamic Pressure (Prandtl's Static Pressure Tube)*

Because of the friction in the fluid the measured dynamic pressure deviates from that of the inviscid flow. The deviation depends on the Reynolds number and the ratio of the diameters $d/D$. It can be corrected with the factor given in the diagram above.

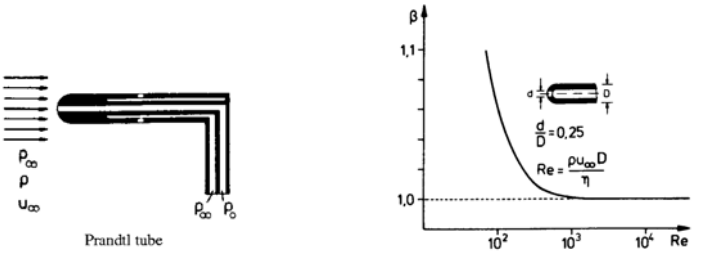


Prandtl's static pressure tube combines the static pressure probe and the Pitot probe for the measurement of the dynamic pressure, which can be determined with Bernoulli's equation from the difference of the total and the static pressure.

$$p_0 - p_\infty = \beta \, \frac{\rho}{2} \, u_\infty^2 \quad \text{with} \quad \beta = \beta \left( Re, \frac{d}{D} \right) \quad . \tag{1.38}$$

*Outflow from a Vessel*

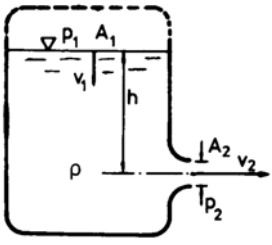


The outflow velocity is

$$v_2 = \sqrt{v_1^2 + 2\,g\,h + \frac{2\,(p_1 - p_2)}{\rho}} \quad . \tag{1.39}$$

For $A_1 >> A_2$ and with $p_2 = p_1$ the outflow velocity becomes $v_2 = \sqrt{2\,g\,h}$ (Torricelli's theorem 1644).

The actual outflow velocity is smaller, caused by the friction forces. The cross section of the stream, in general, is not equal to the geometric cross section of the opening. The stream experiences a contraction $\Psi = A_e/A$, which is called stream contraction; it depends on the shape of the outflow opening and on the Reynolds number.

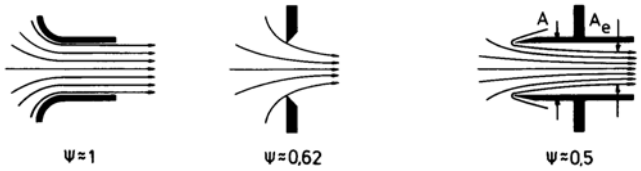


The volume rate of flow is then

$$\dot{Q} = \Psi \, A \sqrt{2 \, g \, h} \quad . \tag{1.40}$$

*Measurement of the Volume Rate of Flow in Pipes*

The volume rate of flow of a steady pipe flow can be obtained by measuring a pressure difference. A sufficiently large pressure difference must be enforced by narrowing the cross section. If $m = A_2/A_1$ designates the area ratio, one obtains for the velocity in the cross section 2

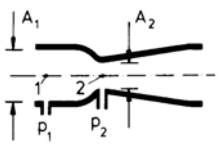


Venturi nozzle

$$v_2 = \sqrt{\frac{1}{(1-m^2)} \, \frac{2\,(p_1 - p_2)}{\rho}} \tag{1.41}$$

and for the volume rate of flow

$$\dot{Q}_{th} = v_2 \, A_2 \quad . \tag{1.42}$$

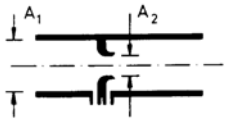


standard nozzle

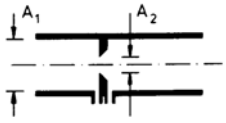


standard orifice

In technical applications mainly the Ventury nozzle, the standard nozzle, and the standard orifice are used for measuring the volume rate of flow. The influence of the friction in the fluid, of the area ratio, and of the shape of the contraction is taken into account in the discharge coefficient $\alpha$.

$$\dot{Q} = \alpha \, A_2 \sqrt{\frac{2}{\rho} \, \Delta p_w} \tag{1.43}$$

The pressure difference $\Delta p_w$ is called differential pressure. The dimensions, the positions of the pressure measurements, the directions for installing, the tolerances, and the discharge coefficients are laid down in the flow-measurement regulations.

## 1.4 One-Dimensional Unsteady Flow

If the velocity in a stream tube not only changes with the path length $s$ but also with the time $t$, then the volume rate of flow also changes with time. Since

$$\dot{Q}(t) = v(s,t) \, A(s) \quad , \tag{1.44}$$

it follows that

$$\frac{\partial \dot{Q}}{\partial t} = \frac{\partial v}{\partial t} \, A \quad . \tag{1.45}$$

Consequently, the interdependence between pressure and velocity is changed. If all other assumptions remain the same as in the derivation of Bernoulli's equation, one obtains the energy equation for unsteady flow for a stream filament to

$$\rho \int \frac{\partial v}{\partial t}\, ds + p + \frac{\rho}{2}\, v^2 + \rho\, g\, z = k(t) \quad . \tag{1.46}$$

If the integral over the local acceleration is small in comparison to the other terms in the above equation, the flow is called quasi-steady.

*Oscillation of a Fluid Column*

A fluid oscillates in a U-tube after displacement from its equilibrium position by the amount $\xi_0$, under the influence of gravity. The energy equation for unsteady inviscid flow gives

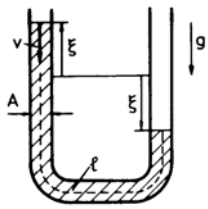


$$\rho\, g\, \xi = -\rho\, g\, \xi + \rho\, \frac{dv}{dt}\, l \quad . \tag{1.47}$$

With $v = -dx/dt$ the differential equation describing the oscillation is

$$\frac{d^2\, \xi}{dt^2} + \frac{2\, g}{l}\, \xi = 0, \tag{1.48}$$

and with the initial conditions

$$v(t=0) = 0, \quad \xi(t=0) = \xi_0 \tag{1.49}$$

the solution is

$$\xi = \xi_0\, \cos(\alpha\, t) \quad \text{with} \quad \alpha = \sqrt{\frac{2\, g}{l}} \quad . \tag{1.50}$$

Therein $\alpha$ is the eigenfrequency of the oscillating fluid column.

*Suction process in a plunger pump*

The pumping process of a periodically working plunger pump can be described with the energy equation for unsteady flows with some simplifying assumptions. In order to avoid cavitation the pressure in the intake pipe should not fall below the vapor pressure $p_V$.
During the suction stroke the pressure attains its lowest value at the piston-head. If it is assumed, that the velocity only depends on the time $t$, the pressure at the piston-head $p_{PH}$ is obtained to

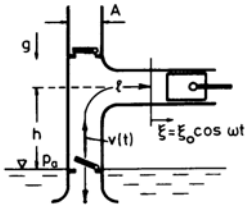


$$\frac{p_{PH}}{\rho\, \omega^2\, l^2} = \frac{p_a - \rho\, g\, h}{\rho\, \omega^2\, l^2} + \frac{\xi_0}{l}\, \left[\cos(\omega\, t) - \frac{1}{2}\, \frac{\xi_0}{l}\, \left(1 - 3\, \cos^2(\omega\, t)\right)\right] \quad . \tag{1.51}$$

In general the piston stroke $\xi_0$ is much smaller than the length of the intake pipe $l$; with this assumption the angular velocity $\omega_V$, at which the pressure at the piston-head reaches the value of the vapor pressure $p_{PH} = p_V$, is

$$\omega_V = \sqrt{\frac{p_a - \rho\, g\, h - p_V}{\rho\, \xi_0\, (l - \xi_0)}} \quad . \tag{1.52}$$

The mean volume rate of flow is

$$\dot{Q} = \frac{\omega}{2\, \pi}\, \int_{\pi/\omega}^{2\, \pi/\omega} v\, A\, dt \qquad \Rightarrow \qquad \dot{Q} = \xi_0\, A\, \frac{\omega}{\pi} \quad . \tag{1.53}$$

## 1.5 Momentum and Moment of Momentum Theorem

The momentum theorem describes the equilibrium between the time rate of change of momentum and external forces and the moment of momentum theorem the equilibium between their moments. For steady as well as for time-averaged flows these theorems involve only the flow conditions on the boundaries of a bounded fluid domain.

### 1.5.1 Momentum Theorem

According to the momentum theorem of mechanics the time rate of change of the momentum is equal to the sum of the acting external forces

$$\frac{d\boldsymbol{I}}{dt} = \sum \boldsymbol{F} \quad . \tag{1.54}$$

For a system with $n$ particles with masses $m_i$ and velocities $\boldsymbol{v}_i$ it follows with

$$\boldsymbol{I} = \sum_{i=1}^{n} m_i \, \boldsymbol{v}_i \tag{1.55}$$

$$\frac{d}{dt} \sum_{i=1}^{n} m_i \, \boldsymbol{v}_i = \sum \boldsymbol{F} \quad . \tag{1.56}$$

If the particles are assumed to form a continuum with density $\rho(x,y,z,t)$ the sum changes into a volume integral. The rate of change of momentum is then

$$\frac{d\boldsymbol{I}}{dt} = \frac{d}{dt} \int_{\tau(t)} \rho \, \boldsymbol{v} \, d\tau \quad . \tag{1.57}$$

The volume $\tau$, which always contains the same particles, changes in a time interval from $\tau(t)$ to $\tau(t + \Delta t)$.

$$\frac{d}{dt} \int_{\tau(t)} \rho \, \boldsymbol{v} \, d\tau = \lim_{\Delta t \to 0} \frac{1}{\Delta t} \left[ \int_{\tau\,(t+\Delta t)} \rho \, \boldsymbol{v} \, (t + \Delta t) \, d\tau - \int_{\tau(t)} \rho \, \boldsymbol{v}(t) \, d\tau \right] \tag{1.58}$$

$$\rho \, \boldsymbol{v} \, (t + \Delta t) = \rho \, \boldsymbol{v}(t) + \frac{\partial(\rho \, \boldsymbol{v})}{\partial t} \, \Delta t + ... \tag{1.59}$$

$$\frac{d\boldsymbol{I}}{dt} = \int_{\tau(t)} \frac{\partial}{\partial t} \, (\rho \, \boldsymbol{v}) \, d\tau + \lim_{\Delta t \to 0} \left( \frac{1}{\Delta t} \int_{\Delta\tau(t)} \rho \, \boldsymbol{v} \, d\tau \right) \tag{1.60}$$

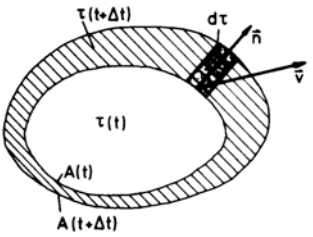


The last integral can be changed into a surface integral over the surface $A(t)$.
Since

$$d\tau = (\boldsymbol{v} \cdot \boldsymbol{n}) \, dA \, \Delta t \quad , \tag{1.61}$$

it follows that

$$\frac{d\boldsymbol{I}}{dt} = \int_{\tau(t)} \frac{\partial}{\partial t} \, (\rho \, \boldsymbol{v}) \, d\tau + \int_{A(t)} \rho \, \boldsymbol{v} (\boldsymbol{v} \cdot \boldsymbol{n}) \, dA \quad . \tag{1.62}$$

For steady flows the time rate of change of momentum is given by the surface integral of the last equation. The surface $A$ of the volume $\tau$ considered is called control surface. The external forces, which are in equilibrium with the time rate of change of momentum, are volume and surface forces, for example, volume forces due to the gravitational force:

$$\boldsymbol{F}_g = \int_\tau \rho\, \boldsymbol{g}\, d\tau \quad . \tag{1.63}$$

The forces which act on the surface are given by the pressure and friction forces. The pressure force is described by the integral

$$\boldsymbol{F_p} = -\int_A p\, \boldsymbol{n}\, dA \quad . \tag{1.64}$$

The friction forces are given by the surface integral extended over the components of the stress tensor $\bar{\bar{\sigma}}'$

$$\boldsymbol{F}_f = -\int_A (\bar{\bar{\sigma}}' \cdot \boldsymbol{n})\, dA \quad . \tag{1.65}$$

If a part of the control surface is given by a rigid wall, then a supporting force $\boldsymbol{F}_s$ is exerted by the wall on the fluid. The supporting force is equal to the force the fluid exerts on the wall, but acts in the opposite direction. The momentum theorem for steady flows then reads

$$\int_A \rho\, \boldsymbol{v}\, (\boldsymbol{v} \cdot \boldsymbol{n})\, dA = \boldsymbol{F}_g + \boldsymbol{F}_p + \boldsymbol{F}_s + \boldsymbol{F}_f \quad . \tag{1.66}$$

The difficult part in the construction of the solution of the momentum theorem mainly consists in the solution of the integrals. If possible, the control surface $A$ has to be chosen in such a way, that the integrals given in (1.63) to (1.66) can be solved. In order to obtain a unique solution the control surface $A$ must be a simply connected surface.

### 1.5.2 Applications of the Momentum Theorem

*Force on a Bent Pipe*

The flow through a horizontal bent pipe is assumed to be inviscid and incompressible. Inlet and outlet cross section, the pressure in the inlet cross section, the external pressure $p_a$, which also prevails in the outlet cross section, and the flow deflection angle $\beta$ have to be known for the solution of the problem. It is advantageous, to choose the control surface as indicated in the sketch by the dashed line.

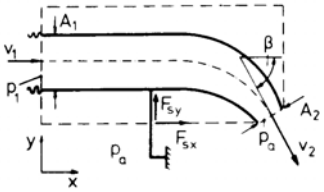


The velocities in the inlet and outlet cross section are determined with Bernoulli's equation and the continuity equation:

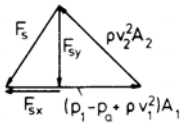


$$v_1 = \sqrt{\frac{2\,(p_1 - p_a)}{\rho}\,\frac{1}{\left(\frac{A_1}{A_2}\right)^2 - 1}} \quad \text{and} \quad v_2 = v_1\,\left(\frac{A_1}{A_2}\right) \quad . \tag{1.67}$$

From the momentum theorem it follows for the $x$-direction

$$-\rho\, {v_1}^2\, A_1 + \rho\, {v_2}^2\, A_2\, \cos\beta = (p_1 - p_a)\, A_1 + F_{sx} \quad , \tag{1.68}$$

and for the $y$-direction

$$-\rho\, {v_2}^2\, A_2\, \sin\beta = F_{sy} \quad . \tag{1.69}$$

The supporting force $\boldsymbol{F_s}$ can be determined from the last two equations.

*Jet Impinging on a Wall*

A horizontal plane fluid jet impinges on a plate under the angle $\beta$ and is deflected to both sides without losses.

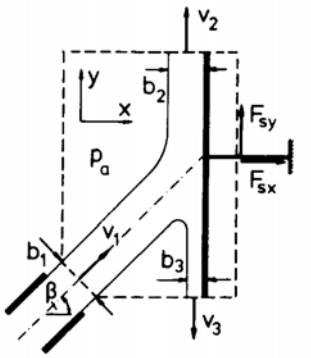


It follows from Bernoulli's equation that the velocity at both ends of the plate is equal to the jet velocity $v_1$, if it is assumed, that the streams leave the plate parallel to it. Then the two components of the supporting force are

$$F_{sx} = -\rho\, v_1^2\, b_1\, \cos\beta \quad \text{and} \quad F_{sy} = 0 \quad . \tag{1.70}$$

The widths of the streams are

$$b_2 = b_1\, \frac{1+\sin\beta}{2} \quad \text{and} \quad b_3 = b_1\, \frac{1-\sin\beta}{2} \quad . \tag{1.71}$$

*Discontinuous Widening of a Pipe*

If a pipe is discontinuously widened from the cross-sectional area $A_1$ to $A_2$, the fluid cannot fill the entire cross-sectional area $A_2$, when entering the widened part of the pipe. Dead water regions are formed in the corner, which extract momentum with the aid of internal friction from the fluid passing by. This loss of momentum results in a pressure loss. The pressure in the entrance cross section also acts on the frontal area $A_2 - A_1$ of the widened part of the pipe.

The losses in the flow can be determined with the continuity equation, Bernoulli's equations, and the momentum theorem, if it is assumed, that downstream from the dead water region the flow properties are constant in every cross section and that the friction caused by the walls can be neglected.

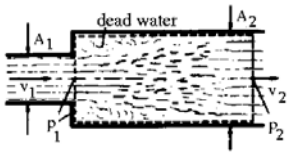


The pressure loss is obtained with the control surface shown in the sketch above by the dashed line to

$$\Delta p_l = p_{01} - p_{02} = (p_1 + \frac{\rho}{2}\, v_1^2) - (p_2 + \frac{\rho}{2}\, v_2^2) \quad , \tag{1.72}$$

with

$$v_1\, A_1 = v_2\, A_2 \quad , \tag{1.73}$$

and

$$\rho\, {v_2}^2\, A_2 - \rho\, {v_1}^2\, A_1 = (p_1 - p_2)\, A_2 \quad , \tag{1.74}$$

and finally to

$$\Delta p_l = \frac{\rho}{2}\, v_1^2\, \left(1 - \frac{v_2}{v_1}\right)^2 \quad . \tag{1.75}$$

The pressure loss, nondimensionalized with the dynamic pressure, is called pressure loss coefficient.

$$\zeta = \frac{\Delta p_l}{\frac{\rho}{2}\, v_1^2} = \left(1 - \frac{A_1}{A_2}\right)^2 \qquad \text{Carnot's equation} \tag{1.76}$$

*Pressure Loss in an Orifice*

After what has been said about the flow through the pipe with a discontinuous widening of the cross section, it can be concluded that the flow through an orifice also must generate a pressure loss. It again can be determined with Carnot's equation. During the passage of the fluid through the orifice the flow contracts and forms a jet, which depends on the shape of the orifice. (geometric opening ratio $m = \frac{A'}{A_1}$). The ratio of the cross section of the bottle neck to the opening cross section of the orifice is called contraction ratio $\Psi = \frac{A_2}{A'}$. The pressure coefficient of the orifice, referenced to the conditions of the oncoming flow in the pipe is

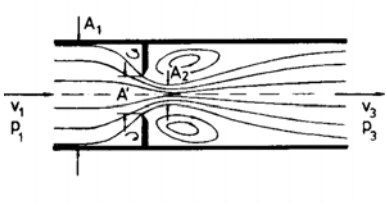


$$\zeta_o = \frac{\Delta p_l}{\frac{\rho}{2} v_1^2} = \left( \frac{1 - \psi\, m}{\psi\, m} \right)^2 \quad . \tag{1.77}$$

In the following table the pressure loss coefficient of the orifice is given for some characteristic values of the product $\Psi\, m$.

| $\Psi\, m$ | 1 | 2/3 | 1/2 | 1/3 |
|---|---|---|---|---|
| $\zeta_o$ | 0 | 1/4 | 1 | 4 |

If the widening of the cross-sectional area is smooth, the losses just discussed can be very much reduced. Then the pressure rises in the flow direction, since the velocity decreases with increasing cross-sectional area. If the opening angle, however, becomes too large, then the flow cannot follow the contour of the widened pipe any longer and a dead-water region similar to the one mentioned previously is generated.

*Resistance of an Installation in a Pipe*

For a pipe with constant cross-section area the continuity equation yields $v_1 = v_2$. The resistance of the body installed results in a pressure drop. The control surface is indicated by the dashed line in the sketch. With the friction forces neglected the resistance is

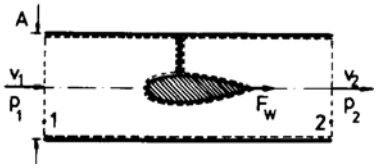


$$F_w = (p_2 - p_1)\, A. \tag{1.78}$$

*Rankine's Slip-Stream Theory*

Performance, thrust, and efficiency of wind-driven rotors and propellers (of ships and airplanes) can be determined with the momentum theorem for one-dimensional flow under the following simplifying assumption:
The rotation of the flow in the slip stream does not influence the axial flow velocity; the driving force is uniformly distributed over the cross section of the slip stream, independent of the number of vanes (infinite number of vanes); the flow is decelerated and accelerated without losses.
The following figure shows the flow through a wind-driven rotor. The following relations are valid for the stream tube with $p_1 = p_2 = p_a$ (atmospheric pressure far away from the rotor).

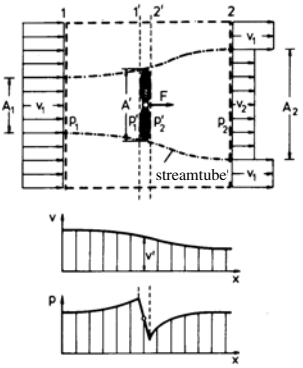


$$\begin{aligned} \rho\, v_1\, A_1 &= \rho\, v'\, A' = \rho\, v_2\, A_2 \\ \frac{\rho}{2}\, {v_1}^2 + p_a &= \frac{\rho}{2}\, {v'_1}^2 + p'_1 \\ \frac{\rho}{2}\, {v_2}^2 + p_a &= \frac{\rho}{2}\, {v'_2}^2 + p'_2 \end{aligned} \tag{1.79}$$

Continuous velocity variation in the slip stream.
Discontinuous pressure change in the cross-sectional plane of the rotor.
The force $F$ exerted by the rotor on the flow in the slip stream is determined from the momentum theorem for the small control volume between the cross section $1'$ and $2'$, immediately upstream and downstream from the cross-sectional plane of the rotor (dark area).

$$F = (p'_2 - p'_1)\, A' \tag{1.80}$$

The force $F$ can also be obtained for the large control surface,, indicated by the dashed line in the last figure

$$F = \rho\, v'\, A'\, (v_2 - v_1) \quad . \tag{1.81}$$

The velocity in the cross-sectional plane of the rotor is obtained with the aid of Bernoulli's equation:

$$v' = \frac{(v_1 + v_2)}{2} \qquad \text{(Froude's Theorem 1883)} \tag{1.82}$$

The energy, which can be extracted from the slip stream per unit time is

$$P = \frac{\rho}{4}\, A'\, {v_1}^3 \left(1 + \frac{v_2}{v_1}\right) \left(1 - \frac{v_2^2}{v_1^2}\right) \quad . \tag{1.83}$$

The extracted power $P$ attains a maximum value for the velocity ratio $\frac{v_2}{v_1} = \frac{1}{3}$. The maximum extracted power, divided by the cross-sectional area of the rotor, is

$$\frac{P_{max}}{A'} = \frac{8}{27}\, \rho\, v_1^3 \quad , \tag{1.84}$$

and the corresponding thrust per unit area is

$$\frac{F}{A'} = -\frac{4}{9}\, \rho\, v_1^2 \quad . \tag{1.85}$$

For air with $\rho = 1.25 kg/m^3$ the following values are obtained for the maximum extracted power and the corresponding thrust per unit cross-sectional area and time, computed for the wind intensities listed.

| $v_1 \quad [m/s]$ | 1 | 5 | 10 | 15 | 20 | 25 | 30 |
|---|---|---|---|---|---|---|---|
| Wind intensity $\quad [BF]$ | 1 | 3 | 6 | 7 | 9 | 10 | 12 |
| $P_{max}/A' \quad [kW/m^2]$ | 0.00037 | 0.0463 | 0.370 | 1.25 | 2.963 | 5.79 | 10.0 |
| $F/A' \quad [N/m^2]$ | 0.555 | 13.88 | 55.55 | 125 | 222 | 347 | 500 |

### 1.5.3 Flows in Open Channels

Flows in rivers and channels are called open channel flows. They differ from pipe flows by their free surface, which is exposed to the atmospheric pressure. For a given volume rate of flow and a given width $b$ of the channel, the depth of the water $h$ can change with the velocity. If inviscid steady flow is assumed, Bernoulli´s equation yields the specific relation for each streamline

$$\frac{v^2}{2\,g} + h' + z = const. \tag{1.86}$$

The sum of the velocity height $v^2/(2\,g)$ and the depth of water $h$ is called energy height $H$. The velocity of the water is assumed to be independent of $z$.

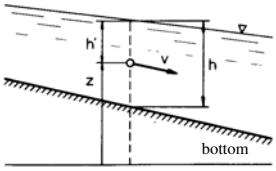


With

$$v = \frac{\dot{Q}}{b\,h} \tag{1.87}$$

there results

$$H = h + \frac{\dot{Q}^2}{2\,g\,h^2\,b^2} \quad . \tag{1.88}$$

If the volume rate of flow and the energy height $H$ are given, (1.88) gives two physically meaningful solutions for the depth of water $h$ and thereby also for the velocity. These two different flow conditions can be found with the relation $H = H(h)$ on both sides of the minimum

$$H_{min.} = \frac{3}{2}\sqrt[3]{\frac{\dot{Q}^2}{g\,b^2}} \tag{1.89}$$

The corresponding critical depth of water is

$$h_{crit.} = \sqrt[3]{\frac{\dot{Q}^2}{g\,b^2}} \quad . \tag{1.90}$$

and the critical velocity is

$$v_{crit.} = \sqrt{g\,h_{crit.}} \quad . \tag{1.91}$$

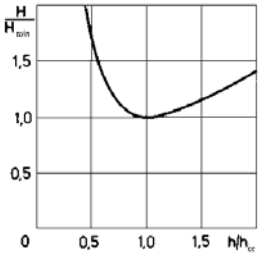


The dimensionless ratio $H/H_{min.}$ is

$$\frac{H}{H_{min.}} = \frac{2}{3}\left[\frac{h}{h_{crit.}} + \frac{1}{2}\left(\frac{h_{crit.}}{h}\right)^2\right] \quad . \tag{1.92}$$

The quantity $c = \sqrt{g\,h}$ is the velocity of propagation of gravitational waves in shallow water, and the ratio $v/c$ is called Froude number

$$Fr = \frac{v}{c} \quad . \tag{1.93}$$

The magnitude of the Froude number determines, which of the two flow conditions prevails.

$Fr < 1 \quad h > h_{crit.} \quad v < v_{crit.}$ subcritical condition
$Fr > 1 \quad h < h_{crit.} \quad v > v_{crit.}$ supercritical condition

For $Fr > 1$ small disturbances cannot travel upstream. According to Bernoulli's equation the sum of the geodetical elevation of the bed and the energy height is constant. If the geodetical

bed elevation is sufficiently increased (undulation of ground), a subcritical open channel flow changes into supercritical motion. If $H$ is the energy height of the channel, the necessary increase of the geodetical bed elevation is

$$Z_{crit.} = H - H_{min.} \quad . \tag{1.94}$$

Also the process in the opposite direction is observed. A supercritical motion ($h < h_{scrit.}$) changes into a subcritical motion with an almost discontinuous increase of the water level (hydraulic jump). This jump is associated with fluid mechanical losses. The water level $h_2$ after the jump can be determined with the momentum theorem and the continuity equation. For an open channel with constant width there results

$$\rho \, (v_2^2 \, h_2 - v_1^2 \, h_1) = \rho \, g \, \left( \frac{h_1^2}{2} - \frac{h_2^2}{2} \right) \tag{1.95}$$

and

$$h_1 \, v_1 = h_2 \, v_2 \quad . \tag{1.96}$$

The ratio of the water levels is

$$\frac{h_2}{h_1} = \sqrt{\frac{1}{4} + \frac{2 \, v_1^2}{g \, h_1}} - \frac{1}{2} \quad . \tag{1.97}$$

A decrease of the water level during the jump ($h_2/h_1 < 1$) is not possible, since then the energy height would have to be increased. The difference of the energy heights $H_1 - H_2$

$$H_1 - H_2 = \frac{h_1}{4} \, \left( \frac{h_1}{h_2} \right) \, \left( \frac{h_2}{h_1} - 1 \right)^3 \tag{1.98}$$

is positive (in the limiting case zero), if $h_2/h_1 \geq 1$. The hydraulic jump can only occur in supercritical motion.

### 1.5.4 Moment of Momentum Theorem

According to the fundamental theorem of mechanics the time rate of change of the moments of momentum is equal to the sum of the acting external moments. For a system of $n$ particles with masses $m_i$, velocities $\boldsymbol{v}_i$, and the distances $\boldsymbol{r}_i$ from a space-bound axis there is obtained

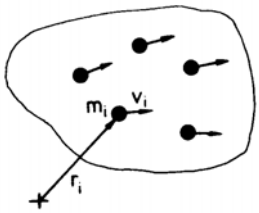


$$\frac{d}{dt} \sum_{i=1}^{n} \boldsymbol{r}_i \times (m_i \, \boldsymbol{v}_i) = \sum \boldsymbol{M} \quad . \tag{1.99}$$

Similar to the derivation of the momentum theorem the transition from the particle system to the continuum is achieved by substituting the sum on the left-hand side of (1.99) by a volume integral

$$\frac{d\boldsymbol{L}}{dt} = \frac{d}{dt} \int_{\tau(t)} \rho \, \boldsymbol{r} \times \boldsymbol{v} \, d\tau \quad . \tag{1.100}$$

The moment of momentum is designated as $\boldsymbol{L}$. Its time rate of change is equal to the sum of the moments of the external forces acting on the fluid considered, referenced to a space bound axis.

For steady flows the volume integral can again be replaced by a surface integral

$$\frac{d\boldsymbol{L}}{dt} = \int_A \rho\,(\boldsymbol{r}\times\boldsymbol{v})\,(\boldsymbol{v}\cdot\boldsymbol{n})\,dA \quad . \tag{1.101}$$

The moment of the external forces results from the moments of the volume forces, the pressure forces, the friction forces, and the supporting force:

$$\begin{aligned}
\boldsymbol{M_g} &= \int_\tau (\boldsymbol{r}\times\rho\,\boldsymbol{g})\,d\tau \quad , \\
\boldsymbol{M_p} &= -\int_A p\,(\boldsymbol{r}\times\boldsymbol{n})\,dA \quad , \\
\boldsymbol{M_f} &= -\int_A \boldsymbol{r}\times(\bar{\bar{\sigma}}'\cdot\boldsymbol{n})\,dA \quad , \\
\boldsymbol{M_s} &= \boldsymbol{r}_s\times\boldsymbol{F}_s
\end{aligned} \tag{1.102}$$

### 1.5.5 Applications of the Moment of Momentum Theorem

*Euler's Turbine Equation (1754)*

If a fluid flows through a duct rotating with constant angular velocity from the outside to the inside in the radial direction (radial turbine),, the moment generated by the flow can be computed with the moment of momentum theorem. The flow is steady with respect to the duct, the walls of which form the control volume. The mass flowing through the duct per unit time is

$$\dot{m} = \rho\,v_1\,A_1\,\sin\delta_1 = \rho\,v_2\,A_2\,\sin\delta_2 \quad . \tag{1.103}$$

With the notation given in the sketch the time rate of change of the angular momentum is

$$\int_A \rho\,(\boldsymbol{r}\times\boldsymbol{v})\,(\boldsymbol{v}\cdot\boldsymbol{n})\,dA = \boldsymbol{k}\,[-\dot{m}\,v_1\,r_1\,\cos\delta_1 + \dot{m}\,v_2\,r_2\,\cos\delta_2] \quad . \tag{1.104}$$

The moment delivered to the turbine shaft is (Moment of reaction)

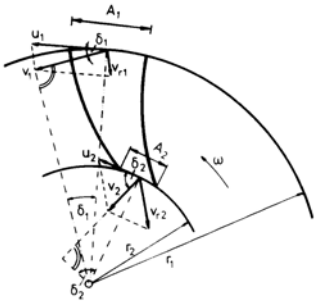


$$M_d = \dot{m}\,[v_1\,r_1\,\cos\delta_1 - v_2\,r_2\,\cos\delta_2] \quad . \tag{1.105}$$

This relation is called Euler's turbine equation. The power delivered to the turbine is with the relations
$u_1 = r_1\,\omega$ and $u_2 = r_2\,\omega$

$$P = M_d\,\omega = \dot{m}\,(v_1\,u_1\,\cos\delta_1 - v_2\,u_2\,\cos\delta_2) \tag{1.106}$$

The largest power output is obtained, when the absolute velocity $v_2$ is normal to the circumferential velocity component $u_2$, i. e. if $\cos\delta_2 = 0$.

*Segner's Water Wheel (1750)*

If a fluid flows from a reservoir into a doubly bent pipe, pivoted about its axis, as sketched in the following drawing, the pipe will start to rotate. The flow generates a moment of rotation, which can be picked up at the pipe. A certain part of this moment is used to overcome the bearing friction. If the fluid motion through the pipe is steady, the moment can be determined with the moment of momentum theorem.

With the notation given in the sketch below the out-flowing mass is

$$\begin{aligned} \dot{m} &= \rho\, v_r\, A \quad \text{,and} \\ M &= \dot{m}\,(v_r - \omega\, R)\, R \quad . \end{aligned} \tag{1.107}$$

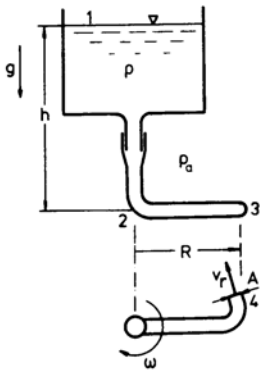


In order to be able to determine the out-flow velocity $v_r$, the flow between the fluid surface in the reservoir and the exit cross section is assumed to be loss-free. The energy equation for the system considered is

$$p_a + \int_1^4 \rho\, \boldsymbol{b}\, d\boldsymbol{s} = p_a + \frac{\rho}{2}\, v_r^2 \quad . \tag{1.108}$$

The integral can be split into two parts

$$\int_1^4 \rho\, \boldsymbol{b} \cdot d\boldsymbol{s} = \int_1^2 \rho\, g\, dz + \int_2^3 \rho\, \omega^2\, r\, dr \quad ; \tag{1.109}$$

therein $\omega^2\, r$ is the centrifugal acceleration.

After integration the out-flow velocity is obtained to

$$v_r = \sqrt{2\, g\, h + \omega^2\, R^2} \quad . \tag{1.110}$$

With the following abbreviations one obtains for $M$

$$\xi = \frac{\omega\, R}{\sqrt{2\, g\, h}} \quad \text{and} \quad M_0 = 2\, \rho\, g\, h\, A\, R \tag{1.111}$$

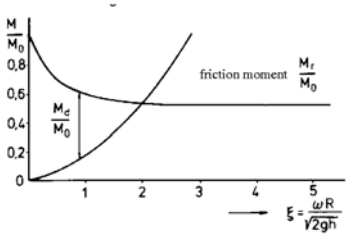


$$\frac{M}{M_0} = \sqrt{1+\xi^2}\, \left(\sqrt{1+\xi^2} - \xi\right) \quad . \tag{1.112}$$

The quantity $M_0$ is the starting moment. If the dependence of the friction moment on the rotational speed is known, the moment $M_d$ delivered to the rotating pipe can be determined.

## 1.6 Parallel Flow of Viscous Fluids

When a fluid is deformed a part of the kinetic energy of the flow is converted into heat (internal friction). For example in pipe flow, the internal friction results in a pressure drop in the flow direction. From a macroscopic point of view, the fluid flows in layers (lat. lamina), and the flow is called laminar flow. The velocity changes from layer to layer, and in the limiting case of infinitesimally thin layers, a continuous velocity profile results. The fluid layers flow past each other and the molecular momentum exchange between them causes tangential stresses,, which are closely related to the velocity gradients. They can be described with a phenomenological ansatz. The form of the ansatz depends on kind of fluid (viscosity law). In the close vicinity to a rigid wall the molecules of the fluid loose the tangential component of the momentum to the bounding surface, and as a consequence the fluid adheres to rigid walls (Stokes' no-slip condition, 1845):

### 1.6.1 Viscosity Laws

*Newtonian Fluid*

Newtonian fluids are fluids in which the tangential stresses are linearly proportional to the velocity gradients. This dependence can be illustrated with the following experiment: The space between two parallel plates is filled with a Newtonian fluid.
If the upper plate is moved with the velocity $u_w$ parallel to the lower plate, as shown in the following sketch, then the velocity increases linearly in the $y$-direction, and the particles in the superjacent layers move with different velocities.

$$u(y) = u_w \frac{y}{h} \tag{1.113}$$

The angle of shear can be determined from their displacement:

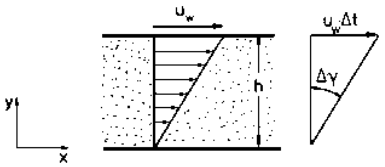


$$\Delta\gamma \approx -\frac{u_w \, \Delta t}{h} \tag{1.114}$$

The rate of strain is obtained by forming the differential quotient

$$\dot{\gamma} = \lim_{\Delta t \to 0} \frac{\Delta\gamma}{\Delta t} = -\frac{u_w}{h} \quad . \tag{1.115}$$

In general, for velocity distributions the rate of strain is

$$\dot{\gamma} = -\frac{du}{dy} \quad . \tag{1.116}$$

The relation between the rate of strain and the tangential or shear stress is obtained by a comparison with a shearing test with a rigid body.

*Shear Experiment*

The shear stress is proportional to the rate of strain. The constant of proportionality is the dynamic shear viscosity $\mu$; it depends on the medium, the pressure, and on the temperature. The ratio $\nu = \frac{\mu}{\rho}$ is called kinematic viscosity.

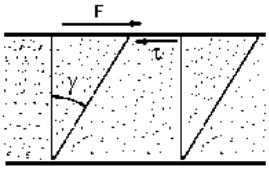


Rigid body $\tau = f(\gamma)$;
$\gamma$ = shear action
Hooke's law: $\tau = G\,\gamma$

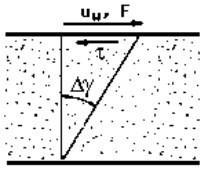


Fluid $\tau = f(\dot{\gamma})$;
$\dot{\gamma}$ = rate of strain
Newton's viscosity law: $\tau = \mu\,\dot{\gamma}$

The following two diagrams show the temperature dependence of the dynamic and the kinematic viscosity of water and air at atmospheric pressure.

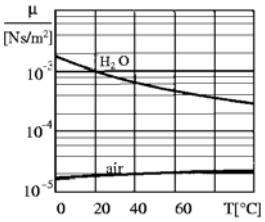


dynamic shear viscosity
$\nu = f(T)$

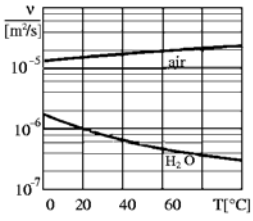


kinematic viscosity
$\nu = f(T)$

*Non-Newtonian Fluids*

Many fluids (for example high-polymeric fluids and suspensions) do not follow Newton's viscosity law. In order to be able to describe the different flow processes with simple relations, numerous empirical model laws were proposed.
The Bingham model describes the flow process of fluids, which below a certain shear stress behave as a rigid body (tooth paste)

$$\tau = \mu\,\dot{\gamma} \pm \tau_0 \quad . \tag{1.117}$$

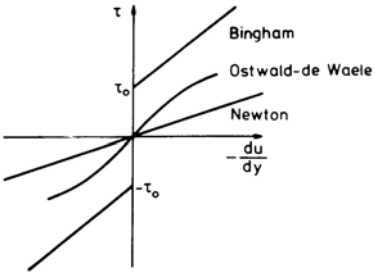


For $|\tau| < \tau_0$ ist $\dot{\gamma} = 0$. The Ostwald-de Waele model can describe nonlinear flow processes

$$\tau = \eta \;|\,\dot{\gamma}\,|^{n-1}\;\dot{\gamma} \quad . \tag{1.118}$$

For $n = 1$ this model is identical with Newton's viscosity law. The three models are shown in the diagram. The deviation of $n$ from unity indicates the deviation of the fluid from Newtonian behavior. For $n < 1$, the behavior is called pseudoplastic, for $n > 1$ the fluid is called dilatant.

### 1.6.2 Plane Shear Flow with Pressure Gradient

In the shear experiment described only shear stresses act in the fluid. In the following example it is shown, how normal stresses together with shear stresses influence the flow. In order to simplify the derivation it is assumed, that the normal stresses are caused by a pressure change in the $x$-direction, and that the shear stresses change only in the $y$-direction. In this parallel shear flow between two plates

$$\tau = \tau(y) \qquad p = p(x) \tag{1.119}$$

the shear stress is assumed to be positive in the $x$-direction, if the normal of the bounding surface points in the negative $y$-direction.
Assume that $L$ is the length in the $x$-direction, over which the pressure changes from $p_1$ to $p_2$. The equilibrium of forces can then be written down for Newtonian and non-Newtonian fluids. The velocity distribution is obtained by inserting the viscosity law and integration in the $y$-direction. For a Newtonian fluid with

$$\tau = -\mu\,\frac{du}{dy} \tag{1.120}$$

there results from the equilibrium of forces

$$\frac{dp}{dx} + \frac{d\tau}{dy} = 0 \quad . \tag{1.121}$$

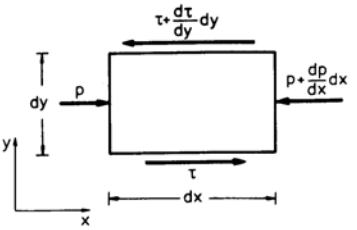


Integration yields

$$\tau(y) = (p_1 - p_2)\,\frac{y}{L} + c_1 \quad . \tag{1.122}$$

The velocity distribution is

$$u(y) = \frac{p_2 - p_1}{2\,\mu\,L}\,y^2 + c_1'\,y + c_2 \quad . \tag{1.123}$$

The constants of integration $c_1'$ and $c_2$ are obtained from the boundary conditions.

$$\left.\begin{array}{ll} y = 0: & u = 0 \\ y = h: & u = u_w \end{array}\right\} \quad \text{Stokes' no-slip condition} \tag{1.124}$$

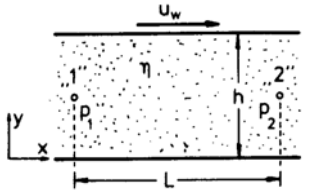


$$u(y) = h^2\,\frac{p_2 - p_1}{2\,\mu\,L}\left[\left(\frac{y}{h}\right)^2 - \frac{y}{h}\right] + u_w\,\frac{y}{h} \tag{1.125}$$

The velocity distribution is determined by the wall velocity $u_w$ and the pressure difference in the $x$-direction $p_1 - p_2$.

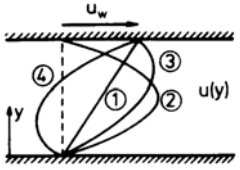


| | | |
|---|---|---|
| ① | $u_w > 0$ | $p_1 - p_2 = 0$ |
| ② | $u_w = 0$ | $p_1 - p_2 > 0$ |
| ③ | $u_w > 0$ | $p_1 - p_2 = 0$ |
| ④ | $u_w > 0$ | $p_1 - p_2 < 0$ |

The wall shear stresses are obtained by differentiation

$$y = 0 \;:\; \tau_w = -\mu\left[\frac{h}{L}\,\frac{p_1 - p_2}{2\,\mu} + \frac{u_w}{h}\right] \tag{1.126}$$

$$y = h \;:\; \tau_w = \mu\left[\frac{h}{L}\,\frac{p_1 - p_2}{2\,\mu} - \frac{u_w}{h}\right] \quad . \tag{1.127}$$

The volume rate of flow is

$$\frac{\dot{Q}}{b} = \int_0^h u(y)\,dy = h^3\,\frac{p_1 - p_2}{12\,\mu\,L} + \frac{u_w\,h}{2} \quad . \tag{1.128}$$

### 1.6.3 Laminar Pipe Flow

A pipe with circular cross section and radius $R$ is inclined at the angle $\alpha$. Laminar flow flows though it. It is assumed that the shear stress depends only on the radial coordinate. The equilibrium of forces yields

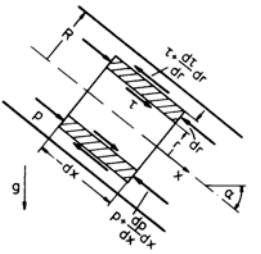


$$-\frac{dp}{dx} + \rho\, g\, \sin\alpha - \frac{1}{r}\,\frac{d}{dr}\,(\tau\, r) = 0 \quad . \tag{1.129}$$

The shear stress is obtained by integration

$$\tau = +\frac{r}{2}\,\left[\frac{p_1 - p_2}{L} + \rho\, g\, \sin\alpha\right] \quad . \tag{1.130}$$

For a Newtonian fluid with $\tau = -\mu\frac{du}{dr}$ the velocity distribution for the Stokes' no-slip condition is

$$u(r) = \frac{R^2}{4\,\mu}\,\left[\frac{p_1 - p_2}{L} + \rho\, g\, \sin(\alpha)\right]\,\left[1 - \left(\frac{r}{R}\right)^2\right] \quad . \tag{1.131}$$

The velocity attains its maximum value at the axis of the pipe ($r = 0$)

$$u_{max} = \frac{R^2}{4\,\mu}\,\left[\frac{p_1 - p_2}{L} + \rho\, g\, \sin\alpha\right] \quad . \tag{1.132}$$

The volume rate of flow through the pipe is

$$\dot{Q} = \int_0^R u(r)\, 2\,\pi\, r\, dr = \frac{\pi\, R^4}{8\,\mu}\,\left[\frac{p_1 - p_2}{L} + \rho\, g\, \sin\alpha\right] \tag{1.133}$$

(Derived by Hagen and Poiseuille about 1840 for $\alpha = 0$). With the volume rate of flow a mean velocity $u_m$ can be defined

$$u_m = \frac{\dot{Q}}{A} = \frac{R^2}{8\,\mu}\,\left[\frac{p_1 - p_2}{L} + \rho\, g\, \sin\alpha\right] = \frac{u_{max}}{2} \quad . \tag{1.134}$$

The pressure difference $p_1 - p_2$ is a measure for the wall shear stress, when the gravitational force can be neglected.

$$\tau_w = \frac{R}{2}\,\frac{p_1 - p_2}{L} \quad . \tag{1.135}$$

The pressure difference referenced to the dynamic pressure of the mean velocity is

$$\frac{p_1 - p_2}{\frac{\rho}{2}\,u_m^2} = \frac{64\,\mu\, l}{\rho\, u_m\, D^2} \quad . \tag{1.136}$$

In the last equation the dimensionless expression $\frac{\rho\, u_m\, D}{\mu}$ is the Reynolds number $Re$,

$$\frac{8\,\tau_w}{\rho\, u_m^2} = \frac{64}{Re} \quad . \tag{1.137}$$

The quotient $8\,\tau_w/(\rho\, u_m^2)$ is called the pipe friction coefficient $\lambda$. It is proportional to the wall shear stress, nondimensionalized with the dynamic pressure of the mean velocity.

$$\lambda = \frac{8\,\tau_w}{\rho\, u_m^2} \quad . \tag{1.138}$$

*Flow in the Intake Region of a Pipe*

If the velocity depends only on the radial coordinate $r$, as for example in the Hagen-Poiseuille law, then the pipe flow is called fully developed. This flow condition is reached only at the end of the intake length $L_i$, which is approximately

$$L_i = 0.029\, Re\, D \quad . \tag{1.139}$$

In the intake region the velocity profiles change as indicated in the following drawing.

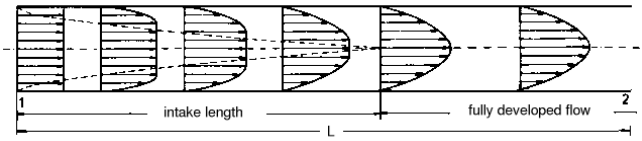


In the intake region an additional pressure loss arises, which can be described by a loss coefficient ($\zeta_i \approx 1.16$)

$$\frac{p_1 - p_2}{\frac{\rho}{2}\, u_m^2} = \lambda\, \frac{L}{D} + \zeta_i \quad . \tag{1.140}$$

In long pipes the intake losses can be neglected, but they have to be taken into account in viscosity measurements in capillary viscometers.
The viscosity can be determined with the aid of the equation derived by Hagen and Poiseeuille, (1.133) for $\alpha = 0$: The validity of this equation was confirmed with extreme accuracy, so that it can be used for viscosity measurements. The experimental set up consists of a pipe with a small diameter and a large diameter-to-length ratio, with the axis positioned horizontally. Then the gravitational acceleration acts normal to the flow direction, and the pressure drop is solely proportional to the dynamic shear viscosity $\mu$ and iversely proportional to the volume rate of flow. The viscosity can be determined by measuring the pressure drop and the volume rate of flow. In order to avoid errors, caused by the variation of the velocity profile in the intake region, the pressure must be measured further downstream. This can be done by computing the entrance length with (1.139) and comparing it with the distance between the position of the boreholes for the pressure measurements and the entrance of the pipe.

## 1.7 Turbulent Pipe Flows

The Hagen-Poiseuille law looses its validity when the Reynols number exceeds a certain value. Experiments show, that irregular velocity fluctuations set in, which cause an intensive intermixing of the various layers in the flow. The momentum exchange normal to the axis of the pipe increases markedly. The profiles of the time-averaged velocity become fuller, and the wall shear stress increases. The pressure drop no longer is proportional to $\dot{Q}$, but approximately to $\dot{Q}^2$. The flow is then called turbulent. In technical pipe flows the transition from laminar to turbulent flow in general occurs at a Reynolds number $Re = 2300$. Under special experimental conditions pipe flows can be kept laminar up to Reynolds number $Re = 20000$ and higher, with the diameter of the pipe again used as the reference length. The flow is then very susceptible to small perturbations and is difficult to maintain.

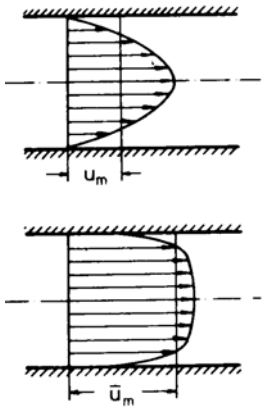

### 1.7.1 Momentum Transport in Turbulent Flows

Following Reynolds (1882) the velocity in turbulent flows can be described with an ansatz, which contains a time-averaged value and a fluctuating part.

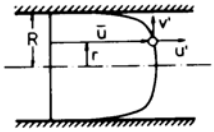


For the fully developed turbulent pipe flow the splitting of the component in the axial direction yields

$$u(r,\Phi,x,t) = \bar{u}(r) + u'(r,\Phi,x,t) \quad , \tag{1.141}$$

and normal to it

$$v(r,\Phi,x,t) = v'(r,\Phi,x,t) \quad . \tag{1.142}$$

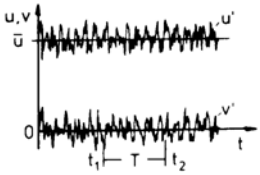


The time-averaged value of the velocity is determined in such a way, that the time-averaged value of the fluctuations vanishes.

In general the time-averaged mean value of the squares and the product of the two components (correlation) of the fluctuation velocity do not vanish. When they are multiplied by the density, they have the dimension of stress. The time-averaged correlation can be interpreted as the transport of momentum per unit area in the radial direction, while the squares represent normal stresses.

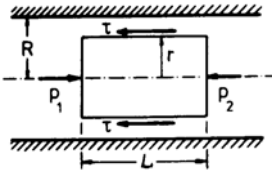


The turbulent momentum transport is mainly determined by the correlation of the velocity fluctuations

$$\overline{u'v'} = \frac{1}{T} \int_0^T (u'v')\, dt. \tag{1.143}$$

This result is obtained with the momentum theorem, written for the control surface indicated by the solid line shown in the drawing above.

$$\int_\tau \frac{\partial}{\partial t}\, \rho\, \boldsymbol{v}\, d\tau + \int_A \rho\, \boldsymbol{v}\, (\boldsymbol{v} \cdot \boldsymbol{n})\, dA = \boldsymbol{F}_p + \boldsymbol{F}_f \tag{1.144}$$

With the velocity

$$\boldsymbol{v} = \boldsymbol{i}\, (\bar{u} + u') + \boldsymbol{j}\, v' \tag{1.145}$$

The time-averaged momentum equation is obtained to

$$\rho \int_A \overline{u'v'}\, dA = 2\, \pi\, r\, L\, \rho\, \overline{u'v'} = \pi\, r^2\, (p_1 - p_2) - \tau\, 2\, \pi\, r\, L \quad , \tag{1.146}$$

which yields with Newton's viscosity law

$$(p_2 - p_1)\, \frac{r}{2\, L} = -\rho\, \overline{u'v'} + \mu\, \frac{d\bar{u}}{dr} \tag{1.147}$$

The quantity $\rho\, \overline{u'v'}$ is called the apparent or turbulent shear stress. If the velocity profile $\bar{u}(r)$ is to be determined, the correlation $\overline{u'v'}$ has to be known. Since the apparent stresses cannot be obtained from (1.147), an additional hypothesis has to be introduced, which constitutes a relation connecting the velocity correlation with the time-averaged velocity.

*Prandtl's Mixing-Length Hypothesis*

In his hypothesis about the turbulent momentum transport Prandtl assumes, that small agglomerations of fluid particles move relative to the surrounding fluid in the main flow direction and normal to it and exchange momentum with their surroundings.

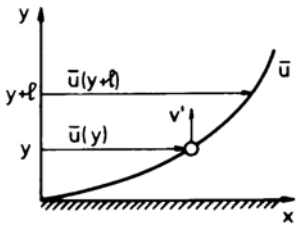


The distance along which the agglomerations loose their excess momentum is called mixing length $l$. Normal to the direction of the main flow the change of velocity between two layers, by the distance $l$ apart from each other, is

$$\Delta u = \bar{u}(y+l) - \bar{u}(y) \approx l\,\frac{d\bar{u}}{dy} \quad . \tag{1.148}$$

This velocity difference can be assumed to be equal to the velocity fluctuation $u'$

$$u' = l\,\frac{d\bar{u}}{dy} \quad . \tag{1.149}$$

The fluctuations in the main flow direction cause fluctuations of the normal velocity component $v'$, which are of equal order of magnitude. A positive fluctuation $u'$ most of the time originates a negative fluctuation $v'$, as can be reasoned from continuity considerations. Hence

$$v' = -cu' \quad , \tag{1.150}$$

where $c$ is a positive constant, which can be included in the mixing length. The turbulent shear stress $\tau_t$ then follows as the mean value of the product of both fluctuations $u'$ and $v'$

$$\tau_t = \rho\,\overline{u'v'} = \rho\,l^2\,\left|\frac{d\bar{u}}{dy}\right|\,\frac{d\bar{u}}{dy} \quad . \tag{1.151}$$

The absolute value of $d\bar{u}/dy$ is introduced, in order to ensure, that the sign of the turbulent shear stress changes with the sign of the velocity gradient.

### 1.7.2 Velocity Distribution and Resistance Law

With the equation for the turbulent shear stress, (1.151), the momentum equation for the turbulent pipe flow reads with a shift of coordinates to $y = R - r$

$$-\frac{p_2 - p_1}{2\,L}\,(R-y) = \mu\,\frac{d\bar{u}}{dy} + \rho\,l^2\,\left|\frac{d\bar{u}}{dy}\right|\,\frac{d\bar{u}}{dy} \quad . \tag{1.152}$$

For $y = 0$ the right-hand side of (1.152) represents the wall shear stress $\tau_w$. The turbulent shear stress vanishes at the wall, as the velocity fluctuations have to vanish there because of Stokes' no-slip condition. The mixing length $l$ therefore has also to vanish in the vicinity of the wall. Prandtl assumed, that in the layer nearest to the wall the mixing length is proportional to the distance from the wall,

$$l = k\,y \quad . \tag{1.153}$$

In the above equation $k$ is a constant. Aside from a very thin layer in the immediate vicinity of the wall, the turbulent shear stress is much larger than the laminar contribution, and hence the latter can be neglected in the integration of (1.152). If finally another of Prandtl's assumptions is introduced, according to which the turbulent shear stress $\tau_t$ remains constant and is equal to the wall shear stress $\tau_w$, then, after integration of (1.152), the universal law of the wall for turbulent pipe flow is obtained

$$\frac{\bar{u}}{u_*} = \frac{1}{k}\,\ln\frac{y\,u_*}{\nu} + C \quad . \tag{1.154}$$

The quantity $u_* = \sqrt{\tau_w/\rho}$ is called friction velocity The constant $k = 0.4$ is named after von Kármán; $k$ and $C$ were determined from experiments. For technically smooth pipes $C = 5.5$.

The logarithmic form of the universal law of the wall shows, that it looses its validity in the immediate vicinity of the wall. Since the mixing length vanishes for $y$ approaching zero, the shear stress in the viscous sublayer is solely given by $\mu\, d\bar{u}/dy$.
With $\tau = \tau_w = const.$, the velocity in the viscous sublayer is

$$\frac{\bar{u}}{u_*} = \frac{y\, u_*}{\nu} \quad . \tag{1.155}$$

Although the logarithmic velocity distribution was derived for the region near the wall, the comparison with experimental data shows, that it is approximately valid over the entire cross section. By eliminating the constant of integration $C$, with $\bar{u} = \bar{u}_{max}(y = R)$ there is obtained

$$\frac{\bar{u}_{max} - \bar{u}}{u_*} = \frac{1}{k} \ln \frac{R}{y} \quad . \tag{1.156}$$

The time-averaged velocity averaged over the cross section is $\bar{u}_m$

$$\frac{\bar{u}_m}{u_*} = \frac{\bar{u}_{max}}{u_*} - 3.75 \quad . \tag{1.157}$$

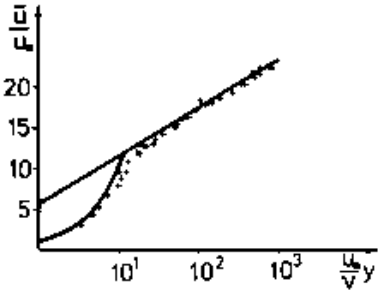


Universal law of the wall

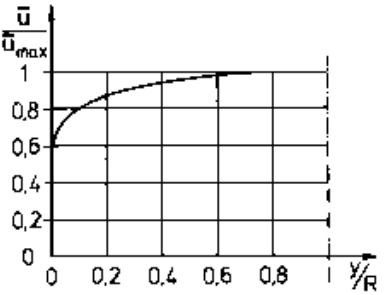


Time-averaged dimensionless radial velocity distribution of the turbulent pipe flow with $\frac{y}{R} = 1 - \frac{r}{R}$.

Experimental data also confirm (1.157), if the constant 3.75 is replaced by the value 4.07.
With the definition of the pipe friction coefficient

$$\lambda = \frac{8\, {u_*}^2}{\bar{u}_m^2} \tag{1.158}$$

and the universal law of the wall, (1.158) can be cast into the form

$$\frac{1}{\sqrt{\lambda}} = 2.035\, \log(Re\, \sqrt{\lambda}) - 0.91 \quad . \tag{1.159}$$

Equation (1.159) agrees with experimental data, if the constants are changed so that

$$\frac{1}{\sqrt{\lambda}} = 2.0\, \log(Re\, \sqrt{\lambda}) - 0.8 \quad . \tag{1.160}$$

This law is called the Prandtl universal resistance law. For Reynolds numbers up to $Re = 10^5$ also the simple relation of Blasius (1911) can be used

$$\lambda = \frac{0.316}{Re^{0.25}} \quad . \tag{1.161}$$

The pipes for which these laws are valid, have to be hydraulically smooth.

*Rough Pipes*

Pipes used in technical applications, in general are not hydraulically smooth. The roughness of the wall influences the flow, such that the pipe friction coefficient is no longer given by Prandtl's law. The friction coefficient then depends on the number of roughness elements per unit area, on their shape, and on their distribution. In order to be able to characterize the roughness in a simplified manner, a parameter $k/R$ (relative roughness) is introduced, which is coordinated with a more accurately defined sand roughness $k_s/R$, such that the pipe friction coefficients agree.

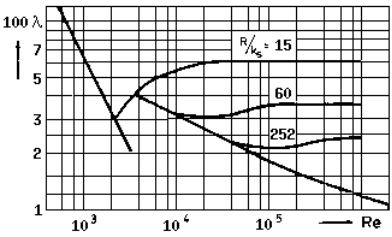


The diagram shows the influence of the relative sand roughness on the pipe friction coefficient. According to this diagram, above a certain Reynolds number the friction coefficient $\lambda$ depends only on $k_s/R$. For completely rough pipes the quadratic resistance law is valid and the pipe friction coefficient can be determined by the following relation.

$$\frac{1}{\sqrt{\lambda}} = 2.0 \log\left(\frac{R}{k_s}\right) + 1.74 \tag{1.162}$$

### 1.7.3 Pipes with Non-circular Cross Section

Experimentally determined resistances of turbulent flows in pipes with non-circular cross sections agree well with the resistance law for circular pipes, if in the equation for the pressure loss and in the definition of the Reynolds number the hydraulic diameter $d_h$ is introduced.

$$d_h = \frac{4\,A}{U} \tag{1.163}$$

$A$ stands for the cross-sectional area and $U$ for the circumference.

$$\Delta p_l = \lambda \frac{L}{d_h} \frac{\rho}{2} \bar{u}_m^2 \qquad Re_h = \frac{\rho\, \bar{u}_m\, d_h}{\mu} \quad . \tag{1.164}$$

As the following diagram shows, the experimental data $\lambda(Re_h)$ follow the Blasius law for turbulent flows. The pressure loss of turbulent flows in open channels can be obtained in the same manner. The hydraulic diameter is then determined from the cross-sectional area of the flow and the wetted circumference of the channel.

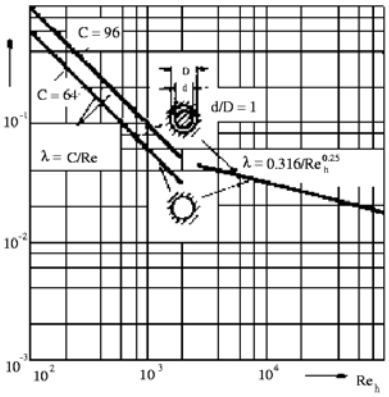


Friction coefficient for laminar and turbulent pipe flow with non-circular cross section

The hydraulic diameter looses its meaning for laminar flows. For laminar flows with non-circular cross section the pipe friction coefficient is determined from the law $\lambda = C/Re$, where the shape of the cross section is accounted for in the constant $C$.

# 2. Fluid Mechanics II

## 2.1 Introduction

A flow is completely determined if the velocity vector $\boldsymbol{v}$ and the thermodynamic properties, the pressure $p$, the density $\rho$, and the temperature $T$ are known everywhere in the flow field. These six quantities, the three velocity components, and the three thermodynamic variables have to be provided for the description of the flow. This can be done by solving the conservation equations for mass, momentum, and energy and the thermal equation of state, which connects the thermodynamic variables with each other. If the latter change markedly, the dynamic shear viscosity, $\mu$, the thermal conductivity $\lambda$, and the specific heat $c$ also have to be prescribed as a function of pressure and temperature. Liquids can be considered as incompressible and their density $\rho$ can be assumed to be constant. This assumption also holds for gases flowing at low speeds.
The conservation laws are presented in the form of partial differential equations ; their solution requires the prescription of initial and boundary conditions.

## 2.2 Fundamental Equations of Fluid Mechanics

### 2.2.1 The Continuity Equation

The mass $m$ of a flowing medium remains constant in a time-dependent volume $\tau(t)$, bounded by the closed surface $A(t)$.

$$\frac{dm}{dt} = \frac{d}{dt}\int_{\tau(t)} \rho \, d\tau = 0 \tag{2.1}$$

The total time derivative of the mass $m$ can be written as

$$\frac{d}{dt}\int_{\tau(t)} \rho d\tau = \lim_{\Delta t \to 0}\left[\frac{1}{\Delta t}\left(\int_{\tau(t+\Delta t)} \rho\,(t+\Delta t)\, d\tau - \int_{\tau(t)} \rho(t)\, d\tau\right)\right] \quad . \tag{2.2}$$

With

$$\rho(t+\Delta t) = \rho(t) + \frac{\partial \rho}{\partial t}\,\Delta t + \ldots \tag{2.3}$$

and

$$d\tau = (\boldsymbol{v}\cdot\boldsymbol{n})\, dA\, dt \tag{2.4}$$

there results

$$\frac{d}{dt}\int_{\tau(t)} \rho \, d\tau = \int_{\tau(t)} \frac{\partial \rho}{\partial t} d\tau + \int_{A(t)} \rho\,(\boldsymbol{v}\cdot\boldsymbol{n})\, dA \quad . \tag{2.5}$$

The surface integral over $A(t)$ can be transformed into a volume integral with the aid of the Gauss divergence theorem, such that the last equation takes on the following form

$$\frac{d}{dt}\int_{\tau(t)} \rho \, d\tau = \int_{\tau(t)} \left[\frac{\partial \rho}{\partial t} + \nabla\cdot(\rho\,\boldsymbol{v})\right] d\tau \quad . \tag{2.6}$$

The above volume integral can vanish only, if the integrand vanishes identically everywhere in the flow field. Hence

$$\frac{\partial \rho}{\partial t} + \nabla \cdot (\rho \, \boldsymbol{v}) = 0 \quad . \tag{2.7}$$

The vanishing of the integral by cancellation of negative with positive parts of the integrand is not meant here. Instead it is required, that the integrand vanishes throughout the flow field. The above equation is known as continuity equation. It can be written in a different form by introducing the total time derivative of the density.

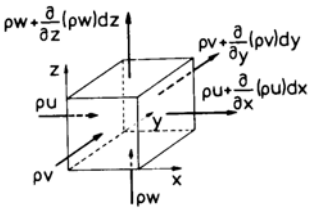


$$\frac{d\rho}{dt} + \rho \, (\nabla \cdot \boldsymbol{v}) = 0 \tag{2.8}$$

For an incompressible fluid there results $\nabla \cdot \boldsymbol{v} = 0$. The continuity equation can also be derived with the aid of a mass balance for a space-bound volume element. The change of mass per unit time in the volume element is equal to the difference between in- and out-flowing mass.

$$-\left[\frac{\partial(\rho \, u)}{\partial x} \, dx \, dy \, dz + \frac{\partial(\rho \, v)}{\partial y} \, dx \, dy \, dz + \frac{\partial(\rho \, w)}{\partial z} \, dx \, dy \, dz\right] = \frac{\partial \rho}{\partial t} \, dx \, dy \, dz \tag{2.9}$$

Again there is obtained

$$\frac{\partial \rho}{\partial t} + \nabla \cdot (\rho \, \boldsymbol{v}) = 0 \quad . \tag{2.10}$$

The change of mass per unit time in the control volume is expressed by the partial derivative $\frac{\partial \rho}{\partial t}$, the mass flow through its surface is given by the expression $\nabla \cdot (\rho \, \boldsymbol{v})$.

### 2.2.2 The Navier-Stokes Equations

The equilibrium of forces acting on a volume element of fluid can be described with the momentum theorem. The time rate of change of the momentum of a closed volume is equal to the sum of the external forces acting on the volume.

$$\frac{d}{dt} \int_{\tau(t)} \rho \, \boldsymbol{v} \, d\tau = \sum \boldsymbol{F} \tag{2.11}$$

The left-hand side of this equation, which is the total time derivative of the volume integral extended over the momentum $\rho \boldsymbol{v}$, can be rearranged similarly to the derivation of the continuity equation. It follows that

$$\frac{d}{dt} \int_{\tau(t)} \rho \, \boldsymbol{v} \, d\tau = \int_{\tau(t)} \left[\frac{\partial \rho \, \boldsymbol{v}}{\partial t} + \nabla \cdot (\rho \, \boldsymbol{v} \, \boldsymbol{v})\right] d\tau = \int_{\tau(t)} \rho \, \left[\frac{\partial \boldsymbol{v}}{\partial t} + (\boldsymbol{v} \cdot \nabla) \, \boldsymbol{v}\right] d\tau \quad . \tag{2.12}$$

The term $(\boldsymbol{v}\boldsymbol{v})$ is the diadic product of the velocity vector $\boldsymbol{v}$. The external forces are the volume force, as, for example, the gravitational force

$$\boldsymbol{F}_g = \int_{\tau(t)} \rho \, \boldsymbol{g} \, d\tau \quad , \tag{2.13}$$

and the surface forces, which result from the stress tensor $\bar{\bar{\sigma}}$.

$$\boldsymbol{F}_\sigma = -\int_{A(t)} (\boldsymbol{n} \cdot \bar{\bar{\sigma}}) dA \tag{2.14}$$

The term $(\boldsymbol{n} \cdot \bar{\bar{\sigma}})$ is the vector product of the normal $\boldsymbol{n}$ and the stress tensor $\bar{\bar{\sigma}}$. The surface integral can again be replaced by a volume integral

$$\boldsymbol{F}_\sigma = -\int_{A(t)} (\boldsymbol{n} \cdot \bar{\bar{\sigma}})\, dA = -\int_{\tau(t)} (\nabla \cdot \bar{\bar{\sigma}})\, d\tau \quad . \tag{2.15}$$

The momentum theorem for an arbitrarily closed volume $\tau$ then reads

$$\int_{\tau(t)} \rho \left[ \frac{\partial \boldsymbol{v}}{\partial t} + (\boldsymbol{v} \cdot \nabla)\, \boldsymbol{v} \right] d\tau = \int_{\tau(t)} \rho\, \boldsymbol{g}\, d\tau - \int_{\tau(t)} (\nabla \cdot \bar{\bar{\sigma}})\, d\tau \quad . \tag{2.16}$$

If the three integrals are lumped together into a single integral, again, it can vanish only, if the integrand vanishes identically:

$$\rho \left[ \frac{\partial \boldsymbol{v}}{\partial t} + (\boldsymbol{v} \cdot \nabla)\, \boldsymbol{v} \right] = \rho\, \boldsymbol{g} - (\nabla \cdot \bar{\bar{\sigma}}) \tag{2.17}$$

The components of this vector equation can be written in arbitrary coordinate systems, suitably chosen for the problem considered. In Cartesian coordinates the following equations result with

$$\bar{\bar{\sigma}} = \begin{pmatrix} \sigma_{xx} & \tau_{xy} & \tau_{xz} \\ \tau_{yx} & \sigma_{yy} & \tau_{yz} \\ \tau_{zx} & \tau_{zy} & \sigma_{zz} \end{pmatrix} \tag{2.18}$$

$$\begin{aligned}
\rho \left( \frac{\partial u}{\partial t} + u \frac{\partial u}{\partial x} + v \frac{\partial u}{\partial y} + w \frac{\partial u}{\partial z} \right) &= \rho\, g_x - \frac{\partial \sigma_{xx}}{\partial x} - \frac{\partial \tau_{xy}}{\partial y} - \frac{\partial \tau_{xz}}{\partial z} \\
\rho \left( \frac{\partial v}{\partial t} + u \frac{\partial v}{\partial x} + v \frac{\partial v}{\partial y} + w \frac{\partial v}{\partial z} \right) &= \rho\, g_y - \frac{\partial \tau_{yx}}{\partial x} - \frac{\partial \sigma_{yy}}{\partial y} - \frac{\partial \tau_{yz}}{\partial z} \\
\rho \left( \frac{\partial w}{\partial t} + u \frac{\partial w}{\partial x} + v \frac{\partial w}{\partial y} + w \frac{\partial w}{\partial z} \right) &= \rho\, g_z - \frac{\partial \tau_{zx}}{\partial x} - \frac{\partial \tau_{zy}}{\partial y} - \frac{\partial \sigma_{zz}}{\partial z} \quad .
\end{aligned} \tag{2.19}$$

These equations describe the relations between the velocity components and the local stresses of the fluid considered. The instantaneous stresses can be related to the velocity field with the aid of the Stokes hypothesis, carried over from theoretical mechanics. In Hooke's law the stresses are assumed to be proportional to the strain, and in fluid mechanics the stresses are assumed to be proportional to the time rate of change of the strain.
Before these relations are established, it is noted, that the above equations of motion state that a small volume element moving with the fluid is accelerated or decelerated by the external forces acting on it. It is seen that the momentum balance is completely equivalent to Newton's second law of motion.
It is also noted, that (2.19) is valid for any fluid either Newtonian or non-Newtonian. In order to use (2.19) for determining the velocity and the pressure, the stresses have to be expressed in terms of the derivatives of the velocity components and the viscosity of the fluid. This will be done next for a Newtonian fluid.

*Stress-Strain Relations*

For the derivation of the relations describing the dependence of the stresses on the time rate of change of the strain, it is assumed. that the normal stresses $\sigma_{xx}$, $\sigma_{yy}$, $\sigma_{zz}$ cause elongations and contractions $\epsilon_x$, $\epsilon_y$, $\epsilon_z$, and the shear stresses $\tau_{xy}, \ldots, \tau_{zy}$ cause angular displacements $\gamma_{xy}, \ldots, \gamma_{zy}$. As indicated in the diagram the components of the time rate of change of the strain are given by the partial derivatives of the velocity components in the direction of the coordinate axes.

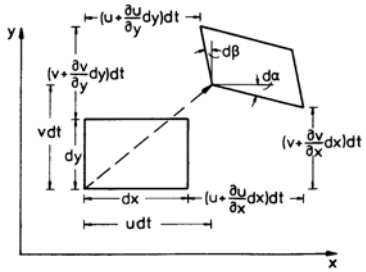


$$\dot{\epsilon}_x = \frac{\partial u}{\partial x} \qquad \dot{\epsilon}_y = \frac{\partial v}{\partial y} \qquad \dot{\epsilon}_z = \frac{\partial w}{\partial z} \tag{2.20}$$

The sum of the components of the time rate of change of the strain yields the relative change in volume, per time interval $dt$ (volume dilatation)

$$\dot{e} = \frac{\partial u}{\partial x} + \frac{\partial v}{\partial y} + \frac{\partial w}{\partial z} = \nabla \cdot \boldsymbol{v}. \tag{2.21}$$

The angular displacements per time interval $dt$ are

$$\dot{\gamma}_{xy} = \frac{d\,\beta + d\,\alpha}{dt} = -\left(\frac{\partial u}{\partial y} + \frac{\partial v}{\partial x}\right) \quad \dot{\gamma}_{yz} = -\left(\frac{\partial v}{\partial z} + \frac{\partial w}{\partial y}\right) \quad \dot{\gamma}_{xy} = -\left(\frac{\partial u}{\partial z} + \frac{\partial w}{\partial x}\right) . \tag{2.22}$$

The normal and tangential stresses are related to the time rate of change of the components of the strain and the angular displacements in a linear ansatz. In the state of rest, in which the time rate of change of the strains and the angular displacements vanish, the normal stresses $\sigma_{xx}$, $\sigma_{yy}$, $\sigma_{zz}$ are independent of the direction, and solely given by the hydrostatic pressure. This behavior of the flow can be expressed by the following hypothesis, introduced by Stokes

$$\begin{aligned} \sigma_{xx} &= p - 2\,\mu\,\dot{\epsilon}_x - \tilde{\lambda}\,\dot{e} \quad , \\ \sigma_{yy} &= p - 2\,\mu\,\dot{\epsilon}_y - \tilde{\lambda}\,\dot{e} \quad , \\ \sigma_{zz} &= p - 2\,\mu\,\dot{\epsilon}_z - \tilde{\lambda}\,\dot{e} \quad , \end{aligned} \tag{2.23}$$

and

$$\tau_{xy} = \mu\,\dot{\gamma}_{xy} \quad , \qquad \tau_{yz} = \mu\,\dot{\gamma}_{yz} \quad , \qquad \tau_{xz} = \mu\,\dot{\gamma}_{xz} \quad . \tag{2.24}$$

Since for reasons of symmetry $\tau_{xy} = \tau_{yx}$,$\tau_{yz} = \tau_{zy}$ and $\tau_{xz} = \tau_{xz}$, only three normal and three tangential stress components of the Stokes stress tensor are unknown. It can therefore be written as

$$\begin{aligned} \bar{\bar{\sigma}} = p \begin{pmatrix} 1 & & \\ & 1 & \\ & & 1 \end{pmatrix} - \tilde{\lambda} \begin{pmatrix} \nabla \cdot \boldsymbol{v} & & \\ & \nabla \cdot \boldsymbol{v} & \\ & & \nabla \cdot \boldsymbol{v} \end{pmatrix} - \\ -2\,\mu \begin{pmatrix} \frac{\partial u}{\partial x} & \frac{1}{2}\left(\frac{\partial u}{\partial y} + \frac{\partial v}{\partial x}\right) & \frac{1}{2}\left(\frac{\partial u}{\partial z} + \frac{\partial w}{\partial x}\right) \\ \frac{1}{2}\left(\frac{\partial u}{\partial y} + \frac{\partial v}{\partial x}\right) & \frac{\partial v}{\partial y} & \frac{1}{2}\left(\frac{\partial v}{\partial z} + \frac{\partial w}{\partial y}\right) \\ \frac{1}{2}\left(\frac{\partial u}{\partial z} + \frac{\partial w}{\partial x}\right) & \frac{1}{2}\left(\frac{\partial v}{\partial z} + \frac{\partial w}{\partial y}\right) & \frac{\partial w}{\partial z} \end{pmatrix} \quad . \end{aligned} \tag{2.25}$$

The coefficient $\tilde{\lambda}$ generally is split into the two parts $\tilde{\lambda} = \hat{\mu} - \frac{2}{3}\,\mu$. The volume viscosity $\hat{\mu}$ takes into account the molecular degrees of freedom; it vanishes for monatomig gases.
The normal stresses are

$$\begin{aligned} \sigma_{xx} &= p - 2\,\mu\,\frac{\partial u}{\partial x} - \left(\hat{\mu} - \frac{2}{3}\,\mu\right)(\nabla \cdot \boldsymbol{v}) \quad , \\ \sigma_{yy} &= p - 2\,\mu\,\frac{\partial v}{\partial y} - \left(\hat{\mu} - \frac{2}{3}\,\mu\right)(\nabla \cdot \boldsymbol{v}) \quad , \\ \sigma_{zz} &= p - 2\,\mu\,\frac{\partial w}{\partial z} - \left(\hat{\mu} - \frac{2}{3}\,\mu\right)(\nabla \cdot \boldsymbol{v}) \quad . \end{aligned} \tag{2.26}$$

Their mean value is

$$\bar{\bar{\sigma}} = \frac{1}{3}\,(\sigma_{xx} + \sigma_{yy} + \sigma_{zz}) = p - \hat{\mu}\,(\nabla \cdot \boldsymbol{v}) \quad . \tag{2.27}$$

For incompressible flows the mean value is simply $\bar{\bar{\sigma}} = p$.
If the stress-strain relations are substituted in the momentum equations, the Navier-Stokes equations are obtained (1823, 1845).

$$\begin{aligned}
\rho \frac{du}{dt} &= -\frac{\partial p}{\partial x} + \frac{\partial}{\partial x}\left[2\,\mu \frac{\partial u}{\partial x} + \tilde{\lambda}\,(\nabla \cdot \boldsymbol{v})\right] + \frac{\partial}{\partial y}\left[\mu\left(\frac{\partial u}{\partial y} + \frac{\partial v}{\partial x}\right)\right] + \frac{\partial}{\partial z}\left[\mu\left(\frac{\partial u}{\partial z} + \frac{\partial w}{\partial x}\right)\right] + \rho\, g_x \\
\rho \frac{dv}{dt} &= -\frac{\partial p}{\partial y} + \frac{\partial}{\partial x}\left[\mu\left(\frac{\partial u}{\partial y} + \frac{\partial v}{\partial x}\right)\right] + \frac{\partial}{\partial y}\left[2\,\mu \frac{\partial v}{\partial y} + \tilde{\lambda}\,(\nabla \cdot \boldsymbol{v})\right] + \frac{\partial}{\partial z}\left[\mu\left(\frac{\partial v}{\partial z} + \frac{\partial w}{\partial y}\right)\right] + \rho\, g_y \\
\rho \frac{dw}{dt} &= -\frac{\partial p}{\partial z} + \frac{\partial}{\partial x}\left[\mu\left(\frac{\partial u}{\partial z} + \frac{\partial w}{\partial x}\right)\right] + \frac{\partial}{\partial y}\left[\mu\left(\frac{\partial v}{\partial z} + \frac{\partial w}{\partial y}\right)\right] + \frac{\partial}{\partial z}\left[2\,\mu \frac{\partial w}{\partial z} + \tilde{\lambda}\,(\nabla \cdot \boldsymbol{v})\right] + \rho\, g_z
\end{aligned}$$

For incompressible flow with constant dynamic shear viscosity $\mu$ the above equations reduce to

$$\begin{aligned}
\rho \frac{du}{dt} &= -\frac{\partial p}{\partial x} + \mu\,\nabla^2 u + \rho\, g_x \quad , \\
\rho \frac{dv}{dt} &= -\frac{\partial p}{\partial y} + \mu\,\nabla^2 u + \rho\, g_y \quad , \\
\rho \frac{dw}{dt} &= -\frac{\partial p}{\partial z} + \mu\,\nabla^2 u + \rho\, g_z \quad . \qquad (2.28)
\end{aligned}$$

### 2.2.3 The Energy Equation

The Bernoulli equation states that the sum of the mechanical energies is constant in incompressible, loss-free, steady flows. In flows with large density and temperature changes in addition to the change of the mechanical energy also the change of the thermal energy has to be included in the balance equation.
The energy $E$ in a closed volume consists out of the internal energy $\rho\, e$ and the kinetic energy $\frac{1}{2}\,\rho\,\boldsymbol{v}^2$.

$$E = \rho\left(e + \frac{\boldsymbol{v}^2}{2}\right) \qquad (2.29)$$

According to the first law of thermodynamics, the internal energy of an arbitrary, always the same mass particles containing volume increases, if the amount of heat, added to the gas through the bounding surface, is larger than the work done against the acting volume and surface forces. Internal heat sources are neglected. Since the time rate of change of the various parts of the energy contributing to the balance is considered, often the notion power $P$ is used. The time rate of change of the total energy of a fluid contained in a volume bounded by a closed surface is

$$\frac{d}{dt}\int_{\tau(t)} \rho\left(e + \frac{\boldsymbol{v}^2}{2}\right) d\tau = \sum P \qquad . \qquad (2.30)$$

The work to be done by the fluid against the volume forces is given by the work, done during the time interval $dt$ by the forces acting along the various particle paths. If the volume force is given by the gravitational force, the corresponding contribution is described by the inner product of the gravitational acceleration $\boldsymbol{g}$ and the velocity $\boldsymbol{v}$.

$$P_\tau = \int_{\tau(t)} \rho(\boldsymbol{g} \cdot \boldsymbol{v}) d\tau \qquad (2.31)$$

The work to be done against the surface forces can be determined with the aid of the work necessary for the displacement of the bounding surface of the volume $\tau$. This contribution is given by the surface integral extended over the inner vector product of the stress tensor $\bar{\bar{\sigma}}$ and the velocity $\boldsymbol{v}$

$$P_A = -\int_A (\bar{\bar{\sigma}} \cdot \boldsymbol{v}) \cdot \boldsymbol{n}\, dA \quad , \tag{2.32}$$

which can again be transformed into a volume integral.

$$P_A = -\int_{\tau(t)} \nabla \cdot (\bar{\bar{\sigma}} \cdot \boldsymbol{v})\, d\tau \tag{2.33}$$

If, as in the derivation of the Navier-Stokes equations, the pressure is separated from the stress tensor, a second integral results, in which the work of the friction forces per unit volume is taken into account by the rest of the stress tensor $\bar{\bar{\sigma}}'$ and the velocity vector

$$P_A = -\int_{\tau(t)} \nabla \cdot (p\, \boldsymbol{v})\, d\tau - \int_{\tau(t)} \nabla \cdot (\bar{\bar{\sigma}}' \cdot \boldsymbol{v})\, d\tau \quad . \tag{2.34}$$

The first integral describes the work of the pressure forces, and the second the work of the friction forces.
The contribution to the energy balance by heat conduction is given by the heat flux through the bounding surface $\boldsymbol{q}$.

$$P_q = -\int_{A(t)} (\boldsymbol{q} \cdot \boldsymbol{n})\, dA \tag{2.35}$$

Thermal radiation is not considered here. With Fourier's law of heat conduction

$$\boldsymbol{q} = -\lambda\, \nabla T \tag{2.36}$$

there is obtained

$$P_q = \int_{A(t)} \lambda\, (\nabla T \cdot \boldsymbol{n}) dA = \int_{\tau(t)} \nabla \cdot (\lambda\, \nabla T)\, d\tau \quad . \tag{2.37}$$

The time rate of change of the total energy contained in the volume of fluid can again be written as a volume integral if the assumptions introduced earlier are retained. Then the energy equation in integral form is

$$\int_{\tau(t)} \left[ \rho\, \frac{d}{dt} \left( e + \frac{\boldsymbol{v}^2}{2} \right) - \rho\, (\boldsymbol{g} \cdot \boldsymbol{v}) + \nabla\, (p \cdot \boldsymbol{v}) + \nabla \left( \bar{\bar{\sigma}}' \cdot \boldsymbol{v} \right) - \nabla \cdot (\lambda\, \nabla \cdot T) \right] d\tau = 0 \tag{2.38}$$

The integral form of the energy equation can be replaced by its differential form if the integrand vanishes identically

$$\rho\, \frac{d}{dt} \left( e + \frac{\boldsymbol{v}^2}{2} \right) = \rho\, (\boldsymbol{g} \cdot \boldsymbol{v}) - \nabla \cdot (p\, \boldsymbol{v}) + \nabla \cdot (\lambda\, \nabla T) - \nabla \cdot (\bar{\bar{\sigma}}' \cdot \boldsymbol{v}) \quad . \tag{2.39}$$

### 2.2.4 Different Forms of the Energy Equation

The energy equation can be written in different forms. The scalar product of the velocity vector and the Navier-Stokes equations yields the following relation

$$\rho\, \frac{d}{dt} \left( \frac{\boldsymbol{v}^2}{2} \right) = \rho\, (\boldsymbol{v} \cdot \boldsymbol{g}) - \boldsymbol{v} \cdot (\nabla \cdot \bar{\bar{\sigma}}) \quad . \tag{2.40}$$

If this equation is subtracted from the energy equation the time rate of change of the internal energy is obtained

$$\rho\, \frac{de}{dt} = \frac{p}{\rho}\, \frac{d\rho}{dt} + \nabla \cdot (\lambda\, \nabla T) + \mu\, \Phi \quad . \tag{2.41}$$

The term $(\frac{p}{\rho})\,(\frac{d\rho}{dt})$ represents the work of compression or expansion of the pressure. The term $\mu\,\Phi$ stands as abbreviation for

$$\mu\,\Phi = \boldsymbol{v}\cdot(\nabla\cdot\bar{\bar{\sigma}}') - \nabla\cdot(\bar{\bar{\sigma}}'\cdot\boldsymbol{v}) \quad . \tag{2.42}$$

The function $\Phi$ is called dissipation function. It represents the amount of the mechanical energy, irreversibly transformed into thermal energy. Another form of the energy equation is obtained by introducing the enthalpy $h$:

$$h = e + \frac{p}{\rho} \tag{2.43}$$

With $h$ there results

$$\rho\,\frac{d}{dt}\left(h + \frac{\boldsymbol{v}^2}{2}\right) = \frac{\partial p}{\partial t} + \rho\;(\boldsymbol{g}\cdot\boldsymbol{v}) + \nabla\cdot\left(\lambda\,\nabla\,T - \bar{\bar{\sigma}}'\cdot\boldsymbol{v}\right) \tag{2.44}$$

In steady flows the stagnation enthalpy remains constant along streamlines, if volume forces can be neglected, and if either the heat conduction and the work done by friction forces per unit volume vanish or if the heat removed by conduction is equal to the work of the friction forces.

$$h_0 = h + \frac{\boldsymbol{v}^2}{2} = \text{const.} \tag{2.45}$$

For perfect gases the enthalpy depends only on the temperature. With

$$dh = c_p\,dT \tag{2.46}$$

the time rate of change of the temperature in the energy equation can be expressed by the time rate of change of the pressure, the divergence of the heat flux, and the dissipation function.

$$\rho\,c_p\,\frac{dT}{dt} = \frac{dp}{dt} + \nabla\cdot(\lambda\,\nabla\,T) + \eta\,\Phi \tag{2.47}$$

In Cartesisan coordinates the equation reads

$$\begin{aligned}
\rho\,c_p\left(\frac{\partial T}{\partial t} + u\,\frac{\partial T}{\partial x} + v\,\frac{\partial T}{\partial y} + w\,\frac{\partial T}{\partial z}\right) &= \frac{\partial p}{\partial t} + u\,\frac{\partial p}{\partial x} + v\,\frac{\partial p}{\partial y} + w\,\frac{\partial p}{\partial z} \\
&+ \frac{\partial}{\partial x}\left(\lambda\,\frac{\partial T}{\partial x}\right) + \frac{\partial}{\partial y}\left(\lambda\,\frac{\partial T}{\partial y}\right) + \frac{\partial}{\partial z}\left(\lambda\,\frac{\partial T}{\partial z}\right) \\
&- \left(\sigma'_{xx}\,\frac{\partial u}{\partial x} + \sigma'_{yy}\,\frac{\partial v}{\partial y} + \sigma'_{zz}\,\frac{\partial w}{\partial z}\right) \\
&- \left[\tau_{xy}\left(\frac{\partial u}{\partial y} + \frac{\partial v}{\partial x}\right) + \tau_{xz}\left(\frac{\partial u}{\partial z} + \frac{\partial w}{\partial x}\right)\right. \\
&+ \left.\tau_{yz}\left(\frac{\partial w}{\partial y} + \frac{\partial v}{\partial z}\right)\right] \quad .
\end{aligned} \tag{2.48}$$

If the components of the Stokes stress tensor are replaced by the relations introduced earlier, the dissipation function $\Phi$ becomes, if $\hat{\mu} = 0$,

$$\begin{aligned}
\Phi &= 2\left[\left(\frac{\partial u}{\partial x}\right)^2 + \left(\frac{\partial v}{\partial y}\right)^2 + \left(\frac{\partial w}{\partial z}\right)^2\right] - \frac{2}{3}\left(\frac{\partial u}{\partial x} + \frac{\partial v}{\partial y} + \frac{\partial w}{\partial z}\right)^2 \\
&+ \left(\frac{\partial u}{\partial y} + \frac{\partial v}{\partial x}\right)^2 + \left(\frac{\partial u}{\partial z} + \frac{\partial w}{\partial x}\right)^2 + \left(\frac{\partial w}{\partial y} + \frac{\partial v}{\partial z}\right)^2 \quad .
\end{aligned} \tag{2.49}$$

The dissipation function is always positive, proving, that an irreversible change of mechanical energy always causes a heating of the fluid or gas.
The conservation equations for mass, momentum, and energy form a system of five coupled, nonlinear, partial differential equations, which require initial and boundary conditions for a solution. For constant density, viscosity, heat conductivity, and heat capacity the energy equation is decoupled from the continuity equation and from the momentum equations, and pressure and velocity can be determined without the use of the energy equation.

## 2.3 Similar Flows

In order to describe flow processes it is necessary to intergrate the conservation laws just derived. Since the integration of these equations in closed form is, in general, not possible because of the inherent mathematical difficulties, flows are often investigated experimentally. Fluid mechanical and thermodynamic data are measured with models geometrically similar to the full-scale configuration, for which the flow is to be determined. However, since in general the models are smaller in size, the measured data have to be applied to the full-scale configuration with the rules of the theory of similitude. This theory makes use of similarity parameters, in which the characteristic quantities with physical dimensions of the flow considered are combined to dimensionless quantities. Two flows about geometrically similar bodies are called similar, if the individual similarity parameters have the same value for both flows. The similarity parameters, that are important for the flow process considered, can either be determined with the method of dimensional analysis applied to the physical properties of the flow or by nondimensionalizing the conservation equations.

### 2.3.1 Derivation of the Similarity Parameters with the Method of Dimensional Analysis

The method of dimensional analysis aims at deriving similarity parameters, which can be used to apply data measured with a model configuration to the geometrically similar full-scale configuration. Thereby the number of necessary experiments can be reduced, which depends on the number the physical quantities influencing the problem. The dimensional analysis also offers the advantage, that the physical quantities can be combined in such a way, that the results are independent of the measuring units. The physical quantities are combined in a product such that dimensionless combinations result. The number of possible combinations is determined by Buckingham's $\Pi$ theorem. According to this theorem $m-n$ dimensionless similarity parameters can be derived from $m$ influence quantities, if $n$ is the number of the fundamental dimensions, entering the problem considered.
In the following the important similarity parameters of the fluid mechanical quantities are derived. If for a flow problem the characteristic values of its length $l$, time $t$, velocity $v$, acceleration $b$, pressure difference $\Delta p$, density $\rho$, and dynamic shear viscosity $\mu$ are known, then the dimensions of these quantities can be described by the three fundamental dimensions length, time, and mass. Each of them can be combined with the other quantities (reference quantities) in a product to form a dimensionless similarity parameter. The reference quantities are chosen to be the length $l$, the velocity $v$, and the density $\rho$. With the aid of Buckingham's $\Pi$ theorem the following four products for the time $t$, the acceleration $b$, the pressure difference $\Delta p$, and the dynamic shear viscosity $\mu$ can be formulated

$$\begin{aligned} K_1 &= t^{\alpha_1}\,\rho^{\beta_1}\,v^{\gamma_1}\,l^{\delta_1} \quad , \\ K_2 &= g^{\alpha_2}\,\rho^{\beta_2}\,v^{\gamma_2}\,l^{\delta_2} \quad , \\ K_3 &= \Delta p^{\alpha_3}\,\rho^{\beta_3}\,v^{\gamma_3}\,l^{\delta_3} \quad , \\ K_4 &= \mu^{\alpha_4}\,\rho^{\beta_4}\,v^{\gamma_4}\,l^{\delta_4} \quad . \end{aligned} \tag{2.50}$$

The gravitational acceleration $g$ is used for $b$. The unknown exponents $\alpha_i$,...,$\delta_i$ have to be determined in such a way, that the similarity parameters $K_i$ are dimensionless. One of each of the exponents can be chosen arbitrarily, for example $\alpha_1 = -1$, $\alpha_2 = -0.5$, $\alpha_3 = 1$, $\alpha_4 = -1$. Then it follows from the equation for $K_1$ by comparison of the exponents of the fundamental dimensions with $[K_1] = L^0\, T^0\, K^0$

$$\begin{aligned} \text{Length L} &: 0 = -3\,\beta_1 + \gamma_1 + \delta_1 \\ \text{Time T} &: 0 = -1 - \gamma_1 \\ \text{Mass M} &: 0 = \beta_1 \quad . \end{aligned} \tag{2.51}$$

This system of equations has the solution

$$\beta_1 = 0. \quad \gamma_1 = -1, \quad \delta_1 = 1 \quad . \tag{2.52}$$

The similarity parameter $K_1$ is obtained to

$$K_1 = \frac{l}{v\,t} \quad . \tag{2.53}$$

The similarity parameters $K_2$ to $K_4$ are determined in similar manner. They are

$$K_2 = \frac{v}{\sqrt{g\,l}}, \quad K_3 = \frac{\Delta p}{\rho\, v^2}, \quad K_4 = \frac{\rho\, v\, l}{\mu} \quad . \tag{2.54}$$

The similarity parameters are named after famous scientists.

$$\begin{aligned} K_1 &= Sr = \frac{l}{v\,t} && \text{Strouhal number,} \\ K_2 &= Fr = \frac{v}{\sqrt{g\,l}} && \text{Froude number,} \\ K_3 &= Eu = \frac{\Delta p}{\rho\, v^2} && \text{Euler number,} \\ K_4 &= Re = \frac{\rho\, v\, l}{\mu} && \text{Reynolds number.} \end{aligned}$$

*Application of the Method of Dimensional Analysis to the Pipe Flow*

As was shown for the pipe flow, its pressure loss $\Delta p$ depends on the density $\rho$, the mean velocity $u_m$, the dynamic shear viscosity $\mu$, the length $l$, the roughness $k$, and the diameter $D$.

$$f(\Delta p,\rho,u_m,\mu,l,k,D) = 0 \tag{2.55}$$

The dimensions of these quantities can be expressed by combinations of the three fundamental dimensions of length, mass, and time. Density, velocity, and length (diameter) are chosen as reference quantities, such that there result four similarity parameters for the remaining four quantities $\Delta p$, $\mu$, $l$, and $k$. If the exponents are set $\alpha_i = 1$, then the products can be formulated as

$$\begin{aligned} K_1 &= \Delta p\, \rho^{\beta_1}\, u_m^{\gamma_1}\, D^{\delta_1} \quad , \\ K_2 &= \mu\, \rho^{\beta_2}\, u_m^{\gamma_2}\, D^{\delta_2} \quad , \\ K_3 &= l\, \rho^{\beta_3}\, u_m^{\gamma_3}\, D^{\delta_3} \quad , \\ K_4 &= k\, \rho^{\beta_4}\, u_m^{\gamma_4}\, D^{\delta_4} \quad . \end{aligned} \tag{2.56}$$

The similarity parameters $K_1$ to $K_4$ are obtained as follows

$$K_1 = \frac{\Delta p}{\rho\, u_m^2}, \quad K_2 = \frac{\mu}{\rho\, u_m\, D}, \quad K_3 = \frac{l}{D}, \quad K_4 = \frac{k}{D} \quad . \tag{2.57}$$

The function $f$ can now be written as

$$f_1\left(\frac{\Delta p}{\rho\, u_m^2},\quad \frac{\mu}{\rho\, u_m\, D},\quad \frac{l}{D},\quad \frac{k}{D}\right)=0 \tag{2.58}$$

or

$$\frac{\Delta p}{\rho\, u_m^2}=f_2\left(Re,\quad \frac{l}{D},\quad \frac{k}{D}\right)\quad . \tag{2.59}$$

The form of the function cannot be determined with the method of dimensional analysis. However, the number of influence quantities has been reduced from six to three.

### 2.3.2 The Method of Differential Equations

The similarity parameters can also be determined by nondimensionalizing the variables in the conservation equations with suitable reference quantities. They are denoted by the subscript 1. The similarity parameters then appear as constant coefficients in the differential equations. To keep the derivation simple, the transport properties $\mu$, $\lambda$, and the specific heat $c_p$ are assumed to be constant. With

$$\begin{gathered}\bar u=\frac{u}{v_1}\quad \bar v=\frac{v}{v_1}\quad \bar\rho=\frac{\rho}{\rho_1}\quad \bar p=\frac{p}{\Delta\, p_1}\\ \bar g_x=\frac{\rho\, g_x}{\rho_1\, g}\quad \bar t=\frac{t}{t_1}\quad \bar x=\frac{x}{l_1}\quad \bar y=\frac{y}{l_1}\quad \bar\mu=\frac{\mu}{\mu_1}\end{gathered} \tag{2.60}$$

the $x$-component of the momentum equation for two-dimensional incompressible flow, written in physical quantities

$$\rho\left(\frac{\partial u}{\partial t}+u\,\frac{\partial u}{\partial x}+v\,\frac{\partial u}{\partial y}\right)=-\frac{\partial p}{\partial x}+\rho\, g_x+\mu\,\nabla^2 u \tag{2.61}$$

is transformed into dimensionless form

$$Sr\,\frac{\partial \bar u}{\partial \bar t}+\bar u\,\frac{\partial \bar u}{\partial \bar x}+\bar v\,\frac{\partial \bar u}{\partial \bar y}=-Eu\,\frac{\partial \bar p}{\partial \bar x}+\frac{1}{Fr^2}\,\bar g_x+\frac{1}{Re}\,\nabla^2\,\bar u\quad . \tag{2.62}$$

This equation contains the similarity parameters $Sr$, $Eu$, $Fr$, and $Re$ already derived. Additional similarity parameters are obtained from the energy equation for compressible flows.

$$\begin{aligned}\rho\, c_p\left(\frac{\partial T}{\partial t}+u\,\frac{\partial T}{\partial x}+v\,\frac{\partial T}{\partial y}\right) &= \lambda\,\nabla^2 T+\left(\frac{\partial p}{\partial t}+u\,\frac{\partial p}{\partial x}+v\,\frac{\partial p}{\partial y}\right)+\\ &+\ 2\,\mu\left[\left(\frac{\partial u}{\partial x}\right)^2+\left(\frac{\partial v}{\partial y}\right)^2\right]\\ &+\ \mu\left(\frac{\partial u}{\partial y}+\frac{\partial v}{\partial x}\right)^2\\ &-\ \frac{2}{3}\,\mu\left(\frac{\partial u}{\partial x}+\frac{\partial v}{\partial y}\right)^2\end{aligned} \tag{2.63}$$

With the additional reference quantities

$$\bar T=\frac{T}{T_1}\qquad ,\quad \Delta\, p_1=\rho_1\, {u_1}^2 \tag{2.64}$$

the dimensionless form of the energy equation is

$$\begin{aligned}\bar{\rho}\left(Sr\,\frac{\partial\bar{T}}{\partial\bar{t}}+\bar{u}\,\frac{\partial\bar{T}}{\partial\bar{x}}+\bar{v}\,\frac{\partial\bar{T}}{\partial\bar{y}}\right) &= \frac{1}{Pr\,Re}\,\bar{\nabla}^2\,\bar{T}+\\ &+ (\gamma-1)\,Ma^2\left[Sr\,\frac{\partial\bar{p}}{\partial\bar{t}}+\left(\bar{u}\,\frac{\partial\bar{p}}{\partial\bar{x}}+\bar{v}\,\frac{\partial\bar{p}}{\partial\bar{y}}\right)\right]\\ &+ (\gamma-1)\,\frac{Ma^2}{Re}\left\{2\left[\left(\frac{\partial\bar{u}}{\partial\bar{x}}\right)^2+\left(\frac{\partial\bar{v}}{\partial\bar{y}}\right)^2\right]\right.\\ &- \left.\frac{2}{3}\left(\frac{\partial\bar{u}}{\partial\bar{x}}+\frac{\partial\bar{v}}{\partial\bar{y}}\right)^2+\left(\frac{\partial\bar{u}}{\partial\bar{y}}+\frac{\partial\bar{v}}{\partial\bar{x}}\right)^2\right\}\quad . \end{aligned} \tag{2.65}$$

The above equation contains the additional similarity parameters

$$\begin{aligned} Pr &= \frac{\mu_1\,c_{p_1}}{\lambda_1} && \text{Prandtl number,}\\ Ma &= \frac{v_1}{a_1}=\frac{v_1}{\sqrt{\gamma\,RT_1}} && \text{Mach number,}\\ \gamma &= \frac{c_{p_1}}{c_{v1}} && . \end{aligned} \tag{2.66}$$

The Mach number is the ratio of the reference velocity to the speed of sound, which for known isentropic exponent $\gamma$ and known gas constant $R$ depends only on the reference temperature $T_1$. The dimensionless variables are the same for all corresponding times and corresponding points of all flow fields which have similar initial and boundary conditions and identical similarity parameters $Sr$, $Eu$, $Fr$, $Re$, $Pr$, $Ma$, and $\gamma$.

### 2.3.3 Physical Meaning of the Similarity Parameters

The similarity parameters derived with the method of dimensional analysis and the method of differential equations can be interpreted from a physical point of view.
The Strouhal number $Sr$ is the ratio of two characteristic times in a time-dependent flow field. If the characteristic time $t$ is large compared to $l/v$, i. e. the time, in which a fluid particle travels the distance $l$, the flow is called quasi-steady ($Sr << 1$). Then the influence of the local acceleration on the flow can be neglected. For periodic flows, (for example arterial circulation in the human body, or flows in pumps) instead of the characteristic time $t$ the frequency $f$ is used.
The Froude number $Fr$ is the ratio of the inertia and gravitational forces. It is of importance for free-surface flows (Gravitational waves, open channel flows).
The Euler number $Eu$ is given by the ratio of pressure and inertia forces, and the Reynolds number $Re$ by the ratio of the inertia and friction forces. If the Reynolds number becomes very large, the friction forces can be neglected. The conservation equations for inviscid flows are called Euler equations and were first derived in 1755. If the Reynolds number is very small, the influence of the inertia forces on the flow can be neglected. Very slow flow motion is often referred to as creeping motion.
The Mach number is a measure for the influence of the compressibility on the flow, which up to $Ma < 0.4$ in general can be neglected. For normal conditions this value corresponds to a velocity of 133 m/s or 480 km/h.
The Prandtl number $Pr$ is the ratio of the product of the dynamic shear viscosity $\mu$ and specific heat $c_p$ and the heat conductivity $\lambda$. For air and also other gases the Prandtl number is almost constant, while for liquids it is strongly temperature dependent.
The isentropic exponent $\gamma$ can also be thought of as a similarity parameter. It depends only on the internal degrees of freedom of the molecules.
It is often difficult in model experiments to satisfy all similarity laws. For example, if in a wind tunnel the influence of the friction forces on the other flow parameters is to be experimentally determined with a model of an airplane, then in incompressible flow only the Reynolds number has

to have the same value as the flow about the full-scale configuration of the airplane. If air is used in the experiment as flow medium, the free-stream velocity of the model is for equal values of the kinematic viscosity $v_M = l\,v/l_M$. Since the model has to be much smaller than the main configuration, in order to satisfy the Reynolds similarity law it would be necessary that $v_M \gg v$. For very large velocities, however, the flow is compressible and would be influenced correspondingly. It is even more difficult if not impossible to satisfy several or all similarity laws simultaneously. If the drag of a ship, which results from friction forces and the generation of waves, is to be determined experimentally, both Reynolds' and Froude's similarity law would have to be satisfied. If in the experiment the same flow medium is used as for the full-scale configuration, then the two laws would contradict each other. With the condition $Re_M = Re$ the length of the model would have to be $l_M = \frac{l\,v}{v_M}$, while Froude's similarity law $Fr_M = Fr$ would require $l_M = l\,v_M^2/v^2$, so that only one of the two laws can be obeyed.

## 2.4 Creeping Motion

Characteristic feature of very slow flow motion is that the friction forces are much larger than the inertia forces. With this supposition the conservation equations or equations of motion can be simplified and a solution be constructed. This is demonstrated with the example of the hydrodynamically lubricated bearing, in which the gap height $h$ is much smaller than the length of the gliding part of the shaft. The bearing is idealized and assumed to be given by an infinitely extended plane wall, which moves with constant velocity $u_\infty$ past the gliding part of the shaft, which can also be assumed to be plane. The lubricant prevents the gliding part of the shaft from touching the wall and reduces the friction force.

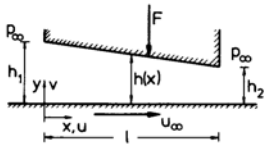


For constant temperature the conservation equations for two-dimensional flow are

$$\begin{aligned}
\frac{\partial u}{\partial x} + \frac{\partial v}{\partial y} &= 0 \\
\rho\left(u\,\frac{\partial u}{\partial x} + v\,\frac{\partial u}{\partial y}\right) &= -\frac{\partial p}{\partial x} + \mu\left(\frac{\partial^2 u}{\partial x^2} + \frac{\partial^2 u}{\partial y^2}\right) \\
\rho\left(u\,\frac{\partial v}{\partial x} + v\,\frac{\partial v}{\partial y}\right) &= -\frac{\partial p}{\partial y} + \mu\left(\frac{\partial^2 v}{\partial x^2} + \frac{\partial^2 v}{\partial y^2}\right) \quad . \qquad (2.67)
\end{aligned}$$

The equations are nondimensionalized with the reference quantities chosen such that the velocity components and their derivatives are of order unity $O(1)$. Since

$$\frac{v}{u_\infty} = O\left(\frac{h_1}{l}\right) \ll 1 \quad , \qquad (2.68)$$

the normal velocity component is streched by $l/h_1$ so that $\bar{v}(x,y) = \frac{v}{u_\infty}\,\frac{l}{h_1}$.
With $Re = \frac{\rho\,u_\infty\,l}{\mu}$ the momentum equations can be solved for the dimensionless pressure gradients

$$\begin{aligned}
\frac{\partial \bar{p}}{\partial \bar{x}} &= \frac{1}{Eu\,Re}\,\frac{l^2}{h_1^2}\left[\frac{\partial^2\,\bar{u}}{\partial\,\bar{y}^2} - Re\,\frac{h_1^2}{l^2}\left(\bar{u}\,\frac{\partial \bar{u}}{\partial \bar{x}} + \bar{v}\,\frac{\partial \bar{u}}{\partial \bar{y}}\right) + \frac{h_1^2}{l^2}\,\frac{\partial^2\,\bar{u}}{\partial \bar{x}^2}\right] \\
\frac{\partial \bar{p}}{\partial \bar{y}} &= \frac{1}{Eu\,Re}\left[\frac{\partial^2 \bar{v}}{\partial \bar{y}^2} - Re\,\frac{h_1^2}{l^2}\left(\bar{u}\,\frac{\partial \bar{v}}{\partial \bar{x}} + \bar{v}\,\frac{\partial \bar{v}}{\partial \bar{y}}\right) + \frac{h_1^2}{l^2}\,\frac{\partial^2\,\bar{v}}{\partial \bar{x}^2}\right] \quad . \qquad (2.69)
\end{aligned}$$

For $Re\,\frac{h_1^2}{l^2} \ll 1$ (Inertia forces $\ll$ friction forces) it follows that

$$\begin{aligned} \frac{\partial \bar{p}}{\partial \bar{x}} &\approx \frac{1}{EuRe}\,\frac{l^2}{h_1^2}\,\frac{\partial^2 \bar{u}}{\partial \bar{y}^2} \\ \frac{\partial \bar{p}}{\partial \bar{y}} &\approx \frac{1}{EuRe}\,\frac{\partial^2 \bar{v}}{\partial \bar{y}^2} \quad . \end{aligned} \tag{2.70}$$

By comparing the right-hand sides it can be concluded that

$$\frac{\partial \bar{p}}{\partial \bar{y}} << \frac{\partial \bar{p}}{\partial \bar{x}} \quad , \tag{2.71}$$

such that it is justified to assume that the variation of the pressure in the $y$-direction can be neglected compared to the variation in the $x$-direction.
With the boundary conditions

$$\begin{array}{lllllll} y = 0 & : & u = u_\infty & & y = h(x) & : & u = 0 \\ x = 0 & : & p = p_\infty & & x = l & : & p = p_\infty \end{array} \tag{2.72}$$

the integration of the simplified first momentum equation yields

$$u = u_\infty \left(1 - \frac{y}{h}\right) - \frac{h^2}{2\,\mu}\,\frac{y}{h}\,\left(1 - \frac{y}{h}\right)\frac{dp}{dx} \quad , \tag{2.73}$$

and the volume rate of flow $\dot{Q}$ is obtained by integrating the last equation in the $y$-Richtung.

$$\dot{Q} = \frac{u_\infty\, h}{2} - \frac{h^3}{12\,\mu}\,\frac{dp}{dx} \quad . \tag{2.74}$$

Since the volume rate of flow is the same for every cross section, the last equation can be integrated in the $x$-direction.

$$p(x) = p_\infty + 6\,\mu\,u_\infty \int_0^x \frac{dx'}{h^2(x')} - 12\,\mu\,\dot{Q} \int_0^x \frac{dx'}{h^3(x')} \tag{2.75}$$

If it is assumed, that the gap height changes linearly with $x$, i. e.

$$h(x) = h_1 - \frac{h_1 - h_2}{l}\,x \quad , \tag{2.76}$$

then it follows that

$$\begin{aligned} \dot{Q} &= u_\infty \frac{h_1\,h_2}{h_1 + h_2} \quad , \\ p(x) &= p_\infty + 6\,\mu\,u_\infty \frac{l}{(h_1^2 - h_2^2)}\,\frac{(h_1 - h)\;(h - h_2)}{h^2}. \end{aligned} \tag{2.77}$$

The total force resulting from the pressure distribution is

$$F_p = \int_0^l p(x)\,dx = \frac{6\,\eta\,u_\infty\,l^2}{(h_1 - h_2)^2}\left[\ln\frac{h_1}{h_2} - \frac{2\;(h_1 - h_2)}{(h_1 + h_2)}\right] \quad . \tag{2.78}$$

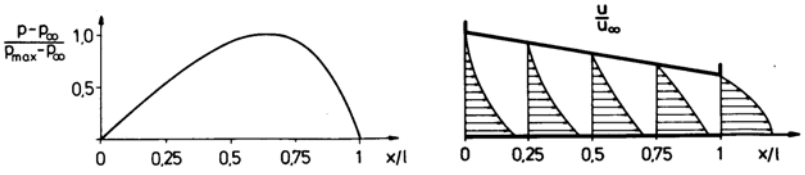

The pressure distribution and the $x$-component of the velocity

$$\frac{u}{u_\infty} = (1 - \frac{y}{h}) \left[1 - 3\,\frac{y}{h}\left(1 - \frac{2\,h_1\,h_2}{(h_1 + h_2)\,h}\right)\right] \tag{2.79}$$

are shown in the diagram above for $\frac{h_2}{h_1} = 0.559$. The $y$-component of the velocity can be obtained by inserting $u$ into the continuity equation and integrating it in the $y$-direction. Equation (2.79) has to be differentiated with respect to $x$, since $u$ enters the continuity equation through its partial derivative. There results a first-order differential equation for $v$, so that only one boundary condition can be satisfied for $v$, e. g.: $y = 0 : v = 0$. Because of the approximative nature of the solution, the second boundary condition for $y = h(x)$ cannot be imposed.

## 2.5 Vortex Theorems

If fluid particles rotate about their axes, the flow is called rotational. Irrotational flows possess a potential and are called potential flows. The important properties of rotational flows and their difference to potential flows is explained in the following.

### 2.5.1 Rotation and Circulation

The rotation of a fluid element is described by its mean angular velocity. With the notation given in the sketch the differential angular changes are

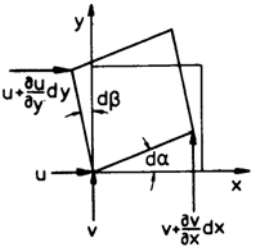


$$\begin{aligned} d\alpha &= \frac{\partial v}{\partial x}\,dt \\ d\beta &= -\frac{\partial u}{\partial y}\,dt \end{aligned} \quad , \tag{2.80}$$

and the mean angular velocity is

$$\zeta = \frac{1}{2}\left(\frac{\partial v}{\partial x} - \frac{\partial u}{\partial y}\right) \quad . \tag{2.81}$$

Generalization of the last equation to three space coordinates leads to the vector of rotation or vorticity

$$\boldsymbol{\omega} = \boldsymbol{i}\,\xi + \boldsymbol{j}\,\eta + \boldsymbol{k}\,\zeta = \frac{1}{2}\,\nabla \times \boldsymbol{v} \quad . \tag{2.82}$$

Analogously to the stream tube and streamline a vortex tube and a vortex line can be defined. In every point of the flow field the direction of a vortex line is given by the direction of the vorticity vector.

$$\frac{dx}{\xi} = \frac{dy}{\eta} = \frac{dz}{\zeta} \tag{2.83}$$

If the vorticity vector is defined everywhere in the flow field, (2.83) can be integrated, from a certain initial point on, to yield a vortex line, of which there are infinitely many. If a closed curve, not a vortex line, is chosen in the flow field, the vortex lines passing through it form a vortex tube, reducing to a vortex filament, when the cross section of the tube tends to zero. The vortex tube is of fundamental importance for measuring the strength of a vortex. An example is shown in the following sketch, where first the flux of vorticity is introduced.
The flux of vorticity $\Omega$ through a surface $A$ is

$$\Omega = \int_A \boldsymbol{\omega} \cdot \boldsymbol{n}\,dA \quad . \tag{2.84}$$

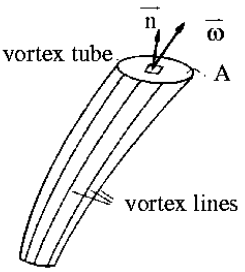


The flux of vorticity is closely related to the circulation $\Gamma$, being defined as the line integral extended over the scalar product of the velocity and the line element of a closed curve $C$.

$$\Gamma = \oint_C \boldsymbol{v} \cdot d\boldsymbol{s} \tag{2.85}$$

In order to elucidate the interrelation between $\Gamma$ and $\Omega$ the circulation $\Gamma$ is computed for an element of a plane surface. It is

$$d\Gamma = \left( \frac{\partial v}{\partial x} - \frac{\partial u}{\partial y} \right) dx\, dy = 2\, \zeta\, dx\, dy \quad . \tag{2.86}$$

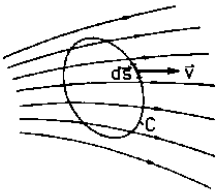


Generalized to the three coordinate directions, there results

$$d\Gamma = 2\, [\xi\ (dy\, dz) + \eta\ (dx\, dz) + \zeta\ (dx\, dy)] \quad . \tag{2.87}$$

Integration of the last equation yields

$$\Gamma = \int_A \boldsymbol{\omega} \cdot \boldsymbol{n}\, dA = 2\, \Omega \tag{2.88}$$

or

$$\oint_C \boldsymbol{v} \cdot d\boldsymbol{s} = \int_A (\nabla \times \boldsymbol{v}) \cdot \boldsymbol{n}\, dA \quad . \tag{2.89}$$

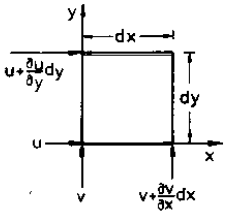


The circulation is equal to twice the value of the flux of vorticity through the surface spanned over a closed curve (Stokes' theorem).
In an incompressible, inviscid flow the circulation does not change, if the volume forces possess a potential $U$. To prove this statement, the total time derivative of the circulation $\Gamma$ is formed

$$\frac{d\Gamma}{dt} = \oint_C \frac{d\boldsymbol{v}}{dt} \cdot d\boldsymbol{s} + \oint_C d\left( \frac{\boldsymbol{v}^2}{2} \right), \tag{2.90}$$

and the Navier-Stokes equations

$$\frac{d\boldsymbol{v}}{dt} = \boldsymbol{g} - \frac{1}{\rho} \nabla p + \nu\, \nabla^2 \boldsymbol{v} \tag{2.91}$$

are introduced with the volume forces assumed to possess a potential $\boldsymbol{g} = \nabla U$. There results

$$\frac{d\Gamma}{dt} = \oint_C d\left( U - \frac{p}{\rho} + \frac{\boldsymbol{v}^2}{2} \right) + \nu \oint_C \left( \nabla^2 \boldsymbol{v} \right) \cdot d\boldsymbol{s} \quad . \tag{2.92}$$

For an inviscid flow ($\nu = 0$) it follows that $\frac{d\Gamma}{dt} = 0$. If $\Gamma(t = 0) = 0$, then the flow is irrotational for all times (Thomson's theorem).

### 2.5.2 Vorticity Transport Equation

For incompressible flow the components of the vorticity vector $\boldsymbol{\omega}$ can easily be introduced in the conservation equations for mass and momentum. There results the vorticity transport equation, which describes the change of the vorticity vector in the flow field. With the aid of a particular integral of the vorticity transport equation a simple ansatz for solutions of the momentum equations for incompressible inviscid flows can be found, without having to solve the nonlinear

momentum equations. The vorticity transport equation is obtained from the Navier-Stokes equations in the following way:

$$\begin{aligned} \frac{du}{dt} &= -\frac{1}{\rho}\frac{\partial p}{\partial x} + g_x + \nu\,\nabla^2 u \\ \frac{dv}{dt} &= -\frac{1}{\rho}\frac{\partial p}{\partial y} + g_y + \nu\,\nabla^2 v \\ \frac{dw}{dt} &= -\frac{1}{\rho}\frac{\partial p}{\partial z} + g_z + \nu\,\nabla^2 w \end{aligned} \tag{2.93}$$

The vorticity component $\zeta$ is introduced by partially differentiating the first equation with respect to $y$ and the second with respect to $x$ and by subtracting the resulting equations from each other.

$$\frac{d\zeta}{dt} = \left(\xi\,\frac{\partial w}{\partial x} + \eta\,\frac{\partial w}{\partial y} + \zeta\,\frac{\partial w}{\partial z}\right) + \nu\,\nabla^2\zeta + \frac{1}{2}\left(\frac{\partial g_y}{\partial x} - \frac{\partial g_x}{\partial y}\right) \tag{2.94}$$

The equations for the other two components $\eta$ and $\xi$ are

$$\begin{aligned} \frac{d\eta}{dt} &= \left(\xi\,\frac{\partial v}{\partial x} + \eta\,\frac{\partial v}{\partial y} + \zeta\,\frac{\partial v}{\partial z}\right) + \nu\,\nabla^2\eta + \frac{1}{2}\left(\frac{\partial g_x}{\partial z} - \frac{\partial g_z}{\partial x}\right) \\ \frac{d\xi}{dt} &= \left(\xi\,\frac{\partial u}{\partial x} + \eta\,\frac{\partial u}{\partial y} + \zeta\,\frac{\partial u}{\partial z}\right) + \nu\,\nabla^2\xi + \frac{1}{2}\left(\frac{\partial g_z}{\partial y} - \frac{\partial g_x}{\partial z}\right) \quad . \end{aligned} \tag{2.95}$$

If the volume forces can be represented by a potential the second bracketed terms on the right-hand side of the equations drop out. The vorticity transport equation, written in vector form reads as follows

$$\frac{d\boldsymbol{\omega}}{dt} = (\boldsymbol{\omega}\cdot\nabla)\;\boldsymbol{v} + \nu\,\nabla^2\,\boldsymbol{\omega} \quad . \tag{2.96}$$

For plane flows the term $(\boldsymbol{\omega}\cdot\nabla)\,\boldsymbol{v}$ vanishes. The rigid body rotation $\boldsymbol{\omega} = \text{const.}$ is a solution of this equation. If in addition the flow is inviscid and steady, the vorticity transport equation reduces to

$$(\boldsymbol{v}\cdot\nabla)\,\boldsymbol{\omega} = 0 \quad . \tag{2.97}$$

This equation shows that $\boldsymbol{\omega}$ is constant along streamlines, it can change only in the direction normal to the streamlines.
As the vorticity transport equation is only a different form of the momentum equations, it can be concluded, that the latter are always satisfied by the condition $\boldsymbol{\omega} = 0$. This solution is only possible, if the flow is inviscid. The potential theory of fluid mechanics rests on this assumption.

## 2.6 Potential Flows of Incompressible Fluids

### 2.6.1 Potential and Stream Function

The condition $\boldsymbol{\omega} = 0$ is identically satisfied, if the velocity vector can be expressed by a potential $\Phi$. The potential is defined by $\boldsymbol{v} = \nabla\,\Phi$. Instead of the velocity now the potential has to be determined with the conservation equations. Since the momentum equations are already satisfied by the condition of irrotationality $\boldsymbol{\omega} = 0$, only the continuity equation can be employed for the determination of $\Phi$. If the definition of $\Phi$ is inserted in the continuity equation, there results

$$\nabla^2\,\Phi = 0 \quad . \tag{2.98}$$

In Cartesian coordinates the corresponding equation read

$$u = \frac{\partial \Phi}{\partial x} \qquad v = \frac{\partial \Phi}{\partial y} \qquad w = \frac{\partial \Phi}{\partial z} \tag{2.99}$$

$$\frac{\partial^2 \Phi}{\partial x^2} + \frac{\partial^2 \Phi}{\partial y^2} + \frac{\partial^2 \Phi}{\partial z^2} = 0 \quad . \tag{2.100}$$

As only inviscid flow is considered, the Stokes no-slip condition cannot be satisfied on rigid impermeable walls. In potential flows as in all inviscid flows only the velocity component $v_n$ vanishes in the direction of the local surface normal $\boldsymbol{n}$ (Kinematic flow condition).

$$v_n = \frac{\partial \Phi}{\partial n} = 0 \tag{2.101}$$

In contrast to the Euler equations the potential equation is linear, and solutions can be superposed. If $\Phi_1$ and $\Phi_2$ satisfy the potential equation, then

$$\Phi = c_1 \, \Phi_1 + c_2 \, \Phi_2 + c_3 \tag{2.102}$$

is also a solution, the quantities $c_1$, $c_2$, and $c_3$ are arbitrary constants.
For two-dimensional flows, instead of the potential a scalar function $\Psi$, the stream function, can be introduced. It satisfies the continuity equation identically. It has to be determined with the condition of irrotationality.
With

$$u = \frac{\partial \Psi}{\partial y} \qquad v = -\frac{\partial \Psi}{\partial x} \tag{2.103}$$

the continuity equation

$$\frac{\partial u}{\partial x} + \frac{\partial v}{\partial y} = 0 \tag{2.104}$$

is satisfied. The condition of irrotationality

$$\frac{\partial v}{\partial x} - \frac{\partial u}{\partial y} = 0 \tag{2.105}$$

leads to the Laplace equation for the stream function.

$$\nabla^2 \, \Psi = 0 \tag{2.106}$$

The differential equation for the streamline follows from the total differential

$$d\Psi = \frac{\partial \Psi}{\partial x} \, dx + \frac{\partial \Psi}{\partial y} \, dy = -v \, dx + u \, dy \tag{2.107}$$

with $\Psi = \text{const}$.

$$\left( \frac{dy}{dx} \right)_{\Psi = konst} = \frac{v}{u} \quad . \tag{2.108}$$

Hence streamlines are given by lines $\Psi(x,y) = \text{const}$. and $d\Psi$ is the fluid volume flowing between two infinitesimally neighboring streamlines. The boundary condition along a rigid wall is

$$\Psi(x,y) = \text{const.} \quad . \tag{2.109}$$

Streamlines ($\Psi = \text{const.}$) and equipotential lines ($\Phi = \text{const.}$) are orthogonal to each other. From $d\Phi = u \, dx + v \, dy$ it follows that

$$\left( \frac{dy}{dx} \right)_{\Phi = const} = -\frac{u}{v} \quad . \tag{2.110}$$

The orthogonality is expressed through the Cauchy-Riemann differential equations.

$$\frac{\partial \Phi}{\partial x} = \frac{\partial \Psi}{\partial y} \qquad \frac{\partial \Phi}{\partial y} = -\frac{\partial \Psi}{\partial x} \tag{2.111}$$

### 2.6.2 Determination of the Pressure

If the potential is known, the pressure distribution can be determined with the Euler equations for the entire flow field. With the identity

$$(\boldsymbol{v} \cdot \nabla)\, \boldsymbol{v} = \nabla\, \frac{\boldsymbol{v}^2}{2} - \boldsymbol{v} \text{ x } (\nabla \text{ x } \boldsymbol{v}) \tag{2.112}$$

the Euler equations can be written as

$$\frac{\partial \boldsymbol{v}}{\partial t} + \nabla\, \frac{\boldsymbol{v}^2}{2} + \frac{1}{\rho}\, \nabla\, p - \boldsymbol{v} \text{ x } (\nabla \text{ x } \boldsymbol{v}) = \boldsymbol{g} \qquad . \tag{2.113}$$

With $\boldsymbol{v} = \nabla\, \Phi$ and $\boldsymbol{g} = \nabla\, U$ there results

$$\nabla\, \left[ \rho\, \frac{\partial \Phi}{\partial t} + \rho\, \frac{\boldsymbol{v}^2}{2} + p - \rho\, U \right] = 0 \quad . \tag{2.114}$$

Integration yields

$$\rho\, \frac{\partial \Phi}{\partial t} + \rho\, \frac{\boldsymbol{v}^2}{2} + p - \rho\, U = c(t) \qquad \text{(Lagrange's integral)} \quad . \tag{2.115}$$

For steady flows the above relation reduces to Bernoulli's equation.

$$\rho\, \frac{\boldsymbol{v}^2}{2} + p - \rho\, U = \text{const.} \quad . \tag{2.116}$$

In potential flows the constant in the Bernoulli equation has one and the same value for the entire flow field and on its boundary. In general the pressure is described in form of a dimensionless pressure coefficient $c_p$. Referenced to free-stream conditions it is defined for vanishing volume forces as

$$c_p = \frac{p - p_\infty}{\frac{1}{2}\, \rho\, u_\infty^2} = 1 - \frac{u^2 + v^2 + w^2}{u_\infty^2} \quad . \tag{2.117}$$

### 2.6.3 The Complex Stream Function

The real and the imaginary part of an analytic function satisfy the Laplace equation. The complex stream function $F(z)$ is defined in such a way, that the potential represents the real part and the stream function the imaginary part.

$$F(z) = F(x + iy) = \Phi(x,y) + i\, \Psi(x,y) \tag{2.118}$$

Repeated partial differentiation of F(z) with respect to $x$ and $y$ gives

$$\frac{\partial^2 F}{\partial\, x^2} + \frac{\partial^2 F}{\partial\, y^2} = 0 \tag{2.119}$$

or

$$\frac{\partial^2 \Phi}{\partial\, x^2} + \frac{\partial^2 \Phi}{\partial\, y^2} + i\, \left( \frac{\partial^2 \Psi}{\partial\, x^2} + \frac{\partial^2 \Psi}{\partial\, y^2} \right) = 0 \qquad . \tag{2.120}$$

The velocity components follow from the total differential

$$\begin{aligned} dF &= \left( \frac{\partial \Phi}{\partial x} + i\, \frac{\partial \Psi}{\partial x} \right)\, dx + \left( \frac{\partial \Phi}{\partial y} + i\, \frac{\partial \Psi}{\partial y} \right)\, dy \\ &= (u - iv)\, (dx + i dy) \\ &= \bar{w} dz \qquad , \end{aligned} \tag{2.121}$$

Therein $\bar{w} = \frac{dF}{dz}$ is the conjugate of the complex velocity $w = u + iv$.

### 2.6.4 Examples for Plane Incompressible Potential Flows

In the following several analytic functions are introduced and their corresponding potential flows are discussed. The other possibility, to describe a flow field by solving the Laplace equation for a given body contour, will not be followed here, as it requires mathematical solution tools, too laborious for an introduction.

*Parallel Flows*

For the analytic function $F(z) = (u_\infty - i\, v_\infty)\, z$ the potential and the stream funktion are

$$\Phi = u_\infty\, x + v_\infty\, y \qquad \Psi = -v_\infty\, x + u_\infty\, y \quad . \tag{2.122}$$

The streamlines ($\Psi = \text{const.}$) are straight lines with the slope

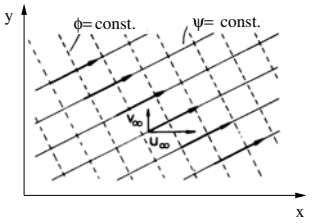


$$\frac{dy}{dx} = \frac{v_\infty}{u_\infty} = \text{const.} \quad . \tag{2.123}$$

The conjugate of the complex velocity

$$\bar{w} = \frac{dF}{dz} = u_\infty - i\, v_\infty \tag{2.124}$$

is constant in the entire flow field.

*Flow in the Vicinity of a Stagnation Point*

The analytic function $F(z) = az^2$ (a real) represents a plane flow in the vicinity of a stagnation point. The potential, the stream function, and the equipotential lines are

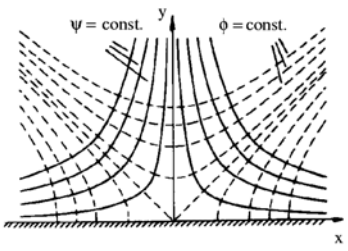


$$\Phi = a\,(x^2 - y^2) \qquad \Psi = 2\, a\, x\, y \quad , \tag{2.125}$$

$$y^2 = c' + x^2 \quad . \tag{2.126}$$

The velocity components are

$$u = 2\, a\, x \qquad v = -2\, a\, y \quad . \tag{2.127}$$

The streamlines are the hyperbolas

$$y = \frac{c}{x} \quad . \tag{2.128}$$

*Source Flow*

The analytic function $F(z) = \frac{E}{2\,\pi\,\ln z}$ describes the flow of a plane source with the conjugate of the complex velocity given by

$$\bar{w} = \frac{E\, x}{2\,\pi\,(x^2 + y^2)} - i\, \frac{E\, y}{2\,\pi\,(x^2 + y^2)} \quad . \tag{2.129}$$

Potential and stream function read in polar coordinates with $z = r\,(\cos\theta + i\,\sin\theta)$

$$\Phi = \frac{E}{2\,\pi}\,\ln r \qquad \Psi = \frac{E}{2\,\pi}\,\theta \quad . \tag{2.130}$$

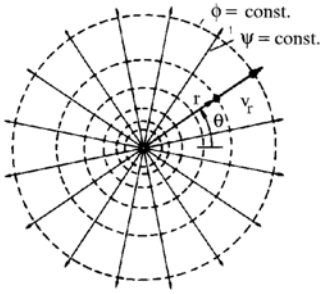


The radial and the azimuthal velocity components are

$$v_r = \frac{E}{2\,\pi\,r} \qquad v_\theta = 0 \quad . \tag{2.131}$$

The constant $E$ is the volume of fluid flowing through the circle with radius $r$. If $E$ is positive, the flow represents a source, if it is negative, the flow is a sink. The point of origin of coordinates is a singular point in the flow field, since the velocity approaches infinity for $r = 0$.

*Potential Vortex*

If stream function and potential of the plane source flow are exchanged, a potential vortex is obtained. The stream function is

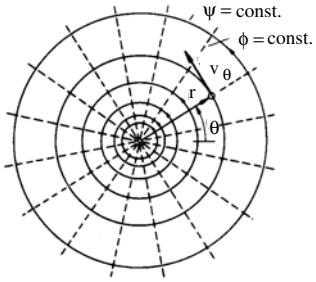


$$F(z) = -\frac{i\,\Gamma}{2\,\pi}\,\ln z \quad . \tag{2.132}$$

The real constant $\Gamma$ is the circulation of the vortex. There result

$$\Phi = \frac{\Gamma}{2\,\pi}\,\theta \qquad \Psi = -\frac{\Gamma}{2\,\pi}\,\ln r \tag{2.133}$$

$$v_r = 0 \qquad v_\theta = \frac{\Gamma}{2\,\pi\,r} \quad . \tag{2.134}$$

The streamlines of the potential vortex are circles around the point of origin of coordinates $r = const.$. The equipotential lines are radial lines.

*Flow Given by a Dipole*

If a source with volume flow $E$ and a sink of equal volume flow are positioned on the $x$-axis and if with decreasing distance $h$ between them $E$ increases in such a way that the product $E\,h = M$ remains constant, there results for the limiting case of $h \to 0$ the analytic function

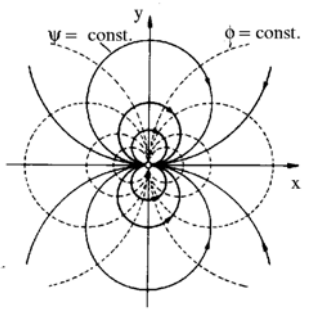


$$F(z) = \frac{M}{2\,\pi}\,\lim_{h\to 0}\frac{\ln(z+h) - \ln z}{h} = \frac{M}{2\,\pi\,z} \quad . \tag{2.135}$$

The quantity $M$ is called the dipole moment and the line, along which source and sink approach each other, is called dipole axis. Potential and stream function are

$$\Phi = \frac{M}{2\,\pi}\,\frac{x}{r^2} \qquad \Psi = -\frac{M}{2\,\pi}\,\frac{y}{r^2} \quad , \tag{2.136}$$

and the velocity components

$$u = -\frac{M}{2\,\pi\,r^2}\,\cos 2\,\theta \qquad v = -\frac{M}{2\,\pi\,r^2}\,\sin 2\,\theta \quad . \tag{2.137}$$

The streamlines are circles, tangent to the $x$-axis in the point of origin of coordinates, with the centers located on the $y$-axis.

*Half Body*

If a parallel flow is superimposed on a source, the flow field about a half body is obtained.

$$\begin{aligned} F(z) &= (u_\infty - i\, v_\infty)\, z + \frac{E}{2\,\pi}\, \ln z + i\, C \\ \Phi &= u_\infty\, x + v_\infty\, y + \frac{E}{2\,\pi}\, \ln r \\ \Psi &= -v_\infty\, x + u_\infty\, y + \frac{E}{2\,\pi}\, \left[\theta - \arctan\left(\frac{v_\infty}{u_\infty}\right)\right] \quad . \end{aligned} \tag{2.138}$$

The oncoming flow is assumed to be parallel to the $x$-axis. The velocity components

$$u = u_\infty + \frac{E\, x}{2\,\pi\, r^2}, \qquad v = \frac{E\, y}{2\,\pi\, r^2} \tag{2.139}$$

vanish for $x_s = -\frac{E}{2\,\pi\, u_\infty}$ (Stagnation point). The streamline through the stagnation point forms the contour of a half body.

$$r_k = \frac{E}{2\,\pi\, r^2}\, \frac{\pi - \theta}{\sin\theta} \tag{2.140}$$

The width of the half body is for $x \to \infty$

$$h = \frac{E}{2\,u_\infty} \quad . \tag{2.141}$$

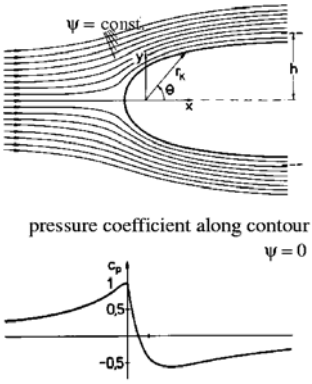


The pressure coefficient

$$c_p = 1 - \left[\left(1 + \frac{h\, x}{\pi\, r^2}\right)^2 + \left(\frac{h\, y}{\pi\, r^2}\right)^2\right] \tag{2.142}$$

along the contour with $\theta' = \pi - \theta$ is

$$c_p = \frac{\sin(2\,\theta')}{\theta'} - \left(\frac{\sin\theta'}{\theta'}\right)^2 \quad . \tag{2.143}$$

For $\theta' = 0$ the pressure coefficient is $c_p = 1$ and for $\theta' = \pi \quad c_p = 0$. For $\theta' = \frac{\pi}{2}$ the pressure coefficient is $c_p = -\frac{4}{\pi^2}$ and approaches asymptotically zero with increasing $x$ after going through a minimum.

*Circular Cylinder*

The superposition of a parallel flow with a dipole results in a flow about a circular cylinder.

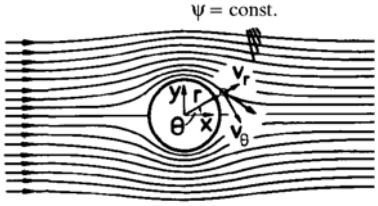


$$\begin{aligned} F(z) &= u_\infty\, z + \frac{M}{2\,\pi\, z} \\ \Phi &= \left(u_\infty + \frac{M}{2\,\pi\, r^2}\right)\, r\, \cos\,\theta \\ \Psi &= \left(u_\infty - \frac{M}{2\,\pi\, r^2}\right)\, r\, \sin\,\theta \end{aligned} \tag{2.144}$$

The streamline $\Psi = 0$ contains the circle around the point of origin of coordinates with radius $R = \sqrt{\frac{M}{2\,\pi\, u_\infty}}$. The azimuthal and the radial velocity component are

$$v_\theta = -u_\infty \left(1 + \frac{M}{2\,\pi\,r^2\,u_\infty}\right) \sin\theta \qquad v_r = -u_\infty \left(1 - \frac{M}{2\,\pi\,r^2\,u_\infty}\right) \cos\theta \quad . \tag{2.145}$$

Along the contour $r = R$, $v_r = 0$ and $v_\theta = -2\,u_\infty \sin\theta$. The flow possesses two stagnation points, one at $\theta = 0$ and the other at $\theta = \pi$; at $\theta = \frac{\pi}{2}$ and $\theta = 3/2\,\pi$ the velocity is twice as large as in the free stream.
The pressure distribution along the contour

$$c_p = 1 - 4\sin^2\theta \tag{2.146}$$

is symmetric with respect to the axes of coordinates and does not exhibit a resulting force (d'Alembert's Paradox 1753).

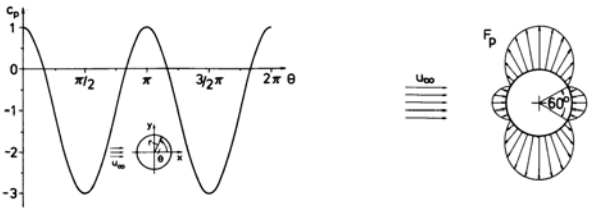


*Circular Cylinder with Circulation (Magnus Effect)*

If a potential vortex is superimposed on the flow about a circular cylinder, the cylinder experiences a force normal to the direction of the free stream.

$$F(z) = u_\infty \left(z + \frac{R^2}{z}\right) - \frac{i\,\Gamma}{2\,\pi}\,\ln z + i\,C$$

$$\Phi = u_\infty \left(r + \frac{R^2}{r}\right) \cos\theta + \frac{\Gamma}{2\,\pi}\,\theta \qquad \Psi = u_\infty \left(r - \frac{R^2}{r}\right) \sin\theta - \frac{\Gamma}{2\,\pi}\,\ln\frac{r}{R} \tag{2.147}$$

From F(z) there now results a velocity field, asymmetric with respect to the $x$-axis with components

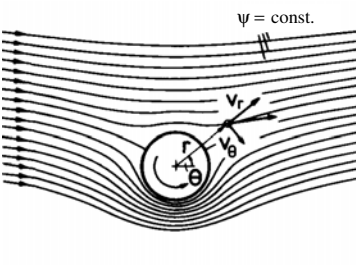


$$\begin{aligned} v_r &= u_\infty \left(1 - \frac{R^2}{r^2}\right) \cos\theta \\ v_\theta &= -u_\infty \left(1 + \frac{R^2}{r^2}\right) \sin\theta + \frac{\Gamma}{2\,\pi\,r} \end{aligned} \tag{2.148}$$

The pressure distribution on the contour $r = R$

$$c_p = 1 - \left(\frac{\Gamma}{2\,\pi\,u_\infty\,R} - 2\,\sin\theta\right)^2 \tag{2.149}$$

depends on the magnitude of the ciculation.

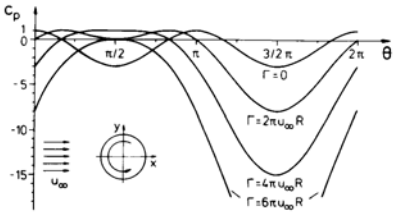


The sign of the circulation determines the direction the resulting force normal to the free stream. For $|\Gamma| < 4\,\pi\,u_\infty\,R$ there exist two stagnation points on the contour, the position of which is given by

$$\sin\theta_s = \frac{\Gamma}{4\,\pi\,u_\infty\,R} \quad . \tag{2.150}$$

If $|\Gamma| > 4\,\pi\,u_\infty\,R$, a free stagnation point is generated in the flow.

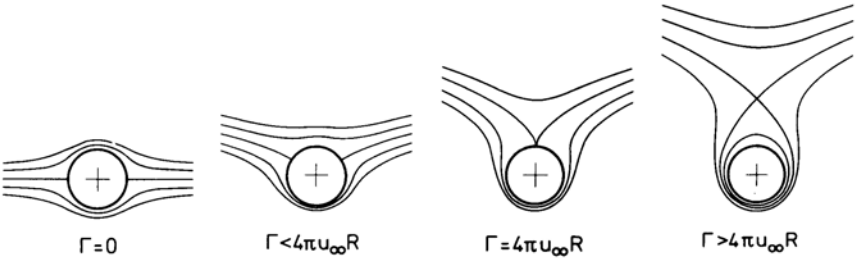


### 2.6.5 Kutta-Joukowski Theorem

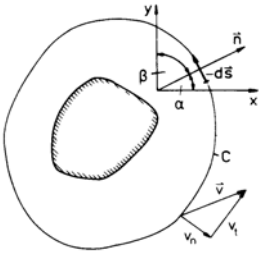


The force acting on an arbitrary body can be determined with the momentum theorem. If the local pressure is eliminated with Bernoulli's equation, the momentum equation yields the force acting on the body.

$$\boldsymbol{F} = -\int_A \rho\, \boldsymbol{v}\ (\boldsymbol{v}\cdot\boldsymbol{n})\ dA + \int_A \rho\, \frac{\boldsymbol{v}^2}{2}\, \boldsymbol{n}\, dA \quad (2.151)$$

The flow is assumed to be two-dimensional, and the potential $\Phi$ be given by

$$\Phi = u_\infty\, x + f(x,y), \quad (2.152)$$

with the function $f(x,y)$ satisfying the Laplace equation. The velocity components are

$$u = u_\infty + \frac{\partial f}{\partial x} \qquad v = \frac{\partial f}{\partial y} \quad . \quad (2.153)$$

Since the partial derivatives $\frac{\partial f}{\partial x}$ and $\frac{\partial f}{\partial y}$ vanish at large distances from the body, the control surface is chosen so far away from the body, that the squares of the partial derivatives can be neglected. The components of the force $\boldsymbol{F}$ are then given by

$$\begin{aligned} F_x &= \rho \int_C \left( \frac{\boldsymbol{v}^2}{2}\, \cos\alpha - u\, v_n \right) ds \\ F_y &= \rho \int_C \left( \frac{\boldsymbol{v}^2}{2}\, \cos\beta - v\, v_n \right) ds \quad . \end{aligned} \quad (2.154)$$

If the velocity components are introduced

$$\begin{aligned} v_n &= \left( u_\infty + \frac{\partial f}{\partial x} \right) \cos\alpha + \frac{\partial f}{\partial y} \cos\beta \\ v_t &= -\left( u_\infty + \frac{\partial f}{\partial x} \right) \cos\beta + \frac{\partial f}{\partial y} \cos\alpha, \end{aligned} \quad (2.155)$$

the expressions for the components of the force become, with the terms of second order neglected

$$\begin{aligned} F_x &= \frac{\rho\, u_\infty^2}{2} \int_C \cos\alpha\, ds - \rho\, u_\infty \int_c v_n\, ds \\ F_y &= \frac{\rho\, u_\infty^2}{2} \int_C \cos\beta\, ds - \rho\, u_\infty \int_c v_t\, ds \quad . \end{aligned} \quad (2.156)$$

With $\cos\alpha = \frac{dy}{ds}$ and $\cos\beta = \frac{dx}{ds}$ the first integrals vanish. The second integral in the expression for $F_x$ also vanishes, since it represents the volume flow through the closed curve $C$. The body does not experience a force in the direction of the free stream (drag).

The force normal to the direction of the free stream is

$$F_y = -\rho\, u_\infty\, \Gamma \quad . \tag{2.157}$$

This result is fundamental for the theory of lift-generating bodies (airfoils).

correct circulation

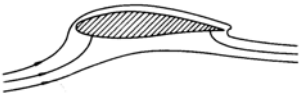

circulation too small

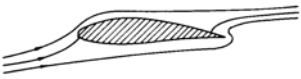

circulation too large

Flows about wing sections can be described by conformal mapping of the potential flow about circular cylinders. The circulation has to be chosen in such a way, that the flow near the trailing edge is tangent to the upper and lower surface (Kutta condition).

If the circulation is too small the stagnation point near the trailing edge is shifted to the lower side, and if the circulation is too large, to the upper side of the wing section.

This flow behavior is not observed in inviscid flow, since the turning of the flow around the sharp trailing edge would imply an infinitely large velocity.

Since, according to Thomson's theorem the circulation in inviscid flow remains constant, two counter-rotating vortices of equal strength must be generated, when a wing begins to move through the air.


$$\Gamma(t=0) = \Gamma(t) = \Gamma_1 + \Gamma_2 = 0 \tag{2.158}$$

The vortex generating the lift of the wing is called bound vortex, and the vortex, remaining at location of the start, starting vortex.

### 2.6.6 Plane Gravitational Waves

The potential flow theory can also be applied to unsteady fluid motion, as for example the description of wave motion of fluids with free surfaces. A suitable ansatz for the description of the wave motion is to choose a potential of the following form

$$\Phi(x,y,t) = f(y)\, \cos(kx - \omega\, t), \tag{2.159}$$

which satisfies the Laplace equation, if the amplitude function $f(y)$ satisfies the differential equation

$$f'' - k^2\, f = 0. \tag{2.160}$$

The quantities $k$ and $\omega$ are constants. The potential is subjected to the following boundary conditions:

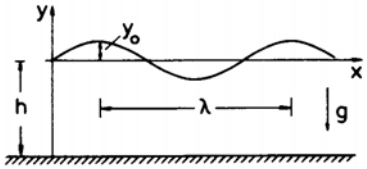


Kinematic flow condition:

$$y = -h: \quad v = \frac{\partial \Phi}{\partial y} = 0 \tag{2.161}$$

Dynamic flow condition:

$$y = y_0(x,t): \quad p = p_0 = \text{const.} \tag{2.162}$$

The quantity $y_0$ is the function describing the free surface.
The general solution of the differential equation for the amplitude function $f$ is

$$f = A\, e^{-k\, y} + B e^{+k\, y} \quad , \tag{2.163}$$

and with the kinematic flow condition there is obtained

$$f = C\, \cosh[k\, (y + h)] \tag{2.164}$$

and

$$\Phi = c\, \cosh[k\, (y + h)]\, \cos(kx - \omega\, t) \quad . \tag{2.165}$$

The velocity of wave propagation $c = \frac{\omega}{k}$ is determined with the dynamic boundary condition for the pressure and with Lagrange's integral. In the following the partial differentials with respect to $t$,$x$, and $y$ are indicated as subscripts.

$$\Phi_t + \frac{1}{2}\, (\Phi_x^2 + \Phi_y^2) + \frac{p_0}{\rho} + g\, y_0 = K(t) \tag{2.166}$$

If the amplitudes are small in comparison to the wave length, then the quadratic terms $\Phi_x^2$, $\Phi_y^2$ can be neglected in comparison to the other terms. The quantities $K(t)$ and $\frac{p_0}{p}$, which do not depend on $x$ and $y$ are included in the potential. There results

$$\Phi_t + g\, y_0 = 0 \quad . \tag{2.167}$$

Since on the surface

$$\frac{dy_0}{dt} = \Phi_y|_{y=y_0}\, , \tag{2.168}$$

it follows, that

$$\Phi_{tt} + g\, \Phi_y = 0 \quad . \tag{2.169}$$

If $\Phi$ is substituted in this equation, the velocity of propagation of the wave crest is obtained (phase velocity).

$$c = \frac{\omega}{k} = \sqrt{\frac{\lambda\, g}{2\, \pi}\, \tanh\, \left(\frac{2\, \pi\, h}{\lambda}\right)} \tag{2.170}$$

The velocity of propagation of the wave depends on the wave length $\lambda = \frac{2\, \pi}{k}$ (Dispersion).
If the depth of the water is large in comparison to the wave length ($h \gg \lambda$), then

$$c = \sqrt{\frac{g\, \lambda}{2\, \pi}} \quad . \tag{2.171}$$

If, vice versa, the water depth is much smaller than the wave length ($h \gg \lambda$), then

$$c = \sqrt{g\, h} \quad . \tag{2.172}$$

Waves in shallow water, as for example, in open channels do not exhibit dispersion.

## 2.7 Laminar Boundary Layers

Closed-form solutions of the conservation equations were primarily found for the limiting cases $Re \to 0$ and $Re \to \infty$.
Many flows are, however, characterized by a very large, but still finite Reynolds number. In these flows the influence of the friction forces is restricted to a thin layer in the immediate vicinity of rigid walls (boundary layer). The flow particles adhere to the wall, while on the outer edge of the boundary layer the flow attains the velocity of the external flow. The partitioning of the entire flow into an inviscid external flow and a viscous boundary-layer flow (The Prandtl boundary-layer hypothesis) enables an essential simplification of the conservation equations.

### 2.7.1 Boundary-Layer Thickness and Friction Coefficient

The boundary-layer thickness $\delta$ can be estimated by requiring the inertia and friction forces to be of the same order of magnitude. The inertia forces per unit volume (e. g. $\rho\, u \frac{\partial u}{\partial x}$) are of the order of magnitude $\frac{\rho\, u_e^2}{l}$, with $u_e$ being the velocity at the outer edge of the boundary layer and $l$ the characteristic length in the streamwise direction. The order of magnitude of the friction forces per unit volume is given by the change of the shear stress in the direction normal to the wall.

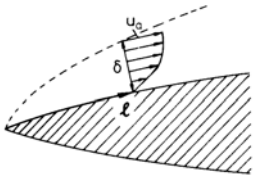


$$\mu\, \frac{\partial^2 u}{\partial\, y^2} \sim \mu\, \frac{u_a}{\delta^2} \tag{2.173}$$

It can then be concluded that

$$\frac{\delta}{l} = O\left(\sqrt{\frac{\mu}{\rho\, u_a\, l}}\right) = O\left(\frac{1}{\sqrt{Re_l}}\right) \quad . \tag{2.174}$$

The nondimensionalized boundary-layer thickness $\frac{\delta}{l}$ is then of the order of magnitude $\frac{1}{\sqrt{Re_l}}$, and consequently, small for large Reynolds numbers.
With this estimate of $\frac{\delta}{l}$ also the order of magnitude of the local skin-friction coefficient $c_f$ can be determined. The shear stress $\tau_w$ acting on the wall is of the order of magnitude $\frac{\mu\, u_a}{\delta}$, such that

$$c_f = \frac{\tau_w}{\rho\, \frac{u_a^2}{2}} = O\left(\frac{1}{\sqrt{Re_l}}\right). \tag{2.175}$$

As the dimensionless boundary-layer thickness the local skin-friction coefficient decreases with increasing Reynolds number.
The flow in the boundary layer can be determined by solving the conservation equations, simplified with the estimate for $\frac{\delta}{l}$ to the boundary-layer equations.

### 2.7.2 Boundary-Layer Equations

For the derivation of the boundary-layer equations, an incompressible, two-dimensional, steady flow along a flat plate is considered. In the conservation equations

$$\begin{aligned}
\frac{\partial u}{\partial x} + \frac{\partial v}{\partial y} &= 0 \\
u\, \frac{\partial u}{\partial x} + v\, \frac{\partial u}{\partial y} &= -\frac{1}{\rho}\, \frac{\partial p}{\partial x} + \nu\, \left(\frac{\partial^2 u}{\partial\, x^2} + \frac{\partial^2 u}{\partial\, y^2}\right) \\
u\, \frac{\partial v}{\partial x} + v\, \frac{\partial v}{\partial y} &= -\frac{1}{\rho}\, \frac{\partial p}{\partial y} + \nu\, \left(\frac{\partial^2 v}{\partial\, x^2} + \frac{\partial^2 v}{\partial\, y^2}\right)
\end{aligned} \tag{2.176}$$

the following dimensionless variables are introduced:

$$\bar{u} = \frac{u}{u_\infty}, \quad \bar{v} = \frac{v}{u_\infty}, \quad \bar{\bar{y}} = \frac{y}{L}, \quad \bar{x} = \frac{x}{L}, \quad \bar{p} = \frac{p}{\rho\, u_\infty^2} \tag{2.177}$$

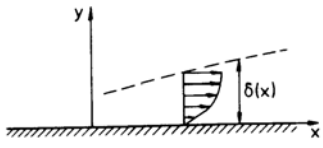


In the boundary layer the coordinate normal to the wall $y$ is $y = O(\delta)$ and hence $\bar{\bar{y}} = O\left(\frac{\delta}{L}\right) = O\left(1/\sqrt{Re_L}\right)$. It follows from the continuity equation, that

$$\bar{\bar{v}} = O\left(\frac{1}{\sqrt{Re_L}}\right) \quad . \tag{2.178}$$

Instead of $\bar{\bar{v}}$ and $\bar{\bar{y}}$ the following quantities

$$\bar{v} = \bar{\bar{v}} \sqrt{Re_L} \quad \text{and} \quad \bar{y} = \bar{\bar{y}} \sqrt{Re_L} \tag{2.179}$$

are introduced. By stretching the normal velocity component and the normal coordinate with the square root of the Reynolds number the magnitude of the dimensionless velocity components and their derivatives are of order unity.
The conservation equations then read

$$\begin{aligned} \frac{\partial \bar{u}}{\partial \bar{x}} + \frac{\partial \bar{v}}{\partial \bar{y}} &= 0 \\ \bar{u}\,\frac{\partial \bar{u}}{\partial \bar{x}} + \bar{v}\,\frac{\partial \bar{u}}{\partial \bar{y}} &= -\frac{\partial \bar{p}}{\partial \bar{x}} + \frac{\partial^2 \bar{u}}{\partial\, \bar{y}^2} + \frac{1}{Re_L}\,\frac{\partial^2 \bar{u}}{\partial\, \bar{x}^2} \\ \frac{1}{Re_L}\left(\bar{u}\,\frac{\partial \bar{v}}{\partial \bar{x}} + \bar{v}\,\frac{\partial \bar{v}}{\partial \bar{y}}\right) &= -\frac{\partial \bar{p}}{\partial \bar{y}} + \frac{1}{Re_L}\,\frac{\partial^2 \bar{v}}{\partial\, \bar{y}^2} + \frac{1}{Re_L^2}\,\frac{\partial^2 \bar{v}}{\partial\, \bar{x}^2} \quad . \end{aligned} \tag{2.180}$$

In (2.180) the barred quantities denote the dimensionless velocity components, pressures, and coordinates. The normal velocity component and coordinate are stretched, and the reciprocal value of the Reynolds number $Re_L$, based on the reference length $L$, appears in both momentum equations. As $Re_L$ is assumed to be large, the equations can be simplified.
The pressure gradient in the $y$-direction is by a factor $\frac{1}{Re_L}$ smaller than the pressure gradient in the $x$-direction. For large Reynolds numbers the second momentum equation can therefore be dropped. In addition, the last term in the first momentum equation can be neglected. There result the boundary-layer equations (Prandtl 1904) for incompressible flows in dimensionless form

$$\begin{aligned} \frac{\partial u}{\partial x} + \frac{\partial v}{\partial y} &= 0 \\ \rho\, u\,\frac{\partial u}{\partial x} + \rho\, v\,\frac{\partial u}{\partial y} &= -\frac{\partial p}{\partial x} + \mu\,\frac{\partial^2 u}{\partial\, x^2} \quad . \end{aligned} \tag{2.181}$$

For the solution of the boundary-layer equations the tangential velocity component at the outer edge of the boundary layer $u_e$ has to be known. For that reason the entire flow is first assumed to be inviscid and the Euler equations have to be solved, for example, for certain flows $u_e$ can be determined with the aid of the potential theory. In a first approximation the velocity of the inviscid flow at the rigid wall is then taken as $u_e$, which is justified, since the thickness of the boundary layer is very small.

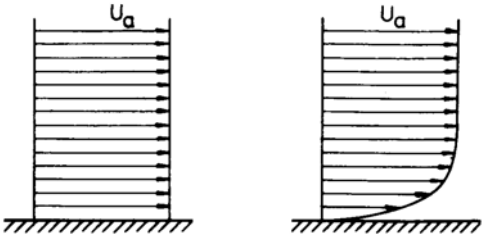


The pressure gradient in the boundary layer is determined with the Bernoulli equation for $y = 0$.

$$\frac{\partial p}{\partial x} = -\rho\, u_e\,\frac{\partial u_e}{\partial x} \tag{2.182}$$

In flows with large density and temperature changes also a thermal boundary layer is generated. Then the energy equation, simplified with the boundary-layer approximation, must also be used for the determination of the flow properties. For two-dimensional, steady, compressible, laminar flows the boundary-layer equations are

$$\frac{\partial(\rho\, u)}{\partial x} + \frac{\partial(\rho\, v)}{\partial y} = 0$$

$$\rho\, u\, \frac{\partial u}{\partial x} + \rho\, v\, \frac{\partial u}{\partial y} = -\frac{\partial p}{\partial x} + \frac{\partial}{\partial y}\left(\mu\, \frac{\partial u}{\partial y}\right)$$

$$\rho\, c_p\, u\, \frac{\partial T}{\partial x} + \rho c_p\, v\, \frac{\partial T}{\partial y} = +\frac{\partial}{\partial y}\left(\lambda\, \frac{\partial T}{\partial y}\right) + u\, \frac{\partial p}{\partial x} + \mu\, \left(\frac{\partial u}{\partial y}\right)^2 \quad . \tag{2.183}$$

In addition to the boundary conditions for the velocity also the temperature has to be prescribed at the outer edge of the boundary layer and at the wall. Instead of the wall temperature also the heat flux through the wall can be prescribed.

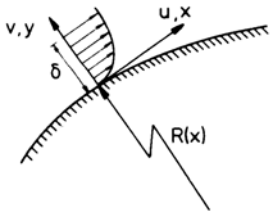


In the following only incompressible boundary layers are considered. The boundary-layer equations as listed above are also valid for flows with curved walls, if $x$ is taken as the coordinate in the tangential direction and $y$ in the direction of the outward normal. The boundary-layer approximation remains valid as long as

$$\frac{\delta}{R} \ll 1 \qquad \frac{dR}{dx} \leq O(1) \quad . \tag{2.184}$$

Corrections have to be introduced, if the curvature becomes large.

### 2.7.3 The von Kármán Integral Relation

The boundary layer is imagined to displace the inviscid external flow from the contour of the body by the amount of the so-called displacement thickness $\delta_1$, being defined as

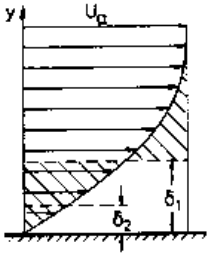


$$\delta_1 = \int_0^\infty \left(1 - \frac{u}{u_e}\right)\, dy \quad . \tag{2.185}$$

Due to the action of the friction forces the momentum of the flow in the boundary layer is reduced. A suitable measure for this effect is the momentum thickness

$$\delta_2 = \int_0^\infty \frac{u}{u_e}\left(1 - \frac{u}{u_e}\right)\, dy \quad . \tag{2.186}$$

The integration of the boundary-layer equations in the $y$-direction yields a differential equation relating $\delta_1$, $\delta_2$, $u_e$ und $\tau_w$. If the normal velocity component in the momentum equation is replaced by the integral of the continuity equation

$$v = -\int_0^y \frac{\partial u}{\partial x}\, dy \tag{2.187}$$

and after integrating the resulting equation in the $y$-direction, there is obtained

$$\int_0^\infty (u_e - u)\, \frac{\partial u}{\partial x}\, dy + \int_0^\infty \left(u_e\, \frac{du_e}{dx} - u\, \frac{\partial u}{\partial x}\right)\, dy = -\frac{1}{\rho}\, \tau(y=0) \quad . \tag{2.188}$$

With

$$(u_e - u)\, \frac{\partial u}{\partial x} = \frac{\partial}{\partial x}\left[(u_e - u)\; u\right] - u\, \frac{\partial (u_e - u)}{\partial x} \tag{2.189}$$

there results

$$\frac{d}{dx}\int_0^\infty (u_e - u)\, u\, dy + \frac{du_e}{dx}\int_0^\infty (u_e - u)\, dy = -\frac{\tau(y=0)}{\rho} \quad . \tag{2.190}$$

This equation can be transformed with the displacement thickness and the momentum thickness to give

$$\frac{d\delta_2}{dx} + \frac{1}{u_e}\frac{d\,u_e}{dx}\,(2\,\delta_2 + \delta_1) + \frac{\tau(y=0)}{\rho\, u_e^2} = 0 \quad . \tag{2.191}$$

If the momentum thickness and the displacement thickness are known, the wall-shear stress can be determined. An approximate solution is possible, if the velocity profile in the boundary layer is assumed to be given by a truncated series

$$\frac{u}{u_e} = \sum_{n=0}^{n=N} a_n \left(\frac{y}{\delta}\right)^n \tag{2.192}$$

with the coefficients determined from the boundary conditions. For the flat plate boundary layer at zero incidence ($\frac{\partial u_e}{\partial x} = 0$), for example with $N = 3$ there results

$$\frac{u}{u_a} = \frac{3}{2}\frac{y}{\delta} - \frac{1}{2}\left(\frac{y}{\delta}\right)^3 \quad , \tag{2.193}$$

and the dimensionless local skin-friction coefficient is obtained by integrating von Kármán's integral relation

$$c_f = \frac{\tau_w}{\frac{\rho}{2}\,u_e^2} = -\frac{\tau(y=0)}{\frac{\rho}{2}\,u_e^2} = \frac{0.648}{\sqrt{Re_x}} \quad . \tag{2.194}$$

### 2.7.4 Similar Solution for the Flat Plate at Zero Incidence

Similar solutions of the boundary-layer equations are solutions in which the dimensionless velocity profiles $\frac{u(x,y)}{u_e(x)}$ at two arbitrary locations $x_1$ and $x_2$ can be made congruent by stretching the normal coordinate $y$ with a scaling function $g(x)$ (Affine velocity profiles).

$$\frac{u(x_1,[\frac{y}{g(x_1)}])}{u_e(x_1)} = \frac{u\left(x_2,[\frac{y}{g(x_2)}]\right)}{u_e(x_2)} \tag{2.195}$$

The incompressible steady flow over a flat plate at zero incidence is the simplest example for a similar solution. Since the pressure gradient vanishes, the boundary-layer equations are

$$\begin{aligned} \frac{\partial u}{\partial x} + \frac{\partial v}{\partial y} &= 0 \\ u\,\frac{\partial u}{\partial x} + v\,\frac{\partial v}{\partial y} &= \nu\,\frac{\partial^2 u}{\partial\, y^2} \end{aligned} \tag{2.196}$$

and the boundary conditions

$$\begin{aligned} y = 0, \quad 0 < x \;&:\; u = v = 0 \\ y \to \infty, \quad 0 < x \;&:\; \lim_{y\to\infty} u = u_\infty \quad . \end{aligned} \tag{2.197}$$

By introducing the stream function

$$u = \frac{\partial \Psi}{\partial y} \qquad v = -\frac{\partial \Psi}{\partial x} \tag{2.198}$$

the continuity equation is identically satisfied and the momentum equation takes on the following form

$$\frac{\partial \Psi}{\partial y}\,\frac{\partial^2 \Psi}{\partial x\,\partial y} - \frac{\partial \Psi}{\partial x}\,\frac{\partial^2 \Psi}{\partial\, y^2} = \nu\,\frac{\partial^3 \Psi}{\partial\, y^3} \quad . \tag{2.199}$$

This equation can be transformed into an ordinary differential equation with a similarity transformation. If the scaling function is assumed to be $g = \sqrt{\frac{\nu\, x}{u_\infty}}$, the dimensionless independent varables are

$$\xi = \frac{x}{L} \qquad \eta = y\,\sqrt{\frac{u_\infty}{\nu\, x}} \quad . \tag{2.200}$$

The stream function is nondimensionalied with $u_\infty\, g$.

$$f(\xi,\eta) = \frac{\Psi}{u_\infty\, g} = \frac{1}{\sqrt{\nu\, x\, u_\infty}}\,\Psi(x,y) \tag{2.201}$$

The velocity components are expressed through the transformed variables

$$u = u_\infty\,\frac{\partial f}{\partial \eta}, \qquad v = -\frac{1}{2}\,\sqrt{\frac{\nu\, u_\infty}{x}}\,\left(f - \eta\,\frac{\partial f}{\partial \eta} + 2\,\xi\,\frac{\partial f}{\partial \xi}\right) \quad . \tag{2.202}$$

The momentum equation then reads

$$2\,\frac{\partial^3 f}{\partial\,\eta^3} + f\,\frac{\partial^2 f}{\partial\,\eta^2} = 2\,\xi\,\left(\frac{\partial f}{\partial \eta}\,\frac{\partial^2 f}{\partial\,\xi\,\partial\,\eta} - \frac{\partial f}{\partial \xi}\,\frac{\partial^2 f}{\partial\,\eta^2}\right) \quad . \tag{2.203}$$

If the flow is to satisfy the similarity condition, i. e. the velocity profiles are affine, then the dimensionless stream function $f$ can only depend on $\eta = \frac{y}{g}$, and the last equation reduces to an ordinary differential equation

$$2\,f''' + f\,f'' = 0 \tag{2.204}$$

with the boundary conditions

$$\eta = 0: \quad f = 0, \quad f' = 0 \qquad\qquad \eta \to \infty: \quad \lim_{\eta\to\infty} f' = 1 \quad . \tag{2.205}$$

The solution (Blasius 1908) is in excellent agreement with experimental data. The local dimensionless skin-friction coefficent can also be determined from the solution.

$$c_f = 2\,\sqrt{\frac{\nu}{u_\infty\, x}}\,f''(\eta = 0) \quad . \tag{2.206}$$

The drag coefficient of the plate with length $L$ is obtained by integrating the local skin friction coefficient.

$$c_D = \frac{1}{L}\,\int_0^L c_f\,dx = \frac{1.328}{\sqrt{Re_L}} \tag{2.207}$$

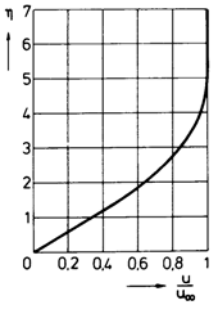


Equations (2.204) and (2.205) represent a two-point boundary-value problem, with boundary conditions to be specified at the wall and at the outer edge of the boundary layer. Because of the nonlinearity of the momentum equation, the solution is obtained by numerical integration. The profile of the tangential velocity component is shown in the following diagram.
The asymptotic behavior of the tangential velocity component near the outer edge of the boundary layer is clearly evidenced. Close to the wall the velocity increases almost linearly, and only for values of $\eta > 2$ is the profile markedly curved.

Because of the asymptotic behavior of the solution of the boundary-layer equations the velocity of the external flow in the transformed plane is attained asymptotically at infinity. The outer edge of the boundary layer is therefore often defined as the location, where $\frac{u}{u_\infty} = 0.99$. The thickness of the boundary layer then is

$$\frac{\delta}{x} = \frac{5.0}{\sqrt{Re_x}} \quad . \tag{2.208}$$

## 2.8 Turbulent Boundary Layers

Boundary layers become turbulent when the Reynolds number exceeds a certain value. As in pipe flow irregular velocity fluctuations set in and cause an additional momentum transport, which is much larger than in laminar flows. As a consequence the time-averaged mean of the velocity profile is fuller and the skin friction increases.

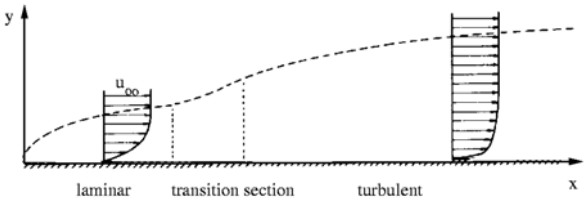


The transition from laminar to turbulent flow is influenced by disturbances in the inviscid flow and in the boundary layer, by the pressure gradient, the curvature and the roughness of the wall, the wall temperature, and density changes in compressible flow.
Theoretical investigations show, that small disturbances always decay below and increase above a certain Reynolds number. For the flow over the flat plate at zero incidence the laminar-turbulent transition is observed at a critical Reynolds number of about $Re = 5 \cdot 10^5$.

### 2.8.1 Boundary-Layer Equations for Turbulent Flow

The turbulent momentum transport in the boundary layer can be described with the aid of the Reynolds hypothesis, according to which the instantaneous flow quantities $f$ can be split into a time-averaged value $\bar{f}$ and a fluctuating part $f'$, for example

$$\begin{aligned} u(x,y,z,t) &= \bar{u}(x,y,z) + u'(x,y,z,t) \\ \bar{u} &= \frac{1}{T}\int_0^T u\, dt \quad . \end{aligned} \tag{2.209}$$

Before the the time-averaged values and the fluctuations are introduced in the momentum equations, it is advantageous to write them in divergence form by making use of the continuity equation. For incompressible flow with the volume forces neglected the equations of motion are

$$\begin{aligned} \frac{\partial u}{\partial x} + \frac{\partial v}{\partial y} + \frac{\partial w}{\partial z} &= 0 \\ \frac{\partial(\rho\, u)}{\partial t} + \frac{\partial}{\partial x}\left(\rho\, u^2 + p\right) + \frac{\partial}{\partial y}\left(\rho\, u\, v\right) + \frac{\partial}{\partial z}\left(\rho\, u\, w\right) &= \mu\, \nabla^2 u \\ \frac{\partial(\rho\, v)}{\partial t} + \frac{\partial}{\partial x}\left(\rho\, u\, v\right) + \frac{\partial}{\partial y}\left(\rho\, v^2 + p\right) + \frac{\partial}{\partial z}\left(\rho\, v\, w\right) &= \mu\, \nabla^2 v \\ \frac{\partial(\rho\, w)}{\partial t} + \frac{\partial}{\partial x}\left(\rho\, u\, w\right) + \frac{\partial}{\partial y}\left(\rho\, v\, w\right) + \frac{\partial}{\partial z}\left(\rho\, w^2 + p\right) &= \mu\, \nabla^2 w \quad . \end{aligned} \tag{2.210}$$

After introducing the Reynolds hypothesis the equations are time-averaged. All terms containing the fluctuations only and not products, the linear terms, drop out in the averaging process. The equations of motion take on the following form for the time-averaged flow quantities

$$\begin{aligned}
\frac{\partial \bar{u}}{\partial x} + \frac{\partial \bar{v}}{\partial y} + \frac{\partial \bar{w}}{\partial z} &= 0 \\
\rho \frac{d\,\bar{u}}{dt} = -\frac{\partial \bar{p}}{\partial x} + \eta\,\nabla^2\,\bar{u} &- \rho \left( \frac{\partial\,\overline{u'^2}}{\partial\,x} + \frac{\partial\,\overline{u'\,v'}}{\partial\,y} + \frac{\partial\,\overline{u'\,w'}}{\partial\,z} \right) \\
\rho \frac{d\,\bar{v}}{dt} = -\frac{\partial \bar{p}}{\partial y} + \eta\,\nabla^2\,\bar{v} &- \rho \left( \frac{\partial\,\overline{u'\,v'}}{\partial\,x} + \frac{\partial\,\overline{v'^2}}{\partial\,y} + \frac{\partial\,\overline{v'\,w'}}{\partial\,z} \right) \\
\rho \frac{d\,\bar{w}}{dt} = -\frac{\partial \bar{p}}{\partial z} + \eta\,\nabla^2\,\bar{w} &- \rho \left( \frac{\partial\,\overline{u'\,w'}}{\partial\,x} + \frac{\partial\,\overline{v'\,w'}}{\partial\,y} + \frac{\partial\,\overline{w'^2}}{\partial\,z} \right) \quad .
\end{aligned} \tag{2.211}$$

The quadratic and cross products of the velocity fluctuations appear in the form of additional stresses. They are called apparent or turbulent stresses. They can be written in form of a tensor, referred to as the Reynolds stress tensor.

$$\rho \begin{pmatrix} \overline{u^2} & \overline{u'\,v'} & \overline{u'\,w'} \\ \overline{u'\,v'} & \overline{v'^2} & \overline{v'\,w'} \\ \overline{u'\,w'} & \overline{v'\,w'} & \overline{w'^2} \end{pmatrix} \tag{2.212}$$

It is known from measurements, that in boundary layers the change of the turbulent stresses is much more pronounced in the direction normal to the wall than in the tangential direction. With this observation and the boundary-layer approximation the following equations are obtained for two-dimensional turbulent boundary layers

$$\begin{aligned}
\frac{\partial \bar{u}}{\partial x} + \frac{\partial \bar{v}}{\partial y} &= 0 \\
\rho \left( \bar{u} \frac{\partial \bar{u}}{\partial x} + \bar{v} \frac{\partial \bar{v}}{\partial y} \right) &= -\frac{\partial \bar{p}}{\partial x} + \mu \frac{\partial^2\,\bar{u}}{\partial y^2} - \rho \frac{\partial\,\overline{u'\,v'}}{\partial y} \quad .
\end{aligned} \tag{2.213}$$

As before in the case of the turbulent pipe flow, the time-averaged cross-product of the velocity fluctuations $\overline{u'\,v'}$ is an additional unknown. If $\bar{u}$ and $\bar{v}$ are to be determined, a relation has to be introduced, which expresses the cross-product through the time-averaged quantities (closure assumption), so that the number of defining equations is equal to the number of unknowns. A simple closure assumption is the Prandtl mixing-length hypothesis, already introduced

$$\overline{u'\,v'} = -l^2 \left| \frac{\partial \bar{u}}{\partial y} \right| \frac{\partial \bar{u}}{\partial y} \quad . \tag{2.214}$$

Since the velocity fluctuations vanish at the wall, the wall shear stress is solely given by the product of the dynamic shear viscosity and the gradient of the time-averaged tangential velocity component.

### 2.8.2 Turbulent Boundary Layer on the Flat Plate at Zero Incidence

In contrast to the laminar boundary layer a similar solution for the turbulent boundary layer on a flat plate can only be arrived at, if rather strong simplifying assumptions are introduced. As in the vicinity of the wall the inertia forces per unit volume and the Stokes stresses are small in comparison to the turbulent stresses, it follows with the assumption of constant shear stress, that

$$\tau_w = \rho\,l^2 \left| \frac{\partial \bar{u}}{\partial y} \right| \frac{\partial \bar{u}}{\partial y} \quad . \tag{2.215}$$

With Prandtl's ansatz for the mixing length $l = 0.4\,y$ the universal law of the wall is again obtained

$$\frac{\bar{u}}{u_*} = 2.5\,\ln\frac{y\,u_*}{\nu} + C \quad . \tag{2.216}$$

The constant $C$ was determined from experimental data to be equal to 5.5. The velocity distribution in the viscous sublayer is given by

$$\frac{\bar{u}}{u_*} = \frac{y\,u_*}{\nu} \quad . \tag{2.217}$$

In the outer part of the boundary layer, which extends over about 85% of the boundary-layer thickness, the fluctuating motions decay, and the velocity distribution follows von Kármán's velocity defect law

$$\frac{\bar{u} - u_\infty}{u_*} = f\left(\frac{y}{\delta}\right) \quad , \tag{2.218}$$

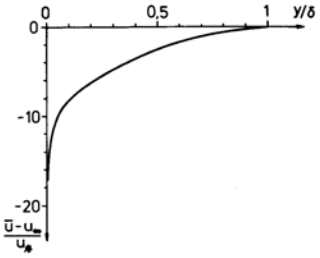


which is shown in the diagram. With the universal law of the wall and the von Kármán integral relation the drag coefficient of the flat plate can be determined as a function of the Reynolds number.
This result, confirmed by experiments up to Reynolds numbers $Re = 5 \cdot 10^8$, was approximated by Schlichting with the simple formula

$$c_D = \frac{0.455}{(\log Re_L)^{2.58}} \tag{2.219}$$

The velocity distribution in the boundary layer can in good agreement with measurements be approximated by a power law of the form:

$$\frac{\bar{u}}{u_\infty} = \left(\frac{y}{\delta}\right)^{\frac{1}{n}} \tag{2.220}$$

The exponent $\frac{1}{n}$ is almost independent of the Reynolds number, and the velocity profiles are therefore almost similar. Over a wide range of the Reynolds numbers $n = 7$. The displacement thickness and the momentum thickness then are

$$\delta_1 = \frac{\delta}{8}, \qquad \delta_2 = \frac{7}{72}\,\delta \quad . \tag{2.221}$$

The 1/7-law looses its validity in the vicinity of the wall. For that reason the wall-shear stress is determined with the aid of the resistance law of the pipe flow, which can be applied to the turbulent flat plate boundary layer.

$$\frac{\tau_w}{\rho\,u_\infty^2} = 0.023\,\left(\frac{\nu}{u_\infty\,\delta}\right)^{0.25} \tag{2.222}$$

If $\tau_w$ and $\delta_2$ are introduced into the von Kármán integral relation, there result

$$\frac{\delta}{x} = \frac{0.37}{\sqrt[5]{Re_x}}, \qquad c_D = \frac{0.074}{\sqrt[5]{Re_L}} \quad . \tag{2.223}$$

In contrast to the laminar boundary layer, the nondimensionalized boundary-layer thickness and the friction coefficient are not proportional to $Re^{-\frac{1}{2}}$, but to $Re^{-\frac{1}{5}}$. In the following diagram the drag coefficient of the flat plate is plotted versus the Reynolds number.

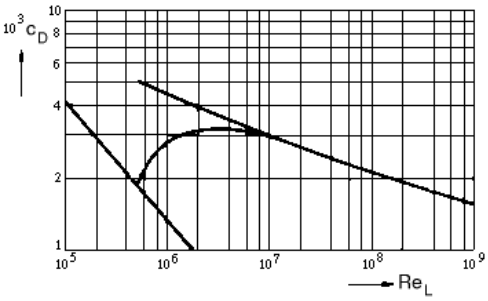


The following interpolation formula suggested by Prandtl can be used for the transition regime from laminar to tubulent flow

$$c_D = \frac{0.074}{\sqrt[5]{Re_L}} - \frac{A}{Re_L} \quad , \qquad (2.224)$$

where $A = 1700$ for $Re_{crit} = 5 \cdot 10^5$.

## 2.9 Separation of the Boundary Layer

Pressure gradients $\frac{\partial p}{\partial x}$ in the external flow can markedly influence the velocity distribution in the boundary layer. The equilibrium of forces acting on an element of fluid is given by inertia, pressure and friction forces, with the inertia and pressure forces prevailing at the outer edge, and the pressure and friction forces near the wall. For incompressible laminar boundary layers the momentum equation reduces for the wall with $y = 0$ to

$$\frac{\partial p}{\partial x} = \mu \left. \frac{\partial^2 u}{\partial y^2} \right|_{y=0} \quad . \qquad (2.225)$$

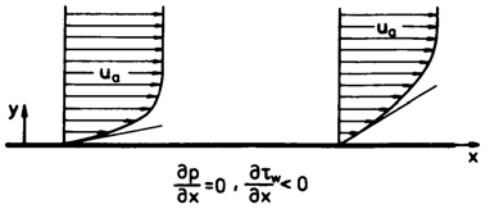


For the flat plate boundary layer, the left-hand side is zero and the velocity profile has a point of inflection at the wall. The flow in the boundary layer is retarded only by friction forces, and the change of the velocity profile in the $x$-direction causes a decrease of the wall shear stress.

If the pressure decreases in the $x$-direction ($\frac{\partial p}{\partial x} < 0$), the flow in the boundary layer is accelerated, and the curvature of the velocity profile at the wall is negative. Depending on the magnitude of the acceleration the following cases have to be distinguished:

1. If the acceleration is small the wall-shear stress decreases in the $x$-direction ($\frac{\partial \tau_w}{\partial x} < 0$).
2. If the deceleration of the flow by the friction forces is just compensated by the pressure forces, the wall-shear stress remains constant ($\frac{\partial \tau_w}{\partial x} = 0$).
3. If the acceleration by the pressure forces is larger than the deceleration by the friction forces, then the wall-shear stress increases ($\frac{\partial \tau_w}{\partial x} > 0$).

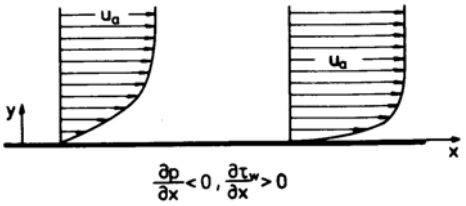


If the pressure gradient is positive, the flow is decelerated by friction and pressure forces, and the curvature of the velocity profile at the wall is positive. The wall-shear stress decreases in the $x$-direction and can become negative. The fluid near the wall then flows in the opposite direction of the main flow, associated with a separation of the flow from the wall (separation and flow reversal) as depicted in the picture below.

Boundary-layer separation by positive pressure gradient:

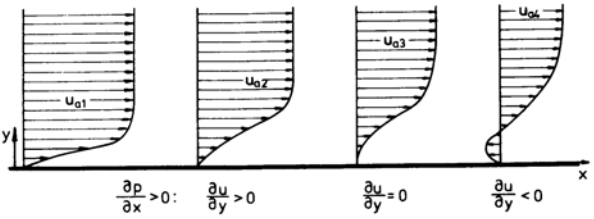


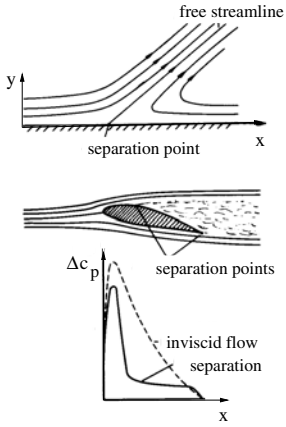


At the $x$-position, where $\tau_w = 0$, the flow separates from the body contour. The reversed flow often leads to formation of vortices downstream from the separation point. In the separated region, also called recirculation or dead-water region, the boundary layer equations are no longer valid. The wall-shear stress can only be determined up to the separation point.

If flow separation occurs, the actual pressure distribution can markedly deviate from the pressure distribution computed for the inviscid flow. For example, on an airfoil flow separation can give rise to a turbulent wake, which begins at the separation point.

At large angles of attack the flow separates on the upper surface of the airfoil near the leading edge, and the lift is greatly reduced.

*Flow Around a Circular Cylinder*

Flows around cylinders and other blunt bodies exhibit substantially different separation behavior as a function of the Reynolds number.

In very slow motion the flow moves around the cylinder without separating. For $Re < 4$ the drag coefficient is nearly inversely proportional to the Reynolds number and the drag itself is proportional to the free-stream velocity. This law looses its validity with increasing Reynolds number.

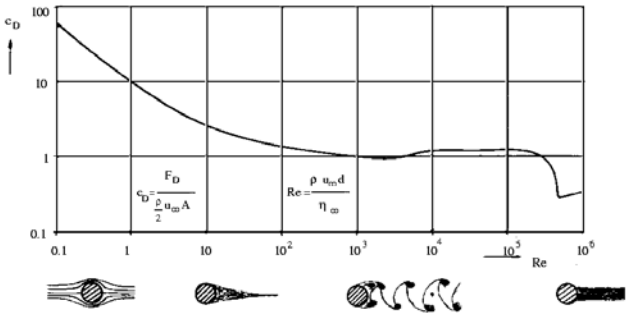


For Reynolds numbers $200 < Re < 10^5$ (subcritical region) the drag coefficient is approximately constant and the drag is proportional to the square of the free-stream velocity. The boundary layer on the cylinder is laminar and separates at an angle of about 83 degrees, measured from the stagnation point. Downstream from the separation points the flow in the wake rolls up into

vortices, which are shed from the cylinder in a alternating pattern (von Kármán vortex street). The Strouhal number, based on the separation frequency $f$ of the vortices, $Sr = \frac{d\,f}{u_\infty}$ is 0.2.

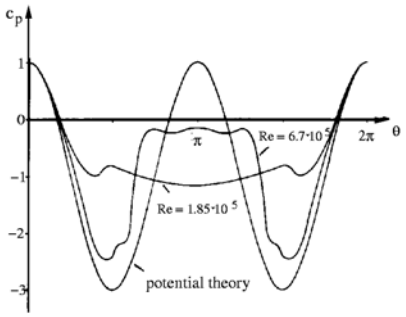


Laminar-turbulent transition of the flow in the boundary layer occurs for Reynolds numbers $10^5 < Re < 5 \cdot 10^5$. Then the kinetic energy of the flow is larger near the wall, and the boundary layer can overcome a larger positive pressure gradient. The separation point moves downstream. The wake, which does no longer exhibit regular vortex shedding, has a smaller cross section. The difference between the actual pressure distribution and that of the potential flow becomes smaller, and the drag coefficient of the cylinder is decreased.

Although the drag due to friction is increased, the total drag is decreased, as the pressure or form drag is reduced by the downstream shift of the separation point.
Disturbances in the free stream and also the surface roughness influence the transition between subcritical and supercritical regime. In the latter, beginning at $5 \cdot 10^5 < Re$ the drag coefficient increases again with the Reynolds number.
Comparable flow situations are observed in the flow around a sphere. However, alternating vortex shedding does not occur.

## 2.10 Selected References

Becker E.: *Technische Strömungslehre*, Teubner, Stuttgart 1977.

Gersten K., Herwig H.: *Strömungsmechanik*, Vieweg-Verlag Braunschweig, Wiesbaden 1992.

Landau L. D., Lifschitz E. M: *Lehrbuch der theoretischen Physik VI - Hydrodynamik,* Akademie-Verlag, Berlin 1974.

Prandtl L., Oswatitsch K., Wieghardt K.: *Führer durch die Strömungslehre*, Vieweg, Braunschweig 1969.

Schlichting H., Gersten K.: *Grenzschicht-Theorie*, Springer, Berlin/Heidelberg 1997.

Tietjens O.: *Strömungslehre*, 2 Bde., Springer, Berlin 1960 - 1970.

Truckenbrodt E.: *Fluidmechanik*, 2 Bde., Springer, Berlin 1980.

Wieghardt K.: *Theoretische Strömungslehre*, Teubner, Stuttgart 1974.

Wuest W.: *Strömungsmeßtechnik*, Vieweg, Braunschweig 1969.

## 2.11 Appendix

The Nabla operator

$$\nabla = \left( \frac{\partial}{\partial x}, \quad \frac{\partial}{\partial y}, \quad \frac{\partial}{\partial z} \right) \tag{2.226}$$

is formally used as a vector. The gradient of a scalar function $p$ is

$$\nabla p = \left( \frac{\partial p}{\partial x}, \quad \frac{\partial p}{\partial y}, \quad \frac{\partial p}{\partial z} \right) \quad , \tag{2.227}$$

the divergence of a vector $\boldsymbol{a}$

$$\nabla \cdot \boldsymbol{a} = \left( \frac{\partial}{\partial x}, \quad \frac{\partial}{\partial y}, \quad \frac{\partial}{\partial z} \right) \begin{pmatrix} a_x \\ a_y \\ a_z \end{pmatrix} = \frac{\partial a_x}{\partial x} + \frac{\partial a_y}{\partial y} + \frac{\partial a_z}{\partial z} \tag{2.228}$$

and the curl

$$\nabla \, \mathrm{x} \, \boldsymbol{a} = \begin{vmatrix} \boldsymbol{i} & \boldsymbol{j} & \boldsymbol{k} \\ \frac{\partial}{\partial x} & \frac{\partial}{\partial y} & \frac{\partial}{\partial z} \\ a_x & a_y & a_z \end{vmatrix} = \begin{pmatrix} (\frac{\partial a_z}{\partial y} - \frac{\partial a_y}{\partial z}) \\ (\frac{\partial a_x}{\partial z} - \frac{\partial a_z}{\partial x}) \\ (\frac{\partial a_y}{\partial x} - \frac{\partial a_x}{\partial y}) \end{pmatrix} \quad . \tag{2.229}$$

The following identities are used:

$$\begin{aligned} \nabla \, \mathrm{x} \, \nabla \, p &= 0 \\ \nabla \, \mathrm{x} \, \nabla^2 \boldsymbol{a} &= \nabla^2 \, (\nabla \, \mathrm{x} \, \boldsymbol{a}) \\ (\boldsymbol{a} \cdot \nabla) \, \boldsymbol{a} &= \nabla \frac{\boldsymbol{a}^2}{2} - \boldsymbol{a} \, \mathrm{x} \, (\nabla \, \mathrm{x} \, \boldsymbol{a}) \quad . \end{aligned} \tag{2.230}$$

The total time derivative is given by the operator

$$\frac{d}{dt} = \frac{\partial}{\partial t} + (\boldsymbol{v} \cdot \nabla) = \frac{\partial}{\partial t} + u \, \frac{\partial}{\partial x} + v \, \frac{\partial}{\partial y} + w \, \frac{\partial}{\partial z} \quad . \tag{2.231}$$

The dyadic product of two vectors is a tensor.

$$(\boldsymbol{a} \, \boldsymbol{b}) = \begin{pmatrix} a_x \, b_x & a_x \, b_y & a_x \, b_z \\ a_y \, b_x & a_y \, b_y & a_y \, b_z \\ a_z \, b_x & a_z \, b_y & a_z \, b_z \end{pmatrix} \tag{2.232}$$

The inner vector product of a vector and a tensor yields a vector.

$$(\boldsymbol{a} \cdot \bar{\bar{\gamma}}) = \begin{pmatrix} a_x & a_y & a_z \end{pmatrix} \begin{pmatrix} \gamma_{xx} & \gamma_{xy} & \gamma_{xz} \\ \gamma_{yx} & \gamma_{yy} & \gamma_{yz} \\ \gamma_{zx} & \gamma_{zy} & \gamma_{xz} \end{pmatrix} = \begin{pmatrix} a_x \, \gamma_{xx} + a_y \, \gamma_{yx} + a_z \, \gamma_{zx} \\ a_x \, \gamma_{xy} + a_y \, \gamma_{yy} + a_z \, \gamma_{zy} \\ a_x \, \gamma_{xz} + a_y \, \gamma_{yz} + a_z \, \gamma_{zz} \end{pmatrix} \tag{2.233}$$

In the derivation of the conservation equations the following transformation of the total time derivative of an integral is used ($\rho$ is the density, $S$ a scalar function of space and time).

$$\begin{aligned} \frac{d}{dt} \int_{\tau(t)} \rho \, S \, d\tau &= \int_{\tau(t)} \left( \rho \, \frac{\partial S}{\partial t} + S \, \frac{\partial \rho}{\partial t} \right) \, d\tau + \int_{A(t)} \rho \, S \, (\boldsymbol{v} \cdot \boldsymbol{n}) \, dA \\ &= \int_{\tau(t)} \left[ S \, \frac{\partial \rho}{\partial t} + \rho \, \frac{\partial S}{\partial t} + S \, \nabla \cdot (\rho \, \boldsymbol{v}) + (\rho \, \boldsymbol{v} \cdot \nabla) \, S \right] \, d\tau \\ &= \int_{\tau(t)} \left[ \rho \, \frac{\partial S}{\partial t} + (\rho \, \boldsymbol{v} \cdot \nabla) \, S \right] \, d\tau \\ &= \int_{\tau(t)} \rho \, \frac{dS}{dt} \, d\tau \end{aligned} \tag{2.234}$$

# 3. Exercises in Fluid Mechanics

## 3.1 Problems

### 3.1.1 Hydrostatics

1.1 The density of a fluid $\rho_f$ is to be determined with a U-tube. One stem is filled with water.

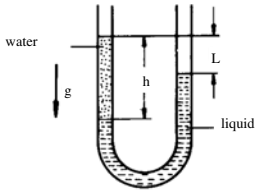


$h = 0.3\,\mathrm{m} \quad L = 0.2\,\mathrm{m} \quad \rho_w = 10^3\,\frac{\mathrm{kg}}{\mathrm{m}^3}$

1.2 In three communicating vessels pistons are exposed to the forces $F_1$, $F_2$ and $F_3$.

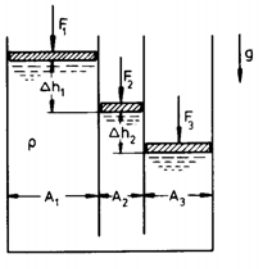


$F_1 = 1100\,\mathrm{N}\; F_2 = 600\,\mathrm{N}\; F_3 = 1000\,\mathrm{N}$
$A_1 = 0.04\,\mathrm{m}^2 \quad A_2 = 0.02\,\mathrm{m}^2$
$A_3 = 0.03\,\mathrm{m}^2 \quad \rho = 10^3\,\frac{\mathrm{kg}}{\mathrm{m}^3} \quad g = 10\,\frac{\mathrm{m}}{\mathrm{s}^2}$
Determine the differences in height $\Delta h_1$ and $\Delta h_2$!

1.3 A cube floats in two laminated fluids, one on top of the other.

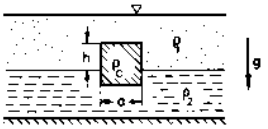


$\rho_1 = 850\,\frac{\mathrm{kg}}{\mathrm{m}^3} \quad \rho_2 = 1000\,\frac{\mathrm{kg}}{\mathrm{m}^3}$
$\rho_C = 900\,\frac{\mathrm{kg}}{\mathrm{m}^3} \quad a = 0.1\,m$
Determine the height $h$!

1.4 A cylindrical vessel floats in another cylindrical vessel, filled with water. After adding a mass $m$ the water surface is raised by $\Delta H$.

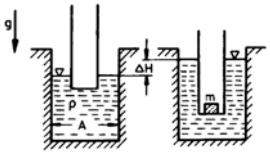


Given: $\rho$, $A$, $m$
Determine the difference in height $\Delta H$!

1.5 A boat with vertical side walls and a weight $W_0$ has a draught in sea water $h_0$ and displaces the volume $\tau_0$. Before entering the mouth of a river the weight of the cargo is reduced by $\Delta W$, in order to avoid the boat running aground. The draught is then $h_1$ and the volume is $\tau_1$. The density of the sea water is $\rho_S$, and that of the water in the river $\rho_R$.

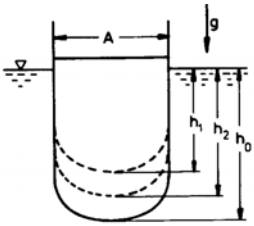


$\rho_S = 1.025 \cdot 10^3\,\frac{\mathrm{kg}}{\mathrm{m}^3} \quad \rho_R = 10^3\,\frac{\mathrm{kg}}{\mathrm{m}^3}$
$W_0 = 1.1 \cdot 10^9\,\mathrm{N} \quad \Delta W = 10^8\,\mathrm{N}$
$h_0 = 11\,\mathrm{m} \quad h_1 = 10.5\,\mathrm{m} \quad g = 10\,\frac{\mathrm{m}}{\mathrm{s}^2}$

Determine
(a) the volume $\tau_0$,
(b) the area of the deck $A$,
(c) the difference $\tau_2 - \tau_1$ of the displaced volumes in fresh water and sea water,
(d) the draught $h_2$ in fresh water!

1.6 A diving bell with the weight $W$ is lowered into the sea.

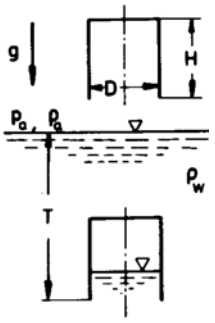


$D = 3\,\mathrm{m} \quad H = 3\,\mathrm{m} \quad T = 22\,\mathrm{m}$
$\rho_a = 1.25\,\frac{\mathrm{kg}}{\mathrm{m}^3} \quad \rho_W = 10^3\,\frac{\mathrm{kg}}{\mathrm{m}^3}$
$p_a = 10^5\,\frac{\mathrm{N}}{\mathrm{m}^2} \quad W = 8 \cdot 10^4\,\mathrm{N} \quad g = 10\,\frac{\mathrm{m}}{\mathrm{s}^2}$

(a) How high does the water in the bell rise if the temperature remains constant?
(b) How large is the force (magnitude and direction) with which the bell must be held?
(c) At what depth of immersion is the force zero?

1.7 A container filled with water is fastened to a plate. It has a small opening in the top.

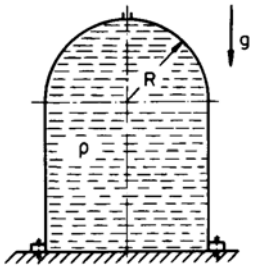


$R = 1\,\mathrm{m} \quad \rho = 10^3\,\frac{\mathrm{kg}}{\mathrm{m}^3} \quad g = 10\,\frac{\mathrm{m}}{\mathrm{s}^2}$

Determine the force in the screws under the assumption that the weight of the container can be neglected!

1.8 A conical plug with density $\rho_s$ closes the outlet of a water basin. The base area of the cone levels with the surface of the fluid.

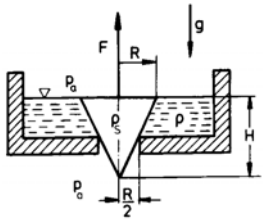


$R = 10^{-2}\,\mathrm{m} \quad H = 10^{-2}\,\mathrm{m} \quad g = 10\,\frac{\mathrm{m}}{\mathrm{s}^2}$
$\rho_s = 2 \cdot 10^3\,\frac{\mathrm{kg}}{\mathrm{m}^3} \quad \rho = 10^3\,\frac{\mathrm{kg}}{\mathrm{m}^3}$
How large must the force be to lift the plug?

1.9 A rectangular sluice gate with the width $B$ separates two sluice chambers.

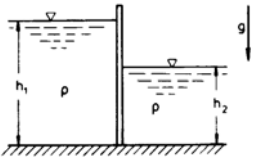


$B = 10\,\mathrm{m} \quad h_1 = 5\,\mathrm{m} \quad h_2 = 2\,\mathrm{m}$
$\rho = 10^3\,\frac{\mathrm{kg}}{\mathrm{m}^3} \quad g = 10\,\frac{\mathrm{m}}{\mathrm{s}^2}$
Determine
(a) the force acting on the sluice gate,
(b) the point of application of force!

1.10 A pivoted wall of a water container with width $B$ is supported with a rod.

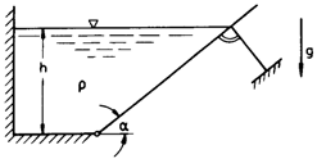


$h = 3\,\mathrm{m} \quad B = 1\,\mathrm{m} \quad \alpha = 30°$
$\rho = 10^3\,\frac{\mathrm{kg}}{\mathrm{m}^3} \quad g = 10\,\frac{\mathrm{m}}{\mathrm{s}^2}$
Determine the force in the rod!

1.11 The triangular opening of a weir is closed with a plate.

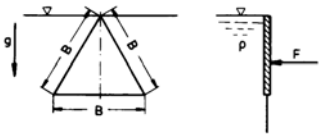


$B = 1\,\mathrm{m} \quad \rho = 10^3\,\frac{\mathrm{kg}}{\mathrm{m}^3} \quad g = 10\,\frac{\mathrm{m}}{\mathrm{s}^2}$

Determine

(a) the closing force,

(b) the point of application of force!

1.12 A fluid with a free surface rotates in an open circular cylindrical vessel with constant angular velocity, large enough, so that the fluid just reaches the edge of the vessel. When the fluid is at rest, it fills the vessel up to the height $h_0$.

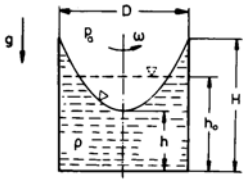


$D = 0.5\,\mathrm{m} \quad h_0 = 0.7\,\mathrm{m} \quad H = 1\,\mathrm{m}$

$\rho = 10^3\,\frac{\mathrm{kg}}{\mathrm{m}^3} \quad p_a = 10^5\,\frac{\mathrm{N}}{\mathrm{m}^2} \quad g = 10\,\frac{\mathrm{m}}{\mathrm{s}^2}$

Determine

(a) the height $h$ and the angular velocity $\omega$,

(b) the pressure distribution at the wall and on the bottom!

Hint:

$$\frac{\partial p}{\partial r} = \rho\,\omega^2\,r \quad \frac{\partial p}{\partial z} = -\rho\,g$$

$$dp = \frac{\partial p}{\partial r}dr + \frac{\partial p}{\partial z}\,dz$$

1.13 Determine the pressure as a function of the height $z$

(a) for an isothermal atmosphere,

(b) for a linear temperature variation $T = T_0 - \alpha\,z$,

(c) for an isentropic atmosphere,

(d) for a height of 3000 m, 6000 m und 11000 m!

$z = 0$ :

$R = 287\,\frac{\mathrm{Nm}}{\mathrm{kg\,K}} \quad T_0 = 287\,\mathrm{K} \quad \gamma = 1.4$

$p_0 = 10\,\frac{\mathrm{N}}{\mathrm{m}^2} \quad \alpha = 6.5 \cdot 10^3\,\frac{\mathrm{K}}{\mathrm{m}} \quad g = 10\,\frac{\mathrm{m}}{\mathrm{s}^2}$

1.14 A metereological balloon of mass $m$ and initial volume $\tau_0$ rises in an isothermal atmosphere. The envelope is slack until the maximum volume $\tau_1$ is attained.

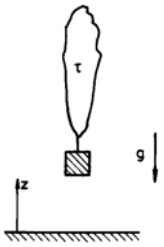


$p_0 = 10^5\,\frac{\mathrm{N}}{\mathrm{m}^2} \quad p_0 = 1.27\,\frac{\mathrm{kg}}{\mathrm{m}^3}$

$m = 2.5\,\mathrm{kg}$

$\tau_0 = 2.8\mathrm{m}^3 \quad \tau_1 = 10\mathrm{m}^3 \quad R = 287\frac{\mathrm{Nm}}{\mathrm{kg\,K}}$

$g = 10\,\frac{\mathrm{m}}{\mathrm{s}^2}$

(a) How large is the force the balloon must be held with before take off?

(b) At what altitude does the balloon attain the volume $\tau_1$?

(c) How high does the balloon rise?

1.15 A balloon with an inelastic envelope has an opening at the bottom for equalization of the pressure with the surrounding air. The weight of the balloon without the gas filling is $W$. Before take off the balloon is held with the force $F_s$.

$W = 1000\,\mathrm{N} \quad F_s = 1720\,\mathrm{N}$

$R = 287\,\frac{\mathrm{Nm}}{\mathrm{kg\,K}}$

$T = 273\,\mathrm{K} \quad g = 10\,\frac{\mathrm{m}}{\mathrm{s}^2}$

Determine the height of rise of the balloon in an isothermal atmosphere!

### 3.1.2 Hydrodynamics

If not mentioned otherwise, the flow is assumed to be loss-free in this chapter.

2.1 Given the velocity field

$u = u_0\,\cos\omega\,t \quad v = v\,\sin\omega\,t$

with $\frac{u_0}{w} = \frac{v_0}{w} = 1\,\mathrm{m}$.

Determine

(a) the streamlines for $\omega\,t = 0, \frac{\pi}{2}, \frac{\pi}{4}$,

(b) the path lines,

(c) the path line of a particle, which at time $t = 0$ is in the point $x = 0$, $y = 1\,\mathrm{m}$!

2.2 Under an iceberg a steady downward flow is initiated by the cooling of the water by the ice. Determine the flow velocity $v$ in the depth $h$ under the assumption, that the cold water (density $\rho_c$) does not mix with the warm water (density $\rho_w$).

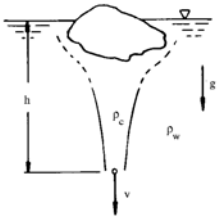


$h = 50\,\mathrm{m} \quad \dfrac{\rho_c - \rho_w}{\rho_c} = 0.01 \quad g = 10\,\dfrac{\mathrm{m}}{\mathrm{s}^2}$

2.3 Hot exhaust air of temperature $T_i$ flows through an open smokestack with a large suction scoop into the atmosphere. The external temperature is $T_a$.

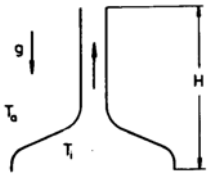


$T_i = 450\,\mathrm{K} \quad T_a = 300\,\mathrm{K}$
$H = 100\,m \quad g = 10\,\dfrac{\mathrm{m}}{\mathrm{s}^2}$

Determine the discharge velocity, taking into account the influence of compressibility!
Hint: Use the Bernoulli equation in differential form:

$$\frac{1}{\rho}\,dp + v\,dv + g\,dz = 0$$

2.4 Determine the free-stream velocity $v_\infty$ of a Prandtl static pressure tube, taking into account the influence of the viscosity for

(a) $\mu = 10^{-3}\,\dfrac{\mathrm{Ns}}{\mathrm{m}^2}$,

(b) $\mu = 10^{-2}\,\dfrac{\mathrm{Ns}}{\mathrm{m}^2}$,

(c) $\mu = 10^{-1}\,\dfrac{\mathrm{Ns}}{\mathrm{m}^2}$.

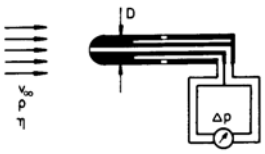


$D = 6 \cdot 10^{-3}\,\mathrm{m} \quad \Delta p = 125\,\dfrac{\mathrm{N}}{\mathrm{m}^2}$
$p = 10^3\,\dfrac{\mathrm{kg}}{\mathrm{m}^3}$

$2.5 \le Re \le 250: \quad \beta = 1 + \frac{6}{Re}$
$250 \le Re: \quad \beta = 1$

2.5 In order to determine the velocity in a pipe flow the pressure difference $\Delta p$ is measured. The pressure difference deviates from the dynamic pressure of the undisturbed flow, if there is a large blockage in the pipe.

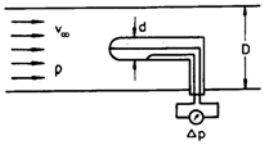


Plot $v_\infty / \sqrt{\frac{2\,\Delta p}{\rho}}$ as a function of $\frac{d}{D}$!

2.6 Water flows out of a large reservoir under the influence of gravity into the open air.

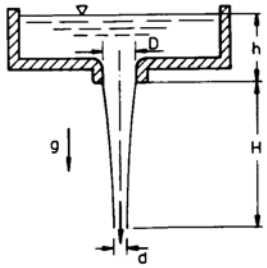


$h = 0.1\,\mathrm{m} \quad H = 1.5\,\mathrm{m} \quad D = 0.1\,\mathrm{m}$
What is the diameter $d$ of the water stream at the position $H$ below the opening?

2.7 Water flows out of a large pressure tank into the open air. The pressure difference $\Delta p$ is measured between the cross sections $A_1$ and $A_2$.

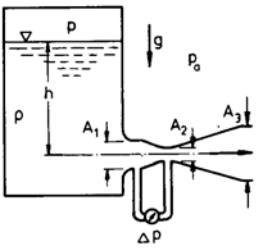


$A = 0.3\,\mathrm{m}^2 \quad A_2 = 0.1\,\mathrm{m}^2 \quad A_3 = 0.2\,\mathrm{m}^2$
$h = 1\,\mathrm{m} \quad \rho = 10^3\,\frac{\mathrm{kg}}{\mathrm{m}^3} \quad p_a = 10^5\,\frac{\mathrm{N}}{\mathrm{m}^2}$
$g = 10\,\frac{\mathrm{m}}{\mathrm{s}^2} \quad \Delta p = 0.64 \cdot 10^5\,\frac{\mathrm{N}}{\mathrm{m}^2}$

The outflow pipe was provided with a variable cross-section distribution in order to enable the measurement for the pressure. The pressure difference $\Delta p$ is measured in the cross sections indicated in the sketch.
Determine
(a) the velocities $v_1$, $v_2$, $v_3$,
(b) the pressures $p_1, p_2, p_3$, and the pressure $p$ above the water surface!

2.8 Water flows out of a large vessel through an opening of width $B$ and height $2a$ into the open air.

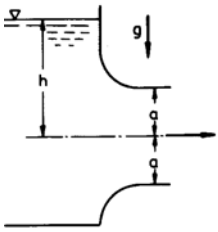


For $\frac{a}{h} \to 0$ the volume flow per unit time is $\dot{Q}_0 = 2\,a\,B\,\sqrt{2\,g\,h}$. Determine the relative error $\frac{\dot{Q}_0 - \dot{Q}}{\dot{Q}}$ for $\frac{a}{h} = \frac{1}{4}, \frac{1}{2}, \frac{3}{4}$!

2.9 Two large reservoirs, one located above the other, are connected with a vertical pipe, with a nozzle attached to its end.

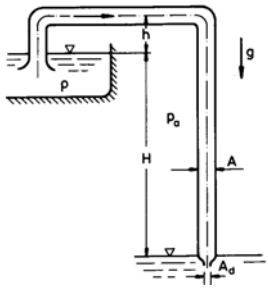


$A = 1\,\mathrm{m}^2 \quad A_d = 0.1\,\mathrm{m}^2 \quad h = 5\,\mathrm{m}$
$H = 80\,\mathrm{m} \quad p_a = 10^5\,\frac{\mathrm{N}}{\mathrm{m}^2} \quad \rho = 10^3\,\frac{\mathrm{kg}}{\mathrm{m}^3}$
$g = 10\,\frac{\mathrm{m}}{\mathrm{s}^2}$

(a) How large is the volume flow per unit time?
(b) Sketch the curve of the static pressure in the pipe!
(c) At what size of the cross section of the exit will vapor bubbles be formed, if the vapor pressure is $p_v = 0.025 \cdot 10^5\,\frac{\mathrm{N}}{\mathrm{m}^2}$?

2.10 Air flows out of a large pressure tank through a well-rounded nozzle and a diffuser into the open air.

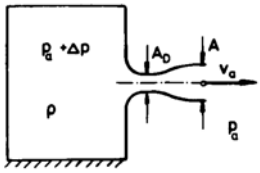


$\rho = 1.25\,\frac{\mathrm{kg}}{\mathrm{m}^3} \quad \Delta p = 10\,\frac{\mathrm{N}}{\mathrm{m}^2}$

Determine the velocity in the throat of the nozzle as a function of the ratio of the cross sections $\frac{A}{A_D}$
(a) for loss-free flow,
(b) for an efficiency of the diffuser of

$$\eta_D = \frac{p_a - p_D}{\frac{\rho}{2}\,(v_D^2 - v_a^2)} = 0.84 \quad !$$

(c) What is the maximum velocity that can be attained for this efficiency of the diffuser?

2.11 Water flows through a nozzle mounted in a pipe (cross-sectional ratio $m_D$, discharge coefficient $\alpha_D$) and an orifice

($m_D$, $\alpha_B$). The mercury gauges show differences in height of $h_D$ and $h_B$.

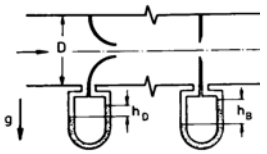


$m_D = 0.5 \quad \alpha_D = 1.08 \quad m_B = 0.6$
$h_D = 1\,\text{m} \quad h_B = 1.44\,\text{m} \quad D = 0.1\,\text{m}$
$\rho_W = 10^3\,\frac{\text{kg}}{\text{m}^3} \quad \rho_{Hg} = 13.6 \cdot 10^3\,\frac{\text{kg}}{\text{m}^3}$
$g = 10\,\frac{\text{m}}{\text{s}^2}$

Determine

1. the volume flow per unit time,
2. the discharge coefficient of the orifice!

2.12 A sluice gate is suddenly opened.

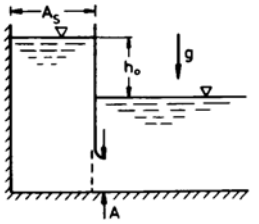


$A_s = 3000\,\text{m}^2 \quad h(t=0) = h_0 = 5\,\text{m}$
$g = 10\,\frac{\text{m}}{\text{s}^2}$

How large must the cross section of the opening $A$ be so that the water level of the bordering lake is attained within 10 minutes, if quasi-steady flow is assumed?

2.13 Two equally large reservoirs, one of which is filled with water, are separated from each other by a wall.

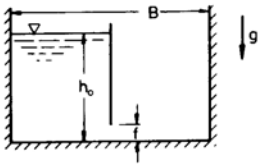


$B = 20\,\text{m} \quad h(t=0) = h_0 = 5\,\text{m}$
$f = 0.05\,\text{m} \quad g = 10\,\frac{\text{m}}{\text{s}^2}$

Determine the time necessary for equalizing the water levels, if the dividing wall is lifted by the amount $f \ll h_0$! Neglegt the contraction of the flow!

2.14 Water flows out of a large reservoir into a lower reservoir, the discharge opening of which is suddenly reduced to one third.

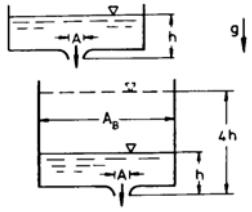


$A = 0.03\,\text{m}^2 \quad A_B = 1\,\text{m}^2$
$h = 5\,\text{m} \quad g = 10\,\frac{\text{m}}{\text{s}^2}$

Determine the time, in which the water level rises to the quadruple value of its initial height $h$!

2.15 A pipe filled with gasoline is held vertically in water and closed at the upper end with a top. A small, well-rounded outlet in the top is opened.

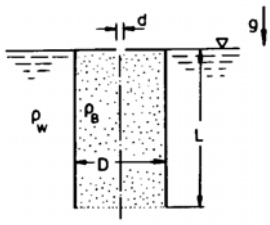


$D = 0.1\,\text{m} \quad d = 0.01\,\text{m}m \quad L = 0.8\,\text{m}$
$\rho_B = 800\,\frac{\text{kg}}{\text{m}^3} \quad \rho_w = 10^3\,\frac{\text{kg}}{\text{m}^3} \quad g = 10\,\frac{\text{m}}{\text{s}^2}$

Since the gasoline is lighter than water, it will begin to flow upward through the small hole. The surface of the water surrounding the pipe is very large compared to the cross-sectional area of the pipe.
How long will it take, until the pipe is completely emptied from gasoline?

2.16 A fluid flows through a pipe with a well-rounded intake. Its velocity is $v_0(t)$.

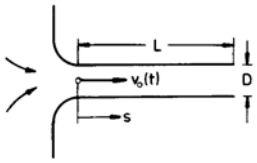


Show that the integral of the local acceleration can be approximated as follows:

$$\int_{-\infty}^{L} \frac{\partial v}{\partial t} ds = \left( \frac{D}{\sqrt{2}} + L \right) \frac{dv_0}{dt}$$

Hint: Assume that for $s < -\frac{D}{\sqrt{8}}$ the fluid flows radially towards the intake with the velocity $v = \frac{\dot{Q}}{2}\, \pi\, s^2$, and that for $s \geq \frac{D}{\sqrt{8}}$ the velocity is equal to $v_0$! For $s = -\frac{D}{\sqrt{8}}$, $v = v_0$.

2.17 Liquid flows out of a large container through a hose, lying horizontally on the ground, in steady motion into the open air. The end of the hose is suddenly lifted up to the height of the liquid level.

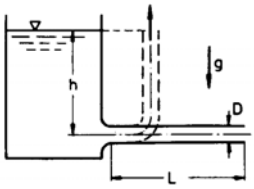


$L = 10\,\text{m} \quad h = 5\,\text{m} \quad D = 0.16\,\text{m}$
$g = 10\,\dfrac{\text{m}}{\text{s}^2}$

Determine

1. the velocity $v_0$ immediately after lifting up the hose,
2. the time, in which the velocity decreases to $\frac{v_0}{2}$,
3. the fluid volume that flowed through the hose during this time!

2.18 The discharge pipe of a large water container is led to a lake. The throttle valve at the end of the pipe is suddenly opened.

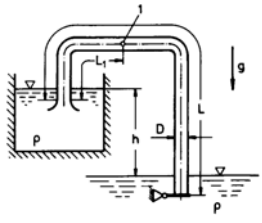


$L = 20\,\text{m} \gg D \quad h = 5\,\text{m} \quad L_1 = 5\,\text{m}$
$p = 10^3\,\dfrac{\text{kg}}{\text{m}^3} \quad g = 10\,\dfrac{\text{m}}{\text{s}^2}$

1. After what time are 99% of the final velocity attained?
2. How much does the pressure at the position 1 differ from its final value?

2.19 A piston is moving sinusoidally in a pipe $s = s_0\, \sin \omega\, t$.

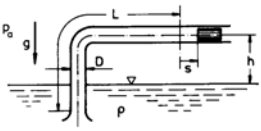


$p_a = 10^5\,\dfrac{\text{N}}{\text{m}^2} \quad L = 10\,\text{m} \gg D \quad h = 2\,\text{m}$
$s_0 = 0.1\,\text{m} \quad \rho = 10^3\,\dfrac{\text{kg}}{\text{m}^3} \quad p_v = 2500\,\dfrac{\text{N}}{\text{m}^2}$
$g = 10\,\dfrac{\text{m}}{\text{s}^2}$

At what angular velocity $\omega$ is the pressure at the piston head equal to the vapor pressure $p_v$?

2.20 In a hydraulic ram the valve I and the valve II are alternatively opened and closed. A part of the water is pumped from the height $h_1$ to the height $h_2$. The other part flows through the valve I.

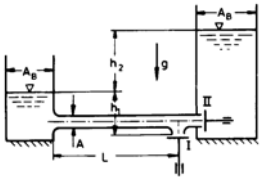


$h_1 = h_2 = 5\,\text{m} \quad L = 10\,\text{m} \gg D$
$A = 0.1\,\text{m}^2 \ll A_B \quad T_1 = 1\,\text{s}$
$g = 10\,\dfrac{\text{m}}{\text{s}^2}$

(a) First the valve I is opened for the time $T$. Determine the volume $Q_I$ of the water discharged!
(b) After closing the valve I, the valve II is opened until the velocity in the pipe is decreased to zero. How large is the discharge volume $Q_{II}$?

2.21 The flap at the end of a discharge pipe of a large container is suddenly opened.

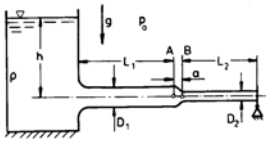


$p_a = 10^5 \dfrac{\mathrm{N}}{\mathrm{m}^2}$ $L_1 = L_2 = 5\,\mathrm{m} \gg a$
$D_1 = 0.1\,\mathrm{m}$ $D_2 = 0.05\,\mathrm{m}$ $h = 2\,\mathrm{m}$
$\rho = 10^3 \dfrac{\mathrm{kg}}{\mathrm{m}^3}$ $g = 10 \dfrac{\mathrm{m}}{\mathrm{s}^2}$

Determine
(a) the time $T$, in which the velocity attains 99% of its final value,
(b) the volume of the fluid discharged,
(c) the pressures $p_A$ and $p_B$ immediately after opening the flap and at time $T$!
(d) Sketch the pressure at the positions $A$ and $B$ as a function of time!

2.22 The pressurized pipe system of a storage power station is closed with a valve. During the closure (shut-down time $T_s$) the discharge volume decreases linearly from $\dot{Q}_0$ to zero.

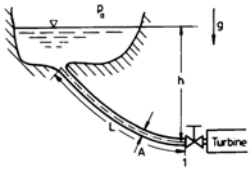


$h = 200\,\mathrm{m}$ $L = 300\,\mathrm{m}$ $A = 0.2\,\mathrm{m}^2$
$\dot{Q} = 3 \dfrac{\mathrm{m}^3}{\mathrm{s}}$ $\rho = 10^3 \dfrac{\mathrm{kg}}{\mathrm{m}^3}$ $g = 10 \dfrac{\mathrm{m}}{\mathrm{s}^2}$
$\Delta p_{save} = (p_1 - p_a)_{save} = 2 \cdot 10^7 \dfrac{\mathrm{N}}{\mathrm{m}^2}$

Determine
(a) the excess pressure in front of the open valve for steady flow,
(b) the pressure variation $p_1(t)$ during closure of the valve (Sketch the result!),
(c) the closure time of the valve so that the excess prssure does not exceed the safe value $\Delta p_{safe}$!

### 3.1.3 Momentum and Moment of Momentum Theorem

In this chapter the friction forces are neglected in comparison to the volume, pressure, and inertia forces, but not the pressure losses, resulting from flow separation.

3.1 Water flows out of a bifurcated pipe into the open air. The pressure in the inflow stem is higher by the amount $\Delta p$ than in the surrounding air.

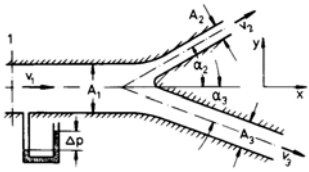


$A_1 = 0.2\,\mathrm{m}^2$ $A_2 = 0.03\,\mathrm{m}^2$
$A_3 = 0.07\,\mathrm{m}^2$ $\alpha_2 = 30°$ $\alpha_3 = 20°$
$\Delta p = 10^4 \dfrac{\mathrm{N}}{\mathrm{m}^2}$ $\rho = 10^3 \dfrac{\mathrm{kg}}{\mathrm{m}^3}$

Determine
(a) the velocities $v_1$, $v_2$, $v_3$,
(b) the force $F$ in the cross section 1,
(c) the angle $\alpha_3$, for which $F_{sy}$ vanishes!

3.2 Water flows out of a large container through a pipe under the influence of gravity in steady motion into the open air. Downstream from the nozzle the water jet is deflected by 180°. The flow is assumed to be two-dimensional.

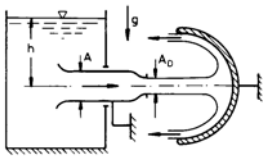


$A = 0.2\,\mathrm{m}^2$ $A_D = 0.1\,\mathrm{m}^2$ $h = 5\,\mathrm{m}$
$\rho = 10^3 \dfrac{\mathrm{kg}}{\mathrm{m}^3}$ $g = 10 \dfrac{\mathrm{m}}{\mathrm{s}}$

Determine the forces retaining the pipe and the guide vane
(a) for the sketched configuration,

(b) for the case that the inlet of the pipe and the nozzle are removed!

3.3 Water flows out of a two-dimensional nozzle in steady motion with the velocity $v_0$ against a guide vane, moving with the velocity $v_r$.

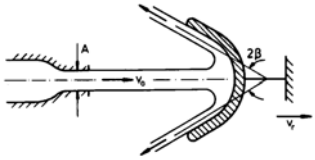


$A = 0.1\,\mathrm{m}^2 \quad v_0 = 60\,\dfrac{\mathrm{m}}{\mathrm{s}} \quad 2\,\beta = 45°$

$\rho = 10^3\,\dfrac{\mathrm{kg}}{\mathrm{m}^3}$

(a) At what velocity $v_r$ does the performance of the vane attain its maximum value?
(b) How large is then the force acting on the vane?

3.4 Two two-dimensional cascades (infinitely many blades) with width $B$ and spacing $t$ deflect a flow by the angle $\alpha$.

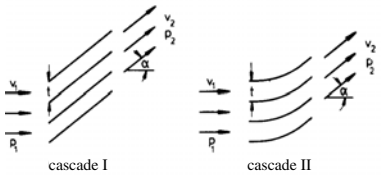


Given: $\rho$, $v_1$, $\alpha$, $B$, $t$
Determine
(a) the velocity $v_2$,
(b) the pressure difference $p_1 - p_2$,
(c) the pressure loss $p_{01} - p_{02}$,
(d) the force exerted by the flow on a blade!

3.5 A rocket moves with constant velocity. The air flowing past the rocket is displaced in the radial direction. The velocity in the jet is $v_A$, around it $v_1$.

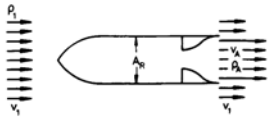


Given: $v_1$, $v_A$, $\rho_1$, $\rho_A$, $A_R$
Determine
(a) the mass of air displaced,
(b) the thrust and the net performance!

3.6 The constant free-stream velocity of a propeller is $v_1$. A certain distance downstream from the propeller the velocity in the slipstream is $v_2$, outside of it $v_1$.

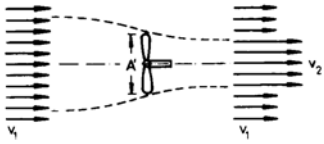


$A' = 7.06\,\mathrm{m} \quad v_1 = 5\,\dfrac{\mathrm{m}}{\mathrm{s}} \quad v_2 = 8\,\dfrac{\mathrm{m}}{\mathrm{s}}$

$\rho = 10^3\,\dfrac{\mathrm{kg}}{\mathrm{m}^3}$

Determine
(a) the velocity $v'$ in the cross-sectional plane of the propeller,
(b) the efficiency!

3.7 A ducted propeller is positioned in a free stream with constant velocity. The inlet lip is well rounded.

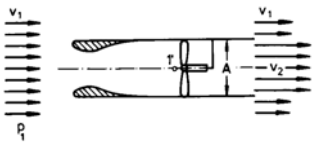


$A = 1\,\mathrm{m}^2 \quad v_1 = 10\,\dfrac{\mathrm{m}}{\mathrm{s}} \quad p_{1'} = 10^5\,\dfrac{\mathrm{N}}{\mathrm{m}^2}$

$\rho = 10^3\,\dfrac{\mathrm{kg}}{\mathrm{m}^3} \quad p_1 = 1.345 \cdot 10^5\,\dfrac{\mathrm{N}}{\mathrm{m}^2}$

(a) Sketch the variation of the static pressure along the axis!
Determine
(b) the mass flow,
(c) the thrust,
(d) the power transferred by the propeller to the flow!

3.8 Two blowers, drawing air from the surroundings, differ in the shape of their inlets.

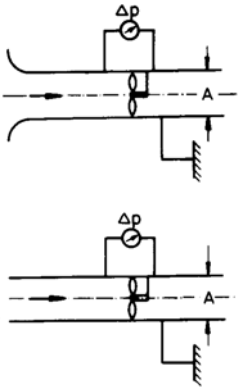


Given: $\rho$, $A$, $\Delta p$
Determine
(a) the discharge volume,
(b) the power of the blowers,
(c) the retaining force!

3.9 A pipe with an inserted nozzle is positioned in a free stream with constant velocity.

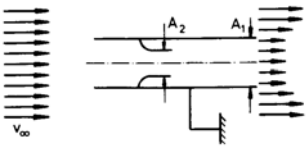


$A_1 = 0.2\,\mathrm{m}^2 \quad A_2 = 0.1\,\mathrm{m}^2 \quad v_\infty = 40\,\dfrac{\mathrm{m}}{\mathrm{s}}$

$\rho = 1.25\,\dfrac{\mathrm{kg}}{\mathrm{m}^3}$

Determine
(a) the velocity in the cross sections $A_1$ and $A_2$,
(b) the retaining force!

3.10 A jet apparatus, which is driven with a blower, sucks the volume rate of flow $\dot{Q}_2$ through a ring-shaped inlet.

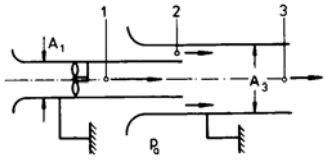


$A_1 = 0.1\,\mathrm{m}^2 \quad A_3 = 0.2\,\mathrm{m}^2$

$p_a = 10^5\,\dfrac{\mathrm{N}}{\mathrm{m}^2}$

$\dot{Q}_2 = 4\,\dfrac{\mathrm{m}^3}{\mathrm{s}} \quad \rho = 1.25\,\dfrac{\mathrm{kg}}{\mathrm{m}^3}$

Determine
(a) the velocity $v_2$ and the pressure $p_{2'}$,
(b) the velocities $v_1$ and $v_{3'}$,
(c) the power of the blower,
(d) the retaining force of the blower casing (traction or compressive force?)!

3.11 Water flows out of a large frictionless supported container through a pipe, with a discontinuous increase of the cross section, into the open air.

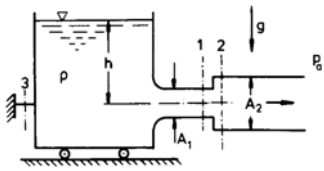


$h = 5\,\mathrm{m} \quad A = 0.1\,\mathrm{m}^2 \quad p_a = 10^5\,\dfrac{\mathrm{N}}{\mathrm{m}^2}$

$\rho = 10^3\,\dfrac{\mathrm{kg}}{\mathrm{m}^3} \quad g = 10\,\dfrac{\mathrm{m}}{\mathrm{s}^2}$

(a) For what cross-sectional area $A_2$ does the volume rate of flow attain its maximum value?
With $A_2$ determined under a) compute
(b) the pressure $p_1$,
(c) the cutting forces $F_{s1}$, $F_{s2}$, $F_{s3}$ (Traction or compressive forces?)!

3.12 A pump is feeding water from a lake into a large pressurized container. The volume rate of flow is measured with a standard nozzle (discharge coefficient $\alpha$).

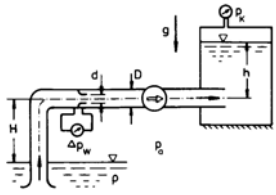


$H = 5\,\mathrm{m} \quad h = 3\,\mathrm{m} \quad d = 0.07\,\mathrm{m}$

$p_K = 2 \cdot 10^5\,\dfrac{\mathrm{N}}{\mathrm{m}^2} \quad \Delta p_w = 3160\,\dfrac{\mathrm{N}}{\mathrm{m}^2}$

$p_a = 10^5\,\dfrac{\mathrm{N}}{\mathrm{m}^2} \quad \rho = 10^3\,\dfrac{\mathrm{kg}}{\mathrm{m}^3} \quad g = 10\,\dfrac{\mathrm{m}}{\mathrm{s}^2}$

$D = 0.1\,\mathrm{m} \quad \alpha = 1.08$

Determine
(a) the velocity in the pipe,
(b) the static pressure upstream and downstream from the pump,
(c) the net performance of the pump!

3.13 Water flows out of a large container through a pipe with a Borda mouthpiece into a lake.

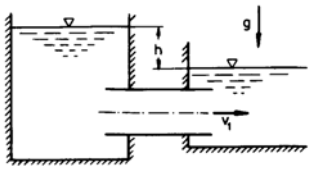


$h = 1\,\mathrm{m} \quad g = 10\,\dfrac{\mathrm{m}}{\mathrm{s}^2}$

Determine
(a) the contraction,
(b) the out-flow velocity $v_1$

3.14 The volume rate of flow of a ventilation blower is measured with an orifice (discharge coefficient $\alpha$, contration coefficient $\Psi$).

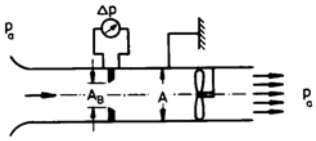


$p_a = 10^5\,\dfrac{\mathrm{N}}{\mathrm{m}^2} \quad \Delta p_w = 300\,\dfrac{\mathrm{N}}{\mathrm{m}^2}$

$\rho = 1.25\,\dfrac{\mathrm{kg}}{\mathrm{m}^3}$

$\alpha = 0.7 \quad \Psi = 0.66 \quad A = 10^{-2}\,\mathrm{m}^2$

$m = \dfrac{A_B}{A} = 0.5$

(a) Sketch the variation of the static and total pressure along the axis of the pipe!
Determine
(b) the volume rate of flow,
(c) the pressure upstream of the blower,
(d) the performance of the blower!

3.15 A hydraulic jump occurs in an open channel.

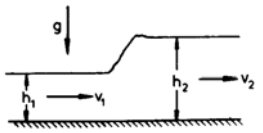


$h_1 = 0.1\,\mathrm{m} \quad h_2 = 0.2\,\mathrm{m} \quad g = 10\,\dfrac{\mathrm{m}}{\mathrm{s}^2}$

Determine
(a) the velocities $v_1$ and $v_2$,
(b) the Froude numbers $Fr_1$ and $Fr_2$,
(c) the energy loss $H_1 - H_2$!

3.16 The volume of water flowing out of a storage pond is controlled with a wicket.

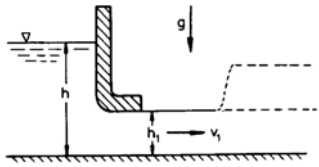


$h = 7.5\,\mathrm{m} \quad g = 10\,\dfrac{\mathrm{m}}{\mathrm{s}^2}$

Determine
(a) the out-flow velocity $v_1$ as a function of the height of level $h_1$ (why is $v_1$ constant in the cross section?),
(b) the height of level, for which the volume rate of flow attains a maximum,
(c) the height of level, for which the hydraulic jump does not occur,
(d) the depth of water and the velocity downstream from the jump for $h_1 = 2.5\,\mathrm{m}$!

3.17 The depth of water $h_1$ of an open channel with constant volume rate of flow is controlled by changing the height $Z_w$ of a weir. For $Z_w = 0$ the depth of water is $h_0$.

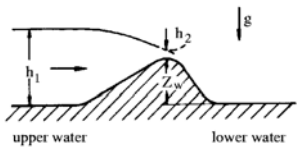

$\dot{Q} = 80\,\frac{\mathrm{m}^3}{\mathrm{s}}$ $B = 20\,\mathrm{m}$ $h_0 = 2\,\mathrm{m}$
$\rho = 3\,\frac{\mathrm{kg}}{\mathrm{m}^3}$

(a) Sketch the variation of the depths of water for $Z_w < Z_{crit.}$ and $Z_w > Z_{crit.}$!
Determine for $Z_w = 1\,m$
(b) the limiting height $Z_{crit.}$ of the dam,
(c) the depths of water $h_1$ and $h_2$,
(d) the difference of the energy heights between upper and lower water,
(e) the force acting on the weir!

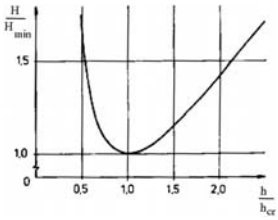


Hint: If a hydraulic jump occurs, it will be at the downstream face of the weir; the depth of the lower water is $h_0$.

3.18 Assume that in a rotating flow pressure and velocity depend only on the radius.

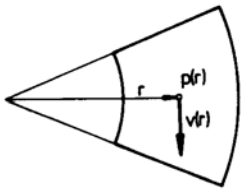


(a) Choose the segment of a circular ring as control surface and, by using the momentum theorem, derive the relation

$$\frac{dp}{dr} = \rho\,\frac{v^2}{r}!$$

(b) For what velocity distribution $v(r)$ does the Bernoulli constant have the same value for all streamlines?

3.19 A lawn sprinkler is fed from a large reservoir. The water jets are inclined to the circumferential direction by the angle $\alpha$. The friction torque of the bearing is $M_r$.

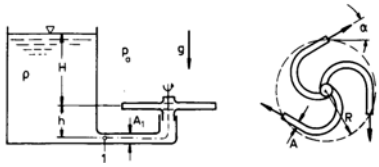


$H = 10\,\mathrm{m}$ $h = 1\,\mathrm{m}$ $R = 0.15\,\mathrm{m}$
$A = 0.5 \cdot 10^4\,\mathrm{m}^2$ $A_1 = 1.5 \cdot 10^4\,\mathrm{m}^2$

$|M_r| = 3.6\,\mathrm{Nm}$ $p_a = 10^5\,\frac{\mathrm{N}}{\mathrm{m}^2}$

$\rho = 10^3\,\frac{\mathrm{kg}}{\mathrm{m}^3}$ $g = 10\,\frac{\mathrm{m}}{\mathrm{s}^2}$ $\alpha = 30°$

Determine
(a) the number of revolutions,
(b) the rate of volume flow,
(c) the pressure $p_1$,
(d) the maximum angular velocity, if the friction torque is assumed to be zero!

### 3.1.4 Laminar Flow of Viscous Fluids

4.1 Determine the following quantities for a fully developed laminar pipe flow of a Newtonian fluid
(a) the velocity distribution

$$\frac{u(r)}{u_{max}} = f(\frac{r}{R}) \quad , \tag{3.1}$$

(b) the ratio

$$\frac{u_m}{u_{max}} \quad , \tag{3.2}$$

(c) the dependence of the pipe friction coefficient on the Reynolds number!

4.2 A Bingham fluid is driven by gravity between two parallel, infinitely wide plates.

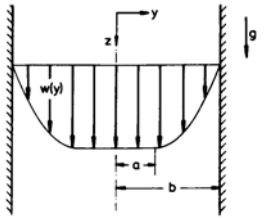

Given: $b$, $\rho$, $\mu$, $\tau_0$, $g$, $\frac{dp}{dz} = 0$

Assume that the flow is fully developed and determine
(a) the distance $a$,
(b) the velocity distribution!

4.3 An oil film of constant thickness and width flows down on an inclined plate.

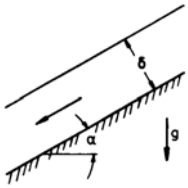


$\delta = 3 \cdot 10^3$ m $\quad B = 1$ m $\quad \alpha = 30°$

$\mu = 30 \cdot 10^{-3} \dfrac{\text{Ns}}{\text{m}^2} \quad \rho = 800 \dfrac{\text{kg}}{\text{m}^3}$

$g = 10 \dfrac{\text{m}}{\text{s}^2}$

Determine the volume rate of flow!

4.4 An oil film is driven by gravity.

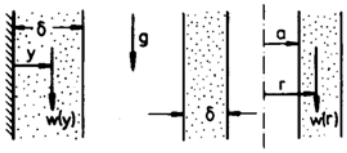


Given: $\delta$, $a$, $\rho$, $\mu$, $g$.

Determine the velocity distribution in the oil film
(a) on a plane vertical wall,
(a) on a wall of a vertically standing circular cylinder!

4.5 A Newtonian fluid flows in the gap between two horizontal plates. The upper plate is moving with the velocity $u_w$, the lower is at rest. The pressure is linearly decreasing in the $x$-direction.

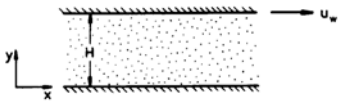


Given: $H$, $u_w$, $\rho$, $\mu$, $\frac{dp}{dx}$

Assume fully developed laminar flow and determine
(a) the velocity distribution,
(b) the ratio of the shear stresses for $y = 0$ and $y = H$,
(c) the volume rate of flow for a width of the plates $B$,
(d) the maximum velocity for $u_w = 0$,
(e) the momentum flux for $u_w = 0$,
(f) the wall-shear stress in dimensionless form for $u_w$
(g) sketch the velocity and shear stress distribution for $u_w > 0$, $u_w = 0$, and $u_w < 0$ !

4.6 A Newtonian fluid flows between two coaxial cylinders.

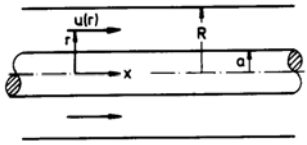


Given: $R$, $a$, $\mu$, $\frac{dp}{dx}$

Assume fully developed laminar flow and determine
(a) the velocity distribution (sketch the result!),
(b) the ratio of the shear stresses for $r = a$ and $r = R$,
(c) the mean velocity!

4.7 A Couette viscosimeter consists out of two concentric cylinders of length $L$. The gap between them is filled with a Newtonian fluid. The outer cylinder rotates with the angular velocity $\omega$, the inner is at rest. At the inner cylinder the torque $M_z$ is measured.

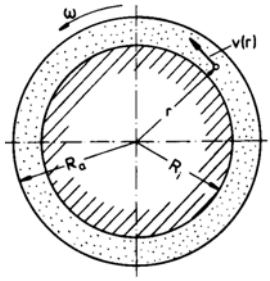

$R_a = 0.11\,\mathrm{m} \quad R_i = 0.1\,\mathrm{m} \quad L = 0.1\,\mathrm{m}$

$\omega = 10\,\dfrac{1}{\mathrm{s}} \quad M_z = 7.246\,10^{-3}\,\mathrm{Nm}$

Determine

(a) the velocity distribution,

(b) the dynamic shear viscosity of the fluid!

Hint: The differential equations for the velocity and shear-stress distributions are:

$$\frac{d}{dr}\left[\frac{1}{r}\frac{d}{dr}\,(rv)\right] = 0 \quad ,$$

$$\tau = -\mu\, r\, \frac{d}{dr}\left(\frac{v}{r}\right)$$

4.8 A gas of thermal conductivity $\lambda$ and specific heats $c_p$ and $c_v$ flows in the gap between two horizontal plates. The upper plate is moving with velocity $u_w$ at temperature $T_w$, the lower is at rest and is thermally isolated.

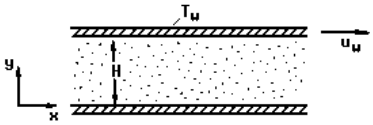


Given: $u_w, \quad H, \quad T_w, \quad \frac{dp}{dx} = 0,$
$\rho, \quad \mu, \quad \lambda, \quad c_p, \quad c_v$

Assume fully developed laminar flow and determine for vanishing convective heat flux and constant material properties

(a) the velocity and temperature distribution,

(b) the heat flux per unit area through the upper plate!

(c) Show that the stagnation enthalpy has the same value everywhere for $Pr = 1$!

(d) Determine the time-dependent temperature variation, if both plates are thermally isolated, and if at the time $t = 0$ the temperature in the flow field is $T_0$!

4.9 A Newtonian fluid with thermal conductivity $\lambda$ flows through a pipe. The wall temperature is kept constant by cooling the wall.

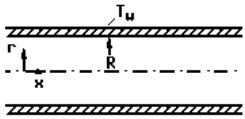


Given: $R, \quad T_w, \quad \lambda, \quad \mu, \quad \frac{dp}{dx}$

(a) Assume fully developed laminar flow and derive the differential equations for the velocity and temperature distribution for a ring-shaped volume element for vanishing convective heat flux and constant material properties! State the boundary conditions!

(b) Determine the temperature distribution

$$\frac{T - T_w}{T_{max} - T_w}$$

4.10 Under a gun slide a plane wall is moving with the velocity $u_\infty$.

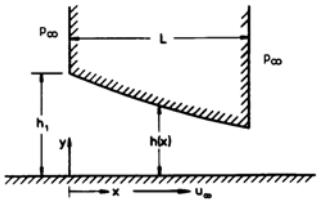


$h(x) = h_1\, e^{-\frac{x}{5\,L}} \quad L = 5 \cdot 10^{-2}\,\mathrm{m}$

$h_1 = 10^{-4}\,\mathrm{m} \quad u_\infty = 1\,\dfrac{\mathrm{m}}{\mathrm{s}} \quad \mu = 10^{-1}\,\dfrac{\mathrm{Ns}}{\mathrm{m}^2}$

$\rho = 800\,\dfrac{\mathrm{kg}}{\mathrm{m}^3}$

Determine

(a) the similarity parameter of the problem,

(b) the volume rate of flow per unit width,

(c) the pressure distribution in the gap,

(d) the pressure force per unit width bearing the gun slide,

(e) the performance loss per unit width $t$ due to bearing friction!

4.11 From the momentum equation in integral form

$$\begin{aligned}\frac{d\boldsymbol{I}}{dt} &= \int_\tau \frac{\partial}{\partial t}\,(\rho\,\boldsymbol{v})\,d\tau + \int_A \rho\,\boldsymbol{v}\,(\boldsymbol{v}\,\boldsymbol{n})dA \\ &= \sum \boldsymbol{F}\end{aligned}$$

derive the differential form of the momentum equation in the $x$-direction for an infinitesimally small volume element

$$\rho\left(\frac{\partial u}{\partial t}+u\frac{\partial u}{\partial x}+v\frac{\partial u}{\partial y}\right)=-\left(\frac{\partial \sigma_{xx}}{\partial x}+\frac{\partial \tau_{xy}}{\partial y}\right)$$

4.12 The $x$-component of the friction force acting on a volume element is given by

$$\begin{aligned} F_{fx} &= \frac{\partial}{\partial x}\left[\mu\left(2\frac{\partial u}{\partial x}-\frac{2}{3}\nabla\cdot\boldsymbol{v}\right)\right]+ \\ &+ \frac{\partial}{\partial y}\left[\mu\left(\frac{\partial u}{\partial y}+\frac{\partial v}{\partial x}\right)\right]+ \\ &+ \frac{\partial}{\partial z}\left[\mu\left(\frac{\partial w}{\partial x}+\frac{\partial u}{\partial x}\right)\quad\right]. \end{aligned}$$

Reduce this equation for an incompressible fluid with constant viscosity!

### 3.1.5 Pipe Flows

5.1 The viscosity of an oil is to be measured with a capillary viscosimeter.
This is done by measuring the time $T$, in which a small part of the oil (volume $\tau$) flows through the capillary. Assume that the flow is loss-free upstream of the position 1!

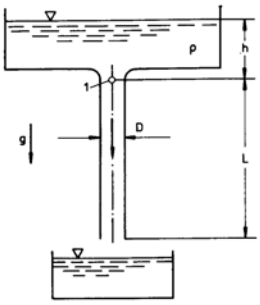


$\tau = 10\,\mathrm{cm}^3 \quad \rho = 900\,\dfrac{\mathrm{kg}}{\mathrm{m}^3} \quad L = 0.1\,\mathrm{m}$
$h = 0.05\,\mathrm{m} \quad D = 1\,\mathrm{mm} \quad T = 254\,\mathrm{s}$
$g = 10\,\dfrac{\mathrm{m}}{\mathrm{s}^2}$

5.2 Water flows out of a large container through a hydraulically smooth pipe, with a nozzle fixed to its end. The pressure upstream of the nozzle is $p_1$. The friction losses in the intake of the pipe and in the nozzle can be neglected. Assume that the flow in the pipe is fully developed!

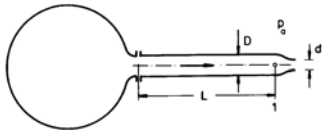


$L = 100\,\mathrm{m} \quad D = 10^{-2}\,\mathrm{m}$
$d = 0.5 \cdot 10^{-2}\,\mathrm{m} \quad p_a = 10^5\,\dfrac{\mathrm{N}}{\mathrm{m}^2}$
$p_1 = 1.075 \cdot 10^5\,\dfrac{\mathrm{N}}{\mathrm{m}^2} \quad \rho = 10^3\,\dfrac{\mathrm{kg}}{\mathrm{m}^3}$
$\mu_1 = 10^{-3}\,\dfrac{\mathrm{Ns}}{\mathrm{m}^2}$

Determine
(a) the velocity in the pipe and at the exit of the nozzle,
(b) the pressure in the container,
(c) the velocity at the exit of the nozzle for $L = 0$ and the same pressure in the container!

5.3 Two containers are connected with each other by 25 pipes with diameter $D_1$ and 25 pipes with diameter $D_2$. A pressure difference of $\Delta p$ is measured between the containers. The pressure-loss coefficient of the intake is $\zeta$.

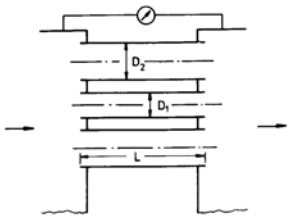


$D_1 = 0.025\,\mathrm{m} \quad D_2 = 0.064\,\mathrm{m}$
$L = 10\,\mathrm{m} \quad \rho = 10^3\,\dfrac{\mathrm{kg}}{\mathrm{m}^3} \quad \lambda = 0.025$
$\Delta p = 10^5\,\dfrac{\mathrm{N}}{\mathrm{m}^2} \quad \zeta = 1$

Determine the volume rate of flow!

5.4 A fluid flows through a hydraulically smooth pipe. The pressure drops by the amount $\Delta p$ over the length $L$.

$L = 100\mathrm{m} \quad D = 0.1\mathrm{m} \quad \Delta p = 5{\cdot}10^4\,\dfrac{\mathrm{N}}{\mathrm{m}^2}$

$$\text{Oil}: \quad \mu = 10^{-1}\,\frac{\text{Ns}}{\text{m}^2} \quad \rho = 800\,\frac{\text{kg}}{\text{m}^3}$$
$$\text{Water}: \quad \mu = 10^{-3}\,\frac{\text{Ns}}{\text{m}^2} \quad \rho = 10^{3}\,\frac{\text{kg}}{\text{m}^3}$$

Determine the velocities of the flow!
Hint: Use the Prandtl resistance law for super-critical Reynolds numbers!

5.5 Compressed air is pumped through a hydraulically smooth pipe. The pressure $p_1$, the density $\rho_1$ and the velocity $\bar{u}_{m1}$ are assumed to be known in the intake cross section.

$D = 10^{-2}\,\text{m} \quad p_1 = 8 \cdot 10^5\,\frac{\text{N}}{\text{m}^2}$

$\bar{u}_{m1} = 10\,\frac{\text{m}}{\text{s}}$

$\rho_1 = 10\,\frac{\text{kg}}{\text{m}^3} \quad \mu = 1.875 \cdot 10^{-5}\,\frac{\text{Ns}}{\text{m}^2}$

(a) Derive the following relation with the aid of the momentum theorem:

$$\frac{dp}{dx} + \rho_1\,\bar{u}_{m1}\,\frac{d\bar{u}_m}{dx} + \frac{\lambda}{D}\,\frac{\rho}{2}\,\bar{u}_m^2 = 0$$

(b) Determine the length, over which the pressure drops by one half of its initial value for compressible flow with constant temperature and for incompressible flow!

5.6 The velocity distribution in the intake region of a laminar pipe flow is described by the following approximation:

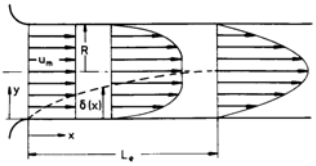


$$\frac{u}{u_m} = \frac{f\left(\frac{y}{\delta}\right)}{1 - \frac{2}{3}\,\frac{\delta}{R} + \frac{1}{6}\,\left(\frac{\delta}{R}\right)^2}$$

$$f\left(\frac{y}{\delta}\right) = \begin{cases} 2\frac{y}{\delta} - \left(\frac{y}{\delta}\right)^2 & 0 \le y \le \delta(x) \\ 1 & \delta(x) \le y \le R \end{cases}$$

Given: $u_m$, $R$, $\rho$, $\mu$

Determine the following quantities for the intake cross section, the end of the intake region, and for $\frac{\delta}{R} = 0.5$

(a) the momentum flux,
(b) the wall shear stress!

5.7 Water flows through a hydraulically smooth pipe with an discontinuous widening of the cross section into the open air.

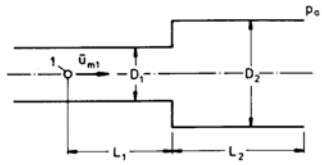


$D = 0.02\,\text{m} \quad D_2 = 0.04\,\text{m} \quad L = 0.2\,\text{m}$

$\bar{u}_{m1} = 0.5\,\frac{\text{m}}{\text{s}} \quad \rho = 10^3\,\frac{\text{kg}}{\text{m}^3}$

$\mu = 10^{-3}\,\frac{\text{Ns}}{\text{m}^2}$

(a) At what length $L_2$ does the pressure difference $p_1 - p_a$ vanish?
(b) How large is the corresponding pressure loss?

Hint: Assume, that the wall shear stress in the widened part of the pipe can be determined with the equations for fully developed pipe flow!

5.8 The feed pipes of a fountain consist out of four straight pipes of total length $L$, two bends (loss coeficient $\zeta_K$) and a valve ($\zeta_V$).

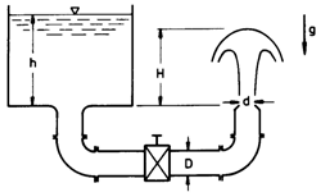


$h = 10\,\text{m} \quad D = 0.05\,\text{m} \quad L = 4\,\text{m}$
$\zeta_K = 0.25 \quad \zeta_V = 4.5 \quad \lambda = 0.025$

Determine the volume rate of flow and the height $H$ for dissipative and nondissipative flow with
(a) $d = \frac{D}{2}$,
(b) $d = D$!

Hint: Assume that the flow in the intake and in the nozzle is loss-free and fully developed in the straight pipes!

5.9 Water flows through a hydraulically smooth pipe.

$D = 0.1\,\mathrm{m} \quad Re = 10^5 \quad \rho = 10^3\,\frac{\mathrm{kg}}{\mathrm{m}^3}$

$\mu = 10^{-3}\,\frac{\mathrm{Ns}}{\mathrm{m}^2}$

Determine

(a) the wall shear stress,

(b) the ratio of the velocities $\frac{\bar{u}_m}{\bar{u}_{max}}$,

(c) the velocity for $\frac{y\,u_*}{\nu} = 5$ and for $\frac{y\,u_*}{\nu} = 50$,

(d) the mixing length for $\frac{y\,u_*}{\nu} = 100$!

5.10 The velocity distribution of a turbulent pipe flow is approximately described by the ansatz

$$\frac{\bar{u}_m}{\bar{u}_{max}} = \left(\frac{y}{R}\right)^{\frac{1}{7}} \quad .$$

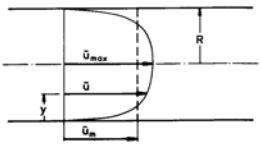


Determine

(a) the ratio of the velocities $\frac{\bar{u}_m}{\bar{u}_{max}}$,

(b) the ratio of the momentum fluxes $\frac{\dot{I}}{\rho\,\bar{u}_m^2\,\pi R^2}$ !

5.11 A pump is feeding water through a rough pipe (equivalent sand roughness $k_s$) from the level $h_1$ to the level $h_2$.

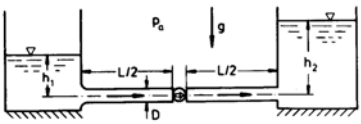


$\dot{Q} = 0.63\,\frac{\mathrm{m}^3}{\mathrm{s}} \quad h_1 = 10\,\mathrm{m} \quad h_2 = 20\,\mathrm{m}$

$L = 20\,\mathrm{km} \quad D = 1\,\mathrm{m} \quad k_s = 2\,\mathrm{mm}$

$\rho = 10^3\,\frac{\mathrm{kg}}{\mathrm{m}^3} \quad \nu = 10^{-6}\,\frac{\mathrm{m}^2}{\mathrm{s}}$

$p_a = 10^5\,\frac{\mathrm{N}}{\mathrm{m}^2} \quad g = 10\,\frac{\mathrm{m}}{\mathrm{s}^2}$

(a) Sketch the variation of the static pressure along the axis of the pipe! Determine

(b) the pressure at the intake of the pump,

(c) the pressure at the exit of the pump,

(d) the net performance of the pump!

5.12 In a fully developed pipe flow with volume rate of flow $\dot{Q}$ a pressure drop $\Delta p$ is measured over the distance $L$.

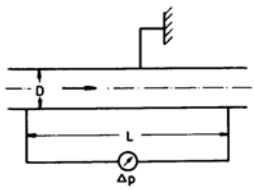


$\dot{Q} = 0.393\,\frac{\mathrm{m}^3}{\mathrm{s}} \quad L = 100\,\mathrm{m} \quad D = 0.5\,\mathrm{m}$

$\Delta p = 12820\,\frac{\mathrm{N}}{\mathrm{m}^2} \quad \rho = 900\,\frac{\mathrm{kg}}{\mathrm{m}^3}$

$\mu = 5 \cdot 10^{-3}\,\frac{\mathrm{Ns}}{\mathrm{m}^2}$

Determine

(a) the pipe friction coefficient,

(b) the equivalent sand roughness of the pipe,

(c) the wall shear stress and the retaining force!

(d) How large would the pressure drop be in a hydraulically smooth pipe?

5.13 Air is to be conveyed through a rough pipe with a well rounded intake with the aid of a blower.

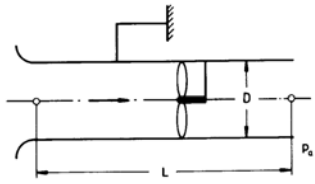


$L = 200\,\mathrm{m} \quad k_s = 1\,\mathrm{mm}$

Determine the ratio of the blower performance for the diameters $D = 0.1\,\mathrm{m}$ and $D = 0.2\,\mathrm{m}$ for the same volume rate of flow and very large Reynolds numbers!

5.14 Water is fed through a system of 100 pipes into a channel with quadratic cross section.

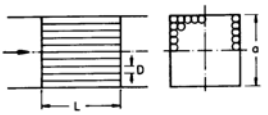


$\dot{Q} = 0.01\,\dfrac{\mathrm{m}^3}{\mathrm{s}}$ $\quad L = 0.5\,\mathrm{m}$ $\quad a = 0.1\,\mathrm{m}$

$D = 0.01\,\mathrm{m}$ $\quad \rho = 10^3\,\dfrac{\mathrm{kg}}{\mathrm{m}^3}$ $\quad \mu = 10^{-3}\,\dfrac{\mathrm{Ns}}{\mathrm{m}^2}$

For what length does the pressure loss of the channel become equal to that of the pipe system?

5.15 An open channel with quadratic cross section is inclined by the angle $\alpha$.


$\dot{Q} = 3 \cdot 10^{-4}\,\dfrac{\mathrm{m}^3}{\mathrm{s}}$ $\quad a = 0.05\,\mathrm{m}$

$\rho = 10\,\dfrac{\mathrm{kg}}{\mathrm{m}^3}$

$\mu = 10^{-3}\,\dfrac{\mathrm{Ns}}{\mathrm{m}^2}$ $\quad g = 10\,\dfrac{\mathrm{m}}{\mathrm{s}^2}$

Determine the angle of inclination and the pressure loss per unit length!

### 3.1.6 Similar Flows

6.1 Derive the dimensionless similarity parameters with the momentum equation for the $x$-direction

$$\rho\left(\frac{\partial u}{\partial t} + u\,\frac{\partial u}{\partial x} + v\,\frac{\partial u}{\partial y}\right) = -\frac{\partial p}{\partial x} + \mu\left(\frac{\partial^2 u}{\partial x^2} + \frac{\partial^2 u}{\partial y^2}\right) \quad !$$

6.2 In hydraulically smooth pipes of different lengths and diameters the pressure loss is measured for different velocities, densities, and viscosities. The flow is fully developed, incompressible, and steady.
How can the results of the measurements be presented in a single curve?

6.3 A fluid flows slowly and steadily through a hydraulically smooth pipe. The flow is laminar and fully developed.
(a) Derive the Hagen-Poisseuille law with the aid of the dimensional analysis from the ansatz

$$\dot{Q} = \left(\frac{\Delta p}{L}\right)^{\alpha} \mu^{\beta}\, D^{\gamma} \quad !$$

(b) Show that the pipe friction coefficient is inversely proportional to the Reynolds number!

6.4 What is the drag of two spheres of different diameter but the same Reynolds number, if one moves in air and the other in water, and if the drag coefficient depends on the Reynolds number only?

$$\frac{\rho_a}{\rho_w} = 0.125 \cdot 10^{-2} \quad \frac{\mu_a}{\mu_w} = 1.875 \cdot 10^{-2}$$

6.5 In an incompressible flow about a circular cylinder the frequency, with which vortices are shed, depends on the free-stream velocity, density, and viscosity. Determine the similarity parameters with the aid of the dimensional analysis!

6.6 The pipes in heat exchangers can oscillate due to excitation by the cross-flow they are exposed to. It is known, that in a flow about a circular cylinder, with its axis normal to the direction of the flow, the Strouhal number is constant for $200 \le Re \le 10^5$.

$D = 0.1\,\mathrm{m}$ $\quad v = 1\,\dfrac{\mathrm{m}}{\mathrm{s}}$ $\quad v' = 3\,\dfrac{\mathrm{m}}{\mathrm{s}}$

$\nu = 10^{-6}\,\dfrac{\mathrm{m}^2}{\mathrm{s}}$ $\quad \nu' = 1.5 \cdot 10^{-5}\,\dfrac{\mathrm{m}^2}{\mathrm{s}}$

Determine
(a) the minimum diameter of the model cylinder,
(b) the excitation frequency $f$, if for the smallest model $f' = 600\,\dfrac{1}{\mathrm{s}}$!

6.7 The power needed to overcome the aerodynamic drag of an automobile with quadratic cross-sectional area $A$ is to be determined in a wind-tunnel

experiment. The cross-sectional area of the model cannot exceed $A_m$ in order to avoid blockage effects in the wind-tunnel.

$A = 4\,\mathrm{m}^2 \quad A_m = 0.6\,\mathrm{m}^2 \quad v = 30\,\dfrac{\mathrm{m}}{\mathrm{s}}$

(a) What speed has to be chosen for the measurement in the wind tunnel?
(b) Determine the power needed, if with a larger model the drag $F' = 810\,\mathrm{N}$ is measured!

6.8 Water flows through a model of a valve (volume rate of flow $\dot{Q}'$). Between intake and exit the pressure difference $\Delta p'$ is measured. The valve is supposed to be used in an air pipe.

$A = 0.18\,\mathrm{m}^2 \quad A' = 0.02\,\mathrm{m}^2$
$\rho = 1.25\,\dfrac{\mathrm{kg}}{\mathrm{m}^3} \quad \rho' = 10^3\,\dfrac{\mathrm{kg}}{\mathrm{m}^3}$
$\mu = 1.875 \cdot 10^{-5}\,\dfrac{\mathrm{Ns}}{\mathrm{m}^2} \quad \mu' = 10^3\,\dfrac{\mathrm{Ns}}{\mathrm{m}^2}$
$\dot{Q}' = 0.2\,\dfrac{\mathrm{m}^3}{\mathrm{s}} \quad \Delta p' = 1.58 \cdot 10^5\,\dfrac{\mathrm{N}}{\mathrm{m}^2}$

(a) For what volume rate of flow are the flows through the model and the full-scale configuration similar?
(b) What is the pressure difference between intake and exit?

6.9 An axial blower (diameter $D$, number of revolutions $n$) is to be designed for air. In a model experiment with water (reduction scale 1:4) the increase of the total pressure $\Delta p'_0$ is measured.

$\dot{Q} = 30\,\dfrac{\mathrm{m}^3}{\mathrm{s}} \quad D = 1\,m \quad n = 12.5\,\dfrac{1}{\mathrm{s}}$
$\rho = 1.25\,\dfrac{\mathrm{kg}}{\mathrm{m}^3} \quad \mu = 1.875 \cdot 10^{-5}\,\dfrac{\mathrm{Ns}}{\mathrm{m}^2}$
$\rho' = 10^3\,\dfrac{\mathrm{kg}}{\mathrm{m}^3} \quad \mu' = 10^{-3}\,\dfrac{\mathrm{Ns}}{\mathrm{m}^2}$
$\Delta p'_0 = 0.3 \cdot 10^5\,\dfrac{\mathrm{N}}{\mathrm{m}^2}$

Determine
(a) the volume rate of flow and the number of revolutions during the experiment,
(b) the change of the total pressure of the blower,
(c) the power and the torque needed for driving the model and the main configuration!

6.10 The power of a propeller of an airplane is to be determined in a wind-tunnel experiment (Model scale 1:4) for the flight velocity $v$. In the test section of the wind tunnel the velocity can be varied between 0 and $300\,\dfrac{\mathrm{m}}{\mathrm{s}}$, the pressure between $0.5 \cdot 10^5\,\dfrac{\mathrm{N}}{\mathrm{m}^2}$ and $5 \cdot 10^5\,\dfrac{\mathrm{N}}{\mathrm{m}^2}$, and the temperature between 250 K and 300 K. The viscosity of air is described by the relation

$$\frac{\mu}{\mu_{300K}} = \left(\frac{T}{300K}\right)^{0.75} \quad .$$

$D = 1\,\mathrm{m} \quad n = 100\,\dfrac{1}{\mathrm{s}} \quad v = 200\,\dfrac{\mathrm{m}}{\mathrm{s}}$
$T = 300\,\mathrm{K} \quad R = 287\,\dfrac{\mathrm{Nm}}{\mathrm{kg\,K}} \quad \gamma = 1.4$
$p = 10^5\,\dfrac{\mathrm{N}}{\mathrm{m}^2}$

(a) Determine an operating point ($v'$, $p'$, $T'$) such that the results of the measurements can be applied to the full-scale configuration!
(b) What number of revolutions must be used in the experiment?
(c) Determine the power, if in the experiment the power $P'$ was measured!

6.11 A model experiment is to be carried out prior to the construction of a tanker (Model scale 1 : 100) in a towing basin.
(a) How large would the ratio of the kinematic viscosities $\frac{\nu'}{\nu}$ have to be?
(b) How large must the towing velocity in water be, if the aerodynamic drag can be neglected and if only the wave drag or only the frictional drag is taken into account?

6.12 A docking pontoon is fastened at the bank of a river. An experiment is to be carried out with a model scaled down to 1 : 16.

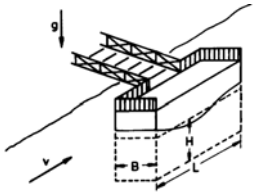

$L = 3.6\,\mathrm{m} \quad B = 1.2\,\mathrm{m} \quad H = 2.7\,\mathrm{m}$
$v = 3\,\dfrac{\mathrm{m}}{\mathrm{s}} \quad F'_D = 4\,\mathrm{N} \quad h' = 2.5\,\mathrm{cm}$
$\rho = 10^3\,\dfrac{\mathrm{kg}}{\mathrm{m}^3}$

Determine
(a) the flow velocity in the model experiment,
(b) the force acting on the pontoon, if the force $F'$ is measured in the experiment,
(c) the drag coefficient of the pontoon,
(d) the height of a wave $h$ to be expected at the side of the pontoon, facing the oncoming flow, if the height $h'$ was measured in the experiment!

6.13 In a refinery oil flows through a horizontal pipe line into a reservoir with pressure $p_R$, with the pressure at the intake being $p_0$. A safety valve is attached to the end of the pipe line, which in the case of emergency can close the pipe line within the time $T$. In a model experiment with water (diminution scale 1 : 10) the maximum pressure in front of the safety valve, measured during the shut-down procedure, is $p'_{max}$.

$p = 1.5 \cdot 10^5\,\dfrac{\mathrm{N}}{\mathrm{m}^2} \quad p_R = p'_R = 10^5\,\dfrac{\mathrm{N}}{\mathrm{m}^2}$
$\rho = 880\,\dfrac{\mathrm{kg}}{\mathrm{m}^3} \quad \rho' = 10^3\,\dfrac{\mathrm{kg}}{\mathrm{m}^3}$
$\mu = 10^{-1}\,\dfrac{\mathrm{Ns}}{\mathrm{m}^2} \quad \mu' = 10^{-3}\,\dfrac{\mathrm{Ns}}{\mathrm{m}^2}$
$T = 0.5\,\mathrm{s} \quad p'_{max} = 1.05 \cdot 10^5\,\dfrac{\mathrm{N}}{\mathrm{m}^2}$

Determine
(a) the pressure $p'_0$ and the shut-down time in the model experiment,
(b) the maximum pressure in the full-scale configuration!

6.14 In a petroleum pipe line (diameter $D$) the volume rate of flow is to be determined with a measuring throttle (diameter $d$). In a model experiment with water (diminution scale 1 : 10) a differential pressure $\Delta p'_D$ and a pressure loss $\Delta p'_l$ is measured at the measuring throttle.

$\dot{Q} = 1\,\dfrac{\mathrm{m}^3}{\mathrm{s}} \quad D = 1\,\mathrm{m} \quad d = 0.4\,\mathrm{m}$
$\rho = 800\,\dfrac{\mathrm{kg}}{\mathrm{m}^3} \quad \mu = 10^{-1}\,\dfrac{\mathrm{Ns}}{\mathrm{m}^2}$
$\rho' = 10^3\,\dfrac{\mathrm{kg}}{\mathrm{m}^3} \quad \mu' = 10^{-3}\,\dfrac{\mathrm{Ns}}{\mathrm{m}^2}$
$\Delta p'_D = 500\,\dfrac{\mathrm{N}}{\mathrm{m}^2} \quad \Delta p'_l = 400\,\dfrac{\mathrm{N}}{\mathrm{m}^2}$

Determine
(a) the flow velocity and the volume rate of flow in the model experiment,
(b) the discharge coefficient and the loss coefficient of the measuring throttle,
(c) the differential pressure and the pressure loss for the full-scale configuration!

### 3.1.7 Potential Flows of Incompressible Fluids

7.1 A cyclone is assumed to have the following velocity distribution:

$$v_\theta(r) = \begin{cases} \omega\, r & r \le r_0 \\ \dfrac{\omega\, r_0^2}{r} & r > r_0 \end{cases} \qquad v_r = 0$$

$r_0 = 10\,\mathrm{m} \quad \omega = 10\,\dfrac{1}{\mathrm{s}}$
$H = 100\,\mathrm{m} \quad \rho = 1.25\,\dfrac{\mathrm{kg}}{\mathrm{m}^3}$

(a) Sketch $v_\theta(r)$!
(b) Determine the circulation for a circle around the axis of the cyclone for $r < r_0$, $r = r_0$ and $r > r_0$!
(c) Show that for $r > r_0$ the flow is irrotational!
(d) How large is the kinetic energy in a cylinder with radius $R = 2\,r_0$ and height $H$?

7.2 (a) State the definitions of potential and stream function for two-dimensional flow! What conditions have to be satisfied so that they can exist?
(b) How are $\nabla \cdot \boldsymbol{v}$ and $\nabla^2 \Phi$ and $\nabla \times \boldsymbol{v}$ and $\nabla^2 \Psi$ related to each other?

7.3 Examine, whether potential and stream function exist for the following velocity fields!
(a) $u = x^2\, y \quad v = y^2\, x$
(b) $u = x \quad v = y$

(c) $u = y \quad v = -x$
(d) $u = y \quad v = x$
Determine potential and stream-function!

7.4 A two-dimensional flow is described by the stream function $\Psi = \left(\frac{U}{L}\right) xy$. In the point $x_{ref} = 0$, $y_{ref} = 1\,\mathrm{m}$ the pressure is $p_{ref} = 10^5\ \dfrac{\mathrm{N}}{\mathrm{m}^2}$.

$U = 2\,\dfrac{\mathrm{m}}{\mathrm{s}} \quad L = 1\,\mathrm{m} \quad \rho = 10^3\,\dfrac{\mathrm{kg}}{\mathrm{m}^3}$

(a) Examine, whether the flow possesses a potential
Determine
(b) the stagnation points, the pressure coefficient, and the isotachs,
(c) velocity and pressure for $x_1 = 2\,m, \quad y_1 = 2\,m$,
(c) the coordinates of a particle, which at time $t = 0$ passes through the point $x_1, y_1$, for the time $t = 0.5\,s$,
(e) the pressure difference between these two points!
(f) Sketch the streamlines!

7.5 Given the potential

$$\Phi = yx^2 - \frac{y^3}{3} \quad .$$

(a) Determine the velocity components and examine, whether the stream function exists!
(b) Sketch the streamlines!

7.6 Determine the velocity fields
$v_r = \frac{c}{r} \quad v_\theta = 0$ and $v_r = 0 \quad v_\theta = \frac{c}{r}$
(a) $\nabla \times \boldsymbol{v}$ and $\nabla \cdot \boldsymbol{v}$,
(b) potential and stream funktion,
(c) the circulation along a curve around the origin!

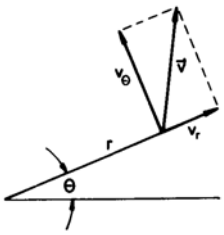


Hint: The following relations are valid for polar coordinates:

$$v_r = \frac{\partial \Phi}{\partial r} = \frac{1}{r}\frac{\partial \Psi}{\partial \theta} \quad v_\theta = \frac{1}{r}\frac{\partial \Phi}{\partial \theta} = -\frac{\partial \Psi}{\partial r}$$

$$\nabla \cdot \boldsymbol{v} = \frac{1}{r}\frac{\partial (r\, v_r)}{\partial r} + \frac{1}{r}\frac{\partial v_\theta}{\partial \theta}$$

$$\nabla \times \boldsymbol{v} = \left(\frac{1}{r}\frac{\partial (r\, v_\theta)}{\partial\, r} - \frac{1}{r}\frac{\partial v_r}{\partial \theta}\right) \boldsymbol{k}$$

7.7 Given the stream function
$\Psi(r,0) = \frac{1}{n}\, r^n \sin(n\,\theta)$.
(a) Sketch the streamlines for $n = 0.5$; $n = 1$ und $n = 2$ !
(b) Determine the pressure coefficient for the point $x = 0$, $y = 0$, if pressure and velocity are known for the point $x_{ref} = 1$, $y_{ref} = 1$!

7.8 Consider a large basin with an outlet. The flow outside of the outlet ($r > R_0$) can be described by superposition of a plane sink and a potential vortex. For $r = R_0$ the in-flow angle is $\alpha$ and the depth of water is $h_0$. The volume rate of flow of the discharging water is $\dot{Q}$.

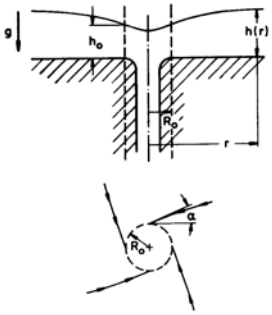


$R_0 = 0.03\,\mathrm{m} \quad h_0 = 0.02\,\mathrm{m} \quad g = 10\,\dfrac{\mathrm{m}}{\mathrm{s}^2}$

$\dot{Q} = 0.5 \cdot 10^{-3}\,\dfrac{\mathrm{m}^3}{\mathrm{s}} \quad \alpha = 30°$

Determine
(a) the circulation $\Gamma$
(b) the shape of the water surface $h(r)$ for $r \geq R_0$,
(c) the depth of water at large distances from the outlet!

Hint: The discharge volume of the sink is to be determined for the radius $r = R_0$!

7.9 The free-stream velocity of a two-dimensional half-body with width $2h$ is $u_\infty$.

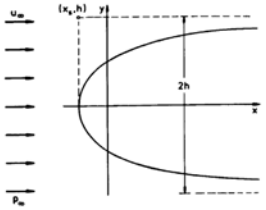


Determine

(a) the stagnation point and the velocity in the point $x = x_s$, $y = h$,
(b) the contour of the half-body,
(c) the pressure distribution on the contour,
(d) the isobars,
(e) the curve along which the pressure is larger by the amount $\frac{\rho}{4}\, u_\infty^2$ than the pressure $p_\infty$ of the free-stream,
(f) the isotachs,
(g) the part of the flow field, in which the velocity component $v$ is larger than $\frac{u_\infty}{2}$,
(h) the curve, which is inclined to the streamlines by 45°,
(i) the maximum deceleration a particle moving along the line of symmetry is experiencing between $x = -\infty$ and the stagnation point!

7.10 Given the stream function

$$\Psi = u_\infty\, y \left(1 - \frac{R^2}{x^2 + y^2}\right) \quad .$$

(a) Sketch the streamlines for $x^2 + y^2 \geq R^2$!
Determine
(b) the pressure distribution on the contour $\Psi = 0$,
(c) the time it takes for a particle to move from the point $x = -3\,R$, $y = 0$ to the point $x = 2\,R$, $y = 0$!

7.11 Consider a parallel free-stream with velocity $u_\infty$ flowing around a circular cylinder with radius $R$, with its axis normal to the direction of the oncoming flow being in the origin of coordinates.
Determine

(a) the curve along which the pressure equals the free-stream pressure $p_\infty$,
(b) the pressure on a circle around the origin of coordinates with radius $2R$!

7.12 The pressure difference $\Delta p$ between two boreholes in a circular cylinder, with its axis normal to the direction of the oncoming flow, is a measure for the angle $\epsilon$ between the free-stream direction and the axis of symmetry.

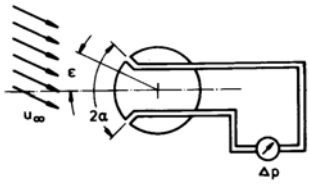


(a) What is the relation between the pressure difference and the angle of attack?
(b) At what angle $\alpha$ does $\Delta p$ attain its maximum value for every $\epsilon$?

7.13 Consider a flow around a bridge pile with circular with cross section. The free-stream velocity is $u_\infty$. The depth of water far upstream is $h_\infty$.

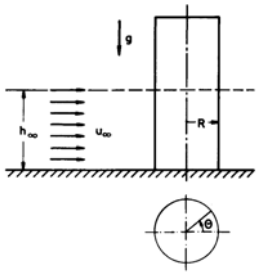


$u_\infty = 1\,\dfrac{\mathrm{m}}{\mathrm{s}} \quad h_\infty = 6\,\mathrm{m} \quad R = 2\,\mathrm{m}$

$\rho = 10^3\,\dfrac{\mathrm{kg}}{\mathrm{m}^3} \quad g = 10\,\dfrac{\mathrm{m}}{\mathrm{s}^2}$

Determine

(a) the height of the water surface at the wall of the pile as function of $\theta$,
(b) the height of the water surface at the stagnation points,
(c) the lowest depth of water, measured from the ground!

Hint: Assume two-dimensional flow!

7.14 The roof (weight $G$) of a hangar of length $L$ and semi-circular cross section rests on the walls of the hangar, without being fixed. The hangar is completely closed except for a small opening on the leeward side.

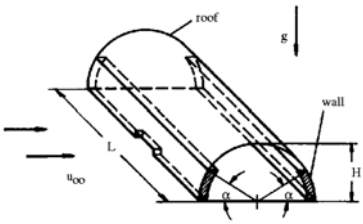


$L = 100\,\text{m} \quad H = 10\,\text{m} \quad G = 10^7\,\text{N}$
$\alpha = 45° \quad u_\infty = 50\,\frac{\text{m}}{\text{s}} \quad \rho = 1.25\,\frac{\text{kg}}{\text{m}^3}$

Investigate, whether the roof has to be anchored to the walls!
Hint: Assume two-dimensional flow!

7.15 Consider a flow around a rotating circular cylinder of length $L$ with its axis normal to the direction of the free-stream with velocity $u_\infty$. The circumferential velocity of the flow on the surface of the cylinder caused by the rotation is $v_t$.

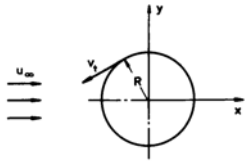


(a) Determine the circulation!
(b) Discuss the flow field for $v_t = u_\infty$!
(c) Determine the force acting on the cylinder!

### 3.1.8 Boundary Layers

8.1 Show that the drag coefficient of the flat plate at zero incidence is proportional to $\frac{1}{\sqrt{Re_L}}$ for a laminar boundary layer!

8.2 The surface of a flat plate is parallel to the direction of a free stream of air.
$u_\infty = 45\,\frac{\text{m}}{\text{s}} \quad \nu = 1.5 \cdot 10^{-5}\,\frac{\text{m}^2}{\text{s}}$
Determine
(a) the transition point for $Re_{crit.} = 5 \cdot 10^5$,
(b) the velocity at the point $x = 0.1\,\text{m}, \quad y = 2 \cdot 10^{-4}\,\text{m}$ with the aid of the Blasius solution! At what coordinate $y$ does the velocity for $x = 0.15\,\text{m}$ attain the same value?
Sketch
(c) the variation of the boundary-layer thickness $\delta(x)$ and a velocity profile for $x < x_{crit.}$ and $x > x_{crit.}$,
(d) the wall-shear stress as a function of $x$ for

$$\frac{dp}{dx} < 0 \quad , \frac{dp}{dx} = 0 \text{ and } \frac{dp}{dx} > 0 \quad !$$

8.3 The surface of a flat plate is parallel to the dircetion of a free stream of water. Formulate the momentum thickness in terms of an integral over the wall-shear stress for a laminar boundary layer

$$-\int_0^x \frac{\tau(x; y=0)}{\rho\, u_\infty^2}\, dx' \text{ dar!}$$

8.4 Air moves past a flat plate (length $L$, width $B$), with its surface parallel to the direction of the free stream.
$u_\infty = 10\,\frac{\text{m}}{\text{s}} \quad L = 0.5\,\text{m} \quad B = 1\,\text{m}$
$\rho = 1.25\,\frac{\text{kg}}{\text{m}^3} \quad \nu = 1.5 \cdot 10^{-5}\,\frac{\text{m}^2}{\text{s}}$
(a) Sketch the velocity profiles $u(y)$ for several values of $x$!
(b) State the boundary conditions for the boundary-layer equations!
(c) Sketch the distribution of the shear stress $\tau(y)$ for the position $x$!
(d) Compute the boundary-layer thickness at the trailing edge of the plate and its drag!

8.5 The velocity profile in the laminar boundary layer of a flat plate at zero incidence (length $L$) can be approximated by a polynomial of fourth degree

$$\frac{u}{u_\infty} = a_0 + a_1 \left(\frac{y}{\delta}\right) + a_2 \left(\frac{y}{\delta}\right)^2 + \\ + a_3 \left(\frac{y}{\delta}\right)^3 + a_4 \left(\frac{y}{\delta}\right)^4 .$$

(a) Determine the coefficients of the polynomial!
(b) Prove the validity of the following relations

$$\begin{aligned} \frac{\delta_1}{\delta} &= \frac{3}{10}, \\ \frac{\delta_2}{\delta} &= \frac{37}{315}, \\ \frac{\delta}{x} &= \frac{5.84}{\sqrt{Re_x}}, \\ c_D &= \frac{1.371}{\sqrt{Re_L}} \end{aligned}$$

8.6 The velocity profile in a laminar boundary layer on a flat plate at zero incidence of length $L$ is approximated by
A) a polynom of fourth degree

$$\frac{u}{u_\infty} = \frac{3}{2}\left(\frac{y}{\delta}\right) - \frac{1}{2}\left(\frac{y}{\delta}\right)^3$$

and
B) a sinosoidal ansatz

$$\frac{u}{u_\infty} = \sin\left(\frac{\pi}{2}\frac{y}{\delta}\right) \quad .$$

(a) Determine $\delta_1$, $\delta_2$, $\delta$, and $c_w$!
(b) Compute the boundary-layer thickness at the trailing edge of the plate and the drag for
$u_\infty = 1\dfrac{\mathrm{m}}{\mathrm{s}}$ $L = 0.5\,\mathrm{m}$ $B = 1\,\mathrm{m}$
$\rho = 10^3\,\dfrac{\mathrm{kg}}{\mathrm{m}^3}$ $\nu = 10^{-6}\,\dfrac{\mathrm{m}^2}{\mathrm{s}}$!

### 3.1.9 Drag

9.1 Two flat plates at zero incidence, one downstream from the other, are exposed to the free-stream velocity $u_\infty$.

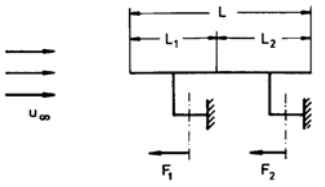


$u_\infty = 1\,\dfrac{\mathrm{m}}{\mathrm{s}}$ $L = L_1 + L_2 = 0.36\,\mathrm{m}$
$B = 1\,\mathrm{m}$ $\rho = 10^3\,\dfrac{\mathrm{kg}}{\mathrm{m}^3}$ $\nu = 10^{-6}\,\dfrac{\mathrm{m}^2}{\mathrm{s}}$

Determine
(a) the retaining forces $F_1$ and $F_2$ for $L_1 = L_2$,
(b) the lengths $L_1$ and $L_1$ for $F_1 = F_2$!

9.2 Two quadratic plates are exposed to a flow, one at zero incidence, the other with its surface normal to the direction of the free stream.

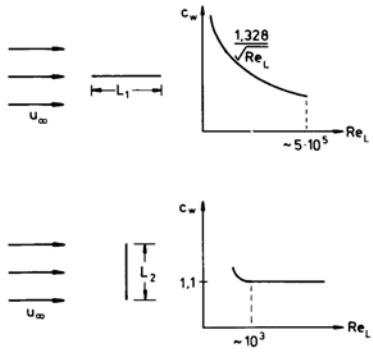


$u_\infty = 5\,\dfrac{\mathrm{m}}{\mathrm{s}}$ $L_1 = 1\,\mathrm{m}$ $\rho = 1.25\,\dfrac{\mathrm{kg}}{\mathrm{m}^3}$
$\nu = 15 \cdot 10^{-6}\,\dfrac{\mathrm{m}^2}{\mathrm{s}}$

(a) Explain the difference between frictional and pressure drag!
(b) How large must $L_2$ be, so that both plates generate the same drag?
(c) How does the drag depend on the free-stream velocity?

9.3 Two flat rectangular plates are exposed to a parallel flow. The plates have the same lateral lengths $L_1$ and $L_2$. The edge of plate 1, with lateral length $L_1$ is parallel to the direction of the free stream, and of plate 2 the edge with lateral length $L_2$. The free-stream velocity is $u_\infty$.

$L_1 = 1\,\mathrm{m}$ $L_2 = 0.5\,\mathrm{m}$ $\nu = 10^{-6}\,\dfrac{\mathrm{m}^2}{\mathrm{s}}$

(a) Determine the ratio of the friction forces for $u_\infty = 0.4\dfrac{\mathrm{m}}{\mathrm{s}}; 0.8\dfrac{\mathrm{m}}{\mathrm{s}}; 1.6\dfrac{\mathrm{m}}{\mathrm{s}}$!
(b) How large would the free-stream velocity for the plate 2 have to be, if the free-stream velocity of plate 1 is $u_\infty = 0.196\,\frac{m}{s}$, and if both drag co-

efficients are supposed to have the same value?

Hints:

$$c_D = \frac{0.074}{Re_L^{\frac{1}{5}}} - \frac{1700}{Re_L}$$

for $5 \cdot 10^5 < Re_L < 10^7$.

9.4 A kite (surface area $A$, weight $W$) generates the force $F$ in the kite string at an angle of attack $\alpha$.

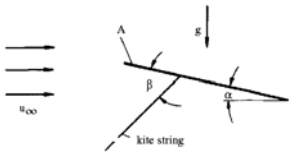


$A = 0.5\,\mathrm{m}^2 \quad W = 10\,\mathrm{N} \quad u_\infty = 10\,\dfrac{\mathrm{m}}{\mathrm{s}}$

$\alpha = 10^\circ \quad \beta = 55^\circ \quad F = 42.5\,\mathrm{N}$

$\rho = 1.25\,\dfrac{\mathrm{kg}}{\mathrm{m}^3}$

Determine the lift and drag coefficient of the kite!

9.5 Assume that the flow around a circular cylinder separates at $\alpha = 120°$, that the pressure distribution up to the separation point can be determined with the potential flow theory, and that the pressure in the dead water region is constant!

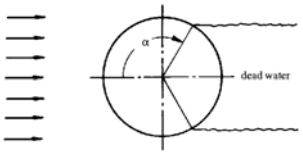


Neglect the frictional drag and determine the drag coefficient of the cylinder!

9.6 A surfboard (width $b$) moves with the velocity $u$ over the surface of quiescent water. The height of the triangular sail is $h$ and its width $b$.

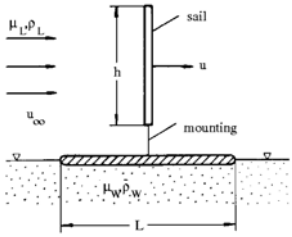


$L = 3.75\,\mathrm{m} \quad B = 0.5\,\mathrm{m} \quad u = 1.5\,\dfrac{\mathrm{m}}{\mathrm{s}}$

$\rho_w = 10^3\,\dfrac{\mathrm{kg}}{\mathrm{m}^3} \quad \mu_w = 10^{-3}\,\dfrac{\mathrm{Ns}}{\mathrm{m}^2}$

$\rho_a = 1.25\,\dfrac{\mathrm{kg}}{\mathrm{m}^3}$

$\mu_a = 1.875 \cdot 10^{-5}\,\dfrac{\mathrm{Ns}}{\mathrm{m}^2} \quad h = 4\mathrm{m} \quad b = 2\mathrm{m}$

Neglect the wave drag , the drag of the sail mounting, and the frictional drag of the upper side of the surfboard and determine

(a) the wind speed $u_\infty$,
(b) the drag of the sail!
(c) How large would the frictional drag of the upper side of the board be?

Hints:

$$\begin{aligned} \text{Board} \quad &: \quad c_D = \frac{0.074}{Re_L^{\frac{1}{5}}} - \frac{1700}{Re_L} \\ (\text{for} \quad &: \quad 5 \cdot 10^5 < Re_L < 10^7) \\ \text{Sail} \quad &: \quad c_D = 1.2 \\ (\text{for} \quad &: \quad Re > 10^3) \end{aligned}$$

9.7 How large must the surface of the equivalent drag of a parachute at least be, in order to avoid the sinking speed in quiescent air to exceed $v$?

$v = 4\,\dfrac{\mathrm{m}}{\mathrm{s}} \quad W = 1000\,\mathrm{N} \quad c_D = 1.33$

$\rho = 1.25\,\dfrac{\mathrm{kg}}{\mathrm{m}^3}$

9.8 A sphere and a circular cylinder of the same material fall with constant velocity in quiescent air. The axis of the cylinder is normal to the direction of the gravitational acceleration. For $0 < Re \leq 0.5$ the drag coefficient of a sphere is given by $c_D = \frac{24}{Re}$ and that of a circular cylinder with its axis normal to the oncoming flow by

$$c_D = \frac{8\,\pi}{Re(2 - \ln Re)} \quad .$$

$\rho = 800\,\frac{\mathrm{kg}}{\mathrm{m}^3}$ $\rho_a = 1.25\,\frac{\mathrm{kg}}{\mathrm{m}^3}$

$\nu_a = 15 \cdot 10^{-6}\,\frac{\mathrm{m}^2}{\mathrm{s}}$ $g = 10\,\frac{\mathrm{m}}{\mathrm{s}^2}$

Determine

(a) the maximum diameters, for which these relations are valid,

(b) the corresponding sink velocities!

9.9 Determine with the aid of the diagram for the drag coefficient of a sphere

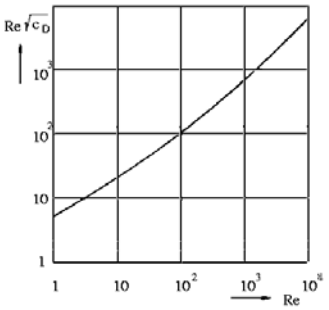


(a) the steady sink velocity of a spherical rain drop of diameter $D$ in air,

(b) the steady ascending velocity of a spherical bubble of air of diameter $D$ in water!

$D = 1\,\mathrm{mm}$ $\rho_w = 10^3\,\frac{\mathrm{kg}}{\mathrm{m}^3}$

$\nu_w = 10^{-6}\,\frac{\mathrm{m}^2}{\mathrm{s}}$

$\rho_a = 1.25\,\frac{\mathrm{kg}}{\mathrm{m}^3}$ $\nu_a = 15 \cdot 10^{-6}\,\frac{\mathrm{m}^2}{\mathrm{s}}$

$g = 10\,\frac{\mathrm{m}}{\mathrm{s}}$

9.10 Spherically shaped dust particles (density $\rho_s$) are to be conveyed with a stream of air against the gravitational force.

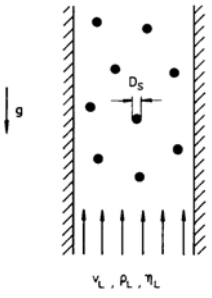


$D_s = 5 \cdot 10^{-5}\,\mathrm{m}$ $\rho_s = 2.5 \cdot 10^3\,\frac{\mathrm{kg}}{\mathrm{m}^3}$

$\rho_a = 1.25\,\frac{\mathrm{kg}}{\mathrm{m}^3}$ $\mu_a = 1.875 \cdot 10^{-5}\,\frac{\mathrm{Ns}}{\mathrm{m}^2}$

$g = 10\,\frac{\mathrm{m}}{\mathrm{s}^2}$

(a) At what velocity of the air $v_1$ are the dust particles suspended?

(b) How large is the velocity of the dust particles if the velocity of the air is $v_a = 3\,\frac{\mathrm{m}}{\mathrm{s}}$?

Hint:

Assume that the dust particles do not influence each other!

$c_D = \frac{24}{Re}\,(1 + \frac{3}{16}\,Re)$ for $0 < Re < 1$

9.11 A spherically shaped fog droplet (diameter $D$) is being suspended by an upward motion of air. At time $t = 0$ the air flow stops and the droplet begins to sink.

$D = 6 \cdot 10^{-5}\,\mathrm{m}$ $\rho_w = 10^3\,\frac{\mathrm{kg}}{\mathrm{m}^3}$

$\rho_a = 1.25\,\frac{\mathrm{kg}}{\mathrm{m}^3}$ $\mu_a = 1.875 \cdot 10^{-5}\,\frac{\mathrm{Ns}}{\mathrm{m}^2}$

$g = 10\,\frac{\mathrm{m}}{\mathrm{s}^2}$

(a) How large is the velocity of the air flow prior to the lull?

(b) After what time does the droplet attain 99% of its steady sink velocity?

Hint: For $Re \leq 0.5$ the law $c_D = \frac{24}{Re}$ is valid for steady and unsteady flow.

9.12 A sphere is falling in steady motion in quiescent air with the velocity $v_1$. A downwash squall increases the velocity to $v_2$.

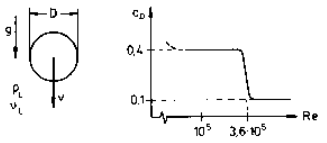


$D = 0.35\,\mathrm{m}$ $G = 4.06\,\mathrm{N}$ $v_1 = 13\,\frac{\mathrm{m}}{\mathrm{s}}$

$v_2 = 18\,\frac{\mathrm{m}}{\mathrm{s}}$ $\rho_a = 1.25\,\frac{\mathrm{kg}}{\mathrm{m}^3}$

$\nu_a = 15 \cdot 10^{-6}\,\frac{\mathrm{m}^2}{\mathrm{s}}$

(a) How large is the drag coefficient prior to the squall?
(b) What steady final velocity does the sphere attain after dying out of the squall?

9.13 A spherically shaped deep-sea probe is heaved with constant velocity from the depth $H$ to the surface of the sea in the time $T_1$.

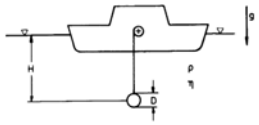

$D = 0.5\,\text{m} \quad H = 4000\,\text{m} \quad T_1 = 3\,\text{h}$
$\rho = 10^3\,\frac{\text{kg}}{\text{m}^3} \quad \mu = 10^{-3}\,\frac{\text{Ns}}{\text{m}^2} \quad g = 10\,\frac{\text{m}}{\text{s}^2}$

Assume constant density of the water, neglect the weight of the cable rope, and determine
(a) the power needed for heaving the probe, if the cable force is $F_1 = 2700$ N,
(b) the weight of the probe and the shortest heaving time, if the cable can take twice the value of the force,
(c) the power then needed!

Hint: Use the diagram of problem 9.12!

9.14 A sphere of diameter $D$ and density $\rho_s$ is vertically shot into quiescent air with initial velocity $v_\infty$.
Assume a constant drag coefficient and determine
(a) the height of rise,
(b) the rise time,
(c) the velocity at impact on the ground,
(d) the falling time!
(e) What values do these quantities attain for a wooden sphere of density $\rho_w$ and for a metal sphere of density $\rho_m$, if $c_D = 0.4$ and $c_w = 0$?

$D = 0.1\,\text{m} \quad v_0 = 30\,\frac{\text{m}}{\text{s}} \quad g = 10\,\frac{\text{m}}{\text{s}^2}$
$\rho_a = 1.25\,\frac{\text{kg}}{\text{m}^3} \quad \rho_w = 750\,\frac{\text{kg}}{\text{m}^3}$
$\rho_m = 7.5 \cdot 10^3\,\frac{\text{kg}}{\text{m}^3}$

## 3.2 Solutions

### 3.2.1 Hydrostatics

1.1

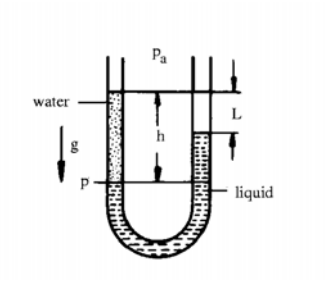


$$
\begin{aligned}
p &= p_a + \rho_w\, g\, h = p_a + \rho_F\, g\, (h - L) \\
\rho_F &= \rho_w\, \frac{h}{h - L} = 3 \cdot 10^3\, \frac{\text{kg}}{\text{m}^3}
\end{aligned}
$$

1.2

$$
\begin{aligned}
p_i &= \frac{F_i}{A_i} + p_a \\
p_2 &= p_1 + \rho\, g\, \Delta h_1 = p_3 - \rho\, g\, \Delta h_2 \\
\Delta h_1 &= \frac{p_2 - p_1}{\rho\, g} = 0.25 \text{ m} \\
\Delta h_2 &= \frac{p_3 - p_2}{\rho\, g} = 0.33 \text{ m}
\end{aligned}
$$

1.3

$$
\begin{aligned}
F_L &= W \\
F_L &= \rho_1\, h a^2\, g + \rho_2\, (a - h)\, a^2\, g \\
W &= \rho_K\, a^3\, g \\
h &= \frac{\rho_2 - \rho_K}{\rho_2 - \rho_1}\, a = 6.67 \cdot 10^{-2} \text{ m}
\end{aligned}
$$

1.4

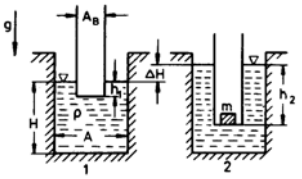


$$
\begin{aligned}
W_1 &= F_{L1} = \rho\, A_B\, h_1\, g \\
W_2 &= F_{L2} = \rho\, A_B\, h_2\, g \\
W_2 &= W_1 + m\, g
\end{aligned}
$$

The volume of the water remains constant.

$$
\begin{aligned}
AH - A_B\, h_1 &= A\, (H + \Delta H) - A_B\, h_2 \\
\Delta H &= \frac{m}{\rho\, A}
\end{aligned}
$$

1.5 (a)

$$
\tau_0 = \frac{W_0}{\rho_m\, g} = 1.07 \cdot 10^5 \text{ m}^3
$$

(b)

$$
\begin{aligned}
\Delta W &= \rho_M\, A\, (h_0 - h_1)\, g \\
A &= 1.95 \cdot 10^4 \text{ m}^2
\end{aligned}
$$

(c)

$$
\begin{aligned}
W_0 - \Delta W &= \rho_M\, \tau_1\, g = \rho_F\, \tau_2\, g \\
\tau_2 - \tau_1 &= \frac{W_0 - \Delta W}{\rho_M\, g} \left( \frac{\rho_M}{\rho_F} - 1 \right) \\
&= 2.44 \cdot 10^3 \text{ m}^3
\end{aligned}
$$

(d)

$$
\begin{aligned}
\tau_2 - \tau_1 &= (h_2 - h_1)\, A \\
h_2 &= 10.625 \text{ m}
\end{aligned}
$$

1.6

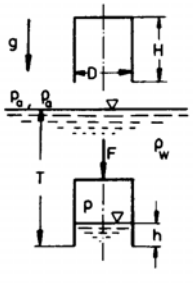


(a)

$$
\begin{aligned}
p_a\, \frac{\pi}{4}\, D^2\, H &= p\, \frac{\pi}{4}\, D^2\, (H - h) \\
p &= p_a + \rho_w\, g\, (T - h)
\end{aligned}
$$

$$
\begin{aligned}
h &= \frac{\rho_w\, g\, (T + h) + p_a}{2\, \rho_w\, g} \\
&\quad - \sqrt{\left( \frac{\rho_w g (T + h) + p_a}{2 \rho_w g} \right)^2 - TH} \\
&= 2 \text{ m}
\end{aligned}
$$

(b)

$$
\begin{aligned}
F &= F_L - W_{air} - W \\
&= \frac{\pi}{4}\, D^2\, g\, [(H - h)\ \rho_w - H\, \rho_a] \\
&\quad - G \\
&= -9.58 \cdot 10^3 \text{ N}
\end{aligned}
$$

(c)

$$
\begin{aligned}
0 &= F_L - W_{air} - W \\
h_0 &= H\left(1 - \frac{\rho_a}{\rho_w}\right) - \frac{4\,W}{\pi\,D^2\,\rho_w\,g} \\
T_0 &= h_0\left(1 + \frac{p_a}{\rho_w\,g\,(H-h_0)}\right) \\
&= 18.3 \text{ m}
\end{aligned}
$$

1.7

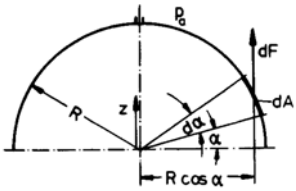


$$
\begin{aligned}
dF &= [p_i(z) - p_a]\,dA\,\sin\alpha \\
dA &= R\,d\alpha\,2\,\pi\,R\,\cos\alpha \\
F &= \frac{\pi}{3}\,R^3\,\rho\,g = 1.05 \cdot 10^4 \text{ N}
\end{aligned}
$$

1.8

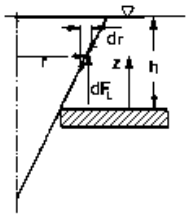


$$
\begin{aligned}
dF_L &= \rho\,g\,(h-z)\,2\pi\,r\,dr \\
\frac{r}{H-h+z} &= \frac{R}{H} \\
F_L &= \frac{\pi}{6}\,R^2\,H\,\rho\,g \\
F &= W - F_L \\
&= \frac{\pi}{3}\,R^2\,H\,(\rho_s - \frac{\rho}{2})\,g \\
&= 1.57 \cdot 10^{-2} \text{ N}
\end{aligned}
$$

1.9

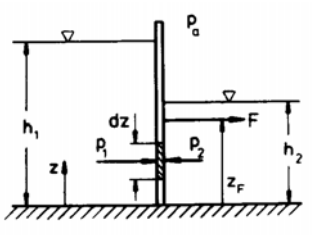


(a)

$$
\begin{aligned}
dF &= [p_1(z) - p_2(z)]\,B\,dz \\
z &\le h_1 : p_1(z) = p_a + \rho g(h_1 - z) \\
z &\le h_2 : p_2(z) = p_a + \rho g(h_2 - z) \\
h_2 &\le z \le h_1 :\ p_2 = p_a \\
F &= \frac{1}{2}\,\rho\,g\,B(h_1^2 - h_2^2) \\
&= 1.05 \cdot 10^6 \text{ N}
\end{aligned}
$$

(b)

$$
\begin{aligned}
F\,z_F &= \int_{z=0}^{z=h_1} z\,dF \\
z_F &= \frac{1}{3}\,\frac{h_1^3 - h_2^3}{h_1^2 - h_2^2} = 1.86 \text{ m}
\end{aligned}
$$

1.10

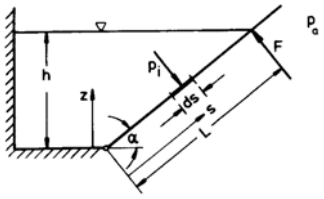


$$
\begin{aligned}
F\,L &= \int_{s=0}^{s=L} s\,dF \\
dF &= [p_i(s) - p_a]\,B\,ds \\
p_i(s) &= p_a + \rho\,g\,[L\,\sin\alpha - z(s)] \\
F &= \frac{\rho\,g\,B\,h^2}{6\,\sin\alpha} = 3 \cdot 10^4 \text{ N}
\end{aligned}
$$

1.11

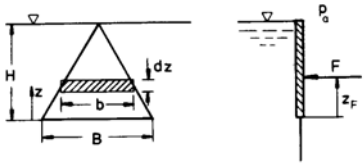


(a)

$$
\begin{aligned}
dF &= [p_i(z) - p_a]\,b(z)\,dz \\
p_i(z) &= p_a + \rho\,g\,(H - z) \\
F &= \frac{1}{4}\,\rho\,g\,B^3 = 2.5 \cdot 10^3 \text{ N}
\end{aligned}
$$

(b)

$$
\begin{aligned}
F\,z_F &= \int_{z=0}^{z=H} z\,dF \\
z_F &= \frac{\sqrt{3}}{8}\,B = 0.217 \text{ m}
\end{aligned}
$$

1.12

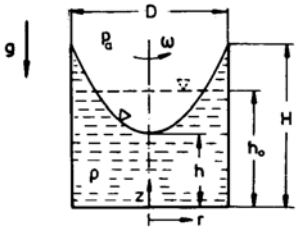


Boundary condition:

$$\begin{aligned} r &= 0, \quad z = h: \quad p = p_a \\ p - p_a &= \rho\, g\, (h - z) + \frac{1}{2}\, \rho\, \omega^2\, r^2 \end{aligned}$$

(a) Surface:

$$\begin{aligned} p &= p_a \\ z_0(r) &= h + \frac{\omega^2\, r^2}{2\, g} \end{aligned}$$

$$\begin{aligned} r = R: \quad z_0 &= H \\ \omega^2 &= 2\, g\, \frac{H - h}{R^2} \\ z_0(r) &= h + (H - h)\, \frac{r^2}{R^2} \end{aligned}$$

Volume of the water:

$$\begin{aligned} \pi R^2 h_0 &= \int_0^R z_0(r)\, 2\, \pi\, r\, dr \\ &= \pi R^2 h + \frac{1}{2} \pi R^2 (H - h) \end{aligned}$$

$$\begin{aligned} h &= 2\, h_0 - H = 0.4\ m \\ \omega &= \sqrt{\frac{4g}{R^2}\, (H - h_0)} = 13.9\ \frac{1}{\mathrm{s}} \end{aligned}$$

(b)

$$\begin{aligned} r = R &: \quad p = p_a + \rho\, g\, (H - z) \\ z = 0 &: \quad p = p_a + \rho\, g\, h + \frac{\rho}{2}\, \omega^2\, r^2 \end{aligned}$$

1.13

$$\frac{dp}{dz} = -\rho(z)\, g$$

(a)

$$\rho(z) = \frac{p(z)}{R\, T_0} \qquad p = p_0\, e^{-\frac{gz}{RT_0}}$$

(b)

$$\begin{aligned} \rho(z) &= \frac{p(z)}{R\, (T_0 - \alpha\, z)} \\ p &= p_0\, \left(1 - \frac{\alpha\, z}{T_0}\right)^{\frac{g}{R\alpha}} \end{aligned}$$

(c)

$$\begin{aligned} \rho(z) &= \rho_0 \left(\frac{p}{p_0}\right)^{\frac{1}{\kappa}} \\ p &= p_0\, \left(1 - \frac{\gamma - 1}{\gamma}\, \frac{gz}{R\, T_0}\right)^{\frac{\kappa}{\kappa - 1}} \end{aligned}$$

(d)

| $p/p_0$ | 3000 m | 6000 m | 11000 m |
|---|---|---|---|
| a) | 0.695 | 0.483 | 0.263 |
| b) | 0.686 | 0.457 | 0.215 |
| c) | 0.681 | 0.442 | 0.186 |

1.14 (a)

$$\begin{aligned} F &= F_L(z = 0) - W \\ &= (\rho_0\, \tau_0 - m)\, g \\ &= 10.6\ \mathrm{N} \end{aligned}$$

(b) for

$$z \le z_1: \quad \begin{aligned} p_1\, \tau_1 &= p_0\, \tau_0 \\ \frac{p_1}{p_0} &= e^{-\frac{g\, z_1}{R\, T_0}} \\ z_1 &= \frac{p_0}{\rho_0\, g}\, \ln \frac{\tau_1}{\tau_0} \\ &= 10.0\ \mathrm{km} \end{aligned}$$

(c)

$$\begin{aligned} F_L(z_2) &= W \\ z_2 &= \frac{p_0}{\rho_0\, g}\, \ln \frac{\rho_0\, \tau_1}{m} \\ &= 12.8\ \mathrm{km} \end{aligned}$$

1.15

$$\begin{aligned} F_L(z) &= W + W_{gas}(z) \\ F_L(0) &= W + W_{gas}(0) + F_s \\ F_L &= \rho\, \tau\, g \\ G_{gas} &= \rho_{gas}\, \tau\, g \\ \frac{\rho_{gas}(z)}{\rho_{gas}(0)} &= e^{-\frac{gz}{RT}} \\ z &= \frac{RT}{g}\, \ln \left(1 + \frac{F_s}{W}\right) \\ &= 7.84\ \mathrm{km} \end{aligned}$$

### 3.2.2 Hydrodynamics

2.1 (a)

$$\begin{aligned}\frac{dy}{dy} &= \frac{v}{u} = -\frac{v_0}{u_0}\,\tan(\omega\,t)\\ y &= \left[-\frac{v_0}{u_0}\,\tan(\omega\,t)\right]\,x + c\end{aligned}$$

Straight lines with slopes $0, -1, -\infty$

(b)

$$\begin{aligned}x(t) &= \int u\,dt + c_1\\ &= \frac{u_0}{\omega}\,\sin(\omega\,t) + c_1\\ y(t) &= \int v\,dt + c_2\\ &= \frac{v_0}{\omega}\,\cos(\omega\,t) + c_2\end{aligned}$$

$$\begin{aligned}\left(\tfrac{\omega}{u_0}\right)^2\,(x-c_1)^2 &+\\ \left(\tfrac{\omega}{v_0}\right)^2\,(y-c_2)^2 &= 1\end{aligned}$$

Circles with radius 1 m.

(c) Circle around the origin

2.2

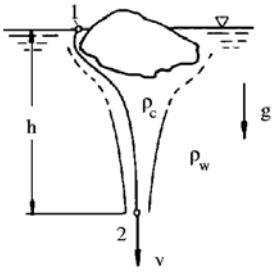


$$\begin{aligned}p_1 + \rho_c\,g\,h &= p_2 + \rho_c\,\frac{v^2}{2}\\ p_2 &= p_1 + \rho_w\,g\,h\\ v &= \sqrt{2\,g\,h\,\frac{\rho_c - \rho_w}{\rho_c}}\\ &= 3.16\,\frac{\mathrm{m}}{\mathrm{s}}\end{aligned}$$

2.3

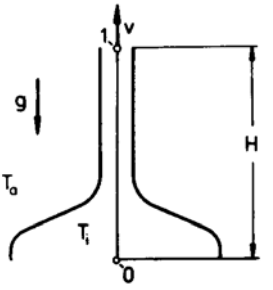


$$\begin{aligned}\frac{dp}{\rho} + \frac{1}{2}\,d\,(v^2) + g\,dz &= 0\\ p &= \rho\,RT\end{aligned}$$

inner:

$$RT_i \ln\left(\frac{p_{1i}}{p_{0i}}\right) + \frac{v^2}{2} + g\,H = 0$$

outer:

$$\begin{aligned}RT_a \ln\left(\frac{p_{1a}}{p_{0a}}\right) + g\,H &= 0\\ v = \sqrt{2\,g\,H\,\left(\frac{T_i}{T_a} - 1\right)} &= 31.6\,\frac{\mathrm{m}}{\mathrm{s}}\end{aligned}$$

2.4

$$\Delta p = \beta\,\frac{\rho}{2}\,v_\infty^2$$

(a) Assumption:

$$\frac{\rho\,v_\infty\,D}{\mu} > 250 \quad v_\infty = 0.5\,\frac{\mathrm{m}}{\mathrm{s}}$$
$$\left(\frac{\rho\,v_\infty\,D}{\mu} = 3000\right)$$

(b) Assumption:

$$\frac{\rho\,v_\infty\,D}{\mu} > 250 \quad v_\infty = 0.5\,\frac{\mathrm{m}}{\mathrm{s}}$$
$$\left(\frac{\rho\,v_\infty\,D}{\mu} = 300\right)$$

(c) Assumption:

$$2.5 < \frac{\rho\,v_\infty\,D}{\mu} < 250$$
$$v_\infty = 0.45\,\frac{\mathrm{m}}{\mathrm{s}} \qquad \left(\frac{\rho\,v_\infty\,D}{\mu} = 27\right)$$

2.5

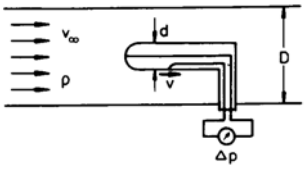


$$\begin{aligned} \Delta p &= \frac{\rho}{2}\, v^2 \\ v_\infty\, D^2 &= v\,(D^2 - d^2) \\ \frac{v_\infty}{\sqrt{\frac{2\,\Delta p}{\rho}}} &= 1 - \frac{d^2}{D^2} \end{aligned}$$

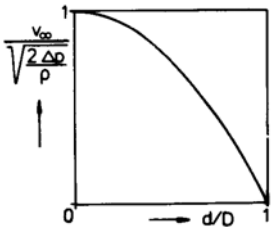


2.6

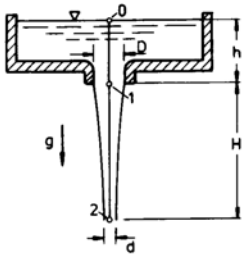


$$\begin{aligned} \rho\, g\,(h+H) &= \rho\, g\, H + \frac{\rho}{2}\, v_1^2 \\ &= \frac{\rho}{2}\, v_2^2 \\ v_1\, D^2 &= v_2\, d^2 \\ d = D\,\sqrt[4]{\frac{h}{h+H}} &= 0.05\ \mathrm{m} \end{aligned}$$

2.7 (a)

$$\begin{aligned} p_1 + \frac{\rho}{2}\, v_1^2 &= p_2 + \frac{\rho}{2}\, v_2^2 \\ v_1\, A_1 &= v_2\, A_2 \\ &= v_3\, A_3 \end{aligned}$$

$$\begin{aligned} v_2 &= \sqrt{\frac{2\,\Delta p}{\rho\left[1 - \left(\frac{A_2}{A_1}\right)^2\right]}} \\ &= 12\ \frac{\mathrm{m}}{\mathrm{s}} \\ v_1 &= 4\ \frac{\mathrm{m}}{\mathrm{s}} \quad v_3 \\ &= 6\ \frac{\mathrm{m}}{\mathrm{s}} \end{aligned}$$

(b)

$$\begin{aligned} p_2 + \frac{\rho}{2}\, v_2^2 &= p_3 + \frac{\rho}{2}\, v_3^2 \\ p_3 = p_a &= 10^5 \frac{\mathrm{N}}{\mathrm{m}^2} \\ p_2 &= 0.46 \cdot 10^5 \frac{\mathrm{N}}{\mathrm{m}^2} \\ p_1 &= 1.1 \cdot 10^5 \frac{\mathrm{N}}{\mathrm{m}^2} \\ p + \rho\, g\, h &= p_a + \frac{\rho}{2}\, v_3^2 \\ p &= 1.08 \cdot 10^5 \frac{\mathrm{N}}{\mathrm{m}^2} \end{aligned}$$

2.8

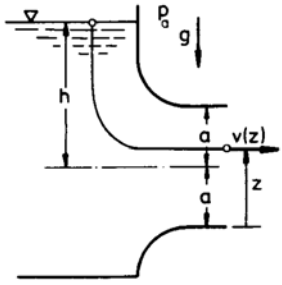


$$p_a + \rho\, g\,(a+h) = p_a + \rho\, g\, z + \tfrac{\rho}{2}\, v(z)^2$$

$$\begin{aligned} \dot{Q} &= \int_0^{2a} v(z)\, B\, dz \\ &= \frac{2}{3}\sqrt{2\,g}\, B\left[\sqrt{(h+a)^3} - \sqrt{(h-a)^3}\right] \end{aligned}$$

$$\frac{\dot{Q}_0 - \dot{Q}}{\dot{Q}} = \frac{3\,\frac{a}{h}}{\sqrt{(1+\frac{a}{h})^3} - \sqrt{(1-\frac{a}{h})^3}} - 1$$

| $a/h$ | 0.25 | 0.5 |
|---|---|---|
| $\frac{\dot{Q}_0 - \dot{Q}}{\dot{Q}}$ | 0.264% | 1.108% |
| $a/h$ | 0.75 | 1.0 |
| $\frac{\dot{Q}_0 - \dot{Q}}{\dot{Q}}$ | 2.728% | 6.066% |

2.9

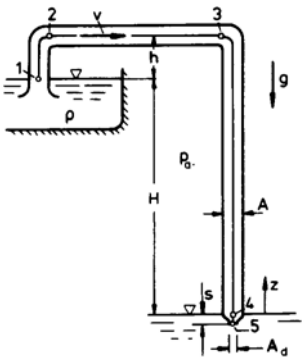


(a)

$$\begin{aligned} p_a + \rho\, g\, H &= p_5 - \rho\, g\, s + \frac{\rho}{2}\, v_5^2 \\ p_5 &= p_a + \rho\, g\, s \\ \dot{Q} &= A_d \sqrt{2\, g\, h} = 4\ \frac{\mathrm{m}^3}{\mathrm{s}} \end{aligned}$$

(b)

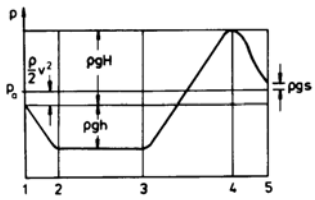


(c) Vapor bubbles are formed, if $p_2 = p_3 = p_v$ .

$$\begin{aligned} v_5^*\, A_d^* &= v^*\, A \\ p_a &= p_v + \rho\, g\, h + \frac{\rho}{2}\, v^{*2} \\ A_d^* &= A \sqrt{\frac{p_a - p_v}{\rho\, g\, H} - \frac{h}{H}} \\ &= 0.244\ \mathrm{m}^2 \end{aligned}$$

2.10

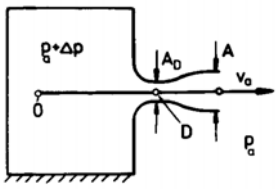


(a)

$$\begin{aligned} v_D\, A_D &= v_a A \\ p_0 = p_a + \Delta p &= p_a + \frac{\rho}{2}\, v_a^2 \\ v_D = \sqrt{\frac{2\,\Delta p}{\rho}}\, \frac{A}{A_D} &= 4\, \frac{A}{A_D}\ \frac{\mathrm{m}}{\mathrm{s}} \end{aligned}$$

(b)

$$\begin{aligned} p_0 - p_a &= (p_0 - p_D) - (p_a - p_D) \\ &= \frac{\rho}{2}\, v_D^2 - \eta_D (\frac{\rho}{2}\, v_D^2 - \frac{\rho}{2}\, v_a^2) \end{aligned}$$

$$\begin{aligned} v_D &= \sqrt{\frac{2\Delta p}{\rho}}\, \frac{A}{A_D} \\ &\quad \cdot \left[ \left( \frac{A}{A_D} \right)^2 (1 - \eta_D) + \eta_D \right]^{-\frac{1}{2}} \\ v_D &= \frac{4\, \frac{A}{A_D}}{\sqrt{0.16\, \left( \frac{A}{A_D} \right)^2 + 0.84}} \end{aligned}$$

(c)

$$\frac{A}{A_D} \to \infty : \quad v_D = 10\ \frac{\mathrm{m}}{\mathrm{s}}$$

2.11

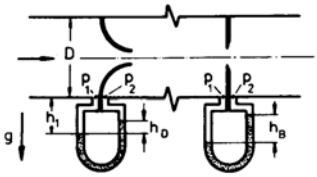


(a)

$$\dot{Q} = m_D\, \frac{\pi\, D^2}{4}\, \alpha_D \sqrt{\frac{2\, (p_1 - p_2)_D}{\rho_w}}$$

$$\begin{aligned} p_1 + \rho_w\, g\, h_1 &= p_2 + \rho_w\, g\, (h_1 - h_D) \\ &\quad + \rho_{Hg}\, g\, h_D \\ \dot{Q} &= 0.07\ \frac{\mathrm{m}^3}{\mathrm{s}} \end{aligned}$$

(b)

$$\begin{aligned} \dot{Q} &= m_B\, \frac{\pi\, D^2}{4}\, \alpha_B \sqrt{\frac{2\, (p_1 - p_2)_B}{\rho_w}} \\ \alpha_B &= \alpha_D\, \frac{m_D}{m_B} \sqrt{\frac{h_D}{h_B}} = 0.75 \end{aligned}$$

2.12

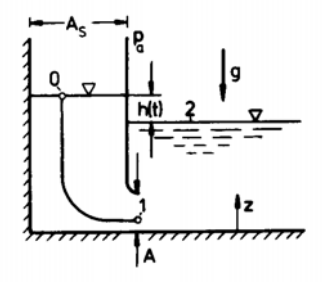


$$
\begin{aligned}
p_a + \rho\, g\, z_0 + \frac{\rho}{2}\, v_0^2 &= p_1 + \rho\, g\, z_1 \\
&\quad + \frac{\rho}{2}\, v_1^2 \\
p_1 + \rho\, g\, z_1 &= p_a + \rho\, g\, z_2
\end{aligned}
$$

The assumption of quasi-steady flow requires that $\frac{A}{A_s} \ll 1$: $v_0^2 \ll v_1^2$.

$$
\begin{aligned}
v_1\, A = v_0\, A_s &= -\frac{dh}{dt}\, A_s \\
T = -\frac{A_s}{A} \int_{h_0}^{0} \frac{dh}{\sqrt{2\, g\, h}} &= \frac{A_s}{A} \sqrt{\frac{2\, h_0}{g}} \\
A = A_s\, \frac{\sqrt{\frac{2\, h_0}{g}}}{T} &= 5\ \mathrm{m}^2
\end{aligned}
$$

2.13

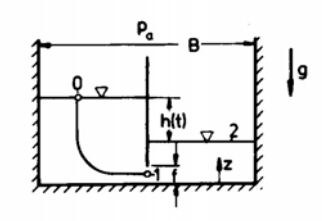


$$
\begin{aligned}
p_a + \rho\, g\, z_0 + \frac{\rho}{2}\, v_0^2 &= p_1 + \rho\, g\, z_1 \\
&\quad + \frac{\rho}{2}\, v_1^2 \\
p_1 + \rho\, g\, z_1 &= p_a + \rho\, g\, z_2
\end{aligned}
$$

$$
\begin{aligned}
v_0^2 &\ll v_1^2 \\
v_1\, f = v_0\, \frac{B}{2} &= -\frac{dz_0}{dt}\, \frac{B}{2} \\
\frac{dz_0}{dt} &= -\frac{dz_2}{dt} \\
\frac{dh}{dt} = \frac{d(z_0 - z_2)}{dt} &= 2\, \frac{dz_0}{dt}
\end{aligned}
$$

$$
\begin{aligned}
T &= -\frac{B}{4f} \int_{h_0}^{0} \frac{dh}{\sqrt{2\, g\, h}} \\
&= \frac{B}{2f} \sqrt{\frac{h_0}{2\, g}} = 100\ \mathrm{s}
\end{aligned}
$$

2.14

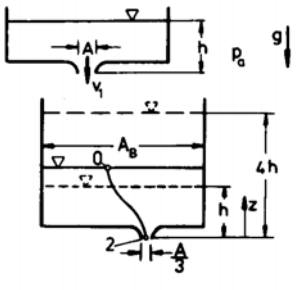


$$
\begin{aligned}
p_a + \rho\, g\, z_0 + \frac{\rho}{2}\, v_0^2 &= p_a + \frac{\rho}{2}\, v_2^2 \\
v_0^2 &\ll v_2^2
\end{aligned}
$$

Volume rate of flow:

$$
\begin{aligned}
\frac{dz_0}{dt}\, A_B &= v_1\, A - v_2\, \frac{A}{3} \\
v_1 &= \sqrt{2\, g\, h}
\end{aligned}
$$

$$
\begin{aligned}
T &= \frac{3}{\sqrt{2\, g}}\, \frac{A_B}{A} \cdot \int_h^{4h} \frac{dz_0}{3\sqrt{h} - \sqrt{z_0}} \\
&= \frac{3}{\sqrt{2\, g}}\, \frac{A_B}{A} \cdot 2 \left[ (3\sqrt{h} - \sqrt{z_0}) - \right. \\
&\quad \left. -3\sqrt{h}\, \ln(3\sqrt{h} - \sqrt{z_0}) \right]_h^{4h} \\
T &= 6\, \frac{A_B}{A} \sqrt{\frac{h}{2\, g}}\, [3 \ln 2 - 1] = 108\ \mathrm{s}
\end{aligned}
$$

2.15

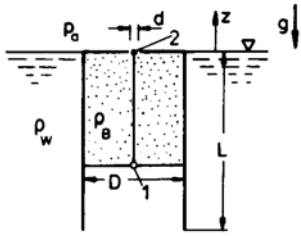


$$
\begin{aligned}
p_1 + \rho_B\, g\, z_1 + \frac{\rho_B}{2}\, v_1^2 &= p_a + \frac{\rho_B}{2}\, v_2^2 \\
p_a &= p_1 + \rho_w\, g\, z_1 \\
v_1^2 &\ll v_2^2 \\
v_2\, d^2 &= v_1\, D^2 \\
&= \frac{dz_1}{dt}\, D^2
\end{aligned}
$$

$$
\begin{aligned}
T &= \left(\frac{D}{d}\right)^2 \sqrt{\frac{\rho_B}{2\,g\,(\rho_w-\rho_B)}} \\
&\quad \int_{-L}^{0} \frac{dz_1}{\sqrt{-z_1}} \\
&= \left(\frac{D}{d}\right)^2 \sqrt{\frac{\rho_B}{\rho_w-\rho_B}} \sqrt{\frac{2\,L}{g}} = 80 \text{ s}
\end{aligned}
$$

2.16

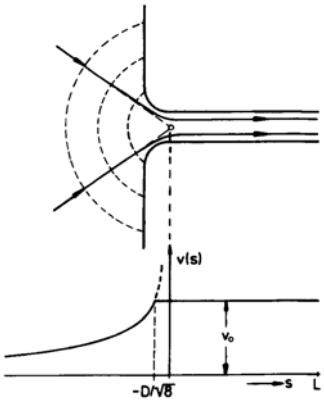


$$
\begin{aligned}
\int_{-\infty}^{L} \frac{\partial v}{\partial t} ds &= \int_{-\infty}^{-\frac{D}{\sqrt{8}}} \frac{\partial}{\partial t} \left(\frac{v_0\,\pi\,D^2}{2\,\pi s^2}\right) ds + \\
&+ \int_{-\frac{D}{\sqrt{8}}}^{L} \frac{\partial v_0}{\partial t}\, ds = \\
&= \left(\frac{D}{\sqrt{2}} + L\right) \frac{dv_0}{dt}
\end{aligned}
$$

2.17

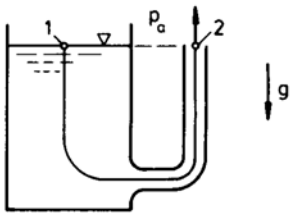


(a)

$$
v_0 = \sqrt{2\,g\,h} = 10\ \frac{\text{m}}{\text{s}}
$$

(b)

$$
p_a + \frac{\rho}{2}\, v_1^2 = p_a + \frac{\rho}{2}\, v_2^2
$$

$$
\begin{aligned}
&+ \rho \int_{s_1}^{s_1} \frac{\partial v}{\partial t}\, ds \\
\int_{s_1}^{s_1} \frac{\partial v}{\partial t}\, ds &\approx L\, \frac{dv_2}{dt} \quad \left(\frac{D}{L} \ll 1\right) \\
T &= -2\,L \int_{v_0}^{\frac{v_0}{2}} \frac{dv_2}{v_2^2} \\
&= \frac{2\,L}{\sqrt{2\,g\,h}} = 2 \text{ s}
\end{aligned}
$$

(c)

$$
\begin{aligned}
Q &= A \int_0^T v_2\, dt \\
&= -2\,A\,L \int_{v_0}^{\frac{v_0}{2}} \frac{dv_2}{v_2} \\
&= \frac{\pi}{2}\, L\, D^2\, \ln 2 = 0.279 \text{ m}^3
\end{aligned}
$$

2.18

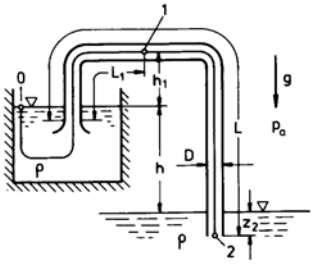


(a)

$$
\begin{aligned}
p_a + \rho_B\, g\, (h + z_2) &= p_a + \rho\, g\, z_2 \\
&+ \frac{\rho}{2}\, v_2^2 \\
&+ \rho \int_{s_0}^{s_2} \frac{\partial v}{\partial t}\, ds \\
\int_{s_0}^{s_2} \frac{\partial v}{\partial t}\, ds &\approx L\, \frac{dv_2}{dt}
\end{aligned}
$$

$$
\begin{aligned}
T &= 2\,L \int_0^{0.99\sqrt{2\,g\,h}} \frac{dv_2}{2\,g\,h - v_2^2} \\
&= \frac{L}{\sqrt{2\,g\,h}} \\
&\quad \ln \left[\frac{\sqrt{2\,g\,h} + v_2}{\sqrt{2\,g\,h} - v_2}\right]_0^{0.99\sqrt{2\,g\,h}} \\
&= 10.6 \text{ s}
\end{aligned}
$$

(b)

$$
\begin{aligned}
p_a &= p_1 + \rho\, g\, h_1 + \frac{\rho}{2}\, v_2^2 \\
&\quad + \rho\, L_1\, \frac{dv_2}{dt} \\
p_a &= p_{1e} = \rho\, g\, h_1 + \frac{\rho}{2}\, v_{2e}^2
\end{aligned}
$$

for:

$$\begin{aligned}\frac{dv_2}{dt} &= \frac{1}{L}\left(g\,h-\frac{v_2}{2}\right)\\ v_2 &= 0.99\sqrt{2\,g\,h}\\ p_1-p_{1e} &= \rho\,g\,h\left(1-0.99^2\right)\cdot\\ &\cdot\ \left(1-\frac{L_1}{L}\right)\\ &= 746\,\frac{\mathrm{N}}{\mathrm{m}^2}\end{aligned}$$

2.19

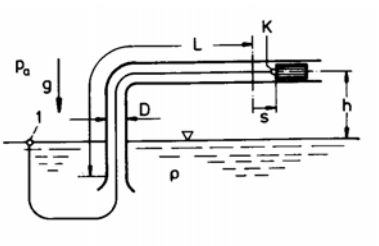


$$\begin{aligned}p_a &= p_p+\rho\,g\,h+\frac{\rho}{2}\,v_p^2\\ &+\ \rho\int_{s_1}^{s_p}\frac{\partial v}{\partial t}\,ds\\ \int_{s_1}^{s_p}\frac{\partial v}{\partial t} &\approx L\,\frac{dv_p}{dt}\quad\left(\frac{s_0}{L}\ll 1\right)\end{aligned}$$

$$\begin{aligned}p_p &= p_a-\rho\,g\,h+\rho\,s_0\,\omega^2\times\\ &\quad\left[L\,\sin\omega t-\frac{s_0}{2}\cos^2\omega t\right]\\ p_{pmin} &= p_v\\ p_p &= p_{pmin}\ \text{with}\ \cos\omega t=0\end{aligned}$$

$$\left(\text{follows from}\frac{dp_p}{dt}=0\right)$$

$$\omega=\sqrt{\frac{p_a-p_v-\rho\,g\,h}{\rho\,s_0\,L}}=8.8\,\frac{1}{\mathrm{s}}$$

2.20

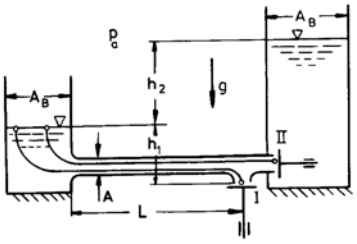


(a)

$$\begin{aligned}p_a+\rho\,g\,h_1 &= p_a+\frac{\rho}{2}\,v^2+\rho\,L\,\frac{dv}{dt}\\ Q_I &= A\int_0^{T_I}v\,dt\\ &= 2\,AL\int_0^{v_I}\frac{v\,dv}{2\,g\,h_1-v^2}\\ &= -AL\ln\left(1-\frac{v_I^2}{2\,g\,h_1}\right)\end{aligned}$$

Determination of $v_I$:

$$\begin{aligned}T_I &= 2\,L\int_0^{v_I}\frac{dv}{2\,g\,h_1-v^2}\\ &= \frac{L}{\sqrt{2\,g\,h_1}}\ln\frac{\sqrt{2\,g\,h_1}+v_I}{\sqrt{2\,g\,h_1}-v_I}\\ v_I &= \sqrt{2\,g\,h_1}\,\frac{e^{\frac{T_I\sqrt{2\,g\,h_1}}{L}}-1}{e^{\frac{T_I\sqrt{2\,g\,h_1}}{L}}+1}\\ Q_I &= 0.240\ \mathrm{m}^3\end{aligned}$$

(b)

$$\begin{aligned}p_a+\rho\,g\,h_1 &= p_a+\rho\,g\,(h_1+h_2)\\ &+\ \frac{\rho}{2}\,v^2+\rho\,L\,\frac{dv}{dt}\end{aligned}$$

$$\begin{aligned}Q_{II} &= A\int_{T_I}^{T_{II}}v\,dt\\ &= -2\,AL\int_{v_I}^{0}\frac{v\,dv}{2\,g\,h_2+v^2}\\ &= AL\ln\left(1+\frac{v_I^2}{2\,g\,h_2}\right)\\ &= 0.194\ \mathrm{m}^3\end{aligned}$$

2.21

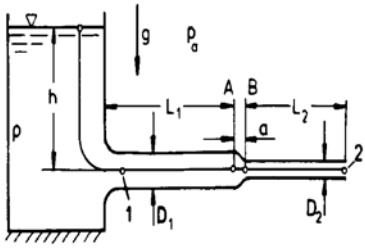


(a)

$$\begin{aligned}p_a+\rho\,g\,h &= p_a+\frac{\rho}{2}\,v_2^2\\ &+\ \rho\left(L_1\frac{dv_1}{dt}+L_2\frac{dv_2}{dt}\right)\end{aligned}$$

$$v_1\, D_1^2 = v_2\, D_2^2$$

$$\begin{aligned} T &= 2\left[L_1\left(\frac{D_2}{D_1}\right)^2 + L_2\right]\cdot \\ &\cdot \int_0^{0.99\sqrt{2\,g\,h}} \frac{dv_2}{2\,g\,h - v_2^2} \\ &= \frac{L_1\left(\frac{D_2}{D_1}\right)^2 + L_2}{\sqrt{2\,g\,h}}\cdot \\ &\cdot \ln\left[\frac{\sqrt{2\,g\,h}+v_2}{\sqrt{2\,g\,h}-v_2}\right]_0^{0.99\sqrt{2\,g\,h}} \\ &= 5.231\ \text{s} \end{aligned}$$

(b)

$$\begin{aligned} Q &= \left[L_1\left(\frac{D_2}{D_1}\right)^2 + L_2\right] A_2 \cdot \\ &\cdot \int_0^{0.99\sqrt{2\,g\,h}} \frac{v_2\, dv_2}{2\,g\,h - v_2^2} \\ &= -\left[L_1\left(\frac{D_2}{D_1}\right)^2 + L_2\right] A_2 \cdot \\ &\cdot \ln\left[2\,g\,h - v_2^2\right]_0^{0.99\sqrt{2\,g\,h}} \\ &= 0.048\ \text{m}^3 \end{aligned}$$

(c)

$$p_A + \frac{\rho}{2}\, v_1^2 = p_a + \frac{\rho}{2}\, v_2^2 + \rho\, L_2 \frac{dv_2}{dt}$$
$$p_B + \frac{\rho}{2}\, v_2^2 = p_a + \frac{\rho}{2}\, v_2^2 + \rho\, L_2 \frac{dv_2}{dt}$$

as shown under (a):

$$\frac{dv_2}{dt} = \frac{2\,g\,h - v_2^2}{2\left[L_1\left(\frac{D_2}{D_1}\right)^2 + L_2\right]}$$

t = 0:

$$\begin{aligned} p_A &= p_B = p_A + \frac{\rho\, g\, h}{1 + \frac{L_1}{L_2}\left(\frac{D_2}{D_1}\right)^2} \\ &= 1.16 \cdot 10^5\ \frac{\text{N}}{\text{m}^2} \end{aligned}$$

t = T:

$$\begin{aligned} p_A &= p_a + \rho\, g\, h\left[0.99^2\left(1 - \frac{D_2^4}{D_1^4}\right)\right. \\ &+ \left.\frac{1 - 0.99^2}{1 + \frac{L_1}{L_2}\left(\frac{D_2}{D_1}\right)^2}\right] \\ &= 1.187 \cdot 10^5\ \frac{\text{N}}{\text{m}^2} \end{aligned}$$

$$\begin{aligned} p_B &= p_a + \frac{1 - 0.99^2}{1 + \frac{L_1}{L_2}\left(\frac{D_2}{D_1}\right)^2}\rho\, g\, h \\ &= 1.003 \cdot 10^5\ \frac{\text{N}}{\text{m}^2} \end{aligned}$$

(d)

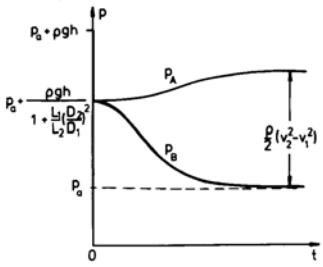


2.22

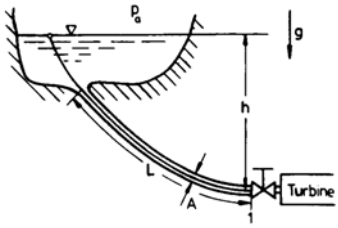


(a)

$$\begin{aligned} p_a + \rho\, g\, h &= p_{1s} + \frac{\rho}{2}\, v_{1s}^2 \\ v_{1s} &= \frac{\dot{Q}_0}{A} \\ p_{1s} - p_a &= \rho\left(g\, h - \frac{\dot{Q}_0^2}{2\, A^2}\right) \\ &= 18.875 \cdot 10^5\ \frac{\text{N}}{\text{m}^2} \end{aligned}$$

(b)

$$\begin{aligned} p_a + \rho\, g\, h &= p_1 + \frac{\rho}{2}\, v_1^2 + \\ &+ \rho\, L\, \frac{Dv_1}{dt} \\ \dot{Q}(t) &= \dot{Q}_0\left(1 - \frac{t}{T_s}\right) \\ p_1(t) &= p_a + \rho\, g\, h + \rho\, L \frac{\dot{Q}_0}{A\, T_S} - \\ &- \frac{\rho}{2}\left(\frac{\dot{Q}_0}{A}\right)^2\left(1 - \frac{t}{T_S}\right)^2 \end{aligned}$$

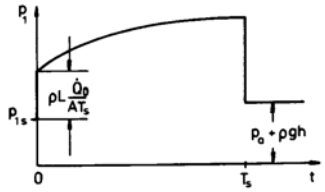


1.

$$\begin{aligned} \Delta p_{zul} &= p_{1max} - p_a \\ &= \rho\, g\, h + \rho\, L \frac{\dot{Q}_0}{A\, T_S} \\ T_S &= 0.25 \text{ s} \end{aligned}$$

### 3.2.3 Momentum and Moment of Momentum Theorem

3.1

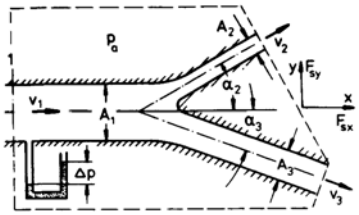


(a)

$$\begin{aligned} p_1 + \frac{\rho}{2} v_1^2 &= p_a + \frac{\rho}{2} v_2^2 = p_a + \frac{\rho}{2} v_3^2 \\ \Delta p &= p_1 - p_a \\ v_1\, A_1 &= v_2\, A_2 + v_3\, A_3 \\ v_1 &= \sqrt{\frac{2\,\Delta p}{\rho} \frac{1}{\left(\frac{A_1}{A_2+A_3}\right)^2 - 1}} \\ &= 2.58 \frac{\text{m}}{\text{s}} \\ v_2 &= v_3 = \frac{A_1}{A_2 + A_3}\, v_1 \\ &= 5.16 \frac{\text{m}}{\text{s}} \end{aligned}$$

(b)

$$\begin{aligned} \rho\, v_3^2\, A_3\, \cos\alpha_3 + \rho\, v_2^2\, A_2\, \cos\alpha_2 \\ -\rho\, v_1^2\, A_1 = (p_1 - p_a)\, A_1 + F_{sx} \\ F_{sx} = -866.4 \text{ N} \end{aligned}$$

$$\begin{aligned} \rho\, v_2^2\, A_2\, \sin\alpha_2 - \rho\, v_3^2\, A_3\, \sin\alpha_3 = F_{sy} \\ F_{sy} = -238.4 \text{ N} \end{aligned}$$

(c)

$$\begin{aligned} A_2\, \sin\alpha_2 - A_3\, \sin\alpha_3^* &= 0 \\ \alpha_3^* &= 12.37^\circ \end{aligned}$$

3.2 (a)

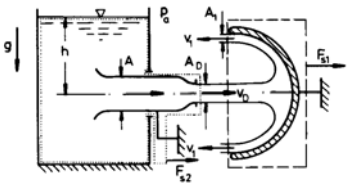


$$-\rho\, v_D^2\, A_D - 2\, \rho\, v_1^2\, A_1 = F_{s1}$$

$$\begin{aligned} v_D &= \sqrt{2\, g\, h} \\ v_D\, A_D &= 2\, v_1\, A_1 \\ p_a + \frac{\rho}{2} v_D^2 &= p_a + \frac{\rho}{2} v_1^2 \\ F_{s1} = -4\, \rho\, g\, h\, A_D &= -2 \cdot 10^4 \text{ N} \end{aligned}$$

$$\begin{aligned} \rho\, v_D^2\, A_D &= (p_a + \rho\, g\, h - p_a)\, A + \\ &+ F_{s2} \\ F_{s2} &= \rho\, g\, h(2\, A_D - A) = 0 \end{aligned}$$

(b)

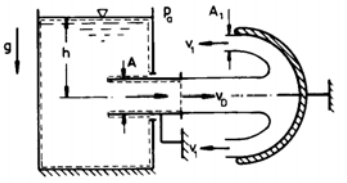


$$\begin{aligned} \rho\, v_D^2\, A_D &= (p_a + \rho\, g\, h - p_a)\, A \\ F_{s1} &= -2\, \rho\, g\, h\, A \\ &= -2 \cdot 10^4 \text{ N} \\ F_{s2} &= 0 \end{aligned}$$

3.3

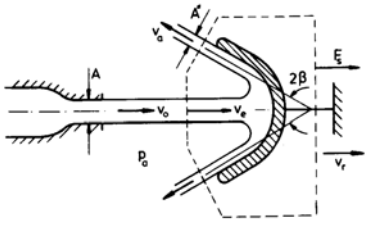

(a)

$$P = -F_S\, v_r$$

Moving control surface:

$$\begin{aligned} -\rho\, v_e^2\, A &= 2\,\rho\, v_a^2\, A^*\, \cos\beta = F_s \\ v_e &= v_0 - v_r \\ p_a + \frac{\rho}{2}\, v_e^2 &= p_a + \frac{\rho}{2}\, v_a^2 \\ v_e\, A &= 2\, v_a\, A^* \end{aligned}$$

$$\begin{aligned} P &= \rho\,(v_0 - v_r)^2\, v_r\, A\,(1+\cos\beta) \\ \frac{dP}{dv_r} &= 0 \\ v_r &= \frac{v_0}{3} = 20\ \frac{\mathrm{m}}{\mathrm{s}} \end{aligned}$$

(b)

$$\begin{aligned} F_s &= -\frac{4}{9}\,\rho\, v_0^2\, A\,(1+\cos\beta) \\ &= 3.08 \cdot 10^5\ \mathrm{N} \end{aligned}$$

3.4

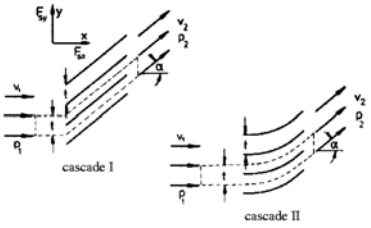


(a)

$$\begin{aligned} v_1\, B\, t &= v_2\, B\, t\, \cos\alpha \\ v_2 &= \frac{v_1}{\cos\alpha} \end{aligned}$$

Cascade I

(b)

$$\begin{aligned} &-\rho\, v_1^2\, B\, t + \rho\, v_1^2\, B\, t\, \cos^2\alpha \\ &\quad = (p_1 - p_2)\, B\, t + F_{sx} \\ &\rho\, v_2^2\, B\, t\, \sin\alpha\, \cos\alpha = F_{sy} \end{aligned}$$

Force normal to the blade:

$$\tan\alpha = -\frac{F_{sx}}{F_{sy}}$$

$$p_1 - p_2 = -\rho\, v_1^2\, \tan^2\alpha$$

(c)

$$\begin{aligned} p_{01} - p_{02} &= (p_1 - p_2) + \frac{\rho}{2}\,(v_1^2 - v_2^2) \\ &= \frac{\rho}{2}\, v_1^2\, \tan^2\alpha \end{aligned}$$

(d)

$$\begin{aligned} F_x &= -F_{sx} = \rho\, v_1^2\, Bt\, \tan^2\alpha \\ F_y &= -F_{sy} = -\rho\, v_1^2\, Bt\, \tan\alpha \end{aligned}$$

Cascade II

(b)

$$\begin{aligned} p_1 + \frac{\rho}{2}\, v_1^2 &= p_2 + \frac{\rho}{2}\, v_2^2 \\ p_1 - p_2 &= \frac{\rho}{2}\, v_1^2\, \tan^2\alpha \end{aligned}$$

(c)

$$p_{01} - p_{02} = 0$$

(d) Momentum equ. as for cascade I

$$\begin{aligned} F_x &= \frac{\rho}{2}\, v_1^2\, Bt\, \tan^2\alpha \\ F_y &= -\rho\, v_1^2\, Bt\, \tan\alpha \end{aligned}$$

3.5

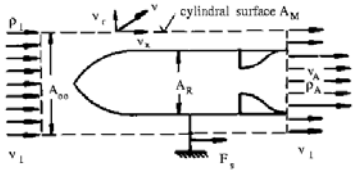


(a)

$$\begin{aligned} \rho_1\, v_1\, A_\infty &= \rho_1\, v_1\,(A_\infty - A_R) \\ &\quad + \Delta\dot{m} \\ \Delta\dot{m} &= \rho_1\, v_1\, A_R \end{aligned}$$

(b)

$$\begin{aligned} &-\rho_1\, v_1^2\, A_\infty + \rho_1\, v_1^2\,(A_\infty - A_R) + \\ &+\rho_A\, v_A^2\, A_R + \int_{A_M} \rho_1\, v_x\, v_r\, dA = F_s \end{aligned}$$

For $\dfrac{A_\infty}{A_R} \gg 1$ : $v_x = v_1$

$$\begin{aligned}\int_{A_M} \rho_1 v_x v_r \, dA &= v_1 \int_{A_M} \rho_1 v_r \, dA \\ &= v_1 \, \Delta \dot{m} \\ F_s &= \rho_A v_A^2 A_R \\ P &= F_s v_1 \\ &= \rho_A v_A^2 v_1 A_R\end{aligned}$$

3.6

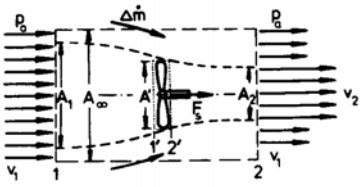


(a)

$$\begin{aligned}p_a + \frac{\rho}{2} v_1^2 &= p_{1'} + \frac{\rho}{2} v'^2 \\ p_{2'} + \frac{\rho}{2} v'^2 &= p_a + \frac{\rho}{2} v_2^2 \\ v_1 A_1 = v' A' &= v_2 A_2\end{aligned}$$

$$\begin{aligned}0 &= (p_{1'} - p_{2'}) A' + F_s \\ &- \rho v_1^2 A_\infty + \rho v_2^2 A_2 \\ &+ \rho v_1^2 (A_\infty - A_2) \\ &- \Delta \dot{m} v_1 = F_s\end{aligned}$$

See problem 4.3

$$\begin{aligned}\rho v_1^2 A_\infty + \Delta \dot{m} &= \rho v_2^2 A_2 \\ &+ \rho v_1^2 (A_\infty - A_2) \\ v' &= \frac{v_1 - v_2}{2} \\ &= 6.5 \, \frac{\text{m}}{\text{s}}\end{aligned}$$

(b)

$$\eta = \frac{F_s v_1}{F_s v'} = \frac{v_1}{v'} = 0.769$$

3.7 (a)

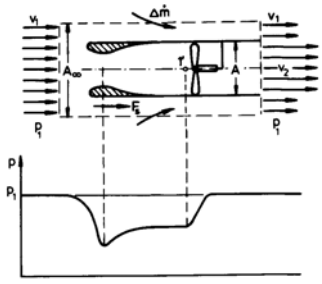


(b)

$$\begin{aligned}p_1 + \frac{\rho}{2} v_1^2 &= p_{1'} + \frac{\rho}{2} v_{1'}^2 \\ v_{1'} = v_2 &= \sqrt{\frac{2}{\rho} (p_1 - p_{1'}) + v_1^2} \\ \dot{m} = \rho A v_{1'} &= 13 \cdot 10^3 \, \frac{\text{kg}}{\text{s}}\end{aligned}$$

(c)

$$\begin{aligned}&-\rho v_1^2 A_\infty - \Delta \dot{m} v_1 + \rho v_2^2 A \\ &\quad + \rho v_1^2 (A_\infty - A) = F_s\end{aligned}$$

See problem 4.5.

$$\begin{aligned}\rho v_1 A_\infty + \Delta \dot{m} &= \rho v_1 (A_\infty - A) \\ &\quad + \rho v_2 A \\ F_s &= \rho v_2 (v_2 - v_1) A \\ &= 0.39 \cdot 10^5 \text{ N}\end{aligned}$$

(d)

$$\begin{aligned}P &= \dot{Q} (p_{02} - p_{01'}) \\ &= \dot{Q} (p_1 - p_{1'}) = 448.5 \text{ kW}\end{aligned}$$

3.8

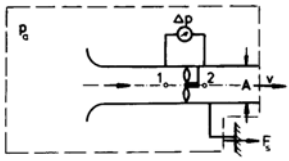


(a)

$$\begin{aligned}p_a &= p_1 + \frac{\rho}{2} v_1^2 \\ \Delta p &= p_2 - p_1 = p_a - p_1 \\ \dot{Q} &= v A = \sqrt{\frac{2 \Delta p}{\rho}} A\end{aligned}$$

(b)

$$P = \dot{Q} (p_{02} - p_{01}) = \sqrt{\frac{2 \Delta p}{\rho}} \Delta p A$$

(c)

$$\rho v^2 A = F_s = 2 \Delta p A$$

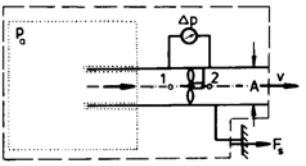


(d)

$$\begin{aligned} \rho\, v^2\, A &= (p_a - p_1)\, A \\ \Delta p = p_2 - p_1 &= p_a - p_1 \\ \dot{Q} = v\, A &= \sqrt{\frac{\Delta p}{\rho}}\, A \end{aligned}$$

(e)

$$P = \dot{Q}\,(p_{02} - p_{01}) = \sqrt{\frac{\Delta p}{\rho}}\, \Delta p\, A$$

(f)

$$\rho\, v^2\, A = F_s = \Delta p\, A$$

3.9

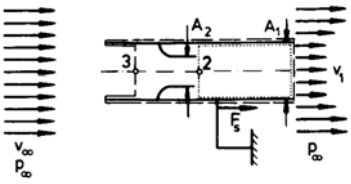


(a)

$$\begin{aligned} p_\infty + \frac{\rho}{2}\, v_\infty^2 &= p_2 + \frac{\rho}{2}\, v_2^2 \\ -\rho\, v_2^2\, A_2 + \rho\, v_1^2\, A_1 &= (p_2 - p_\infty)\, A_1 \\ v_2\, A_2 &= v_1\, A_1 \end{aligned}$$

$$\begin{aligned} v_2 &= \frac{v_\infty}{\sqrt{1 - 2\,\frac{A_2}{A_1} + 2\,\left(\frac{A_2}{A_1}\right)^2}} \\ &= 56.6\ \frac{\mathrm{m}}{\mathrm{s}} \\ v_1 &= 28.3\ \frac{\mathrm{m}}{\mathrm{s}} \end{aligned}$$

(b)

$$-\rho v_3^2 A_1 + \rho v_1^2 A_1 = (p_3 - p_\infty) A_1 + F_s$$

$$\begin{aligned} p_\infty + \frac{\rho}{2}\, v_\infty^2 &= p_3 + \frac{\rho}{2}\, v_3^2 \\ v_3 &= v_1 \\ F_s = \frac{\rho}{2}\,(v_1^2 - v_\infty^2)\, A_1 &= -100\ \mathrm{N} \end{aligned}$$

3.10

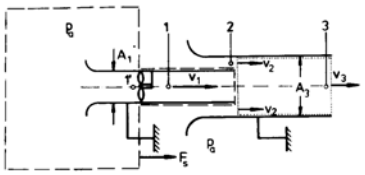


(a)

$$\begin{aligned} v_2 &= \frac{\dot{Q}_2}{A_3 - A_1} = 40\ \frac{\mathrm{m}}{\mathrm{s}} \\ p_a &= p_2 + \frac{\rho}{2}\, v_2^2 \\ p_2 &= 0.99 \cdot 10^5\ \frac{\mathrm{N}}{\mathrm{m}^2} \end{aligned}$$

(b)

$$\begin{aligned} -\rho\, v_1^2\, A_1 - \rho\, v_2^2\, A_2 + \rho\, v_3^2\, A_3 &= (p_2 - p_a)\, A_3 \\ v_1\, A_1 + v_2\, A_2 &= v_3\, A_3 \end{aligned}$$

$$\begin{aligned} v_1 &= \left(1 + \sqrt{\frac{1}{2\,\frac{A_1}{A_3}\,\left(1 - \frac{A_1}{A_3}\right)}}\right) v_2 \\ &= 96.6\ \frac{\mathrm{m}}{\mathrm{s}} \\ v_3 &= v_1\,\frac{A_1}{A_3} + v_2\left(1 - \frac{A_1}{A_3}\right) \\ &= 68.3\ \frac{\mathrm{m}}{\mathrm{s}} \end{aligned}$$

(c)

$$\begin{aligned} P &= \dot{Q}_1\,(p_{01} - p_{01'}) \\ &= \dot{Q}_1\,(p_1 - p_{1'}) \\ p_1 &= p_2 \\ p_a &= p_{1'} + \frac{\rho}{2}\, v_1^2 \\ p &= \frac{\rho}{2}\left(v_1^2 - v_2^2\right)\, v_1\, A_1 \\ &= 46.6\ \mathrm{kW} \end{aligned}$$

(d)

$$\begin{aligned} \rho\, v_1^2\, A_1 &= (p_a - p_2)\, A_1 + F_s \\ F_s &= \rho\left(v_1^2 - \frac{v_2^2}{2}\right) A_1 \\ &= 1066\ \mathrm{N} \end{aligned}$$

(Traction force)

3.11

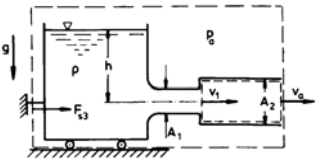


(a)

$$\begin{aligned} -\rho\, v_1^2\, A_1 + \rho\, v_a^2\, A_2 &= (p_1 - p_a)\, A_2 \\ p_a + \rho\, g\, h &= p_1 + \frac{\rho}{2}\, v_1^2 \\ v_1\, A_1 &= v_a\, A_2 \end{aligned}$$

$$\dot{Q} = \frac{\sqrt{2\, g\, h}\, A}{\sqrt{2\, \left(\frac{A_1}{A_2}\right)^2 - 2\, \frac{A_1}{A_2} + 1}}$$

$$\begin{aligned} \frac{d\dot{Q}}{dA_2} &= 0 \\ A_2 &= 2\, A_1 = 0.2\ \mathrm{m}^2 \end{aligned}$$

(b)

$$p_1 = p_a - \rho\, g\, h = 5\, 10^4\, \frac{\mathrm{N}}{\mathrm{m}^2}$$

(c)

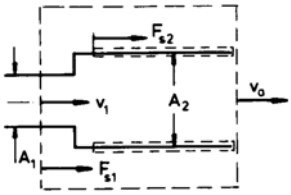


$$\begin{aligned} -\rho\, v_1^2\, A_1 + \rho\, v_a^2\, A_2 &= (p_1 - p_a)\, A_1 \\ &\quad + F_{s1} \end{aligned}$$

$$\begin{aligned} F_{s1} &= -\rho\, g\, h\, A_1 \\ &= -5\, 10^3\ \mathrm{N\ (Traction\ force)} \end{aligned}$$

$$\begin{aligned} F_{s2} &= 0 \\ \rho\, v_a^2\, A_2 &= F_{s3} \end{aligned}$$

$$\begin{aligned} F_{s3} &= 2\, \rho\, g\, h\, A_1 \\ &= 10^4\ \mathrm{N\ (Compressive\ force)} \end{aligned}$$

3.12

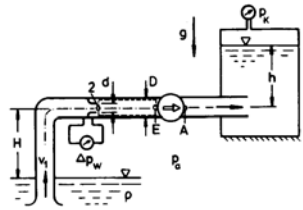


(a)

$$\begin{aligned} \dot{Q} &= v_1\, \frac{\pi\, D^2}{4} = \alpha\, \frac{\pi\, D^2}{4}\, \sqrt{\frac{2\, \Delta\, p_w}{\rho}} \\ v_1 &= \alpha\, \frac{d^2}{D^2}\, \sqrt{\frac{2\, \Delta\, p_w}{\rho}} = 1.33\ \frac{\mathrm{m}}{\mathrm{s}} \end{aligned}$$

(b)

$$\begin{aligned} -\rho\, v_2^2\, A_2 &+ \rho\, v_1^2\, A_1 = (p_2 - p_E)\, A_1 \\ p_a &= p_2 + \rho\, g\, H + \frac{\rho}{2}\, v_2^2 \\ v_2\, A_2 &= v_1\, A_1 \end{aligned}$$

$$\begin{aligned} p_E &= p_a - \frac{\rho}{2}\, v_1^2 \left[ \left( \frac{D^2}{d^2} - 1 \right)^2 + 1 \right] \\ &\quad - \rho\, g\, H = 0.482 \cdot 10^5\ \frac{\mathrm{N}}{\mathrm{m}^2} \\ p_A &= p_K + \rho\, g\, h = 2.3 \cdot 10^5\ \frac{\mathrm{N}}{\mathrm{m}^2} \end{aligned}$$

(c)

$$\begin{aligned} P &= v_1\, \frac{\pi\, D^2}{4}\, (p_{oA} - p_{oE}) \\ &= 1.9 \cdot 10^3\ \mathrm{kW} \end{aligned}$$

3.13

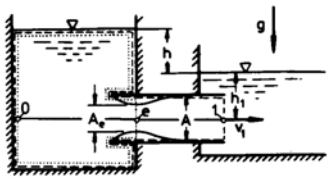


(a)

$$\begin{aligned} \rho\, v_e^2\, A_e &= (p_0 - p_e)\, A \\ p_0 &= p_e + \frac{\rho}{2}\, v_e^2 \\ \Psi &= \frac{A_e}{A} = 0.5 \end{aligned}$$

(b)

$$\begin{aligned} \rho\, v_1^2\, A &= (p_0 - p_1)\, A \\ p_0 &= p_a + \rho\, g\, (h + h_1) \\ p_1 &= p_a + \rho\, g\, h_1 \\ v_1 &= \sqrt{g\, h} = 3.16\ \frac{\mathrm{m}}{\mathrm{s}} \end{aligned}$$

3.14 (a)

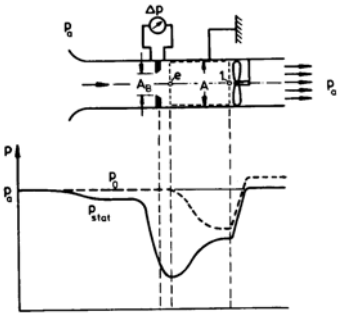


(b)

$$\begin{aligned} \dot{Q} &= \alpha\, m\, A \sqrt{\frac{2\, \Delta\, p_w}{\rho}} \\ &= 7.67 \cdot 10^{-2}\ \frac{\mathrm{m}^3}{\mathrm{s}} \end{aligned}$$

(c)

$$\begin{aligned} -\rho\, v_e^2\, A_e + \rho\, v_1^2\, A &= (p_e - p_1)\, A \\ p_a &= p_e + \frac{\rho}{2}\, v_e^2 \end{aligned}$$

$$\begin{aligned} \dot{Q} &= v_1\, A_1 = v_e\, A_e = v_e\, \Psi\, m\, A \\ p_1 &= p_a - \alpha^2\, m^2 \cdot \\ &\quad \cdot\ \Delta\, p_w \left[ \left( 1 - \frac{1}{\Psi\, m} \right)^2 + 1 \right] \\ &= 0.998 \cdot 10^5\ \frac{\mathrm{N}}{\mathrm{m}^2} \end{aligned}$$

(d)

$$P = \dot{Q}\, (p_a - p_1) = 14.4\ \mathrm{W}$$

3.15

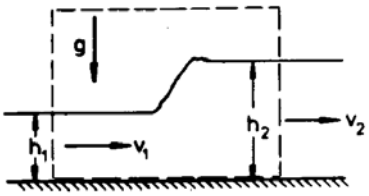


(a)

$$\begin{aligned} -\rho\, v_1^2\, B\, h_1 + \rho\, v_2^2\, B\, h_2 &= \rho\, g\, B\, \frac{h_1^2}{2} - \\ &\quad - \rho\, g\, B\, \frac{h_2^2}{2} \end{aligned}$$

$$\begin{aligned} v_1\, B\, h_1 &= v_2\, B\, h_2 \\ v_1 &= \sqrt{\frac{g}{2}\, \frac{h_2}{h_1}\, (h_1 + h_2)} \\ &= 1.73\ \frac{\mathrm{m}}{\mathrm{s}} \\ v_2 &= 0.87\ \frac{\mathrm{m}}{\mathrm{s}} \end{aligned}$$

(b)

$$\begin{aligned} Fr_1 &= \frac{v_1}{\sqrt{g\, h}} = 1.73 \\ Fr_2 &= 0.61 \end{aligned}$$

(c)

$$\begin{aligned} H_1 - H_2 &= h_1 - h_2 + \frac{1}{2\, g}\, (v_1^2 - v_2^2) \\ &= \frac{(h_2 - h_1)^3}{4\, h_1\, h_2} = 0.0125\ \mathrm{m} \end{aligned}$$

3.16

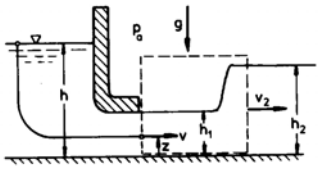


(a) For each streamline it is,

$$\begin{aligned} p_a + \rho\, g\, h &= p + \rho\, g\, z + \frac{\rho}{2}\, v^2 \\ p + \rho\, g\, z &= p_a + \rho\, g\, h_1 \\ v &= \sqrt{2\, g\, (h - h_1)} \\ &= v_1 (\text{independent of z}) \end{aligned}$$

(b)

$$\begin{aligned} \dot{Q} &= v_1\, B\, h_1 \\ \frac{d\dot{Q}}{dh_1} &= 0 \\ h_{1max} = \frac{2}{3}\, h &= 5\ \mathrm{m} \end{aligned}$$

(b)

$$\begin{aligned} Fr_1 &= \frac{v_1}{\sqrt{g\, h}} = 1 \\ h_{1gr} &= \frac{2}{3}\, h = 5\ \mathrm{m} \end{aligned}$$

(c)

$$\begin{aligned}\rho g B\left(\frac{h_1^2}{2}-\frac{h_2^2}{2}\right) &= -\rho v_1^2 B h_1 + \\ &\quad +\rho v_2^2 B h_2 \\ v_1 B h_1 &= v_2 B h_2\end{aligned}$$

$$\begin{aligned}h_2 &= \frac{h_1}{2}\left(\sqrt{1+16\left(\frac{h}{h_1}-1\right)}-1\right) \\ &= 5.93 \text{ m} \\ v_2 &= 4.22 \frac{\text{m}}{\text{s}}\end{aligned}$$

3.17 (a)

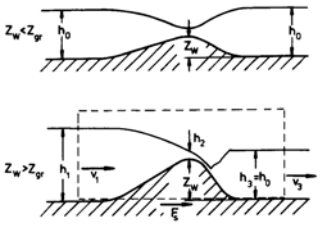


(b)

$$Z_{crit.} + H_{min} = H_0$$

$$\begin{aligned}Z_{crit.} &= h_0 + \frac{\dot{Q}^2}{2 g B^2 h_0^2} - \frac{3}{2}\sqrt[3]{\frac{\dot{Q}^2}{g B^2}} \\ &= 0.446 \text{ m}\end{aligned}$$

(c) $z_W > z_{crit.}$ :

$$\begin{aligned}h_2 &= h_{crit.} = \sqrt[3]{\frac{\dot{Q}^2}{g B^2}} \\ &= 1.170 \text{ m} \\ H_1 &= Z_W + H_{min} \\ \frac{H_1}{H_{min}} &= \frac{Z_W}{H_{min}} + 1 = 1.570\end{aligned}$$

from diagram:

$$\begin{aligned}\frac{h_1}{h_{crit.}} &= 2.26 \\ h_1 &= 2.64 \text{ m}\end{aligned}$$

(Elevation of the upper water)

(d)

$$\begin{aligned}H_1 - H_3 &= H_1 - H_0 \\ &= Z_W - Z_{crit.} \\ &= 0.554 \text{ m}\end{aligned}$$

(e)

$$\begin{aligned}&-\rho v_1^2 B h_1 + \rho v_3^2 B h_3 \\ &= \rho g B\left(\frac{h_1^2}{2} - \frac{h_3^2}{2}\right) + F_s\end{aligned}$$

$$\begin{aligned}F = - F_s &= \frac{\rho g B}{2}(h_1 - h_0)\cdot \\ &\cdot \left(h_1 + h_0 - \frac{2\dot{Q}^2}{g B^2 h_1 h_0}\right) \\ &= 2.60 \cdot 10^5 \text{ N}\end{aligned}$$

3.18

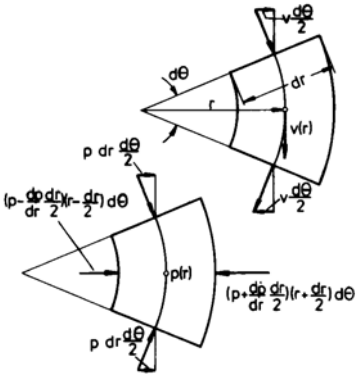


(a)

$$\begin{aligned}&- \rho v^2 dr \frac{d\theta}{2} - \rho v^2 dr \frac{d\theta}{2} = \\ &= \left(p - \frac{dp}{dr}\frac{dr}{2}\right)\left(r - \frac{dr}{2}\right)d\theta - \\ &- \left(p + \frac{dp}{dr}\frac{dr}{2}\right)\left(r + \frac{dr}{2}\right)d\theta + \\ &+ 2 p\, dr \frac{d\theta}{2}\end{aligned}$$

$$\frac{dp}{dr} = \rho \frac{v^2}{r}$$

(b)

$$\begin{aligned}\frac{d}{dr}\left(p + \frac{\rho}{2} v^2\right) &= 0 \\ \frac{dp}{dr} = -\rho v \frac{dv}{dr} &= \rho \frac{v^2}{r} \\ v &= \frac{const.}{r}\end{aligned}$$

3.19 (a)

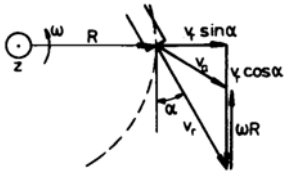


$$\begin{aligned} M_r &= 3\,\rho\, v_r A\,(\boldsymbol{r}\ \mathrm{x}\ \boldsymbol{v}_a)_z \\ &= 3\,\rho\, v_r A\, R(-v_r\,\cos\alpha + \omega\, R) \end{aligned}$$

Determination of $v_r$ :

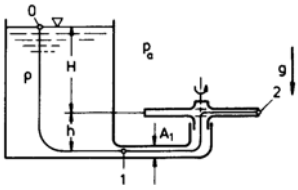


$$\begin{aligned} p_a &= p_a + \frac{\rho}{2}\, v_r^2 - \int_{s_0}^{s_2} \rho\,(\boldsymbol{b}\cdot d\boldsymbol{s}) \\ &= p_a + \frac{\rho}{2}\, v_r^2 - \rho\left(gH + \frac{\omega^2\, R^2}{2}\right) \\ v_r &= \sqrt{2\,g\,H + 2\,\omega^2\, R^2} \end{aligned}$$

with

$$\begin{aligned} \xi &= \frac{\omega\, R}{\sqrt{2\,g\,h}} \text{ and} \\ M_0 &= -3\,\rho\, A\, R\, 2\,g\, H\,\cos\alpha \quad : \\ \frac{M_r}{M_0} &= \sqrt{1+\xi^2}\left(\sqrt{1+\xi^2} - \frac{\xi}{\cos\alpha}\right) \end{aligned}$$

$$\xi^2 = \frac{2\,\frac{M_r}{M_0} + \tan^2\alpha - 1}{2\tan^2\alpha} \cdot \left[\sqrt{1 + \left(\frac{\left(1-\frac{M_r}{M_0}\right)\,2\,\tan\alpha}{2\,\frac{M_r}{M_0} + \tan^2\alpha - 1}\right)^2} - 1\right]$$

$$\begin{aligned} \xi &= 0.07 \\ n &= 1.05\,\frac{1}{\mathrm{s}} \end{aligned}$$

(b)

$$\dot{Q} = 3\, v_r\, A = 2.13\cdot 10^{-3}\ \frac{\mathrm{m}^3}{\mathrm{s}}$$

(c)

$$\begin{aligned} p_a + \rho\, g\,(h+H) &= p_1 + \frac{\rho}{2}\, v_1^2 \\ v_1 &= \frac{\dot{Q}}{A_1} \\ p_1 &= 1.095\cdot 10^5\ \frac{\mathrm{N}}{\mathrm{m}^2} \end{aligned}$$

(d)

$$\begin{aligned} \xi_0 &= \frac{1}{\tan\alpha} = 1.73 \\ \omega_0 &= 163\,\frac{1}{\mathrm{s}} \end{aligned}$$

### 3.2.4 Laminar Flow of Viscous Fluids

4.1

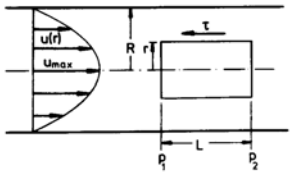


(a)

$$(p_1 - p_2)\,\pi\, r^2 - \tau\, 2\,\pi\, r\, L = 0$$

$$\begin{aligned} \tau &= -\mu\,\frac{du}{dr} \\ r = R: \quad u &= 0 \\ \frac{u(r)}{u_{max}} &= 1 - \left(\frac{r}{R}\right)^2 \end{aligned}$$

(b)

$$\begin{aligned} \frac{u(m)}{u_{max}} &= \frac{\dot{Q}}{u_{max}\,\pi\, R^2} \\ &= 2\int_0^1 \left[1 - \left(\frac{r}{R}\right)^2\right] \times \\ &\quad \times \frac{r}{R}\, d\left(\frac{r}{R}\right) \\ &= \frac{1}{2} \end{aligned}$$

(c)

$$\begin{aligned} \lambda &= \frac{8\,\tau_w}{\rho\, u_m^2} \\ \tau_w &= \frac{4\,\mu\, u_m}{R} \\ \lambda &= \frac{64}{Re} \end{aligned}$$

4.2 For $y \le a$ the fluid behaves as a rigid body.

(a)

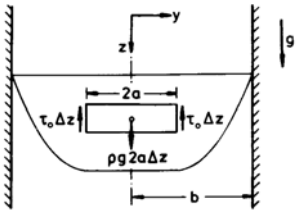


$$\rho\, g\, a\, \Delta z = \tau_0 \Delta z$$
$$a = \frac{\tau_0}{\rho\, g}$$

(b)

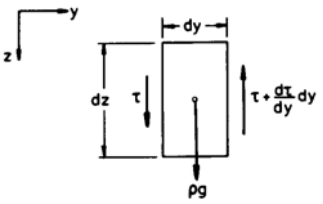


$$a \le y \le b: \quad \frac{d\tau}{dy} = \rho\, g$$
$$\tau = -\mu \frac{dw}{dy} + \tau_0$$
$$y = a: \quad \tau = \tau_0$$
$$y = b: \quad w = 0$$

$$w(y) = \frac{\rho\, g}{2\,\mu}[(b-a)^2 - (y-a)^2]$$

$$0 \le y \le a: \quad w(y) = \frac{\rho\, g}{2\,\mu}(b-a)^2$$

4.3

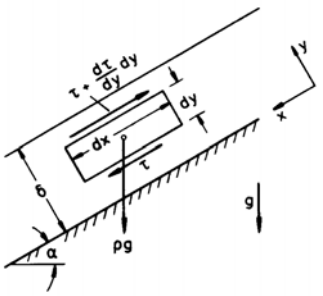


$$\dot{Q} = B \int_0^\delta u(y)\, dy$$
$$\frac{d\tau}{dy} = \rho\, g \sin\alpha$$
$$\tau = -\mu \frac{du}{dy}$$
$$y = 0: \quad u = 0$$
$$y = \delta: \quad \tau = 0$$

$$u(y) = \frac{\rho\, g \sin\alpha}{\mu}\left[\delta y - \frac{y^2}{2}\right]$$
$$\dot{Q} = \frac{\rho\, g\, B \sin\alpha}{3\,\mu}\,\delta^3$$
$$= 1.2 \cdot 10^{-3}\ \frac{\mathrm{m}^3}{\mathrm{s}}$$

4.4 (a)

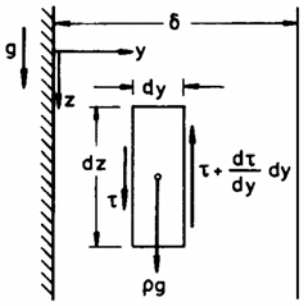


$$-\frac{d\tau}{dy} + \rho\, g = 0$$
$$\tau = -\mu \frac{dw}{dy}$$
$$\frac{d^2w}{dy^2} + \frac{\rho\, g}{\mu} = 0$$
$$y = 0: \quad w = 0$$
$$y = \delta: \quad \tau = 0$$

$$w(y) = \frac{\rho\, g}{\mu}\,\delta^2\left[\frac{y}{\delta} - \frac{1}{2}\left(\frac{y}{\delta}\right)^2\right]$$

(b)

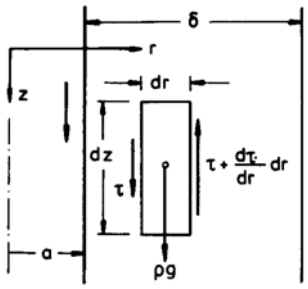


$$\tau\, 2\,\pi\, dz - \left(\tau + \frac{d\tau}{dr}\, dr\right) 2\,\pi\,(r+dr)\, dz + \rho\, g\, \pi \left[(r+dr)^2 - r^2\right] dz = 0$$

$$\begin{aligned} -r\,\frac{d\tau}{dr} - \tau + \rho\, g\, r &= 0 \\ \tau &= -\mu\,\frac{dw}{dr} \end{aligned}$$

$$\begin{aligned} \frac{d}{dr}\left(r\,\frac{dw}{dr}\right) + \frac{\rho\, g}{\mu}\, r &= 0 \\ r = a \;:\quad w &= 0 \\ r = a+\delta \;:\quad \tau &= 0 \end{aligned}$$

$$w(r) = \frac{\rho\, g}{2\,\mu} \times \times \left[(a+\delta)^2 \ln\frac{r}{a} + \frac{a^2 - r^2}{2}\right]$$

4.5 (a)

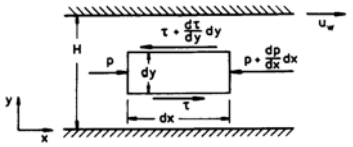


$$\begin{aligned} \frac{dp}{dx} + \frac{d\tau}{dy} &= 0 \\ \tau &= -\mu\,\frac{du}{dy} \\ \frac{d^2u}{dy^2} &= \frac{1}{\mu}\,\frac{dp}{dx} \\ y = 0 :\quad u &= 0 \\ y = H :\quad u &= u_w \end{aligned}$$

$$u(y) = \frac{1}{2\ mu}\,\frac{dp}{dx}\, H^2 \left[\left(\frac{y}{H}\right)^2 - \frac{y}{H}\right] + + u_w\,\frac{y}{H}$$

(b)

$$\frac{\tau(y=H)}{\tau(y=0)} = \frac{u_w + \frac{1}{2\,\mu}\frac{dp}{dx}\, H^2}{u_w - \frac{1}{2\,\mu}\frac{dp}{dx}\, H^2}$$

(c)

$$\begin{aligned} \dot{Q} &= u_m\, B\, H = B \int_0^H u(y)\, dy \\ &= \left(\frac{u_w}{2} - \frac{dp}{dx}\,\frac{H^2}{12\,\mu}\right) BH \end{aligned}$$

(d)

$$u_{max} = -\frac{dp}{dx}\,\frac{H^2}{8\,\mu}$$

(e)

$$\frac{dI_x}{dt} = B \int_0^H \rho\, u(y)^2\, dy = \frac{6}{5}\,\rho\, u_m^2\, BH$$

(f)

$$\frac{\tau_w}{\frac{\rho}{2}\, u_m^2} = \frac{12}{Re}$$

(g)

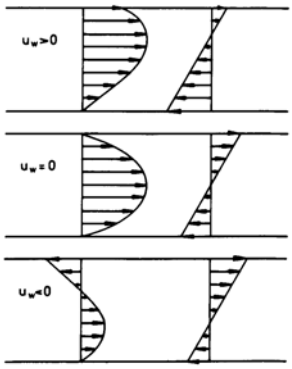


4.6

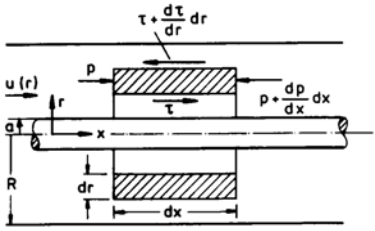

(a)

$$\frac{dp}{dx} + \frac{1}{r}\frac{d(\tau\, r)}{dr} = 0$$

Compare problem 5.4b

$$\tau = -\mu\,\frac{du}{dr}$$

$$\frac{1}{r}\frac{d}{dr}\left(r\,\frac{du}{dr}\right) - \frac{1}{\mu}\frac{dp}{dx} = 0$$

$$r = a: \quad u = 0$$

$$r = R: \quad u = 0$$

$$\begin{aligned} u(r) &= -\frac{1}{4\,\mu}\frac{dp}{dx}\,(R^2 - a^2)\,\times \\ &\times \left[\frac{R^2 - r^2}{R^2 - a^2} - \frac{\ln\left(\frac{r}{R}\right)}{\ln\left(\frac{a}{R}\right)}\right] \end{aligned}$$

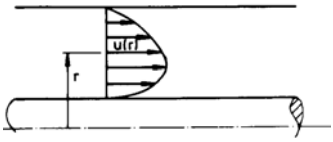


(b)

$$\frac{\tau(r=a)}{\tau(r=R)} = \frac{R}{a}\,\frac{2\,a^2\,\ln\frac{a}{R} + R^2 - a^2}{2\,R^2\,\ln\frac{a}{R} + R^2 - a^2}$$

(c)

$$\begin{aligned} u_m &= \frac{\dot{Q}}{\pi\,(R^2 - a^2)} \\ &= \frac{1}{\pi\,(R^2 - a^2)}\int_a^R u(r)\,2\pi r\,dr \\ &= -\frac{1}{8\mu}\frac{dp}{dx}\,R^2\left[1 + \left(\frac{a}{R}\right)^2 + \right. \\ &\quad \left. + \frac{1 - \left(\frac{a}{R}\right)^2}{\ln\left(\frac{a}{R}\right)}\right] \end{aligned}$$

4.7 (a)

$$\frac{d}{dr}\left[\frac{1}{r}\frac{d}{dr}\,(r\,v)\right] = 0$$

$$r = R_i \;: \quad v = 0$$

$$r = R_a \;: \quad v = \omega\, R_a$$

$$v(r) = \frac{\omega\, R_a^2}{r}\,\frac{r^2 - R_i^2}{R_a^2 - R_i^2}$$

(b)

$$\begin{aligned} \mu &= \left.\frac{\tau}{-r\,\frac{d}{dr}\left(\frac{v}{r}\right)}\right|_{r=R_i} \\ M_z &= -\tau(r = R_i)\,2\pi\, R_i^2\, L \\ \mu &= \frac{M_z}{4\,\pi\,\omega R_i^2\, L}\left[1 - \left(\frac{R_i}{R_a}\right)^2\right] \\ &= 10^{-2}\,\frac{\mathrm{Ns}}{\mathrm{m}^2} \end{aligned}$$

4.8

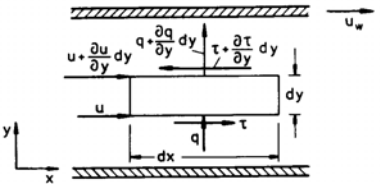


$$\rho\,\frac{de}{dt}\,dx\,dy =$$

$$\begin{aligned} &= \left[q - \left(q + \frac{\partial q}{\partial y}\,dy\right)\right]\,dx + \tau\,u\,dx - \\ &- \left(\tau + \frac{\partial \tau}{\partial y}\,dy\right)\left(u + \frac{\partial u}{\partial y}\,dy\right)\,dx \end{aligned}$$

$$\begin{aligned} \frac{d\tau}{dy} &= 0 \\ q &= -\lambda\,\frac{\partial T}{\partial y} \\ \tau &= -\mu\,\frac{\partial u}{\partial y} \\ \rho\,\frac{de}{dt} &= \lambda\,\frac{\partial^2 T}{\partial y^2} + \mu\left(\frac{\partial u}{\partial y}\right)^2 \end{aligned}$$

(a) It follows from problem 5.5a):

$$\begin{aligned} u(y) &= u_w\frac{y}{H} \\ \rho\,\frac{de}{dt} &= \rho\, c_v\left(\frac{\partial T}{\partial t} + u\,\frac{\partial T}{\partial x} + v\,\frac{\partial T}{\partial y}\right) \\ &= 0 \\ \frac{d^2T}{dy^2} &= -\frac{\mu}{\lambda}\left(\frac{u_w}{H}\right)^2 \\ y &= H: \quad T = T_w \\ y &= 0: \quad q = 0 \\ T(y) &= T_w + \frac{\mu}{2\,\lambda}\left(\frac{u_w}{H}\right)^2 (H^2 - y^2) \end{aligned}$$

(b)

$$q_w = -\lambda \left.\frac{dT}{dy}\right|_{y=H} = \frac{\mu\, u_w^2}{H}$$

(c)

$$\begin{aligned}
h_0 &= c_p\, T + \frac{\boldsymbol{v}^2}{2} = c_p\, T + \frac{u^2}{2} \\
h_0 &= \text{const:} \quad \nabla\, h_0 = 0 \\
\frac{\partial h_0}{\partial x} &= c_p\, \frac{\partial T}{\partial x} + \frac{\partial(\frac{u^2}{2})}{\partial x} = 0 \\
\frac{\partial h_0}{\partial y} &= c_p\, \frac{\partial T}{\partial y} + \frac{\partial(\frac{u^2}{2})}{\partial y} \\
&= c_p\, \frac{dT}{dy} + u\, \frac{du}{dy} \\
&= \left(1 - \frac{\mu\, c_p}{\lambda}\right) \left(\frac{u_w}{H}\right)^2 y \\
Pr &= \frac{\mu\, c_p}{\lambda} = 1: \quad \frac{\partial h_0}{\partial y} = 0
\end{aligned}$$

(d)

$$\begin{aligned}
\frac{\partial T}{\partial y} &= 0 \\
\frac{dT}{dt} &= \frac{\mu}{\rho\, c_v} \left(\frac{u_w}{H}\right)^2 \\
t &= 0: \quad T = T_0 \\
T(t) &= T_0 + \frac{\mu}{\rho\, c_v} \left(\frac{u_w}{H}\right)^2 t
\end{aligned}$$

4.9 (a)

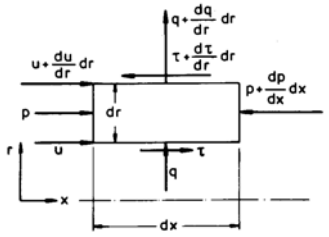


Velocity distribution:

$$\begin{aligned}
\tau + r\, \frac{dp}{dx} + r\, \frac{d\tau}{dr} &= 0 \\
\tau &= -\mu\, \frac{du}{dr}
\end{aligned}$$

$$r\, \frac{dp}{dx} - \mu\, \frac{d}{dr}\left(r\, \frac{du}{dr}\right) = 0$$

$$\begin{aligned}
r = R &: \quad u = 0 \\
r = 0 &: \quad \frac{du}{dr} = 0
\end{aligned}$$

Temperature distribution:

$$\begin{aligned}
0 &= q\, 2\, \pi\, r\, dx + \tau\, u\, 2\pi\, r\, dx - \\
&- \left(q + \frac{dq}{dr}\, dr\right)\, 2\pi\, (r + dr)\, dx - \\
&- \left(\tau + \frac{d\tau}{dr}\, dr\right) \left(u + \frac{du}{dr}\, dr\right) \cdot \\
&\cdot \quad 2\, \pi\, (r + dr)\, dx + \\
&+ \left[p - \left(p + \frac{dp}{dx}\, dx\right)\right] \cdot \\
&\cdot \quad u\, \pi\, \left[(r + dr)^2 - r^2\right]
\end{aligned}$$

$$\begin{aligned}
q &= -\lambda \frac{dT}{dr} \\
\lambda\, \frac{d}{dr}\left(r\, \frac{dT}{dr}\right) &+ \mu\, r \left(\frac{du}{dr}\right)^2 = 0 \\
r = R &: \quad T = T_w \\
r = 0 &: \quad \frac{dT}{dr} = 0
\end{aligned}$$

(b) It follows from problem 5.1a

$$\begin{aligned}
\frac{u(r)}{u_{max}} &= 1 - \left(\frac{r}{R}\right)^2 \\
T - T_w &= \frac{\mu\, u_{max}^2}{4\, \lambda} \left[1 - \left(\frac{r}{R}\right)^4\right]
\end{aligned}$$

$r = 0$ :

$$\begin{aligned}
T_{max} - T_w &= \frac{\mu\, u_{max}^2}{4\, \lambda} \\
\frac{T - T_w}{T_{max} - T_w} &= 1 - \left(\frac{r}{R}\right)^4
\end{aligned}$$

4.10 (a)

$$Re \left(\frac{h_1}{L}\right)^2 = 1.6 \cdot 10^{-3}$$

(b)

$$\begin{aligned}
\frac{\dot{Q}}{B} &= \int_0^{h(x)} u(x,y)\, dy \\
&= const. \\
\frac{dp}{dx} &= \mu\, \frac{\partial^2 u}{\partial y^2} \\
y = 0 &: \quad u = u_\infty \\
y = h(x) &: \quad u = 0
\end{aligned}$$

$$u(x,y) = u_\infty \left(1 - \frac{y}{h(x)}\right) -$$
$$-\frac{h^2(x)}{2\,\eta}\,\frac{y}{h(x)}\left(1-\frac{y}{h(x)}\right)\frac{dp}{dx}$$
$$\frac{\dot{Q}}{B} = \frac{u_\infty\,h(x)}{2} - \frac{h^3(x)}{12\,\mu}\,\frac{dp}{dx}$$

$$x = 0: \quad p = p_\infty$$

$$\begin{aligned} p(x) &= p_\infty + 6\,\mu\,u_\infty \int_0^x \frac{dx'}{h^2(x')} - \\ &- 12\,\mu\left(\frac{\dot{Q}}{B}\right)\int_0^x \frac{dx'}{h^3(x')} \end{aligned}$$

With $p(x=L) = p_\infty$ yields:

$$\begin{aligned} \frac{\dot{Q}}{B} &= \frac{u_\infty}{2}\,\frac{\int_0^L \frac{dx}{h^2(x)}}{\int_0^L \frac{dx}{h^3(x)}} \\ \frac{\dot{Q}}{B} &= \frac{3}{4}\,u_\infty\,h_1\frac{e^{\frac{2}{5}}-1}{e^{\frac{3}{5}}-1} \\ &= 4.49\cdot 10^{-5}\,\frac{\mathrm{m}^2}{\mathrm{s}} \end{aligned}$$

(c) With

$$\begin{aligned} K &= \frac{e^{\frac{2}{5}}-1}{e^{\frac{3}{5}}-1}: \\ p(x) &= p_\infty + 15\frac{\mu\,u_\infty}{h_1}\frac{L}{h_1}\cdot \\ &\cdot \quad \left[e^{\frac{2x}{5L}} - K\,e^{\frac{3x}{5L}} + K - 1\right] \end{aligned}$$

(d)

$$\frac{F_{py}}{B} = \int_0^L (p(x) - p_\infty)\,dx$$

$$= 15\mu\,u_\infty\left(\frac{L}{h_1}\right)^2\left[\frac{5}{6}\,(e^{\frac{2}{5}}-1)+K-1\right]$$

$$= 3035\,\frac{\mathrm{N}}{\mathrm{m}}$$

(e)

$$\begin{aligned} \frac{P}{B} &= u_\infty \int_0^L \tau_{xy}(x, y=0)\,dx \\ \tau_{xy} &= -\mu\,\frac{du}{dr} \end{aligned}$$

$$\begin{aligned} &= \frac{\mu\,u_\infty}{h(x)}\left[1 + 3\left(1 - \frac{3K}{2}\,\frac{h_1}{h(x)}\right)\times\right. \\ &\left.\times\left(1 - 2\,\frac{y}{h(x)}\right)\right] \end{aligned}$$

$$\begin{aligned} \frac{P}{B} &= 20\,\mu\,u_\infty^2\,\frac{L}{h_1}\times \\ &\times\left[e^{\frac{1}{5}} - 1 - \frac{9K}{16}\,(e^{\frac{2}{5}}-1)\right] \\ &= 55.9\,\frac{\mathrm{W}}{\mathrm{m}} \end{aligned}$$

4.11

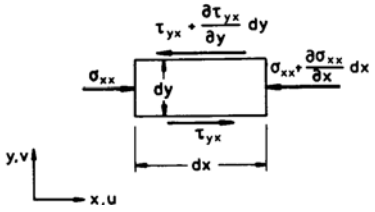


$$\begin{aligned} \frac{dI_x}{dt} &= \int_\tau \frac{\partial(\rho\,u)}{\partial t}\,d\tau + \int_A \rho\,u\,(\boldsymbol{v}\cdot\boldsymbol{n})\,dA \\ &= \sum F_x \end{aligned}$$

$$\int_\tau \frac{\partial(\rho\,u)}{\partial t}\,d\tau = \left(\rho\,\frac{\partial u}{\partial t} + u\,\frac{\partial \rho}{\partial t}\right)dx\,dy\,dz$$

$$\int_A \rho\,u\,(\boldsymbol{v}\cdot\boldsymbol{n})\,dA =$$
$$\left[-\rho\,u^2 + \left(\rho\,u^2 + \frac{\partial(\rho\,u^2)}{\partial x}\,dx\right)\right]\,dy\,dz -$$
$$-\left[-\rho\,uv + \left(\rho\,uv + \frac{\partial(\rho\,uv)}{\partial y}\,dy\right)\right]dx\,dz$$

$$\begin{aligned} &= \left[\rho\,u\,\frac{\partial u}{\partial x} + \rho\,v\,\frac{\partial u}{\partial y} + \right. \\ &\left. + u\left(\frac{\partial(\rho\,u)}{\partial x} + \frac{\partial(\rho\,v)}{\partial y}\right)\right]\times \\ &\times dx\,dy\,dz \end{aligned}$$

Continuity equation:

$$\frac{\partial \rho}{\partial t} + \frac{\partial(\rho\,u)}{\partial x} + \frac{\partial(\rho\,v)}{\partial y} = 0$$

$$\sum F_x = -\left(\frac{\partial \sigma_{xx}}{\partial x} + \frac{\partial \tau_{xy}}{\partial y}\right) dx\, dy\, dz$$

$$(\tau_{yx} = \tau_{xy})$$

$$\rho\left(\frac{\partial u}{\partial t} + u\frac{\partial u}{\partial x} + v\frac{\partial u}{\partial y}\right) = -\left(\frac{\partial \sigma_{xx}}{\partial x} + \frac{\partial \tau_{xy}}{\partial y}\right)$$

4.12

$$\begin{aligned} \mu &= const.: \\ F_{rx} &= \mu\left(\frac{\partial^2 u}{\partial x^2} + \frac{\partial^2 u}{\partial y^2} + \frac{\partial^2 u}{\partial z^2}\right) + \\ &\quad + \frac{\mu}{3}\frac{\partial}{\partial x}(\nabla \cdot \boldsymbol{v}) \\ \rho &= const.: \\ F_{rx} &= \mu\left(\frac{\partial^2 u}{\partial x^2} + \frac{\partial^2 u}{\partial y^2} + \frac{\partial^2 u}{\partial z^2}\right) \end{aligned}$$

### 3.2.5 Pipe Flows

5.1

$$\begin{aligned} \mu &= \frac{\rho\, \bar{u}_m\, D}{Re} \\ \bar{u}_m &= \frac{4\,\tau}{\pi\, D^2\, T} \\ \rho\, g\,(h+L) &= (1 + \lambda\frac{L}{D} + \zeta_e)\frac{\rho}{2}\,\bar{u}_m^2 \end{aligned}$$

Assumption: Laminar flow

$$\begin{aligned} \zeta_e &= 1.16 \\ \lambda &= 11.92 \\ Re &= \frac{64}{\lambda} = 5.37 \end{aligned}$$

Intake region:

$$\begin{aligned} L_e &= 0.029\, Re\, D \\ &= 0.16 \cdot 10^{-3}\ \mathrm{m} \ll L \\ \mu &= 8.40 \cdot 10^{-3}\ \frac{\mathrm{Ns}}{\mathrm{m}^2} \end{aligned}$$

5.2

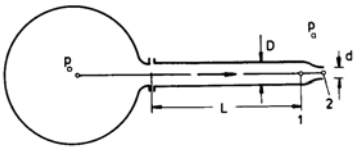


(a)

$$p_1 + \frac{\rho}{2}\,\bar{u}_{m1}^2 = p_a + \frac{\rho}{2}\,\bar{u}_{m2}^2$$

$$\begin{aligned} \bar{u}_{m1}^2\,\frac{\pi\, D^2}{4} &= \bar{u}_{m2}^2\,\frac{\pi\, d^2}{4} \\ \bar{u}_{m1}^2 &= \sqrt{\frac{2(p_1 - p_a)}{\rho}\,\frac{1}{\left(\frac{D}{d}\right)^4 - 1}} \\ &= 1\ \frac{\mathrm{m}}{\mathrm{s}} \\ \bar{u}_{m2} &= 4\ \frac{\mathrm{m}}{\mathrm{s}} \end{aligned}$$

(b)

$$\begin{aligned} p_0 &= p_1 + (1 + \lambda\,\frac{L}{D})\,\frac{\rho}{2}\,\bar{u}_{m1}^2 \\ Re_1 &= \frac{\rho\,\bar{u}_{m1}\,D}{\mu} = 10^4 \\ \lambda &= \frac{0.316}{\sqrt[4]{Re}} = 0.0316 \\ p_0 &= 2.66 \cdot 10^5\ \frac{\mathrm{N}}{\mathrm{m}^2} \end{aligned}$$

(c)

$$\bar{u}_{m2} = \sqrt{\frac{2\,(p_0 - p_a)}{\rho}} = 18.22\ \frac{\mathrm{m}}{\mathrm{s}}$$

5.3

$$\begin{aligned} \dot{Q} &= 25\frac{\pi}{4}\,(\bar{u}_{m1}\,D_1^2 + \bar{u}_{m2}\,D_2^2) \\ \Delta p &= (1 + \lambda\,\frac{L}{D_1} + \zeta)\frac{\rho}{2}\,\bar{u}_{m1}^2 \\ &= (1 + \lambda\,\frac{L}{D_2} + \zeta)\frac{\rho}{2}\,\bar{u}_{m2}^2 \\ \bar{u}_{m1} &= \sqrt{\frac{2\,\Delta p}{\rho\,(1 + \lambda\,\frac{L}{D_1} + \zeta)}} \\ \bar{u}_{m2} &= \sqrt{\frac{2\,\Delta p}{\rho\,(1 + \lambda\,\frac{L}{D_2} + \zeta)}} \\ \dot{Q} &= 0.518\ \frac{\mathrm{m}^3}{\mathrm{s}} \end{aligned}$$

5.4

$$\begin{aligned} \Delta p &= \lambda\,\frac{L}{D}\,\frac{\rho}{2}\,\bar{u}_m^2 \\ \bar{u}_m &= \frac{1}{\sqrt{\lambda}}\sqrt{\frac{2\,\Delta p}{\rho}\,\frac{D}{L}} \end{aligned}$$

$$\begin{aligned}
\bar{u}_m \frac{\rho\, D}{\mu}\sqrt{\lambda} &= Re\sqrt{\lambda} \\
&= \sqrt{\frac{2\,\Delta p}{\rho}\frac{D}{L}}\frac{\rho\, D}{\mu} \\
(Re\,\sqrt{\lambda})_{crit} &= 2300\sqrt{\frac{64}{2300}} = 384
\end{aligned}$$

Oil:

$$\begin{aligned}
Re\,\sqrt{\lambda} &= 283 \\
\frac{1}{\sqrt{\lambda}} &= \frac{Re\,\sqrt{\lambda}}{64} \\
u_m &= 1.56\ \frac{\mathrm{m}}{\mathrm{s}}
\end{aligned}$$

Water:

$$\begin{aligned}
Re\,\sqrt{\lambda} &= 3.16\cdot 10^4 \\
\frac{1}{\sqrt{\lambda}} &= 2.0\,\log(Re\,\sqrt{\lambda}) - 0.8 \\
\bar{u}_m &= 2.59\ \frac{\mathrm{m}}{\mathrm{s}}
\end{aligned}$$

5.5 (a)

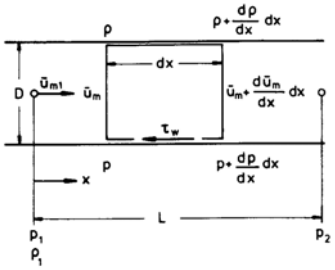


$$\begin{aligned}
\rho\,\bar{u}_m &= \left(\rho + \frac{d\rho}{dx}\,dx\right)\times \\
&\quad \times\left(\bar{u}_m + \frac{d\bar{u}_m}{dx}dx\right) \\
&= \rho_1\,\bar{u}_{m1}
\end{aligned}$$

$$\begin{aligned}
\left(\rho + \frac{d\rho}{dx}\,dx\right)\left(\bar{u}_m + \frac{d\bar{u}_m}{dx}dx\right)^2\frac{\pi D^2}{4} - \\
-\rho\,\bar{u}_m^2\frac{\pi D^2}{4} = -\tau_w\,\pi\,D\,dx + \\
+\left[p - \left(p + \frac{dp}{dx}dx\right)\right]\frac{\pi D^2}{4}
\end{aligned}$$

$$\begin{aligned}
\lambda &= \frac{8\,\tau_w}{\rho\,\bar{u}_m^2} \\
\frac{dp}{dx} &+ \rho_1\,\bar{u}_{m1}\frac{d\bar{u}_m}{dx} + \frac{\lambda}{D}\frac{\rho}{2}\,\bar{u}_m^2 = 0
\end{aligned}$$

(b) Compressible flow:

$$\rho\frac{d\bar{u}_m}{dx} + \bar{u}_m\frac{d\rho}{dx} = 0$$

(Continuity equation)

$$\begin{aligned}
\rho &= \frac{\rho_1}{p_1}\,p \quad (T = const.) \\
\frac{d\rho}{dx} &= \frac{\rho_1}{p_1}\,\frac{dp}{dx} \\
\frac{dp}{dx} &- \frac{\rho_1\,p_1\,\bar{u}_{m1}^2}{p^2}\,\frac{dp}{dx} \\
&+ \frac{\lambda}{2\,D}\frac{\rho_1\,p_1\,\bar{u}_{m1}^2}{p} \\
&= 0
\end{aligned}$$

$$\begin{aligned}
Re &= Re_1 = 0.533\cdot 10^5 \\
\lambda &= \frac{0.316}{\sqrt[4]{Re}} = 0.0208
\end{aligned}$$

$$\begin{aligned}
\int_1^2 p\,dp &- \rho_1\,p_1\,\bar{u}_{m1}^2\int_1^2\frac{dp}{p} + \\
&+ \frac{\lambda}{2\,D}\,\rho_1\,p_1\,\bar{u}_{m1}^2\int_1^2 dx \\
&= 0
\end{aligned}$$

$$\begin{aligned}
L &= \frac{D}{\lambda}\frac{p_1}{\rho_1\,\bar{u}_{m1}^2}\left[1 - \left(\frac{p_2}{p_1}\right)^2\right] - \\
&- \frac{D}{\lambda}\,\ln\left(\frac{p_1}{p_2}\right)^2 = 287.9\ \mathrm{m}
\end{aligned}$$

Incompressible flow:

$$\begin{aligned}
\frac{d\bar{u}_m}{dx} &= 0 \\
\frac{dp}{dx} &= -\frac{\lambda}{D}\frac{\rho_1}{2}\,\bar{u}_{m1}^2 \\
L &= 2\,\frac{D}{\lambda}\,\frac{p_1 - p_2}{\rho_1\,\bar{u}_{m1}^2} = 384.7\ \mathrm{m}
\end{aligned}$$

5.6 (a)

$$r = R - y$$

$$\begin{aligned}
\dot{I} &= \int_0^R \rho\,u^2\,2\pi\,r\,dr \\
&= 2\rho\,u_m^2\,\pi\,R\int_0^1\left(\frac{u}{u_m}\right)^2\frac{r}{R}d\left(\frac{r}{R}\right)
\end{aligned}$$

$$
\begin{aligned}
\delta &= 0: \quad \frac{u}{u_m} = 1 \\
\dot{I} &= \rho\, u_m^2\, \pi\, R^2 \\
\delta &= R: \\
\frac{u}{u_m} &= 2\left[1 - \left(\frac{r}{R}\right)^2\right] \\
\dot{I} &= 1.33\, \rho\, u_m^2\, \pi\, R^2
\end{aligned}
$$

$$
\begin{aligned}
\delta &= \frac{R}{2}: \\
\frac{u}{u_m} &= \begin{cases} \frac{96\,r}{17R}\left(1-\frac{r}{R}\right) & \frac{R}{2} \le r \le R \\ \frac{24}{17} & 0 \le r \le \frac{R}{2} \end{cases}
\end{aligned}
$$

$$
\begin{aligned}
\dot{I} &= 2\rho\, u_m^2 \pi\, R^2 \times \\
&\quad \times \left[\int_0^{0.5} \left(\frac{24}{17}\right)^2 \frac{r}{R}\, d\left(\frac{r}{R}\right) + \right. \\
&\quad \left. + \int_{0.5}^{1} \left[\frac{96}{17}\,\frac{r}{R}\left(1-\frac{r}{R}\right)\right]^2 \times \right. \\
&\quad \left. \times \frac{r}{R}\, d\left(\frac{r}{R}\right)\right] \\
&= 1.196\, \rho\, u_m^2\, \pi\, R^2
\end{aligned}
$$

(b)

$$
\tau_w = \mu\, u_m\, \frac{\frac{2}{\delta}}{1 - \frac{2}{3}\,\frac{\delta}{R} + \frac{1}{6}\left(\frac{\delta}{R}\right)^2}
$$

$$
\begin{aligned}
\delta \to 0 &: \quad \tau_w \to \infty \\
\delta \to R &: \quad \tau_w = 4\frac{\mu\, u_m}{R} \\
\delta \to \frac{R}{2} &: \quad \tau_w = 5.65\frac{\mu\, u_m}{R}
\end{aligned}
$$

5.7 (a)

$$
\begin{aligned}
p_1 + \frac{\rho}{2}\,\bar{u}_{m1}^2 &= p_a + \left(1 + \lambda_2 \frac{L_2}{D_2}\right) \times \\
&\quad \times \frac{\rho}{2}\,\bar{u}_{m2}^2 + \\
&\quad + \left(\zeta + \lambda_1\,\frac{L_1}{D_1}\right)\,\frac{\rho}{2}\,\bar{u}_{m1}^2 \\
\zeta &= \left(1 - \frac{D_1^2}{D_2^2}\right)^2 \\
\bar{u}_{m1}\, D_1^2 &= \bar{u}_{m2}\, D_2^2
\end{aligned}
$$

$$
\begin{aligned}
Re_1 &= 10^4 \qquad \lambda_1 = 0.0316 \\
Re_2 &= 5 \cdot 10^3 \quad \lambda_1 = 0.0376
\end{aligned}
$$

$$
\begin{aligned}
L_2 &= \frac{D_2}{\lambda_2}\left[\left(2\,\frac{D_1^2}{D_2^2} - \lambda_1\,\frac{L_1}{D_1}\right) \times \right. \\
&\quad \left. \times \frac{D_2^4}{D_1^4} - 2\right] \\
&= 1.0\ \mathrm{m}
\end{aligned}
$$

(b)

$$
\begin{aligned}
\Delta p_v &= p_1 - p_a + \left(1 - \frac{D_1^4}{D_2^4}\right)\frac{\rho}{2}\,\bar{u}_{m1}^2 \\
&= 117.2\ \frac{\mathrm{N}}{\mathrm{m}^2}
\end{aligned}
$$

5.8

$$
\begin{aligned}
\rho\, g\, h &= \left(\lambda\frac{L}{D} + 2\,\zeta_K + \zeta_v\right)\,\frac{\rho}{2}\,\bar{u}_m^2 + \\
&\quad + \frac{\rho}{2}\,u_d^2 \\
u_d\, d^2 &= \bar{u}_m\, D^2 \\
\dot{Q} &= u_d\,\frac{\pi\, d^2}{4}
\end{aligned}
$$

$$
= \sqrt{\frac{2\, g\, h}{1 + \left(\frac{d}{D}\right)^4 \left(\lambda\,\frac{L}{D} + 2\,\zeta_K + \zeta_V\right)}}\,\frac{\pi\, d^2}{4}
$$

$$
H = \frac{u_d^2}{2\, g}
$$

with losses:
(a)

$$
\dot{Q} = 5.79 \cdot 10^{-3}\ \frac{\mathrm{m}^3}{\mathrm{s}} \qquad H = 6.96\ m
$$

(b)

$$
\dot{Q} = 9.82 \cdot 10^{-3}\ \frac{\mathrm{m}^3}{\mathrm{s}} \qquad H = 1.25\ m
$$

loss-free:
(a)

$$
\dot{Q} = 6.94 \cdot 10^{-3}\ \frac{\mathrm{m}^3}{\mathrm{s}} \qquad H = h
$$

(b)

$$
\dot{Q} = 27.77 \cdot 10^{-3}\ \frac{\mathrm{m}^3}{\mathrm{s}} \qquad H = h
$$

5.9 (a)

$$\lambda = \frac{0.316}{\sqrt[4]{Re}}$$

$$\bar{u}_m = \frac{\mu}{\rho\, D}\, Re$$

$$\tau_w = \frac{\lambda\, \rho\, \bar{u}_m^2}{8} = 2.22\ \frac{\mathrm{N}}{\mathrm{m}^2}$$

(b)

$$\frac{\bar{u}_m}{u_*} = \frac{\bar{u}_{max}}{u_*} - 4.07$$

$$\lambda = 8\left(\frac{u_*}{\bar{u}_m}\right)^2$$

$$\frac{\bar{u}_m}{\bar{u}_{max}} = \frac{1}{1 + 4.07\sqrt{\frac{\lambda}{8}}} = 0.84$$

(c)

$$\frac{y\, u_*}{\nu} = 5 = \frac{\bar{u}}{u_*} \quad \text{(Viscous sub-layer)}$$

$$\bar{u} = 5\sqrt{\frac{\lambda}{8}}\, \bar{u}_m = 0.236\ \frac{\mathrm{m}}{\mathrm{s}}$$

(for y = 0.11 mm)

$$\frac{y\, u_*}{\nu} = 50$$

(Logarithmic velocity distribution)

$$\frac{\bar{u}}{u_*} = 2.5\, \ln\left(\frac{y\, u_*}{\nu}\right) + 5.5$$

$$\bar{u} = 0.720\ \frac{\mathrm{m}}{\mathrm{s}}$$

(for y = 1.1 mm)

(d)

$$l = 0.4\, y = 0.4\, \frac{y\, u_*}{\nu}\, \frac{\nu}{\sqrt{\frac{\lambda}{8}}\, \bar{u}_m}$$

$$= 0.85\ \mathrm{mm}$$

5.10 (a)

$$r = R - y$$

$$\frac{\bar{u}_m}{\bar{u}_{max}} = \frac{\dot{Q}}{\pi\, R^2\, \bar{u}_{max}}$$

$$= 2\int_0^1 \left(1 - \frac{r}{R}\right)^{\frac{1}{7}} \frac{r}{R}\, d\left(\frac{r}{R}\right)$$

$$= \frac{49}{60}$$

(b)

$$\frac{\dot{I}}{\rho\, \bar{u}_m\, \pi\, R^2} = \frac{\int_0^R \rho\, \bar{u}^2\, 2\, \pi\, r\, dr}{\rho\, \bar{u}_m^2\, \pi\, R^2}$$

$$= 2\left(\frac{\bar{u}_{max}}{\bar{u}}\right)^2 \cdot$$

$$\cdot \int_0^1 \left(1 - \frac{r}{R}\right)^{\frac{2}{7}} \frac{r}{R}\, d\left(\frac{r}{R}\right)$$

$$= \frac{50}{49}$$

5.11 (a)

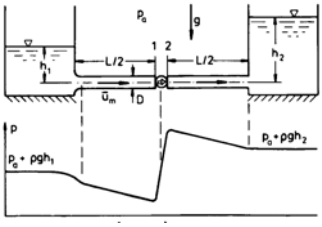


(b)

$$p_a + \rho\, g\, h_1 = p_1 + \left(1 + \lambda\frac{L}{2D}\right)\frac{\rho}{2}\, \bar{u}_m^2$$

$$\dot{Q} = \bar{u}_m\, \frac{\pi\, D^2}{4}$$

$$Re = \frac{\bar{u}_m\, D}{\nu} = 8 \cdot 10^5$$

$$\frac{R}{k_s} = 250$$

(From diagram, page 29)

$$\lambda = 0.024$$

$$p_1 = 1.22 \cdot 10^5\ \frac{\mathrm{N}}{\mathrm{m}^2}$$

(c)

$$p_2 = p_a + \rho\, g\, h_2 + \lambda\, \frac{L}{2D}\, \frac{\rho}{2}\, \bar{u}_m^2$$

$$= 3.77 \cdot 10^5\ \frac{\mathrm{N}}{\mathrm{m}^2}$$

(d)

$$P = \dot{Q}(p_2 - p_1) = 160.5\ \mathrm{kW}$$

5.12

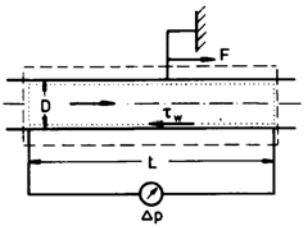


(a)

$$\begin{aligned} \Delta p &= \lambda \frac{L}{D} \frac{\rho}{2} \bar{u}_m^2 \\ \dot{Q} &= \bar{u}_m \frac{\pi D^2}{4} \\ \lambda &= \frac{\pi^2 \Delta p D^5}{8 \rho L \dot{Q}^2} = 0.0356 \end{aligned}$$

(b)

$$Re = \frac{\rho \bar{u}_m D}{\eta} = 1.8 \cdot 10^5$$

(From diagram, page 29)

$$\begin{aligned} \frac{R}{k_s} &= 60 \\ k_s &= 4.2 \text{ mm} \end{aligned}$$

(c)

$$\begin{aligned} \Delta p \frac{\pi D^2}{4} - \tau_w \pi DL &= 0 \\ \tau_w = \Delta p \frac{D}{4L} &= 16 \frac{\text{N}}{\text{m}^2} \\ F = -\Delta p \frac{\pi D^2}{4} &= -2517 \text{ N} \end{aligned}$$

(d)

$$\lambda = 0.016$$

(From diagram page 29)

$$\Delta p = 5.8 \cdot 10^3 \frac{\text{N}}{\text{m}^2}$$

5.13

$$\begin{aligned} \frac{P_1}{P_2} &= \frac{\left(1 + \lambda_1 \frac{L}{D_1}\right) \frac{\rho}{2} \bar{u}_{m1}^2}{\left(1 + \lambda_2 \frac{L}{D_2}\right) \frac{\rho}{2} \bar{u}_{m2}^2} \\ \dot{Q} &= \bar{u}_m \frac{\pi D^2}{4} \\ \frac{1}{\sqrt{\lambda}} &= 2.0 \log\left(\frac{R}{k_s}\right) + 1.74 \\ \frac{P_1}{P_2} &= \frac{1 + \lambda_1 \frac{L}{D_1}}{1 + \lambda_2 \frac{L}{D_2}} \left(\frac{D_2}{D_1}\right)^4 = 39.2 \end{aligned}$$

5.14

$$\begin{aligned} \lambda_{ps} \frac{L}{D} \frac{\rho}{2} \bar{u}_{mps}^2 &= \lambda_{ch} \frac{L_{ch}}{d_h} \frac{\rho}{2} \bar{u}_{mch}^2 \\ d_h &= a \end{aligned}$$

$$Re_{ch} = \frac{\rho a}{\mu} \frac{\dot{Q}}{a^2} = 10^5 \qquad \lambda_{ch} = 0.018$$

$$\begin{aligned} Re_{ps} &= \frac{\rho D}{\mu} \frac{\dot{Q}}{100 \frac{\pi D^2}{4}} \qquad \lambda_{ch} = 0.030 \\ &= 1.27 \cdot 10^4 \end{aligned}$$

$$L_{ch} = 13.57 \text{ m}$$

5.15

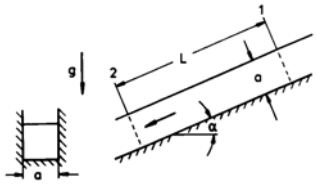


$$\rho g L \sin\alpha + \frac{\rho}{2} \bar{u}_m^2 = \left(1 + \lambda \frac{L}{d_h}\right) \frac{\rho}{2} \bar{u}_m^2$$

$$d_h = \frac{4 a^2}{3 a}$$

$$\begin{aligned} Re_h &= \frac{\rho d_h}{\mu} \frac{\dot{Q}}{a^2} = 8 \cdot 10^3 \quad \lambda = 0.033 \\ \alpha &= 0.02^\circ \\ \frac{\Delta p_v}{L} &= \lambda \frac{1}{d_h} \frac{\rho}{2} \left(\frac{\dot{Q}}{a^2}\right)^2 = 3.61 \frac{\text{N}}{\text{m}^3} \end{aligned}$$

### 3.2.6 Similar Flows

6.1

$$\bar{u} = \frac{u}{v_1}, \quad \bar{v} = \frac{v}{v_1}, \quad \bar{p} = \frac{p}{\Delta p_1}, \quad \bar{\rho} = \frac{\rho}{\rho_1},$$
$$\bar{\mu} = \frac{\mu}{\mu_1}, \quad \bar{x} = \frac{x}{L_1}, \quad \bar{y} = \frac{y}{L_1}, \quad \bar{t} = \frac{t}{t_1}$$

$$\begin{aligned} &\bar{\rho} \left(Sr \frac{\partial \bar{u}}{\partial t} + \bar{u} \frac{\partial \bar{u}}{\partial \bar{x}} + \bar{v} \frac{\partial \bar{u}}{\partial \bar{y}}\right) \\ &= -Eu \frac{\partial \bar{p}}{\partial \bar{x}} + \frac{\bar{\mu}}{Re} \left(\frac{\partial^2 \bar{u}}{\partial \bar{x}^2} + \frac{\partial^2 \bar{u}}{\partial \bar{y}^2}\right) \end{aligned}$$

$$Sr = \frac{L_1}{v_1 t_1}, \quad Eu = \frac{\Delta p_1}{\rho_1 v_1^2},$$
$$Re = \frac{\rho_1 v_1 L_1}{\mu_1}$$

6.2

$$f_1(Re,Eu) = 0: \quad Eu = f_2(Re)$$
$$\lambda = \frac{D}{L}\,\frac{\Delta p}{\frac{\varrho}{2}\,u_m^2} = 2\frac{D}{L}\,Eu = f_3(Re)$$

6.3 (a)

$$\begin{aligned} L^3\,T^{-1} &= (M\,L^{-2}\,T^{-2})^\alpha \\ &\cdot\ (M\,L^{-1}\,T^{-1})^\beta\,L^\gamma \\ \alpha &= 1 \quad \beta = -1 \quad \gamma = 4 \\ \dot{Q} &\sim \frac{\Delta p\,D^4}{L\,\mu} \end{aligned}$$

(b)

$$\begin{aligned} \lambda &= \frac{D}{L}\,\frac{\Delta p}{\frac{\varrho}{2}\,u_m^2} \\ \frac{\Delta p\,D}{L} &\sim \frac{\dot{Q}\,\eta}{D^3} \sim \frac{u_m\,\mu}{D} \\ \lambda &\sim \frac{1}{Re} \end{aligned}$$

6.4

$$\begin{aligned} \frac{F_{Da}}{F_{Dw}} &= \frac{c_{Da}\,\frac{\pi}{4}\,D_a^2\,\frac{\rho_a}{2}\,u_{\infty L}^2}{c_{Dw}\,\frac{\pi}{4}\,D_w^2\,\frac{\rho_W}{2}\,u_{\infty w}^2} \\ &= \frac{c_{Da}\,\mu_a^2\,\frac{\rho_w}{2}\,Re_a^2}{c_{Dw}\,\mu_w^2\,\frac{\rho_a}{2}\,Re_w^2} \\ Re_a &= Re_w: \quad c_{Da} = c_{Dw} \\ \frac{F_{Da}}{F_{Dw}} &= 0.281 \end{aligned}$$

6.5

$$F(f,\mu,\rho,u_\infty,D) = 0$$
$$K_1 = f^{\alpha_1}\,\rho^{\beta_1}\,u_\infty^{\gamma_1}\,D^{\delta_1}$$

Take $\alpha_1 = 1$:

$$\begin{aligned} \beta_1 &= 0. \quad \gamma_1 = -1, \quad \delta_1 = 1 \\ K_1 &= \frac{fD}{u_\infty} = Sr \\ K_2 &= \mu^{\alpha_2}\,\rho^{\beta_2}\,u_\infty^{\gamma_2}\,D^{\delta_2} \end{aligned}$$

Take $\alpha_2 = -1$:

$$\begin{aligned} \beta_2 &= 1, \quad \gamma_1 = 1, \quad \delta_2 = 1 \\ K_2 &= \frac{\rho\,u_\infty\,D}{\mu} = Re \end{aligned}$$

6.6 (a)

$$\begin{aligned} Sr' &= Sr: \quad Re'_{min} = 200 \\ D'_{min} &= Re'_{min}\,\frac{\nu'}{v'} = 1\ mm \end{aligned}$$

(b)

$$Sr = Sr': \quad f = \frac{v\,D'_{min}}{v'\,D}\,f' = 2\,\frac{1}{s}$$

6.7 (a)

$$Re = Re': \quad v' = \sqrt{\frac{A}{A'}}\,v$$

Small, so that flow in wind-tunnel remains incompressible:

$$A' = A_m: v' = 77.46\ \frac{\mathrm{m}}{\mathrm{s}}$$

(b)

$$\begin{aligned} P &= \frac{F_D}{F'_D}\,F'_D\,v \\ &= \frac{c_D\frac{\varrho}{2}\,v^2\,A}{c_{D'}\frac{\varrho}{2}\,v'^2\,A_m}\,F'_D\,v \\ Re &= Re': \quad c_D = c'_D \\ P &= F'_D\,v = 24.3\ \mathrm{kW} \end{aligned}$$

6.8 (a)

$$\begin{aligned} Re = Re': \quad & \\ \dot{Q} &= \frac{vA}{v'A'}\,\dot{Q}' \\ &= \frac{\mu\,\rho'\,D'A}{\mu'\,\rho\,DA'}\,\dot{Q}' \\ \frac{A}{A'} &= \left(\frac{D}{D'}\right)^2 \\ \dot{Q} &= 9\ \frac{\mathrm{m}^3}{\mathrm{s}} \end{aligned}$$

(b)

$$\begin{aligned} Eu = Eu':\ \Delta p &= \frac{\rho\,v^2}{\rho'\,v'^2}\,\Delta p' \\ &= \frac{\rho\,\dot{Q}^2\,A'^2}{\rho'\,\dot{Q}'^2\,A^2}\Delta p' \\ &= 4.94\cdot 10^3\ \frac{\mathrm{N}}{\mathrm{m}^2} \end{aligned}$$

6.9 (a)

$$\begin{aligned} Re = Re' :\ \dot{Q}' &= \frac{v'\,D'^2}{v\,D^2}\,\dot{Q} \\ &= \frac{\eta'\,\rho\,D'}{\eta\,\rho'\,D}\,\dot{Q} \\ &= 0.5\ \frac{\mathrm{m}^3}{\mathrm{s}} \\ Sr = Sr' :\ n' &= \frac{v'\,D}{v\,D'}\,n \\ &= 13.3\ \frac{1}{\mathrm{s}} \end{aligned}$$

(b)

$$Eu = Eu' :\ \Delta p_0 = \frac{\rho\,v^2}{\rho'\,v'^2}\,\Delta p_0 = 527\ \frac{\mathrm{N}}{\mathrm{m}^2}$$

(c)

$$\begin{aligned} P &= \dot{Q}\Delta p_0 = 15.82\ \mathrm{kW} \\ P' &= \dot{Q}'\Delta p_0' = 15\ \mathrm{kW} \\ M &= \frac{P}{2\,\pi\,n} = 201\ \mathrm{Nm} \\ M' &= \frac{P'}{2\,\pi\,n'} = 179\ \mathrm{Nm} \end{aligned}$$

6.10 (a)

$$\begin{aligned} T' = T :\quad \mu' &= \mu_{300\ K} \\ Ma = Ma' :\quad v' &= v = 200\ \frac{\mathrm{m}}{\mathrm{s}} \\ Re = Re' :\quad p' &= \frac{\rho'}{\rho}\,p = \frac{D}{D'}\,p \\ &= 4 \cdot 10^5\ \frac{\mathrm{N}}{\mathrm{m}^2} \end{aligned}$$

(b)

$$Sr = Sr' :\quad n' = \frac{v'\,D}{v\,D'}\,n = 400\ \frac{1}{\mathrm{s}}$$

(c)

$$P = \frac{\frac{\rho}{2}\,v^3\,D^2}{\frac{\rho'}{2}\,v'^3\,D'^2}\,P' = 4\,P'$$

6.11 (a)

$$\begin{aligned} Re = Re' :\quad \frac{\nu'}{\nu} &= \frac{v'\,L'}{v\,L} \\ Fr = Fr' :\quad \frac{v'}{v} &= \sqrt{\frac{L'}{L}} \\ \frac{\nu'}{\nu} &= 10^{-3} \quad (!) \end{aligned}$$

(b)

$$Fr = Fr' :\quad \frac{v'}{v} = \sqrt{\frac{L'}{L}} = 0.1$$

oder

$$Re = Re' :\quad \frac{v'}{v} = \frac{L}{L'} = 100$$

6.12 (a)

$$\begin{aligned} Fr_L = Fr_L' :\quad v' &= v\,\sqrt{\frac{L'}{L}} \\ &= 0.75\ \frac{\mathrm{m}}{\mathrm{s}} \end{aligned}$$

(b)

$$\begin{aligned} c_D &= c_D' \\ F_D &= \frac{\frac{\rho}{2}\,v^2\,B\,H}{\frac{\rho}{2}\,v'^2\,B'\,H'}\,F_D' \\ &= 1.64 \cdot 10^4\ \mathrm{N} \end{aligned}$$

(c)

$$c_D = 1.12$$

(d)

$$\frac{v}{\sqrt{g\,h}} = \frac{v'}{\sqrt{g\,h'}} :\ h = 16\,h' = 0.4\ \mathrm{m}$$

6.13 (a)

$$\begin{aligned} Eu &= Eu', \quad Re = Re' : \\ \frac{p_0' - p_R}{p_0 - p_R} &= \frac{\rho'\,v'^2}{\rho\,v^2} = \frac{\rho\,D^2\,\mu'^2}{\rho'\,D'^2\,\mu'^2} \\ p_0' - p_R &= 440\ \frac{\mathrm{N}}{\mathrm{m}^2} \\ Sr &= Sr' : \\ T' &= \frac{v\,D'}{v'\,D}\,T = 0.57\ \mathrm{s} \end{aligned}$$

(b) Analogously to a)

$$P_{max} = 6.68 \cdot 10^5\ \frac{\mathrm{N}}{\mathrm{m}^2}$$

6.14 (a)

$$\begin{aligned} Re = Re' :\quad v' &= \frac{\rho\,\mu'\,D}{\rho'\,\mu\,D'}\,\frac{\dot{Q}}{\frac{\pi}{4}\,D^2} \\ &= 0.1\ \frac{\mathrm{m}}{\mathrm{s}} \\ \dot{Q} &= 8 \cdot 10^{-4}\ \frac{\mathrm{m}^3}{\mathrm{s}} \end{aligned}$$

(c)

$$\alpha = \frac{\frac{4\dot{Q}}{\pi d^2}}{\sqrt{\frac{2\,\Delta p'_D}{\rho}}} = \frac{\left(\frac{D}{d}\right)^2}{\sqrt{2\,Eu_D}}$$

$$\begin{aligned} Eu_D &= Eu'_D: \quad \alpha = \alpha' = 0.6366 \\ Eu_l &= Eu'_l: \quad \zeta = \zeta' = 77.1 \end{aligned}$$

(d)

$$\begin{aligned} \Delta p_D &= \frac{\rho\, v^2}{\rho'\, v'^2}\, \Delta p'_D \\ &= 0.625 \cdot 10^5\, \frac{\mathrm{N}}{\mathrm{m}^2} \\ \Delta p_l &= \frac{\rho\, v^2}{\rho'\, v'^2}\, \Delta p'_l \\ &= 0.5 \cdot 10^5\, \frac{\mathrm{N}}{\mathrm{m}^2} \end{aligned}$$

### 3.2.7 Potential Flows of Incompressible Fluids

7.1 (a)

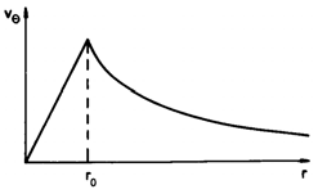


(b)

$$\begin{aligned} \Gamma &= \oint_c \boldsymbol{v}\, d\boldsymbol{s} \\ &= \int_0^{2\pi} v_\theta(r)\, r\, d\theta \\ &= \begin{cases} 2\,\pi\omega\, r^2 & r \le r_0 \\ 2\,\pi\omega\, r_0^2 & r > r_0 \end{cases} \end{aligned}$$

(c)

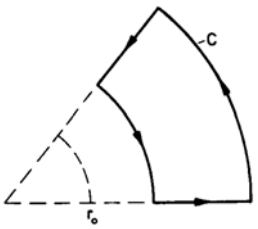


$$\begin{aligned} \Gamma &= \oint_c \boldsymbol{v}\, d\boldsymbol{s} = 0 \\ \boldsymbol{\omega} &= 0 \end{aligned}$$

(d)

$$\begin{aligned} E &= \int_0^{2\,r_0} \frac{\rho}{2}\, v_\theta^2\, H\, 2\,\pi\, r\, dr \\ &= \pi\,\rho\, H\, \omega^2\, r_0^2\, (0.25 + \ln 2) \\ &= 3.7 \cdot 10^8\ \mathrm{Nm} \end{aligned}$$

7.2 (a)

$$u = \frac{\partial \Phi}{\partial x} \qquad v = \frac{\partial \Phi}{\partial y}$$

Potential $\Phi$ exists, if

$$\nabla \times \boldsymbol{v} = 0\ .$$

$$u = \frac{\partial \Psi}{\partial y} \qquad v = -\frac{\partial \Psi}{\partial x}$$

Stream function exists, if,

$$\nabla \cdot \boldsymbol{v} = 0\ .$$

(b)

$$\begin{aligned} \nabla \cdot \boldsymbol{v} &= \nabla^2 \Phi \\ \nabla \times \boldsymbol{v} &= -\nabla^2 \Psi\, \boldsymbol{k} \end{aligned}$$

7.3

| | $\nabla \cdot \boldsymbol{v}$ | $\lvert \nabla \times \boldsymbol{v} \rvert$ |
|---|---|---|
| a) | 4xy | $y^2 - x^2$ |
| b) | 2 | 0 |
| c) | 0 | -2 |
| d) | 0 | 0 |

Stream function exists, for c) and d), the potential for b) and d).

Determination of the stream function:
(a)

$$\begin{aligned} \Psi &= \int u\, dy + f(x) = \frac{y^2}{2} + f(x) \\ v &= -\frac{\partial \Psi}{\partial x} = -f'(x) = -x \\ \Psi &= \frac{1}{2}(x^2 + y^2) + c \end{aligned}$$

(b)

$$\Psi = \frac{1}{2}(y^2 - x^2) + c$$

Determination of the potential:

(c)

$$\begin{aligned} \Phi &= \int u\,dx + f(y) = \frac{x^2}{2} + f(y) \\ v &= \frac{\partial \Phi}{\partial y} = f'(y) = y \\ \Phi &= \frac{1}{2}(x^2 + y^2) + c \end{aligned}$$

(d)

$$\Phi = xy + c$$

7.4 (a)

$$|\ \nabla \text{ x } \boldsymbol{v}\ | = 0: \quad \text{Potential exists.}$$

(b)

$$u = \frac{U}{L}\,x \qquad v = -\frac{U}{L}\,y$$

Stagnation points:

$$u = v = 0: \quad x = y = 0$$

Pressure coefficient:

$$\begin{aligned} c_p &= \frac{p - p_{ref}}{\frac{\rho}{2}\,\boldsymbol{v}_{ref}^2} \\ &= 1 - \frac{u^2 + v^2}{u_{ref}^2 + v_{ref}^2} \\ &= 1 - \frac{x^2 + y^2}{x_{ref}^2 + y_{ref}^2} \end{aligned}$$

Isotachs:

$$\boldsymbol{v}^2 = u^2 + v^2 = \left(\frac{U}{L}\right)^2 (x^2 + y^2)$$

$$x^2 + y^2 = \left(\frac{\boldsymbol{v}\,L}{U}\right)^2$$

Circles around the origin of coordinates with radius

$$\frac{|\ \boldsymbol{v}\ |\ L}{U}$$

(c)

$$u_1 = 4\ \frac{\text{m}}{\text{s}} \quad v_1 = -4\ \frac{\text{m}}{\text{s}}$$

$$|\ \boldsymbol{v}_1\ | = 5.66\ \frac{\text{m}}{\text{s}}$$

$$\begin{aligned} p_1 &= p_{ref} + c_{p1}\,\frac{\rho}{2}\,\boldsymbol{v}_{ref}^2 \\ &= 0.86 \cdot 10^5\ \frac{\text{N}}{\text{m}^2} \end{aligned}$$

(d)

$$t = \int_{x_1}^{x_2} \frac{dx}{u} = \frac{L}{U} \ln \frac{x_2}{x_1}$$

$$x_2 = 5.44 \text{ m}$$

$$\Psi = const: \quad x_1\,y_1 = x_2\,y_2$$

$$y_2 = 0.74 \text{ m}$$

(e)

$$\begin{aligned} p_1 - p_2 &= (c_{p1} - c_{p2})\,\frac{\rho}{2}\,\boldsymbol{v}_{ref}^2 \\ &= 0.442 \cdot 10^5\ \frac{\text{N}}{\text{m}^2} \end{aligned}$$

(f)

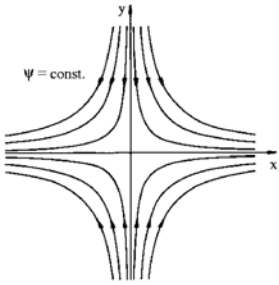


7.5 (a)

$$\begin{aligned} u &= 2\,x\,y \qquad v = x^2 - y^2 \\ \nabla \cdot \boldsymbol{v} &= 0: \text{Stream function exists.} \end{aligned}$$

(b)

$$\Psi = x\,y^2 - \frac{x^3}{3} + c$$

$$\text{Streamlines: } \Psi = const.$$

$$y = \pm\sqrt{\frac{x^3}{3} + \frac{k}{x}} \quad (x \neq 0)$$

Asymptotes:

$$x \to \pm\infty: \quad y = \pm\frac{x}{\sqrt{3}}$$

$$x \to \pm 0: \quad y \to \pm\infty$$

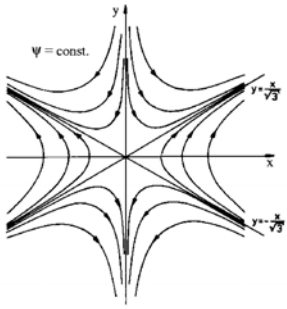

7.6

$$v_r = \frac{c}{r} \qquad v_\theta = 0$$

(a)

$$\nabla \text{ x } \boldsymbol{v} = 0$$
$$\nabla \cdot \boldsymbol{v} = 0$$

(b)

$$\begin{aligned} \Phi &= \int v_r \, dr + f_1(\theta) \\ &= c \ln r + f_1(\theta) \\ \frac{\partial \Phi}{\partial \theta} &= 0: \quad f_1(\theta) = k_1 \\ \Psi &= \int r \, v_r \, d\theta = c\theta + f_2(r) \\ \frac{\partial \Psi}{\partial r} &= 0: \quad f_2(r) = k_2 \end{aligned}$$

(c) Circle with radius r:

$$\begin{aligned} \Gamma &= \int_0^{2\pi} v_\theta \, r \, d\theta = 0 \\ v_r &= 0 \qquad v_\theta = \frac{c}{r} \end{aligned}$$

(a)

$$\begin{aligned} \nabla \text{ x } \boldsymbol{v} &= 0 \\ \nabla \cdot \boldsymbol{v} &= 0 \end{aligned}$$

(b)

$$\begin{aligned} \Phi &= c\,\theta + k_3 \\ \Psi &= -c \, \ln x + k_4 \end{aligned}$$

(c)

$$\Gamma = 2\,\pi\,c$$

7.7 (a) n = 0.5:

$$\begin{aligned} \Psi &= 2\sqrt{r} \sin\left(\frac{\theta}{2}\right) \\ \Psi &= 0: \quad \theta = 0.2\,\pi \\ \Psi &= c: \quad r = \left(\frac{c}{2}\right)^2 \sin^{-2}\left(\frac{\theta}{2}\right) \end{aligned}$$

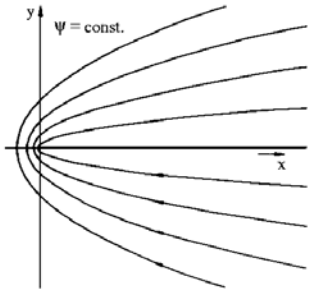


Parallel flow:

$$\begin{aligned} n &= 1: \Psi = r \, \sin\theta = y \\ n &= 2: \Psi = \frac{1}{2} r^2 \, \sin(2\,\theta) = xy \end{aligned}$$

See problem 8.4.

(b)

$$\begin{aligned} c_p &= \frac{p - p_{ref}}{\frac{\rho}{2}\,\boldsymbol{v}_{ref}^2} = 1 - \frac{\boldsymbol{v}^2}{\boldsymbol{v}_{ref}^2} \\ v_\theta &= -r^{n-1} \, \sin(n\,\theta) \\ v_r &= r^{n-1} \, \cos(n\,\theta) \\ c_p &= 1 - \left(\frac{x^2 - y^2}{2}\right)^{n-1} \\ n &= 1: \quad c_p(0.0) = 0 \\ n &> 1: \quad c_p(0.0) = 1 \\ n &< 1: \quad c_p(0.0) = -\infty \end{aligned}$$

7.8 (a)

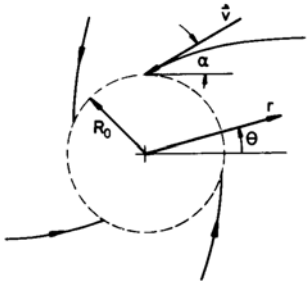


$$\begin{aligned} \Psi &= \frac{E}{2\,\pi}\,\theta - \frac{\Gamma}{2\,\pi} \, \ln\frac{r}{R} \\ v_r &= \frac{E}{2\,\pi\,r} \\ v_\theta &= \frac{\Gamma}{2\,\pi\,r} \end{aligned}$$

$$\tan\alpha = -\frac{v_r}{v_\theta}\Big|_{r=R_0}$$

$$\begin{aligned} E &= -\frac{\dot{Q}}{h_0} \\ \Gamma &= \frac{\dot{Q}}{h_0 \tan\alpha} = 4.33 \cdot 10^{-2}\ \frac{\mathrm{m}^2}{\mathrm{s}} \end{aligned}$$

(b)

$$\begin{aligned} \rho\, g\, h + \frac{\rho}{2}\boldsymbol{v}^2 &= \rho\, g\, h_0 + \frac{\rho}{2}\boldsymbol{v}_0^2 \\ \boldsymbol{v}^2 &= v_r^2 + v_\theta^2 \\ \boldsymbol{v}_\theta^2 &= \boldsymbol{v}_{r=R_0}^2 \end{aligned}$$

$$h(r) = h_0 + \frac{1}{8g}\left(\frac{\dot{Q}}{\pi\, R_0\, h_0\, \sin\alpha}\right)^2 \cdot \cdot\left[1 - \left(\frac{R_0}{r}\right)^2\right]$$

(c)

$$\begin{aligned} \lim_{r\to\infty} h(r) &= h_0 + \frac{1}{8g}\left(\frac{\dot{Q}}{\pi\, R_0\, h_0\, \sin\alpha}\right)^2 \\ &= 2.35 \cdot 10^{-2}\ \mathrm{m} \end{aligned}$$

7.9

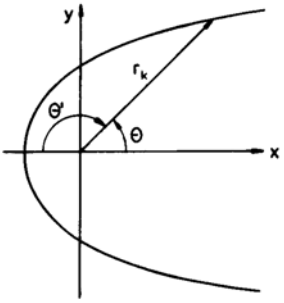


(a)

$$\begin{aligned} \Psi &= u_\infty\, y + \frac{E}{2\,\pi}\,\theta + c \\ &= u_\infty\left[y + \frac{h}{\pi}\arctan\left(\frac{y}{x}\right)\right] + c \\ u &= u_\infty\left(1 + \frac{h}{\pi}\,\frac{x}{x^2+y^2}\right) \\ v &= u_\infty\frac{h}{\pi}\frac{y}{x^2+y^2} \end{aligned}$$

Stagnation point: $u = v = 0$ :

$$\begin{aligned} x_s &= -\frac{h}{\pi}, \quad y_s = 0 \\ u(x_s,h) &= u_\infty\frac{\pi^2}{1+\pi^2} \\ v(x_s,h) &= u_\infty\frac{\pi^2}{1+\pi^2} \end{aligned}$$

(b) Contour: Streamline through stagnation point

$$r_C = \frac{h}{\pi}\,\frac{\pi-\theta}{\sin\theta} = \frac{h}{\pi}\,\frac{\theta'}{\sin\theta}$$

with

$$\theta' = \pi - \theta$$

(c)

$$\begin{aligned} c_p &= 1 - \frac{u^2+v^2}{u_\infty^2} = -\frac{h}{\pi}\frac{2x + \frac{h}{\pi}}{x^2+y^2} \\ c_{pC} &= \frac{\sin(2\,\theta')}{\theta'} - \left(\frac{\sin\theta'}{\theta'}\right)^2 \end{aligned}$$

(d)

$$c_p = \text{const:}$$

$$\left(x + \frac{h}{\pi\, c_p}\right)^2 + y^2 = (1-c_p)\left(\frac{h}{\pi\, c_p}\right)^2$$

Circles around $\left(-\frac{h}{\pi\, c_p}.0\right)$ with radius $\frac{h\sqrt{1-c_p}}{\pi\, c_p}$

(e)

$$c_p = \frac{1}{2} : \left(x + \frac{2h}{\pi}\right)^2 + y^2 = 2\left(\frac{h}{\pi}\right)^2$$

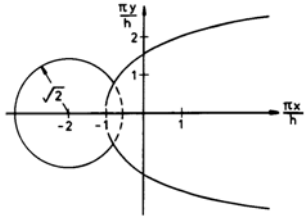

(f)

$$\frac{\sqrt{u^2+v^2}}{u_\infty} = k$$

$$\left(x-\frac{\frac{h}{\pi}}{k^2-1}\right)^2+y^2 = \left(\frac{\frac{kh}{\pi}}{k^2-1}\right)^2$$

Circles around $\left(\frac{h}{\pi\,(k^2-1)}.0\right)$ with radius $\frac{kh}{\pi\,(k^2-1)}$

(g)

$$v = u_\infty \frac{h}{\pi}\frac{y}{x^2+y^2} > \frac{u_\infty}{2}$$

$$x^2+\left(y-\frac{h}{\pi}\right)^2 < \left(\frac{h}{\pi}\right)^2$$

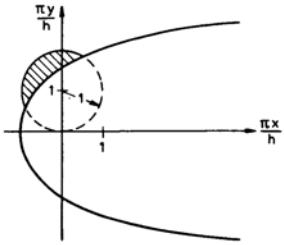


(h)

$$\tan\alpha = \frac{v}{u} = 1$$

$$\left(x+\frac{h}{2\,\pi}\right)^2+\left(y-\frac{h}{2\pi}\right)^2=\frac{1}{2}\left(\frac{h}{\pi}\right)^2$$

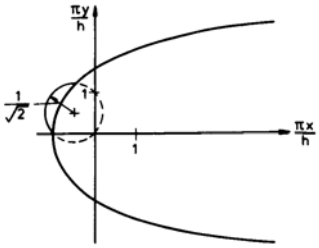


(i) Acceleration along the $x$-Axis:

$$b = \frac{du}{dt} = u\,\frac{\partial du}{\partial dx}$$

$$= -u_\infty \frac{h}{\pi}\left(\frac{1}{x^2}+\frac{h}{\pi}\,\frac{1}{x^3}\right)$$

$$\frac{db}{dx}=0: \quad x_{max} = -\frac{3}{2}\,\frac{h}{\pi}$$

$$b_{max} = -\frac{4}{27}\,\frac{\pi}{h}\,u_\infty^2$$

7.10 (a)

$$\Psi = 0: \quad y = 0$$

$$x^2+y^2 = R^2$$

(Parallel flow)

$$r=\sqrt{x^2+y^2}\to\infty: \quad \Psi \to u_\infty\, y$$

Stream function describes the flow around a cylinder.

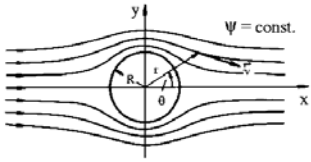


(b)

$$c_p = 1-\frac{v_r^2+v_\theta^2}{u_\infty^2}$$

$$v_r = u_\infty\left[1-\left(\frac{R}{r}\right)^2\right]\cos\theta$$

$$v_\theta = -u_\infty\left[1+\left(\frac{R}{r}\right)^2\right]\sin\theta$$

$$r=R: \quad c_p = 1-4\,\sin^2\theta$$

(c)

$$\Delta t = \int_{-3R}^{2R}\frac{dx}{u(x.0)}$$

$$u(x.0) = u_\infty\left(1-\frac{R^2}{x^2}\right)$$

$$\Delta t = \frac{1}{u_\infty}\left[x+\frac{R}{2}\,\ln\,\frac{x-R}{x+R}\right]_{-3R}^{-2R}$$

$$= \frac{R}{u_\infty}\,(1+0.5\,\ln 1.5)$$

7.11 Determination of velocity components see problem 8.10.

$$c_p = \left(\frac{R}{r}\right)^2\left[2\,\cos(2\,\theta)-\left(\frac{R}{r}\right)^2\right]$$

(a)

$$c_p = 0$$

$$r = \frac{R}{\sqrt{2\,\cos(2\,\theta)}} \quad \text{or}$$

$$\left(\frac{\sqrt{2}\,x}{R}\right)^2-\left(\frac{\sqrt{2}\,y}{R}\right)^2=1$$

Hyperbola

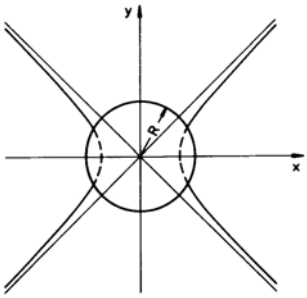


(b)

$$c_p = \frac{7}{16} - \sin\theta$$

7.12 (a)

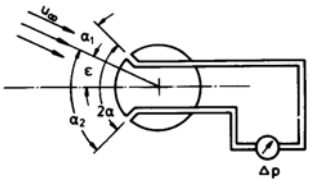


$$\begin{aligned} \Delta p &= (c_{p1} - c_{p1})\frac{\rho}{2} u_\infty^2 \\ c_p &= 1 - 4\,\sin^2\alpha \\ \sin^2\alpha_2 - \sin^2\alpha_1 &= \sin(\alpha_1+\alpha_2) \\ &\cdot\ \sin(\alpha_2-\alpha_1) \end{aligned}$$

$$\Delta p = 2\,\rho\,u_\infty^2\,\sin(2\,\alpha)\,\sin(2\,\epsilon)$$

(b)

$$\alpha = \frac{\pi}{2}$$

7.13 (a)

$$\begin{aligned} \rho\,g\,h_\infty + \frac{\rho}{2}\,u_\infty^2 &= \rho\,g\,h(\theta) + \frac{\rho}{2}\,\boldsymbol{v}^2 \\ r = R : \boldsymbol{v}^2 &= v_\theta^2 = 4u_\infty^2 \sin^2\theta \\ h(\theta) - h_\infty &= \frac{u_\infty^2}{2g}(1 - 4\sin^2\theta) \end{aligned}$$

(b) Stagnation points:

$$\theta = 0 \text{ und } \theta = \pi$$

$$h = h_\infty + \frac{u_\infty^2}{2\,g} = 6.05 \text{ m}$$

(c)

$$\theta_{min} = \frac{\pi}{2}, \quad \frac{3\,\pi}{2}$$

$$h_{min} = h_\infty - \frac{3\,u_\infty^2}{2\,g} = 5.85 \text{ m}$$

7.14

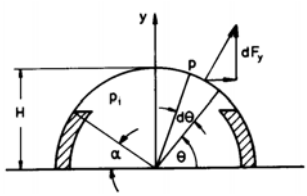


$$\begin{aligned} dF_y &= (p_i - p)\,LH\,\sin\theta\,d\theta \\ p_i &= p_\infty + \frac{\rho}{2}\,u_\infty^2 \\ p &= p_\infty + c_p\,\frac{\rho}{2}\,u_\infty^2 \\ &= p_\infty + (1 - 4\,\sin^2\theta)\,\frac{\rho}{2}\,u_\infty^2 \\ F_y &= \int_{\frac{\pi}{4}}^{\frac{3\,\pi}{4}} 2\,\rho\,u_\infty^2\,LH\,\sin^3\theta\,d\theta \\ &= 2\,\rho\,u_\infty^2\,LH\,\left[-\frac{1}{3}\,\sin^2\theta\,\cos\theta - \right. \\ &\quad \left. -\frac{2}{3}\,\cos\theta\right]_{\frac{\pi}{4}}^{\frac{3\,\pi}{4}} \\ &= 7.37 \cdot 10^6 \text{ N} < G \end{aligned}$$

Mooring not necessary.

7.15 (a)

$$\begin{aligned} \Psi &= u_\infty\,r\,\sin\theta\left[1 - \left(\frac{R}{r}\right)^2\right] - \\ &\quad -\frac{\Gamma}{2\,\pi}\,\ln\frac{r}{R} \\ v_r &= u_\infty\left[1 - \left(\frac{R}{r}\right)^2\right]\cos\theta \\ v_\theta &= -u_\infty\left[1 + \left(\frac{R}{r}\right)^2\right]\sin\theta * \\ &\quad +\frac{\Gamma}{2\,\pi\,r} \\ r &= R: \quad v_{\theta\ vortex} = v_t = \frac{\Gamma}{2\,\pi\,R} \\ \Gamma &= 2\,\pi\,R\,v_t \end{aligned}$$

(b) Flow field for $v_t = u_\infty$:

$$\begin{aligned} \Psi &= u_\infty\,r\,\sin\theta\left(1 - \left(\frac{R}{r}\right)^2\right) - \\ &- u_\infty\,R\ln\frac{r}{R} \\ v_r &= u_\infty\left[1 - \left(\frac{R}{r}\right)^2\right]\cos\theta \\ v_\theta &= u_\infty\left[\frac{R}{r} - \left[1 + \frac{R^2}{r^2}\right]\sin\theta\right] \\ \Psi &= 0: \end{aligned}$$

Contour: Circle around the origin of coordinates with radius R. 2 Stagnation points on the contour ($r = R$): $\theta_s = \frac{\pi}{6}, \frac{5\pi}{6}$; nor free Stagnation points

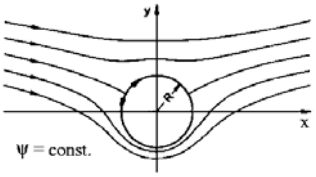


(c)

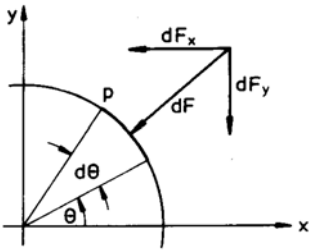


$$
\begin{aligned}
dF_x &= -pLR\cos\theta\, d\theta \\
dF_y &= -pLR\sin\theta\, d\theta \\
p &= p_\infty + c_p \frac{\rho}{2} u_\infty^2 \\
r &= R: \\
& \quad c_p = 1 - \left(\frac{v_t}{u_\infty} - 2\sin\theta\right)^2
\end{aligned}
$$

$$
\begin{aligned}
F_x &= -LR \int_0^{2\pi} \frac{\rho}{2} u_\infty^2 \times \\
&\times \left[1 - \left(\frac{v_t}{u_\infty} - 2\,\sin\theta\right)^2\right] \times \\
&\times \cos\theta\, d\theta - \\
&- LR \int_0^{2\pi} p_\infty \cos\theta\, d\theta = 0 \\
F_y &= -LR \int_0^{2\pi} \frac{\rho}{2} u_\infty^2 \times \\
&\times \left[1 - \left(\frac{v_t}{u_\infty} - 2\,\sin\theta\right)^2\right] \times \\
&\times \sin\theta\, d\theta - \\
&- LR \int_0^{2\pi} p_\infty \sin\theta\, d\theta \\
&= -2\,\pi\,\rho LR\, v_t\, u_\infty \\
&= -\rho\, u_\infty\, \Gamma\, L
\end{aligned}
$$

### 3.2.8 Boundary Layers

8.1

$$
\begin{aligned}
c_D &\sim \frac{F_D}{\rho\, u_\infty^2\, BL} \sim \frac{\bar{\tau}_w}{\rho\, u_\infty^2} \\
&\sim \frac{\frac{\eta\, u_\infty}{\delta}}{\rho\, u_\infty^2} \sim \frac{\mu}{\rho\, u_\infty\, \delta}
\end{aligned}
$$

Inertia and frictional forces of equal order of magnitude:

$$
\begin{aligned}
\frac{\rho\, u_\infty^2}{L} &\sim \frac{\bar{\tau}_w}{\delta} \\
c_D &\sim \frac{1}{\sqrt{Re_L}}
\end{aligned}
$$

8.2 (a)

$$
x_{crit.} = \frac{\nu\, Re_{crit}}{u_\infty} = 0.167 \text{ m}
$$

(b)

$$
\begin{aligned}
\eta = \frac{y}{x}\sqrt{Re_x} &= 1.095 \\
\frac{u}{u_\infty} = 0.36 : u &= 16.2\ \frac{\text{m}}{\text{s}}
\end{aligned}
$$

from diagram, page 60

$$
\begin{aligned}
x = 0.15\ m &: \ Re_x = 4.5 \cdot 10^5 \\
\frac{y}{x}\sqrt{Re_x} = 1.095 &: \ y = 2.45 \cdot 10^{-4}\text{m}
\end{aligned}
$$

(c)

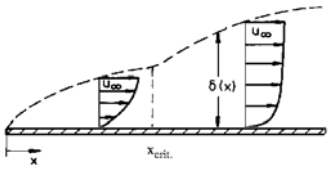


(d)

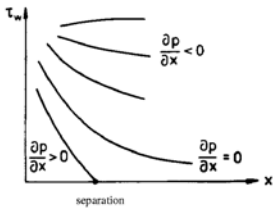

8.3

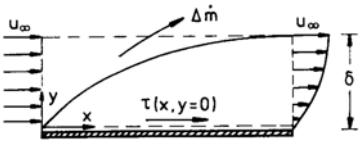


$$-\rho\, u_\infty^2\, \delta + \rho \int_0^\delta u^2\, dy + \Delta\, \dot{m}\, u_\infty =$$
$$= \int_0^x \tau(x',y=0)\, dx'$$
$$\Delta\, \dot{m} = \rho \int_0^\delta (u_\infty - u)\, dy$$

$$\int_0^\delta \frac{u}{u_\infty}\left(1 - \frac{u}{u_\infty}\right) =$$
$$= \delta_2 = -\int_0^x \frac{\tau(x',y=0)}{\rho\, u_\infty^2}\, dx'$$

8.4 (a)

$$Re_L = 3.33\, 10^5 :$$

Boundary layer laminar

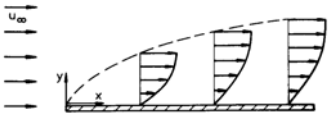


(b)

$$y = 0 \;:\quad u = v = 0$$
$$y \to \infty \;:\quad u \to u_\infty$$

(c)

From boundary-layer equation:

$$\frac{\partial \tau}{\partial y} = 0 \quad \text{for } y = 0 \text{ und } y = \delta$$

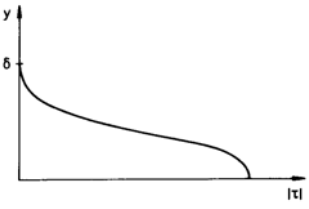


(d) From Blasius solution:

$$\begin{aligned}
\delta(x = L) &= \frac{5L}{\sqrt{Re_L}} \quad c_f = \frac{0.664}{\sqrt{Re_x}} \\
\delta(x = L) &= 4.33 \text{ mm} \\
F_w &= 2 \int_0^L B\, \tau_w\, dx \\
&= \rho\, u_\infty^2\, B \int_0^L c_f\, dx \\
&= 0.144 \text{ N}
\end{aligned}$$

8.5 (a) Boundary conditions:

$$\begin{aligned}
\frac{y}{\delta} &= 0 : \quad \frac{u}{u_\infty} = 0, \quad \frac{v}{u_\infty} = 0 \\
\frac{y}{\delta} &= 1 : \quad \frac{u}{u_\infty} = 1
\end{aligned}$$

From boundary-layer equation:

$$\rho\left(u\,\frac{\partial u}{\partial x} + v\,\frac{\partial u}{\partial y}\right) = \eta\,\frac{\partial^2 u}{\partial y^2} :$$

$$\begin{aligned}
\frac{y}{\delta} = 0 : \quad u = v &= 0 : \\
\frac{\partial^2 \left(\frac{u}{u_\infty}\right)}{\partial \left(\frac{y}{\delta}\right)^2} &= 0 \\
\frac{y}{\delta} = 1 : \quad \frac{\partial u}{\partial x} = \frac{\partial u}{\partial y} &= 0 : \\
\frac{\partial^2 \left(\frac{u}{u_\infty}\right)}{\partial \left(\frac{y}{\delta}\right)^2} &= 0
\end{aligned}$$

Inviscid external flow

$$\begin{aligned}
\frac{y}{\delta} &= 1 : \quad \tau \sim \frac{\partial \left(\frac{u}{u_\infty}\right)}{\partial \left(\frac{y}{\delta}\right)} = 0 \\
\frac{u}{u_\infty} &= 2\left(\frac{y}{\delta}\right) - 2\left(\frac{y}{\delta}\right)^3 + \left(\frac{y}{\delta}\right)^4
\end{aligned}$$

(b)

$$\begin{aligned}
\frac{\delta_1}{\delta} &= \int_0^1 \left(1 - \frac{u}{u_\infty}\right)\, d\left(\frac{y}{\delta}\right) \\
&= \frac{3}{10} \\
\frac{\delta_2}{\delta} &= \int_0^1 \frac{u}{u_\infty}\left(1 - \frac{u}{u_\infty}\right)\, d\left(\frac{y}{\delta}\right) \\
&= \frac{37}{315}
\end{aligned}$$

Von Kármán integral relation

$$\frac{d\delta_2}{dx} + \frac{\tau(y=0)}{\rho\, u_\infty} = 0$$

$$\begin{aligned}\tau(y=0) &= -\frac{\mu\, u_\infty^2}{\delta}\left.\frac{d\left(\frac{u}{u_\infty}\right)}{d\left(\frac{y}{\delta}\right)^2}\right|_{\frac{y}{\delta}=0} \\ &= -2\,\frac{\mu\, u_\infty}{\delta}\end{aligned}$$

Integration:

$$\begin{aligned}\frac{\delta}{x} &= \frac{5.84}{\sqrt{Re_x}} \\ c_D &= \frac{2}{L}\int_0^L \frac{\tau_w}{\rho\, u_\infty^2}\, dx \\ &= -\frac{2}{L}\int_0^L \frac{\tau(y=0)}{\rho\, u_\infty^2}\, dx \\ &= \frac{1.371}{\sqrt{Re_L}}\end{aligned}$$

8.6 (a) Solution see problem 9.5

A)

$$\begin{aligned}\frac{\delta_1}{\delta} &= \frac{3}{8}, \\ \frac{\delta_2}{\delta} &= \frac{39}{280}, \\ \frac{\delta}{x} &= \frac{4.641}{\sqrt{Re_x}}, \\ c_D &= \frac{1.293}{\sqrt{Re_L}}\end{aligned}$$

B)

$$\begin{aligned}\frac{\delta_1}{\delta} &= 1 - \frac{2}{\pi} = 0.363 \\ \frac{\delta_2}{\delta} &= \frac{2}{\pi} - \frac{1}{2} = 0.137 \\ \frac{\delta}{x} &= \frac{\sqrt{\frac{2\,\pi^2}{4-\pi}}}{\sqrt{Re_x}} = \frac{4.795}{\sqrt{Re_x}} \\ c_D &= \frac{2\sqrt{2-\frac{\pi}{2}}}{\sqrt{Re_L}} = \frac{1.310}{\sqrt{Re_L}}\end{aligned}$$

(b) A)

$$\begin{aligned}\delta(x=L) &= 3.288 \text{ mm} \\ F_D &= c_D\, \rho\, u_\infty^2\, 2\, L\, B \\ &= 0.91\ N\end{aligned}$$

B)

$$\begin{aligned}\delta(x=L) &= 3.39 \text{ mm} \\ F_D &= 0.93 \text{ N}\end{aligned}$$

### 3.2.9 Drag

9.1 (a)

$$\begin{aligned}F_1 &= c_{D1}\,\frac{\rho}{2}\, u_\infty^2\, 2\, L_1\, B \\ Re_{L1} &= 1.8 \cdot 10^5 < Re_{crit.} \\ c_{D1} &= \frac{1.328}{\sqrt{Re_{L1}}} = 3.13 \cdot 10^{-3} \\ F_1 &= 0.564 \text{ N} \\ Re_L &= 3.6 \cdot 10^5 < Re_{crit.} \\ F_{tot} &= F_1 + F_2 \\ &= \frac{1.328}{\sqrt{Re_L}}\,\frac{\rho}{2}\, u_\infty^2\, 2\, L\, B \\ F_2 &= 0.233 \text{ N}\end{aligned}$$

(b)

$$\begin{aligned}F_{tot} &= 2\, F_1 \\ L_1 &= \frac{L}{4} = 0.09 \text{ m} \\ L_2 &= 0.27 \text{ m}\end{aligned}$$

9.2 (a) The frictional drag results from the shear stresses acting on the body, the pressure drag results from change of the potential pressure distribution caused by the frictional force.

(b)

$$\begin{aligned}c_{D1}\,\frac{\rho}{2}\, u_\infty^2\, 2\, L_1^2 &= c_{D2}\,\frac{\rho}{2}\, u_\infty^2\, 2\, L_2^2 \\ Re_1 = \frac{u_\infty\, L_1}{\nu} &= 3.33 \cdot 10^5 \\ c_{D1} = \frac{1.328}{\sqrt{Re_1}} &= 2.30 \cdot 10^{-3}\end{aligned}$$

Assumption:

$$\begin{aligned}Re_2 &= \frac{u_\infty\, L_2}{\nu} > 10^3: \quad c_{D2} = 1.1 \\ L_2 &= L_1\sqrt{\frac{2\, c_{D1}}{c_{D2}}} = 6.47 \cdot 10^{-2} \text{ m} \\ Re_2 &= 2.16 \cdot 10^4 > 10^3\end{aligned}$$

(c)

$$\begin{aligned}F_{D1} &= \frac{1.328}{\sqrt{Re_1}}\,\frac{\rho}{2}\, u_\infty^2\, 2\, L_1^2 \sim u_\infty^{\frac{3}{2}} \\ F_{D2} &= 1.1\,\frac{\rho}{2}\, u_\infty^2\, L_2^2 \sim u_\infty^2\end{aligned}$$

9.3 (a)

$$\frac{F_{D1}}{F_{D2}} = \frac{c_{D1}}{c_{D2}}$$

| $u_\infty$ | $Re_1$ | $10^3\, c_{D1}$ |
|---|---|---|
| $0.4\ \frac{\mathrm{m}}{\mathrm{s}}$ | $4 \cdot 10^5$ | 2.10 |
| $0.8\ \frac{\mathrm{m}}{\mathrm{s}}$ | $8 \cdot 10^5$ | 2.76 |
| $1.6\ \frac{\mathrm{m}}{\mathrm{s}}$ | $1.6 \cdot 10^5$ | 3.19 |
| $Re_1$ | $10^3\, c_{D2}$ | $\frac{F_{D1}}{F_{D2}}$ |
| $2 \cdot 10^5$ | 2.97 | 0.707 |
| $4 \cdot 10^5$ | 2.10 | 1.313 |
| $8 \cdot 10^5$ | 2.76 | 1.156 |

(b)

$$\begin{aligned} Re_1 &= 1.96 \cdot 10^5 \\ c_{D1} &= c_{D2} = 3.0 \cdot 10^{-3} \end{aligned}$$

1)

$$Re_2 = Re_1 : \quad u_{\infty 2} = 0.392\ \frac{\mathrm{m}}{\mathrm{s}}$$

2)

$$Re_2 \approx 1.3 \cdot 10^6 : u_{\infty 2} = 2.6\ \frac{\mathrm{m}}{\mathrm{s}}$$

3)

$$Re_3 \approx 9 \cdot 10^6 : \quad u_{\infty 2} = 18\ \frac{\mathrm{m}}{\mathrm{s}}$$

(2) and 3) from diagram page 64).

9.4

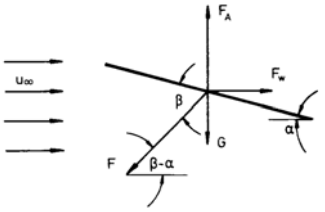


$$\begin{aligned} c_L &= \frac{F_L}{\frac{\varrho}{2}\, u_\infty^2\, A} \\ F_L &- W - F\, \sin(\beta - \alpha) = 0 \\ c_L &= \frac{W + F\, \sin(\beta - \alpha)}{\frac{\varrho}{2}\, u_\infty^2\, A} = 1.28 \\ c_D &= \frac{F_D}{\frac{\varrho}{2}\, u_\infty^2\, A} \\ F_D &- F\, \cos(\beta - \alpha) = 0 \\ c_D &= \frac{F\, \cos(\beta - \alpha)}{\frac{\varrho}{2}\, u_\infty^2\, A} = 0.96 \end{aligned}$$

9.5

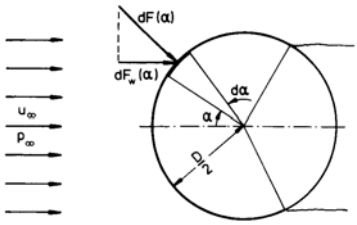


$$\begin{aligned} c_D &= \frac{2 \int_0^\pi dF_w(\alpha)}{\frac{\varrho}{2}\, u_\infty^2\, DL} \\ dF_D(\alpha) &= dF(\alpha)\, \cos\alpha \\ &= p(\alpha)\, L\, \frac{D}{2}\, \cos\alpha\, d\alpha \\ p(\alpha) &= c_p(\alpha)\, \frac{\rho}{2}\, u_\infty^2 + p_\infty \end{aligned}$$

$$0 \le \alpha \le \frac{2}{3}\, \pi :$$

$$p(\alpha) = (1 - 4\, \sin^2\alpha)\, \frac{\rho}{2}\, u_\infty^2 + p_\infty$$

$$\frac{2}{3} \le \alpha \le \pi :$$

$$\begin{aligned} p(\alpha) &= \left[1 - 4\, \sin^2(\frac{2}{3}\, \pi)\right]\, \frac{\rho}{2}\, u_\infty^2 + p_\infty \\ &= -2\, \frac{\rho}{2}\, u_\infty^2 + p_\infty \\ c_D &= \sqrt{3} \end{aligned}$$

9.6 (a)

$$F_{DS} = F_{DB}$$

$$\begin{aligned} c_{DB} \frac{\rho_w}{2} u^2 LB &= c_{DS}\, \frac{\rho_a}{2} \times \\ &\quad \times (u_\infty - u)^2 \frac{hb}{2} \\ Re_L &= \frac{\rho_W\, u\, L}{\mu_W} \\ &= 5.625 \cdot 10^6 \\ c_{DB} &= \frac{0.074}{Re_L^{\frac{1}{5}}} - \frac{1700}{Re_L} \\ &= 3.0 \cdot 10^{-3} \end{aligned}$$

Assumption:

$$\begin{aligned} Re_b &= \frac{\rho_a\,(u_\infty - u)\,b}{\mu_a} > 10^3 \\ c_{DS} &= 1.2 \\ u_\infty &= u\left(1 + \sqrt{\frac{c_{DB}}{c_{DS}}\,\frac{\rho_W}{\rho_a}\,\frac{2\,LB}{hb}}\right) \\ &= 2.95\ \frac{\mathrm{m}}{\mathrm{s}} \\ Re_b &= 1.94 \cdot 10^5 > 10^3 \end{aligned}$$

(b)

$$F_{DS} = 6.33\ \mathrm{N}$$

(c)

$$\begin{aligned} F^*_{DB} &= c^*_{DB}\,\frac{\rho_a}{2}\,\left(u_\infty - u^2\right)\,LB \\ Re^*_L &= \frac{\rho_a\,(u_\infty - u)\,L}{\mu_a} = 3.63 \cdot 10^5 \\ c^*_{DB} &= \frac{1.328}{\sqrt{Re^*_L}} = 2.20 \cdot 10^{-3} \\ F^*_{DB} &= 5.45 \cdot 10^{-3} \ll F_{DB} \end{aligned}$$

9.7

$$\begin{aligned} c_D\,\frac{\rho}{2}\,v^2\,A &= W \\ A = \frac{W}{c_D\,\frac{\rho}{2}\,v^2} &= 75.2\ \mathrm{m}^2 \end{aligned}$$

9.8 (a)

$F_D = W$ (Lift can be neglected)

Sphere:

$$c_D\,\frac{\rho_a}{2}\,v^2\,\frac{\pi\,D_S^2}{4} = \rho\,\frac{\pi\,D_S^3}{6}\,g$$

$$\begin{aligned} v &= Re\,\frac{\nu_a}{D_S} \\ D_S &= \sqrt[3]{18\,Re\,\frac{\rho_L}{\rho}\,\frac{\nu_a^2}{g}} \end{aligned}$$

$$Re = 0.5:$$
$$D_{Smax} = 6.81 \cdot 10^{-2}\ \mathrm{mm}$$

Cylinder (Length L):

$$c_D\,\frac{\rho_a}{2}\,v^2\,D_C\,L = \rho\,\frac{\pi\,D^2}{4}\,L\,g$$
$$D_C = \sqrt[3]{\frac{16\,Re}{2 - \ln Re}\,\frac{\rho_a}{\rho}\,\frac{\nu_a^2}{g}}$$

$$Re = 0.5:$$
$$D_{Cmax} = 4.71 \cdot 10^{-2}\ \mathrm{mm}$$

(b)

$$\begin{aligned} v_S &= 0.110\ \frac{\mathrm{m}}{\mathrm{s}} \\ v_C &= 0.159\ \frac{\mathrm{m}}{\mathrm{s}} \end{aligned}$$

9.9

$$v = Re\,\frac{\nu}{D}$$

(a) (Lift can be neglected:)

$$\begin{aligned} F_D &= W = \rho_W \frac{\pi\,D^3}{6}\,g \\ F_D &= c_D\,\frac{\rho_a}{2}\,v^2\,\frac{\pi\,D^2}{4} \\ &= c_D\,Re^2\,\frac{\pi}{8}\rho_a\,v_a^2 \\ Re\,\sqrt{c_D} &= \sqrt{\frac{8\,F_D}{\pi\,\rho_a}}\frac{1}{\nu_a} \\ &= \sqrt{\frac{4}{3}\,\frac{\rho_W}{\rho_a}\,D\,g}\,\frac{D}{\nu_a} \\ &= 217.7 \end{aligned}$$

from diagram: $Re = 250$

$$v = 3.75\ \frac{\mathrm{m}}{\mathrm{s}}$$

(b) (Weight can be neglected)

$$\begin{aligned} F_D &= F_L = \rho_W \frac{\pi\,D^3}{6}\,g \\ F_D &= c_D\,\frac{\rho_W}{2}\,v^2\,\frac{\pi\,D^2}{4} \\ Re\,\sqrt{c_D} &= \sqrt{\frac{4}{3}\,D\,g}\,\frac{D}{\nu_W} = 115 \\ Re &= 113 \\ v &= 0.11\ \frac{\mathrm{m}}{\mathrm{s}} \end{aligned}$$

9.10

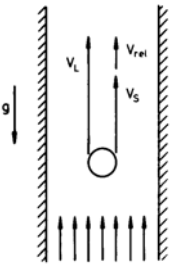

$$W = F_D \quad \text{(Lift can be neglected)}$$
$$v_{rel} = v_a - v_s$$

(a)

$$v_s = 0$$
$$c_{DW}\,\frac{\rho_a}{2}\,v_1^2\,\frac{\pi\,D_S^2}{4} = \rho_S\,\frac{\pi\,D_S^3}{6}\,g$$
$$\text{Assumption: } Re = \frac{\rho_a\,v_1\,D_S}{\mu_a} < 1$$

$$v_1 = -\frac{24}{9}\,\frac{\mu_a}{\rho_a\,D_S} + \sqrt{\left(\frac{24\,\mu_a}{9\,\rho_a\,D_S}\right)^2 + \frac{8}{27}\,\frac{\rho_S}{\rho_a}\,D_S\,g}$$
$$= 0.168\ \frac{\text{m}}{\text{s}}$$
$$Re = 0.559 < 1$$

(b)

$$v_{rel} = v_1$$
$$v_s = v_a - v_1 = 2.832\ \frac{\text{m}}{\text{s}}$$

9.11 (a)

$$F_D = W$$

(Lift can be neglected)

$$c_D\,\frac{\rho_a}{2}\,v_a^2\,\frac{\pi\,D^2}{4} = \rho_W\,\frac{\pi\,D^3}{6}\,g$$

Assumption:

$$Re = \frac{\rho_a\,v_a\,D}{\mu_a} < 0.5$$
$$v_a = \frac{\rho_W\,g\,D^2}{18\,\mu_L} = 0.107\ \frac{\text{m}}{\text{s}}$$
$$Re = 0.427 < 0.5$$

(b)

$$\rho_W\,\frac{\pi\,D^3}{6}\,\frac{dv}{dt} = \rho_W\,\frac{\pi\,D^3}{6}\,g - \frac{24\,\mu_a}{\rho_a\,v\,D}\,\frac{\rho_a}{2}\,v^2\,\frac{\pi\,D^2}{4}$$

Steady sinking velocity:

$v_s = v_a$

$$\frac{1}{g}\,\frac{dv}{dt} = 1 - \frac{v}{v_a}$$
$$T = -\frac{v_a}{g}\,\ln\left(1 - \frac{v}{v_a}\right)_0^{0.99\,v_a}$$
$$= 0.049\,\text{s}$$

9.12 (a)

$$W = F_{D1}$$

(Lift can be neglected)

$$F_{D1} = c_{D1}\,\frac{\rho_a}{2}\,v_1^2\,\frac{\pi\,D^2}{4}$$
$$c_{D1} = 0.4 \qquad (Re_1 = 3.03 \cdot 10^5)$$

(b)

$$Re_2 = \frac{v_2\,D}{\nu_a} = 4.2 \cdot 10^5$$
$$\text{from diagram: } c_{D2} = 0.1$$

$$F_{D2} = c_{D2}\,\frac{\rho_a}{2}\,v_2^2\,\frac{\pi\,D^2}{4}$$
$$= 1.95\ \text{N} < W$$

Acceleration $v_3$, so that

$$G = F_{D3}$$
$$G = c_{D3}\,\frac{\rho_a}{2}\,v_3^2\,\frac{\pi\,D^2}{4}$$

$$\text{from diagram: } c_{D3} = 0.1$$
$$v_3 = 26.0\ \frac{\text{m}}{\text{s}}$$

9.13 (a)

$$P_1 = F_1\,v_1 = F_1\,\frac{H}{T_1} = 1000\,\text{W}$$

(b)

$$W = F_1 + F_L - F_{D1}$$
$$= F_1 + \rho\,\frac{\pi\,D^3}{6}\,g - c_D\,\frac{\rho}{2}\left(\frac{H}{T_1}\right)^2\,\frac{\pi\,D^2}{4}$$
$$Re = \frac{\rho\,H\,D}{\mu\,T_a} = 1.85 \cdot 10^5$$

$$\text{from diagram: } c_{D1} = 0.4$$
$$G = 3349\ \text{N}$$

(c)

$$F_{D2} = c_{D2}\,\frac{\rho}{2}\left(\frac{H}{T_2}\right)^2\,\frac{\pi\,D^2}{4}$$
$$= 2\,F_1 + F_L - W$$

Assumption:

$$Re_2 = \frac{\rho\, H\, D}{\mu\, T_2} > 3.6 \cdot 10^5$$

from diagram: $c_{D2} = 0.1$

$$\begin{aligned} T_2 &= HD\sqrt{\frac{\pi\,\rho\,c_{D2}}{8\,(F_1+F_{D1})}} \\ &= 241.0 \text{ s} \\ Re_2 &= 8.3 \cdot 10^6 \end{aligned}$$

(d)

$$P_2 = 2\,F_1\,\frac{H}{T_2} = 89.64 \text{ kW}$$

9.14 (a)

$$\begin{aligned} \rho_W\,\frac{\pi\,D^3}{6}\,\frac{dv}{dt} &= -\rho_S\,\frac{\pi\,D^3}{6}\,g - \\ &- c_{D2}\,\frac{\rho_a}{2}\,v^2\,\frac{\pi\,D^2}{4} \end{aligned}$$

Introduce steady sinking velocity:

$$\begin{aligned} v_s^2 &= \frac{4}{3}\,\frac{\rho_S}{\rho_a}\,\frac{D\,g}{c_D} - \\ -\frac{1}{g}\,\frac{dv}{1+\left(\frac{v}{v_s}\right)^2} &= dt = \frac{dz}{v} \end{aligned}$$

$$\begin{aligned} H &= -\frac{1}{g}\int_{v_0}^{0}\frac{v\,dv}{1+\left(\frac{v}{v_s}\right)^2} \\ &= \frac{v_s^2}{2\,g}\,\ln\left[1+\left(\frac{v}{v_s}\right)^2\right] \end{aligned}$$

(b)

$$\begin{aligned} T_H &= -\frac{1}{g}\int_{v_0}^{0}\frac{dv}{1+\left(\frac{v}{v_s}\right)^2} \\ &= \frac{v_s^2}{g}\,\arctan\frac{v_0}{v_s} \end{aligned}$$

(c)

$$\begin{aligned} \rho_S\frac{\pi\,D^3}{6}\,g\frac{dv}{dt} &= -\ c_D\frac{\rho_a}{2}\,v^2\frac{\pi\,D^2}{4} + \\ &+\ \rho_S\,\frac{\pi\,D^3}{6}\,g \\ \frac{1}{g}\,\frac{dv}{1-\left(\frac{v}{v_s}\right)^2} &= dt = \frac{dz}{v} \end{aligned}$$

$$\begin{aligned} H &= \frac{1}{g}\int_0^{v_B}\frac{v\,dv}{1-\left(\frac{v}{v_s}\right)^2} \\ &= -\frac{v_s^2}{2\,g}\,\ln\left[1-\left(\frac{v_B}{v_s}\right)^2\right] \\ v_B &= \frac{v_s}{\sqrt{1+\left(\frac{v}{v_s}\right)^2}} \end{aligned}$$

(d)

$$\begin{aligned} T_B &= -\frac{1}{g}\int_0^{v_B}\frac{dv}{1-\left(\frac{v}{v_s}\right)^2} \\ &= \frac{v_s^2}{g}\,\ln\frac{v_s+v_B}{v_s-v_B} \end{aligned}$$

(e)

| | $c_D = 0.4$ | | $c_w = 0$ |
|---|---|---|---|
| | wooden sphere | metal sphere | |
| $H$ [m] | 37.2 | 44.0 | 45 |
| $T_H$ [s] | 2.64 | 2.96 | 3 |
| $v_B$ [$\frac{\text{m}}{\text{s}}$] | 24.9 | 29.3 | 30 |
| $T_H$ [s] | 2.81 | 2.98 | 3 |

# 4. Gasdynamics

## 4.1 Introduction

In the first part of this chapter, which is a continuation of fluid mechanics II, after a short repetition of the important thermodynamic relations, one- dimensional, steady, isentropic flows of compressible gases in a stream tube with variable cross-section are described. Then normal compression shocks in one-dimensional supersonic flows associated with a discontinuous increase of entropy will be explained. It will be shown, that the increase of entropy is due to heat conduction and disspation of mechanical energy in the shock.
The description of normal shocks quite naturally leads to oblique shocks, which are discussed as third topic. The properties of strong and weak shocks are explained with the aid of the shock polar diagram, and the jump conditions for weak shocks are subsequently used as starting point for the derivation of the relations for isentropic flows, the expansion around a corner after Prandtl and Meyer, and the reverse, the isentropic compression. The jump conditions for oblique shocks and the Prandtl-Meyer expansion are then employed to determine lift and wave drag of airfoil profiles at angle of attack in supersonic flow.
In the next chapter an introduction to the computation of supersonic flows is given. Beginning with the fundamental equation of gasdynamics, the theory of characteristics is explained. Thereafter, compressible potential flows are discussed. These considerations include plane and axially symmetric supersonic and subsonic flows about slender bodies.
Finally the similarity rules of gasdynamics are discussed. First the similarity rules for two-dimensional flows are derived with the aid of the linearized potential equation, together with several examples of their application. The chapter closes with the extension of the similarity rules to axially symmetric and transonic flows.
The various topics presented are again supplemented by exercises in gasdynamics in Chap. 5. Several examples are given to illustrate the application of the laws for one-dimensional steady flows. The abrupt changes of the flow quantities across normal and oblique shocks are delt with in the following two subsections. Prandtl-Meyer expansions and their interaction with oblique compression shocks is studied in detail for several flow configurations, followed by exercises concerned with the determination of lift and wave drag in the frame of the small-perturbation theory. Finally the application of the theory of characteristics and the computation of potential compressible flows together with the similarity rules are demonstrated.

## 4.2 Thermodynamic Relations

In flows of compressible gases, in addition to the rate of change of the mechanical energy also the rate of change of the thermal energy has to be considered. It is therefore necessary to define the thermodynamic state of the gas with state variables, e. g. the pressure $p$, the density $\rho$, and the temperature $T$. Their interdependence is described by the thermal equation of state. If the law given by Boyle, Mariotte, and Gay-Lussac is used, i. e.

$$p = \rho\, R\, T \quad , \tag{4.1}$$

the gas is called thermally perfect. For thermally non-perfect gases other relations must be used, as for example the Van der Waals law. The specific gas constant $R$ depends on the molecular weight of the gas. For air it is $R = 287 \frac{J}{kgK}$.

Another state variable is the internal energy. It is defined by two thermodynamic quantities, the temperature $T$ and the specific volumen $v = \frac{1}{\rho}$.

$$e = e(v,T) \tag{4.2}$$

This relation is known as the caloric equation of state. The total derivative is

$$de = \left(\frac{\partial e}{\partial v}\right)_T dv + \left(\frac{\partial e}{\partial T}\right)_v dT \quad . \tag{4.3}$$

The internal energy of thermally perfect gases depends on the temperature only. It then follows that

$$de = \left(\frac{\partial e}{\partial T}\right)_v dT \quad , \quad c_v = \left(\frac{\partial e}{\partial T}\right)_v \quad . \tag{4.4}$$

The quantity $\left(\frac{\partial e}{\partial T}\right)_v$ is called specific heat $c_v$ at constant volume. If $c_v$ is constant, the gas is called calorically perfect, and the internal energy is given by

$$e = c_v\, T + e_r \quad . \tag{4.5}$$

The quantity $e_r$ is a reference value. The enthalpy $h$ is another important state variable:

$$h = e + p\, v \tag{4.6}$$

As the internal energy, the enthalpy of thermally perfect gases depends on the temperature only.

$$dh = c_p\, dT \tag{4.7}$$

The quantity $c_p$ is the specific heat at constant pressure

$$c_p = \left(\frac{\partial h}{\partial T}\right)_p \quad . \tag{4.8}$$

It follows from the relation for the specific heats $c_v$ and $c_p$

$$c_p = c_v + R \tag{4.9}$$

for calorically perfect gases, that $c_p =$ is constant. Hence

$$h = c_p\, T + h_r \quad , \tag{4.10}$$

where $h_r$ is again a reference value.
The ratio of the specific heats $\frac{c_p}{c_v} = \gamma$ is – according to the gas-kinetic theory – given by the number $n$ of degrees of freedom

$$\gamma = \frac{n+2}{n} \quad . \tag{4.11}$$

For monatomic gases ($n = 3$) $\gamma = 1.667$, and for diatomic gases ($n = 5$) $\gamma = 1.4$. At high temperatures additional degrees of freedom are excited, and the ratio $\frac{c_p}{c_v}$ decreases. For air at a temperature of 300 $K$ $\gamma = 1.4$, and for 3000 $K$ is $\gamma = 1.292$.
The entropy $s$ is introduced as another state variable with the second law of thermodynamics

$$T\, ds = d\, e + p\, dv \quad . \tag{4.12}$$

For a thermally perfect gas it follows that

$$ds = c_v \frac{dp}{p} - c_p \frac{d\rho}{\rho} \quad . \tag{4.13}$$

This relation can be integrated for a calorically perfect gas.

$$s = s_r + c_v \ln \left[ \frac{\left(\frac{p}{p_r}\right)}{\left(\frac{\rho}{\rho_r}\right)^\gamma} \right] \tag{4.14}$$

The quantities $p_r$, $\rho_r$ are reference values.
If the entropy is constant $s = s_r$, there results the isentropic relation

$$\frac{p}{\rho^\gamma} = \frac{p_r}{{\rho_r}^\gamma} \quad . \tag{4.15}$$

In flows in which the entropy is constant, the pressure varies only with the density $\rho$, with the relationship depending on the isentropic exponent $\gamma$.

## 4.3 One-Dimensional Steady Gas Flow

Consider the one-dimensional flow of a compressible, inviscid gas without heat exchange. The gas is assumed to be thermally and calorically perfect.

### 4.3.1 Conservation Equations

With the assumptions stated the conservation equations for mass, momentum, and energy are:

$$\begin{aligned} d\left[\rho\, u\right] &= 0 \\ d\left[\rho\, u^2 + p\right] &= 0 \\ d\left[\rho\, u \left(h + \frac{u^2}{2}\right)\right] &= 0 \quad . \end{aligned} \tag{4.16}$$

The quantities in the square brackets represent the mass, momentum, and energy fluxes. The system of equations is closed by introducing the thermal equation of state; density, pressure, enthalpy, and velocity can now be determined.

$$p = \rho\, RT \tag{4.17}$$

If only continuous changes of the state variables are admitted, it follows from the second law of thermodynamics, that the entropy remains constant.

$$ds = \frac{1}{T} \left( dh - \frac{dp}{\rho} \right) = 0 \tag{4.18}$$

One of the conservation equations can then be replaced by the isentropic relation:

$$\frac{p}{\rho^\gamma} = \frac{p_0}{\rho_0^\gamma} \tag{4.19}$$

The quantities $p_0$ and $\rho_0$ are the values of pressure and density, which the gas attains in the state of rest after isentropic compression.

### 4.3.2 The Speed of Sound

The Mach number $Ma$ is an important similarity parameter for the description of compressible flows. It is given by the ratio of the local flow velocity and the speed of sound. Distinguished are subsonic, supersonic, and transonic flows. Since each of the flows exhibits its own particularities, the Mach number has to be known for the description of flows.
In a compressible medium pressure disturbances travel with finite speed. The speed of propagation of small pressure disturbances is the speed of sound. The changes of the state variables caused by the propagation of sound occur at constant entropy.

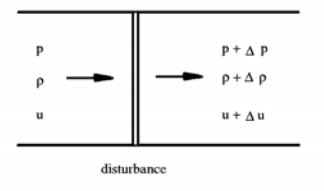


The compression of a gas by an explosion does not take place without losses, and the speed of propagation is larger than the speed of sound. Consider a small disturbance moving with the velocity $u$ through a gas at rest. For an observer moving with the flow, the flow process is steady. The mass and momentum balance

$$\begin{aligned} \rho\, u &= (\rho + \Delta\rho)(u + \Delta u) \\ -\rho\, u^2 + (\rho + \Delta\rho)(u + \Delta u)^2 &= p - (p + \Delta p) \end{aligned} \qquad (4.20)$$

yield

$$u^2 = \frac{1}{1 + \frac{\Delta u}{u}} \frac{\Delta p}{\Delta \rho} \quad . \qquad (4.21)$$

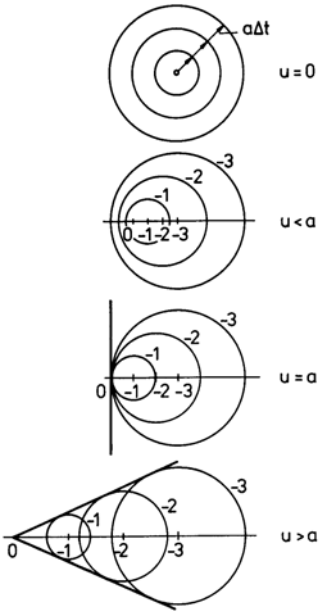


If the changes of the flow quantities are assumed to be infinitesimally small, then the expression for the speed of sound is

$$a = \sqrt{\left(\frac{\partial p}{\partial \rho}\right)_{s=const.}} \quad , \qquad (4.22)$$

which for incompressible media is infinitely large as $\Delta\rho \to 0$. In the above derivation it was tacidly assumed, that the influence of friction forces can be neglected; (4.22) can therefore only be applied, if the disturbances are small enough so that the assumption is valid. Disturbances caused by sound are small, and friction forces can be left out.
It then follows that the motion in a sound wave can be considered as isentropic, as the entropy production is proportional to the squares of the velocity and temperature gradients. For perfect gases, with the isentropic relation $dp/p = \gamma\, d\rho/\rho$ and the thermal equation of state $p/\rho = R\,T$, one obtains

$$a = \sqrt{\gamma\, \frac{p}{\rho}} = \sqrt{\gamma\, RT} \quad . \qquad (4.23)$$

The speed of sound depends on the temperature of the gas only. Since it is finite, the propagation of sound is influenced by the speed of the sound source. Consider a punctiform sound source: If it is at rest, the sound waves propagate in concentric circles and spread out in the entire space. If the source is set in motion and moves with subsonic speed, the sound waves propagate in excentric circles. If the source moves with the speed of sound, the waves can propagate only

in the space downstream from the source, and for supersonic speed, the sound can spread out only in the so-called Mach cone, the half angle of which is given by

$$\alpha = \arcsin\left(\frac{1}{Ma}\right). \tag{4.24}$$

An observer can therefore hear a sound source moving with supersonic speed only after it has passed him.

### 4.3.3 Integral of the Energy Equation

It follows from the conservation equations for one-dimensional, steady, compressible flow, that the sum of the kinetic energy $\frac{u^2}{2}$ and the static enthalpy $h$ remains constant. The value of this constant is given by the stagnation enthalpy

$$h_0 = h + \frac{u^2}{2} \quad . \tag{4.25}$$

For calorically perfect gases the enthalpy can be replaced by the product of static temperature and the specific heat at constant pressure $c_p\,T$.

$$c_p\,T_0 = c_p\,T + \frac{u^2}{2} \tag{4.26}$$

Introducing the thermal equation of state there results

$$\frac{\gamma}{\gamma-1}\frac{p_0}{\rho_0} = \frac{\gamma}{\gamma-1}\frac{p}{\rho} + \frac{u^2}{2} \tag{4.27}$$

and with the definition of the speed of sound

$$\frac{a_0^2}{\gamma-1} = \frac{a^2}{\gamma-1} + \frac{u^2}{2} \quad . \tag{4.28}$$

If the isentropic relation is combined with the expression for the speed of sound,

$$a^2 = a_0^2\left(\frac{p}{p_0}\right)^{\frac{\gamma-1}{\gamma}} \quad , \tag{4.29}$$

(4.27) takes on the following form

$$\frac{\gamma}{\gamma-1}\frac{p_0}{\rho_0} = \frac{\gamma}{\gamma-1}\left(\frac{p_0}{\rho_0}\right)\left(\frac{p}{p_0}\right)^{\frac{\gamma-1}{\gamma}} + \frac{u^2}{2} \quad . \tag{4.30}$$

This equation is often called the Bernoulli equation for compressible flow. Because of the isentropic change of the state the dependence of the static pressure on the kinetic energy is not linear as it is in incompressible flow. If the last equation is divided by the square of the speed of sound, pressure, temperature, density, and speed of sound can be expressed in a simple manner by the Mach number and the stagnation quantities:

$$\begin{aligned}
\frac{p}{p_0} &= \left(1 + \frac{\gamma-1}{2}\,Ma^2\right)^{-\frac{\gamma}{\gamma-1}} \\
\frac{T}{T_0} &= \left(1 + \frac{\gamma-1}{2}\,Ma^2\right)^{-1} \\
\frac{\rho}{\rho_0} &= \left(1 + \frac{\gamma-1}{2}\,Ma^2\right)^{-\frac{1}{\gamma-1}} \\
\frac{a}{a_0} &= \left(1 + \frac{\gamma-1}{2}Ma^2\right)^{-\frac{1}{2}}
\end{aligned} \tag{4.31}$$

### 4.3.4 Sonic Conditions

If the local flow velocity is equal to the speed of sound, pressure, temperature, and density attain specific values, which solely depend on the stagnation conditions of the gas. The sonic condition, also refered to as the critical state, is designated by an asterisk:

$$\begin{aligned} \frac{p^*}{p_0} &= \left(\frac{2}{\gamma+1}\right)^{\frac{\gamma}{\gamma-1}} \\ \frac{T^*}{T_0} &= \left(\frac{2}{\gamma+1}\right) \\ \frac{\rho^*}{\rho_0} &= \left(\frac{2}{\gamma+1}\right)^{\frac{1}{\gamma-1}} \\ \frac{a^*}{a_0} &= \left(\frac{2}{\gamma+1}\right)^{\frac{1}{2}} \end{aligned} \tag{4.32}$$

For air with $\gamma = 1.4$ the critical values are as follows:

$$\frac{p^*}{p_0} = 0.528; \qquad \frac{T^*}{T_0} = 0.833; \qquad \frac{\rho^*}{\rho_0} = 0.634; \qquad \frac{a^*}{a_0} = 0.913 \tag{4.33}$$

Instead of the local speed of sound $a$ also the critical speed of sound can be used to define a Mach number, which is called the critical Mach number

$$Ma^* = \frac{u}{a^*}. \tag{4.34}$$

The relation between the local Mach number $Ma = \frac{u}{a}$ and the critical Mach number is given by the energy equation. If therein $a_0$ is replaced by $a^*$, after division by $u^2$, there is obtained

$$Ma^{*2} = \frac{\gamma+1}{\gamma-1+\frac{2}{Ma^2}} \quad . \tag{4.35}$$

For $Ma \to \infty$ the critical Mach number $Ma^*$ approaches the limiting value

$$\lim_{Ma\to\infty} Ma^* = \sqrt{\frac{\gamma+1}{\gamma-1}} \quad . \tag{4.36}$$

With these relations the ratios of the pressure, temperature, density, and speed of sound, refered to their stagnation values, can be expressed by the critial Mach number :

$$\begin{aligned} \frac{p}{p_0} &= \left(1-\frac{\gamma-1}{\gamma+1}\,Ma^{*2}\right)^{\frac{\gamma}{\gamma-1}} \\ \frac{T}{T_0} &= \left(1-\frac{\gamma-1}{\gamma+1}\,Ma^{*2}\right) \\ \frac{\rho}{\rho_0} &= \left(1-\frac{\gamma-1}{\gamma+1}\,Ma^{*2}\right)^{\frac{1}{\gamma-1}} \\ \frac{a}{a_0} &= \left(1-\frac{\gamma-1}{\gamma+1}\,Ma^{*2}\right)^{\frac{1}{2}} \end{aligned} \tag{4.37}$$

With $Ma^* = 1$ these relations reduce to those given for the critial state.

### 4.3.5 The Limiting Velocity

A flow attains its maximum velocity, if the gas is expanded into vacuum. The resulting limiting velocity $u_g$ depends only on the stagnation conditions. To show this, the Bernoulli equation for compressible flow is solved for the velocity $u$

$$u = \sqrt{\frac{2\,\gamma\,RT_0}{\gamma - 1}\left[1 - \left(\frac{p}{p_0}\right)^{\frac{\gamma-1}{\gamma}}\right]} \quad . \tag{4.38}$$

This relation was first derived by de Saint-Venant and Wantzel in 1839. If the pressure is lowered to zero, the limiting velocity is given by

$$u_g = \lim_{p\to 0} u = \sqrt{\frac{2\,\gamma\,R\,T_0}{\gamma - 1}} \quad . \tag{4.39}$$

The corresponding Mach number $Ma_g$ is infinitely large, the critical Mach number has the finite value, already stated

$$Ma_g^* = \sqrt{\frac{\gamma + 1}{\gamma - 1}} \quad . \tag{4.40}$$

The limiting velocity can also be used to define the pressure, density, temperature, and speed of sound in terms of the local velocity and the stagnation conditions:

$$\begin{aligned}
\frac{p}{p_0} &= \left(1 - \frac{u^2}{u_g^2}\right)^{\frac{\gamma}{\gamma-1}} \\
\frac{T}{T_0} &= \left(1 - \frac{u^2}{u_g^2}\right) \\
\frac{\rho}{\rho_0} &= \left(1 - \frac{u^2}{u_g^2}\right)^{\frac{1}{\gamma-1}} \\
\frac{a}{a_0} &= \left(1 - \frac{u^2}{u_g^2}\right)^{\frac{1}{2}}
\end{aligned} \tag{4.41}$$

The ratio of the limiting velocity and the speed of sound at stagnation conditions is

$$\frac{u_g}{a_0} = \sqrt{\frac{2}{\gamma - 1}} \quad . \tag{4.42}$$

The numerical values of the quantities discussed here are given in the appendix as a function of the Mach number $Ma$. The data can be used to compute one-dimensional isentropic flows, if the stagnation conditions are prescribed.

### 4.3.6 Stream Tube with Variable Cross-Section

The influence of the compressibility on one-dimensional isentropic flow in a stream tube with slowly varying cross-section $A$ can be investigated with the conservation equations given previously. The continuity equation can be written in the form

$$\frac{d\rho}{\rho} + \frac{du}{u} + \frac{dA}{A} = 0 \quad . \tag{4.43}$$

The differential of the density can be eliminated with the aid of the momentum equation:

$$-u\,du = \frac{dp}{\rho} = a^2\,\frac{d\rho}{\rho} \tag{4.44}$$

There results

$$\frac{du}{u} = -\frac{1}{(1-Ma^2)}\,\frac{dA}{A} \quad . \tag{4.45}$$

Three cases can be distinguished:

1. Subsonic flow (Ma $< 1$)
   The velocity increases with decreasing cross section.
2. Supersonic flow (Ma $> 1$)
   The velocity decreases with increasing cross section.
3. Transonic flow (Ma $= 1$)
   Sonic velocity can only be attained in the stream tube, if $dA$ vanishes locally.

According to this result supersonic flow can only be generated, if the stream tube has a convergent-divergent distribution of the cross section (Laval nozzle). The cross section with minimum area, where the local velocity is equal to the speed of sound, is called critical cross section or throat. The local velocity can be computed with the Bernoulli equation for compressible flow as a function of the pressure ratio:

$$u = \sqrt{\frac{2\,\gamma}{\gamma-1}\,\frac{p_0}{\rho_0}\left[1-\left(\frac{p}{p_0}\right)^{\frac{\gamma-1}{\gamma}}\right]} \quad . \tag{4.46}$$

The local Mach number is obtained by dividing by the local speed of sound

$$Ma = \sqrt{\frac{2}{\gamma-1}\left[\left(\frac{p_0}{p}\right)^{\frac{\gamma-1}{\gamma}}-1\right]} \quad . \tag{4.47}$$

The rate of mass flow through every cross section is constant. For the following derivation it is advantageous to choose the critical rate of mass flow as reference value.

$$\rho\,u\,A = \rho^*\,a^*\,A^* \quad . \tag{4.48}$$

With this relation, the interdependence between static pressure, Mach number, and cross-sectional area can be formulated. If (4.48) is solved for $\frac{A^*}{A}$ and if the stagnation quantities are introduced as reference values, there results

$$\frac{A^*}{A} = \frac{\rho}{\rho_0}\,\frac{\rho_0}{\rho^*}\,\frac{u}{a_0}\,\frac{a_0}{a^*} \quad . \tag{4.49}$$

The critical cross-sectional area ratio $\frac{A^*}{A}$ can be expressed by the pressure ratio $\frac{p}{p_0}$

$$\frac{A^*}{A} = \frac{\left(\frac{p}{p_0}\right)^{\frac{1}{\gamma}}\sqrt{1-\left(\frac{p}{p_0}\right)^{\frac{\gamma-1}{\gamma}}}}{\sqrt{\frac{\gamma-1}{2}\left(\frac{2}{\gamma+1}\right)^{\frac{\gamma+1}{\gamma-1}}}} \tag{4.50}$$

or by the local Mach number

$$\frac{A^*}{A} = \frac{Ma}{\left[\frac{2}{\gamma+1}\left(1+\frac{\gamma-1}{2}\,Ma^2\right)\right]^{\frac{\gamma+1}{2\,(\gamma-1)}}} \quad . \tag{4.51}$$

The last equation shows, that $\frac{A^*}{A}$ tends to zero for small Mach numbers ($Ma \to 0$) and also for very large Mach numbers ($Ma \to \infty$). The critical area ratio is plotted in the following

diagramm for $\gamma = 1.4$ as a function of the Mach number and of the pressure ratio. The maximum $\frac{A^*}{A} = 1$ is attained for a pressure ratio of $\frac{p^*}{p_0} = 0.528$. The two branches of the curve correspond to subsonic and supersonic flow. If the cross section is chosen to first converge and then diverge, and if the flow entering the stream tube is subsonic, it is then accelerated and becomes sonic, and finally in the divergent part supersonic.

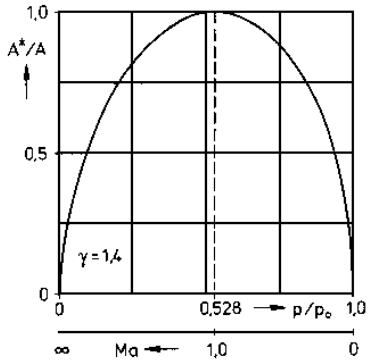


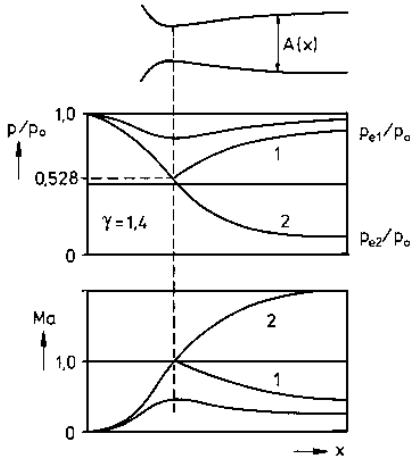


According to the assumptions introduced, (4.50) and (4.51) are valid only for isentropic flow, since the variation of the density is assumed to be isentropic.

Mach number and pressure distribution can be determined for an area distribution prescribed in the streamwise direction.

The flow in the nozzle solely depends on the pressure in the exit cross section.

If the pressure drop in the exit cross section is small $p_{e1} < p_e < p_0$, the flow in the nozzle remains subsonic.

If the pressure in the exit cross section is reduced to $p_{e1}$, the speed in the critical cross section will be equal to the speed of sound. An isentropic supersonic flow in the divergent part of the nozzle can exist only if the pressure in the exit cross section is at least reduced to $p_{e2}$.

If the pressure in the exit cross section is between $p_{e1}$ and $p_{e2}$, the flow cannot adjust isentropically to the conditions existing in the exit cross section. Then a discontinuous increase of the density, pressure, and temperature occurs in the supersonic part of the nozzle, known as normal compression shock. The flow is decelerated to subsonic speed. This discontinuous process causes losses, which result in an increase in entropy.

## 4.4 Normal Compression Shock

Compression shocks can be viewed as a discontinuous change of all flow quantities. The corresponding changes can be obtained with the integrals of the conservation equations.

### 4.4.1 The Jump Conditions

Consider a plane supersonic flow with a normal compression shock in a chanel with constant sross-sectional area; the integrals of the conservation equations given earlier can be written in the following form:

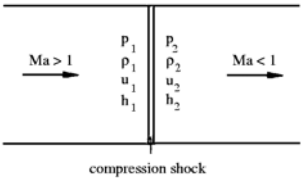


$$\begin{aligned} \rho_1\, u_1 &= \rho_2\, u_2 \\ p_1 + \rho_1\, u_1^2 &= p_2 + \rho_2\, u_2^2 \\ h_1 + \frac{u_1^2}{2} &= h_2 + \frac{u_2^2}{2} \end{aligned} \tag{4.52}$$

In order to determine the density ratio $\frac{\rho_2}{\rho_1}$ the velocity difference is first obtained from the continuity and the momentum equation.

$$u_1 - u_2 = \frac{a_2^2}{\gamma\, u_2} - \frac{a_1^2}{\gamma\, u_1} \tag{4.53}$$

The local speed of sound is expressed through the critical speed of sound $a^*$ and the flow velocity $u$. The intergal of the energy equation yields

$$a^2 = \frac{\gamma+1}{2}\, a^{*2} - \frac{\gamma-1}{2}\, u^2 \quad . \tag{4.54}$$

Combining the last equations gives the Prandtl relation

$$u_1\, u_2 = a^{*2} \text{ or } Ma_1^* = \frac{1}{Ma_2^*} \quad . \tag{4.55}$$

The Prandtl relation shows that a normal shock decelerates a supersonic flow always to a subsonic flow. The density ratio follows from the continuity equation

$$\frac{\rho_2}{\rho_1} = \frac{u_1}{u_2} = Ma_1^{*2} = \frac{(\gamma+1)\, Ma_1^2}{2 + (\gamma-1)\, Ma_1^2} \quad . \tag{4.56}$$

The pressure ratio $\frac{p_2}{p_1}$ is obtained by first solving the momentum equation for the pressure difference $p_2 - p_1$ and expressing the velocity ratio $\frac{u_1}{u_2}$ by $Ma_1$.

$$\frac{p_2}{p_1} = 1 + \frac{2\,\gamma}{\gamma+1}(Ma_1^2 - 1) \tag{4.57}$$

For high Mach numbers $Ma_1$ the pressure ratio $\frac{p_2}{p_1}$ tends to infinity, while the density ratio approaches the finite value $\frac{\gamma+1}{\gamma-1}$. The increase of entropy across the compression shock follows from (4.14). It is

$$\frac{s_2 - s_1}{R} = \ln\left[\left(\frac{p_2}{p_1}\right)^{\frac{1}{\gamma-1}} \left(\frac{\rho_2}{\rho_1}\right)^{\frac{-\gamma}{\gamma-1}}\right] \quad . \tag{4.58}$$

If the Mach number is introduced in the expression for the pressure and density ratio, the entropy difference across the compression shock becomes

$$\frac{s_2 - s_1}{R} = \ln\left\{\left[1 + \frac{2\,\gamma}{\gamma+1}\,(Ma_1^2 - 1)\right]^{\frac{1}{\gamma-1}} \left[\frac{(\gamma+1)\, Ma_1^2}{2 + (\gamma-1)\, Ma_1^2}\right]^{-\frac{\gamma}{\gamma-1}}\right\} \quad . \tag{4.59}$$

The condition $s_2 - s_1 \geq 0$ shows, that compression shocks can exist only in supersonic flows. The nozzle flow discussed earlier can now be explained for the case of the non-adjusted pressure in the exit cross section with the aid of the normal-shock relations. If the pressure $p_e$ is not equal to the value, required for an isentropic supersonic flow in the divergent part of the nozzle, a normal compression shock is generated at a certain location in the nozzle, with the pressure jump just large enough, such that the pressure in the exit cross section can be matched. The flow velocity between the normal shock and the exit cross section is – according to the shock

relations – everywhere smaller than the local speed of sound. The following diagram shows the pressure and Mach number distribution in the streamwise direction in the nozzle.
The photographic picture taken in a supersonic wind tunnel shows the compression shock as thick dark line in the flow, almost normal to the line of symmetry of the two-dimensional nozzle. Also visible are several Mach lines, originated at the wall of the nozzle. Small disturbances, caused by grooves in the wall propagate along these lines into the flow.

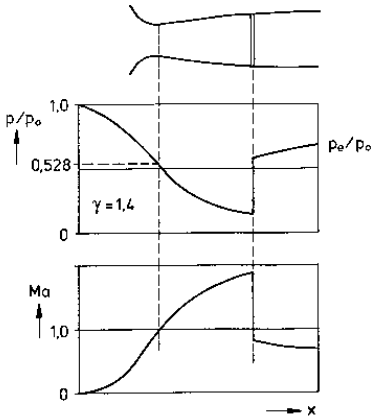


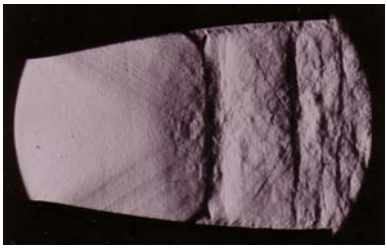

Supersonic flow with compression shock in a Laval nozzle. Mach lines can be noted upstream of the shock, which are originated on the wall of the nozzle.

### 4.4.2 Increase of Entropy Across the Normal Compression Shock

Assuming that the compression shock represents a discontinuity is only an approximation. In reality the shock has a thickness $\delta$ of the order of magnitude of several free mean paths. If the gas flowing through the shock can be assumed to be a continuum, the Navier-Stokes equations can be employed for the description of the flow between the upstream and downstream edge of the compression shock. The flow quantities do not change discontinuously in form of a jump, but in a continuous transition from the free-stream conditions to the flow conditions downstream from the shock.

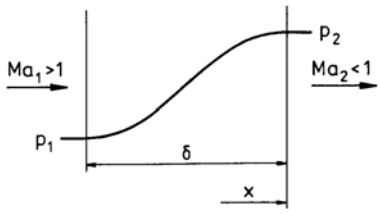


The increase of the entropy can now be explained as an action of the frictional forces and the heat conduction within the shock region of finite thickness. The conservation equations for one-dimensional, steady, viscous, and heat conducting flow are

$$\begin{aligned} d\left[\rho\, u\right] &= 0 \\ d\left[\rho\, u^2 + p - \frac{4}{3}\,\mu\,\frac{du}{dx}\right] &= 0 \\ d\left[\rho\, u\,\left(h + \frac{u^2}{2}\right) - \lambda\,\frac{dT}{dx} - \frac{4}{3}\,\mu\, u\,\frac{du}{dx}\right] &= 0 \quad . \end{aligned} \tag{4.60}$$

The terms in the square brackets represent the mass, momentum, and energy fluxes. They remain constant, and the introduction of frictional forces and heat conduction does not affect this result. If the flow variables are constant upstream of and downstream from the shock, the terms describing the shear stresses and the heat flux vanish outside of the shock.
The increase of entropy can be explained with the aid of the first law of thermodynamics in the form

$$ds = \frac{1}{T}\left(dh - \frac{1}{\rho}\,dp\right). \tag{4.61}$$

If the momentum equations is solved for $dp$ and the energy equation for $dh$ and if the resulting expressions are inserted in the second law of thermodynamics, there results

$$\rho\, u\, \frac{ds}{dx} = \frac{1}{T}\left[\frac{d}{dx}\left(\lambda\,\frac{dT}{dx}\right) + \frac{4}{3}\,\mu\,\left(\frac{du}{dx}\right)^2\right] \tag{4.62}$$

As the mass flux is constant, the last equation can be written in the following form:

$$\rho_1\, u_1\, (s_2 - s_1) = \int_1^2 \frac{\lambda}{T^2}\,\left(\frac{dT}{dx}\right)^2 dx + \frac{4}{3}\int_1^2 \frac{\mu}{T}\,\left(\frac{du}{dx}\right)^2 dx \tag{4.63}$$

The integrals in the above equation represent the contributions of the heat conduction and the dissipation of mechanical energy. They can be determined, if the local gradients $\frac{du}{dx}$ and $\frac{dT}{dx}$ are known. They, in turn, can be obtained by repeated integration of (4.60), with the boundary conditions given by (4.52). If it is assumed, that the Prandtl number is $Pr = \mu\,\frac{c_p}{\lambda} = 0.75$, then the total enthalpy $h_0$ remains constant. The continuity and the momentum equation can then be combined to yield

$$\frac{\gamma+1}{2\,\gamma}\,\rho_1\, u_1\,(u - u_1)\,\left(1 - \frac{a^{*2}}{u_1\, u}\right) - \frac{4}{3}\,\mu\,\frac{du}{dx} = 0 \tag{4.64}$$

The solution of this equation would provide the velocity distribution $u(x)$ within the shock. The temperature distribution $T(x)$ can be obtained from the energy equation in the form of (4.60) and also the integrands in (4.63). A closed-form solution is, however, not possible. The thickness of the shock can be estimated from (4.64). For transonic speeds it is of the order of magnitude

$$\delta \sim \frac{\eta}{\rho\, a}\,\frac{u_1}{(u_1 - u_2)} \quad . \tag{4.65}$$

### 4.4.3 Normal Shock in Transonic Flow

The shock relations can considerably be simplified for low supersonic speeds. If in the relation

$$\frac{s_2 - s_1}{R} = \ln\left\{\left[1 + \frac{2\,\gamma}{\gamma+1}\,\left(Ma_1^2 - 1\right)\right]^{\frac{1}{\gamma-1}}\,\left[\frac{(\gamma+1)\,Ma_1^2}{(\gamma-1)\,Ma_1^2 + 2}\right]^{-\frac{\gamma}{\gamma-1}}\right\} \tag{4.66}$$

the square of the Mach number $Ma_1^2$ is replaced by $1 + m$, with $m$ assumed to be small compared to unity, the expression of the right-hand side of (4.66) can be expanded in a power series. Collecting the resulting expressions in increasing powers of $m$, it is seen that the terms of first and second order vanish, and one obtains

$$\frac{s_2 - s_1}{R} = \frac{2\,\gamma}{(\gamma+1)^2}\,\frac{(Ma_1^2 - 1)^3}{3} + \ldots \quad . \tag{4.67}$$

This results shows, that the entropy increase across a normal compression shock is small at low supersonic Mach numbers. It increases with $(Ma_1^2 - 1)^3$. All changes of the state are therefore almost isentropic. The relation for the pressure change across the normal compression shock

$$\frac{p_2 - p_1}{p_1} = \frac{2\,\gamma}{\gamma+1}\,(Ma_1^2 - 1) \tag{4.68}$$

reduces to

$$\frac{p_2 - p_1}{p_1} = \left(\frac{12\,\gamma^2}{\gamma+1}\right)^{\frac{1}{3}}\,\left(\frac{s_2 - s_1}{R}\right)^{\frac{1}{3}} \quad . \tag{4.69}$$

The change of pressure can thereby directly be related to the increase of entropy.

## 4.5 Oblique Compression Shock

In addition to normal compression shocks, also oblique shocks can occur in supersonic flow. They are inclined by a certain angle, the shock angle $\sigma$, with respect to the direction of the free-stream flow.

### 4.5.1 Jump Conditions and Turning of the Flow

As for the normal shock, the jump conditions for the oblique shock can be obtained from the Euler equations for two-dimensional flow. It is advantageous, to use Cartesian coordinates, oriented normally and tangentially to the shock.
For uniform free-stream conditions and constant inclination of the shock, the jump conditions follow from the continuity equation, the two momentum equations, and the energy equation:

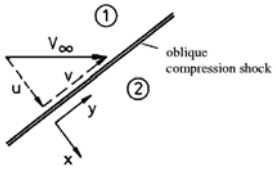


$$\begin{aligned}
\rho_1\, u_1 &= \rho_2\, u_2 \\
\rho_1\, u_1\, v_1 &= \rho_2\, u_2\, v_2 \\
\rho_1\, u_1^2 + p_1 &= \rho_2\, u_2^2 + p_2 \\
\rho_1\, u_1 \left[h_1 + \frac{1}{2}\left(u_1^2 + v_1^2\right)\right] &= \rho_2\, u_2 \left[h_2 + \frac{1}{2}\left(u_2^2 + v_2^2\right)\right]
\end{aligned} \tag{4.70}$$

The jump conditions for the oblique compression shock correspond to those for the normal shock. Mass, momentum, and energy fluxes normal to the shock remain constant during the passage of the flow through the shock. The tangential velocity component remains unchanged. The following sketch shows a part of an oblique shock, indicated by the thick black line. Shown is also the velocity upstream of the shock $V_1$, and downstream $V_2$, both decomposed into components normal and tangential to the shock $u_1$ and $v_1$, and $u_2$ and $v_2$. As $u_2$ is smaller than $u_1$, and as $v_2$ is equal to $v_1$, the direction of the oncoming velocity is changed, as the velocity triangles indicate. Thus an oblique shock always causes a turning of the flow towards the shock.

The flow is turned by the angle $\beta$. The jump conditions can again be used to derive the relations for the density, pressure, temperature, and velocity changes across the shock.
The density ratio can be expressed with the shock intensity $\frac{u_1}{a_1} = Ma_1 \sin\sigma$ as

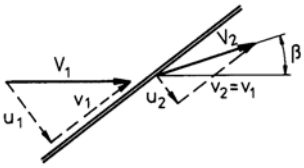


$$\frac{\rho_2}{\rho_1} = \frac{(\gamma+1)\, Ma_1^2\, \sin^2\sigma}{(\gamma-1)\, Ma_1^2\, \sin^2\sigma + 2} \quad , \tag{4.71}$$

the increase of pressure as

$$\frac{p_2 - p_1}{p_1} = \frac{2\,\gamma}{(\gamma+1)}\left(Ma_1^2\, \sin^2\sigma - 1\right) \quad , \tag{4.72}$$

the temperature ratio as

$$\frac{T_2}{T_1} = \frac{a_2^2}{a_1^2} = 1 + 2\,\frac{(\gamma-1)}{(\gamma+1)^2}\left(\frac{\gamma\, Ma_1^2\, \sin^2\sigma + 1}{Ma_1^2\, \sin^2\sigma}\right)\left(Ma_1^2\, \sin^2\sigma - 1\right) \quad , \tag{4.73}$$

the increase of entropy as

$$\frac{s_2 - s_1}{R} = \ln \left\{ \left[ 1 + 2\,\frac{\gamma}{\gamma+1}\,\left( Ma_1^2\,\sin^2\sigma - 1 \right) \right]^{\frac{1}{\gamma-1}}\,\left[ \frac{(\gamma+1)\,Ma_1^2\,\sin^2\sigma}{(\gamma-1)\,Ma_1^2\,\sin^2\sigma + 2} \right]^{-\frac{\gamma}{\gamma-1}} \right\} \quad , \tag{4.74}$$

and the Mach number downstream from the shock as

$$Ma_2^2\,\sin^2(\sigma-\beta) = \frac{2 + (\gamma-1)\,Ma_1^2\,\sin^2\sigma}{2\,\gamma\,Ma_1^2\,\sin^2\sigma - (\gamma-1)} \quad . \tag{4.75}$$

From the velocity diagram shown above, the normal components of the velocity $u_1$ and $u_2$ are

$$\frac{u_1}{v} = \tan\sigma \quad \text{and} \quad \frac{u_2}{v} = \tan(\sigma-\beta) \quad . \tag{4.76}$$

The ratio of these two expressions yields, together with the jump condition for the mass flux

$$\frac{\tan(\sigma-\beta)}{\tan\sigma} = \frac{(\gamma-1)\,Ma_1^2\,\sin\sigma^2 + 2}{(\gamma+1)\,Ma_1^2\,\sin\sigma^2} \quad . \tag{4.77}$$

The turning angle $\beta$ can now be expressed as follows

$$\beta = \arctan\left[ \frac{2\,\cot\sigma\,(Ma_1^2\,\sin^2\sigma - 1)}{Ma_1^2\,(\gamma + \cos(2\,\sigma)) + 2} \right] \quad . \tag{4.78}$$

The equation for the increase of entropy, (4.74), with $\Delta s \geq 0$, indicates that the shock intensity has to satisfy the condition

$$Ma_1\,\sin\sigma \geq 1 \quad . \tag{4.79}$$

The shock angle $\sigma$ is bounded from below by the Mach angle $\alpha$

$$\alpha = \arcsin\frac{1}{Ma_1}. \tag{4.80}$$

Then $\sigma$ can vary within the limits

$$\alpha \leq \sigma \leq \frac{\pi}{2} \tag{4.81}$$

The turning angle $\beta$ vanishes for both limits $\sigma = \frac{\pi}{2}$ and $\sigma = \alpha$; it attains an extremum value in between. For $Ma_1 \to \infty$ the expression for $\beta$ reduces to

$$\tan\beta \to \frac{\sin 2\sigma}{\gamma + \cos(2\sigma)} \quad , \tag{4.82}$$

so that with $\gamma = 1.4$ the maximum turning angle results to $\beta_{max} \approx 45°$ and the corresponding shock angle to $\sigma = 67.5°$. Similarly, it can be shown, that a maximum turning angle exists for every finite Mach number.

Another interesting relation results from (4.75), if $Ma_2$ is set equal to unity. Then for every free-stream Mach number $Ma_1$ and flow turning angle $\beta$ there exists a shock angle $\sigma$, which yields sonic conditions immediately downstream from the shock. It can also be expected, that the shock angle $\sigma$ of flows with $Ma_2 = 1$ is close to $\sigma_{max}$ as then the shock tends to be close to normal, with subsonic flow conditions downstream.

In the following diagram the dependence of the shock angle $\sigma$ is shown for several Mach numbers as a function of $\beta$.

According to the diagram, the jump conditions yield two solutions, which are characterized by different shock angles and shock intensities. The solutions are known as the weak and strong solution. The strong solution describes a flow which is subsonic downstream from the shock, the weak solution a flow which is supersonic with the exception of $\beta \sim \beta_{max}$. This region is bounded by the line $Ma_2 = 1$.

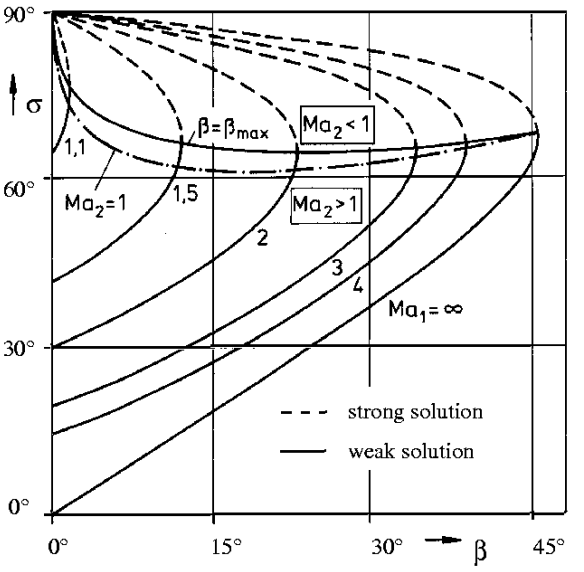


### 4.5.2 Weak and Strong Solution

The supersonic flow over a wedge is described by the weak solution for $\beta < \beta_{max}$.

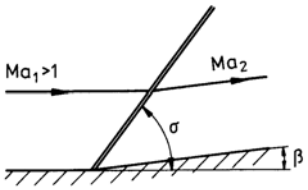


The turning angle $\beta$ is equal to the wedge angle. All flow quantities downstream from the oblique shock can be determined with the relations obtained from the jump conditions. The weak solution is also valid for a double wedge with nose angle $\beta$.

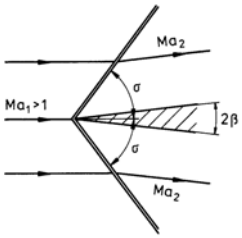


The flow quantities downstream from the shock can also be determined for a double wedge at angle of attack. With vanishing turning or nose angle of the wedge the shock intensity $Ma_1\ sin\sigma$ tends to unity, and the shock deteriorates to a sonic line.

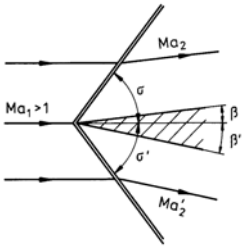


If the nose angle of the wedge $\beta$ is $\beta > \beta_{max}$, the shock is detached from the wedge and deforms into a bow shock in front of the wedge.

A closed-form solution of the conservation equations does not exist for the flow field between the bow shock and the wedge. In a certain point on the shock, the tangent of the shock is normal to the direction of the free-stream velocity.

The shock angle $\sigma$ then attains all possible values, from $\sigma = \frac{\pi}{2}$ to the value corresponding to the maximum turning angle, further to the angle, corresponding to the speed of sound immediately downstream from the shock, until it decreases to the Mach angle of the free stream $\alpha$ at large distances from the wedge. The strong solution is valid for that part of the shock between the points $S$ and $S'$.

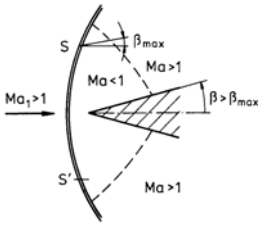


### 4.5.3 Heart-Curve Diagram and Hodograph Plane

Due to the non-linearity of the jump conditions the pressure ratio cannot explicitly be formulated in terms of the turning angle. However, the pressure ratio $\frac{p_2}{p_1}$ and the turning angle $\beta$ can be computed for all values of the shock intensity, so that a plot of $\frac{p_2}{p_1} = f(\beta)$ can be provided. The shape of the curve is similar to that of the contour of the heart, the lower part of which representing the weak solution and the upper part the strong solution. With the aid of the heart-curve diagram the pressure ratio across the oblique shock can easily be determined for every turning angle.

A supplement for the description of the flow in the physical plane is the so-called hodograph plane, with the velocity components as coordinates. The hodograph plane enables a simple representation of the solution of the jump conditions for the normal and the oblique compression shock.

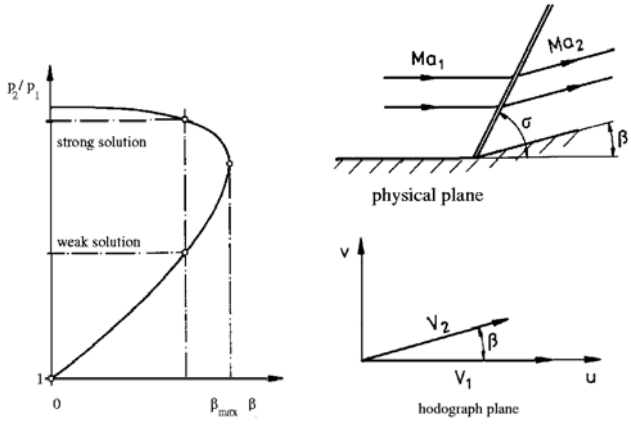


The velocity vectors downstream from the oblique shock are first plotted for all values of the turning angle at a constant free-stream Mach number. The resulting curve is called the shock polar. Most of the time it is plotted in the form of the velocity components, nondimensionalized with the critical speed of sound $a^*$. The hodograph plane is bounded by a circle with radius $R = [\frac{\gamma+1}{\gamma-1}]^{\frac{1}{2}}$. The sonic line is represented by a circle with radius unity. The weak solution is given by the point $B$, the strong solution by the point $B'$; the velocity of the flow containing a normal shock is given by the point $A'$. There exists a shock polar for every free-stream Mach number $Ma_1$.

In order to determine the dimensionless downstream velocity $\frac{v_2}{a^*}$ the turning angle $\beta$ is plotted, intersecting the shock polar in the point $B$. The tangential and the two normal velocity components are obtained by constructing the normal from the origin of the coordinates to the extension of the line $A - B$.

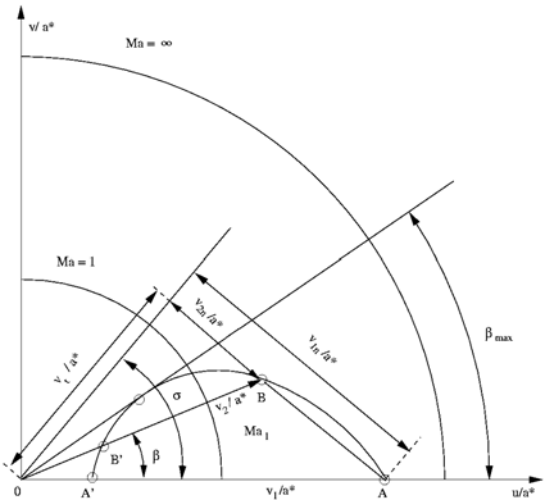


### 4.5.4 Weak Compression Shocks

Compression shocks are termed weak, if the shock intensity $Ma_1 \sin\sigma$ approaches unity. The jump conditions can be simplified with this assumption. First the relation for the turning angle $\beta$ is solved for $Ma_1^2 \sin^2\sigma$:

$$Ma_1^2 \sin^2\sigma = \frac{2 \tan\sigma}{(\gamma+1)\tan(\sigma-\beta) - (\gamma-1)\tan\sigma} \tag{4.83}$$

For weak shocks the shock angle $\sigma$ does not differ much from the Mach angle $\alpha$, and the turning angle $\beta$ tends to zero. One obtains for small angles $\beta$

$$Ma_1^2 \sin^2\sigma \approx 1 + \frac{\gamma+1}{2} \frac{Ma_1^2}{\sqrt{Ma_1^2-1}} \beta \quad . \tag{4.84}$$

The dimensionless pressure difference is approximately

$$\frac{p_2 - p_1}{p_1} = \frac{\gamma\, Ma_1^2}{\sqrt{Ma_1^2-1}} \beta \quad . \tag{4.85}$$

Also the expression for the increase of the entropy can be approximated:

$$\frac{s_2 - s_1}{R} \approx \frac{\gamma+1}{12\,\gamma^2} \left( \frac{\gamma\, Ma_1^2}{\sqrt{Ma_1^2-1}} \right)^3 \beta^3 \tag{4.86}$$

The square of the velocity ratio $\frac{v_2}{v_1}$ is

$$\left(\frac{v_2}{v_1}\right)^2 = \frac{\left(\frac{u_2}{v}\right)^2 + 1}{\left(\frac{u_1}{v}\right)^2 + 1} = \frac{\tan^2(\sigma-\beta)+1}{\tan^2\sigma + 1} = \frac{\cos^2\sigma}{\cos^2(\sigma-\beta)} \quad . \tag{4.87}$$

With the approximation $\sigma \to \alpha$, $\beta \to 0$ there results

$$\left(\frac{v_2}{v_1}\right)^2 \approx (1 - 2\,\tan\alpha\beta) \approx \left[1 - \frac{\beta}{\sqrt{Ma_1^2-1}}\right]^2 \tag{4.88}$$

and finally

$$\frac{v_2 - v_1}{v_1} = \frac{\Delta v}{v_1} = -\frac{\beta}{\sqrt{Ma_1^2 - 1}} \quad . \tag{4.89}$$

The last relation shows, that the velocity is decreased, if the turning angle $\beta$ is increased. The decrease of the velocity simultaneously causes an increase of the pressure and of the density. The compression can be enforced either by one or several weak oblique compression shocks.

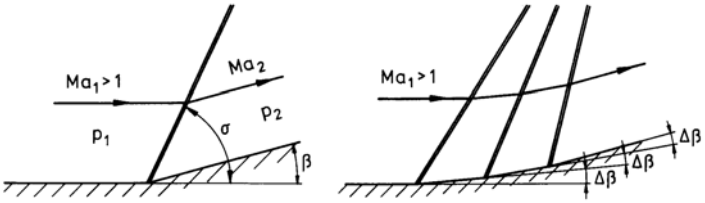


If the compression is designed in such a way, that the turning of the flow is the same in both cases, i. e. $\beta = n\,\Delta\,\beta$, then the pressure after the $n$-th turning is

$$p_n = p_1 + \ \mathrm{O}(n\,\Delta\,\beta) \quad . \tag{4.90}$$

The increase of entropy

$$s_n = s_1 + O(n\,\Delta\,\beta^3) = O\left(\frac{\beta^3}{n^2}\right) \tag{4.91}$$

can substantially be reduced, if the number of the turning elements is increased and approaches infinity in the limiting case. Very weak shocks then reduce asymptotically to so-called Mach waves. The width of each of the compression elements is infinitesimally small. The contour is continuously curved. Along the Mach lines the Mach number and the turning angle are constant. The flow cannot be influenced against the main flow direction, and disturbances cannot propagate upstream. A certain distance away from the contour, the Mach waves coalesce to an oblique compression shock.

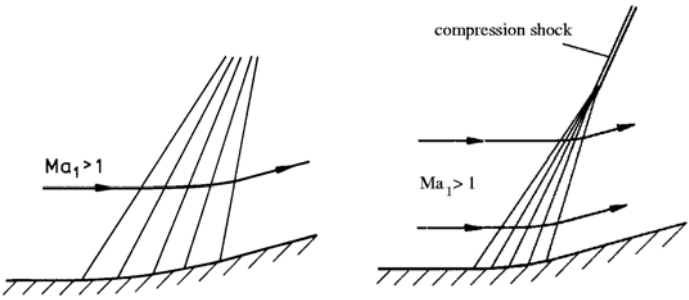


## 4.6 The Prandtl-Meyer Flow

As just shown, the entropy remains constant if an inviscid supersonic flow is continuously turned by infinitesimally weak oblique compression shocks. An increase of the total turning angle causes a decrease of the velocity and an increase of the static pressure. Vice versa, the turning angle can be decreased, the velocity increased, and the pressure decreased. Then the gas is said to expand.

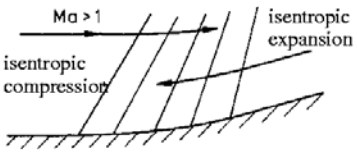


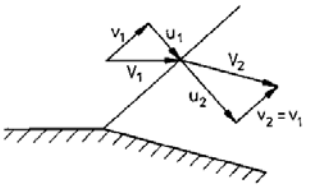


In a supersonic flow a continuously curved contour therefore generates an isentropic compression, if the turning angle is increased, and an expansion, if the turning angle is decreased.

If a discontinuous expansion would be assumed, as indicated in the sketch, the normal velocity component would have to increase and pressure and temperature would have to decrease. The shock relations would then require a decreasee of entropy, which would contradict the second law of thermodynamics; it is for this reason, that an expansion can occur only in isentropic flow with continuous turning.

### 4.6.1 Isentropic Change of Velocity

The equation for the change of the velocity across a weak compression shock reduces to a differential equation of the following form if isentropic flow is assumed

$$\sqrt{Ma^2 - 1}\,\frac{dv}{v} = \cot\alpha\,\frac{dv}{v} = -d\beta \quad . \tag{4.92}$$

The integral of this equation was first published by Prandtl and Meyer in 1908. In order to facilitate the integration, the square of the velocity is expressed through the Mach angle with the aid of the energy equation

$$v^2 = \frac{a^{*2}}{\sin^2\alpha + b^2\,\cos^2\alpha} \quad . \tag{4.93}$$

The quantity $b^2$ is an abbreviation of $\frac{\gamma-1}{\gamma+1}$. By differentiation of this expression the differential equation for the velocity change can be cast into the following form:

$$\frac{b^2 - 1}{b^2 + \tan^2\alpha}\,d\alpha = -d\beta \tag{4.94}$$

The integration of the left-hand side of this equation yields an angle $\nu(Ma)$, which became known as the Prandtl-Meyer angle.

$$\nu(Ma) = \alpha - \frac{1}{b}\left[\frac{\pi}{2} - \arctan(b\cot\alpha)\right] + C \tag{4.95}$$

The constant of integration $C$ is so chosen, such that the Prandtl-Meyer angle vanishes for $Ma = 1$.

$$\nu(Ma) = \sqrt{\frac{\gamma+1}{\gamma-1}}\,\arctan\left[\sqrt{\frac{\gamma-1}{\gamma+1}\,(Ma^2-1)}\right] - \arctan\left[\sqrt{Ma^2-1}\right] \tag{4.96}$$

For $Ma \geq 1$ there exists a uniquely defined value of $\nu$, which with increasing Mach number monotonically tends to

$$\lim_{Ma\to\infty}\nu = \nu_{max} = \frac{\pi}{2}\left(\sqrt{\frac{\gamma+1}{\gamma-1}} - 1\right). \tag{4.97}$$

For example, for $\gamma = 1.4 \quad \nu_{max} = 130.5°$.
The integral of the right-hand side of the differential equation for the velocity change completes the relation between the Prandtl-Meyer angle $\nu(Ma)$ and the turning angle:

$$\nu - \nu_1 = \beta_1 - \beta \tag{4.98}$$

With these relations isentropic expansion and compression of the Prandtl-Meyer flow can easily be determined:

$$\begin{aligned} \text{Expansion:} \qquad & \beta < \beta_1, \quad \nu > \nu_1 \\ & \nu = \nu_1 + \mid \beta - \beta_1 \mid \\ \text{Compression:} \qquad & \beta > \beta_1, \quad \nu < \nu_1 \\ & \nu = \nu_1 - \mid \beta - \beta_1 \mid \end{aligned} \tag{4.99}$$

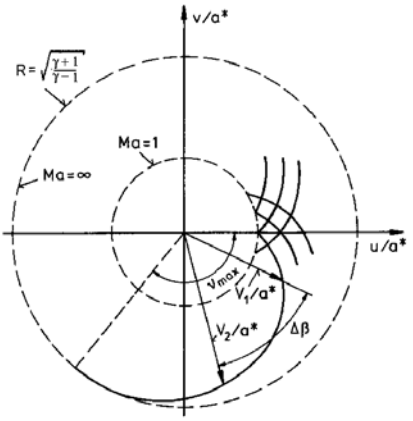


The Prandtl-Meyer angle $\nu(Ma)$ is tabulated in the appendix as a function of the Mach number. The solution can easily be plotted in the hodograph plane. The Prandtl-Meyer integral represents an epicycloid, extending from the sonic circle ($Ma = 1$) to the circle of the limiting velocity ($Ma \to \infty$). Expansion and compression, which are given by a certain turning of the flow $\Delta\beta$, can simply be entered in the hodogragh plane and the corresponding velocity change can be read off.

### 4.6.2 Corner Flow

A uniform supersonic flow with a Mach number $Ma_1 \geq 1$ over a plane wall, by kinking of the wall at an arbitrary point $P$ into a convex corner, can be turned by the amount $\Delta\beta$. After the turn the gas moves with the Mach number $Ma_2$ parallel to the bent part of the wall. The flow can be determined with the aid of the Prandtl-Meyer integral.

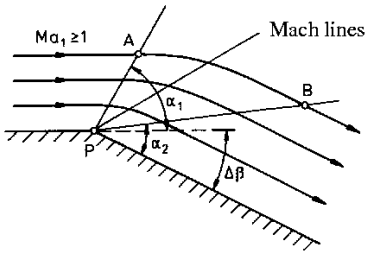


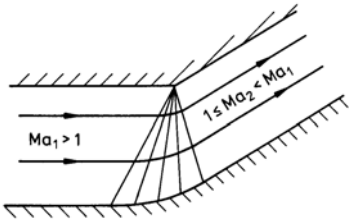


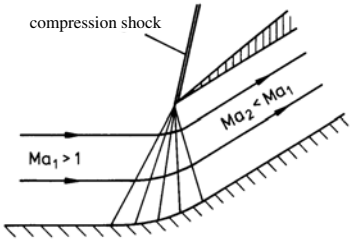

In the region bounded by the Mach lines $PA$ and $PB$ the flow quantities are constant along each Mach line, but change from line to line. It is in this region that the flow expands from $Ma_1$ to $Ma_2$. The solution is singular in the point $P$, where all flow conditions corresponding to $Ma_1 \leq Ma \leq Ma_2$ can be found.
The gas can also be thought of to flow in the opposite direction. In this form the Prandtl-Meyer flow provides the principle for an isentropic inlet diffuser, used on supersonic airplanes. The previous sketch shows the flow reversal (compression by solidification of a streamline). The flow field on the right demonstrates how a supersonic inlet diffuser can be constructed with the Prandtl-Meyer corner flow.
Expansion and compression are illustrated with two numerical examples: Assume that a plane supersonic flow with a Mach number $Ma_1 = 3$ is given. The corresponding Prandtl-Meyer angle $\nu$ is $\nu = 49.76°$. The oncoming flow is assumed not to have been turned, so that $\beta_1 = 0°$. If the flow is to be decelerated to sonic speed, it has to be turned by $\beta_{Ma=1} = 49.76°$.
In the second example it is assumed, that a plane supersonic flow with a free-stream Mach number $Ma_1 = 2$ ($\nu_1 = 26.38°$) is turned by 10°. For an expansion there results a Prandtl-Meyer angle of $\nu_2 = 36.38°$, corresponding to a Mach number $Ma_2 = 2.386$, and for a compression, the Prandtl-Meyer angle is $\nu_2 = 16.38°$, and the Mach number is $Ma_2 = 1.652$.

### 4.6.3 Interactions Between Shock Waves and Expansions

Prandtl-Meyer flows and oblique compression shocks can interact with each other. To be distinguished are shock-shock and shock-expansion interactions.

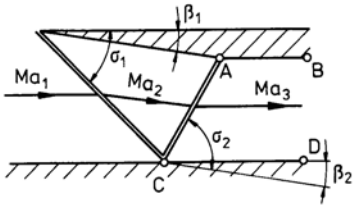


In the following sketch the reflexion of an oblique compression shock on a rigid wall is shown. If a shock impinges on a wall, it is reflected, as the wall affects the oncoming flow as a wedge.
The reflected shock has the shock angle $\sigma_2$, which differs from $\sigma_1$, although $\beta_1$ and $\beta_2$ have the same value. The gas can only flow off parallel to the walll $CD$, if the wall $AB$ is parallel to $CD$. The pressure ratio $\frac{p_3}{p_1}$ is given by the shock intensities $Ma_1 \sin\sigma_1$ and $Ma_2 \sin\sigma_2$.
If the flow is mirrored at the wall $CD$ and if the wall is replaced by a streamline, the intersection of two oblique compression shocks of equal intensity results. The shocks are bent when they intersect each other. For the flow shown the gas flows off parallel to the oncoming flow.
The intersection of two oblique shocks of different intensity is also possible. If both shocks are assumed to be weak, the flow pattern is different from the one just discussed. The streamline through the point of intersection divides the flow into two regions of different stagnation pressures, as the shock intensities are no longer the same on both sides of the dividing streamline. As a consequence, the two regions have different entropy levels and also the other flow variables attain different values, with the exception of the static pressure. Hence the flow cannot maintain the direction of the free stream. It is found that the streamline through the point of intersection is inclined to the direction of the oncoming flow by the angle $\delta$ (Page 160, a).
The angle $\delta$ results from the condition, that the static pressure on both sides of the streamline through the point of intersection has to have the same value.

$$\frac{p_3}{p_1} = \frac{p_3'}{p_1} = \frac{p_3\, p_2}{p_2\, p_1} = \frac{p_3'\, p_2'}{p_2'\, p_1} \tag{4.100}$$

Because of the different shock intensities the increase of entropy $s_3' - s_1$ is not equal to the increase of entropy $s_3 - s_1$. The streamline through the point of intersection represents a line of discontinuity of the entropy, the density, the velocity, and the temperature.

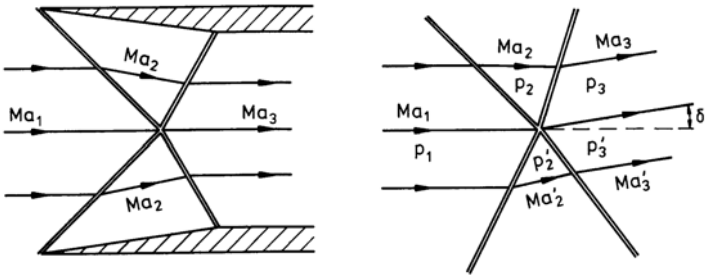


a)

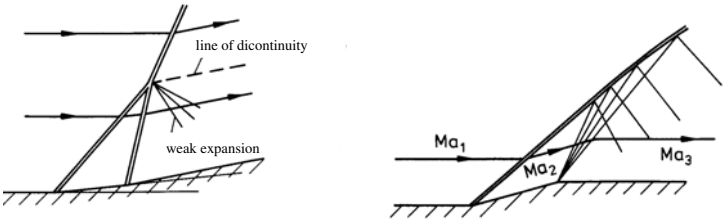


b)

If two oblique shocks are generated by two wedges, one downstream from the other (see sketch b), they coalesce and form a single shock, which approximately produces the same rise of the static pressure as the two other oblique shocks. A mutual pass through of the shocks is not possible, and a weak expansion or compression can arise downstream from the point of intersection to balance the static pressure.
If a Prandtl-Meyer flow interacts with an oblique compression shock, the shock is being curved. The Mach waves are reflected at the shock and interact with each other.
If an oblique compression shock impinges on a wall at an shock angle $\sigma$, for which at $Ma_2$ $\beta > \beta_{max}$, the reflected shock can no longer be attached to the wall. This type of reflection is called Mach reflection. An almost normal compression shock is originated in the immediate vicinity of the wall, which joins the impinging and the reflected shock in the triple point.

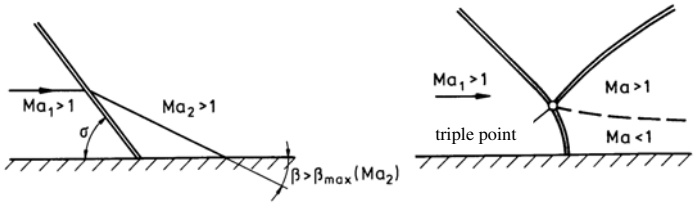


Again a line of discontinuity of entropy is formed downstream from the triple point. The static pressure has the same value on both sides of the line, but all other flow quantities attain different values.

## 4.7 Lift and Wave Drag in Supersonic Flow

With the jump conditions for oblique compression shocks and the Prandtl-Meyer flow pressure distributions can be determined for airfoil sections moving in supersonic flow.

### 4.7.1 The Wave Drag

Airfoils in inviscid supersonic flow generate drag, which is caused by the compression shocks.

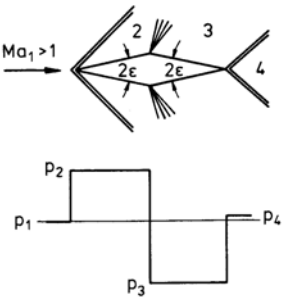


For example, the flow over the front part of a double-wedge profile is compressed by the oblique shock, attached to the leading edge, and the pressure is $p_2$. The gas expands at the shoulder of the profile in a Prandtl-Meyer corner flow, and the pressure on the rear part of the profile is lowered to $p_3$. Finally, the pressure is increaed again at the trailing edge, when the flow passes through the recompression shock, downstream of which the pressure is $p_4$. Caused by the overpressure on the front part and the lower pressure on the rear part of the profile, a drag per unit length results, which is

$$F_D = (p_2 - p_3)d \quad . \tag{4.101}$$

The quantity $d$ is the maximum thickness of the profile. The drag is called wave drag of supersonic flow. Pressure drag caused by flow separation and frictional drag have to be determined separately.

### 4.7.2 Lift of a Flat Plate at Angle of Attack

A flat plate, inclined in an inviscid supersonic flow at the angle of attack $\beta$, generates lift in addition to the wave drag. Both, lift and wave drag can be determined with the jump conditions of oblique compression shocks and the Prandtl-Meyer flow:

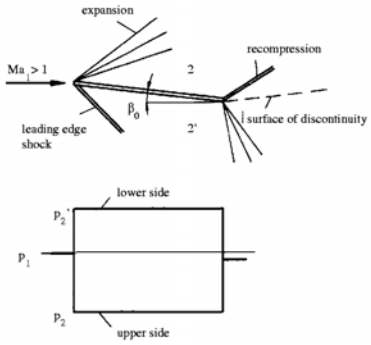


$$\begin{aligned} F_L &= (p_2' - p_2)\, t\, \cos\beta \\ F_D &= (p_2' - p_2)\, t\, \sin\beta \end{aligned} \tag{4.102}$$

The quantity $t$ is the chord of the profile. Since wing sections in general are thin and since their angles of attack are small, approximate solutions can be constructed for the determination of lift and wave drag. Because of the different shock intensities of the oblique shock at the leading edge and the recompression shock at the trailing edge, a surface of discontinuity of the entropy is generated at the trailing edge of the flat plate.

### 4.7.3 Thin Profiles at Angle of Attack

With the approximation for the pressure jump for weak oblique compression shocks

$$\frac{\Delta p}{p_1} \approx \frac{\gamma Ma_1^2}{\sqrt{Ma_1^2 - 1}}\, \Delta\beta \tag{4.103}$$

the pressure coefficient can be determined for small angles of attack as a function of the free-stream Mach number.

$$c_p = \frac{p - p_1}{\frac{\rho_1}{2}\, v_1^2} = \frac{2}{\gamma\, Ma_1^2}\, \frac{\Delta p}{p_1} \approx \frac{2\,\beta}{\sqrt{Ma_1^2 - 1}} \tag{4.104}$$

Lift and wave drag of the flat plate result from the pressure difference between lower and upper side of the plate.

$$c_{pl} - c_{pu} = \frac{4\,\beta}{\sqrt{Ma_1^2 - 1}} \tag{4.105}$$

The lift coefficient is

$$c_L = (c_{pl} - c_{pu}) \cos\beta = \frac{4\,\beta}{\sqrt{Ma_1^2 - 1}} \tag{4.106}$$

and the drag coefficient

$$c_D = (c_{pl} - c_{pu}) \sin\beta = \frac{4\,\beta^2}{\sqrt{Ma_1^2 - 1}} \quad . \tag{4.107}$$

The ratio

$$\frac{c_D}{c_L^2} = \frac{1}{4}\sqrt{Ma_1^2 - 1} \tag{4.108}$$

is independent of the angle of attack $\beta$.
For the double-wedge profile with nose angle $2\epsilon$ and vanishing angle of attack, the approximation yields for the front and rear part of the profile

$$c_p = \pm\frac{2\,\epsilon}{\sqrt{Ma_1^2 - 1}} \quad . \tag{4.109}$$

The drag coefficient is

$$c_D = \frac{4}{\sqrt{Ma_1^2 - 1}} \left(\frac{d}{l}\right)^2 . \tag{4.110}$$

With the approximation for thin profiles, lift and wave drag can also be determined for non-zero angles of attack, variable thickness distribution, and camber.

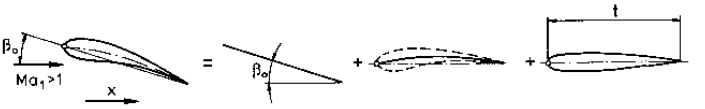


angle of attack camber thickness distribution

The local angle of attack consists out of three parts: The angle of attack of the chord $\beta_0$, the angle of attack of the mean camber line $\Delta\beta_c(x)$ with respect to $\beta_0$, and the angle of attack of the thickness distribution $\Delta\beta_t(x)$, with respect to the mean camber line

$$\beta = \beta_0 + \Delta\beta_c + \Delta\beta_t \quad . \tag{4.111}$$

The lift of the profile is

$$F_L = \frac{\rho_1}{2}\, v_1^2 \int_0^t (c_{pu} - c_{po})\, dx \quad . \tag{4.112}$$

The other integrals vanish with $\Delta\beta_c(x) \approx \frac{dy_c}{dx}$ and $\Delta\beta_t(x) \approx \frac{dy_t}{dx}$, and the expression for the lift coefficient is

$$c_L = \frac{4\,\beta_0}{\sqrt{Ma_1^2 - 1}} \quad . \tag{4.113}$$

The wave drag of the profile is

$$F_D = \frac{\rho_1\, v_1^2}{2} \int_0^t \left[ \left( \frac{dy_u}{dx} \right)^2 + \left( \frac{dy_l}{dx} \right)^2 \right] dx \, \frac{2}{\sqrt{Ma_1^2 - 1}} \quad , \tag{4.114}$$

and the drag coefficient can be written in the following form:

$$c_D = \frac{4}{\sqrt{Ma_1^2 - 1}} \left( \beta_0^2 + \overline{\Delta\beta_c^2} + \overline{\Delta\beta_t^2} \right) \tag{4.115}$$

The quantities $\overline{\Delta\beta_c^2}$ and $\overline{\Delta\beta_t^2}$ are the squares of the angular variations, averaged over the chord of the profile. In general the wave drag consists out of three parts, which result from the angle of attack, the camber, and the thickness distribution.

## 4.8 Theory of Characteristics

If two Prandtl-Meyer flows interact with each other, the flow cannot be described by superposition of the Prandtl-Meyer solutions, since they describe only simple waves, but not their intersections. A solution for non-simple regions can be constructed with the conservation equations for two-dimensional flows.
The following sketch shows the simple and non-simple regions of two Prandtl-Meyer flows superposed on each other. Close to the two corners the flows do not interact with each other, but downstream from the first intersection of the Mach lines the flow is influenced by both corners.

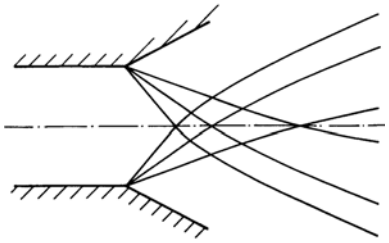

Non-simple regions also exist on the downstream side of curved compression shocks. Then the changes of the entropy have to be included in the determination of the pressure, density, temperature, and velocity. The interdependence between the distribution of entropy and the velocity field is described in the Crocco vorticiy theorem.

### 4.8.1 The Crocco Vorticity Theorem

With the second law of thermodynamics

$$T ds = dh - \frac{dp}{\rho} \tag{4.116}$$

and the energy equation the total derivative of the entropy can be expressed through the total derivatives of velocity and pressure. If it is assumed, that the stagnation temperature is constant throughout the entire flow field, it follows that

$$T ds = -\left( u\, du + v\, dv + \frac{dp}{\rho} \right) \quad . \tag{4.117}$$

For a two-diemnsional steady flow the total derivatives of the velocity components are

$$du = \frac{\partial u}{\partial x}dx + \frac{\partial u}{\partial y}dy \quad \text{and} \quad dv = \frac{\partial v}{\partial x}dx + \frac{\partial v}{\partial y}dy \quad . \tag{4.118}$$

Introduction of the momentum equations leads to the following expression for $Tds$

$$Tds = -\left[\left(\frac{v}{u} - \frac{dy}{dx}\right)\left(\frac{\partial v}{\partial x} - \frac{\partial u}{\partial y}\right)\right] udx \quad . \tag{4.119}$$

The ratio $\frac{dy}{dx}$ can be viewed as the slope of arbitrary unknown sets of curves. If the slope is chosen to be identical with the slope of the streamlines

$$\frac{dy}{dx} = \frac{v}{u} \quad , \tag{4.120}$$

it can be concluded, that the entropy remains constant along streamlines.

$$ds = \frac{\partial s}{\partial x}dx + \frac{\partial s}{\partial y}dy = 0 \qquad u\,\frac{\partial s}{\partial x} + v\,\frac{\partial s}{\partial y} = 0 \tag{4.121}$$

Streamlines are therefore called the characteristic lines of the entropy. The entropy remains constant in the entire flow field, if the second bracketed term $\frac{\partial v}{\partial x} - \frac{\partial u}{\partial y}$, representing one of the components of the vorticity vector, vanishes. This is the contents of the Crocco vorticity theorem, which also holds for three-dimensional flows: If in the second law of thermodynamics in the form

$$T\,\nabla\, s = \nabla h - \frac{\nabla p}{\rho} \tag{4.122}$$

the gradient of the static enthalpy is eliminated with the energy equation

$$\nabla\, h = -\nabla\,\frac{v^2}{2} + \nabla\, h_0 \quad , \tag{4.123}$$

and if the momentum equation is introduced in vector form

$$\frac{\partial \boldsymbol{v}}{\partial t} + (\boldsymbol{v}\cdot\nabla)\,\boldsymbol{v} = -\frac{\nabla p}{\rho}, \tag{4.124}$$

one obtains the Crocco vorticty theorem for three-dimensional flow

$$T\,\nabla s + \boldsymbol{v}\ \mathrm{x}\ (\nabla\ \mathrm{x}\ \boldsymbol{v}) = \frac{\partial \boldsymbol{v}}{\partial t} + \nabla h_0 \quad . \tag{4.125}$$

According to this theorem the entropy remains constant along streamlines, even in three-dimensional flows, as long as the the velocity and the stagnation enthalpy do not change with time. This becomes clear, if the scalar product of (4.125) and the velocty vector $\boldsymbol{v}$ is obtained; then the second term of the left-hind side of the last equation vanishes. For otherwise equal conditions the entropy remains constant in irrotational flows.

### 4.8.2 The Fundamental Equation of Gasdynamics

The partial derivative of the density, pressure, and temperature can be eliminated from the conservation equations for mass, momentum, and energy, so that only the velocity components and their partial derivatives remain in the resulting equation. This equation is called the fundamental equation of gasdynamics. It will first be derived for two-dimensional steady flows, but

will then be extended to three-dimensional flows. The continuity equation and the momentum equations read

$$\begin{aligned} \frac{\partial u}{\partial x} + \frac{\partial v}{\partial y} + \frac{1}{\rho}\left(u\,\frac{\partial \rho}{\partial x} + v\,\frac{\partial \rho}{\partial y}\right) &= 0 \\ u\,\frac{\partial u}{\partial x} + v\,\frac{\partial u}{\partial y} + \frac{1}{\rho}\,\frac{\partial p}{\partial x} &= 0 \\ u\,\frac{\partial v}{\partial x} + v\,\frac{\partial v}{\partial y} + \frac{1}{\rho}\,\frac{\partial p}{\partial y} &= 0 \quad . \end{aligned} \tag{4.126}$$

The energy equation in the form $h_0 = const.$ and the differential of the thermal equation of state

$$dp = \frac{p}{\rho}\,d\rho + \frac{p}{T}dT \tag{4.127}$$

yield the following relation:

$$u\,\frac{\partial p}{\partial x} + v\,\frac{\partial p}{\partial y} = -\frac{u\,p}{c_p\,T}\left(u\,\frac{\partial u}{\partial x} + v\,\frac{\partial v}{\partial x}\right) - \frac{v\,p}{c_p\,T}\left(u\,\frac{\partial u}{\partial x} + v\,\frac{\partial v}{\partial x}\right) - p\,\left(\frac{\partial u}{\partial x} + \frac{\partial v}{\partial y}\right) \quad . \tag{4.128}$$

Multiplying the first momentum equation with $u$ and the second with $v$ and adding the resulting relations yields

$$u\,\frac{\partial p}{\partial x} + v\,\frac{\partial p}{\partial y} = -\left[\rho\,u^2\,\frac{\partial u}{\partial x} + \rho\,u\,v\,\left(\frac{\partial u}{\partial y} + \frac{\partial v}{\partial x}\right) + \rho\,v^2\,\frac{\partial v}{\partial y}\right] \quad . \tag{4.129}$$

The fundamental equation of gasdynamics for two-dimensional steady flow is obtained by subtracting (4.129) from (4.128)

$$(u^2 - a^2)\,\frac{\partial u}{\partial x} + v\,u\,\left(\frac{\partial u}{\partial y} + \frac{\partial v}{\partial x}\right) + \left(v^2 - a^2\right)\,\frac{\partial v}{\partial y} = 0 \quad . \tag{4.130}$$

In the above equation, $a$ is the local speed of sound. For three-dimensional flows, one obtains with the aid of the energy equation, the thermal equation of state, and the continuity equation, a relation for $\boldsymbol{v} \cdot \nabla\, p$

$$\boldsymbol{v} \cdot \nabla\, p = -\frac{p}{c_p\,T}\,\boldsymbol{v} \cdot \nabla\,\left(\frac{\boldsymbol{v}^2}{2}\right) - p\,(\nabla \cdot \boldsymbol{v}) \quad , \tag{4.131}$$

which is inserted into the equation for the mechanical energy:

$$\boldsymbol{v} \cdot \nabla\left(\frac{\boldsymbol{v}^2}{2}\right) = -\frac{\boldsymbol{v}}{\rho} \cdot \nabla\, p \tag{4.132}$$

After collecting terms, the last equation, written in Cartesian coordinates, becomes:

$$\begin{aligned} (u^2 - a^2)\,\frac{\partial u}{\partial x} + (v^2 - a^2)\,\frac{\partial v}{\partial y} + (w^2 - a^2)\,\frac{\partial w}{\partial z} + \\ + vw\left(\frac{\partial v}{\partial z} + \frac{\partial w}{\partial y}\right) + uv\left(\frac{\partial u}{\partial y} + \frac{\partial v}{\partial x}\right) + uw\left(\frac{\partial u}{\partial z} + \frac{\partial w}{\partial x}\right) = 0 \end{aligned} \tag{4.133}$$

In comparison to the equation derived previously, the fundamental equation of gasdynamics contains three additional terms for three-dimensional flows.

### 4.8.3 Compatibility Conditions for Two-Dimensional Flows

According to the Crocco vorticty theorem, in inviscid steady flows the entropy remains constant along streamlines. It is therefore advantageous, to introduce streamline coordinates $\xi$ and $\eta$, which are oriented in the direction of the streamlines and normal to them. Since $\frac{\partial s}{\partial \xi} = 0$, the derivative of the entropy in the direction normal to the streamlines can be written as total derivative

$$\frac{ds}{d\eta} = \frac{1}{v}\left(u\,\frac{\partial s}{\partial y} - v\,\frac{\partial s}{\partial x}\right). \tag{4.134}$$

The partial derivatives $\frac{\partial s}{\partial x}$ and $\frac{\partial s}{\partial y}$ are substituted with the aid of the Crocco vorticity theorem

$$\frac{\partial s}{\partial x} = -\frac{v}{T}\left(\frac{\partial v}{\partial x} - \frac{\partial u}{\partial y}\right) \quad , \qquad \frac{\partial s}{\partial y} = \frac{u}{T}\left(\frac{\partial v}{\partial x} - \frac{\partial u}{\partial y}\right) \quad , \tag{4.135}$$

so that the partial derivative $\frac{\partial v}{\partial x}$ is replaced by $\frac{\partial u}{\partial y}$ and the entropy gradient $\frac{ds}{d\eta}$

$$\frac{\partial v}{\partial x} = \frac{\partial u}{\partial y} + \frac{T}{v}\,\frac{ds}{d\eta} \quad . \tag{4.136}$$

This expression is inserted into the fundamental equation of gasdynamics. There is obtained

$$(u^2 - a^2)\,\frac{\partial u}{\partial x} + (v^2 - a^2)\,\frac{\partial v}{\partial y} + 2vu\,\frac{\partial u}{\partial y} + \frac{vuT}{v}\,\frac{ds}{d\eta} = 0 \quad . \tag{4.137}$$

The last step consists in the elimination of the partial derivatives of the velocity components. The total derivatives

$$du = \frac{\partial u}{\partial x}dx + \frac{\partial u}{\partial y}dy \quad \text{and} \quad dv = \frac{\partial v}{\partial x}dx + \frac{\partial v}{\partial y}dy \tag{4.138}$$

are solved for $\frac{\partial u}{\partial x}$ and $\frac{\partial v}{\partial y}$:

$$\frac{\partial u}{\partial x} = \frac{du}{dx} - y'\,\frac{\partial u}{\partial y} \quad ; \quad \frac{\partial v}{\partial y} = \frac{1}{y'}\left(\frac{dv}{dx} - \frac{\partial v}{\partial x}\right) \tag{4.139}$$

The quantity $y'$, written as abbreviation for $\frac{dy}{dx}$, can, as in the derivation of the Crocco vorticity theorem, be thought of as the unknown local slope of sets of curves. With the last two equations the fundamental equation of gasdynamics can be written as

$$\begin{aligned}(u^2 - a^2)\frac{du}{dx} + (v^2 - a^2)\,\frac{1}{y'}\,\frac{dv}{dx} \quad &- \quad \left[y'\,(u^2 - a^2) + \frac{1}{y'}\,(v^2 - a^2) - 2\,u\,v\right]\frac{\partial u}{\partial y} \\ &- \quad \left[\frac{1}{y'}\,(v^2 - a^2) - u\,v\right]\frac{T}{v}\,\frac{ds}{d\eta} = 0 \quad .\end{aligned} \tag{4.140}$$

The slope $y'$ is now chosen in such a way, that the bracketed term multiplying $\frac{\partial u}{\partial y}$, vanishes:

$$y' = \frac{uv \pm a\,\sqrt{u^2 + v^2 - a^2}}{u^2 - a^2} \tag{4.141}$$

For supersonic flows $Ma > 1$ the fundamental equation reduces to a system of nonlinear ordinary differential equations with real coefficients. If in the expression for $y'$ the inclination of the velocity vector, given by the angle $\beta$, and the Mach angle $\alpha$ are introduced, it is seen, that $y'$ is identical with the slope of the Mach lines.

$$\frac{dy}{dx} = \tan(\beta \pm \alpha) \quad . \tag{4.142}$$

The Mach lines are called the characteristic curves of the fundamental equation of gasdynamics. Along these curves the change of the velocity can be expressed by total derivatives. With the expressions obtained for $y'$ substituted into the fundamental equation, with $u = v\ \cos\beta$ and $v = v\ \sin\beta$ the compatibility conditions for the velocity take on the form

$$\cot\alpha \frac{dv}{v} \mp d\beta + \sin\alpha\ \cos\alpha \frac{ds}{\gamma\, R} = 0. \tag{4.143}$$

These relations are valid along the Mach lines, the characteristic curves, given by the equations

$$\frac{dy}{dx} = \tan(\beta \pm \alpha) \quad . \tag{4.144}$$

The differential $ds$ must be determined with the compatibility condition for the entropy.

$$ds = 0 \qquad \text{along the streamlines} \qquad \frac{dy}{dx} = \tan\beta \quad . \tag{4.145}$$

The solution of the equations describing the compatibility conditions along the characteristic curves, in general, is only possible with numerical methods for ordinary differential equations. For isentropic flows, (4.142) can be integrated, since the term $\cot\alpha \frac{dv}{v}$ represents the differential of the Parndtl-Meyer angle $\nu$.
The compatibility conditions then reduce to the simple form

$$d(\nu \mp \beta) = 0, \tag{4.146}$$

or

$$\nu \mp \beta = \text{const.} \qquad \text{(Riemann invariants)} \tag{4.147}$$

for

$$\frac{dy}{dx} = \tan(\beta \pm \alpha) \quad . \tag{4.148}$$

The difference or the sum of the Prandtl-Meyer angle and the local flow inclination angle, respectively, are constant along the corresponding Mach lines.

### 4.8.4 Computation of Supersonic Flows

With the Riemann invariants and the equations describing the slope of the characteristic curves, supersonic isentropic flows can be determined. This is explained in the following example. Given are the flow quantities in two neighboring points $P_1$ and $P_2$, which are not supposed to lie on a Mach line. The Prandtl-Meyer angle $\nu$ and the flow inclination angle $\beta$ at the point of intersection of the characteristic curves $P_3$, can be determined with the integrals of the compatibiliy conditions.

$$\begin{aligned} \nu_2 - \beta_2 &= \nu_3 - \beta_3 \\ \nu_1 + \beta_1 &= \nu_3 + \beta_3 \end{aligned} \tag{4.149}$$

With the notation adopted, one obtains

$$\begin{aligned} \nu_3 &= \frac{1}{2}\ [(\nu_1 + \nu_2) + (\beta_1 - \beta_2)] \\ \beta_3 &= \frac{1}{2}\ [(\nu_1 - \nu_2) + (\beta_1 + \beta_2)] \end{aligned} \tag{4.150}$$

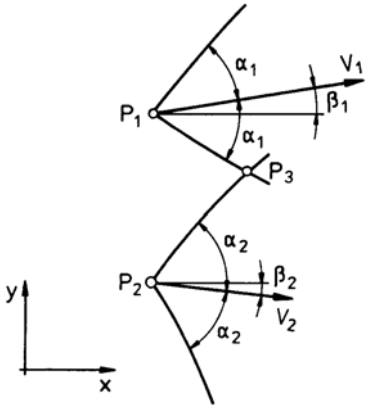


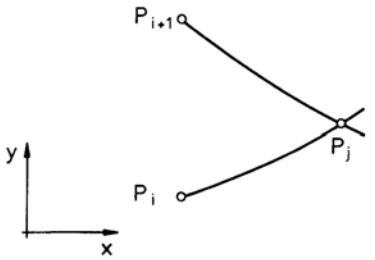


With the Prandtl-Meyer angle $\nu_3$ known, the Mach number $Ma_3$ and the other flow quantities can be determined. The location of the point $p_3$ is computed with a difference-solution of the characteristic equations.

For the computation of a supersonic flow field it is assumed that $n$ neighboring points (not on the same Mach line) are given in a supersonic flow.

At these points the flow quantities are known, i. e. $\nu_1$, $\nu_2$,..., $\nu_i$, ...,$\nu_n$ and $\beta_1$, $\beta_2$, ...,$\beta_i$, ... , $\beta_n$. With $\nu_i$, $\nu_{i+1}$ and $\beta_i$, $\beta_{i+1}$ of two neighboring points, $\nu_j$ and $\beta_j$ of a third point $P_j$ in the vicinity of the points $P_i$ and $P_{i+1}$ can be determined. The position of the point $P_j$ is obtained by discretizing the equations for the characteristic curves and solving the difference equations for small distances from the points $P_i$ and $P_{i+1}$. The coordinates of the new point are:

$$\begin{aligned} x_j &\approx \frac{(y_{i+1} - y_i + m_i^+ x_i - m_{i+1}^- x_{i+1})}{(m_i^+ - m_{i+1}^-)} \\ y_j &\approx y_{i+1} + m_{i+1}^- (x_j - x_{i+1}) \end{aligned} \qquad (4.151)$$

The quantities $m^+$ and $m^-$ are abbreviations of the slopes of the characteristic curves. For the determination of the coordinates of the point $P_j$ mean values of the slopes can be employed

$$\begin{aligned} m_i^+ &= \frac{1}{2}\left[\tan(\beta+\alpha)_i + \tan(\beta+\alpha)_j\right] \\ m_{i+1}^- &= \frac{1}{2}\left[\tan(\beta-\alpha)_{i+1} + \tan(\beta-\alpha)_j\right] \quad . \end{aligned} \qquad (4.152)$$

Only a certain part of the flow field depends on the initial data prescribed. This region is called the domain of dependence, sketched in the following figure. The flow outside of the domain of dependence cannot be determined without additional information.

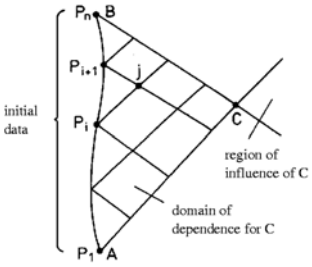


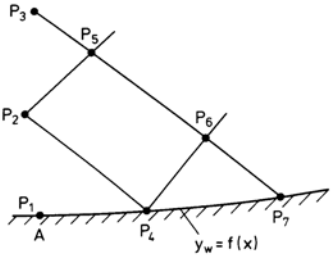


It is therefore necessary to prescribe boundary conditions for the computation of the other parts of the flow field. Two kinds of boundary conditions, representing streamlines of the flow field, are to be distinguished: the rigid wall and the free boundary, for example the edge of a

supersonic jet. For a rigid wall the curve of the contour of the wall $y_w = f(x)$ has to be known. If the point $P_1$ is a point on the contour, all other points on the contour, for which the flow quantities have to be determined, can be obtained by intersection of a characteristic with the curve describing the contour of the wall $y_w = f(x)$. For the points $P_4$ and $P_7$ the local flow inclination angle is known from the relation (see sketch)

$$\frac{dy_w}{dx} = f'(x) = \tan \beta_w. \tag{4.153}$$

The Prandtl-Meyer angle is obtained from the one Riemann invariant, corresponding to the Mach line intersecting the contour:

$$\nu_4 = \nu_2 + \beta_2 - \beta_4 \quad . \tag{4.154}$$

After determining the flow quantities at the point $P_4$, the quantities at all other points on the contour, for example, at the points $P_6$ and $P_7$, or at all points between the points $A$ and $D$ are computed.

$$\nu_7 = \nu_6 + \beta_6 - \beta_7 \tag{4.155}$$

Along a free boundary the static pressure $p_s$ is known, but not the flow inclination angle $\beta_s$. Since the stagnation pressure $p_0$ of an isentropic flow is constant in the entire flow field, the pressure ratio $\frac{p_s}{p_0}$ can be computed for the edge of the jet, also the Mach number $Ma_s$, and the Prandtl-Meyer angle $\nu_s$. The compatibility condition then yields the flow inclination angle $\beta_s$. If $B$ is a point on the edge of the jet, it follows that

$$\beta_s = \beta_{n-1} + \nu_s - \nu_{n-1} \quad . \tag{4.156}$$

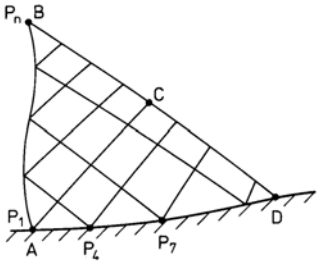


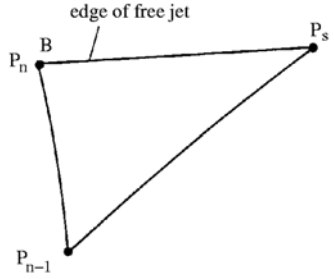


The location of the point $P_s$ is determined by letting the streamline through the point $B$ intersect the Mach line through the point $P_{n-1}$.

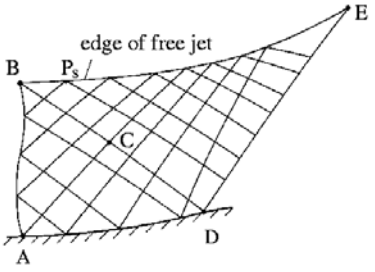


With the procedure described, the flow in the region $B - D - E$ can be determined, one side of which is bounded by the edge of the jet (free boundary), and the other by the Mach line, originated in the point $D$. If the boundary conditions downstream from the points $D$ and $E$ are known, the computation of the flow can be continued.

It is often required, for example for nozzle flows, to prescribe constant flow quantities along the characteristic curve through the point $D$.

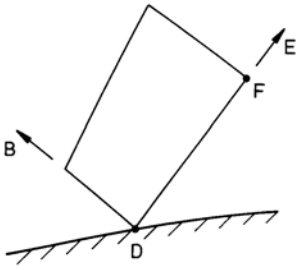


Then the computation begins in the point $F$, which is assumed to lie on the characteristic curve through the point $D$ in its vicinity. The computation is continued in the direction towards the free boundary along the characteristic $D-B$. The flow in the region $A-B-D$ is not influenced by the flow condition prescribed.

If two characteristic curves of the same kind intersect, the computation cannot be continued. In the point of intersection a compression shock is originated, causing a change of entropy, which is not included in the method of computation described here.

## 4.9 Compressible Potential Flows

The condition of irrotationality admits the introduction of a potential $\Phi$ for the description of compressible flows. However, in contrast to incompressible flows, the partial differential equation for the determination of the potential $\Phi$ is not linear.

### 4.9.1 Simplification of the Potential Equation

The fundamental equation of gasdynamics, in which only partial derivatives of the velocity components are contained, will be used to derive a simplified partial differential equation for the determination of the unknown potential $\Phi$.
The potential, defined by

$$u = \frac{\partial \Phi}{\partial x} \qquad v = \frac{\partial \Phi}{\partial y} \qquad w = \frac{\partial \Phi}{\partial z} \quad , \tag{4.157}$$

inserted into the fundamental equation of gasdynamics, yields the exact potential equation for steady compressible flows:

$$\begin{aligned} (u^2 - a^2)\,\frac{\partial^2 \Phi}{\partial x^2} + (v^2 - a^2)\,\frac{\partial^2 \Phi}{\partial y^2} + (w^2 - a^2)\,\frac{\partial^2 \Phi}{\partial z^2} \quad + \\ +2\,u\,v\frac{\partial^2 \Phi}{\partial x \partial y} + 2\,u\,w\frac{\partial^2 \Phi}{\partial x \partial z} + 2\,v\,w\frac{\partial^2 \Phi}{\partial y \partial z} \quad = \quad 0 \end{aligned} \tag{4.158}$$

The nonlinearity of this equation is immediately evident, if the velocity components appearing in the coefficients are replaced by (4.157). A closed-form solution is therefore not possible.
Since in flows about slender bodies the velocity components $v$ and $w$ are small and $u$ deviates only little from the free-stream velocity, the exact potential equation can be simplified. With the aid of the perturbation velocities

$$u' = u - u_\infty \qquad v' = v \qquad w' = w \tag{4.159}$$

a perturbation potential can be defined:

$$u' = \frac{\partial \Phi}{\partial x} \qquad v' = \frac{\partial \Phi}{\partial y} \qquad w' = \frac{\partial \Phi}{\partial z} \quad . \tag{4.160}$$

In order to simplify (4.158) the speed of sound is eliminated by employing the energy equation

$$\frac{a^2}{a_\infty^2} = 1 - \frac{\gamma - 1}{2}\,Ma_\infty^2 \left[ \frac{2u'}{u_\infty} + \left(\frac{u'}{u_\infty}\right)^2 + \left(\frac{v'}{u_\infty}\right)^2 + \left(\frac{w'}{u_\infty}\right)^2 \right] \quad . \tag{4.161}$$

This relation is introduced together with the definition of the perturbation potential into the exact potential equation. If terms of the order

$$O(Ma_\infty^2 \frac{u'^2}{u_\infty^2}), \qquad O(Ma_\infty^2 \frac{v'^2}{u_\infty^2}), \qquad O(Ma_\infty^2 \frac{w'^2}{u_\infty^2}) \tag{4.162}$$

are dropped, one obtains

$$\begin{aligned}(1 - Ma_\infty^2)\,\frac{\partial^2\Phi}{\partial x^2} + \frac{\partial^2\Phi}{\partial y^2} + \frac{\partial^2\Phi}{\partial z^2} &= (\gamma+1)\,Ma_\infty^2\,\frac{u'}{u_\infty}\,\frac{\partial^2\Phi}{\partial x^2} + \\ &+ (\gamma-1)\,Ma_\infty^2\,\frac{u'}{u_\infty}\left(\frac{\partial^2\Phi}{\partial y^2} + \frac{\partial^2\Phi}{\partial z^2}\right) + \\ &+ 2\,Ma_\infty^2\left[\frac{v'}{u_\infty}\,\frac{\partial^2\Phi}{\partial x\partial y} + \frac{w'}{u_\infty}\,\frac{\partial^2\Phi}{\partial x\partial z}\right] \quad .\end{aligned} \tag{4.163}$$

It is seen, that the simplified equation still contains nonlinear terms, and only if terms of the order

$$O(Ma_\infty^2 \frac{u'}{u_\infty}), \qquad O(Ma_\infty^2 \frac{v'}{u_\infty}), \qquad O(Ma_\infty^2 \frac{w'}{u_\infty}) \tag{4.164}$$

are neglected, a linear differential equation results for the determination of the perturbation potential

$$(1 - Ma_\infty^2)\,\frac{\partial^2\Phi}{\partial x^2} + \frac{\partial^2\Phi}{\partial y^2} + \frac{\partial^2\Phi}{\partial z^2} = 0 \quad . \tag{4.165}$$

This linearization is not valid for transonic flows. For $Ma_\infty \to 1$ the term

$$(1 - Ma_\infty^2)\,\frac{\partial^2\Phi}{\partial x^2}$$

tends to zero faster than the term

$$(\gamma+1)\,Ma_\infty^2\,\frac{u'}{u_\infty}\,\frac{\partial^2\Phi}{\partial x^2} \quad .$$

It is for this reason, that the last terms cannot be omitted in the computation of transonic flows, since

$$\lim_{Ma_\infty \to 1}\left[1 - Ma_\infty^2 - (\gamma+1)\,Ma_\infty^2\,\frac{u'}{u_\infty}\right]\frac{\partial^2\Phi}{\partial x^2} = -(\gamma+1)\,\frac{u'}{u_\infty}\,\frac{\partial^2\Phi}{\partial x^2} \quad . \tag{4.166}$$

For $Ma_\infty \to 1$ the simplified potential equation therefore reads

$$(1 - Ma_\infty^2)\,\frac{\partial^2\Phi}{\partial x^2} + \frac{\partial^2\Phi}{\partial y^2} + \frac{\partial^2\Phi}{\partial z^2} = (\gamma+1)\,Ma_\infty^2\,\frac{u'}{u_\infty}\,\frac{\partial^2\Phi}{\partial x^2} \quad . \tag{4.167}$$

This equation must be employed for transonic flows, while for subsonic and supersonic flows the linearized potential equation can be used.

### 4.9.2 Determination of the Pressure Coefficient

For the linearized potential equation and also for the transonic approximation the relation, describing the pressure coefficient

$$c_p = \frac{2}{\gamma\,Ma_\infty^2}\left(\frac{p}{p_\infty} - 1\right) \tag{4.168}$$

can be simplified.

Equation (4.168) can be rearranged for isentropic flows with the aid of the energy equation:

$$c_p = \frac{2}{\gamma\, Ma_\infty^2} \left\{ \left[ 1 + \frac{\gamma - 1}{2}\, Ma_\infty^2 \left( 1 - \frac{u^2 + v^2 + w^2}{u_\infty^2} \right) \right]^{\frac{\gamma}{\gamma - 1}} - 1 \right\} \quad . \tag{4.169}$$

A series development of the last equation yields for the terms of first and second order

$$c_p = - \left[ \frac{2\, u'}{u_\infty} + (1 - Ma_\infty^2) \left( \frac{u'}{u_\infty} \right)^2 + \left( \frac{v'}{u_\infty} \right)^2 + \left( \frac{w'}{u_\infty} \right)^2 \right] \quad . \tag{4.170}$$

If the second-order terms are neglected as in the derivation of the linearized potential equation, one obtains for the pressure gradient

$$c_p = -2 \frac{u'}{u_\infty} = -\frac{2}{u_\infty} \frac{\partial \Phi}{\partial x} \quad . \tag{4.171}$$

This relation is also valid for transonic flows.
If the perturbation potential is known from a solution of the linearized potential equation or the transonic approximation, the pressure distribution (for example on a body) can be computed with the last equation.

### 4.9.3 Plane Supersonic Flows About Slender Bodies

The linearized potential equation for supersonic flows for determining the perturbation potential $\Phi$ in the form

$$\frac{\partial^2 \Phi}{\partial x^2} - \frac{1}{Ma_\infty^2 - 1} \frac{\partial^2 \Phi}{\partial y^2} = 0 \tag{4.172}$$

can be solved with the ansatz of d'Alembert for the solution of the wave equation

$$\Phi(x,y) = f(\xi) + g(\eta). \tag{4.173}$$

The functions $f(\xi)$ and $g(\eta)$ must be twice differentiable functions. Their arguments are defined as follows:

$$\xi = x - \lambda y \qquad \eta = x + \lambda y \tag{4.174}$$

For the solution of the linearized potential equation $\lambda$ is the constant

$$\lambda = \sqrt{Ma_\infty^2 - 1} \quad . \tag{4.175}$$

For $\xi = \text{const.}$ one obtains

$$y = \frac{x}{\lambda} - \text{const} \quad . \tag{4.176}$$

The curves described by this relation are straight lines with the slope

$$\frac{dy}{dx} = \frac{1}{\sqrt{Ma_\infty^2 - 1}} \tag{4.177}$$

They are identical with the Mach lines of the free stream with positive inclination.
For $\eta = \text{const.}$ there results

$$y = -\frac{x}{\lambda} + \text{konst.} \tag{4.178}$$

and

$$\frac{dy}{dx} = -\frac{1}{\sqrt{Ma_\infty^2 - 1}} \quad . \tag{4.179}$$

The lines $\eta = \text{const.}$ are the Mach lines of the free stream with negative inclination.

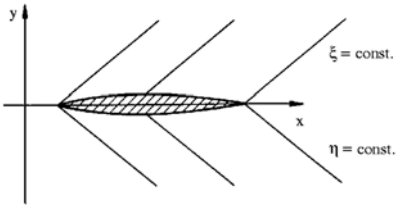


The curvature of the Mach lines caused by their mutual interaction cannot be grasped by the linearized theory.

The perturbations caused by a slender body propagate along the lines $\xi = x - \lambda y = const.$ on its upper side, and on its lower side along the lines $\eta = x + \lambda y = const.$

The solution is therefore split into two parts:

$$\begin{aligned} 0 \;&\leq\; y \qquad \Phi(x,y) = f(x - \lambda y) \\ 0 \;&\geq\; y \qquad \Phi(x,y) = g(x + \lambda y) \end{aligned} \tag{4.180}$$

The still unknown functions $f(\xi)$ and $g(\eta)$ are determined from the boundary conditions. The kinematic flow condition requires the velocity vector to be normal to the surface normal of the contour of the body. If the surface is described by the equation $F(x,y) = 0$, the kinematic flow condition can be written as

$$v \cdot \nabla F(x,y) = 0 \tag{4.181}$$

or

$$(u_\infty + u')\frac{\partial F}{\partial x} + v'\frac{\partial F}{\partial y} = 0 \quad . \tag{4.182}$$

With $u' \ll u_\infty$, the slope of the contour of the body is approximately

$$\left.\frac{dy}{dx}\right|_c = \tan\beta_c \approx \frac{v'}{u_\infty} = -\frac{\frac{\partial F}{\partial x}}{\frac{\partial F}{\partial y}} \quad . \tag{4.183}$$

Since the body is slender, a series development for $y = 0$ can be employed:

$$v'(x,y) = v'(x,o) + \frac{\partial v'}{\partial y}(x,o)y + \; ... \tag{4.184}$$

One obtains

$$u_\infty \left.\frac{dy}{dx}\right|_c \approx v'(x,o) = \frac{\partial \Phi}{\partial y}(x,o) \quad . \tag{4.185}$$

If the contour on the upper side is specified by $F_u(x,y) = 0$, the derivative of the function $f(\xi)$ is determined by

$$u_\infty \left.\frac{dy}{dx}\right|_u = -\lambda \frac{df}{d\xi}(x,o). \tag{4.186}$$

The function $f(\xi)$ is then obtained by integration. The pressure coefficient for the upper side is

$$c_{pu} = -\frac{2\,\frac{\partial \Phi}{\partial x}(x,o)}{u_\infty} = -\frac{2}{u_\infty}\frac{df}{d\xi}(x,o) \quad , \tag{4.187}$$

and with (4.186)

$$c_{pu} = \frac{2}{\sqrt{Ma_\infty^2}} \left.\frac{dy}{dx}\right|_u \quad . \tag{4.188}$$

The pressure coefficient for the lower side is obtained analogously:

$$c_{pl} = -\frac{2}{\sqrt{Ma_\infty^2}} \left.\frac{dy}{dx}\right|_l \tag{4.189}$$

With the pressure coefficient for the upper and lower side of the body known, wave drag and lift can be computed for supersonic free-stream conditions.

### 4.9.4 Plane Subsonic Flow About Slender Bodies

Solutions of the linearized potential equation can also be constructed for compressible subsonic flows. Since the partial differential equation for the perturbation potential

$$(1 - Ma_\infty^2)\,\frac{\partial^2 \Phi}{\partial x^2} + \frac{\partial^2 \Phi}{\partial y^2} = 0 \tag{4.190}$$

differs from the exact potential equation for incompressible flow only by a constant factor, solutions available for incompressible flows can be used. The adaption of such a solution to compressible flow is demonstrated here for a symmetric airfoil profile at zero angle of attack. The thickness distribution of the profile can be described by positioning sources and sinks along the axis of symmetry. For an incompressible flow they are given by the following relation:

$$\Phi(x,y) = \frac{E}{2\,\pi} \ln \sqrt{(x-\xi)^2 + y^2} \tag{4.191}$$

In this equation the positions of the sources or sinks are given by the points $(x = \xi, y = 0)$. The constant $E$ is positive, if a source is considered, and negative if a sink is to be described. Equation (4.191) also satisfies the linearized potential equation for compressible flow, if the coordinate $y$ is replaced by $y\sqrt{1 - Ma_\infty^2}$. Since the differential equation is linear, solutions can be superposed. With this ansatz an arbitrary contour can be generated with a distribution of sources and sinks along the line of symmetry. The potential then is of the form

$$\Phi(x,y) = \sum_{i=1}^{n} \frac{E_i}{2\,\pi} \ln \sqrt{(x-\xi_i)^2 + m^2\,y^2} \tag{4.192}$$

with $m^2 = 1 - M_\infty^2$.
Also a continuous distribution of sources and sinks can be thought of. The sum is then exchanged with an integral:

$$\Phi(x,y) = \frac{1}{\pi\,m} \int_0^t f(\xi) \ln \sqrt{(x-\xi)^2 + m^2\,y^2}\, d\xi \tag{4.193}$$

The source function $f(\xi)$ has to be determined in such a way, that the contour of the profile forms a streamline. It follows from the boundary condition that

$$\frac{v'(x,o)}{u_\infty} = \left.\frac{dy}{dx}\right|_c = \frac{1}{u_\infty} \frac{\partial \Phi(x,o)}{\partial y} = \lim_{y\to 0} \frac{1}{\pi\,u_\infty} \int_0^t f(\xi) \frac{m\,y\,d\xi}{(k-\xi)^2 + m^2\,y^2} \quad . \tag{4.194}$$

The limit process gives the simple relation $f(x) = u_\infty \frac{dy_c}{dx}$. Then the expression for the potential becomes

$$\Phi(x,y) = \frac{u_\infty}{\pi\, m} \int_0^t \left(\frac{dy_c}{dx}\right) \ln\sqrt{(x-\xi)^2 + m^2\, y^2}\, d\xi, \tag{4.195}$$

and the pressure coefficient is

$$c_p(x,o) = -2\,\frac{u'}{u_\infty}(x,0) = -\frac{2}{\pi\, m} \int_0^t \left(\frac{dy_k}{dx}\right)_{x=\xi} \frac{d\xi}{x-\xi} \quad . \tag{4.196}$$

The application of the solution is illustrated for the subsonic compressible flow about a double parabolic wing section:

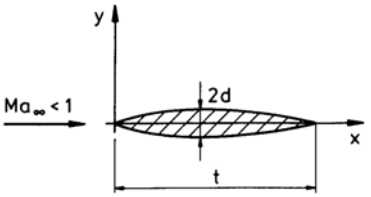


$$y_c = 4d\left(\frac{x}{t} - \left(\frac{x}{t}\right)^2\right) \tag{4.197}$$

In the first step the source function $f(x)$ is determined from the contour of the body.

$$f(x) = u_\infty \frac{dy_c}{dx} = 4\frac{d}{t}\, u_\infty\, (1 - 2\,\frac{x}{t}) \tag{4.198}$$

The perturbation velocity for $y = 0$ is

$$u'(x,0) = 4\,\frac{d}{t}\,\frac{u_\infty}{\pi\, m} \int_0^t (1 - 2\frac{\xi}{t})\,\frac{1}{(x-\xi)} d\xi \quad , \tag{4.199}$$

and the expression for the pressure coefficient becomes

$$c_p(x,0) = -8\,\frac{d}{t}\,\frac{1}{\pi\, m} \left(2 - \left(1 - 2\,\frac{x}{t}\right) \ln\left|\frac{1-\frac{x}{t}}{\frac{x}{t}}\right|\right). \tag{4.200}$$

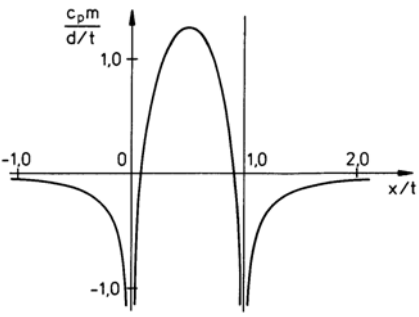


The plot of the pressure coefficient exhibits singular behavior of the solution at the leading and trailing edges. The failure of the solution at these points can be traced back to the simplifications intoduced by the linearization of the potential equation. Another point to be mentioned is, that the solution provides the same values for the product $c_p\, m$, as long as the thickness ratio $\frac{d}{t}$ retains the same value. In other words, similar profiles have similar pressure distributions.

### 4.9.5 Flows about Slender Bodies of Revolution

A slender body of revolution is an axially symmetric body, the local radius $R(x)$ of which everywhere being much smaller than its length $L$. For pointed bodies solutions of the simplified potential equation for compressible flow can be constructed in a manner similar to that of two-dimensional flows. The velocity components in the axial, radial, and azimuthal direction are again expressed with a perturbation potential:

$$u' = \frac{\partial\Phi}{\partial x} \qquad v' = \frac{\partial\Phi}{\partial r} \qquad w' = \frac{1}{r}\,\frac{\partial\Phi}{\partial\theta} \tag{4.201}$$

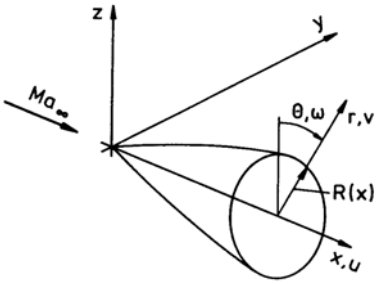


The linearized potential equation for bodies of revolution, in comparison to plane flows, contains an additional term, which results from the continuity equation, written in cylindrical coordinates: For a volume element of the flow in cylindrical coordinates the mass balance for steady flow yields the continuity equation in the following form

$$\frac{1}{r}\frac{\partial}{\partial r}(\rho\, v\, r) + \frac{\partial}{\partial x}(\rho\, u) + \frac{1}{r}\frac{\partial}{\partial \theta}(\rho\, w) = 0 \quad . \tag{4.202}$$

The term containing the radial velocity component deviates in form from its counterpart for two-dimensional flow. This is also reflected in the linearized potential equation:

$$(1 - Ma_\infty^2)\frac{\partial^2 \Phi}{\partial x^2} + \frac{\partial^2 \Phi}{\partial r^2} + \frac{1}{r}\frac{\partial \Phi}{\partial r} + \frac{1}{r^2}\frac{\partial^2 \Phi}{\partial \theta^2} = 0 \tag{4.203}$$

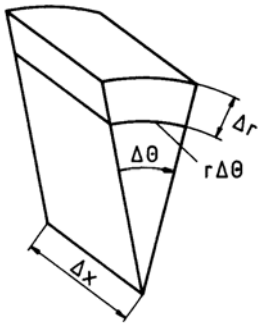


The last term in the above equation vanishes for axially symmetric flows ; the second-last term approaches the limit for $r \to 0$

$$\lim_{r\to 0}\frac{1}{r}\frac{\partial \Phi}{\partial r} = \left.\frac{\partial^2 \Phi}{\partial r^2}\right|_{r=0} = 0 \quad . \tag{4.204}$$

Equation (4.184) show, that the boundary condition for the body of revolution is given by the second derivative of the potential in comparison to the first for two-dimensional flow, see (4.185).

Also the formulation of the boundary conditions for the body contour deviates from the formulation for plane flows.

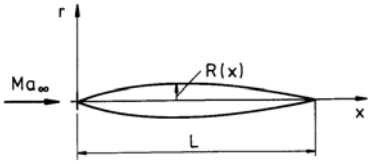


If the contour of the body is specified by a certain distribution of the local radius over the length of the body $L$, the exact boundary conditon is

$$\frac{dR}{dx} = \left(\frac{v'}{u_\infty + u'}\right)_R \quad . \tag{4.205}$$

If the boundary conditon is to be prescribed again in an approximation as in the case of the two-dimensional flow, along the axis, then the series development for $v(r,x)$ for $r = 0$ must take into account the different variation of the radial velocity component manifested in the continuity equation. If the continuity equation is written in the form

$$\frac{\partial}{\partial r}(\rho\, v\, r) = -r\frac{\partial}{\partial x}(\rho\, u) \quad , \tag{4.206}$$

it is seen that, if $\frac{\partial}{\partial x}(\rho\, u)$ remains finite in the vicinity of the axis, for $r \to 0$ there results

$$\lim_{r\to 0}\frac{\partial}{\partial r}(\rho\, v\, r) \to 0 \quad . \tag{4.207}$$

In the neighborhood of the axis the product $\rho\, v\, r$ is a function of the axial coordinate $x$, and the series development of the radial velocity component has the form:

$$v\, r = a_0(x) + a_1(x)r + a_2(x)r^2 + ... \tag{4.208}$$

The approximation of the exact boundary condition then reduces to

$$R\,\frac{dR}{dx} = \left(\frac{v'R}{u_\infty + u'}\right)_R \approx \frac{a_0(x)}{u_\infty}. \tag{4.209}$$

Also the expression for the pressure coefficient differs from its counter part of plane flows. Since $v'$ and $u'$ for $r \to 0$ are of different order of magnitude, the expression for the pressure coefficient for axially symmetric flows in the neighborhood of the axis is

$$c_p = -2\frac{u'}{u_\infty} - \frac{v'^2}{u_\infty^2} \quad . \tag{4.210}$$

The solution of the linearized potential equation for axially symmetric, compressible flows about slender bodies can again be constructed by superposition of fundamental solutions. The thickness distribution of slender bodies of revolution is, as before, generated by a distribution of sources and sinks along the axis, given by the following relation

$$\Phi(x,r) = \sum_{i=1}^{n} \frac{E_i}{\sqrt{(x-\xi_i)^2 + r^2}} \tag{4.211}$$

for incompressible flows, with the constants $E_i$ having positive (sources) and negative (sinks) values. For a continuous source-sink distribution along the axis the sum is replaced by an integral, so that

$$\Phi(x,r) = \int_0^L \frac{f(\xi)\,d\xi}{\sqrt{(x-\xi)^2 + r^2}} \quad . \tag{4.212}$$

The source function $f(\xi)$ is determined with the boundary conditions, as described earlier. The solution for the compressible flow is adjusted by stretching the radial coordinate by the quantity $m = \sqrt{(1 - Ma_\infty^2)}$. The potential is of the form

$$\Phi(x,r) = \int_0^L \frac{f(\xi)\,d\xi}{\sqrt{(x-\xi)^2 + (mr)^2}} \quad . \tag{4.213}$$

The solution can formally be extended to supersonic flows. With $\lambda^2 = Ma_\infty^2 - 1 \to 0$ the linearized potential equation

$$\frac{\partial^2\Phi}{\partial r^2} + \frac{1}{r}\,\frac{\partial\Phi}{\partial r} - \lambda^2\,\frac{\partial^2\Phi}{\partial x^2} = 0 \tag{4.214}$$

changes over into the form of the wave equation, the solution of which can be obtained by superposition of fundamental solutions for source-sink distributions along the axis

$$\Phi(x,r) = \frac{E_i}{\sqrt{(x-\xi_i)^2 - (\lambda\,r)^2}}. \tag{4.215}$$

The potential becomes imaginary, if $\lambda^2\,r^2 \to (x-\xi_i)^2$. Since an imaginary potential does not represent a physically meaningful solution, the integration for the continuous source-sink distribution can only be carried out up to the upper limit

$$\xi \le x - \lambda\,r. \tag{4.216}$$

The integral representation of the potential is then

$$\Phi(x,r) = \int_0^{x-\lambda r} \frac{f(\xi)\,d\xi}{\sqrt{(x-\xi)^2 - (\lambda\,r)^2}} \quad . \tag{4.217}$$

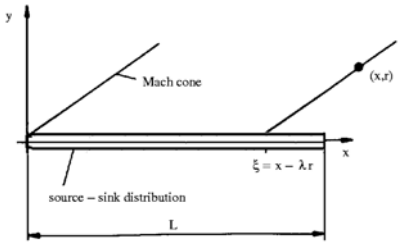


The change of the upper limit of integration is necessitated by the finite extent of the region of influence of supersonic flows. A point $P(x,r)$ on the surface of the Mach cone, given by $\xi = x - \lambda\, r$, cannot be influenced by the sources and sinks further downstream.

## 4.10 Similarity Rules

Similar flows exhibit physically similar behavior for geometrically similar conditions. Ratios of two kinds of forces or energies have to have the same value at corresponding points in flows to be compared. The laws for carrying over a result obtained in one flow to another are given, for example, by the similarity laws of Euler, Strouhal, Reynolds, and Mach. It is well known that not all of the similarity laws can be obeyed, if measured data are to be applied to the full-scale configuration.
In gasdynamics the similarity laws of Euler and Mach are extended to similarity rules for steady inviscid flows in the frame of the simplified potential theory by combining the similarity laws with geometric parameters. In the following the similarity rules will briefly be discussed.

### 4.10.1 Similarity Rules for Plane Flows After the Linearized Theory

Assume a compressible subsonic flow, which can be described by a solution of the linearized potential equation:

$$\frac{\partial^2 \Phi_1}{\partial x_1^2} + \frac{1}{1 - Ma_1^2}\,\frac{\partial^2 \Phi_1}{\partial y^2} = 0 \tag{4.218}$$

The free-stream Mach number is $Ma_1$ and the perturbation potential $\Phi_1(x_1,y_1)$. It satisfies the boundary condition

$$\frac{\partial \Phi_1}{\partial y_1}(x_1,0) = u_1 \left.\frac{dy_1}{dx_1}\right|_c = u_1\,\frac{d_1}{t_1}\,f_1'\!\left(\frac{x_1}{t_1}\right) \quad . \tag{4.219}$$

The quantities $d_1$ and $t_1$ are the maximum thickness and the length of the body, $u_1$ is the free-stream velocity, and $f_1(\frac{x_1}{t_1})$ the function describing the contour of the body, which is assumed to be slender. The pressure coefficient is

$$c_{p1} = -\frac{2}{u_1}\left(\frac{\partial \Phi_1}{\partial x_1}\right) \quad . \tag{4.220}$$

A second flow with the potential $\Phi_2(x_2,y_2)$ satisfies the linearized potential equation for a different free-stream Mach number $Ma_2$:

$$\frac{\partial^2 \Phi_2}{\partial x_2^2} + \frac{1}{1 - Ma_2^2}\,\frac{\partial^2 \Phi_2}{\partial y_2^2} = 0 \tag{4.221}$$

The corresponding boundary condition is

$$\frac{\partial^2 \Phi_2}{\partial y_2^2}(x_2,0) = u_2 \left.\frac{dy_2}{dx_2}\right|_c = u_2\,\frac{d_2}{t_2}\,f_2'\left(\frac{x_2}{t_2}\right) \quad , \tag{4.222}$$

and the pressure coefficient is given by

$$c_{p2} = -\frac{2}{u_2}\,\frac{\partial \Phi_2}{\partial x_2} \quad . \tag{4.223}$$

The potential $\Phi_1$ and also the pressure coefficient $c_{p1}$ are assumed to be known. It will be shown, that $c_{p2}$ can be expressed through $c_{p1}$. First the differential equation for the potential $\Phi_1$ is transformed into the differential equation for the potential $\Phi_2$. In order to be able to do so, it is necessary, to determine the dependencies $x_2 = x_2(x_1)$ and $y_2 = y_2(y_1)$. This is done by expressing the differential operator $\frac{\partial^2}{\partial x_1^2}$ by $x_2$:

$$\frac{\partial^2}{\partial x_1^2} = \left(\frac{\partial x_2}{\partial x_1}\right)^2 \frac{\partial^2}{\partial x_2^2} + \frac{\partial^2 x_2}{\partial x_1^2}\,\frac{\partial}{\partial x_2} \tag{4.224}$$

Since the first derivative of the potential does not appear in the differential equation, the term $\frac{\partial^2 x_2}{\partial x_1^2}$ has to vanish. Hence the relation connecting $x_2$ with $x_1$ is linear, such that $x_2 = a\,x_1$, with $a$ being a constant. the same is true for $y_2$ and $y_1$, and $y_2 = b\,y_1$. The differential equation for $\Phi_1$ can then be written in the form

$$a^2\,\frac{\partial^2 \Phi_1}{\partial x_2^2} + \frac{b^2}{1 - Ma_2^2}\,\frac{\partial^2 \Phi_1}{\partial y_2^2} = 0 \quad , \tag{4.225}$$

and the boundary condition transforms into the relation

$$b\,\frac{\partial \Phi_1}{\partial y_2} = u_1\,\left(\frac{d_1}{t_1}\right)\,f_1'\,\left(\frac{x_1}{t_1}\right) \quad . \tag{4.226}$$

The pressure coefficient becomes

$$c_{p1} = -\frac{2}{u_1}\,a\,\left(\frac{\partial \Phi_1}{\partial x_2}\right) \quad . \tag{4.227}$$

Since the simplified potential equation is linear and homogeneous, every solution can be multiplied by an arbitrary constant. In order to express $\Phi_1$ through $\Phi_2$, a linear relation can therefore be used to connect the two solutions:

$$\Phi_1(x_1,y_1) = A\;\Phi_2(x_2,y_2) \tag{4.228}$$

The quantity $A$ is an unknown constant. If $\Phi_1$ is substituted by (4.228) in the differential equation, (4.225), it is seen, that the original equation for $\Phi_1$ is transformed into the differential equation for $\Phi_2$, if the ratio $\frac{b}{a}$ is given by

$$\frac{b}{a} = \sqrt{\frac{1 - Ma_1^2}{1 - Ma_2^2}}. \tag{4.229}$$

The boundary condition for $\Phi_1$ then reads

$$\frac{\partial \Phi_2}{\partial y_2}(x_2,0) = \frac{u_2}{b\,A}\,\left(\frac{d_1}{t_1}\right)\,f_1'\,\left(\frac{x_1}{t_1}\right) \quad . \tag{4.230}$$

The boundary condition for $\Phi_2$ with an arbitrarily assumed thickness ratio $\frac{d_2}{t_2}$ is

$$\frac{\partial \Phi_2}{\partial y_2}(x_2,0) = u_2\,\left(\frac{d_2}{t_2}\right)\,f_2'\,\left(\frac{x_2}{t_2}\right) \quad . \tag{4.231}$$

For bodies of the same geometric family $f_1\left(\frac{x_1}{t_1}\right) = f_2\left(\frac{x_2}{t_2}\right)$ the constant $A$ is obtained to

$$A = \frac{1}{b}\,\frac{u_1}{u_2}\,\frac{d_1}{t_1}\,\frac{t_2}{d_2} \quad . \tag{4.232}$$

On the other hand the constant $A$ can be chosen and the thickness ratio $\frac{d_2}{t_2}$ thereby be fixed. The following relation holds for the pressure coefficients

$$c_{p1} = -\frac{2\,a\,A}{u_1}\left(\frac{\partial \Phi_2}{\partial x_2}\right) = \frac{u_2}{u_1}\,A\,a\,c_{p2} \quad . \tag{4.233}$$

Finally there results

$$c_{p1}\,\frac{\sqrt{1-Ma_1^2}}{\frac{d_1}{t_1}} = c_{p2}\,\frac{\sqrt{1-Ma_2^2}}{\frac{d_2}{t_2}} \quad . \tag{4.234}$$

Since the left-hand side of (4.234) was assumed to be known, the subscripts on the right-hand side can be dropped:

$$c_p\,\frac{\sqrt{1-Ma_1^2}}{\frac{d_1}{t_1}} = \text{const.} \quad . \tag{4.235}$$

The last relation provides four similarity rules for bodies, described by the contour $f(\frac{x}{t})$:

1. The pressure coefficient $c_p$ remains constant, if the ratio $\frac{(1-M_\infty^2)^{\frac{1}{2}}}{(\frac{d}{t})}$ remains constant.
2. The pressure coefficient $c_p$ varies with $(1-Ma_\infty^2)^{-\frac{1}{2}}$, if the thickness ratio $\frac{d}{t}$ remains constant (Prandtl-Glauert rule).
3. The pressure coefficient $c_p$ varies with $\frac{d}{t}$, if the free-stream Mach number is kept constant.
4. The pressure coefficient $c_p$ varies with $(1-Ma_\infty^2)^{-1}$, if the thickness ratio $\frac{d}{t}$ varies with $(1-Ma_\infty^2)^{-\frac{1}{2}}$ (Göthert rule).

These rules are also valid for supersonic flows.

### 4.10.2 Application of the Similarity Rules to Plane Flows

If the pressure distribution on an airfoil section was measured for a certain free-stream Mach number, the results of the measurements can be converted to other free-stream Mach number with the Prandtl-Glauert rule. According to this rule the product of the pressure coefficient and $(1-Ma_\infty^2)^{\frac{1}{2}}$ remains constant:

$$c_{p2} = c_{p1}\,\sqrt{\frac{1-Ma_1^2}{1-Ma_2^2}} \quad . \tag{4.236}$$

If, for example $Ma_1$ is $Ma_1 = 0.4$, one obtains for a second Mach number, say $Ma_2 = 0.7 \Rightarrow c_{p2} = 1.283\,c_{p1}$. Another application of the Prandtl-Glauert rule is demonstrated with the example of determining the critical free-stream Mach number for an airfoil profile.
If the free-stream velocity about an airfoil profile is subsonic, in general the pressure on the upper side of the profile is lowered, and the flow can locally attain sonic or even supersonic velocity. The particular free-stream Mach number, for which locally the speed of sound is attained for the first time, is called critical free-stream Mach number. From the expression for the pressure coefficient

$$c_p = \frac{2}{\gamma\,Ma_\infty^2}\left\{\left[\frac{2+(\gamma-1)\,Ma_\infty^2}{2+(\gamma-1)\,Ma^2}\right]^{\frac{\gamma}{\gamma-1}} - 1\right\} \tag{4.237}$$

the critical value of the pressure coefficient is obtained by setting $Ma = 1$:

$$c_{pcrit} = \frac{2}{\gamma\, Ma_\infty^2} \left\{ \left[ \frac{2 + (\gamma - 1)\, Ma_\infty^2}{\gamma + 1} \right]^{\frac{\gamma}{\gamma - 1}} - 1 \right\} \tag{4.238}$$

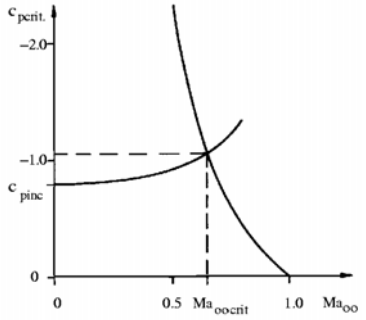


This relation is independent of the airfoil profile considered. The critical free-stream Mach number of an airfoil profile can be determined with the Prandtl-Glauert rule, if the pressure distribution is known for another Mach number, for example $Ma_\infty = 0$. Then the expression for the pressure coefficient can be written as

$$c_p = \frac{c_{pinc}}{\sqrt{1 - Ma_\infty^2}} \quad . \tag{4.239}$$

With (4.239) The critical Mach number can be determined by intersecting the curve obtained with (4.238) with the curve obtained with (4.239) as shown in the diagram.

The application of the Göthert rule will be shown as the third example. According to this rule the product of the thickness ratio $\frac{d}{t}$ and $(1 - Ma_\infty^2)^{\frac{1}{2}}$ remains constant.

If the pressure distribution of a wing, known for a given angle of attack in incompressible flow, is to be converted to a compressible subsonic flow, the chord of the wing $t$ is changed for constant maximum thickness to

$$t = t_{inc.} \sqrt{1 - Ma_\infty^2} \quad . \tag{4.240}$$

The corresponding angle of attack is

$$\alpha = \frac{\alpha_{inc.}}{\sqrt{1 - Ma_\infty^2}} \quad . \tag{4.241}$$

Equations (4.240) and (4.241) are graphically illustrated in the following sketch. The corresponding angle of attack $\alpha$ in compressible subsonic flow is larger than in incompressible flow and the chord is shortened as a result of the Prandtl-Glauert transformation.

This result shows already, that the similarity rules play an important role in the design of wing sections and wings for compressible subsonic flow, illustrated in the following sketches.

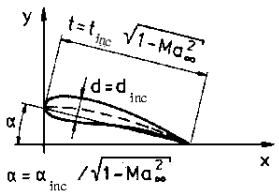


compressible flow
$Ma_\infty < 1$

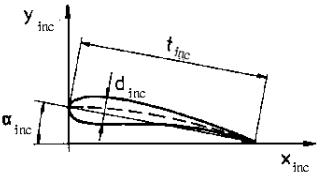


incompressible flow
$Ma_\infty = 0$

For delta wings also the planform has to be changed.

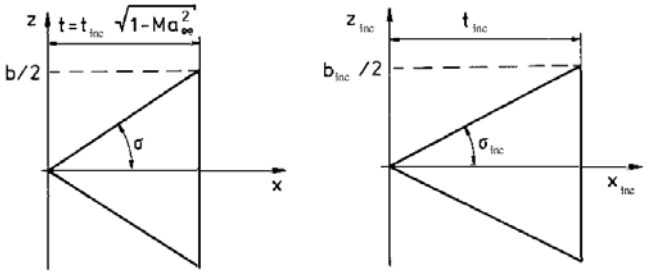


compressible flow incompressible flow

The sweep angle $\sigma$ for compressible flows is

$$\sigma = \arctan\left(\tan\frac{\sigma_{inc.}}{\sqrt{1-Ma_\infty^2}}\right) \quad . \tag{4.242}$$

The similarity rules loose their validity in the vicinity of stagnation points, since the linearized theory is not valid there.

### 4.10.3 Similarity Rules for Axially Symmetric Flows

If $\Phi_1(x_1,r_1)$ and $\Phi_2(x_2,r_2)$ are solutions of the linearized potential equation for axially symmetric flows

$$\frac{\partial^2\Phi}{\partial x^2} + \left(\frac{1}{1-Ma_\infty^2}\right)\left(\frac{\partial^2\Phi}{\partial r^2} + \frac{1}{r}\frac{\partial\Phi}{\partial r}\right) = 0 \quad , \tag{4.243}$$

the relations $x_2 = a\,x_r, \quad r_2 = b\,r_1$ are valid as for two-dimensional flows with

$$\frac{b}{a} = \sqrt{\frac{1-Ma_1^2}{1-Ma_2^2}} \text{ and } \Phi_1(x_1,r_1) = A\,\Phi_2(x_2,r_2) \quad . \tag{4.244}$$

Differences are encountered in the conversion of the boundary conditions. The boundary condition for the potential $\Phi_1(x_1,r_1)$ is with

$$R_1 = \left(\frac{R_{max}}{l}\right)_1 l_1\, f_1\left(\frac{x_1}{l_1}\right)$$

$$\frac{\partial\Phi_1}{\partial r_1}(x_1,r_1 = R_1) = u_1\left(\frac{R_{max}}{l}\right)_1 f_1'\left(\frac{x_1}{l_1}\right) \quad . \tag{4.245}$$

If $\Phi_1$ and $r_2$ are replaced with the ansatz above, there is obtained

$$bA\,\frac{\partial\Phi_2}{\partial r_2}(x_2,r_2 = bR_1) = u_1\left(\frac{R_{max}}{l}\right)_1 f_1'\left(\frac{x_1}{l_1}\right). \tag{4.246}$$

The boundary condition for the potential $\Phi_2$ is with $R_2 = \left(\frac{R_{max}}{l}\right)_2 l_2\, f_2\left(\frac{x_2}{l_2}\right)$

$$\frac{\partial\Phi_2}{\partial r_2}(x_2,r_2 = R_2) = u_2\left(\frac{R_{max}}{l}\right)_2 f_2'\left(\frac{x_2}{l_2}\right) \quad . \tag{4.247}$$

By comparing the last three equations it is seen, that for bodies of the same family $f_1\left(\frac{x_1}{l_1}\right) = f_2\left(\frac{x_2}{l_2}\right)$ the thickness ratios have to satisfy the condition

$$\left(\frac{R_{max}}{l}\right)_2 = \sqrt{\frac{1-Ma_1^2}{1-Ma_2^2}}\left(\frac{R_{max}}{l}\right)_1 . \tag{4.248}$$

As a consequence the constant $A$ is fixed by the boundary conditions:

$$A = \frac{u_1}{u_2}\frac{\left(\frac{R_{max}}{l}\right)_1}{\left(\frac{R_{max}}{l}\right)_2}\frac{1}{b} \tag{4.249}$$

The pressure coefficient $c_{p1}$

$$c_{p1} = -\frac{2}{u_1}\frac{\partial \Phi_1}{\partial x} - \frac{1}{u_1^2}\left(\frac{\partial \Phi_1}{\partial r_1}\right)^2 , \tag{4.250}$$

after replacing $\Phi_1$ by $\Phi_2$ and $r_1$ by $r_2$, takes on the following form:

$$c_{p1} = \frac{1-Ma_1^2}{1-Ma_2^2}\left[-\frac{2}{u_2}\frac{\partial \Phi_2}{\partial x} - \frac{1}{u_2^2}\left(\frac{\partial \Phi_2}{\partial r_2}\right)^2\right] \tag{4.251}$$

The content of the square bracketed term represents the pressure coefficient $c_{p2}$. The similarity rule, which results from this relation, has the form

$$c_p = \frac{\text{const.}}{1-Ma_\infty^2} \quad . \tag{4.252}$$

The last equation can also be written in the following form with the condition for the maximum radii

$$c_p = \frac{\text{const.}\left(\frac{R_{max}}{l}\right)}{\sqrt{1-Ma_\infty^2}} \quad , \tag{4.253}$$

which is equal to the similarity rules for plane flows.

### 4.10.4 Similarity Rules for Plane Transonic Flows

Instead of the linearized potential eqaution the nonlinear approximation for transonic flows must be used

$$\frac{\partial^2 \Phi}{\partial x^2} + \frac{1}{1-Ma_\infty^2}\frac{\partial^2 \Phi}{\partial y^2} = \frac{(\gamma+1)\,Ma_\infty^2}{(1-Ma_\infty^2)}\frac{1}{u_\infty}\frac{\partial \Phi}{\partial x}\frac{\partial^2 \Phi}{\partial x^2} \quad . \tag{4.254}$$

With the same ansatz as employed previously the constant $A$ is already fixed by the right-hand side of the differential equation

$$A = \frac{(\gamma_2+1)\,Ma_2^2\,(1-Ma_1^2)}{(\gamma_1+1)\,Ma_1^2\,(1-Ma_2^2)} \quad , \tag{4.255}$$

and the expression for the pressure coefficient becomes:

$$\frac{c_{p1}\,(\gamma_1+1)\,Ma_1^2}{1-Ma_1^2} = \frac{c_{p2}\,(\gamma_2+1)\,Ma_2^2}{1-Ma_2^2} \tag{4.256}$$

Since the constant $A$ is fixed, these considerations cannot be carried over to axially symmetric flows.

## 4.11 Selected References

Ganzer, U.: *Gasdynamik* Springer Verlag, 1988.

Liepmann, H.W., Roshko, A.: *Elements of Gasdynamics* John Wiley Verlag, 1957.

Oswatitsch K.: *Gasdynamics* Academic Press Inc., 1956.

Sauer, R.: *Einführung in die theoretische Gasdynamik*, Springer Verlag, 1960.

Shapiro, A.H.: *The Dynamics and Thermodynamics of* Compressible Fluid Flow, Vol.1 John Wiley Verlag, 1953.

Zierep, J.: *Theoretische Gasdynamik, Band 1* Braun Verlang, 3. Auflage, 1976.

# 5. Exercises in Gasdynamics

## 5.1 Problems

### 5.1.1 One-Dimensional Steady Flows of Gases

1.1 Consider an inviscid flow of gas without heat exchange through a stream tube.

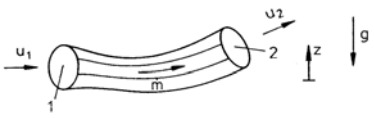


(a) Formulate the first law of thermodynamics for this system!
(b) What kinds of energies interact
1. in compressible fluid flow
2. in incompressible fluid flow?

1.2 An airplane flies over an observer in level flight.

$H = 577\,\mathrm{m} \quad v = 680\,\dfrac{\mathrm{m}}{\mathrm{s}} \quad T = 287\,\mathrm{K};$

$R = 287\,\dfrac{\mathrm{Nm}}{\mathrm{kg\,K}} \quad \gamma = 1.4$

(a) Determine the Mach number!
(b) What distance did the aeroplane cover, before it was heard by the observer?
(c) When was the noise generated the observer heard?

1.3 Determine for an isentropic flow ($\gamma = 1.4$)
(a) the critical temperature ratio,
(b) the critical pressure ratio,
(c) the limiting value of the critical Mach number $Ma^* = \frac{u}{a^*}$ for $Ma \to \infty$!

How large is the change of temperature across the normal compression shock?

1.4 A small pressure disturbance moves through a gas at rest. Derive the expression for the speed of propagation!

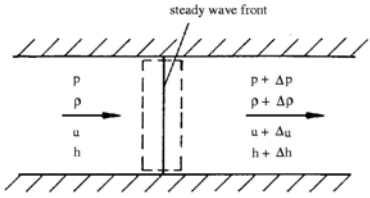


$$a^2 = \left(\frac{\partial p}{\partial \rho}\right)_s$$

1.5 A jet-propelled airplane passes a second jet-plane at a distance $b$.

$v_A = 510\,\dfrac{\mathrm{m}}{\mathrm{s}} \quad v_B = 680\,\dfrac{\mathrm{m}}{\mathrm{s}} \quad b = 170\,\mathrm{m};$

$T = 287\,\mathrm{K} \quad R = 287\,\dfrac{\mathrm{Nm}}{\mathrm{kg\,K}} \quad \gamma = 1.4$

After what time would the pilot of the overtaken airplane have been able to hear the noise generated by the faster flying airplane?

1.6 Gas flows isentropically and steadily through a vertical pipe with cylindrical cross section against the direction of the gravitational acceleration.

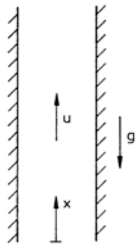


Derive the expression describing the convective acceleration, and state, how the velocity changes for
(a) $Ma(x = 0) < 1$
(b) $Ma(x = 0) > 1$

1.7 Derive the expression relating $Ma^*$ to $Ma$ for a one-dimensional isoenergetic flow with the aid of the energy equation and show, that for $\gamma = const.$

$$\lim_{Ma\to\infty} Ma^* = \sqrt{\frac{\gamma+1}{\gamma-1}}.$$

1.8 Derive the relation describing the dependence of the area ratio $\frac{A}{A^*}$ on the Mach number $Ma$ and the isentropic exponent $\gamma$ for an isentropic nozzle flow!

1.9 The relation between the mass flow $\Theta$ and the local velocity $v$, nondimensionalized with the speed of sound at stagnation conditions $a_0$, is shown in the following diagram for one-dimensional, isentropic and isoenergetic flow.

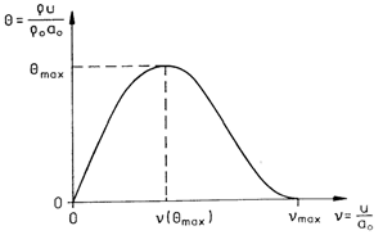


Determine:
(a) the maximum mass flow,
(b) the velocity, corresponding to this value of the mass flow,
(c) the maximum velocity, nondimensionalized with the speed of sound at stagnation conditions.

1.10 Viscous flow of air passes through a thermally isolated pipe with cylindrical cross section at subsonic speed.

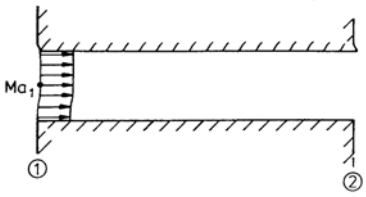


$$Ma_1 < 1; \quad \frac{p_{01}}{p_{02}} = 2; \quad \gamma = 1.4$$

(a) Determine the ratio of the critical cross sections $\frac{A_2^*}{A_1^*}$
(b) How does the Mach number vary in the direction of the flow?
(c) To what value can $Ma_{1max}$ increase?

1.11 Air flows out of a large container through a nozzle into the open air. The flow in the nozzle is steady and isentropic. The Mach number in the throat is smaller than unity.

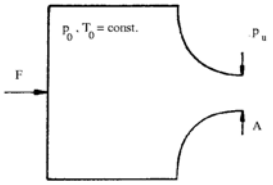


(a) Derive the function $f$ describing the retaining force $F$

$$\frac{F}{A\,p_0} = f\left(\gamma, \frac{p_u}{p_0}\right) \quad .$$

(b) Develop the function in a power series for the case $p_u \approx p_0$, and compare the result with the corresponding relation for incompressible flow!

1.12 Consider an inviscid nozzle flow of a perfect gas with constant specific heats. Determine $\frac{T}{T_0}$, $\frac{p}{p_0}$, and $\frac{\rho}{\rho_0}$ as a function of the Mach number for adiabatic conditions!

1.13 In the nozzle sketched below a flow is accelerated to supersonic speed corresponding to a Mach number $Ma = 2$.

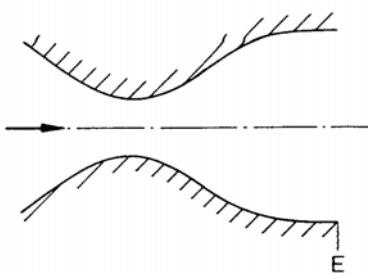

(a) Sketch the pressure distribution $\frac{p}{p_0}$, the variation of the Mach number $Ma$, and the ratio of the mass flow $\frac{\rho\, u}{\rho^*\, u^*}$ along the axis of the nozzle.
(b) Determine for the exit cross section:
1. the cross-sectional ratio $\frac{A^*}{A_E}$
2. the pressure ratio $\frac{p_E}{p_0}$,
3. the temperature ratio $\frac{T_E}{T_0}$,
4. the mass-flow ratio $\frac{\rho_E\, u_E}{\rho^*\, u^*}$

1.14 Air is sucked through a convergent nozzle into a large container.

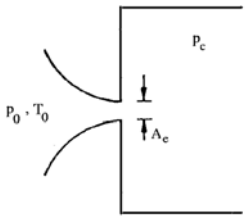


$p_0 = 10^5$ Pa; $T_0 = 300$ K; $\gamma = 1.4$;
$R = 287 \frac{\text{Nm}}{\text{kg K}}$; $A_e = 0.02\,\text{m}^2$

Determine the mass flow for
(a) $p_c = 7 \cdot 10^4\ Pa$,
(b) $p_c = 2 \cdot 10^4\ Pa$!
(c) Sketch the variation of the mass-flow ratio $\frac{\dot{m}}{\rho_0\, a_0\, A_e}$, as a function of the pressure in the container $\frac{p_c}{p_0}$!

1.15 Consider a large pressurized vessel filled with air, that flows through a nozzle sketched below into the surrounding air.

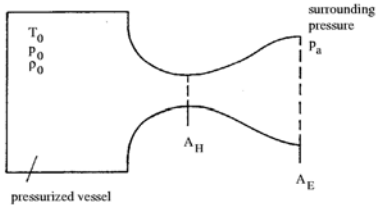


$p_a = 10^5$ Pa; $T_0 = 288$ K; $\gamma = 1.4$;
$R = 287 \frac{\text{Nm}}{\text{kg K}}$; $A_H = 1\,\text{cm}^2$

Determine for $p_{0outl.} = 7.824 \cdot 10^5\ Pa$ and $p_0 = 1.086 \cdot 10^5\ Pa$
(a) the stagnation density $\rho_0$,
(b) the quantities $Ma$, $Ma^*$, $p$, $\rho$, $T$, $u$, and $\dot{m}$ in the cross section of the throat $A_H$ and in the exit cross section $A_E$ assuming isentropic flow in the nozzle!

1.16 Gas flows through a thermally isolated pipe with constant cross section.
(a) Derive the relation

$$h + \frac{C_1}{2\,\rho^2} = C_2;\ \ C_1, C_2 = \text{const.}\ (*)!$$

(b) With the relation $(*)$ the so-called "Fanno"- curve is obtained in the h-s diagram (see sketch).
1. Prove that the Mach number is unity in the point $P$!
2. Caused by wall friction, the stagnation pressure decreases in the direction of the flow.

Plot the direction of the change of state along the "Fanno"- curve for supersonic and subsonic flow!

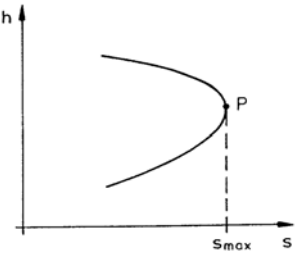


1.17 Consider the inviscid flow of a gas through a thermally non-isolated pipe with constant cross section.
(a) Derive the following relations for this flow!

$$P = \frac{C_1}{\rho} + C_2;\quad C_1, C_2 = \text{const.}(*)$$

(b) The relation $(*)$ yields the "Raleigh"-curve in the h-s diagram.

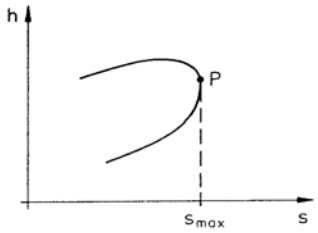


1. Determine the Mach number in the point $P$!
2. Mark the branches of the curve, indicating supersonic and subsonic flow!
3. Indicate the direction of the change of state on the branches of the curve, if the pipe is heated!

### 5.1.2 Normal Compression Shock

2.1 How large can the density ratio $\frac{\varrho_2}{\rho_1} = f(\gamma)$ across a nomal compression shock become? $\gamma$ =const.

2.2 The free-stream velocity in front of a normal compression shock is $u_1 = 300 \frac{\mathrm{m}}{\mathrm{s}}$ and the critical Mach number $Ma_1^* = 1.25$.

Compute the velocity $u_2$ downstream from the shock, without using a diagram!

2.3 A normal compression shock moves through air resting in a thermally isolated pipe with pressure $p_1$ and temperature $T_1$, with velocity $u$.

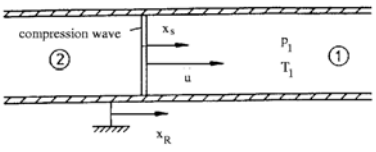


$p_1 = 10^5$ Pa; $T_1 = 293$ K; $\gamma = 1.4$;
$R = 287 \frac{\mathrm{Nm}}{\mathrm{kg\,K}}$; $u = 515 \frac{\mathrm{m}}{\mathrm{s}}$

The flow is unsteady with respect to coordinates fixed to the pipe $x_R$; for an observer moving with the shock ($x_s$) the flow is steady. Determine the quantities $p$, $p_0$, $T$, $T_0$, $Ma$, and also $u$ upstream of (Index "1") and downstream (Index "2") from the shock for:

(a) the system of coordinates moving with the shock $x_s$,
(b) the coordinate system fixed to the pipe $x_R$.

2.4 A normal compression shock moves through quiescent air with temperature $T_1$ and pressue $p_1$ in a thermally isolated shock tube with velocity $u$. The static pressure downstream from the shock wave is $p_2$.

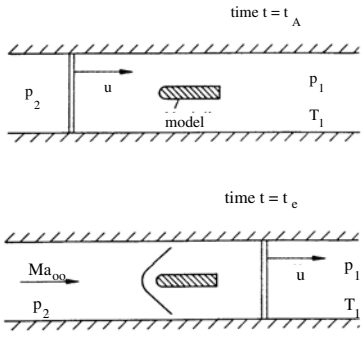


$p_1 = 10^5$ Pa; $T_1 = 300$ K; $\gamma = 1.4$;
$p_0 = 10^5$ Pa; $R = 287 \frac{\mathrm{Nm}}{\mathrm{kg\,K}}$

1.) Determine the velocity of the shock u (for t = $t_A$).
2.) Determine for $t = t_B$,
   (a) the Mach number $Ma_\infty$,
   (b) the stagnation temperature $T_{0\infty}$,
   (c) the stagnation pressure $p_{0\infty}$.

2.5 An airplane flies at supersonic speed. A shock wave is formed, which is normal in front of the nose of the airplane.

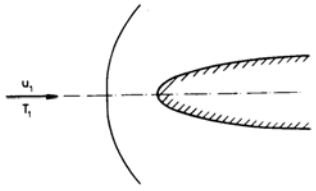

$\gamma = 1.4 \quad R = 287 \dfrac{\text{Nm}}{\text{kg K}} \quad T = 287\,\text{K}$
$u_1 = 680 \dfrac{\text{m}}{\text{s}}$

How large is the temperature change of the air across the shock?

2.6 A normal compression shock was generated in the divergent part of a plane Laval nozzle between the cross sections $A_A$ and $A_B$, for which the Mach numbers $Ma_A$ and $Ma_B$ are known.

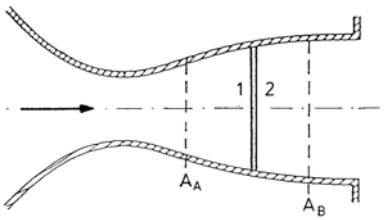


$Ma_A = 2.2; \quad Ma_B = 0.6; \quad \frac{A_B}{A_A} = 1.8;$
$\gamma = 1.4$

Determine:
(a) the ratio of the stagnation pressures $\frac{p_{01}}{p_{02}}$,
(b) the ratio of the static pressures $\frac{p_2}{p_1}$ immediately upstream of and downstream from the shock,
(c) the pressure ratio $\frac{p_B}{p_A}$.

2.7 A turbo engine sucks air out of the atmosphere. The pressure in front of the compressor is $p_1$.

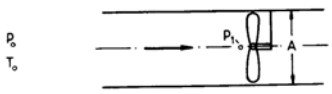


$\gamma = 1.4 \quad R = 287 \dfrac{\text{Nm}}{\text{kg K}} \quad T = 287\,\text{K}$
$p_0 = 10^5 \dfrac{\text{N}}{\text{m}^2} \quad p_1 = 0.74 \cdot 10^5 \dfrac{\text{N}}{\text{m}^2};$
$A = 9 \cdot 10^{-3}\,\text{m}^2$

Determine the mass flow through the engine!

2.8 An engine equipped with a Laval nozzle is tested on a test stand. The engine is designed for the Mach number $Ma_{Edesign1}$. The pressure in the chamber $p_v$ can be varied.

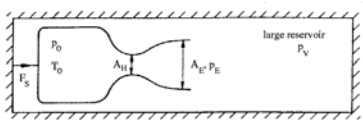


$Ma_{Edesign1} = 2.3; \quad p_0 = 10^5\,\text{Pa};$
$\gamma = 1.4; \quad R = 287 \dfrac{\text{Nm}}{\text{kg K}};$
$T_0 = 280\,\text{K}; \quad A_H = 1\,\text{cm}^2$

Assume isentropic flow in the nozzle and determine:
(a) $p_{Edesign1}$ and $\frac{A_H}{A_E}$,
(b) the lowest pressure $p_{v1}$, for which the flow in the nozzle is subsonic everywhere, and also $Ma_{E1}$,
(c) the pressure in the chamber $p_{v2}$, at which a normal shock is formed in the exit cross section $A_E$,
(d) the thrust $F_s$, for $p_v = p_{Edesign}$ and $p_v = p_{v2}$.
(e) Sketch the variation of $p$ and $Ma$ along the axis of the nozzle for $p_v = p_{v1}$ and $p_v = p_{Edesign}$.

2.9 During the test procedure of a jet engine equipped with a Laval nozzle the chamber pressure $p_v$ and the pressure $p_E$ at the exit of the nozzle are varied. The stagnation pressure at the exit of the nozzle $p_{0E}$ is measured with a pitot tube.

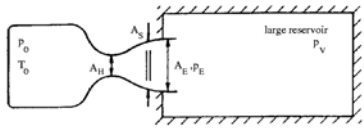


$p_0 = 10^5\,\text{Pa}; \quad T_0 = 280\,\text{K};$
$A_H = 1\,\text{cm}^2; \quad Ma_{Edesign} = 2.3;$
$R = 287 \dfrac{\text{Nm}}{\text{kg K}}; \quad \gamma = 1.4;$

Determine the position of the normal compression shock $\frac{A^*}{A_s}$, the mass flow $\dot{m}$, and the Mach number at the exit of the nozzle $Ma_E$ for:

(a) $p_{va} = 0.645 \cdot 10^5\ Pa$ ;
$p_{0Ea} = 0.721 \cdot 10^5\ Pa$ ,
(b) $p_{vb} = 0.816 \cdot 10^5\ Pa$ ;
$p_{0Eb} = 0.876 \cdot 10^5\ Pa$ .
(c) Compute the ratio $\frac{\Delta s_a}{\Delta s_b}$.
(d) Sketch the variation of $p$, $p_0$, and $Ma$ along the axis of the nozzle.
(e) At the pressure $p_{ve}$ a normal compression shock is observed at $\frac{A_*}{A_E} = 0.9$. Determine $Ma_1^*$, ahead of the shock, $Ma_2^*$ downstream from the shock, $Ma_E$, and the pressure $p_{ve}$.

2.10 Air is sucked from the surroundings into a supersonic wind tunnel, equipped with a Laval nozzle and variable diffuser, and from there into a large container (volume $V_v$) with constant temperature $T_v$. The Mach number in the test section for the design condition is $Ma_M = 2.3$.

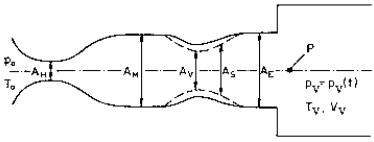


$p_0 = 10^5$ Pa; $T_0 = T_v = 280$ K;
$R = 287 \frac{\text{Nm}}{\text{kg K}}$; $V_v = 1000\ \text{m}^3$;
$A_E = A_M$; $A_H = 0.1\ \text{m}^2$;
$\gamma = 1.4$; $Ma_{Edesign} = 2.3$

(a) A normal compression shock is observed in the exit cross section of the diffuser. Determine the pressure in the container $p_{c1}$!
(b) A normal compression shock is observed at $A_s = 0.57\ A_E$.
Determine:
1. the Mach number $Ma_s^*$ and the static pressure $p_s$ downstream from the shock,
2. the pressure in the container $p_{c2}$!
(c) Sketch the variation of the Mach number $Ma$ along the axis of the nozzle up to the point $P$ for both cases!
(d) 1. How must the throat of the diffuser $A_v$ be adjusted, to maximize the testing time for a test Mach number $Ma_M = 2.3$?
2. Compute the gain in testing time for this case and compare it to the situation that the wind tunnel is operated without a diffuser!

2.11 Air flows isentropically ($\gamma = 1.4$) out of a large, frictionless supported container through a well-rounded nozzle into the surroundings.

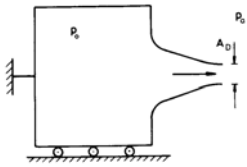


(a) Determine the dimensionless thrust $\frac{F_s}{p A_D}$ for the pressure ratios $\frac{p_a}{p_0} = 1$; 0.6; 0.2; 0 !
(b) How large are the corresponding values for incompressible flow?

2.12 An adiabatic wind tunnel sucks air from the surroundings into an adiabatic container (volume $V_c$). The Mach number $Ma_M$ in the test section is controlled by adjusting the throat $A_L$ of the Laval nozzle.
$p_a = 10^5$ Pa; $T_a = 300$ K; $\gamma = 1.4$;
$R = 287 \frac{\text{Nm}}{\text{kg K}}$; $V_c = 400\ \text{m}^3$;
$A_E = 0.508\ \text{m}^2$; $A_M = 0.2\ \text{m}^2$;

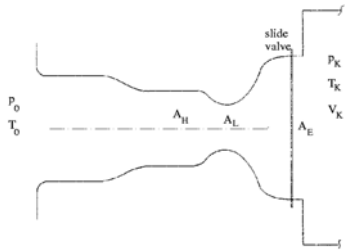


(a) the tunnel is started by opening a slide valve and at time $t = t_0$ a steady flow has built up in the test section. The Mach number $Ma_E$ in the exit cross section $A_E$ of the

Laval nozzle is at this time equal to the design Mach number. Determine the cross sectional area of the throat $A_L$ of the Laval nozzle, so that the Mach number in the test section $Ma_M$ is $Ma_M = 0.8$. How large are then the Mach number $Ma_E$ and the static pressure $p_E$ in the exit cross section $A_E$?

(b) Determine the maximum measuring time $t_{max}$, for which the Mach number in the test section is constant $Ma_M = 0.8$.

(c) A loss of stagnation pressure $\Delta p_0 = 0.020 p_a$ is caused by installations in the test section. How large is now the Mach number $Ma'_M$ in the test section, if the cross section of the throat $A_L$ of the Laval nozzle is the same as before? How has the cross section of the throat $A'_L$ of the Laval nozzle to be adjusted, so that the Mach number in the test section is again $Ma_M = 0.8$?

### 5.1.3 Oblique Compression Shock

3.1 A supersonic flow is turned by the contour sketched below by the angle $\beta$.

Physical plane:

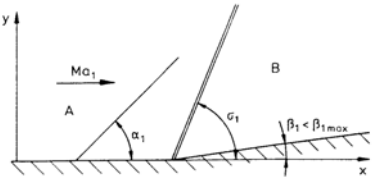


Sketch:

(a) the variation of the turning angle $\beta$ as a function of the shock angle $\sigma$, and plot the state $B$ in the physical plane,

(b) the geometric construction for determining the state $B$ in the hodograph plane ($u$, $v$ velocity components in the $x$, $y$ directions),

(c) the flow field for $\beta_1 > \beta_{max}$!

3.2 The velocity $V_1$ upstream of a straight compression shock is given by its normal component $u_{n1} = 400 \dfrac{\text{m}}{\text{s}}$ and the tangential component $u_{t1} = 300 \dfrac{\text{m}}{\text{s}}$. Across the shock the static temperature is increased to $T_2 = 1.2\, T_1$

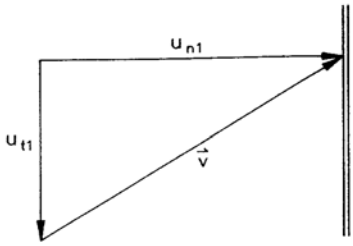


Determine with $\gamma = 1.4$ and $R = 287$ Nm/kgK:

(a) the Mach number $Ma_1$ and the static temperature $T_1$ upstream of the shock,

(b) the velocity components $u_{n2}$ and $u_{t2}$, the Mach number $Ma_2$, and the turning angle $\beta$ downstream from the shock,

(c) the velocity components $u_{n1}$ and $u_{t1}$ for $Ma_1 = \text{const.}$, so that $Ma_2 = 1$. How large is the turning angle $\beta$ now?

3.3 Air is sucked out of the atmosphere through a supersonic wind tunnel into a vacuum container (see sketch). The Laval nozzle is designed for the Mach number $Ma_E$ in the test section.

$p = 10^5$ Pa; $T = 280$ K; $\gamma = 1.4$;

$R = 287 \dfrac{\text{Nm}}{\text{kg K}}$; $A_H = 0.1\ \text{m}^2$;

$V_v = 1000\ \text{m}^3$; $Ma_E = 2.3$

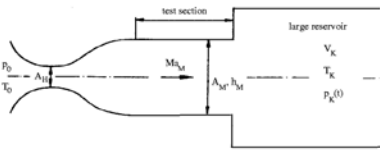


During the test the temperature in the container is $T_v = 280$ K $= \text{const}$. At time $t = 0$ the pressure in the container is $p_v(t = 0) = 0.08 \cdot 10^5$ Pa.

(a) Determine the available testing time $\Delta t$ (undisturbed flow in the test section, $Ma_E = 2.3$).
(b) Determine the following quantities: Shock angle $\sigma$, turning angle $\beta$, $p_{02}$, $Ma_2$, $T_2$, $T_{02}$, and the velocity $V_2$ downstream from the shock for the pressure in the container $p_v = 0.16 \cdot 10^5$ Pa.
(c) A wedge with nose angle $2\,\beta_w = 40°$ is mounted in the test section.

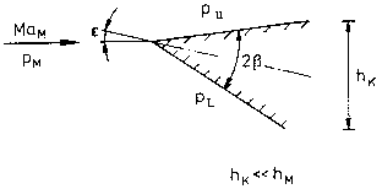


How large can the angle of attack $\epsilon$ be, without detachment of the compression shock? How large are the pressure difference $p_l - p_u$, and the Mach numbers $Ma_u$ and $Ma_l$ for this case?

3.4 Determine for the sketched flow field ($Ma_\infty$, $h_0 = \text{const.}$):

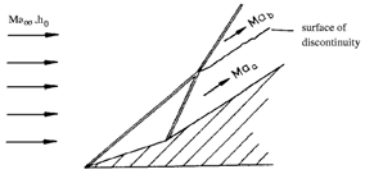


$Ma_a = 2$; $Ma_b = 1.8$; $\gamma = 1.4$;
$R = 287 \dfrac{\text{Nm}}{\text{kg K}}$

(a) the entropy difference $\Delta s = s_b - s_a$,
(b) the ratio of the velocities $|\,V_a\,| \,/\, |\,V_b\,|$,
(c) the density ratio $\rho_a/\rho_b$.

3.5 In the combustion chamber of a slender rocket a steady state with the stagnation pressure $p_0$ is attained after ignition.

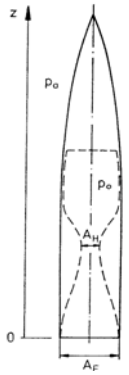


The flow is assumed to be two-dimensional and inviscid. The pressure in the atmosphere is given by:

$$\frac{p_a(z)}{p_a(0)} = \left(1 - \frac{\gamma - 1}{\gamma}\, a\, z\right)^{\frac{\gamma}{\gamma - 1}}$$

Rocket: $p_0 = 15 \cdot 10^5\ Pa$; $A_E = 1\ m^2$;
$A_H = 0.15\ m^2$; $\gamma = 1.4$
surroundings: $p_a(0) = 10^5$ Pa; $\gamma = 1.4$
$a = 1.1 \cdot 10^{-4}\ \dfrac{1}{\text{m}}$;

1. Determine for lift-off:
   (a) the Mach number $Ma_E$ and the pressure $p_E$ in the exit cross section $A_E$,
   (b) the shock angle $\sigma$ of all shocks and the Mach numbers downstream from the shocks!
   (c) Sketch the flow field downstream from the exit cross section! Sketch the shocks, the streamlines, and the Mach lines!
2. What is the height of the design condition of the rocket?

3.6 The flow in a two-dimensional supersonic wind tunnel is compressed by the shock configuration shown in the following sketch.

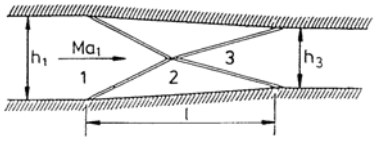


$Ma_1 = 3$; $\rho_2/\rho_1 = 1.85$; $\gamma = 1.4$

Determine the ratio of heights of the tunnel $h_3/h_1$ and the ratio $h_1/l$.

3.7 Given is the detached shock of a blunt symmetric body as sketched below.

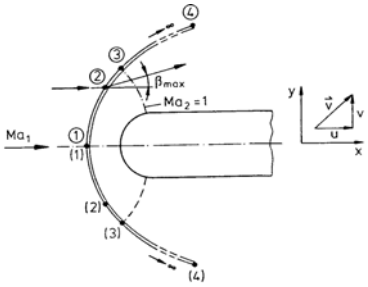


Sketch the shock polar and the heart-curve diagram. Plot the points 1 to 4 in the diagrams.

3.8 Consider a two-dimensional curved compression shock (see sketch). The shock angles $\sigma_A$ and $\sigma_B$ are known for the points $A$ and $B$, the verticle distance between them is $\Delta\, y$. Determine (approximately) the vorticity of the flow downstream from the shock for the streamline in the middle between the points $A$ and $B$.

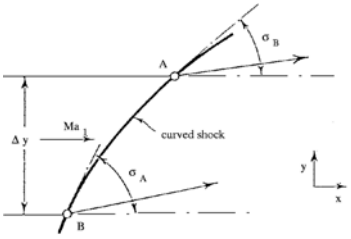


$Ma_1 = 2$; $\Delta\, y = 3$ cm; $T_0 = 300$ K;
$\sigma_A = 35°$; $\sigma_B = 55°$;
$R = 287 \dfrac{\text{Nm}}{\text{kg K}}$; $\gamma = 1.4$

Hint: Component of the vorticity in the $x$-$y$-plane:

$$\nabla \text{ x } \boldsymbol{v} = \left(\frac{\partial v}{\partial x} - \frac{\partial u}{\partial y}\right) \boldsymbol{k} \approx \left(\frac{\Delta\, v}{\Delta\, x} - \frac{\Delta\, u}{\Delta\, y}\right) \boldsymbol{k}$$

Consider the shock as straight line with an averaged slope between the points $A$ and $B$ for the determination of $\Delta\, x$.

### 5.1.4 Expansions and Compression Shocks

4.1 The radial component $u_r$ and the tangential component $u_t$ of the velocity are given for a point $P$ inside of a Prandtl-Meyer expansion.

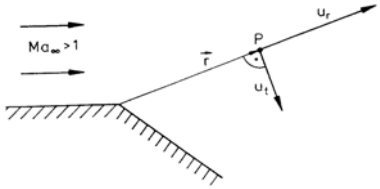


$u_r = 500 \dfrac{\text{m}}{\text{s}}$; $u_t = 250 \dfrac{\text{m}}{\text{s}}$;
$R = 287 \dfrac{\text{Nm}}{\text{kg K}}$; $\gamma = 1.4$

Determine:
(a) the Mach number $Ma_p$ for the point $P$
(b) and the temperature $T_p$!

4.2 Derive $\frac{\partial v_r}{\partial \Phi} = f(a)$ for the sketched Prandtl-Meyer expansion; $a$ = speed of sound.

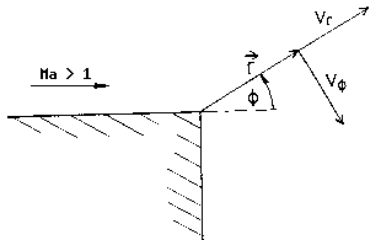


Hint:

$$\nabla \text{ x } \boldsymbol{v} = \frac{1}{r}\,\frac{\partial}{\partial r}\,(r\, v_\Phi) - \frac{1}{r}\,\frac{\partial v_r}{\partial \Phi}$$

4.3 The flow in the sketched supersonic wind tunnel is accelerated from $Ma_1$ to $Ma_3$ by two Prandtl-Meyer expansions. The first and the last characteristic lines of both expansions are plotted in the drawing.

The flow is expected to leave the tunnel parallel to the direction of the oncoming flow. Determine the length of the distances $AB'$ and $AC'$ and their inclination to the horizontal line.

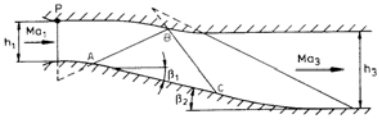


$Ma_1 = 1$; $Ma_3 = 2.06$; $h_1 = 0.1$ m; $\gamma = 1.4$

4.4 Consider the plane supersonic flow sketched below.

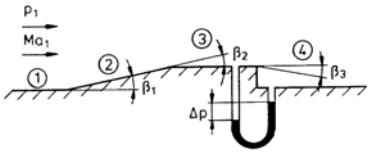


$Ma_1 = 2.5$; $\beta_1 = \beta_2 = 12°$;
$p_1 = 0.541 \cdot 10^5$Pa; $\Delta p = 0.304 \cdot 10^5$Pa;
$\gamma = 1.4$; $R = 287 \dfrac{\text{Nm}}{\text{kg K}}$

Determine:
(a) $Ma_2$, $\sigma$, $p_{02}$, and $p_2$,
(b) $Ma_3$ and $p_3$,
(c) $Ma_4$, $\beta_3$.
(d) Sketch streamlines, shock waves, and expansion fans.

4.5 An oblique compression shock is observed at the exit of a plane Laval nozzle for the pressure in the surrounding atmosphere $p_u$. The shock angle $\sigma_1$ is 40° and the turning angle $\beta_1 = 10°$.

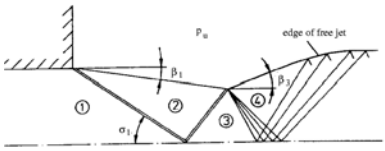


$p_a = 0.2 \cdot 10^5$ Pa; $R = 287 \dfrac{\text{Nm}}{\text{kg K}}$;
$\gamma = 1.4$;

Determine:
(a) the Mach numbers $Ma_1$ and $Ma_3$, and the static pressure $p_2$,
(b) the angle $\beta_3$!
(c) Sketch the flow field for $p_a = 0.28 \cdot 10^5$ Pa!
(d) At what surrounding pressure in the atmosphere is a normal shock to be observed in the exit cross section of the nozzle?

4.6 A plane inlet diffuser of a jet engine is so designed, that the front shock hits the lip at a free-stream Mach number $Ma_1 = 3$. The center body has a wedge angle of $\beta_1$. The flow is decelerated in the diffuser with a Prandtl-Meyer compression to the speed of sound.

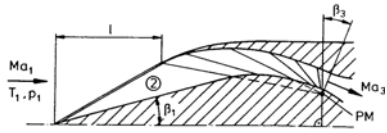


$Ma_1 = 3$; $T_1 = 250$ K; $\gamma = 1.4$;
$Ma_3 = 1$; $R = 287 \dfrac{\text{Nm}}{\text{kg K}}$; $\beta_1 = 15°$;
$l = 1$ m; $p_1 = 0.54 \cdot 10^5$ Pa;
width $b = 0.5$ m

(a) Determine for the design condition:
  1. $Ma_2$; $p_2$; $T_2$; $T_{02}$; $p_{02}$; and $\frac{\Delta s}{R}$,
  2. $\beta_3$, $p_3$, and the mass flow $\dot{m}$.
(b) How high would the static pressure $p_{3is.}$ be for isentropic compression from $Ma_1 = 3$ down to $Ma_3 = 1$?
(c) At what free-stream Mach number $Ma_{1c}$ would the compression shock still be attached to the center body?

4.7 A plane three-shock diffuser is designed for the free-stream Mach number $Ma_1$. The compression of the air from "3" to "4" (see sketch below) is enforced by a normal compression shock.

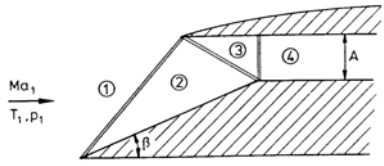

$Ma_1 = 3$; $T_1 = 300\,\mathrm{K}$; $\gamma = 1.4$;
$A = 0.1\,\mathrm{m}^2$; $p_1 = 0.5 \cdot 10^5\,\mathrm{Pa}$;
$R = 287\,\dfrac{\mathrm{Nm}}{\mathrm{kg\ K}}$; $\beta = 16^\circ$

Determine:

(a) the static pressure $p_4$ and the Mach number $Ma_4$,

(b) and the mass flow $\dot{m}$ through the inlet diffuser.

(c) How large would the mass flow $\dot{m}$ and the static pressure $p_{4is.}$ be for isentropic compression from $Ma_1$ down to $Ma_4$?

4.8 The contour shown below decreases the Mach number $Ma_1 > 1$ of the free stream by a Prandtl-Meyer compression down to $Ma = 1$.

(a) Sketch the flow field for $Ma_1$ and for a Mach number $Ma_2$, with $1 < Ma_2 < Ma_1$


(b) Sketch the supersonic flow field about a flat plate at angle of attack, (shocks, expansion fans, and streamlines).


(c) Sketch the flow field for the given wall contour with shocks, expansion fans, and streamlines for $\beta > \beta_{max}$.


4.9 A plane supersonic jet is deflected with a baffleplate. Sketch the flow field with shocks, expansion fans and streamlines.

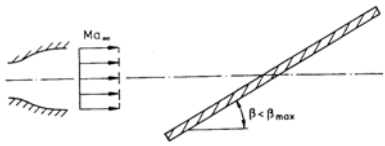


4.10 (a) Sketch the supersonic flow field about the body, shown below, including shocks, expansion fans, and streamlines.

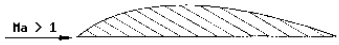


(b) Sketch the supersonic flow field about the body, shown below, including shocks, expansion fans, and streamlines.

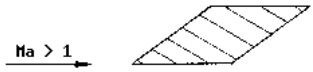


4.11 (a) Sketch the supersonic flow field over the contour, shown below, including shocks, Mach lines, and streamlines!


(b) Sketch the supersonic flow field about a cambered plate, shown below, including shocks, Mach lines, and streamlines.

### 5.1.5 Lift and Wave Drag – Small-Perturbation Theory

5.1 Consider the two-dimensional inviscid supersonic flow with free-stream Mach number $Ma_\infty$ about a double wedge profile and a pair of profiles with the same thickness ratio $d/l$.

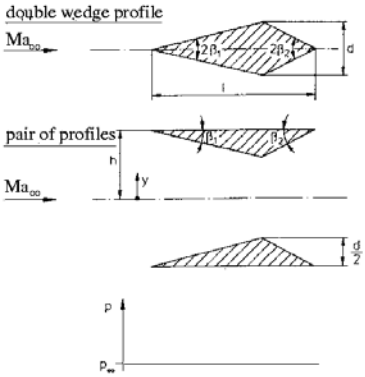


$Ma_\infty = 2.5$; $\beta_1 = 12°$; $\beta_2 = 15°$;
$l = 1\,\mathrm{m}$; $d = 0.24\,\mathrm{m}$;
$\gamma = 1.4$; $R = 287\,\dfrac{\mathrm{Nm}}{\mathrm{kg\,K}}$

(a) Sketch a streamline of the flow about the pair of profiles somewhere between $0 < y < h$ and indicate the variation of the static pressure along this streamline.
(b) Sketch the flow field about the double-wedge profile with shocks, expansion fans, and streamlines.
(c) Sketch the static pressure distribution on the surface of the double-wedge profile.
(d) Determine the drag coefficient $c_D$ of the double-wedge profile and for the pair of profiles (approximately).

$$c_D = \frac{F_D}{\frac{\varrho}{2}\,u_\infty^2\,b\,l}$$
$$b = \text{wing span}$$

5.2 Air flows through a two-dimensional tunnel with a velocity twice the speed of sound. For reasons of reconstruction the cross section of the tunnel has to be widened and the flow be redirected, as sketched below. Use the linearized theory and compute the turning angle $\beta_2$ and the Mach number $Ma_2$!

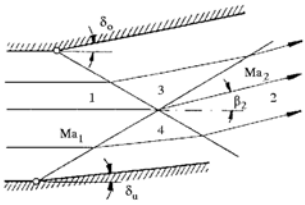


$Ma_1 = 2$; $\delta_u = 5°$; $\delta_o = 10°$;
$\gamma = 1.4$; $R = 287\,\dfrac{\mathrm{Nm}}{\mathrm{kg\,K}}$
Hint (linearized theory):
$$\frac{\Delta p}{p_1} = \frac{\gamma\,Ma_1^2}{\sqrt{Ma_1^2 - 1}}\,\Delta\beta$$

5.3 The contours of the upper and lower side, $y_u(x)$ and $y_l(x)$, respectively, of a thin airfoil profile with $h \ll t$ are given. Derive the expressions for determining the lift and drag coefficients $c_L$ and $c_D$ for supersonic free-stram conditions with the linearized theory!
Show, that the lift coefficient $c_L$ depends only on the free-stream Mach number and the angle of attack $\epsilon$.

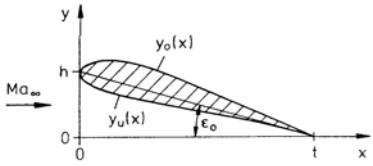


5.4 Air flows through a two-dimensional cascade. The lower side of the blades are flat, the contour of the upper side is given by the relation $\frac{y}{t} = \frac{h}{t}\,cos(\frac{\pi}{2}\,\frac{x}{t})$.

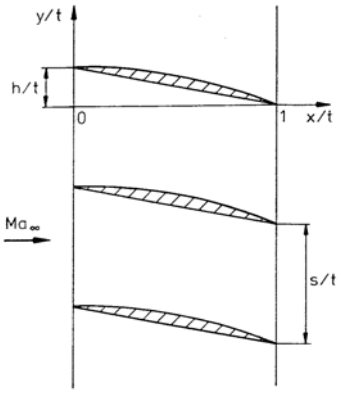


$Ma_\infty = 3$; $p_\infty = 10^5$ Pa;
$\gamma = 1.4$; $h/t = 0.05$
width of the blades: $b = 1$ m
chord: $t = 1$ m

Determine with the linearized theory:

(a) the spacing $s/t$ such that the blades do not interfere with each other,

(b) the pressure coefficients $c_{pu} = c_{pu}(x/t)$ and $c_{pl} = c_{pl}(x/t)$ for the upper and lower side of a blade and sketch their variation,

(c) the forces $F_x$ and $F_y$.

5.5 Use the linearized theory and compute the ratio of lift and drag coefficient $c_L/c_D$ for a profile with angle of attack $\epsilon_o$ and thickness distribution for supersonic flow with $Ma_\infty$, as sketched below!

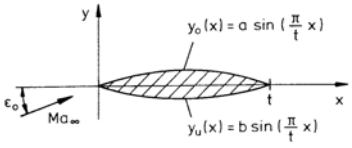


Given: $Ma_\infty$; $\epsilon_o$; $a$; $b$; $t$

5.6 Consider thin, two-dimensional profiles in supersonic flow at $Ma_\infty$. Determine lift and drag coefficient with the approximation for slender airfoils.

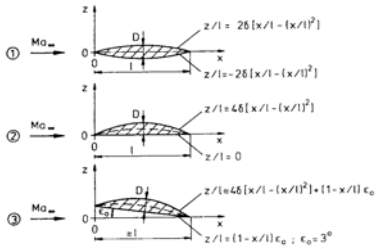


$Ma_\infty = \sqrt{2}$; $\delta = D/l = 0.1$

5.7 1.) Determine the drag coefficient $c_D$ of the double-wedge profile, sketched below, for inviscid, two-dimensional supersonic flow without any approximation.

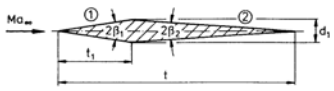


$Ma_\infty = 3$; $\beta_1 = 10°$; $\beta_2 = 4°$;
$\frac{d}{t} = 0.10$ m; $\gamma = 1.4$

2.) Determine with the linearized theory:

(a) the pressure coefficient $c_{p1}$ on the front and rear part $c_{p2}$, and the drag coefficient $c_D$ for $Ma_\infty = 3$;

(b) the lift coefficient $c_L$ and the drag coefficient $c_D$ for an angle of attack $\epsilon = 5°$ ($Ma_\infty = 3$).

5.8 An airplane flies in level flight at a Mach number $Ma_1$ and an altitude $H_1$ (static pressure $p_1$). Lift and drag are generated by a wing with a thin double-wedge profile at an angle of attack $\epsilon_1$ and a thickness ratio $\delta$. The airplane climbs to an altitude $H_2$ with the static pressure $p_2$ and flies then again in level flight.

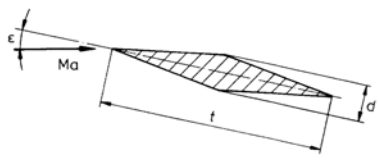

$Ma_1 = \sqrt{2}$; $\epsilon_1 = 2°$; $\delta = \frac{d}{t} = 0.03$; $p_2 = \frac{p_1}{\sqrt{2}}$; $\gamma = 1.4$

Determine for the altitude $H_2$:

(a) the angle of attack $\epsilon_2$, if the Mach number is kept constant ($Ma_2 = Ma_1$),

(b) the Mach number $Ma_2$, if the angle of attack remains unchanged ($\epsilon_2 = \epsilon_1$; give reasons for the solution),

(c) the ratio of drag and lift $F_D/F_L$ for the wing,

(d) the ratio of the necessary propulsive powers $P_a/P_b$ ($T_\infty = \text{const.}$) ($P_a$ = propulsive power for $Ma_2 = Ma_1$, see part a), $P_b$ = propulsive power for $\epsilon_2 = \epsilon_1$, see part b),

(e) the ratio of the energies $W_a/W_b$ necessary for the same route of flight (notation same as under d).

### 5.1.6 Theory of Characteristics

6.1 (a) Under what angle $\gamma$ are characteristics reflected at the edge of a jet?

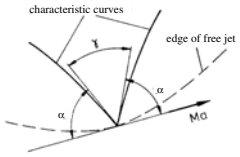


(b) Discuss, how the flow direction is determined at the edge of a jet and how the Mach number is determined along a rigid wall.

6.2 A plane jet impinges on a concave wall (see sketch below).
The flow is assumed to be isentropic. The Mach number downstream from the characteristic line 4–5 is supposed to be constant.
Determine the turning angle $\beta_3$ and the Mach number $Ma_3$ for the point $P_3$!

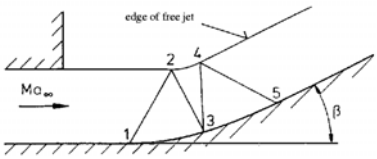


6.3 In the flow field shown below the line $OA$ is the first, and the line $OB$ the last charakteristic of an expansion fan.

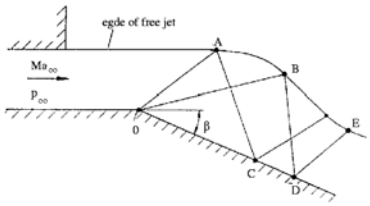


$Ma_\infty = 2$; $p_\infty = 10^5$ Pa; $|\beta| = 10°$
$\gamma = 1.4$; $R = 287 \frac{\text{Nm}}{\text{kg K}}$

Determine:

(a) the pressure and the Mach number for the point $C$,

(b) the slope of the streamline for the point $E$.

6.4 In the flow field sketched below the line 01 is the first, and the line 02 the last characteristic of the Prandtl-Meyer corner in the point 0.

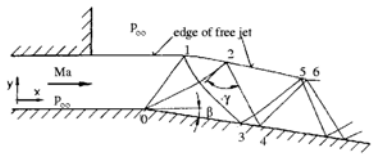


$Ma_\infty = 1.7$; $|\beta| = 7°$
$\gamma = 1.4$; $R = 287 \frac{\text{Nm}}{\text{kg K}}$

Determine:

(a) the direction of the flow in the points 2 and 6,

(b) the Mach numbers in the points 3 and 4,

(c) the angle $\gamma$ and the pressure ratio $p_4/p_\infty$!

6.5 Air flows through a plane symmetric nozzle, the contour consisting out of two circular sectors, isentropically into a large container (see the following sketch).

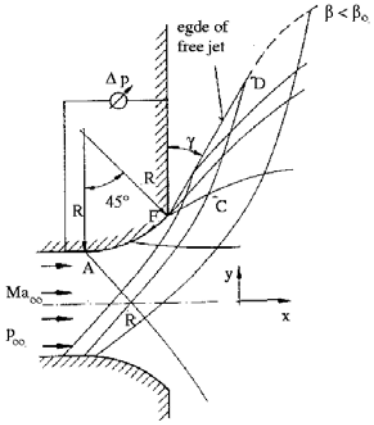


$Ma_\infty = 1.34$; $p_\infty = 10^5$ Pa;
$\Delta p_\infty = 0.98 \cdot 10^5$ Pa;
$\gamma = 1.4$; $R = 287 \dfrac{\text{Nm}}{\text{kg K}}$

(a) State the differential equation describing the two characteristics as a function of the flow angle $\beta$ and the Mach angle $\alpha$.
(b) The region $ABCEA$ is a simple region. Prove that all right-running characteristics in this region are straight lines!
(c) Determine the Mach number at the edge of the jet and the angle $\gamma$ between the edge of the jet and the wall!
(d) Show that the flow angle $\beta$ downstream from the point $D$ first has to decrease!

6.6 Air flows through a divergent two-dimensional channel with straight walls. Along the circular segment with radius $r^*$ the Mach number is $Ma = 1$.

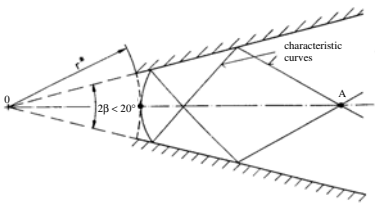


Determine for $\gamma = 1.4$ :
(a) the Mach number $Ma_A$ for the point $A$ with the method of characteristics,
(b) the ratio $r_A/r^*(r_A = \text{distance } 0-A)$.

6.7 Consider the flow field sketched below.

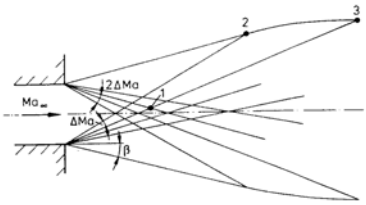


$Ma_\infty$; $\beta$; $\Delta\, Ma$

Determine the Prandtl-Meyer angle and the flow angle in the points 1 to 3.

6.8 A plane jet ($Ma_\infty = 3$) is symmetrically turned by a wedge with nose angle $2\,\beta = 28°$ (see sketch below).

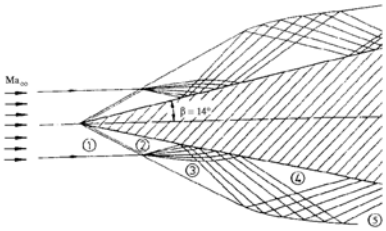


Determine $\beta_3$, $Ma_3$, $\beta_4$, $Ma_4$, and $Ma_e$!

### 5.1.7 Compressible Potential Flows and Similarity Rules

7.1 Reflexion of Mach waves

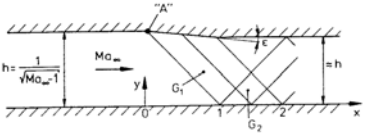


Determine the pressure coefficient $c_p(x,y)$ for $0 \le x \le 2$ for the lower wall!

7.2 Consider a supersonic flow in a wind tunnel . The flow is turned by the angle $\epsilon$ in the point $A$.

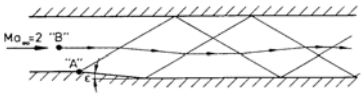


Draw the streamline through the point $B$, based on the linearized theory.

7.3 Supersonic flow flows through a cascade, consisting out of thin flat plates at small angle of attack $\epsilon_0$.

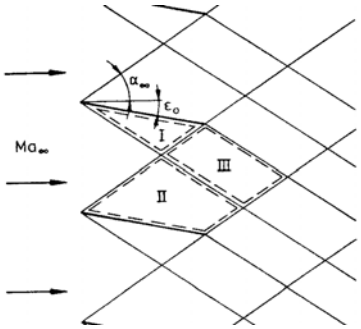


Formulate:

(a) the solutions for the linearized potential equation $(Ma_\infty^2 - 1)\,\varphi_{xx} - \varphi_{yy} = 0$ for the regions I, II, and III,

(b) the boundary conditions for the potentials in the regions I and II!

Determine:

(c) the potential function $\varphi(x,y)$ for the regions I, II, and III,

(d) the magnitude of the perturbation velocities and the direction of the outflow in the region III!

7.4 Consider the flow field sketched below.

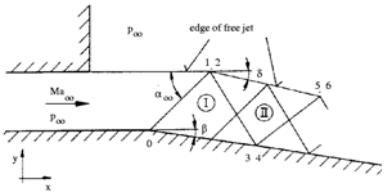


(a) Formulate the solution of the linearized potential equation for the regions I and II!

(b) State the expression for the pressure coefficient $c_p$ and the boundary condition at the edge of the jet for the region II!

(c) Determine the angle $\delta$ as a funcrion of $\beta$!

7.5 A two-dimensional supersonic flow is turned by a rigid wall as indicated in the sketch. The discontinuity surface, marked in the sketch, separates two flow regimes of equal pressure and flow direction, but with different velocities.

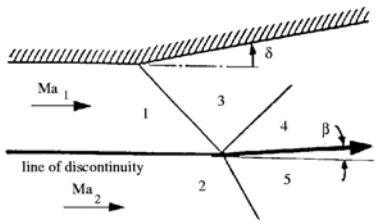


$p_1$; $\delta$; $\gamma$; $Ma_1$; $Ma_2$;
$Ma_1 > 1$; $Ma_2 > 1$;
$Ma_1 \neq Ma_2$; $p_4 = p_6$ .

Determine the turning angle of the flow $\beta$ and the static pressure $p_6$ with the linearized potential theory in the region 5. Hint: First formulate the solution for the perturbation potential and the boundary conditions in the regions 3, 4, and 5.

7.6 For the incompressible flow about an elliptic profile at zero angle of attack, the relation below describes the dependence of the maximum velocity along the contour, $(V_{max})$, on the free-stream velocity $U_\infty$, and the normalized thickness $\delta$:

$$\frac{V_{max}}{U_\infty} = 1 + \delta \qquad .$$

Determine the free-stream Mach number of the compressible subsonic flow, at which locally the speed of sound is attained on the surface of an ellipse with $\delta = 0.25$; use the following diagram for the solution.

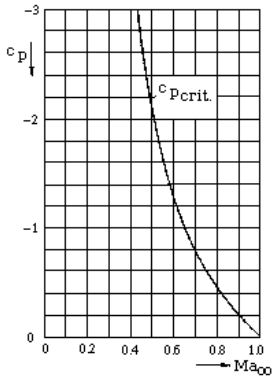


7.7 Consider a transonic flow at $Ma_1 = 0.95$ about a wing section with the relative thickness $\delta_1 = 0.05$. The minimum pressure on the contour is measured to be $c_{p1min} = 0.3$. Use the von Kármán similarity rule and compute the relative thickness $\delta_2$ and the pressure coefficient $c_{p2min}$ of a second wing section for a free-stream Mach number $Ma_2 = 0.9$.

7.8 The critical Mach number of a thin wing section is $Ma_{\infty crit.} = 0.7$. The lift coefficient measured at this Mach number is $c_L = 0.3$.

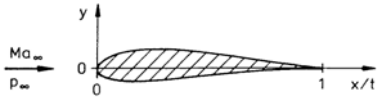


$p_\infty = 10^5$ Pa; $\gamma = 1.4$;
$R = 287 \dfrac{\text{Nm}}{\text{kg K}}$

(a) Determine the lowest local pressure on the contour and the critical pressure coefficient $c_{pcrit.}$.

(b) For what free-stream Mach number $Ma_{\infty\, b}$ is the sketched pressure distribution measured with the same wing section?

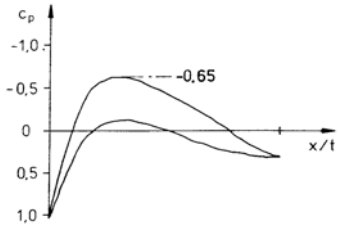


(c) Determine the lift coefficients $c_{Lcomp.}$ at $Ma_{\infty\, c} = 0.4$ and $c_{ainc.}$ for incompressible flow!

7.9 A model experiment is carried out in incompressible flow in order to determine the pressure distribution of a compressible flow over a cambered wall.

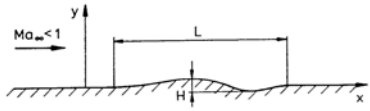


What similarity rule
$c_p/c_{pinc.} = f(Ma_\infty)$ should be used for the application of the results of the measurements and what geometric dimensions $L_{inc.}/L$ and $H_{inc.}/H$ are determined for the model?
Use the solution of the linearized potential equation for compressible flow and a sinosoidal wall:

$$c_p = \frac{2\,\pi\, d/l}{\sqrt{1 - Ma_{\infty^2}}}\, e^{-2\,\pi\, y\, H\, \sqrt{1-Ma_{\infty^2}}} \times \\ \times \; sin\left(\frac{2\,\pi\, x}{l}\right) \quad ,$$

with $d$ = maximum amplitude.

7.10 1. According to the linearized theory for plane flows the following similarity rule is valid for bodies of the same family:
$\dfrac{c_p}{A} = \text{const.}$, if $\dfrac{d/t}{A\sqrt{|\, Ma_\infty^2 - 1\,|}} = \text{const.}$, and A arbitrary.

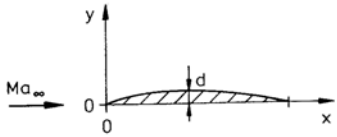


Determine $A$ in such a way, that the transformation of the body contour is identical with the coordinate transformation

$x = \text{const}$; $y\sqrt{|\, Ma_\infty^2 - 1\,|} = \text{const.}$

What similarity rule is obtained?

2. An equivalent formulation of (1) is

$$\frac{c_p \sqrt{|\, Ma_\infty^2 - 1\,|}}{d/t} = \text{const.}$$

   (a) Derive the corresponding similarity rule for the lift coefficient $c_L$!
   (b) Show, that the relation

$$\frac{\epsilon}{d/t} = \text{const.}$$

   is valid for supersonic flow, if $\epsilon$ designates the angle of attack!
3. Name three classes of flows, fo which the above similarity rules are not valid!

7.11 (a) An airfoil with thickness ratio $\delta_a = 0.1$ generates a lift coefficient $c_{L1} = 0.325$ at $Ma_{\infty 1} = 0.6$. At what free-stream Mach number $Ma_{\infty 2}$ is the lift coefficient $c_{L2} = 0.37$?
   (b) How large is the thickness ratio $\delta_b$ of a wing of the same family for incompressible flow, if its lift coefficient $c_{Linc.} = c_{L1}$ for $Ma_{\infty 1} = 0.6$?

7.12 An airplane generates its lift with a thin wing with a double-wedge profile. It flies steadily in level flight.

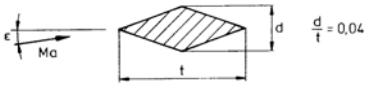


A. Assume linearized plane supersonic flow ($Ma > 1$):
   1. The lift coefficient is $c_{a1} = 0.1$ at the free-stream Mach number $Ma_{\infty 1} = 1.5$. Determine the angle of attack $\epsilon_1$ of the wing!
   2. The Mach number is increased to $Ma_{\infty 2} = 3$. Determine the angle of attack $\epsilon_2$ and the drag coefficient $c_{D2}$!

B. Linearized plane subsonic flow ($Ma_\infty < 1$):
   3. How large does the lift coefficient $c_{L3}$ at $Ma_{\infty 3} = 0.75$ have to be? How large is the drag coefficient $c_{D3}$ at this free-stream Mach number?
   4. How large is the lift coefficient $c_{L4}$ for the same geometry ($\epsilon$ = const., $\delta$ = const.) in incompressible flow?
   5. How large do the ratios $\delta_{5inc.}/\delta$ and $\epsilon_{5inc.}/\epsilon_3$ have to be in incompressible flow, so that $c_{L5inc.}$ is $c_{L5inc.} = c_{L3}$?

## 5.2 Solutions

### 5.2.1 One-Dimensional Steady Flows of Gases

1.1 (a) Law of thermodynamics for steady processes

$$\begin{aligned} h_2 &- h_1 + \frac{u_2^2}{2} - \frac{u_1^2}{2} \\ &+ g\,(z_2 - z_1) = 0 \end{aligned}$$

with:

$$h_2 - h_1 = e_2 - e_1 + \frac{p_2}{\rho 2} - \frac{p_1}{\rho_1}$$

(b) 1.

$$\Delta e \leftrightarrow \Delta\, g\, z + \Delta\, \frac{u_2^2}{2} + \Delta\, \frac{p}{\rho}$$

In compressible flows internal energy is transformed into kinetic energy, potential energy, and compression work.

2.

$$\Delta e = 0$$

The internal energy is constant in incompressible fluids, which, for thermally perfect gases ($e = f(T)$) implies a constant temperature. There is only an exchange between mechanical energies.

1.2 (a)

$$Ma = \frac{v}{\sqrt{\gamma\, R\, T}} = 2.0$$

(b)

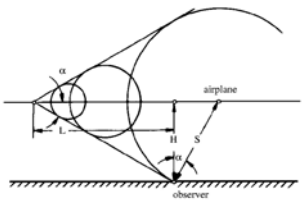


$$\begin{aligned} L &= \frac{H}{\tan\alpha} \\ \alpha &= \arctan\left(\frac{1}{Ma}\right) \\ L &= 1001\ \text{m} \end{aligned}$$

(c)

$$\begin{aligned} \Delta t &= \frac{S}{a} \\ \cos\alpha &= \frac{H}{S} \\ \Delta t &= 1.96\ \text{s} \end{aligned}$$

prior to flying over the observer.

1.3 (a)

$$\begin{aligned} c_p\, T_0 &= c_p\, T^* + \frac{a^{*2}}{2} \\ a^{*2} &= \gamma\, R\, T \\ c_p &= \frac{\gamma\, R}{\gamma - 1} \\ \frac{T^*}{T_0} &= \frac{2}{\gamma + 1} = 0.833 \end{aligned}$$

(b)

$$\frac{p^*}{p_0} = \left(\frac{T^*}{T_0}\right)^{\frac{\gamma}{\gamma-1}} = 0.528$$

(c)

$$\begin{aligned} Ma \to \infty &: \quad T \to 0 \\ c_p\, T_0 &= \frac{u_{max}^2}{2} \\ \lim_{Ma\to\infty} Ma^* &= \sqrt{\frac{\gamma+1}{\gamma-1}} = 2.45 \end{aligned}$$

1.4

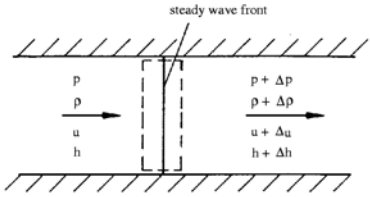


$$\begin{aligned} \rho\, u &= (\rho + \Delta\,\rho)\,(u + \Delta\, u) \\ &\Rightarrow\ u\, d\rho = -\rho\, du \\ p - (p + \Delta\, p) &= (\rho + \Delta\,\rho)\,(u + \Delta\, u)^2 \\ &- \rho\, u^2 \\ \Rightarrow 2\,\rho\, u\, du &+ u^2\, d\rho = -dp \\ \Rightarrow u^2 &= \frac{dp}{d\rho} \end{aligned}$$

$$
\begin{aligned}
h + \frac{u_2^2}{2} = (h + \Delta h) &+ \frac{1}{2}(u + \Delta u)^2 \\
\Rightarrow dh + udu &= 0 \\
Tds &= dh - \frac{dp}{\rho} \\
\text{with} \qquad udu &= -\frac{dp}{\rho} \\
\Rightarrow Tds &= 0 \\
\Rightarrow u^2 &= \left(\frac{\partial p}{\partial \rho}\right)_s = a^2
\end{aligned}
$$

1.5

$$
\begin{aligned}
\Delta t &= \frac{b}{(v_B - v_A)\tan\alpha} \\
Ma_B &= 2: \quad \alpha = 30^\circ \\
\Delta t &= 1.73 \text{ s}
\end{aligned}
$$

1.6

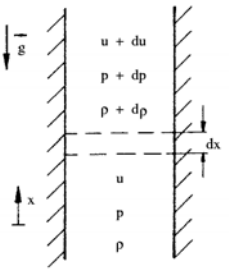


$$
\begin{aligned}
d(\rho u^2) &= -dp - \rho g dx \\
d(\rho u) &= 0 \\
\Rightarrow u\frac{du}{dx} &= -\frac{1}{\rho}\frac{dp}{dx} - g \\
a^2 &= \frac{dp}{d\rho} \\
\Rightarrow u\frac{du}{dx} + \frac{a^2}{\rho}\frac{d\rho}{dx} &= -g \\
\Rightarrow u\frac{du}{dx} &= -\frac{Ma^2}{Ma^2 - 1}\, g
\end{aligned}
$$

with $u > 0 \quad dx > 0$ it follows for
a) $Ma < 1 \quad du > 0$
b) $Ma > 1 \quad du < 0$

1.7

$$
\begin{aligned}
h_0 = \frac{u^2}{2} + c_p T &= \text{const.} \\
c_p &= \frac{\gamma}{\gamma - 1} R
\end{aligned}
$$

$$
\begin{aligned}
\frac{u^2}{2} + \frac{\gamma}{\gamma - 1} RT &= \frac{a^{*2}}{2} + \frac{\gamma}{\gamma - 1} RT^* \\
\Rightarrow \frac{u^2}{2} + \frac{a^2}{\gamma - 1} &= \frac{1}{2}\frac{\gamma + 1}{\gamma - 1} a^{*2} \\
Ma^{*2} &= \frac{\frac{\gamma+1}{\gamma-1}}{1 + \frac{2}{\gamma-1}\frac{1}{Ma^2}} \\
\Rightarrow \lim_{Ma\to\infty} Ma^{*2} &= \frac{\gamma + 1}{\gamma - 1}
\end{aligned}
$$

1.8

$$
\begin{aligned}
\frac{A}{A^*} = \frac{\rho^* a^*}{\rho u} \quad \frac{\rho^*}{\rho} &= \left(\frac{T^*}{T}\right)^{\frac{1}{\gamma-1}} \\
\Rightarrow \frac{A}{A^*} &= \left(\frac{T^*}{T}\right)\frac{1}{Ma^*} \\
c_p T + \frac{u^2}{2} &= c_p T^* + \frac{a^{*2}}{2} \\
\Rightarrow \frac{T^*}{T} &= \frac{1 + \frac{\gamma-1}{2} Ma^2}{1 + \frac{\gamma-1}{2}}
\end{aligned}
$$

After problem 1.7

$$
\begin{aligned}
Ma^{*2} &= \frac{\gamma + 1}{\gamma - 1 + \frac{2}{Ma^2}} \\
\frac{A}{A^*} &= \left(\frac{1 + \frac{\gamma-1}{2} Ma^2}{1 + \frac{\gamma-1}{2}}\right)^{\frac{1}{\gamma-1}} \cdot \\
&\quad \cdot \left(\frac{\gamma + 1}{\gamma - 1 + \frac{2}{Ma^2}}\right)^{-\frac{1}{2}}
\end{aligned}
$$

1.9 (a)

$$
\begin{aligned}
\Theta_{max} &= \frac{\rho^* a^*}{\rho_0 a_0} = \frac{\rho^*}{\rho}\sqrt{\frac{T^*}{T_0}} \\
&= \left(\frac{2}{\gamma + 1}\right)^{\frac{1}{\gamma-1}} \left(\frac{2}{\gamma + 1}\right)^{\frac{1}{2}} \\
\Theta_{max} &= \left(\frac{2}{\gamma + 1}\right)^{\frac{\gamma+1}{2(\gamma-1)}}
\end{aligned}
$$

(b)

$$
v(\Theta_{max}) = \frac{a^*}{a_0} = \sqrt{\frac{T^*}{T}} = \sqrt{\frac{2}{\gamma + 1}}
$$

(c)

$$
\begin{aligned}
\frac{u_{max}^2}{2} &= c_p\, T_0 = \frac{\gamma}{\gamma - 1} RT_0 \\
v_{max} &= \frac{u_{max}}{a_0} = \sqrt{\frac{2}{\gamma + 1}}
\end{aligned}
$$

1.10 (a)

$$\begin{aligned} \rho_1^* a_1^* A_1^* &= \rho_2^* a_2^* A_2^* \\ T_1^* = T_2^* &\Rightarrow a_1^* = a_2^* \\ \Rightarrow \frac{A_2^*}{A_1^*} &= \frac{p_{01}}{p_{02}} = 2 \end{aligned}$$

(b)

$$\begin{aligned} &\frac{A_2^*}{A} = 2\,\frac{A_1^*}{A}; \quad Ma_1 < 1 \\ &\Rightarrow Ma_2 > Ma_1 \end{aligned}$$

(c)

$$\begin{aligned} Ma_{2max} &= 1 \\ \left(\frac{A_1^*}{A}\right)_{max} &= \frac{A_1^*}{A_2^*} \quad \left(\frac{A_2^*}{A}\right)_{max} \\ &= \frac{1}{2} \\ \Rightarrow Ma_{1max} &= 0.3 \end{aligned}$$

1.11 (a) Momentum:

$$\begin{aligned} F &= \gamma p_a Ma^2 A \\ \Rightarrow \frac{F}{Ap_0} &= \gamma \frac{p_a}{p_0} Ma^2 \end{aligned}$$

Energy:

$$\begin{aligned} \frac{T_0}{T} &= 1 + \frac{\gamma - 1}{2}\, Ma^2 \\ \frac{T_0}{T} &= \left(\frac{p_0}{p}\right)^{\frac{\gamma-1}{\gamma}} \\ \Rightarrow \frac{F}{Ap_0} &= \frac{2\gamma}{\gamma - 1}\left(\frac{p_a}{p_0}\right) \cdot \\ &\quad \cdot \left[\left(\frac{p_a}{p_0}\right)^{-\frac{1}{\gamma-1}} - 1\right] \quad . \end{aligned}$$

(b)

$$\begin{aligned} &\frac{p_a}{p_0} = 1 - \frac{p_0 - p_a}{p_0} = 1 - \epsilon; \quad \epsilon \ll 1 \\ &(1-\epsilon)^{-\frac{\gamma-1}{\gamma}} = 1 + \frac{\gamma - 1}{\gamma}\,\epsilon \\ &\quad + \frac{\frac{\gamma-1}{\gamma}\left(\frac{\gamma-1}{\gamma} + 1\right)}{2!}\,\epsilon^2 \pm ... \\ &\Rightarrow \frac{F}{Ap_0} = 2\epsilon + 0(\epsilon^2) \\ &\quad = 2\frac{p_0 - p_a}{p_0} + 0(\epsilon^2) \end{aligned}$$

incompressible

$$\begin{aligned} \left(\frac{F}{Ap_0}\right)_{ink} &= 2\frac{p_0 - p_a}{p_0} \\ \Rightarrow \frac{F}{Ap_0} - \left(\frac{F}{Ap_0}\right)_{ink} &= \Delta\left(\frac{F}{Ap_0}\right) \\ &= 0(\epsilon^2) \end{aligned}$$

Table of solution in the Appendix.

1.12

$$\begin{aligned} c_p\, T_0 &= c_p\, T + \frac{u^2}{2} \\ c_p &= \frac{\gamma\, R}{\gamma - 1} \\ \frac{T}{T_0} &= \left(\frac{\gamma - 1}{2}\, Ma^2 + 1\right)^{-1} \\ \frac{\rho}{\rho_0} &= \left(\frac{T}{T_0}\right)^{\frac{1}{\gamma-1}} \\ &= \left(\frac{\gamma - 1}{2}\, Ma^2 + 1\right)^{\frac{1}{1-\gamma}} \\ \frac{p}{p_0} &= \left(\frac{T}{T_0}\right)^{\frac{\gamma}{\gamma-1}} \\ &= \left(\frac{\gamma - 1}{2}\, Ma^2 + 1\right)^{\frac{\gamma}{1-\gamma}} \end{aligned}$$

1.13 (a)

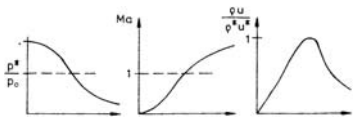


(b)

$$\begin{aligned} 1.\ \frac{A^*}{A_E} &= 0.593; \\ 2.\ \frac{p_E}{p_0} &= 0.128; \\ 3.\ \frac{T_E}{T_0} &= 0.556; \\ 4.\ \frac{\rho_E\, u_E}{\rho^*\, u^*} &= \frac{A^*}{A_E} = 0.593 \end{aligned}$$

1.14

$$\begin{aligned} \frac{\dot{m}}{\rho_0\, a_0\, A} &= \frac{\rho u}{\rho_0 a_0} \\ \frac{\rho}{\rho_0} &= \left(\frac{p}{p_0}\right)^{\frac{1}{\gamma}} \end{aligned}$$

$$\frac{u^2}{2}+\frac{a^2}{\gamma-1} = \frac{a_0^2}{\gamma-1}$$

$$\Rightarrow u^2 = \frac{2\,a_0^2}{\gamma-1}\left[1-\left(\frac{a}{a_0}\right)^2\right]$$

$$= \frac{2\,a_0^2}{\gamma-1}\left[1-\left(\frac{p}{p_0}\right)^{\frac{\gamma-1}{\gamma}}\right]$$

$$\Rightarrow \frac{\dot m}{\rho_0\,a_0\,A} = \left(\frac{p}{p_0}\right)^{\frac{1}{\gamma}}\sqrt{\frac{2}{\gamma-1}}\cdot \cdot \sqrt{\left(1-\left(\frac{p}{p_0}\right)^{\frac{\gamma-1}{\gamma}}\right)}$$

critical state

$Ma_e = 1$

$$\Rightarrow p_e = \frac{p^*}{p_0}\,p_0 = \left(\frac{2}{\gamma-1}\right)^{\frac{\gamma-1}{\gamma}}\,p_0$$

$$= 0.528\cdot 10^5\ \text{Pa}$$

(a)

$$\frac{p_c}{p_0} = 0.7 > 0.528 \Rightarrow \text{subcritical}$$

$$\dot m = \frac{p_0}{RT_0}\sqrt{\gamma RT_0}\,A_e\left(\frac{p_c}{p_0}\right)^{\frac{1}{\gamma}}\cdot \cdot \sqrt{\frac{2}{\gamma-1}\left(1-\left(\frac{p_c}{p_0}\right)^{\frac{\gamma-1}{\gamma}}\right)}$$

$$= 4.35\ \frac{kg}{s}$$

(b)

$$\frac{p_c}{p_0} = 0.2 < 0.528 \Rightarrow \text{supercritical}$$

$$p_e = p^*$$

$$\dot m = \frac{p_0}{RT_0}\sqrt{\gamma RT_0}\,A_e\left(\frac{2}{\gamma+1}\right)^{\frac{1}{2}\frac{\gamma+1}{\gamma-1}}$$

$$= 4.67\ \frac{\text{kg}}{\text{s}}$$

(c)

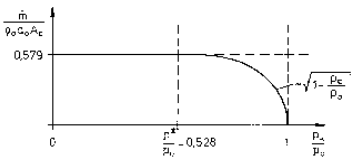


$$\frac{p_c}{p_0} \le \frac{p^*}{p_0} = 0.528$$

$$\Rightarrow \frac{\dot m}{\rho_0 a_0 A_e} = \text{const.} = 0.579$$

$$\frac{p_c}{p_0} > \frac{p^*}{p_0}$$

$$\Rightarrow \frac{\dot m}{\rho_0 a_0 A_e} = \left(\frac{p_c}{p_0}\right)^{\frac{1}{\gamma}}\sqrt{\frac{2}{\gamma-1}}\cdot \cdot \sqrt{\left(1-\left(\frac{p_c}{p_0}\right)^{\frac{\gamma-1}{\gamma}}\right)}$$

with

$$p_c \to p_0 : Ma \to 0;\quad \rho \approx \rho_0$$

$$u_e \approx \sqrt{\frac{2}{\rho}\,(p_0-p_c)}$$

$$\Rightarrow \frac{\dot m}{\rho_0\,a_0\,A_e} \sim \sqrt{1-\frac{p_c}{p_0}}$$

1.15 (a) for: $p_0 = 7.824\cdot 10^5$ Pa

$$\Rightarrow \rho_0 = \frac{p_0}{RT_0} = 9.47\ \frac{\text{kg}}{\text{m}^3}$$

(b)

$$p_0 = 7.824\cdot 10^5\,Pa;\quad A_H = A^*;$$

$$Ma = Ma^* = 1$$

$$\frac{p^*}{p_0} = 0.528 \Rightarrow p_H = 4.13\cdot 10^3\,Pa$$

$$\frac{\rho^*}{\rho_0} = 0.634 \Rightarrow \rho_H = 6.00\ \frac{\text{kg}}{\text{m}^3}$$

$$\frac{T^*}{T_0} = 0.833 \Rightarrow T_H = 240\ \text{K}$$

$$u_H = a^* = \sqrt{\gamma RT^*} = 310.5\ \frac{\text{m}}{\text{s}}$$

$$\dot m^* = \rho^*\,a^*\,A^* = 0.186\ \frac{\text{kg}}{\text{s}}$$

$$p_E = 10^5\ \text{Pa}$$

$$\Rightarrow \frac{p_E}{p_0} = 0.1278$$

$$Ma_E = 2;\quad Ma_E^* = 1.63$$

$$\frac{\rho_E}{\rho_0} = 0.230$$

$$\Rightarrow \rho_E = 2.18\ \frac{\text{kg}}{\text{m}^3}$$

$$\frac{T_E}{T_0} = 0.556 \Rightarrow T_E = 160\ \text{K}$$

$$u_E = Ma_E\,a_E = 507.1\ \frac{\text{m}}{\text{s}}$$

$$\dot m_E = \dot m^* = 0.186\ \frac{\text{kg}}{\text{s}}$$

(a) for: $p_0 = 1.064 \cdot 10^5$ Pa

$$\Rightarrow \rho_0 = 1.29 \ \frac{\text{kg}}{\text{m}^3}$$

(b) $p_0$ is only slightly higher than $p_a$
⇒ Subsonic flow in the entire nozzle! The throat is no longer a special cross section!

$$A_E : \frac{p_E}{p_0} = 0.9398$$
$$\Rightarrow Ma_E = 0.3; \ Ma_E^* = 0.326$$

with isentropic relation

$$\frac{p}{\rho^\gamma} = \text{const., it follows:}$$
$$\frac{\rho_E}{\rho_0} = 0.956$$
$$\Rightarrow \rho_E = 1.23 \ \frac{\text{kg}}{\text{m}^3}$$
$$\frac{T_E}{T_0} = 0.982$$
$$\Rightarrow T_E = 283 \text{ K}$$
$$u_E = 101.2 \ \frac{\text{m}}{\text{s}};$$
$$\dot{m} = 2.1 \cdot 10^{-2} \ \frac{\text{kg}}{\text{s}}$$
$$A_H \neq A^*$$
$$\frac{A_f^*}{A_E} = \frac{\rho_e \, u_E}{\rho_f^* \, a_f^*} = 0.492$$
$$\frac{A_f^*}{A_H} = 0.83$$
$$\Rightarrow Ma_H = 0.59; \quad Ma_H^* = 0.62$$
$$\frac{p_0}{p_H} = 1.26$$
$$\Rightarrow p_H = 0.79 \cdot 10^5 \text{ Pa}$$

Isentropic condition:

$$\rho_H = 1.09 \ \frac{\text{kg}}{\text{m}^3}; \ T_H = 269.2 \text{ K}$$
$$u_H = 194 \ \frac{\text{m}}{\text{s}}; \ \dot{m}_h = 2.1 \cdot 10^{-2} \ \frac{\text{kg}}{\text{s}}$$

1.16 (a)

$$h_0 = \text{const.} = h + \frac{u^2}{2} = C_2$$
$$\rho u = \text{const.} = \sqrt{C_1}$$
$$\Rightarrow h + \frac{C_1}{2\rho^2} = C_2$$

(b)

$$(Tds)_P = 0 = \left(dh - a^2 \frac{d\rho}{\rho}\right)_P$$
$$dh = u^2 \, \frac{d\rho}{\rho}$$
$$\Rightarrow (u_p^2 - a^2) \left(\frac{d\rho}{\rho}\right)_P = 0$$
$$\Rightarrow Ma = 1$$

$2^{nd}$ and $3^{rd}$

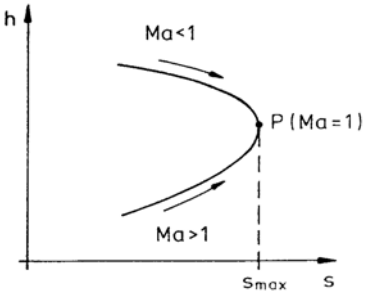


1.17 (a)

$$\rho u = \text{const.}$$
$$\rho u^2 + p = \text{const.}$$
$$\Rightarrow p + \frac{C_1}{\rho} = C_2; \quad C_1 = (\rho u)^2$$

(b)

$$\left(\frac{dp}{d\rho}\right)_P = \left(\frac{\partial dp}{\partial d\rho}\right)_s = a_P^2$$
$$\left(\frac{dp}{d\rho}\right)_P = u_P^2$$
$$\Rightarrow Ma_P = 1$$

$2^{nd}$ and $3^{rd}$

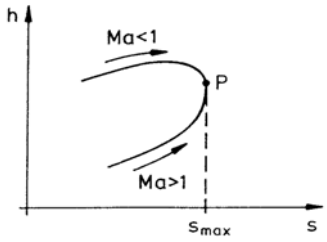

### 5.2.2 Normal Compression Shock

2.1 Continuity equation: $u_1\rho_1 = u_2\rho_2$
Prandtl relation : $u_1u_2 = a^{*2}$

$$\begin{aligned} \Rightarrow \frac{\rho_2}{\rho_1} = \frac{u_1}{u_2} = \frac{u_1^2}{a^{*2}} &= Ma_1^{*2} \\ \Rightarrow \left(\frac{\rho_2}{\rho_1}\right)_{max} = {Ma_{1max}^*}^2 &= \frac{\gamma+1}{\gamma-1} \end{aligned}$$

2.2

$$\begin{aligned} u_1u_2 &= a^{*2} \\ \Rightarrow u_2 = \frac{a^{*2}}{u_1^2} = \frac{u_1}{Ma_1^{*2}} &= 192\ \frac{\mathrm{m}}{\mathrm{s}} \end{aligned}$$

2.3 (a)

$$\begin{aligned} Ma_1 = \frac{u_1}{a_1} &= \frac{u_1}{\sqrt{\gamma RT_1}} = 1.5 \\ \frac{p_1}{p_{01s}} &= 0.272 \\ \Rightarrow p_{01s} &= 3.67\cdot 10^5\ \mathrm{Pa} \\ T_{01s} = 425\ \mathrm{K};\ p_{2s} &= 2.45\cdot 10^5\ \mathrm{Pa} \\ T_{2s} = 387\ \mathrm{K};\ p_{02s} &= 3.4\cdot 10^5\ \mathrm{Pa} \\ T_{02s} &= T_{01s} \end{aligned}$$

$$\begin{aligned} Ma_{2s}^* &= \frac{1}{Ma_{1s}^*} = 0.7328 \\ \Rightarrow Ma_{2s} &= 0.71 \\ u_{2s} &= Ma_{2s}\sqrt{\gamma RT_{2s}} \\ &= 280\ \frac{\mathrm{m}}{\mathrm{s}} \end{aligned}$$

(b)

$$\begin{aligned} u_{1R} &= Ma_{1R} = 0 \\ p_{01R} &= p_1;\quad T_{01R} = T_1 \\ p_{2R} &= p_{2s};\quad T_{2R} = T_{2s} \\ u_{2R} &= u - u_{2s} = 235\ \frac{\mathrm{m}}{\mathrm{s}} \\ &\Rightarrow Ma_{2R} = 0.596 \\ &\Rightarrow \frac{p_{2R}}{p_{02R}} = 0.78 \\ &\Rightarrow p_{02R} = 3.14\cdot 10^5\ \mathrm{Pa} \\ \frac{T_{2R}}{T_{02R}} &= 0.94 \Rightarrow T_{02R} = 399\ \mathrm{K} \end{aligned}$$

2.4 1) Coordinates moving with shock: Index "s"

$$\begin{aligned} \frac{p_2}{p_1} &= 10.2 \Rightarrow Ma_{1s} = 3 \\ u &= Ma_{1s}\sqrt{\gamma RT_1} = 1042\ \frac{\mathrm{m}}{\mathrm{s}} \end{aligned}$$

2) (a)

$$\begin{aligned} Ma_{2s}^* &= \frac{1}{Ma_{1s}^*} = 0.509 \\ \Rightarrow Ma_{2s} &= 0.47 \\ T_2 &= \frac{T_2}{T_1}T_1 = 795\ \mathrm{K} \end{aligned}$$

$$\begin{aligned} u_{2s} &= Ma_{2s}\sqrt{\gamma RT_2} \\ &= 265.6\ \frac{\mathrm{m}}{\mathrm{s}} \\ Ma_\infty &= \frac{u - u_{2s}}{\sqrt{\gamma RT_1}} = 1.37 \end{aligned}$$

(b)

$$\begin{aligned} Ma_\infty &= 1.37 \Rightarrow \frac{T_2}{T_{0\infty}} = 0.72 \\ \Rightarrow T_{0\infty} &= 1104\ \mathrm{K} \end{aligned}$$

(c)

$$p_{0\infty} = \frac{p_{0\infty}}{p_2}p_2 = 30.9\cdot 10^5\ \mathrm{Pa}$$

2.5

$$\begin{aligned} c_p\,T_1 + \frac{u_1^2}{2} &= c_p\,T_2 + \frac{u_2^2}{2} \\ \frac{u_1}{u_2} &= \frac{(\gamma+1)\,Ma_1^2}{2+(\gamma-1)\,Ma_1^2} \\ c_p &= \frac{\gamma\,R}{\gamma-1} \\ T_2 - T_1 &= \frac{(\gamma-1)(u_1^2-u_2^2)}{2\,\gamma\,R} \\ &= 197.9\ \mathrm{K} \end{aligned}$$

2.6 (a)

$$\frac{p_{01}}{p_{02}} = \frac{A_2^*}{A_1^*} = \frac{A_2^*}{A_B}\,\frac{A_A}{A_1^*}\,\frac{A_B}{A_A} = 3.04$$

(b)

$$\begin{aligned} \frac{p_{01}}{p_{02}} &= 3.04 \\ \Rightarrow Ma &= 3 \Rightarrow \frac{p_2}{p_1} = 10 \end{aligned}$$

(c)

$$\frac{p_B}{p_A} = \frac{p_B}{p_{02}} \frac{p_{01}}{p_A} \frac{p_{02}}{p_{01}} = 2.76$$

2.7

$$\dot{m} = \rho_1 v_1 A_1 = \sqrt{\frac{\gamma}{R T_1}}\, p_1 Ma_1 A$$

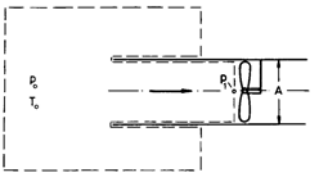


$$\begin{aligned}
\rho_1 v_1^2 A_1 &= (p_0 - p_1) A \\
Ma_1 &= \sqrt{\frac{1}{\gamma}\left(\frac{p_0}{p_1} - 1\right)} \\
c_p T_0 &= c_p T_1 + \frac{v_1^2}{2} \\
T_1 &= \frac{T_0}{1 + \frac{\gamma-1}{2} Ma_1^2} \\
\dot{m} &= 1.41 \frac{\text{kg}}{\text{s}}
\end{aligned}$$

2.8 (a)

$$\begin{aligned}
Ma_{Edesign} &= 2.3 \\
\Rightarrow p_{Edesign} &= \frac{p_E}{p_0} p_0 = 0.08 \cdot 10^5 \text{ Pa} \\
\frac{A_H}{A_E} &= \frac{A^*}{A_E} = 0.456
\end{aligned}$$

(b) Subsonic flow in the nozzle

$$\begin{aligned}
\frac{A^*}{A_E} &= 0.456 \\
\Rightarrow p_{v1} &= \frac{p_E}{p_0} p_0 = 0.95 \cdot 10^5 \text{ Pa} \\
Ma_{E1} &= 0.28
\end{aligned}$$

(c)

$$p_{v2} = \frac{p_{v2}}{p_{Edesignl}} p_{Edesignl} = 0.48 \cdot 10^5 \text{ Pa}$$

/d)

$$\begin{aligned}
A_E \rho_E u_E^2 &= (p_v - p_E) A_E + F_s \\
A_E \rho_E u_E^2 &= A_E \rho_E \gamma Ma_E^2 \\
p_v &= p_E
\end{aligned}$$

1.

$$\begin{aligned}
F_{Sdesign} &= A_E \rho_{E\ design} \times \\
&\quad \times \gamma Ma_{E\ design}^2 \\
&= 13 \text{ N}
\end{aligned}$$

2.

$$\begin{aligned}
F_{spv2} &= A_E \rho_{E2} u_{E2} \\
&= A_E \frac{u_{E2}^2}{u_{E1}^2} u_{E1}^2 \frac{\rho_{E2}}{\rho_{E1}} \rho_{E2} \\
F_{spv2} &= F_{s1} \frac{1}{Ma_1^{*2}} = 4.2 \text{ N}
\end{aligned}$$

(e) for isentropic flow $p_E = p_K$

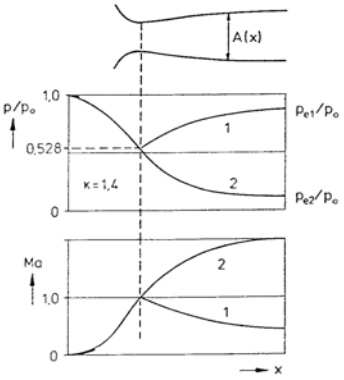


2.9 (a)

$$\begin{aligned}
\frac{p_0}{p_{0Ea}} &= 1.387 \\
\Rightarrow Ma_{Ea} &= 2 \Rightarrow \frac{A^*}{A_{sa}} = 0.593 \\
\dot{m} = \rho^* A^* u^* &= p^* \gamma A^* Ma^* \frac{1}{a^*} \\
&= \frac{p^*}{p_0} p_0 \gamma A^* \times \\
&\quad \times \frac{1}{\sqrt{\gamma R \frac{T^*}{T_0} T_o}} \\
&= 0.0242 \frac{\text{kg}}{\text{s}} \\
\frac{p_{ka}}{p_{0Ea}} &= 0.895 \\
&\Rightarrow Ma_{Ea} = 0.4
\end{aligned}$$

(b) see (a)

$$\begin{aligned}
\dot{m} &= 0.0242 \frac{\text{kg}}{\text{s}};\ Ma_{Eb} = 0.32; \\
\frac{A^*}{A_{sb}} &= 0.77
\end{aligned}$$

(c)

$$\frac{\Delta s}{R} = ln\frac{p_{01}}{p_{02}} \Rightarrow \frac{\Delta s_a}{\Delta s_b} = 2.5$$

(d)

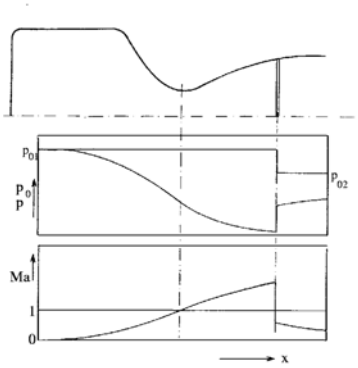


(e)

$$\begin{aligned}
\frac{A_H}{A_s} &= \frac{A_E}{A_s}\frac{A_H}{A_E} = 0.507 \\
\Rightarrow Ma_{a1}^{*\,2} &= 1.71 \Rightarrow Ma_{a2}^{*\,2} = 0.585 \\
\frac{A_2^*}{A_H} &= \frac{p_{01}}{p_{02}} = 1.58 \\
\frac{A_2^2}{A_E} &= \frac{A_2^*}{A_H}\frac{A_H}{A_E} = 0.72 \\
\Rightarrow Ma_E &= 0.47 \\
p_E &= \frac{p_E}{p_{02}} p_{02} = 0.538 \cdot 10^5\ Pa
\end{aligned}$$

2.10 (a) 1.

$$\begin{aligned}
Ma_E &= Ma_M = 2.3 \\
\Rightarrow p_{v1} &= \frac{p_{v1}}{p_E}\frac{p_E}{p_0} p_0 = 0.48 \cdot 10^5\ \text{Pa}
\end{aligned}$$

(b)

$$\begin{aligned}
\frac{A_H}{A_S} &= \frac{A_E}{A_S}\frac{A^*}{A_E} = 0.8 \\
\Rightarrow Ma_1^* &= 1.425 \Rightarrow Ma_s^* = 0.7 \\
p_s &= \frac{p_s}{p_1}\frac{p_1}{p_0} p_0 = 0.66 \cdot 10^5\ \text{Pa}
\end{aligned}$$

2.

$$\begin{aligned}
\frac{A_2^*}{A_E} &= \frac{A_2^*}{A_H}\frac{A_H}{A_E} = \frac{p_{01}}{p_{02}}\frac{A_H}{A_E} \\
&= 0.511 \\
\Rightarrow Ma_{2E} &= 0.311 \\
p_{v2} &= \frac{p_{k2}}{p_{02}}\frac{p_{02}}{p_{01}} p_{01} \\
&= 0.82 \cdot 10^5\ \text{Pa}
\end{aligned}$$

(c)

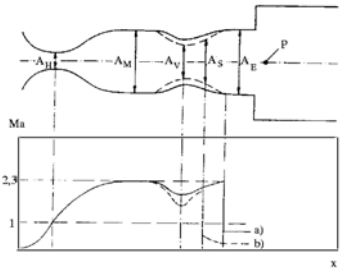


(d) 1.

$$A_v = A^* = A_H$$

2.

$$\begin{aligned}
\Delta t &= \frac{\Delta m}{\dot m} \\
\Delta m &= (p_{vmax} - p_{v1})\frac{V_v}{T_v R} \\
\frac{p_{kmax}}{p_0} &= 0.95 \\
\Rightarrow \Delta m &= 585\ \text{kg} \\
\dot m &= \rho^* A^* u^* = \frac{A_H \gamma \frac{p^*}{p_0} p_0}{\sqrt{\gamma R \frac{T^*}{T_0} T_o}} \\
&= 24.15\ \frac{\text{kg}}{\text{s}} \\
\Rightarrow \Delta t &= 24.22\ \text{s}
\end{aligned}$$

2.11

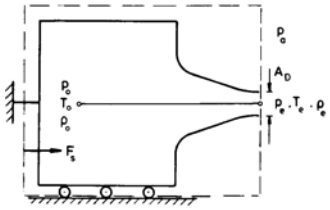


(a)

$$\begin{aligned}
\rho_e\, v_e^2\, A_D &= (p_a - p_e)\, A_D + F_s \\
v_e^2 &= 2\, c_p\, (T_0 - T_e) \\
c_p &= \frac{\gamma\, R}{\gamma - 1}
\end{aligned}$$

$$\begin{aligned}
\frac{F_s}{p_0\, A_D} &= \frac{2\,\gamma}{\gamma - 1}\frac{\rho_e}{\rho_0}\left(1 - \frac{T_e}{T_0}\right) \\
&\quad - \frac{p_a}{p_0} + \frac{p_e}{p_0} \\
\frac{T}{T_0} &= \left(\frac{\rho}{\rho_0}\right)^{\gamma-1} = \left(\frac{p}{p_0}\right)^{\frac{\gamma}{1-\gamma}}
\end{aligned}$$

$$\begin{aligned}\frac{F_s}{p_0\,A_D} &= \frac{2\,\gamma}{\gamma-1}\left(\frac{p_e}{p_0}\right)^{\frac{1}{\gamma}} \\ &- \frac{\gamma+1}{\gamma-1}\frac{p_e}{p_0} - \frac{p_a}{p_0}\end{aligned}$$

$$\begin{aligned}\text{subcritical}: \; p_e &= p_a \\ \text{supercritical}: \; p_e &= p^* \\ &= 0.528\,p_0\end{aligned}$$

(see problem 1.3)

(b)

$$\begin{aligned}F_s &= \rho_e\,v_e^2\,A_D \\ v_e^2 &= \frac{2\,(p_0-p_a)}{\rho} \\ \frac{F_s}{p_0\,A_D} &= 2\left(1-\frac{p_a}{p_0}\right)\end{aligned}$$

| $\frac{p_a}{p_0}$ | $\frac{F_s}{p_0\,A_D}$ a) compr. | b) incompr. |
|---|---|---|
| 1 | 0 | 0 |
| 0.6 | 0.66 | 0.8 |
| 0.2 | 1.07 | 1.6 |
| 0 | 1.27 | 2 |

2.12 (a)

$$\begin{aligned}\frac{A^*}{A_H} &= 0.963 \\ A^* = A_L &= 0.193\ \text{m}^2 \\ \frac{A^*}{A_E} &= 0.38 \Rightarrow Ma_E = 2.5 \\ \frac{p_E}{p_a} &= \frac{p_E}{p_0} = 0.0585 \\ \Rightarrow p_E &= 0.0585 \cdot 10^5\ \text{Pa}\end{aligned}$$

(b)

$$t_{max} = \frac{\Delta m}{\dot m};\quad T_c = T_0 = T_a$$

$$= (p_{Emax} - p_E(t=t_0))\frac{V_c}{\dot m R T_K}$$

$$\begin{aligned}\dot m = A_L\rho^* u^* &= 45\ \frac{\text{kg}}{\text{s}} \\ \frac{A_L}{A_E} &= 0.3793 \\ \Rightarrow Ma_E(t=t_{max}) &= 0.23 \\ \Rightarrow p_E(t=t_{max}) &= 0.96\cdot 10^5\ \text{Pa} \\ \Rightarrow t_{max} &= 9.3\ \text{s}\end{aligned}$$

(c)

$$\begin{aligned}\frac{A'_L}{A_L} &= \frac{p_a - 0.02p_a}{p_a} = 0.98 \\ \frac{A'_L}{A_M} &= \frac{A'_L}{A_L}\frac{A_L}{A_M} = 0.944 \\ \Rightarrow Ma'_M &= 0.76 \\ \frac{A'_L}{A_M} &= 0.963 \\ A'_L &= \frac{A_L}{A'_L}\frac{A'_L}{A_M}A_M \\ &= 0.197\ \text{m}^2\end{aligned}$$

### 5.2.3 Oblique Compression Shock

3.1

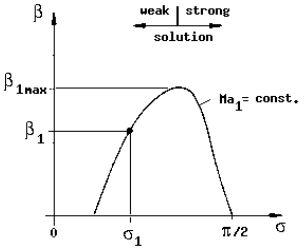


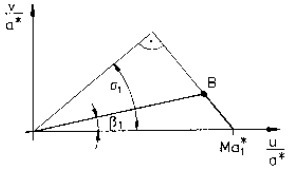


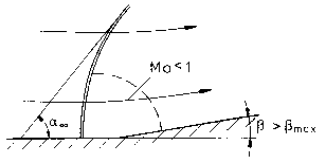


3.2 (a)

$$\begin{aligned}Ma_1\,\sin\sigma &= 1.32 \\ \sigma = \arctan\frac{u_{n1}}{u_{t1}} &= 53.1^\circ \\ Ma_1 = \frac{V_1}{a_1} &= 1.65 \\ \Rightarrow T_1 &= 228.5\ \text{K}\end{aligned}$$

(b)

$$\begin{aligned} u_{t2} &= u_{n1} \\ Ma_1 \sin\sigma &= 1.32 \Rightarrow u_{n2} = 259\ \frac{\mathrm{m}}{\mathrm{s}} \\ Ma_1^* &= 1.45 \Rightarrow Ma_2^* = 1.16 \\ Ma_2 &= 1.2; \quad \beta = 12^\circ \end{aligned}$$

(c) Shock polar

$$\begin{aligned} \frac{u_{n1}}{a^*} &= 1.28; \quad \frac{u_{t1}}{a^*} = 0.69; \\ \beta &= 15^\circ \\ a^* &= \sqrt{\gamma R \frac{T^*}{T_0}\frac{T_0}{T_1}\,T_1} = 344\ \frac{\mathrm{m}}{\mathrm{s}} \\ \Rightarrow u_{n1} &= 440\ \frac{\mathrm{m}}{\mathrm{s}}; \quad u_{t1} = 237.4\ \frac{\mathrm{m}}{\mathrm{s}} \end{aligned}$$

3.3 (a)

$$\begin{aligned} \Delta t &= \frac{\Delta m}{\dot m} \\ \dot m &= \rho^* A_H u^* = 24.15\ \frac{\mathrm{kg}}{\mathrm{s}} \\ \Delta m &= \frac{V_v}{RT_v}(p_{kmax} - p_v(t=0)) \\ p_{vmax} &= 0.48 \cdot 10^5\ \mathrm{Pa} \end{aligned}$$

(normal shock in exit cross section)

$$\Rightarrow \Delta m = 497.6\,\mathrm{kg} \Rightarrow \Delta t = 20.6\ \mathrm{s}$$

(b)

$$\begin{aligned} p_E &= \frac{p_E}{p_0}\,p_0 = 0.08 \cdot 10^5\ \mathrm{Pa} \\ \Rightarrow \frac{p_v}{p_E} &= 2 \Rightarrow Ma_E \sin\sigma = 1.36 \\ \Rightarrow \sigma &= 36.25^\circ; \quad \beta = 11.5^\circ \\ \frac{p_v}{p_{02}} &= 0.165 \Rightarrow Ma_2 = 1.83 \\ T_2 &= \frac{T_2}{T_1}\frac{T_1}{T_0}T_0 = 167\ \mathrm{K} \\ V_2 &= Ma_2\, a_2 = 474\ \frac{\mathrm{m}}{\mathrm{s}} \end{aligned}$$

(c)

$$\begin{aligned} \beta_{max}(Ma = 2.3) &= 27.5^\circ \\ \Rightarrow \epsilon_{max} &= 7.5^\circ \\ \beta_{0b} &= 12.5^\circ \Rightarrow \sigma_{0b} = 37^\circ \\ \Rightarrow Ma_E \sin\sigma_{0b} &= 1.384 \\ \beta_u &= 27.5^\circ \Rightarrow \sigma_u = 62^\circ \\ \Rightarrow Ma_E \sin\sigma_u &= 2.03 \end{aligned}$$

$$\begin{aligned} p_u - p_{0b} &= \left(\frac{p_u}{p_E} - \frac{p_{0b}}{p_E}\right)p_E \\ &= 0.22 \cdot 10^5\ \mathrm{Pa} \\ Ma_{0b}^* = 1.55 &\Rightarrow Ma_{0b} = 1.85 \\ Ma_u^* = 0.92 &\Rightarrow Ma_{0b} = 0.94 \end{aligned}$$

3.4 (a)

$$\begin{aligned} \Delta s &= R \ln\left(\frac{p_{0a}}{p_{0b}}\right) \\ &= R\, ln\left(\frac{p_{0a}}{p_a}\frac{p_b}{p_{0b}}\right) \end{aligned}$$

$$p_a = p_b; \quad \Delta s = 88.62\ \frac{\mathrm{J}}{\mathrm{kg\,K}}$$

(b)

$$\begin{aligned} |\,\boldsymbol{V_a}\,| / |\,\boldsymbol{V_b}\,| &= \frac{Ma_a}{Ma_b}\sqrt{\frac{T_a}{T_b}} \\ &= \frac{Ma_a}{Ma_b}\sqrt{\frac{T_a}{T_{0a}}\frac{T_{0b}}{T_b}} \\ &= 1.063 \\ (T_{0a} &= T_{0b}) \end{aligned}$$

(c)

$$\frac{\rho_a}{\rho_b} = \frac{T_b}{T_a} = 1.092$$

3.5 1) (a)

$$\frac{A_H}{A_E} = 0.15 \Rightarrow Ma_{EAusl.} = 3.5$$

(b)

$$\begin{aligned} \frac{p_{a(0)}}{p_E} &= 5.13 \\ \Rightarrow Ma_E \sin\sigma_1 &= 2.12 \\ \Rightarrow \sigma &= 37.3^\circ \\ Ma_E^* &= 2.06 \\ \Rightarrow Ma_1^* &= 1.71 \\ & (\beta_1 = 22^\circ) \\ \Rightarrow Ma_1 &= 2.2 \\ \beta_2 = \beta_1 &\Rightarrow \sigma_2 = 53^\circ \\ Ma_2^* = 1.2 &\Rightarrow Ma_2 = 1.25 \end{aligned}$$

(c)

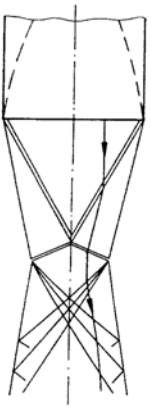

2) (a)

$$\begin{aligned} p_a(z) &= p_{Edesignl} \\ &= 0.195 \cdot 10^5 \text{ Pa} \\ z &= \left[1 - \left(\frac{p_{Edesignl}}{p_a(0)}\right)^{\frac{\gamma-1}{\gamma}}\right] \times \\ &\times \frac{\gamma}{(\gamma-1)a} \\ &= 11.9 \text{ km} \end{aligned}$$

3.6

$$\begin{aligned} v_1\,\rho_1\,h_1 &= v_3\,\rho_3\,h_3 \\ \Rightarrow \frac{h_3}{h_1} &= \frac{Ma_1^*}{Ma_3^*}\frac{\rho_1}{\rho_3} \\ \frac{\rho_2}{\rho_1} &= 1.85 \\ \Rightarrow Ma_1 \sin\sigma_1 &= 1.5 \\ \Rightarrow \sigma_1 = 30°; \quad Ma_1^* &= 1.964 \\ \Rightarrow \beta = 13°; \quad Ma_2^* &= 1.78; \\ Ma_2 &= 2.4 \\ Ma_3^* = 1.56; \quad \sigma &= 37° \\ \Rightarrow Ma_2 \sin\sigma_2 &= 1.44 \\ \frac{\rho_3}{\rho_2} &= 1.75 \\ \frac{\rho_1}{\rho_3} &= \frac{\rho_1}{\rho_2}\frac{\rho_2}{\rho_3} = 0.309 \\ \Rightarrow \frac{h_3}{h_1} &= 0.389 \end{aligned}$$

$$\begin{aligned} \tan\beta &= \frac{h_1 - h_3}{2l} = \frac{h_1}{l}\,\frac{1 - \frac{h_3}{h_1}}{2} \\ \Rightarrow \frac{h_1}{l} &= \frac{2\tan\beta}{1 - \frac{h_3}{h_1}} = 0.756 \end{aligned}$$

3.7

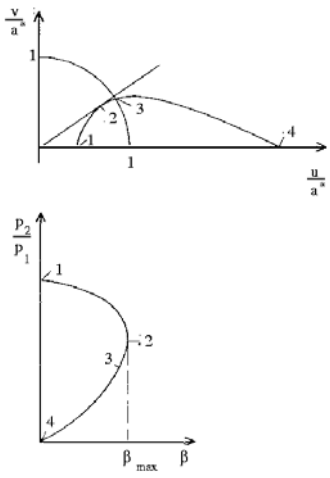


3.8

$$\begin{aligned} \Delta x &= \frac{2\Delta y}{\tan\sigma_A + \tan\sigma_B} \\ &= 2.8 \text{ cm} \\ Ma_1^* &= 1.63 \Rightarrow \beta_A = 5.5°; \\ \beta_B &= 21° \\ \Rightarrow Ma_{A2}^* &= 1.54; \quad Ma_{B2}^* = 1.13 \\ a^* &= \sqrt{\gamma R \frac{T^*}{T_0} T_0} = 316.94 \ \frac{\text{m}}{\text{s}} \\ v_{A2} &= Ma_{A2}^*\, a^* \sin\beta_A \\ &= 46.78 \ \frac{\text{m}}{\text{s}} \\ u_{A2} &= Ma_{A2}^*\, a^* \cos\beta_A \\ &= 485.84 \ \frac{\text{m}}{\text{s}} \\ v_{B2} &= Ma_{B2}^*\, a^* \sin\beta_B \\ &= 128.35 \ \frac{\text{m}}{\text{s}} \\ u_{B2} &= Ma_{B2}^*\, a^* \cos\beta_B \\ &= 334.35 \ \frac{\text{m}}{\text{s}} \\ \Rightarrow \nabla \text{ x } \boldsymbol{v} &= -7960 \ \frac{1}{\text{s}} \end{aligned}$$

### 5.2.4 Expansions and Compression Shocks

4.1 (a) $\boldsymbol{r}$ is a Mach line

$$\begin{aligned} \tan\alpha &= \frac{u_t}{u_r} \Rightarrow \alpha = 26.57^\circ \\ Ma_p &= \frac{1}{\sin\alpha} = 2.24 \end{aligned}$$

(b)

$$\begin{aligned} u_t &= a_p \\ \Rightarrow T_p &= \frac{u_t^2}{\gamma R} = 155 \text{ K} \end{aligned}$$

4.2 P.-M. flow = plane, isentropic flow

$$\begin{aligned} \Rightarrow rot\, \boldsymbol{V} &= 0 \\ \frac{\partial v_r}{\partial \Phi} &= \frac{\partial}{\partial r}(r v_\Phi) \\ \Rightarrow v_\Phi + r\frac{\partial v_\Phi}{\partial r} - \frac{\partial v_r}{\partial \Phi} &= 0 \\ \frac{\partial v_\Phi}{\partial r} = 0 \text{ and } v_\Phi &= a \Rightarrow \frac{\partial v_r}{\partial \Phi} = a \end{aligned}$$

4.3

$$\begin{aligned} \nu_3 = \nu_1 + 2 \mid \beta \mid; \quad \nu_3 = 28^\circ; \quad \nu_1 = 0^\circ \\ \Rightarrow \beta = 14^\circ \\ \nu_2 = \nu_1 + \mid \beta \mid = 14^\circ \\ \Rightarrow Ma_2 = 1.57; \quad \alpha_2 = 39.5^\circ \\ \text{Conti: } a^*\, h\, \rho^* = \overline{AB}\, u_2\, \rho_2\, \sin\alpha_2 \\ \frac{A^*}{A} = \frac{h}{\overline{AB}\sin\alpha_2} = 0.82 \\ \Rightarrow \overline{AB} = 0.192 \text{ m} \\ \overline{AC} = 2\,\overline{AB}\cos\alpha_2 = 0.296 \text{ m} \\ \delta_{AB} = \alpha_2 - \beta = 25.5^\circ \\ \delta_{AC} = \beta = 14^\circ \end{aligned}$$

4.4 (a)

$$\begin{aligned} Ma_1 = 2.5; \quad \beta_1 = 12^\circ \\ \Rightarrow \sigma = 34^\circ; \quad Ma_2 = 2; \quad \frac{p_{02}}{p_{01}} = 0.96 \\ p_{02} = \frac{p_{02}}{p_{01}}\frac{p_{01}}{p_1} p_1 = 8.87 \cdot 10^5 \text{ Pa} \\ p_2 = \frac{p_2}{p_{02}} p_{02} = 1.13 \cdot 10^5 \text{ Pa} \end{aligned}$$

(b) P.-M. flow = isentropic flow

$$\begin{aligned} \Rightarrow p_{02} = p_{03} = p_{04} \\ \nu_3 = \nu_2 + \mid \beta_2 \mid \\ \nu_2 = 26.4^\circ \Rightarrow \nu_3 = 38.4^\circ \\ \Rightarrow Ma_3 = 2.47 \\ p_3 = \frac{p_3}{p_{03}} p_{03} = 0.546 \cdot 10^5 \text{ Pa} \end{aligned}$$

(c)

$$\begin{aligned} \frac{p_4}{p_{03}} = \frac{p_3 - \Delta p}{p_{04}} = 0.0273 \\ \Rightarrow Ma_4 = 3; \quad \nu_4 = 49.8^\circ \\ \Rightarrow \mid \beta \mid = \nu_4 - \nu_3 = 11.4^\circ \end{aligned}$$

(d)

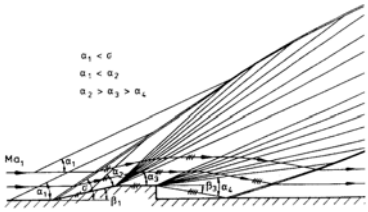


4.5 (a)

$$\begin{aligned} \beta_1 = 10^\circ; \quad \sigma_1 = 40^\circ \Rightarrow Ma_1 = 2 \\ Ma^{*2} = 1.44; \quad \beta_2 = \beta_1 \\ \Rightarrow Ma_3^* = 1.2; \quad Ma_3 = 1.26 \\ p_1 = \frac{p_1}{p_a} p_a = 0.11 \cdot 10^6 \text{ Pa} \end{aligned}$$

(b)

$$\begin{aligned} \beta_3 &= \nu_4 - \nu_3 \\ \frac{p_4}{p_{04}} &= \frac{p_4}{p_3}\frac{p_3}{p_{03}}; \\ p_{03} &= p_{04}; \quad p_4 = p_2 = p_u \\ Ma_2 &= 1.62; \quad \sigma_2 = 51^\circ \\ \Rightarrow \frac{p_3}{p_2} &= 1.69 \\ \Rightarrow p_3 &= 0.388 \cdot 10^5 \text{ Pa} \\ Ma_3 &= 1.26 \\ \Rightarrow \frac{p_3}{p_{03}} &= 0.38; \quad \nu_3 = 5.1^\circ \\ \Rightarrow \frac{p_4}{p_{04}} &= 0.225 \\ \Rightarrow Ma_4 &= 1.63; \quad \nu_4 = 15.7^\circ \\ \Rightarrow \beta_3 &= 10.6^\circ \end{aligned}$$

(c)

$$\begin{aligned} \frac{p_{ac}}{p_1} &= 2.5 \\ \Rightarrow Ma_1 \sin\sigma_1 &= 1.51 \\ \Rightarrow \sigma = 49°; \quad \beta_1 &= 17.5°; \\ Ma_2 &= 1.32 \\ \Rightarrow \beta_1 > \beta_{max}(Ma_2) &= 7° \end{aligned}$$

$\Rightarrow$ Mach reflexion

(d)

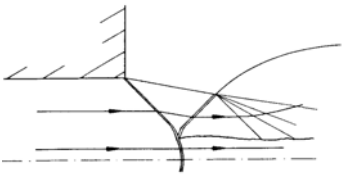

(e)

$$Ma_1 \sin\sigma = 2$$
$$p_{ad} = \frac{p_{ad}}{p_1} p_1 = 0.5 \cdot 10^5 \text{ Pa}$$

4.6 (a) 1.

$$\begin{aligned} Ma_1^* &= 1.96; \quad \beta_1 = 15° \\ \Rightarrow Ma_2^* &= 1.73; \quad \sigma = 33° \\ \Rightarrow Ma_2 &= 2.25; \\ Ma_1 \sin\sigma &= 1.634 \\ p_2 &= \frac{p_2}{p_1} p_1 \\ &= 1.57 \cdot 10^5 \text{ Pa} \\ T_2 &= \frac{T_2}{T_1} T_1 \\ &= 350 \text{ K} \end{aligned}$$

$$\begin{aligned} T_{02} &= T_{01} = \frac{T_{01}}{T_1} T_1 = 700 \text{ K} \\ p_{02} &= \frac{p_{02}}{p_{01}} \frac{p_{01}}{p_1} p_1 \\ &= 17.71 \cdot 10^5 \text{ Pa} \\ p_{01} &= \frac{p_{01}}{p_1} p_1 = 19.84 \cdot 10^5 \text{ Pa} \\ \frac{\Delta s}{R} &= ln\left(\frac{p_{01}}{p_{02}}\right) = 0.1134 \end{aligned}$$

2.

$$\begin{aligned} \nu_3 = 0 &= \nu_2 - |\beta_2| \\ \Rightarrow \beta_2 &= 33.02° \\ \beta_3 = \beta_2 - \beta_1 &= 18.02° \\ p_3 = \frac{p_3}{p_{03}} p_{02} &= 9.36 \cdot 10^5 \text{ Pa} \\ \dot{m} &= u_1 \rho_1 b l \tan\sigma_1 \\ &= 232.4 \frac{\text{kg}}{\text{s}} \end{aligned}$$

(b)

$$p_{3is} = \frac{p_{3is}}{p_{01}} p_{01} = 10.48 \cdot 10^5 \text{ Pa}$$

(c)

$$Ma_{1min}(\beta_1 = 15°) = 1.62$$

4.7 (a) from shock polar

| | $Ma$ | $Ma^*$ | $\beta$ | $\sigma$ | $Ma \sin\sigma$ | $\frac{\hat{p}}{p}$ |
|---|---|---|---|---|---|---|
| 1 | 3 | 1.96 | 16° | 33.3° | 1.65 | 3 |
| 2 | 2.21 | 1.72 | 16° | 42.4° | 1.49 | 2.41 |
| 3 | 1.59 | 1.42 | 0° | 90° | 1.59 | 2.77 |
| 4 | 0.67 | 0.71 | | | | |

$$p_4 = \frac{p_4}{p_3} \frac{p_3}{p_2} \frac{p_2}{p_1} p_1 = 10.03 \cdot 10^5 \text{ Pa}$$

(b)

$$\begin{aligned} \dot{m} &= \rho_4 u_4 A \\ &= \frac{p_4}{RT_4} Ma_4 \sqrt{\gamma RT_4}\, A \\ &= p_4 Ma_4 \sqrt{\frac{\gamma}{RT_1} \frac{T_1}{T_0} \frac{T_0}{T_4}} A \\ &= 169.9 \frac{\text{kg}}{\text{s}} \end{aligned}$$

1.

$$\begin{aligned} p_{4is} &= \frac{p_4}{p_0} \frac{p_0}{p_1} p_1 = 13.56 \cdot 10^5 \text{ Pa} \\ \dot{m}_{is} &= \dot{m} \frac{p_{4is}}{p_4} = 229.7 \frac{\text{kg}}{\text{s}} \end{aligned}$$

4.8 (a)

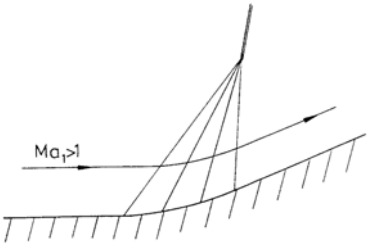


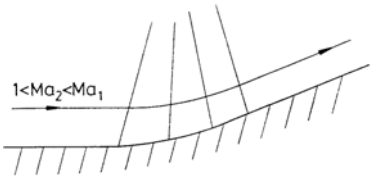


(b)

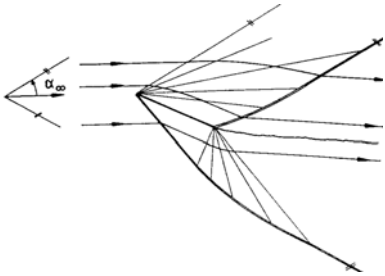


(c)

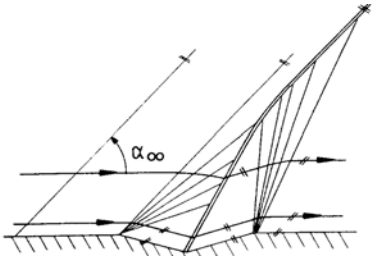


4.9

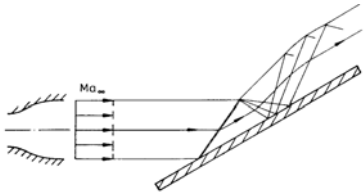


4.10 (a)

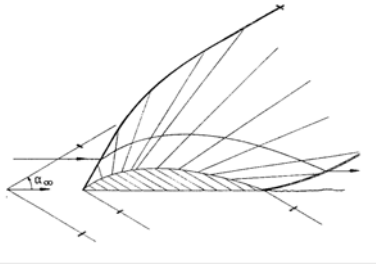


(b)

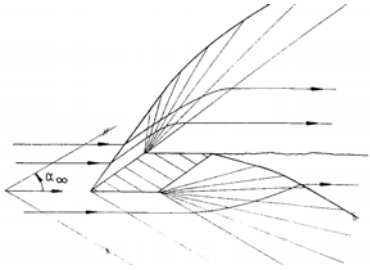


4.11 (a)

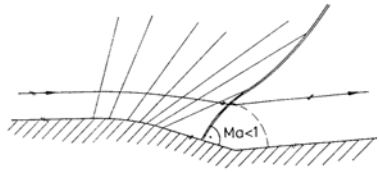


(b)

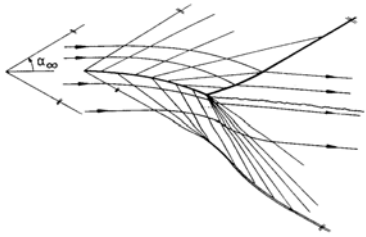

### 5.2.5 Lift and Wave Drag – Small-Perturbation Theory

5.1 (a)

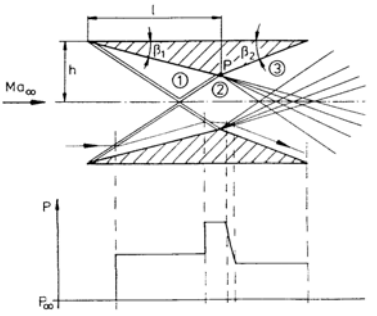


(b)(c)

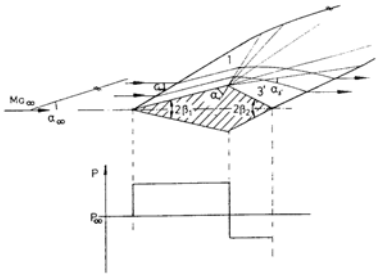


(d) Table of solution in the Appendix

*Pair of profiles*

$$
\begin{aligned}
c_D &= \frac{2F_D}{\gamma p_\infty Ma_\infty^2 lb} \\
F_D &= (p_1 - p_3)db \\
\Rightarrow c_D &= \frac{2}{\gamma Ma_{infty}^2}\left(\frac{p_1}{p_\infty} - \frac{p_3}{p_\infty}\right)\frac{d}{l} \\
&= 0.016 \\
\frac{p_1}{p_\infty} &= 2.1 \\
p_{03} &= p_{02}; \\
\frac{p_3}{p_\infty} &= \frac{p_3}{p_{03}}\frac{p_{02}}{p_2}\frac{p_2}{p_1}\frac{p_1}{p_\infty} \\
&= 1.8
\end{aligned}
$$

*Double wedge*

$$
\begin{aligned}
F_D &= (p_1 - p_{3'})db \\
\Rightarrow c_D &= \frac{2}{\gamma Ma_\infty^2}\left(\frac{p_1}{p_\infty} - \frac{p_{3'}}{p_\infty}\right)\frac{d}{l} \\
&= 0.096 \\
\frac{p_1}{p_\infty} &= 2.1 \\
p_{03'} &= p_{02}; \\
\frac{p_{3'}}{p_\infty} &= \frac{p_{3'}}{p_{03'}}\frac{p_{01}}{p_1}\frac{p_1}{p_\infty} \\
&= 0.345
\end{aligned}
$$

5.2

$$
\begin{aligned}
\frac{p_3 - p_1}{p_1} &= K(-\delta_o); \\
K &= \frac{\gamma Ma_1^2}{\sqrt{Ma_1^2 - 1}} \\
\frac{p_2 - p_3}{p_1} &= K(-(\delta_o - \beta)) \\
\Rightarrow \frac{p_2 - p_1}{p_1} &= K(\beta - 2\delta_o) \\
\frac{p_4 - p_1}{p_1} &= K\delta_u \\
\frac{p_2 - p_4}{p_1} &= K(-(\beta - \delta_u)) \\
\Rightarrow \frac{p_2 - p_1}{p_1} &= K(2\delta_u - \beta) \\
\Rightarrow 2\delta_u - \beta &= \beta - 2\delta_o \\
\Rightarrow \beta &= \delta_o + \delta_u = 15^\circ
\end{aligned}
$$

$$
\frac{p_2}{p_0} = \frac{p_1}{p_0}\left[1 + \frac{\gamma Ma_1^2}{\sqrt{Ma_1^2 - 1}}(\delta_u - \delta_o)\right]
$$

$$
\begin{aligned}
&= 0.0918 \\
\Rightarrow Ma_2 &= 2.22
\end{aligned}
$$

5.3

$$
\begin{aligned}
c_{pu} &= \frac{2}{\sqrt{Ma_\infty^2 - 1}}\left(\frac{dy}{dx}\right)_u \\
c_{pl} &= -\frac{2}{\sqrt{Ma_\infty^2 - 1}}\left(\frac{dy}{dx}\right)_l \\
c_L &= \frac{1}{t}\int_0^t (c_{pl} - c_{pu})dx \\
&= \frac{4\epsilon}{\sqrt{Ma_\infty^2 - 1}}
\end{aligned}
$$

$$
c_D = \frac{1}{t}\int_0^t \left[c_{pu}\left(\frac{dy}{dx}\right)_u + c_{pl}\left(-\frac{dy}{dx}\right)_l\right]dx
$$

$$
= \frac{2}{\sqrt{Ma_\infty^2 - 1}}\frac{1}{t}\int_0^t \left[\left(\frac{dy}{dx}\right)_u^2 + \left(\frac{dy}{dx}\right)_l^2\right]dx
$$

5.4 (a)

$$\frac{s}{t} = \frac{h}{t} + \tan\left(\arcsin\frac{1}{Ma_1}\right) = 0.4$$

(b)

$$\begin{aligned} c_{pu}\left(\frac{x}{t}\right) &= \frac{2}{\sqrt{Ma_1^2-1}}\left(\frac{dy}{dx}\right)_u \\ &= \frac{\pi}{\sqrt{Ma_1^2-1}}\frac{h}{t}\sin\left(\frac{\pi}{2}\frac{x}{t}\right) \\ c_{pl}\left(\frac{x}{t}\right) &= \frac{2}{\sqrt{Ma_1^2-1}}\left(\frac{h}{t}\right) \end{aligned}$$

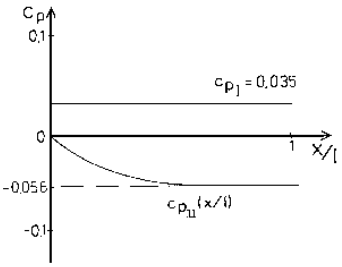


(c)

$$\begin{aligned} F_y &= c_L\, b\, t\, \frac{\rho_\infty}{2}\, u_\infty^2 \\ &= \frac{1}{2}\, c_L\, b\, t\, \gamma\, Ma_1^2\, p_\infty \\ c_L &= \frac{4\frac{h}{t}}{\sqrt{Ma_1^2-1}} = 0.0707 \\ \Rightarrow F_y &= 44.55 \text{ kN} \\ F_x &= \frac{1}{2}\, c_D\, b\, t\, \gamma\, Ma_1^2\, p_\infty \end{aligned}$$

$$\begin{aligned} c_D &= \frac{2}{\sqrt{Ma_\infty^2-1}} \times \\ &\times \int_0^t \left[\left(\frac{dy}{dx}\right)_u^2 + \left(\frac{dy}{dx}\right)_l^2\right] d\left(\frac{x}{t}\right) \\ &= 0.004 \Rightarrow F_x = 2.52 \text{ kN} \end{aligned}$$

5.5

$$\begin{aligned} c_L &= \frac{4\,\epsilon_0}{\sqrt{Ma_\infty^2-1}} \\ c_D &= \frac{2}{\sqrt{Ma_\infty^2-1}} \times \\ &\times \left[2\epsilon^2 + \frac{1}{t}\int_0^t \left[\left(\frac{dy}{dx}\right)_u^2 + \left(\frac{dy}{dx}\right)_l^2\right] dx\right] \\ &= \frac{4\,\epsilon_0^2}{\sqrt{Ma_\infty^2-1}} + \frac{a^2+b^2}{\sqrt{Ma_\infty^2-1}}\left(\frac{\pi}{t}\right)^2 \\ &\Rightarrow \frac{c_L}{c_D} = \frac{4\epsilon_o}{4\epsilon_0^2 + (a^2+b^2)\left(\frac{\pi}{t}\right)^2} \end{aligned}$$

5.6

$$\begin{aligned} c_L &= \frac{4\,\epsilon_0}{\sqrt{Ma_\infty^2-1}} \\ c_D &= \frac{4}{\sqrt{Ma_\infty^2-1}} \times \\ &\times \left[\epsilon_0^2 + \overline{\epsilon_s^2(x)} + \overline{\left(\frac{d\,d(x)}{dx}\right)^2}\right] \end{aligned}$$

$$\begin{aligned} c_{L1} &= 0; \\ c_{D1} &= \frac{16}{3}\,\delta^2\,\frac{1}{\sqrt{Ma_\infty^2-1}} = 0.05 \\ c_{L2} &= 0; \\ c_{D2} &= 0.11 = 2c_{D1} \\ c_{L3} &= 0.21; \\ c_{D3} &= \frac{4}{\sqrt{Ma_\infty^2-1}}\left(\frac{8}{3}\delta^2 + \epsilon_0^2\right) \\ &= 0.12 \end{aligned}$$

5.7 (a) 1.

$$\begin{aligned} c_D &= \left(1-\frac{p_2}{p_1}\right) \times \\ &\times \frac{p_1}{p_\infty}\frac{2}{\gamma\, Ma_\infty^2}\frac{d}{t} \\ \frac{p_1}{p_\infty} &= 2.08; \\ \frac{p_2}{p_1} &= \frac{p_2}{p_{02}}\frac{p_{01}}{p_1} \\ Ma_1 &= 2.45 \\ \nu_2 &= \nu_1 + |\,\beta_1 + \beta_2\,| \\ &= 52.9^\circ \\ \Rightarrow Ma_2 &= 3.18 \\ \frac{p_2}{p_{02}} &= 0.024; \\ \frac{p_1}{p_{01}} &= 0.0603 \\ \Rightarrow \frac{p_2}{p_1} &= 0.38 \Rightarrow c_D = 0.0204 \end{aligned}$$

2.

$$
\begin{aligned}
c_{p1} &= \frac{2\tan\beta_1}{\sqrt{Ma_\infty^2-1}} = 0.125\\
c_{p2} &= \frac{2\tan\beta_2}{\sqrt{Ma_\infty^2-1}} = -0.0494\\
c_D &= (c_{p1}-c_{p2})\frac{d}{t} = 0.0174
\end{aligned}
$$

(b)

$$
\begin{aligned}
c_L &= \frac{4\,\epsilon}{\sqrt{Ma_\infty^2-1}} = 0.1237\\
c_D &= c_{D\,a)} + \frac{4\,\epsilon^2}{\sqrt{Ma_\infty^2-1}}\\
&= 0.0282
\end{aligned}
$$

5.8 (a)

$$
\begin{aligned}
F_L &= \rho_\infty\,\gamma\,Ma_\infty^2\,A_w\,\frac{4\,\epsilon}{\sqrt{Ma_\infty^2-1}}\\
&= \text{ const.}\\
&\Rightarrow\ p_\infty\,\epsilon\,\frac{Ma_\infty^2}{\sqrt{Ma_\infty^2-1}} = \text{const.}\\
&\Rightarrow\ p_1\,\epsilon_1 = p_2\,\epsilon_2\\
&\Rightarrow\ \epsilon_2 = \epsilon_1\,\sqrt{2} = 2.8^\circ
\end{aligned}
$$

(b)

$$
\begin{aligned}
\epsilon_2 &= \epsilon_1\\
&\Rightarrow\ \frac{Ma_2^2}{\sqrt{Ma_2^2-1}}p_2 = \frac{Ma_1^2}{\sqrt{Ma_1^2-1}}p_1\\
&\Rightarrow\ Ma_2^4 - 8\,Ma_2^2 + 8 = 0\\
&\Rightarrow\ Ma_{2_{1.2}} = \sqrt{4\pm\sqrt{8}}\\
&\Rightarrow\ Ma_{2_1} = 2.61 \wedge Ma_{2_2} = 1.08
\end{aligned}
$$

(transonic regime, for which

$c_L\dfrac{\sqrt{Ma^2-1}}{\epsilon} =$ const. is not valid!)

(c)

$$\frac{F_D}{F_L} = \frac{c_D}{c_L} = \frac{\delta^2+\epsilon^2}{\epsilon}$$

(d)

$$
\begin{aligned}
&P = u_\infty\,F_D; \quad F_L = \text{ const.}\\
&\frac{P_a}{P_b} = \frac{\delta^2+\epsilon_a^2}{\delta^2+\epsilon_b^2}\frac{\sqrt{Ma_b^2-1}}{\sqrt{Ma_a^2-1}}\frac{Ma_a^3}{Ma_b^3} = 0.6
\end{aligned}
$$

(e)

$$
\begin{aligned}
W &= P\,t; \quad s = u\,t\\
\Rightarrow \frac{W_a}{W_b} &= \frac{P_a}{Ma_a}\,\frac{Ma_b}{P_b} = 1.11
\end{aligned}
$$

### 5.2.6 Theory of Characteristics

6.1 (a)

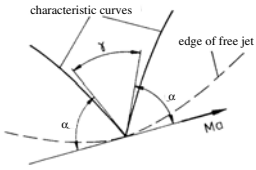


$$
\begin{aligned}
\gamma &= 180^\circ - 2\alpha\\
\alpha &= \arcsin\frac{1}{Ma}
\end{aligned}
$$

(b) Edge of free boundary:

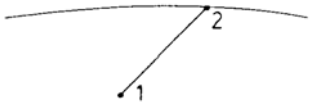


$$
\begin{aligned}
\nu_1 - \beta_1 &= \nu_2 - \beta_2\\
\frac{p_u}{p_o} &\Rightarrow \nu_2\\
\Rightarrow \beta_2 &= \nu_2 - \beta_1 - \nu_1
\end{aligned}
$$

Rigid wall:

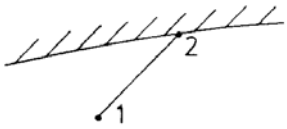


$$
\begin{aligned}
&\beta_2 \text{ is known}\\
&\nu_2 = \nu_1 - \beta_1 + \beta_2
\end{aligned}
$$

6.2

$$
\begin{aligned}
\nu_2 + \beta_2 &= \nu_3 + \beta_3\\
\nu_2 &= \nu_\infty\\
\beta_2 &= \beta_1 = 0\\
\Rightarrow \nu_3 + \beta_3 &= \nu_\infty
\end{aligned}
$$

$$\begin{aligned}
\nu_3 - \beta_3 &= \nu_4 - \beta_4 \\
\nu_4 &= \nu_\infty \\
\beta_4 = \beta_5 &= \beta \\
\Rightarrow \nu_3 - \beta_3 &= \nu_\infty - \beta \\
\Rightarrow \nu_3 &= \nu_\infty - \frac{\beta}{2} \\
\beta_3 &= \frac{\beta}{2}
\end{aligned}$$

6.3 (a)

$$\begin{aligned}
\nu_\infty + \beta_A &= \nu_c + \beta_c \\
\nu_\infty = 26.38^\circ; \quad \beta_c = 10^\circ; \quad \beta_A &= 0 \\
\Rightarrow \nu_c = 36.38^\circ; \quad Ma_c &= 2.4 \\
p_c = \frac{p_3}{p_0}\frac{p_0}{p_\infty} p_\infty &= 0.535 \cdot 10^5 \text{ Pa}
\end{aligned}$$

(b)

$$\begin{aligned}
\nu_D - \beta_D &= \nu_\infty - \beta_E \\
\nu_D + \beta_D &= \nu_\infty + \beta_E \\
\nu_\infty + \mid \beta \mid - \beta &= \nu_\infty - \beta_B \\
\Rightarrow \beta_B = 2\,\beta &= -20^\circ \\
\Rightarrow \nu_D = 16.38^\circ; \quad \beta_E &= 0 \\
\Rightarrow \left[\frac{dy}{dx}\right]_E &= 0
\end{aligned}$$

6.4 (a)

$$\begin{aligned}
\nu_2 - \beta_2 &= \nu_\infty + \mid \beta \mid - \beta \\
\nu_2 = \nu_\infty &\rightarrow \beta_2 = -14^\circ \\
\nu_6 - \beta_6 = \nu_4 - \beta_4; \quad \beta_4 &= \beta \\
\nu_4 + \beta &= \nu_\infty + \beta_2 \\
\Rightarrow \nu_4 = 10.81^\circ; \quad \beta_6 &= 0
\end{aligned}$$

(b)

$$\begin{aligned}
\nu_3 + \beta_3 &= \nu_1 + \beta_1 \\
\beta_1 = 0 \quad \nu_1 = \nu_\infty, \quad \beta_3 &= \beta \\
\Rightarrow \nu_3 = 24.81^\circ \Rightarrow Ma_3 &= 1.94 \\
\nu_4 + \beta_4 &= \nu_2 + \beta_2 \\
\Rightarrow \nu_4 = 10.81 \Rightarrow Ma_4 &= 1.46
\end{aligned}$$

(c)

$$\begin{aligned}
\gamma = 180^\circ - 2\,\alpha_2 &= 107.94^\circ \\
\frac{p_4}{p_\infty} = \frac{p_4}{p_0 4}\frac{p_{0\infty}}{p_\infty} &= 1.43
\end{aligned}$$

6.5 (a)

$$\left[\frac{dy}{dx}\right]_{Ch.} = \tan(\beta \pm \alpha)$$

$+$ : left running characteristic

$-$ : right running characteristic

(b)

$$\begin{aligned}
\nu_1 + \beta_1 &= \nu_2 + \beta_2 \\
\nu_\infty &= \nu_1 - \beta_1 \\
\nu_\infty &= \nu_2 - \beta_2 \\
\Rightarrow \nu_1 = \nu_2; \quad \beta_1 &= \beta_2
\end{aligned}$$

For arbitrary points 1, 2 in region ABCEA: it follows from $\nu_1 = \nu_2$ $\alpha_1 = \alpha_2$.

$$\begin{aligned}
\Rightarrow \left[\frac{dy}{dx}\right]_{1-2} &= \tan(\beta_1 - \alpha_1) \\
&= \tan(\beta_2 - \alpha_2) = \text{ const.}
\end{aligned}$$

(c)

$$\begin{aligned}
\frac{p_{Fr.}}{p_0} = \frac{p_\infty}{p_0}\frac{p_\infty - \Delta p}{p_\infty} &= 0.0066 \\
\Rightarrow Ma_{Fr.} = 4; \quad \nu_{Fr.} &= 65.78^\circ \\
\nu_{Fr.} = \nu_\infty + 90^\circ - \gamma & \\
\Rightarrow \gamma = 31.5^\circ &
\end{aligned}$$

(d)

$$\begin{aligned}
\nu_\infty &= \nu_F - \beta_D \\
\nu_2 - \beta_2 &= \nu_F - \beta_{D2} \\
\nu_2 = \nu_\infty + \mid \beta_2 \mid &= \nu_\infty - \beta_2 \\
-2\,\beta_2 &= -\beta_{D2} + \beta_D \\
\Rightarrow \beta_{D2} = \beta_D + 2\,\beta_2 &< \beta_D
\end{aligned}$$

6.6 (a)

$$\begin{aligned}
\nu_2 + (-10^\circ) &= 0 \\
\Rightarrow \nu_2 &= 10^\circ \\
\nu_3 - 10^\circ &= \nu_2 - (-10^\circ) \\
\Rightarrow \nu_3 &= 30^\circ \\
\nu_4 = \nu_3 + 10^\circ &= 40^\circ \\
\Rightarrow Ma_4 &= 2.54
\end{aligned}$$

(b) Continuity equation:

$$\begin{aligned}
A^*\, u^*\, \rho^* &= A_A\, u_A\, \rho_A \\
\frac{A^*}{A}(Ma_A = 2.54) &= 0.36 \\
\Rightarrow r_A &= 2.8 r^*
\end{aligned}$$

6.7

$$\begin{aligned}
\nu_2 = \nu_3 = \nu_\infty + \mid \beta \mid \\
\nu_2 - \beta_2 = \nu_\infty \\
\Rightarrow \beta_2 = \nu_3 - \nu_\infty = \mid \beta \mid \\
\nu_0 = \nu\,(Ma_\infty + 2\Delta Ma) \\
\nu_u = \nu\,(Ma_\infty + \Delta Ma) \\
\nu_u - \beta_u = \nu_1 - \beta_1; \quad \beta_u = \nu_\infty - \nu_u \\
\nu_o + \beta_o = \nu_1 + \beta_1; \quad \beta_o = \nu_o - \nu_\infty \\
\Rightarrow \nu_1 = \nu_o + \nu_u - \nu_\infty \\
\beta_1 = \nu_o - \nu_u \\
\nu_1 - \beta_1 = \nu_3 - \beta_3 \\
\Rightarrow \beta_3 = \mid \beta \mid + 2\,(\nu_\infty - \nu_u)
\end{aligned}$$

6.8

$$\begin{aligned}
Ma_1 = 3; \quad \mid \beta \mid = 14^\circ \Rightarrow \sigma = 31.5^\circ \\
\Rightarrow Ma_1 \sin\sigma = 1.57 \\
\Rightarrow \frac{p_{01}}{p_{02}} = 1.09 \\
Ma_2^* = 1.75; \quad \nu_2 = 34^\circ \\
p_3 = p_1; \quad p_{03} = p_{02} \\
\frac{p_3}{p_{03}} = \frac{p_1}{p_{01}}\frac{p_{01}}{p_{02}} = 0.0299 \\
\Rightarrow Ma_3 = 2.94; \quad \nu_3 = 48.5^\circ \\
\nu_3 + \beta_3 = \nu_2 + \beta_2 \\
\Rightarrow \beta_3 = -28.5^\circ \\
\nu_4 - \beta_4 = \nu_3 - \beta_3 \\
\beta_4 = -14^\circ \rightarrow \nu_4 = 63^\circ; \quad Ma_4 = 3.8 \\
\nu_5 + \beta_5 = \nu_4 + \beta_4 \\
\nu_5 = \nu_3 \rightarrow \beta_5 = 0.5^\circ \\
\nu_e - \beta_e = \nu_5 - \beta_5 \\
\Rightarrow \nu_e = 34^\circ; \quad Ma_e = 2.29 = Ma_2
\end{aligned}$$

### 5.2.7 Compressible Potential Flows and Similarity Rules

7.1

$$\begin{aligned}
c_p &= -2\frac{u'}{u_\infty} \\
0 \le x \le 1; \quad u' &= 0 \\
\Rightarrow c_p(0 \le x \le 1, y = 0) &= 0
\end{aligned}$$

$G_1$:

$$\begin{aligned}
\varphi_1 = g(x) + \lambda y) &= g(\eta) \\
\text{with} \qquad \lambda &= \sqrt{Ma_\infty^2 - 1}
\end{aligned}$$

B.C.:

$$\begin{aligned}
\frac{v'}{u_\infty} &= \left(\frac{dy}{dx}\right)_c = -\epsilon \\
v' &= \frac{\partial g}{\partial y} = \lambda\frac{dg}{d\eta} = -\epsilon u_\infty \\
\Rightarrow \frac{dg}{d\eta} &= -\frac{\epsilon u_\infty}{\lambda}
\end{aligned}$$

$G_2$:

$$\varphi_2 = g(\eta) + f(\xi); \quad \xi = (x - \lambda y)$$

B.C.:

$$\begin{aligned}
v' &= 0 = \frac{\partial \varphi_2}{\partial y} = \lambda\frac{dg}{d\eta} - \lambda\frac{df}{d\xi} \\
&\Rightarrow \frac{df}{d\xi} = \frac{dg}{d\eta} = -\frac{\epsilon u_\infty}{\lambda} \\
&\Rightarrow c_{p2} = \frac{4\epsilon}{\lambda}
\end{aligned}$$

$$c_p(1 \le x \le 2; \quad y = 0) = \frac{4\epsilon}{\lambda}$$

7.2

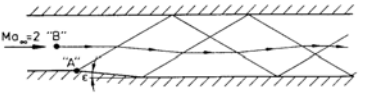


7.3 (a)

$$\begin{aligned}
\varphi_I = g(x + \lambda y) \\
\varphi_{II} = f(x - \lambda y) \\
\varphi_{II} = f(x - \lambda y) + g(x + \lambda y)
\end{aligned}$$

(b)

$$\begin{aligned}
\frac{v}{u_\infty} &= \left(\frac{dy}{dx}\right)_c = \\
&= \epsilon = \frac{1}{u_\infty}\frac{\partial \varphi_I}{\partial y} = \frac{1}{u_\infty}\frac{\partial \varphi_{II}}{\partial y}
\end{aligned}$$

(c)

$$\begin{aligned}
\epsilon &= \frac{g'\lambda}{u_\infty} \\
\Rightarrow g &= \frac{\epsilon u_\infty}{\lambda}(x + \lambda y) + c_I \\
\epsilon &= -\frac{1}{u_\infty} f'\,\lambda \\
\Rightarrow f &= -\frac{\epsilon u_\infty}{\lambda}(x - \lambda y) + c_{II} \\
\Rightarrow \varphi_I &= \frac{\epsilon u_\infty}{\lambda}(x + \lambda y) + c_I \\
\varphi_{II} &= -\frac{\epsilon u_\infty}{\lambda}(x - \lambda y) + c_{II} \\
\varphi_{III} &= 2\,\epsilon\,u_\infty\,y + c_{III}
\end{aligned}$$

(d)

$$u' = \frac{\partial \varphi_{III}}{\partial x} = 0$$
$$v' = \frac{\partial \varphi_{III}}{\partial y} = 2\,\epsilon\,u_\infty$$
$$\left(\frac{dy}{dx}\right)_{\text{Streamline in } G_{III}} = 2\,\epsilon$$

7.4 (a)

$$\varphi_I = f_I(x - \lambda y)$$
$$\varphi_{II} = f_{II}(x - \lambda y) + g_{II}(x + \lambda y)$$

(b)

$$p_{Fr.} = p_\infty \Rightarrow c_{pFr.} = 0$$
$$\Rightarrow u'_{Fr} = \left(\frac{\partial \varphi_{II}}{\partial x}\right)_{Fr.} = 0$$

(c)

$$\begin{aligned}
\frac{df_I}{d\xi} &= \frac{df_{II}}{d\xi} \\
v'_K &= u_\infty\,\beta \\
&= -\lambda\left(\frac{df_{II}}{d\xi}\right)_k \\
v'_{Fr.} &= u_\infty\,\delta \\
&= -\lambda\left(\frac{df_{II}}{d\xi} - \frac{dg_{II}}{d\eta}\right)_{Fr.}
\end{aligned}$$

$$\begin{aligned}
\left(\frac{\partial \varphi_{II}}{\partial x_{Fr.}}\right) &= 0 \\
\Rightarrow \left(\frac{df_{II}}{d\xi} + \frac{dg_{II}}{d\eta}\right)_{Fr.} &= 0 \\
\Rightarrow v'_{Fr.} &= -2\,\lambda\frac{df_{II}}{d\xi} \\
\Rightarrow \delta &= 2\,\beta
\end{aligned}$$

7.5

$$\begin{aligned}
\varphi_3 &= g_3(\eta_3); \quad \eta_3 = x + \lambda_1 y; \\
\lambda_1 &= \sqrt{Ma_1^2 - 1} \\
\frac{\partial \varphi_3}{\partial y} &= v'_3 = \frac{dy}{dx}\,u_1 \\
&= \delta u_1 = \left(\frac{dg_3}{d\eta_3}\right)\lambda_1 \\
\frac{\partial \varphi_5}{\partial y} &= \beta_5 u_2 = \left(\frac{dg_5}{d\eta_5}\right)\lambda_2
\end{aligned}$$

$$\begin{aligned}
\varphi_4 &= f_4(\xi_4) + g_4(\eta_4) \\
\frac{\partial \varphi_4}{\partial y} &= v'_4 = \beta_4 u_1 \\
&= \frac{dg_4}{d\eta_4}\lambda_1 + \frac{df_4}{d\xi_4}(-\lambda_1) \\
\frac{g_4}{\eta_4} &= \frac{dg_3}{d\eta_3} = \frac{\delta u_1}{\lambda_1} \\
\Rightarrow \frac{df_4}{d\xi_4} &= \frac{u_1}{\lambda_1}(\delta - \beta_4)
\end{aligned}$$

$$\begin{aligned}
c_{p4} &= -\frac{2}{u_1}\frac{\partial \varphi_4}{\partial x} \\
&= -\frac{2}{u_1}\left(\frac{dg_4}{d\eta_4} + \frac{df_4}{d\xi_4}\right) \\
&= -\frac{2}{u_1}\left(\frac{\delta u_1}{\lambda_1} + \frac{u_1}{\lambda_1}\,(\delta - \beta_4)\right) \\
&= -\frac{2}{\lambda_1}(2\,\delta - \beta_4) \\
c_{p5} &= -\frac{2}{u_2}\frac{\partial \varphi_5}{\partial x} = -\frac{2}{\lambda_2}\beta_5 \\
c_{p4} &= \frac{2}{\gamma Ma_1^2}\left(\frac{p_4}{p_1} - 1\right) \\
c_{p5} &= \frac{2}{\gamma Ma_2^2}\left(\frac{p_5}{p_1} - 1\right) \\
p_4 &= p_5 \Rightarrow c_{p4}\,Ma_1^2 = c_{p5}\,Ma_2^2 \\
c_{p4}Ma_1^2 &= -\frac{2Ma_1^2}{\lambda_1}(2\,\delta - \beta_4) \\
&= -\frac{2Ma_2^2}{\lambda_2}\beta_5 \\
\beta_4 &= \beta_5 = \beta \\
\Rightarrow \beta &= \frac{2\,\delta Ma_1^2}{Ma_1^2 + Ma_2^2\,\frac{\lambda_1}{\lambda_2}} \\
\frac{p_5}{p_1} &= c_{p5}\frac{\gamma Ma_2^2}{2} + 1
\end{aligned}$$

$$Ma_1^2 = 1 - \frac{2\,\delta\,\gamma\,Ma_2^2 Ma_1^2}{Ma_1^2\sqrt{Ma_2^2 - 1} + Ma_2^2\sqrt{Ma_2^2 - 1}}$$

7.6

$$c_p = \frac{p - p_\infty}{\frac{\varrho}{2}u_\infty^2}; \quad V_{max} = u_\infty(1 + \delta)$$
$$\text{incomp.:} \frac{\rho_\infty}{2}u_\infty^2 + p_\infty = \frac{\rho_\infty}{2}V_{max}^2 + p_{min}$$
$$\Rightarrow \frac{\rho_\infty}{2}u_\infty^2 + p_\infty = \frac{\rho_\infty}{2}u_\infty^2(1 + \delta)^2 + p_{min}$$
$$\Rightarrow c_{pmin,\ inc.} = 1 - (1 + \delta)^2 = -0.5626$$

$$c_{pmin,comp.} = \frac{c_{pmin,inc.}}{\sqrt{1 - Ma_\infty^2}}$$

$\rightarrow$ in diagram

$\rightarrow$ intersection with curve for $c_{pcrit.}$

$\Rightarrow \quad Ma_{\infty,crit.} = 0.7$

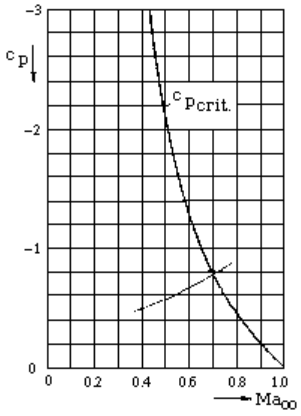


7.7

$$\begin{aligned}
\delta_1 \frac{Ma_1^2}{(1 - Ma_1^2)^{\frac{3}{2}}} &= \delta_2 \frac{Ma_2^2}{(1 - Ma_2^2)^{\frac{3}{2}}} \\
&\Rightarrow \quad \delta_2 = 0.15 \\
\frac{Ma_1^2}{1 - Ma_1^2}\, c_{p1} &= \frac{Ma_2^2}{1 - Ma_2^2} c_{p2} \\
&\Rightarrow \quad c_{p2} = 0.651
\end{aligned}$$

7.8 (a)

$$\begin{aligned}
p_{min} &= p^* = \frac{p^*}{p_0} \frac{p_0}{p_\infty} p_\infty \\
&= 0.733 \cdot 10^5 \text{ Pa} \\
c_{pcrit.} &= \frac{2}{\gamma\, Ma_{\infty crit.}} \left( \frac{p^*}{p_\infty} - 1 \right) \\
&= -0.778
\end{aligned}$$

(b)

$$c_{pbmin} = -0.65$$

from diagram

$$\begin{aligned}
c_{pbmin} \sqrt{1 - Ma_{\infty b}^2} \\
= c_{pamin} \sqrt{1 - Ma_{\infty a}^2} \\
\Rightarrow Ma_{\infty b} = 0.519
\end{aligned}$$

(c)

$$\begin{aligned}
c_L = \frac{1}{t} \int_0^t (c_{pl} - c_{pu}) dx \\
\Rightarrow c_{Lc} \sqrt{1 - Ma_{\infty c}^2} \\
= c_{La} \sqrt{1 - Ma_{\infty a}^2} \\
\Rightarrow c_{Lc} = 0.2246; \quad c_{Linc.} = 0.214
\end{aligned}$$

7.9

$$\begin{aligned}
\frac{c_p}{c_{pinc.}} &= f(Ma_\infty) \\
\left( \frac{x}{l} \right) &= \left( \frac{x}{l} \right)_{inc} \\
\left( \frac{y}{l} \right) &= \left( \frac{y}{l} \right)_{inc} \frac{1}{\sqrt{1 - Ma_\infty^2}} \\
\Rightarrow \frac{L}{L_{inc.}} = 1; \quad \frac{H}{H_{inc.}} &= \frac{1}{\sqrt{1 - Ma_\infty^2}} \\
\frac{c_p}{c_{pinc.}} &= \frac{1}{1 - Ma_\infty^2}
\end{aligned}$$

7.10 1.

$$\begin{aligned}
x = \text{ const.} \Rightarrow t &= \text{ const.} \\
y \sqrt{|\, Ma_\infty^2 - 1 \,|} &= \text{ const.} \\
\rightarrow d \sqrt{|\, Ma_\infty^2 - 1 \,|} &= \text{ const.} \\
\Rightarrow A = \frac{1}{|\, Ma_\infty^2 - 1 \,|} \\
\Rightarrow c_p \,|\, Ma_\infty^2 - 1 \,| &= \text{ const.};
\end{aligned}$$

Göthert rule

2. (a)

$$\begin{aligned}
c_L = \frac{1}{t} \int_0^t (c_{pl} - c_{pu}) dt \\
\Rightarrow \frac{c_L \sqrt{|\, Ma_\infty^2 - 1 \,|}}{d/t} = \text{ const.}
\end{aligned}$$

(b)

$$\begin{aligned}
c_L = \frac{4\,\epsilon}{\sqrt{|\, Ma_\infty^2 - 1 \,|}} \\
\Rightarrow \frac{\epsilon}{d/t} = \text{ const.}
\end{aligned}$$

(c) transonic flows
hypersonic flows

7.11 (a)

$$\begin{aligned}
c_L \sqrt{|\, Ma_\infty^2 - 1 \,|} &= \text{ const.} \\
\Rightarrow Ma_{\infty 2} = 0.711
\end{aligned}$$

(b)

$$c_L \frac{\sqrt{|\ 1 - Ma_\infty^2\ |}}{\delta} = \text{ const.}$$
$$c_{L1} = c_{Linc.}$$
$$\Rightarrow \delta_{inc.} = \frac{\delta_1}{\sqrt{|\ Ma_\infty^2 - 1\ |}} = 0.125$$

7.12 (a) 1.

$$c_L = \frac{4\,\epsilon}{\sqrt{Ma_\infty^2 - 1}}$$
$$\rightarrow \epsilon = 0.028 \hat{=} 1.6^\circ$$

2.

$$F_L = \text{ const. } (T_\infty, p_\infty = \text{ const. })$$
$$\Rightarrow c_{L1}\, Ma_{\infty 1}^2 = c_{L2}\, Ma_{\infty 2}^2$$

$$\begin{aligned} \Rightarrow c_{L2} &= 0.025 \\ \rightarrow \epsilon_2 &= 0.0177 \hat{=} 1.013^\circ \\ c_D &= \frac{4}{\sqrt{Ma_\infty^2 - 1}} \times \\ &\quad \times \left[ \left( \frac{d}{l} \right)^2 + \epsilon^2 \right] \\ &= 0.0027 \end{aligned}$$

(b) 3.

$$c_{L3} Ma_{\infty 3}^2 = c_{L1} Ma_{\infty 1}^2$$
$$\Rightarrow c_{L3} = 0.4; \quad c_{D3} = 0!$$

4.

$$c_{L4} = c_{L3} \sqrt{1 - Ma_{\infty 3}^2} = 0.265$$

5.

$$\begin{aligned} \frac{c_{L5}}{\delta_5} &= c_{L3} \frac{\sqrt{1 - Ma_{\infty 3}^2}}{\delta} \\ \Rightarrow \frac{\delta_5}{\delta} &= \frac{1}{\sqrt{1 - Ma_{\infty 3}^2}} = 1.512 \\ \Rightarrow \delta_5 &= 0.06 \\ \epsilon &= \frac{\epsilon_3}{\sqrt{1 - Ma_{\infty 3}^2}} \\ &= 0.042 \hat{=} 2.4^\circ \end{aligned}$$

## 5.3 Appendix

### Tables and Diagrams

Table of solution problem 1.11

| Ma | $\epsilon$ | $\epsilon^2$ | $\frac{F}{Ap_0}$ | $\left(\frac{F}{Ap_0}\right)_{inc}$ | $\Delta\left(\frac{F}{Ap_0}\right)$ | $\frac{\Delta\left(\frac{F}{Ap_0}\right)}{\frac{F}{Ap_0}}$ [%] |
|---|---|---|---|---|---|---|
| 0 | 0 | 0 | 0 | 0 | 0 | - |
| 0.05 | $1.8 \cdot 10^{-3}$ | $3.1 \cdot 10^{-6}$ | $3.496 \cdot 10^{-3}$ | $3.496 \cdot 10^{-3}$ | $-2.2 \cdot 10^{-6}$ | -0.06 |
| 0.10 | $7.0 \cdot 10^{-3}$ | $4.9 \cdot 10^{-5}$ | $1.390 \cdot 10^{-2}$ | $1.394 \cdot 10^{-2}$ | $-3.5 \cdot 10^{-5}$ | -0.25 |
| 0.15 | $1.6 \cdot 10^{-2}$ | $2.4 \cdot 10^{-4}$ | $3.101 \cdot 10^{-2}$ | $3.118 \cdot 10^{-2}$ | $-1.7 \cdot 10^{-4}$ | -0.56 |
| 0.20 | $2.8 \cdot 10^{-2}$ | $7.6 \cdot 10^{-4}$ | $5.446 \cdot 10^{-2}$ | $5.501 \cdot 10^{-2}$ | $-5.5 \cdot 10^{-4}$ | -1.00 |
| 0.30 | $6.1 \cdot 10^{-2}$ | $3.7 \cdot 10^{-3}$ | $1.184 \cdot 10^{-1}$ | $1.211 \cdot 10^{-1}$ | $-2.7 \cdot 10^{-3}$ | -2.30 |
| 0.40 | $1.0 \cdot 10^{-1}$ | $1.1 \cdot 10^{-2}$ | $2.006 \cdot 10^{-1}$ | $2.088 \cdot 10^{-1}$ | $-8.2 \cdot 10^{-3}$ | -4.10 |
| 0.60 | $2.2 \cdot 10^{-1}$ | $4.7 \cdot 10^{-2}$ | $3.951 \cdot 10^{-1}$ | $4.320 \cdot 10^{-1}$ | $-3.7 \cdot 10^{-2}$ | -9.30 |
| 0.80 | $3.4 \cdot 10^{-1}$ | $1.2 \cdot 10^{-1}$ | $5.878 \cdot 10^{-1}$ | $6.879 \cdot 10^{-1}$ | $-1.0 \cdot 10^{-1}$ | -22.00 |
| 1.00 | $4.7 \cdot 10^{-1}$ | $2.2 \cdot 10^{-1}$ | $7.396 \cdot 10^{-1}$ | $9.434 \cdot 10^{-1}$ | $-2.0 \cdot 10^{-1}$ | -28.00 |

Table of solution 5.1 (d)

*Pair of profiles*

| | $Ma$ | $Ma^*$ | $\beta$ | $\sigma$ | $\nu$ | $Ma \sin\sigma$ | $\frac{p_i}{p_{0i}}$ | $\frac{p_i}{p_{i-1}}$ | $\frac{p_{0i}}{p_{0i-1}}$ |
|---|---|---|---|---|---|---|---|---|---|
| $\infty$ | 2.5 | 1.83 | 12° | 34° | | 1.39 | 0.059 | | |
| 1 | 2.0 | 1.63 | 12° | 42° | | 1.33 | 0.128 | 2.1 | 0.96 |
| 2 | 1.56 | 1.40 | 15° | | 13° | | 0.250 | 1.9 | 0.97 |
| 3 | 2.1 | 1.68 | | | 28° | | 0.113 | 0.452 | 1 |

Table of solution 5.1 (d)

*Double wedge profile*

| | $Ma$ | $Ma^*$ | $\beta$ | $\nu$ | $\frac{p_i}{p_{0i}}$ | $\frac{p_i}{p_{i-1}}$ | $\frac{p_{0i}}{p_{0i-1}}$ |
|---|---|---|---|---|---|---|---|
| 1 | 2.0 | 1.63 | 12° | 26° | 0.128 | 2.1 | 0.96 |
| 3 | 3.2 | 2.01 | | 53° | 0.021 | 0.164 | 1 |

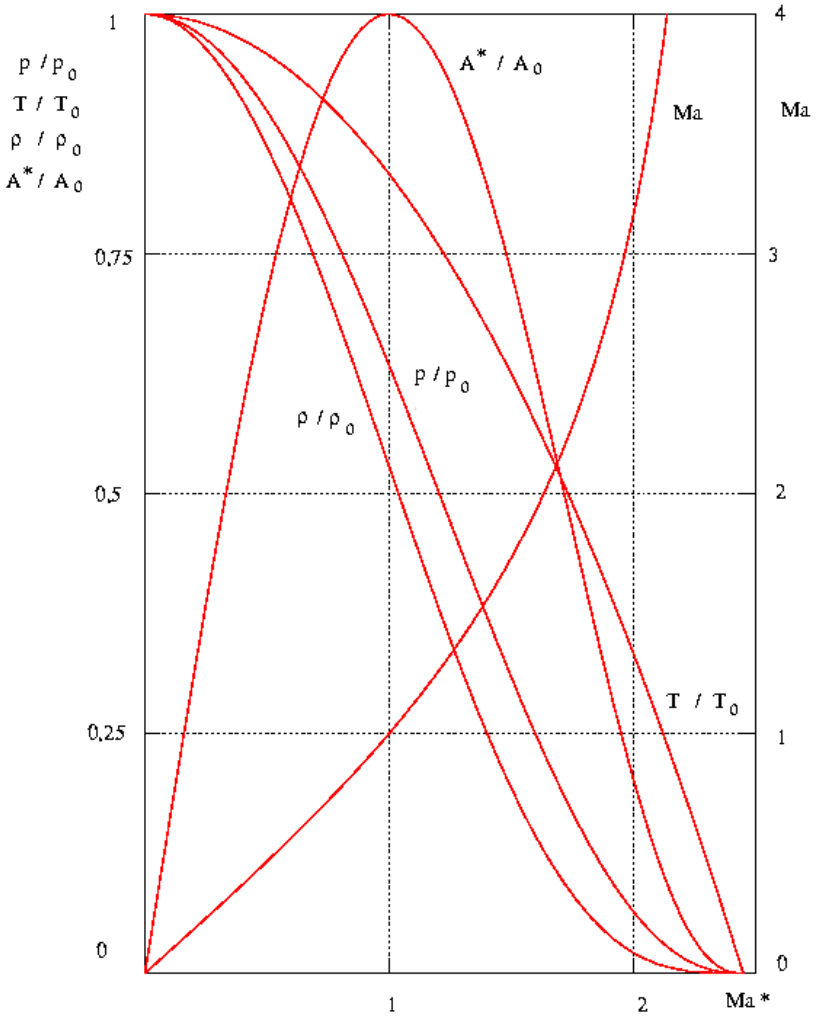


Gasdynamic quantities of the Laval-nozzle flow ($\gamma = 1.4$)

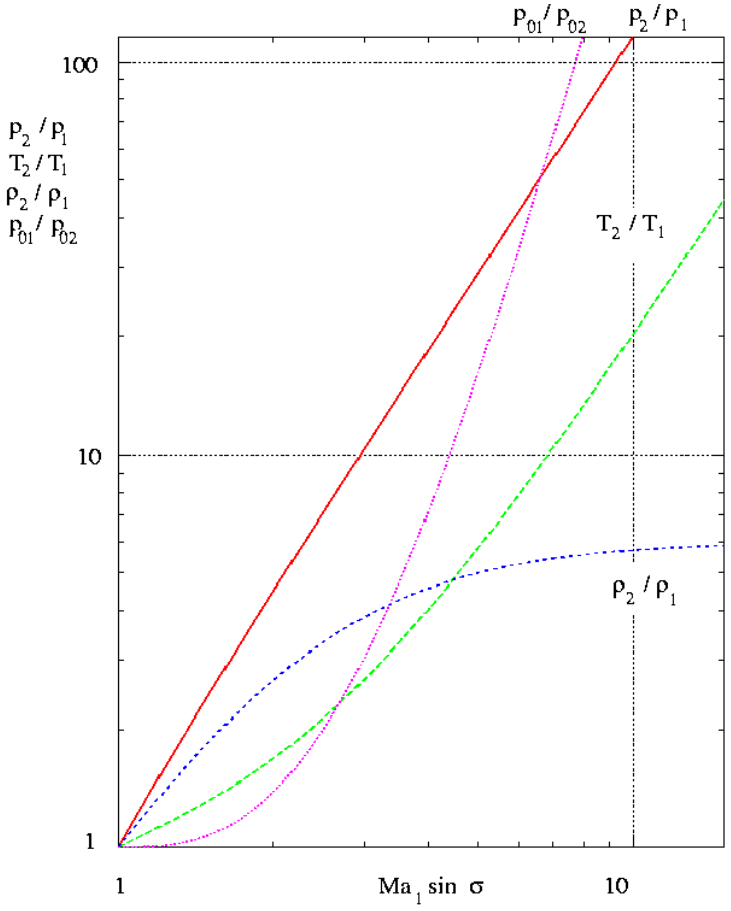


Gasdynamic quantities for compression shock

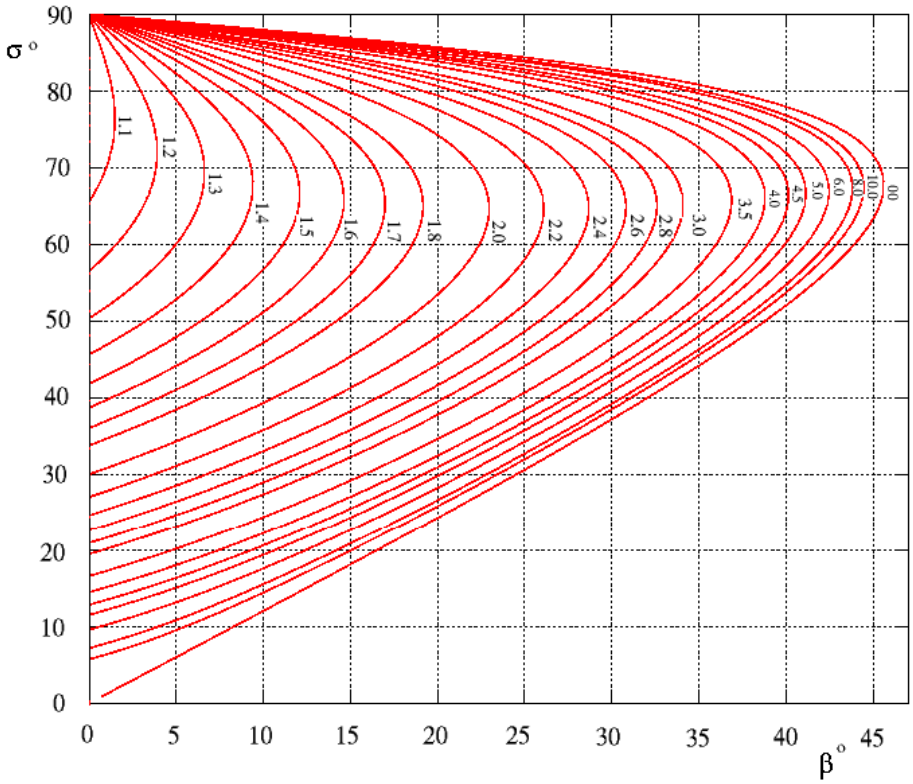


Oblique compression shock

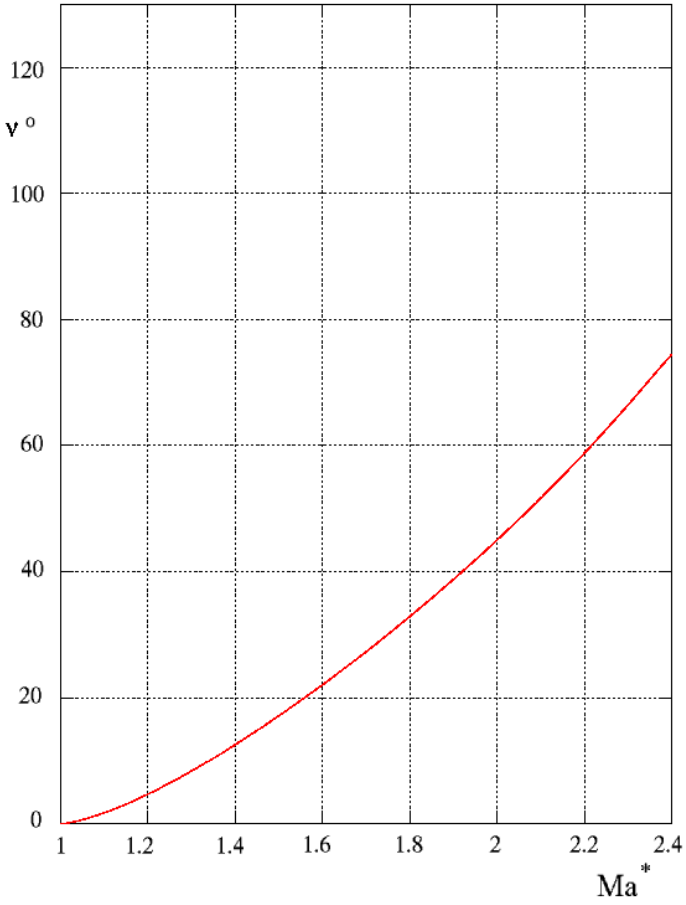


Prandtl-Meyer-Function $\nu(Ma^*)$

$$\begin{aligned}
\nu(Ma^*) &= \sqrt{\frac{\gamma+1}{\gamma-1}} \cdot \arctan \sqrt{\frac{\frac{\gamma-1}{2}(Ma^{*2}-1)}{1-\frac{\gamma-1}{2}(Ma^{*2}-1)}} \\
&- \arctan \sqrt{\frac{\frac{\gamma+1}{2}(Ma^{*2}-1)}{1-\frac{\gamma-1}{2}(Ma^{*2}-1)}} \\
\nu(Ma) &= \sqrt{\frac{\gamma+1}{\gamma-1}} \cdot \arctan \sqrt{\frac{\gamma-1}{\gamma+1}(Ma^2-1)} \\
&- \arctan \sqrt{Ma^2-1}
\end{aligned}$$

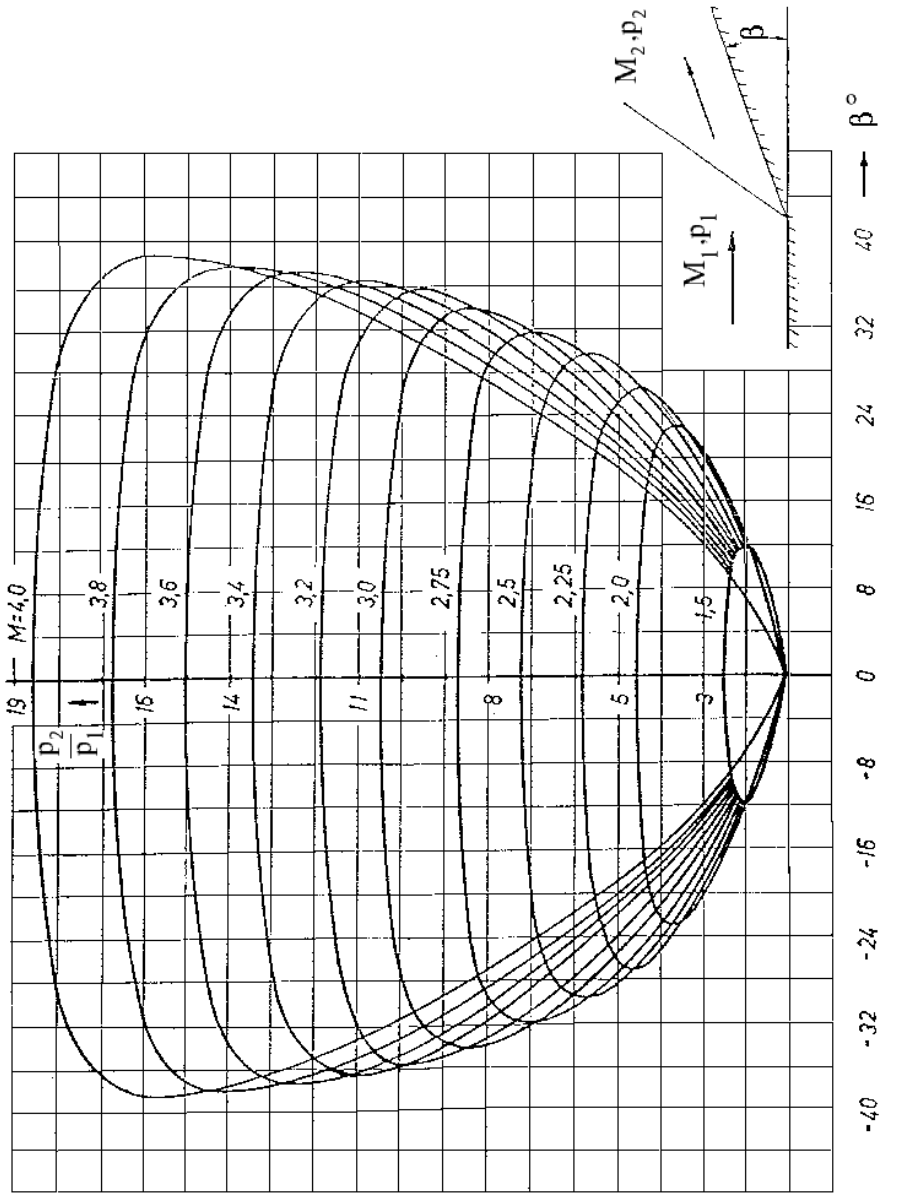


Oblique compression shock: Heart-curve diagram

One-dimensional nozzle flow
Perfect gas with const. spec. heats, $\gamma = 1.4$

| $Ma$ | $Ma^*$ | $\frac{p}{p_0}$ | $\frac{\rho}{\rho_0}$ | $\frac{T}{T_0}$ | $\frac{A^*}{A}$ |
|---|---|---|---|---|---|
| 0.00 | 0.00000 | 1.0000000 | 1.000000 | 1.00000 | 0.000000 |
| 0.01 | 0.01095 | 0.9999300 | 0.999950 | 0.99998 | 0.017279 |
| 0.10 | 0.10944 | 0.9930314 | 0.995017 | 0.99800 | 0.171767 |
| 0.20 | 0.21822 | 0.9724967 | 0.980277 | 0.99206 | 0.337437 |
| 0.30 | 0.32572 | 0.9394697 | 0.956380 | 0.98232 | 0.491385 |
| 0.40 | 0.43133 | 0.8956144 | 0.924274 | 0.96899 | 0.628875 |
| 0.50 | 0.53452 | 0.8430192 | 0.885170 | 0.95238 | 0.746356 |
| 0.60 | 0.63481 | 0.7840040 | 0.840452 | 0.93284 | 0.841610 |
| 0.70 | 0.73179 | 0.7209279 | 0.791579 | 0.91075 | 0.913766 |
| 0.80 | 0.82514 | 0.6560216 | 0.739992 | 0.88652 | 0.963178 |
| 0.90 | 0.91460 | 0.5912601 | 0.687044 | 0.86059 | 0.991215 |
| 1.00 | 1.00000 | 0.5282818 | 0.633939 | 0.83333 | 1.000000 |
| 1.10 | 1.08124 | 0.4683542 | 0.581696 | 0.80515 | 0.992137 |
| 1.20 | 1.23114 | 0.4123770 | 0.531142 | 0.77640 | 0.910459 |
| 1.30 | 1.29987 | 0.3609139 | 0.482903 | 0.74738 | 0.937818 |
| 1.40 | 1.29987 | 0.3142409 | 0.437423 | 0.71839 | 0.896921 |
| 1.50 | 1.36458 | 0.2724031 | 0.394984 | 0.68966 | 0.850219 |
| 1.60 | 1.42539 | 0.2352712 | 0.355730 | 0.66138 | 0.799850 |
| 1.70 | 1.48247 | 0.2025935 | 0.319693 | 0.63371 | 0.747604 |
| 1.80 | 1.53598 | 0.1740403 | 0.286818 | 0.60680 | 0.694936 |
| 1.90 | 1.58609 | 0.1490396 | 0.256991 | 0.58072 | 0.642981 |
| 2.00 | 1.63299 | 0.1278045 | 0.230048 | 0.55556 | 0.592593 |
| 2.10 | 1.67687 | 0.1093532 | 0.205803 | 0.53135 | 0.544383 |
| 2.20 | 1.71791 | 0.0935217 | 0.184051 | 0.50813 | 0.498759 |
| 2.30 | 1.75629 | 0.0799726 | 0.164584 | 0.48591 | 0.455969 |
| 2.40 | 1.79218 | 0.0683997 | 0.147195 | 0.46468 | 0.416129 |
| 2.50 | 1.82574 | 0.0585277 | 0.131687 | 0.44444 | 0.379259 |
| 2.60 | 1.85714 | 0.0501152 | 0.117871 | 0.42517 | 0.345307 |
| 2.70 | 1.88653 | 0.0429500 | 0.105571 | 0.40683 | 0.314168 |
| 2.80 | 1.91404 | 0.0368483 | 0.097626 | 0.38941 | 0.285704 |
| 2.90 | 1.93981 | 0.0316515 | 0.084889 | 0.37286 | 0.416129 |
| 3.00 | 1.96396 | 0.0272237 | 0.076226 | 0.35714 | 0.236152 |
| 3.50 | 2.06419 | 0.0131109 | 0.045233 | 0.28986 | 0.147284 |
| 4.00 | 2.13809 | 0.0065861 | 0.027662 | 0.23810 | 0.093294 |
| 4.50 | 2.19360 | 0.0034553 | 0.017446 | 0.19802 | 0.060378 |
| 5.00 | 2.23607 | 0.0018900 | 0.011340 | 0.16667 | 0.040000 |
| 6.00 | 2.29528 | 0.0006334 | 0.005194 | 0.12195 | 0.018804 |
| 7.00 | 2.33333 | 0.0002416 | 0.002609 | 0.09259 | 0.009602 |
| 8.00 | 2.35907 | 0.0001024 | 0.001414 | 0.07246 | 0.005260 |
| 9.00 | 2.37722 | 0.0000474 | 0.000815 | 0.05814 | 0.003056 |
| 10.00 | 2.39046 | 0.0000236 | 0.00495 | 0.04762 | 0.001866 |

Prandtl-Meyer angle ($\nu$ in °, $\gamma = 1.4$)

| $Ma$ | $\nu$ | $Ma$ | $\nu$ | $Ma$ | $\nu$ | $Ma$ | $\nu$ | $Ma$ | $\nu$ |
|---|---|---|---|---|---|---|---|---|---|
| 1.00 | 0.00 | 1.60 | 14.48 | 2.55 | 40.28 | 4.10 | 67.08 | 7.10 | 91.49 |
| 1.02 | 0.13 | 1.62 | 15.45 | 2.60 | 41.41 | 4.20 | 68.33 | 7.20 | 92.00 |
| 1.04 | 0.35 | 1.64 | 16.04 | 2.65 | 42.53 | 4.30 | 69.54 | 7.30 | 92.49 |
| 1.06 | 0.64 | 1.66 | 16.64 | 2.70 | 43.62 | 4.40 | 70.70 | 7.40 | 92.97 |
| 1.08 | 0.97 | 1.68 | 17.22 | 2.75 | 44.69 | 4.50 | 71.83 | 7.50 | 93.44 |
| 1.10 | 1.34 | 1.70 | 17.81 | 2.80 | 45.74 | 4.60 | 72.92 | 7.60 | 93.90 |
| 1.12 | 1.73 | 1.72 | 18.40 | 2.85 | 49.78 | 4.70 | 73.97 | 7.70 | 94.34 |
| 1.14 | 2.16 | 1.74 | 18.98 | 2.90 | 47.79 | 4.80 | 74.98 | 7.80 | 94.76 |
| 1.16 | 2.61 | 1.78 | 19.56 | 2.95 | 48.78 | 4.90 | 75.97 | 7.90 | 95.21 |
| 1.18 | 3.07 | 1.80 | 20.15 | 3.00 | 49.76 | 5.00 | 76.92 | 8.00 | 95.62 |
| 1.20 | 3.56 | 1.82 | 20.72 | 3.05 | 50.71 | 5.10 | 77.84 | 8.50 | 97.57 |
| 1.22 | 4.03 | 1.84 | 21.30 | 3.10 | 51.65 | 5.20 | 78.73 | 9.00 | 99.32 |
| 1.24 | 4.57 | 1.86 | 22.45 | 3.15 | 52.57 | 5.30 | 79.59 | 9.50 | 100.98 |
| 1.26 | 5.09 | 1.88 | 23.02 | 3.20 | 53.47 | 5.40 | 80.43 | 10.00 | 102.31 |
| 1.28 | 5.63 | 1.90 | 23.59 | 3.25 | 54.35 | 5.50 | 81.24 | 11.00 | 104.79 |
| 1.30 | 6.17 | 1.92 | 24.15 | 3.30 | 55.22 | 5.60 | 82.03 | 12.00 | 106.88 |
| 1.32 | 6.76 | 1.94 | 24.71 | 3.35 | 56.07 | 5.70 | 82.79 | 13.00 | 108.65 |
| 1.34 | 7.28 | 1.96 | 25.27 | 3.40 | 56.91 | 5.80 | 83.54 | 14.00 | 110.18 |
| 1.36 | 7.84 | 1.98 | 25.83 | 3.45 | 57.72 | 5.90 | 84.26 | 15.00 | 111.51 |
| 1.38 | 8.41 | 2.00 | 26.38 | 3.50 | 58.53 | 6.00 | 84.95 | 16.00 | 112.64 |
| 1.40 | 8.99 | 2.05 | 27.75 | 3.55 | 59.32 | 6.10 | 85.63 | 17.00 | 113.71 |
| 1.42 | 9.56 | 2.10 | 29.10 | 3.60 | 30.09 | 6.20 | 86.29 | 18.00 | 114.63 |
| 1.44 | 10.15 | 2.15 | 30.42 | 3.65 | 60.85 | 6.30 | 86.94 | 19.00 | 115.43 |
| 1.46 | 10.73 | 2.20 | 31.73 | 3.70 | 61.59 | 6.40 | 87.56 | 20.00 | 116.19 |
| 1.48 | 11.32 | 2.25 | 33.02 | 3.75 | 62.35 | 6.50 | 88.17 | 21.00 | 116.87 |
| 1.50 | 11.90 | 2.30 | 34.28 | 3.80 | 63.04 | 6.60 | 88.76 | 22.00 | 117.48 |
| 1.52 | 12.49 | 2.35 | 35.52 | 3.85 | 63.75 | 6.70 | 89.33 | 23.00 | 118.04 |
| 1.54 | 13.09 | 2.40 | 36.75 | 3.90 | 64.44 | 6.80 | 89.89 | 24.00 | 118.55 |
| 1.56 | 13.68 | 2.45 | 37.94 | 3.95 | 65.12 | 6.90 | 90.44 | 25.00 | 119.03 |
| 1.58 | 14.27 | 2.50 | 39.15 | 4.00 | 65.78 | 7.00 | 90.97 | $\infty$ | 130.45 |

# 6. Aerodynamics Laboratory

## 6.1 Wind Tunnel for Low Speeds (Göttingen-Type Wind Tunnel)

*Abstract*

The wind tunnel for low speeds of the Aerodynamisches Institut of the RWTH Aachen is a Göttingen-type wind tunnel. It is a continuously running closed-circuit tunnel, in which the the air is circulated with a single-stage axial-flow fan with a maximum power of 100 kW. The test section is open and has a diameter of 1.2 m. The maximum attainable air speed is 60 m/s (216 km/h).
Generally a wind tunnel has to be built in such a way that:

1. an air flow is generated in the test section with constant velocity distribution in time and space,
2. the losses caused by the closed-circuit circulation are as small as possible.

The objective of this experiment is to examine the quality of this wind tunnel. In order to do so, the velocity distribution in the test section is measured with a Prandtl tube. The dependence of the accuracy of the measurement on the free-stream direction is tested by turning the Prandtl tube with respect to the direction of the oncoming flow. Also, the quality coefficient of the wind tunnel (ratio of the power of the air stream and the power of the axial-flow fan) is determined as a function of the flow velocity.

### 6.1.1 Preliminary Remarks

The prerequisits for the usability of wind tunnels for fluid-mechanical investigations are the following:

1. The similarity laws can be applied, so that the results obtained with models in the wind tunnel can be transfered to flows about full-scale configurations, especially to flows about airplanes in free flight.
2. The boundary conditions for the flows about the models in the wind tunnel and the full-scale configurations, especially for those in free flight, have to be similar.

In general, complete similarity cannot be attained in a single experiment. For this reason, it is necessary to determine the similarity parameter, which is of greatest importance for the problem to be investigated, and only obey the corresponding similarity law in the experiment. For steady low speeds, it is sufficient to keep

$$Re = \frac{v\, l\, \rho}{\mu} = \frac{\text{Inertia force}}{\text{Frictional force}} \tag{6.1}$$

constant.
In order to obey the similarity law, it is necessary to provide similar initial and boundary conditions, e. g.:

1. the ratio of the width of the air stream in the wind tunnel and the size of the model compared to the infinite width of the air stream in free flight,
2. the roughness of the surface of the model,
3. the intensity of turbulence of the flow in the wind tunnel, and others.

The flow velocity of the Göttingen-type tunnel of the Aerodynamisches Institut is small compared to the speed of sound. The influence of the compressibility of the air on the flow can therefore not be investigated.

### 6.1.2 Wind Tunnels for Low Speeds

Wind tunnels for low speeds (with air as working medium at atmospheric temperatures: $v \leq 80\,\mathrm{m/s}$) are continuously operated, i. e. a fan generates a flow for an arbitrary duration of the test. Two basic types of tunnels are known:

1. The Göttingen-type (after Prandtl) wind tunnel: Tunnel circulating the air with either open or closed test section.
2. The Eiffel-type wind tunnel : Tunnel without air circulation with open or closed test section.

The Eiffel-type tunnel is briefly described next.

#### Eiffel-Type Wind Tunnel

The Eiffel tunnel in its simplest design consists of a tube with a fan. Air is sucked from the surroundings; Eiffel tunnels are used for determining wind loads on buildings (low construction costs for large dimensions; the air speed is low – only up to $40\,\mathrm{m/s}$). Most of the available tunnels are built at higher expenditures.
In order to generate a uniform velocity profile with low turbulent intensity in the test section, a nozzle with a contraction ratio of $A_c/A_n = 5 \div 20$ is necessary. A further improvement of the velocity distribution is possible by positioning guiding vanes and screens upstream of the test section: A high contraction yields a relatively low velocity in the settling chamber and small losses caused by installations.
In order to keep the operating costs low, diffusers are used for pressure recovery (in a simple wind tunnel the entire dynamic pressure of the test section $\rho\, v^2/2$ must be counted as loss).
The pressure in the measuring cross section is below atmospheric. An underpressure chamber is needed for an open test section; the air flows through a diffuser back into the open air. A recirculation is possible inside of a hangar, and testing is then independent of the weather coditions. Most of the time the fan is mounted at the end of the wind tunnel. A long diffuser enables a high pressure recovery, but this is also associated with higher construction costs; in very long diffusers the losses due to wall friction are increased.
The advantages of an Eiffel-type tunnel are its simple construction and its low construction costs. A high quality coefficient can only be obtained, if a refined diffuser with large opening angle – up to $35^o$ – and internal guide vanes are used, in order to avoid flow separation. The guide vanes can cause fouling of the tunnel.
The disadvantage of the Eiffel-type tunnel is given by the necessity, that with an open test section the air stream has to be enclosed by an underpressure chamber. The advantage of low construction costs is then at least in part outweighed by a lower quality coefficient and higher operating costs.

#### Göttingen-Type Wind Tunnel

In wind tunnels of the Göttingen-type after Prandtl the flow medium is circulated from the measuring cross section back to the settling chamber with the aid of diffusers and guide vanes. The optimal widening of the diffusers ($\alpha_{opt}/2 = 3 \div 4^\circ$) requires a minimum length for a given cross section of the test section and a prescribed contration ratio. The fan is to be installed as far away as posible from the test section, so that the disturbances caused by spiralling of the flow and non-uniformities caused by the hub, have space enough to decay.
The advantages of this type of tunnel are the following: If the tunnel has an open test section, the pressure in the air stream is atmospheric and the test section is easily accessible. The quality

coefficient - in particlar with a closed test section - can attain maximum values. The operation is independent of the conditions in the surroundings, as temperature and humidity of the air. The disadvantages are, that the construction costs are high, and a minimum space is needed; if foreign substances are added to the air, e. g. smoke for flow visualization, fouling has to be controlled.

### 6.1.3 Charakteristic Data of a Wind Tunnel

The power of the fan $P_{eff}$ needed for a continuously operated wind tunnel is proportional to the power of the air stream $P_{Str}$ in the test section.
The power of the air stream is $P_{Str} = \dot{m}\, v_\infty^2/2 = \rho\, A_{Str}\, v_\infty^3/2$ (The subscript "$\infty$" denotes the test section).
The constant of proportionality is called the quality coefficient. It is defined as

$$\xi = \frac{P_{Str}}{P_{eff}} \quad . \tag{6.2}$$

The quality coefficient is not the same as an efficiency. In general it exceeds unity and is the higher the smaller the mechanical losses of the wind tunnel are. The electric power needed is usually smaller than the power of the air stream.

$$P_{eff} = \frac{1}{\xi}\frac{\rho}{2}\, A_{Str}\, v_\infty^3 \tag{6.3}$$

Since the power of the air stream is proportional to the third power of $v_\infty$, the power of the fan can increase rapidly to large values. The required power is given in the following table. The values are calculated for a wind tunnel with a cross section of the test section of $A_{Str} = 1\,\mathrm{m}^2$ with atmospheric conditions inside (pressure, density, and temperature).

| $v_\infty$ [ m/s ] | $Ma[-]$ | $P_{Str}$ [ kW ] |
|---|---|---|
| 80 | 0.24 | 314 |
| 340 | 1.0 | $2.5\ 10^4$ |
| 680 | 2.0 | $2.0\ 10^6$ |

With these data it can easily be estimated, that a Göttingen-type wind tunnel needs its own power plant for high subsonic and supersonic velocities to satisfy its power requirements.
The power of the air stream is also proportional to the measuring cross section $A_{Str}$. It is reasonable to assume, that the diameter of the test section is approximately equal to the length of the model, as the following example shows. If the Reynolds similarity law is to be obeyed, one obtains for the length of the models considered:

| | | | |
|---|---|---|---|
| Original e. g. | Automobile | $l = 5$ m; $v = 100$ km/h; | $Re \approx 10^7$ |
| | Airplane | $l = 20$ m; $v = 300$ km/h; $H = 3$ km; | $Re \approx 10^8$ |
| Modell e. g. | Automobile | $l = Re\ \mu/\rho\, v = 1.85$ m | |
| | Airplane | $l = 18.5$ m | |

For the above examples it is assumed, that these Reynolds numbers can be attained at atmospheric conditions and at most at a maximum speed of $v_\infty = 80\ m/s$ in the model tests.
Wind tunnels for low speeds therefore have to be as large as possible, so that the similarity laws can be obeyed. The exceptions to be mentioned here are flows about bodies, of which the force coefficient does not strongly depend on the Reynolds number.

#### Power Balance of a Göttingen-Type Wind Tunnel

The power to be provides by the fan is:

$$P_{eff} = \dot{Q}\, \Delta p_{tot.} = A_{Str}\, v_\infty\, \Delta p_{tot.} \tag{6.4}$$

$\dot{Q}$ = Volume rate of flow
$\Delta p_{tot.}$ = Difference of the total pressure up- and downstream from the fan

$$\Delta p_{tot.} = \Delta p_{Loss} = \sum \zeta_i \frac{\rho}{2} v_i^2 \quad . \tag{6.5}$$

The subscript "$i$" refers to the corresponding components causing the losses, e.g. diffuser, turning corner, etc. To be able to compare, all loss coefficients are referenced to the dynamic pressure $\rho\, v_\infty^2/2$ in the test section.

$$\Delta p_{Loss} = \sum \zeta_{i\infty} \frac{\rho}{2} v_\infty^2 \tag{6.6}$$

The quality coefficient is

$$\xi = \frac{1}{\sum \zeta_{i\infty}} \tag{6.7}$$

**Losses of Mechanical Energy in a Göttingen-Type Wind Tunnel**

The characteristic orders of magnitudes of the losses of mechanical energy in a Göttingen-type wind tunnel are listed in the following table:

| Nr. compare. page 240 | construction part | $\zeta_i$ | $\zeta_{i\infty}$ | Percentage % |
|---|---|---|---|---|
| 9 | Test section open<br>(Test section closed) | 0.11<br>(0.016) | 0.11 | 33 |
| 10 | Collector (friction) | s.u. | | |
| 11 | 1. Diffuser | 0.06 | 0.06 | 18 |
| 12 | 1. Turning corner | 0.15 | 0.03 | 9 |
| 1 | Fan | 0.05 | 0.007 | 2 |
| 2 | 2. Turning corner | 0.15 | 0.03 | 9 |
| 3 | 2. Diffuser | 0.06 | 0.025 | 7.5 |
| 4 | 3. Turning corner | 0.15 | 0.006 | 1.75 |
| 5 | 4. Turnng corner | 0.15 | 0.006 | 1.75 |
| 6 | Screens a. Straightener | 3.0+0.2 | 0.04 | 12 |
| 7 | Nozzle (friction) | s. b. | | |
| 8 | Edge of nozzle<br>Friction ($\lambda = 0.01$) | | 0.02 | 6 |
| | | | $\sum = 0.334$ | $\sum = 100\%$ |

9 Test section: The air stream in an open test section causes much larger losses due to the mixing at its edge, than in a closed test section, which causes only wall friction.

10 Collector: Variable Geometry or slots guarantee proper ouflow for different volume flow.

11, 3 Diffuser: To avoid separation an opening angle of $\alpha/2 = 3 \div 4°$ cannot be exceeded; this requirement may result in large construction lengths. Short diffusers with large opening angles are also built; flow separation is avoided by guide vanes.

12, 2, 4, 5 Turning corners: For structural reasons, most of the time they are built as profiled cascades; curved plates, used as cambered surfaces can bring about substantial improvements.

1 Fan: The size of the hub, the motor can be mounted in, also depends on structural and acoustic conditions; disturbances due to swirl in the flow are compensated by guide wheels. Instead of a large fan, often several smaller fans are used for better controllability. Adjustable blades are also installed, in order to attain a optimal efficiency at partial load.

6 Screens and straighteners: Several screens with different mesh size exhibit a more favorable ratio of the damping of the turbulent fluctuations and the drag than a comparable single screen. Straighteners often are built out of honeycomb profiled cascades. Empirically determined standard values are available for the ratios of the spacing, diameter of the tunnel, and the chord of the cascade.

7 Nozzle: The contraction ratio and the contour are the most important quantities that determine the flow uniformity in the test section.

Small winglets, also called Seiferth wings, are mounted near the edge of the nozzle to avoid the formation of vortex rings and velocity oscillations in the air stream.

Friction: The inner walls of the tunnel should be as smooth as possible; steps between the various parts of the tunnel should be avoided.

For the example given in the table there results

$$\xi = \frac{1}{\sum \zeta_{i\infty}} = \frac{1}{0.334} = 3$$

The electric power needed for this tunnel with $A_{Str} = 1\,\mathrm{m}^2$ and atmospheric conditions of the air in the stream would be

$$P_{el} = \frac{P_{Str}}{\xi\, \eta_{el}\, \eta_{fan}} = \frac{314\ \mathrm{kW}}{3 \cdot 0.94 \cdot 0.8} = 140\ \mathrm{kW}$$

### 6.1.4 Method of Test and Measuring Technique

For determining the characteristic data of the tunnel the following measurements were carried out in the experiment:

1. Measurement of the velocity distribution in the measuring cross section at a fixed distance from the edge of the nozzle.
2. Investigation of the directional sensitivity of the Prandtl tube.
3. Determination of the quality coefficient of the wind tunnel for several wind speeds.

#### Measurement of the Velocity with a Prandtl Tube

The difference between the total pressure and the static pressure at free-stream conditions is measured at two points, the stagnation point and a point on the wall, parallel to the direction of the free stream (sketch see page 241)

$$p_{tot.} - p_\infty = \frac{\rho}{2} v_\infty^2 = q_\infty \quad . \tag{6.8}$$

In the experiment the pressure difference $q_\infty$ is measured with a liquid manometer. In order to obtain $v_\infty$ the density $\rho$ has to be determined

$$\rho = \frac{p}{R\,T} = \frac{Ba\ g \cdot 13.6}{R\,T}\ \frac{\mathrm{Ns}^2}{\mathrm{mm\ Hg\ m}^3} \quad . \tag{6.9}$$

The barometric pressure $Ba$ [mm Hg] and the temperature T [K] are measured. The gas constant of air is for 1 bar and 273 K

$$R = 287\ \frac{\mathrm{m}^2}{\mathrm{s}^2\mathrm{K}} \quad .$$

**Liquid Manometer (U-Tube Prinziple)**

**Betz-Manometer:** In comparison to the simple U-tube the Betz-Manometer (sketched on page 241) has one narrow stem (measuring tube) and a wide stem (pot).
Principle:

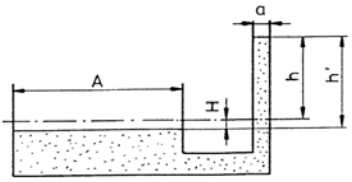


$$h\,a = H\,A \tag{6.10}$$

$$h + H = h' \tag{6.11}$$

$$h/h' = \frac{1}{1 + a/A} \tag{6.12}$$

The data are read on a scale, which is attached to a float and moves with the fluid column in the stem. The scale division $h$ is distorted, compared to the actual height of the fluid $h$'. There is only one reading position.

**Inclined-Tube Manometer:** In order to increase the accuracy of the reading, the scale stem of the inclined-tube manometer is inclined (see sketch on page 242).

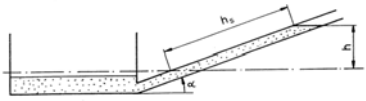


$$h_s = \frac{h}{\sin\alpha}\ ; \qquad \alpha \text{ for large } h_s$$

**Stagnation Tube – Venturi Tube**

The sensitivity of the stagnation tube is limited:
In air: 4 m/s is equivalent to 1 mm $H_2O$
1 m/s is equivalent to 0.0625 mm $H_2O$ at atmospheric conditions of the air.
In comparison to the stagnation tube the reading sensitivity of the Venturi tube can be improved by changing the ratio of the cross sections of the two measuring positions (see the following sketch).

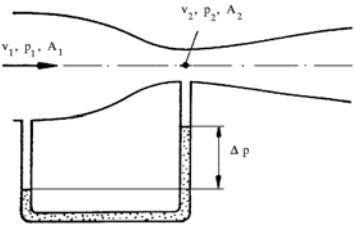


$$p_1 - p_2 = \frac{\rho}{2} v_1^2 \left[ \left( \frac{A_1}{A_2} \right)^2 - 1 \right] \tag{6.13}$$

$$\text{Theor.: } p_1 = p_\infty (v_1 = v_\infty) \tag{6.14}$$

$$\Rightarrow \quad \underbrace{\Delta p = \frac{\rho}{2} v_\infty^2}_{\text{for stagnation tube}} \quad \left[ \left( \frac{A_1}{A_2} \right)^2 - 1 \right] \tag{6.15}$$

**Nozzle-Calibration Factor**

The nozzle-calibration factor is defined as

$$\vartheta = \frac{q_\infty}{\Delta p_{sc}} \quad . \tag{6.16}$$

The quantity $\Delta p_{sc}$ is proportional to the dynamic pressure $q_\infty$. It is important for measurements, since it can be used to determine the velocity without having a measuring probe interfere with the model.

$$\Delta p_{sc} = p_{sc} - p_a, \qquad q_\infty = p_g - p_\infty \tag{6.17}$$

The pressure in the settling chamber $p_{sc}$ (compare. test assembly page 242) is approximately equal to the total pressure $p_g(v = 0)$. Often the static pressure in the air stream is set equal to the ambient pressure, which is only approximately true. In reality the surrounding air is entrained into the air stream. Thereby the edge-streamline of the air stream is curved, and the following can be observed:

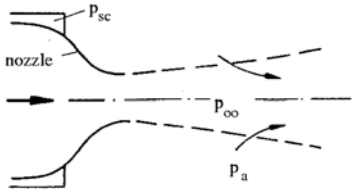


$$p_\infty > p_a; \qquad p_\infty - p_a > 0 \tag{6.18}$$

$$\Delta p_{sc} = q_\infty + p_\infty - p_a \tag{6.19}$$

$$\Delta p_{sc} > q_\infty \tag{6.20}$$

**Measurement of the Quality Coefficient**

$$\text{Quality Coefficient} = \frac{\text{Power of air stream}}{\text{Power of fan}} = \frac{P_{Str}}{P_{eff}} = \xi \tag{6.21}$$

$$\text{Power of air stream} = P_{Str} = \frac{\rho}{2} A_{Str} v_\infty^3 \tag{6.22}$$

The power of the air stream can be obtained from the measurement of the velocity, the barometric pressure, and the temperature. The power of the fan, $P_{eff}\,\eta_{el}\,\eta_G$, is determined by measuring the voltage and the current of the armature and the exciter field of the direct-current motor of the wind tunnel. The ratio of these two quantities yields the quality coefficient.

**Other Methods for Measuring the Velocity**

With the Prandtl and the Venturi tube, the velocity is determined by measuring a pressure difference. Methods which use other principles are:

1. Measurement of a force: The drag of a body – its dependence on the free-stream velocity is assumed to be known – is measured (Example: The Robinson anemometer).
2. Heat-transfer measurement: The larger the velocity of the flow over a heated body, the larger the heat transfer from the body to the cold flow becomes (Example: hot film, hot wire).
3. Optical Doppler effect: The frequency shift of an incident light ray and its reflexion from particles, moving with the velocity of a flow, can be used to determine the flow velocity (Example: Laser-Doppler anemometer).

**Selected References:**

Prandtl, L.: *Führer durch die Strömungslehre, 6. Aufl.*, Vieweg-Verlag, 1965, S.301 ff.

Wuest, W.: *Strömungsmeßtechnik,* Vieweg-Verlag, 1969.

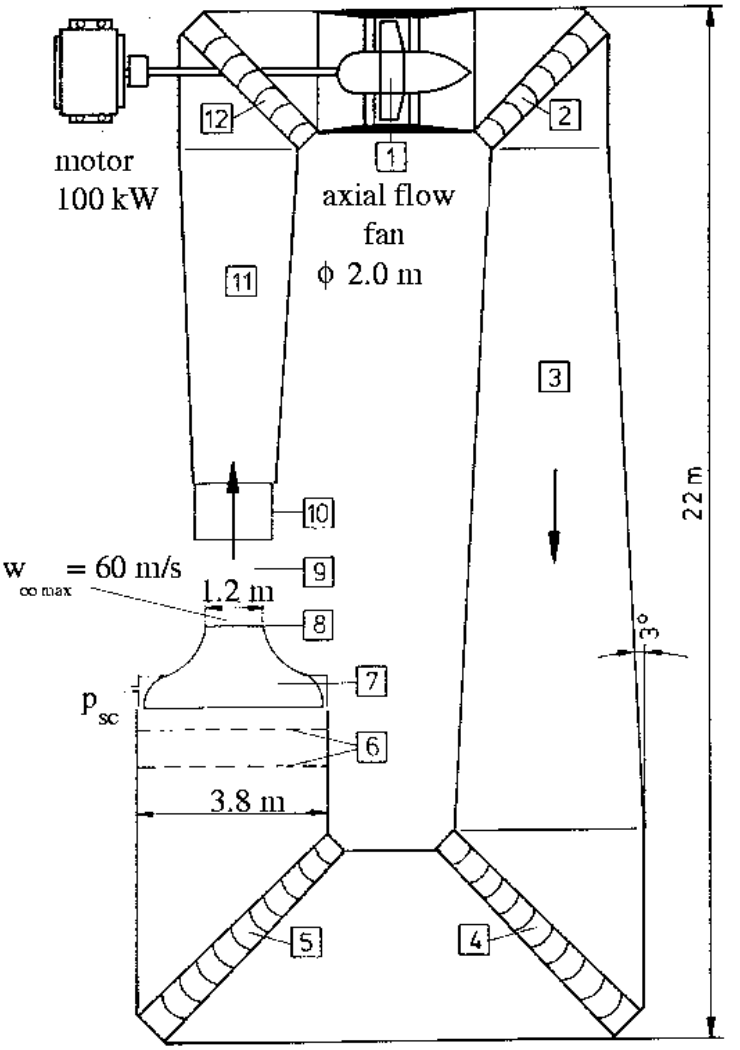


Wind tunnel of the Aerodynamisches Institut

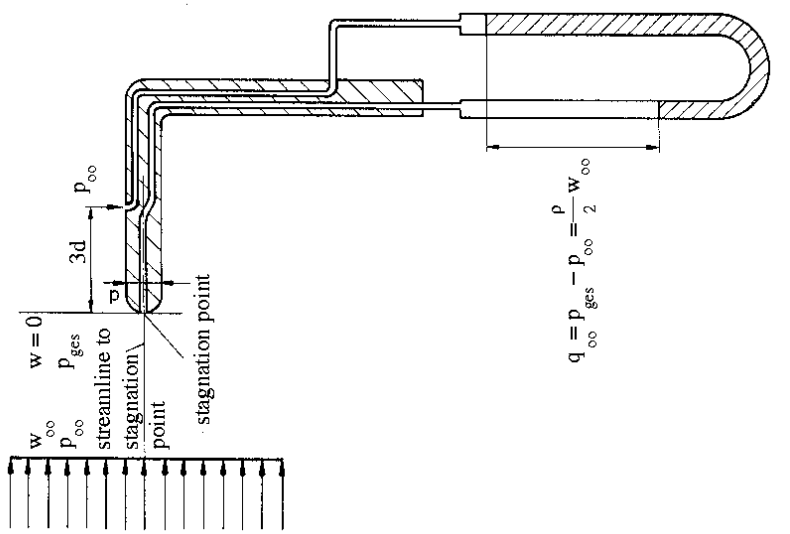


Prandtl tube

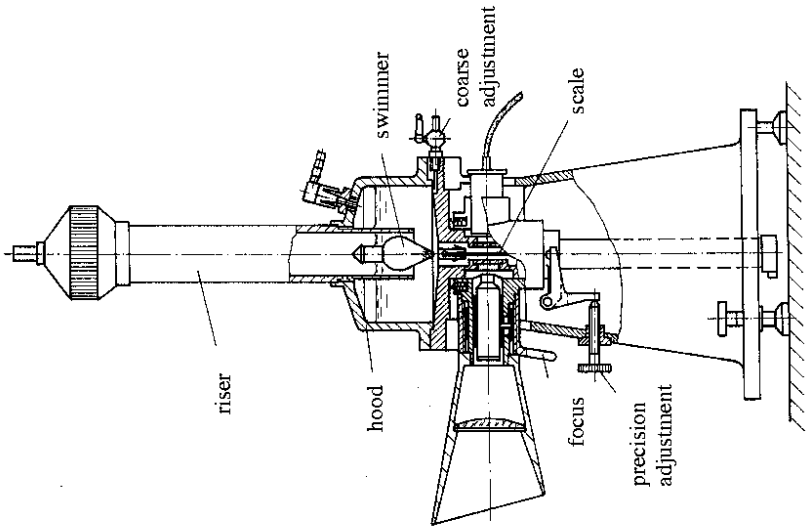


Projection-manometer after Betz

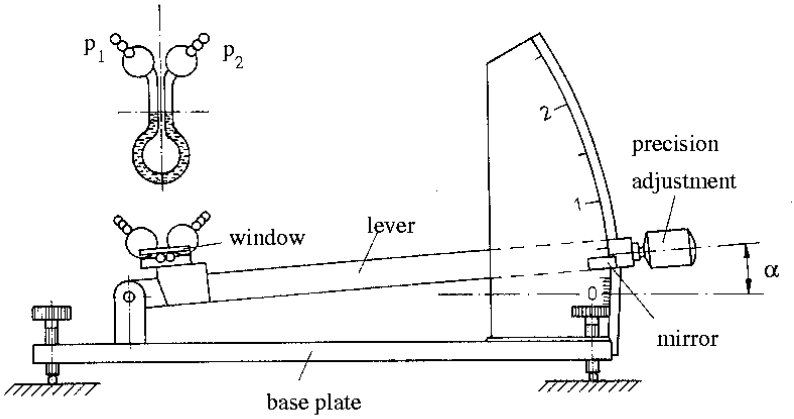


Lever micro manometer after Betz

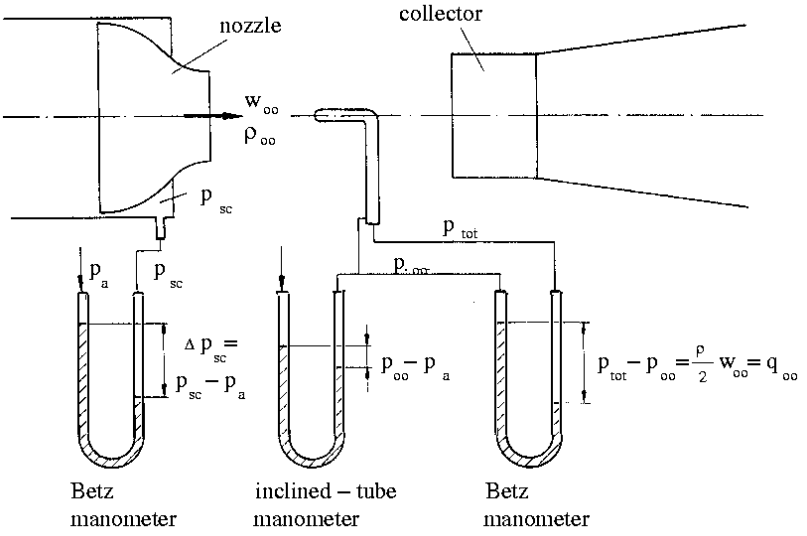


Test assembly

### 6.1.5 Evaluation

1. Draw the following diagram of the measured data:

$$q_\infty = f(z)_{\beta=0^\circ,\ x=\text{const.}}$$

$$q_\infty = f(\beta)_{z=0,\ \text{const.}}$$

$$\xi = f(v_\infty)$$

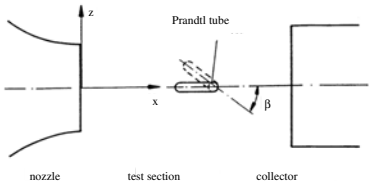


| Quantity | Formula | Dimension | Measured data | | | | | |
|---|---|---|---|---|---|---|---|---|
| $\Delta p_{sc}$ | Measurement | mm $H_2O$ | 20 | 40 | 60 | 80 | 120 | 160 |
| $q_\infty$ | Measurement | mm $H_2O$ | s. b. | | | | | |
| $Ba$ | Measurement | mm Hg | 749.44 | | | | | |
| $p_a \approx p_\infty$ | $Ba\ 13.6\ g\ \frac{\text{N s}^2}{\text{mm Hg m}^3}$ | N / $m^2$ | $0.99987\ 10^5$ | | | | | |
| $t_\infty$ | Measurement | °C | 22.4 | 22.5 | 22.8 | 23.1 | 23.4 | 24.2 |
| $\rho_\infty$ | $p_\infty / R\,T_\infty$ | kg / $m^3$ | 1.18 | 1.179 | 1.178 | 1.178 | 1.176 | 1.172 |
| $v_\infty$ | $\sqrt{2\,q_\infty\,g/\rho_\infty}$ | m / s | 18.2 | 25.8 | 31.6 | 36.5 | 44.7 | 51.75 |
| $\dot{Q}_\infty$ | $A_{Str.}\ v_\infty$ | $m^3$ / s | 21.7 | 30.8 | 37.7 | 43.6 | 53.4 | 61.8 |
| $n$ | Measurement | $\text{min}^{-1}$ | 239.5 | 335.6 | 409.1 | 469.7 | 567.9 | 659.2 |
| $u$ | $\pi n D_p/60$ | m / s | 25.1 | 35.14 | 42.8 | 49.2 | 59.5 | 69.0 |
| $\lambda$ | $\frac{\dot{Q}_\infty}{u\,D_p^2\,\pi/4[1-(d_N/D_p)^2]}$ | −− | 0.37 | 0.37 | 0.37 | 0.38 | 0.38 | 0.38 |
| $\eta_G(\lambda)$ | from diagram | −− | 0.8 | 0.8 | 0.8 | 0.77 | 0.77 | 0.77 |
| $I_A$ | Measurement | $A$ | 55 | 90 | 128 | 165 | 240 | 330 |
| $U_A$ | Measurement | $V$ | 63 | 89 | 108 | 124 | 150 | 167 |
| $I_E$ | Measurement | $A$ | 3 | 3 | 3 | 3 | 3 | 3 |
| $U_E$ | Measurement | $V$ | 204 | 205 | 204 | 206 | 205 | 206 |
| $P_A$ | $I_A\,U_A$ | $W$ | 3465 | 8010 | 13824 | 20460 | 36000 | 55110 |
| $P_{We}$ | $P_A\,\eta_{el}$ | $W$ | 3181 | 7353 | 12690 | 18782 | 33048 | 50591 |
| $P_{eff}$ | $P_{We}\,\eta_G$ | $W$ | 2544.8 | 5882.4 | 10152.0 | 11462 | 25447 | 38955 |
| $P_{Str}$ | $A_{Str}\,\rho_\infty/2\,v_\infty^3$ | $W$ | 4247 | 12088 | 22191 | 34169 | 62705 | 96969 |
| $\xi$ | $P_{Str}/P_{eff}$ | −− | 1.67 | 2.1 | 2.2 | 2.36 | 2.5 | 2.5 |
| $\Delta p_{sc}$ | $\approx q_\infty$ | $\frac{\text{N}}{\text{m}^2}$ | 196.2 | 394.4 | 588.6 | 784.8 | 1177.2 | 1569.6 |
| | | | | | | | | |

| $\lambda$ | 0.2 | 0.25 | 0.3 | 0.35 | 0.4 |
|---|---|---|---|---|---|
| $\eta_G$ | 0.83 | 0.89 | 0.89 | 0.85 | 0.72 |

$A_{Str} = A_n = 1.194\,\text{m}^2$ ; $D_p = 2\,\text{m}$ ; $d_N/D_p = 0.5$ ;

$\eta_{el} = 0.918$ ; $\lambda$ = ratio of forward circumferential velocity $= \dfrac{\text{Axial velocity}}{\text{circumferential velocity}}$

$1\,\text{mm Hg} = 13.6\,\text{mm } H_2O$; $1\,\text{mm } H_2O = 1\,\text{kp / m}^2$ ; $1\,\text{kp} = 9.81\,\text{N}$;

$1\,\text{Nm} = 1\,H_2O = 1\,\text{J}$; $R = 287\dfrac{\text{Nm}}{\text{kg K}} = 287\dfrac{\text{m}^2}{\text{s}^2\ \text{K}}$ for air at 1 bar and 273 K

$q_\infty = f(z)$

| $z$[m] | $q_\infty$[mm $H_2O$] | $q_\infty$[N/m$^2$] |
|---|---|---|
| 0 | 116.6 | 1143.85 |
| 0.1 | 116.9 | 1146.79 |
| 0.2 | 117.2 | 1149.73 |
| 0.3 | 117.4 | 1151.69 |
| 0.4 | 117.4 | 1151.69 |
| 0.5 | 117.6 | 1153.66 |
| 0.55 | 117.4 | 1151.69 |
| 0.575 | 114.7 | 1125.21 |
| 0.6 | 48.5 | 475.79 |
| 0.625 | 1.0 | 9.81 |
| 0.65 | 0 | 0 |

$$1\text{mm } H_2O = 1\,\frac{\text{kp}}{\text{m}^2} = 9.81\,\frac{\text{kg}}{\text{sec}^2\,\text{m}} = 9.81\,\frac{\text{N}}{\text{m}^2}$$

$q_\infty = f(\beta)$

| $\beta$[<°] | $q_\infty$[mm $H_2O$] | $q_\infty$[N/m$^2$] |
|---|---|---|
| 0 | 116.5 | 1142.87 |
| 5 | 116.9 | 1146.79 |
| 10 | 115.1 | 1129.13 |
| 15 | 109.6 | 1075.18 |
| 20 | 100.6 | 986.89 |
| 25 | 92.3 | 905.46 |
| 30 | 79.3 | 777.93 |

a)

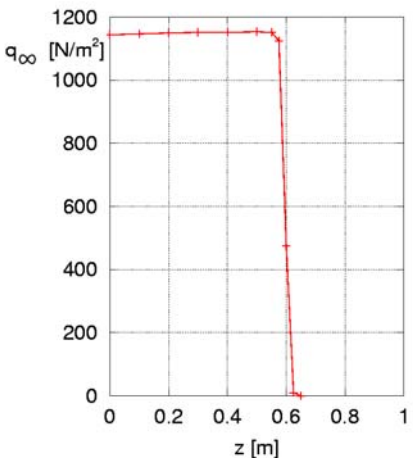

b)

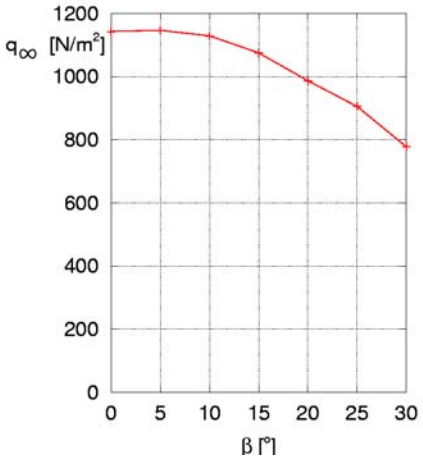


c)

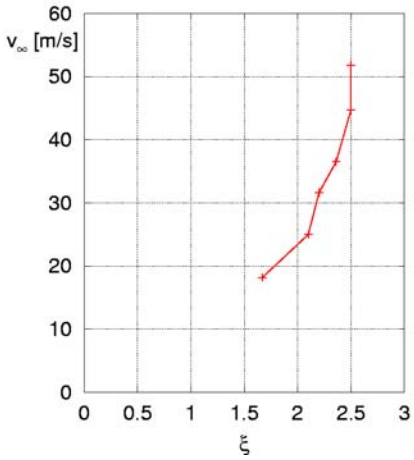


The dynamic pressure $q_\infty$ was not measured for this series of measurements, since

$$q_\infty = p_g - p_\infty \text{ and } p_\infty \approx p_a.$$

With

$$p_g \approx p_{sc} \text{ and } \Delta p_{sc} = p_{DV} - p_a$$

there results

$$\Delta p_{sc} = q_\infty + p_\infty - p_a$$
$$\Rightarrow q_\infty = \Delta p_{sc} \quad .$$

2. How large is the nozzle-calibration factor $\vartheta$?

$$\vartheta = \frac{q_\infty}{\Delta p_{sc}} \quad \text{with} \quad q_\infty = 1143.85\,\frac{\text{N}}{\text{m}^2}$$

(from series of measurements for diagram 1.a)

$$\Delta p_{sc} = 120\,\text{mm}\ H_2O = 1177.2\frac{\text{N}}{\text{m}^2}$$
$$\Rightarrow \vartheta = 0.972 \quad .$$

3. The power needed for a Göttingen-type, return-circuit wind tunnel is approximately 180 kW for a velocity of 80 m/s and a measuring cross section of the air stream of 1.2 m$^2$, all losses included.

a) What power would be needed for an Eiffel-type tunnel with 80 m/s and 1.2 m$^2$ cross section, which sucks the air through a straight tube out of the open air and returns it without pressure recovery? The frictional losses can be neglected! ($\rho = 1.25\,\text{kg/m}^3$)

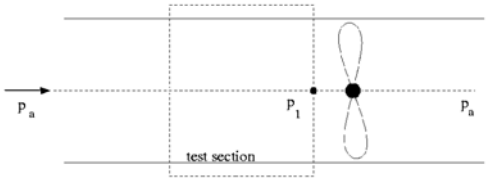


$$v_\infty = 80\,\frac{\text{m}}{\text{s}}; \quad A_{Str.} = 1.2\,\text{m}$$
$$\Rightarrow N_{Str.} = \frac{9}{2}\,A_{Str.} v_\infty^3 = 384\,\text{kW}$$
$$N_{eff} = 180\,\text{kW} \text{ Göttingen-type tunnel}$$
$$Ma = 0.24 \Rightarrow \text{ air } \approx \text{ incompressible}$$

Momentum equation

$$\begin{aligned} \rho\, v^2\, A &= (p_a - p_1)\, A \\ \Delta p &= p_2 - p_1 = p_a - p_1 \end{aligned}$$

$$\begin{aligned} P &= \dot{Q}\,(p_{02} - p_{01}) \\ \dot{Q} &= v\, A_{Str.} \end{aligned}$$

$$p_{02} - p_{01} = p_2 + \frac{\rho}{2}\, v^2 - p_1 - \frac{\rho}{2}\, v^2 = \Delta p$$

$$\begin{aligned} P &= v\, A_{Str.}\, \Delta p \\ P &= \rho\, v^2\, A_{Str.} \\ P &= 770\,\text{kW} \end{aligned}$$

b) What power is needed for the same Eiffel tunnel, if a short diffuser is installed downstream from the test section? The length of the short diffuser is assumed to be 2 m, its angle of inclination is $\alpha/2 = 3°$. Flow separation is avoided by guide vanes; wall friction can be neglected.

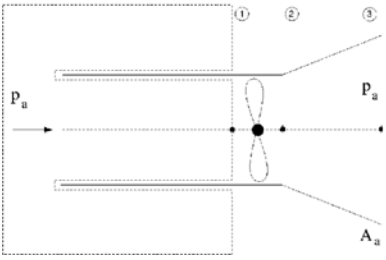


Momentum equation:

$$\rho\, v_1^2\, A_{Str.} = \Delta\, A_{Str.}$$

$$\Delta p = p_a - p_1 = 8000\,\frac{\text{N}}{\text{m}^2}$$

Bernoulli equation for cross sections $2 \to 3$:

$$\begin{aligned} p_2 + \frac{\rho}{2}\, v_2^2 &= p_a + \frac{\rho}{2}\, w_3^2; \quad v_1 = v_2 \quad v_3 = v_1 \frac{A_{Str.}}{A_n} \\ p_2 - p_1 &= p_a + \frac{\rho}{2}\, v_1^2 \left(\frac{A_{Str.}}{A_n}\right)^2 - \frac{\rho}{2}\, v_1^2 - p_a + \Delta p \\ p_2 - p_1 &= \Delta p + \frac{\rho}{2}\, v_1^2 \left[\left(\frac{A_{Str.}}{A_n}\right)^2 - 1\right] \\ N_{eff} &= \dot{Q}\,(p_2 - p_1) = v_1\, A_n \left[\Delta p + \frac{\rho}{2}\, v_1^2 \left[\left(\frac{A_{Str.}}{A_n}\right)^2 - 1\right]\right] \\ N_{eff} &= 485\,\text{kW} \end{aligned}$$

4. If a subsonic wind tunnel of the Göttingen type is built as compressed-air tunnel, the Reynolds number can be increased by increasing the density $\rho$. To what value is the Reynolds number increased, if for the same power of the fan the density is raised to three times of its original value? The temperature of the air is assumed to be the same, and the loss coefficients $\sum \zeta_i$ of the tunnel are assumed to be independent of the Reynolds number.

$$N_{eff} = A_{Str.}\, v_\infty^3 \sum \xi_{i1}\, \frac{\rho}{2} = const. \Rightarrow v_1^3\, \rho_1 = v w_2^3\, \rho_2$$

$$\begin{aligned} &\text{Subscript 1} \;:\; \rho_1 \\ &\text{Subscript 2} \;:\; \rho_2 = 3\,\rho_1 \end{aligned}$$

$$\begin{aligned} \frac{Re_1}{Re_2} &= \frac{v_1\, l_1\, \rho_1}{\mu_1}\, \frac{\mu_2}{v_2\, l_2\, \rho_2} = \frac{v_1}{v_2}\, \frac{\rho_1}{\rho_2} = \sqrt[3]{\frac{\rho_2}{\rho_1}}\, \frac{\rho_1}{\rho_2} = \sqrt[3]{3}\, \frac{1}{3} = 0.48 \\ \left(\frac{v_1}{v_2}\right)^3 &= \frac{\rho_2}{\rho_1} \Rightarrow Re_2 = 2.08\, Re_1 \end{aligned}$$

## 6.2 Pressure Distribution on a Half Body

*Abstract*

In this experiment the distribution of the static pressure on the surface of an axially symmetric half body is measured in an incompressible flow. An analytic expression is derived for the description of the contour with the aid of the potential theory by superposing a spherical source and a parallel flow. The theoretical pressure distribution is compared with experimentally determined values. In the experiment the Betz projection, the multiple-tubed, the inclined-tube, and the micromanometer are used. The Hele-Shaw flow is discussed for flow visualization purposses .

### 6.2.1 Determination of the Contour and the Pressure Distribution

#### Derivation of the Equation for the Contour with the Potential Theory

In the experiment the pressure distribution is measured on the rounded part of a half body, i. e. of a half-infinitely long, cylindrical body. Such a body can be generated with the potential theory by superposing a spherical source, positioned on the $z$-axis with a flow, parallel to the $z$-axis.

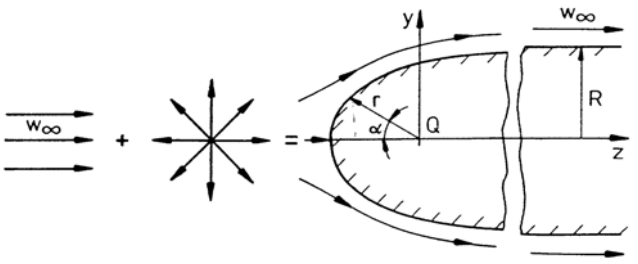


$$\phi_{superp.} = v_\infty \, z - \frac{Q}{4\pi r} \tag{6.23}$$

The expressions for the velocity componets can be written as:

$$v_x = \frac{\partial \phi}{\partial x} = \frac{Q}{4\pi} \frac{x}{r^3} \tag{6.24}$$

$$v_y = \frac{\partial \phi}{\partial y} = \frac{Q}{4\pi} \frac{y}{r^3} \tag{6.25}$$

$$v_z = \frac{\partial \phi}{\partial z} = \frac{Q}{4\pi} \frac{z}{r^3} + v_\infty \tag{6.26}$$

For reasons of continuity the fluid leaving the source can flow only inside the half body. There results

$$Q = \pi \, v_\infty \, R^2 \qquad . \tag{6.27}$$

The part of the parallel flow, that flows in a cylinder of radius $y$ about the $z$-axis, is equal to that part of the source flow, that flows in the opposite direction of the oncoming parallel flow inside the cylinder.

$$\pi\, y^2\, v_\infty = \frac{Q\,(1-\cos\alpha)}{2} \tag{6.28}$$

The flow is axially symmetric with respect to the $z$-axis. In order to determine the contour of the half body, the meridional plane is considered, and with (6.28) one obtains the equation describing the contour in the following form:

$$\frac{r}{R} = \frac{\sin\alpha/2}{\sin\alpha} = \frac{1}{2\cdot\cos\alpha/2} \quad , \tag{6.29}$$

The angle $\alpha$ is the angle between the negative $z$-axis and the projection of the radius vector $r$ on the meridional plane.

**Derivation of the Equation for the Pressure Distribution**

Since in a potential flow the Bernoulli equation is valid in the entire flow field and on its boundary, the pressure and the dimensionless pressure coefficient can immediately be determined for the contour of the half body:

$$c_p = \frac{p-p_\infty}{\rho/2\cdot v_\infty^2} = 1-\left(\frac{v}{v_\infty}\right)^2 \tag{6.30}$$

with

$$v^2 = v_x^2 + v_y^2 + v_z^2 \quad .$$

The components of the local velocity vector $w$ again result from the superposition of the source flow with the parallel flow. Equation (6.29) inserted into (6.30) yields the expression for the pressure coefficient

$$c_p = 1 - 4\sin^2\frac{\alpha}{2} + 3\sin^4\frac{\alpha}{2} \quad . \tag{6.31}$$

### 6.2.2 Measurement of the Pressure

In the experiment the static pressure is measured at 12 measuring points on the half body just described, through small boreholes in the surface, which are connected with manometers. Four manometers with different sensitivity are used:

| | Measuring range [mm $H_2O$] | Accuracy of measurement |
|---|---|---|
| Multiple-tubed manometer | 800 | 5/10 |
| Betz projection manometer | 400 | 1/10 |
| Inclined-tube manometer | 80 | 1/10 |
| Betz lever micro manometer | 2.5 | 1/100 |

**Error Sources**

1. The angle between the surface normal and the axis of the borehole is not exactly zero.

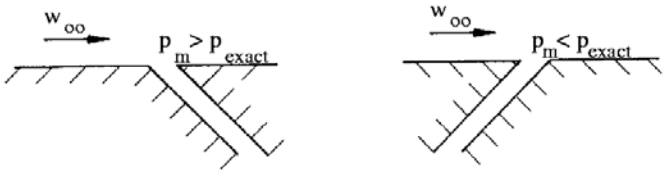

2. The roughness, or burr, and chamfers or radii at the edge of the borehole disturb the flow in the borehole and falsify the measurement.
3. Dimension size of the boreholes:
   Some of the influences of the dimension sizes of the borehole on the error of measurement are described by Wuest in [Wuest 1969]. According to his findings the error of measurement increases approximately linear with the diameter of the borehole $d$ (the measured values are too large). The following relation is often used for describing the error of measurement $\Delta p$:

$$\frac{\Delta p}{\tau_0} = f\left(Re_\tau, \frac{l}{d}\right) \qquad \text{with} \qquad Re_\tau = \frac{d}{\nu}\sqrt{\frac{\tau_0}{\rho}} \tag{6.32}$$

($\tau_0$ = wall shear stress)

Also the depth of the borehole $l$ is of importance. In the following two diagrams, taken from [Wuest 1969], curves describing the influence of the ratio $l/d$ and of the ratio burr height to diameter $\varepsilon/d$ on the error of measurement, are depicted:

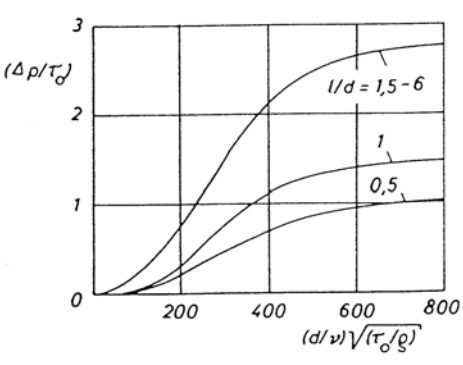


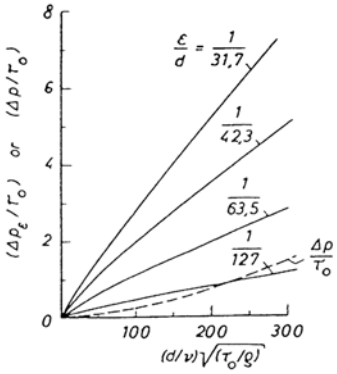


According to [Liepmann 1967] the diameter $d$ should be smaller than one fifth of the boundary-layer thickness, otherwise the borehole could produce disturbances in the outer flow.
The connecting tube between borehole and manometer should be as short as possible in order to keep the transit time of the pressure measuring system as short as possible. The flow restistance in the tubes and the elasticity of the tubes result in finite measuring times: The exact pressure can only asymptotically be registered by the measuring device [Wuest 1969].

**Comparison of the Results**

Differences between the pressure distribution determined with the potential theory and the experimental data are explained by the fact, that the influence of the boundary layer on the pressure distribution was not taken into account. In the boundary layer the velocity increases from zero at the wall (Stokes no-splip condition), asymptotically to the local value of the external flow, which can be considered as inviscid and therefore be computed with the potential flow theory. In the boundary layer the pressure is constant in the direction normal to the wall, and the static pressure along the wall is therefore imposed by the external flow. The external flow is displaced by the boundary layer away from the body.

### 6.2.3 The Hele-Shaw Flow

The Hele-Shaw flow [Schlichting und Gersten 1997] is a creeping flow between two parallel flat plates, separated from each other by a small distance. Although the flow is governed by viscous forces, it can be described with a solution, which in form is identical with that of the potential

theory. If it is assumed that the Reynolds number is small and that the ratio of the distance between the plates and the length of the plates $h/L << 1$, the equations of motion can be simplified.

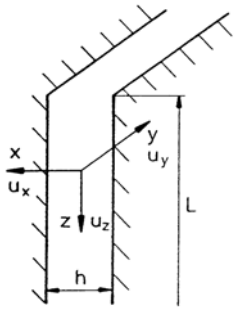


$$0 = -\frac{\partial p}{\partial x}$$

$$0 = -\frac{\partial p}{\partial y} + \mu \frac{\partial^2 w_y}{\partial x^2} \tag{6.33}$$

$$0 = -\frac{\partial p}{\partial z} + \mu \frac{\partial^2 w_z}{\partial x^2} + \rho g \tag{6.34}$$

It follows from (6.34) that the pressure does not depend on $x$. The other two equations can be integrated in the $x$-direction, with the boundary conditions given by the no-slip condition on the plates, and the velocity field can be obtained.

$$u_y = \frac{1}{2\mu}\frac{\partial p}{\partial y}\left(x^2 - \frac{h^2}{4}\right) \quad ; \qquad u_z = \frac{1}{2\mu}\left(\frac{\partial p}{\partial z} - \rho g\right)\left(x^2 - \frac{h^2}{4}\right) \tag{6.35}$$

The results reveal the following properties of the Hele-Shaw flow:

1. The streamlines exhibit the same patterns in all planes $x = \text{const.}$
2. In every plane $x = \text{const.}$ the velocity can be expressed by the gradient of a scalar function, i.e.

$$u_y = \frac{\partial \varphi}{\partial y} \quad ; \qquad u_z = \frac{\partial \varphi}{\partial z} \quad \text{with} \quad \varphi = \frac{1}{2\eta}\left(p - \rho g z\right)\left(x^2 - \frac{h^2}{4}\right) \quad . \tag{6.36}$$

**Selected References**

Schlichting, H., Truckenbrodt, E.: *Aerodynamik des Flugzeugs 1. Band,* 2. Aufl., Springer-Verlag, 1967, S. 62 ff.

Truckenbrodt, E. *Strömungsmechnanik*, Springer Verlag. 1968, S. 104.

Wieghardt, K. *Theoretische Strömungslehre*, Teubner Studienbücher, 1969.

Wuest, W. *Strömungsmesstechnik,* Uni-Tex, Vieweg-Verlag, 1969.

Liepmann, H.W, Roshko, A.: *Elements of gasdynamics,* 8th printing, Wiley, Galcit Aeronautical Series, 1967.

Schlichting H., Gersten K.: *Grenzschicht-Theorie*, Verlag-Springer, Berlin/Heidelberg 1997.

### 6.2.4 Evaluation

1. Draw the contour of the half body in the scale 1:1, and plot the measured and theoretically determined pressure distribution ($c_p$) versus the $z$-coordinate.

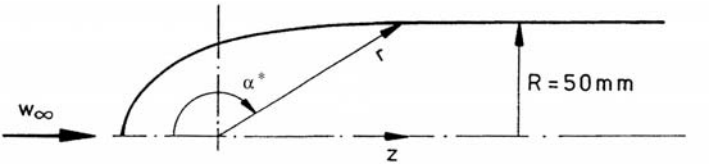


| $\alpha^*[^o]$ | 0 | 20 | 30 | 45 | 60 | 90 | 110 | 120 | 135 | 150 | 160 | 180 |
|---|---|---|---|---|---|---|---|---|---|---|---|---|
| | | | | | | | | | | | | |
| $r$[mm] | 25 | 25.4 | 25.9 | 27 | 28.9 | 35.3 | 43.6 | 50 | 65.3 | 96.5 | 144 | $\infty$ |
| $c_{p_{Pot}}$ | 1 | 0.882 | 0.745 | 0.478 | 0.187 | –0.25 | –0.334 | –0.312 | –0.224 | –0.12 | –0.057 | 0 |

| Meas. position | $z$ [mm] | * $\Delta p$ [mm $H_2O$] | $c_{p_{exp}}$ | Measuring instrument Measuring range / Accuracy [mm $H_2O$] |
|---|---|---|---|---|
| 1 | –25 | 80 | 1 | Betz projection manometer ( 400 / ~ 1/10 ) |
| 2 | –23 | 62 | 0.772 | Multiple-tubed manometer ( 800 / ~ 5/10 ) |
| 3 | –17 | 26 | 0.324 | |
| 4 | –10 | –2 | –0.025 | |
| 5 | + 5 | –23 | –0.286 | |
| 6 | +20 | –25 | –0.311 | |
| 7 | +40 | –18 | –0.224 | |
| 8 | +75 | –11 | –0.137 | |
| 9 | +125 | –5 | –0.062 | |
| 10 | +195 | –1.3 | –0.016 | Betz projection manometer |
| 11 | +275 | –1.01 | –0.0126 | inclined-tube manometer |
| 12 | +355 | 0.03 | 0.0004 | micro manometer 2.5 / ~ 1/100 |

* Measuring position 1–10 [mm $H_2O$]
11–12 [mm Alk.]

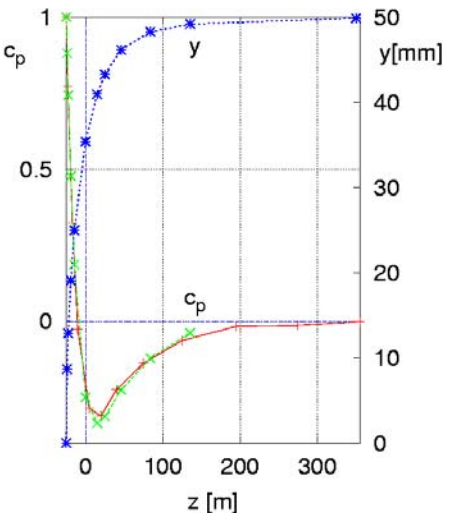


$$c_{p_{exp}}: \quad q_\infty = \vartheta\ \Delta p_{sc}$$

$$\begin{aligned} c_p &= \frac{p - p_\infty}{\frac{\varrho}{2} v_\infty^2} = \frac{p - p_\infty}{q_\infty} \\ c_{pi} &= \frac{p_i - p_a}{\Delta p_{sc}}\ \frac{1}{\vartheta} + 1 - \frac{1}{\vartheta} \\ \vartheta &\approx 1 \\ c_{pi} &= \frac{p_i - p_a}{\Delta p_{sc}} \end{aligned}$$

With:

$$\Delta p_{sc} = 80.3 \text{ mm Wg} = 787.74\ \frac{\text{N}}{\text{m}^2}$$

$$\begin{aligned} v_\infty &= \sqrt{\frac{2\ q_\infty}{\rho}} = 36.2\ \frac{\text{m}}{\text{s}} \\ \rho &= \frac{Ba[\text{mm Hg}]\ 13.6\ \text{g}}{R\ T} = 1.2\ \frac{\text{kg}}{\text{m}^3} \end{aligned}$$

2. Sketch the multiple-tubed manometer and state why the reading of the pressure difference does not depend on the pressure above the measuring fluid in the supply container.

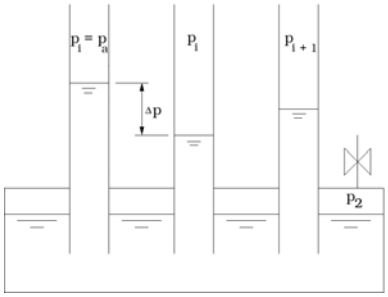


$$\Delta p = p_i - p_1 = \rho\ g\ (h_i - h_1) \neq f(p_2)$$

Only pressure differences are measured, and consequently the reading is independent of the constant pressure $p_2$.

3. Determine the position (angle $\alpha$) on the contour of the half body, where the pressure is equal to $p_\infty$. Consider the Prandtl tube: Why is the borehole for measuring the static pressure not placed in this position?
$p = p_\infty \Rightarrow c_p = 0$
$c_{p0} = 1 - 4\ \sin^2(\frac{\alpha_0}{2}) + 3\ \sin^4(\frac{\alpha_0}{2}) = 0;$
the zero position is determined numerically with the method of interval bisecting for $\alpha_0\ \varepsilon\ [69°, 70°]$ from diagram resp. interpolation; $\Delta\alpha = 0{,}1;\ \epsilon = 0.0001.$
$\alpha_0 = 69.54°$; from diagram: $\alpha_0 = 69°$
It can be seen in the diagram, that $dc_p/d\alpha$ and $dc_p/dz$ are large at the position in question, so that small errors can cause large inaccuracies in the measurement of the pressure with the Prandtl tube.
4. Why can it not be expected – not even for a technically perfect pressure measurement – that the measured data agree completely with the results computed with the potential theory?
In order to be able to apply the potential theory it is necessary to assume inviscid flow. The actual flow is viscous, and for a sufficiently high Reynolds number a boundary layer is formed on the measuring probe, which causes a displacement of the inviscid external flow. This influence is not taken into account in the potential theory.
5. Can a three-dimensional potential flow be visualized with the Hele-Shaw flow?
The Hele-Shaw flow is a creeping motion between two parallel plane plates, a small distance apart from each other. A three-dimensional potential flow cannot be visualized with the Hele-Shaw flow, since the curl of the velocity vector does not vanish because of the influence of the viscous forces.

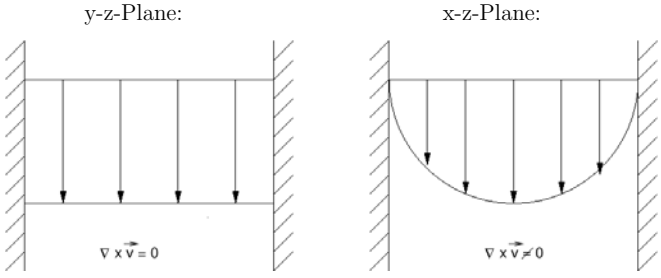


It can be shown, that the velocity components, averaged over the gap between the plates can be derived from a potential, and it can be concluded that the flow of a viscous fluid is analogous to an irrotational flow with regards to the velocity components averaged over the gap between the two plates.

## 6.3 Sphere in Incompressible Flow

*Abstract*

The drag coefficient of the sphere is to be measured in a wind tunnel as a function of the Reynolds number of the free stream *Re*. The flow velocity of the air is less than 50 m/s, and compressibility effects do not come into play. The variation of the drag coefficient with the Reynolds number *Re* will be discussed, also the influence of the intensity of turbulence of the air stream, the roughness of the surface of the sphere, and the support of the sphere in the wind tunnel.

### 6.3.1 Fundamentals

#### Flow Around the Sphere According to the Potential Theory

The flow around the sphere can be determined with the potential theory by superposing a three-dimensional dipole with a parallel flow.

$$\phi = u_\infty x + \frac{M}{4\pi r^2}\cos\Theta \tag{6.37}$$

With this ansatz the pressure distribution on the sphere is

$$c_p = \frac{p - p_\infty}{\frac{\rho}{2}u_\infty^2} = 1 - \frac{9}{4}\sin^2\Theta \quad . \tag{6.38}$$

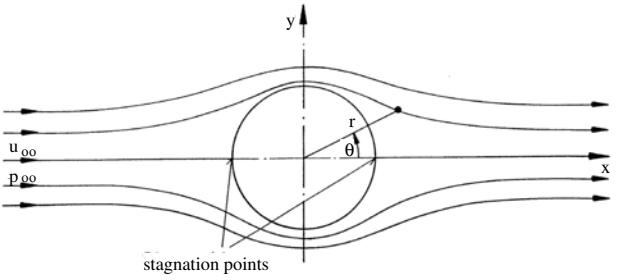


The pressure distribution is symmetric with respect to the $y$-axis; it follows that the resulting drag force is zero – in contrast to all experience – (*The d'Alembert Paradox*).
In the following diagram the pressure distribution obtained with the potential theory is compared with the results of measurements by O. Flachsbart [Flachsbart 1927].

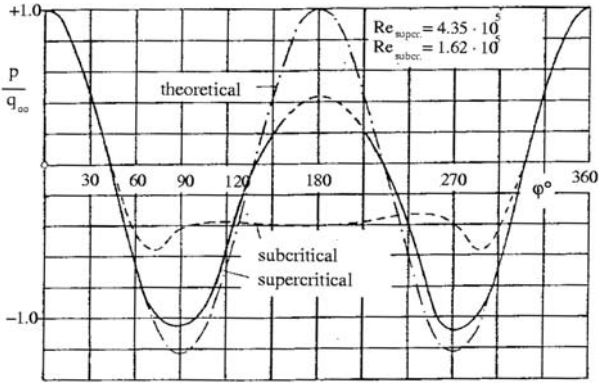

**Viscous Flow Around a Sphere**

If a sphere is positioned into an air stream, the flow exerts a force in the direction of the oncoming flow (drag), which is usually described by the drag coefficient.

$$c_D = \frac{F_D}{\frac{\rho}{2} u_\infty^2 A} \tag{6.39}$$

with

$$\begin{aligned} F_D &= \text{Drag force} \\ \frac{\rho}{2} u_\infty^2 &= \text{Dynamic pressure of the free stream} \\ A &= \text{Cross-sectional area} \end{aligned}$$

The drag coefficient $c_D$ was determined in numerous experiments as a function of the Reynolds number $Re$ [Wieselsberger 1914, Bacon 1924, Reid 1924, Flachsbart 1927, Fage 1936, Möller 1937, Achenbach 1972, Bailey 1974].
At moderate Reynolds numbers, ranging from $10^3$ to $10^6$, the drag coefficient $c_D$ can be measured in relatively small wind tunnels (e.g. in the wind tunnel of the Aerodynamisches Institut). Very low and very high Reynolds numbers require other experimental techniques:
At very low Reynolds numbers the drag coefficient $c_D$ is determined by measuring the sinking speed of small spheres in highly viscous fluids; Reynolds numbers $Re > 10^6$ can be obtained either in wind tunnels with a large measuring cross section, compressed-air tunnels, or in towing experiments in the free atmosphere.
Stokes was able to obtain a closed-form solution for very low Reynolds numbers (creeping motion), by neglecting the inertia forces in comparison to the frictional forces. The result of his theory is

$$c_D = \frac{24}{Re} \quad , \tag{6.40}$$

which agrees well with experimental data for Reynolds numbers $Re < 1$. An extension of the Stokes theory by Oseen, who considered the influence of the inertia forces on the flow in the far field, yielded a solution similar to the one provided by Stokes, but it could not be applied to higher Reynolds numbers. For high Reynolds numbers the value of the drag coefficient mainly depends on the position of the separation point of the boundary layer.

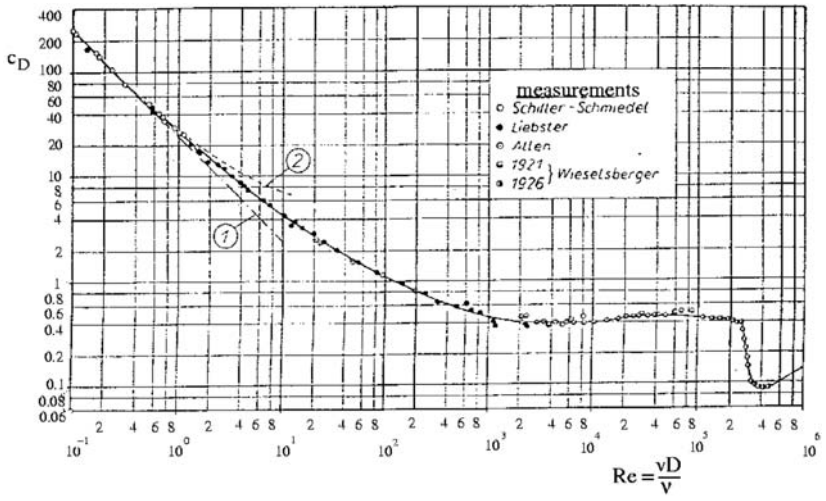

The above diagram shows the drag coefficient as a function of the Reynolds number after H. Schlichting [1982]; curve(1): Theory of Stokes; curve(2): Theory of Oseen.
For $10^3 < Re < 2 \cdot 10^5$, $c_D$ remains almost constant at $\approx 0.4$. This regime is called the *subcritical* regime, since the boundary layer on the sphere remains laminar. On the front part of the sphere the flow is accelerated, and a part of the mechanical energy is used up by the friction forces in the boundary layer. The pressure rise on the rear part strongly decelerates the flow; the kinetic energy of the flow in the boundary layer is diminished and the flow cannot attain the the total pressure at the rearward stagnation point as predicted by the potential theory. The flow separates, and a large "dead-water region" is formed. With increasing Reynolds number the separation point moves downstream on the sphere close to the equator ($\alpha \approx .80°$).
Since in the dead-water region the static pressure is approximately equal to the value obtained with the potential theory for the separation point, the pressure distribution on the sphere is asymmetrical, and a high pressure drag results.

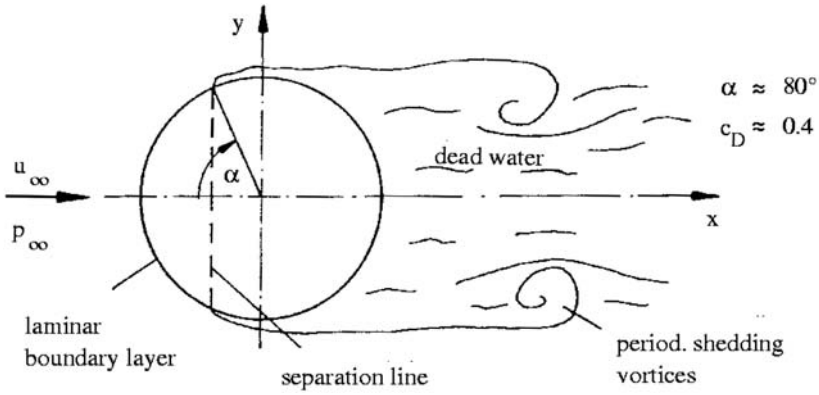


In the supercritical regime $4 \cdot 10^5 < Re < 10^6$ the laminar boundary layer undergoes transition to turbulent flow on the front part of the sphere, a certain distance downstream from the stagnation point.
Due to the turbulent momentum transport in the boundary layer, additional kinetic energy is transported into the fluid layers near the wall, replacing a part of the energy consumed by the frictional forces. The velocity profile is now fuller. The boundary layer can now longer withstand the increasing pressure and separates further downstream ($\alpha \approx .120°$). The diameter of the dead-water region is smaller, and the pressure is higher, so that the drag of the sphere is reduced (see the following sketch).
The laminar-turbulent transition can already be enforced in the subcritical Reynolds number regime by imposing a disturbance on the laminar boundary layer. A ring of a thin wire (called tripping wire) is mounted along a "parallel of latitude", shortly upstream of the equator. With this experiment Prandtl proved his hypothesis, according to which the abrupt drop of the drag coefficient $c_D$ is caused by the flow in the boundary layer.
The regime between the sub- and supercritical regime is called the *critical* regime, in which the drag coefficient decreases rapidly. The position and the shape of the curve of the drag coefficient in this regime are influenced by several factors, as reflected in the deviation of the results of various experimentators from each other (see the following diagram, provided by Achenbach).

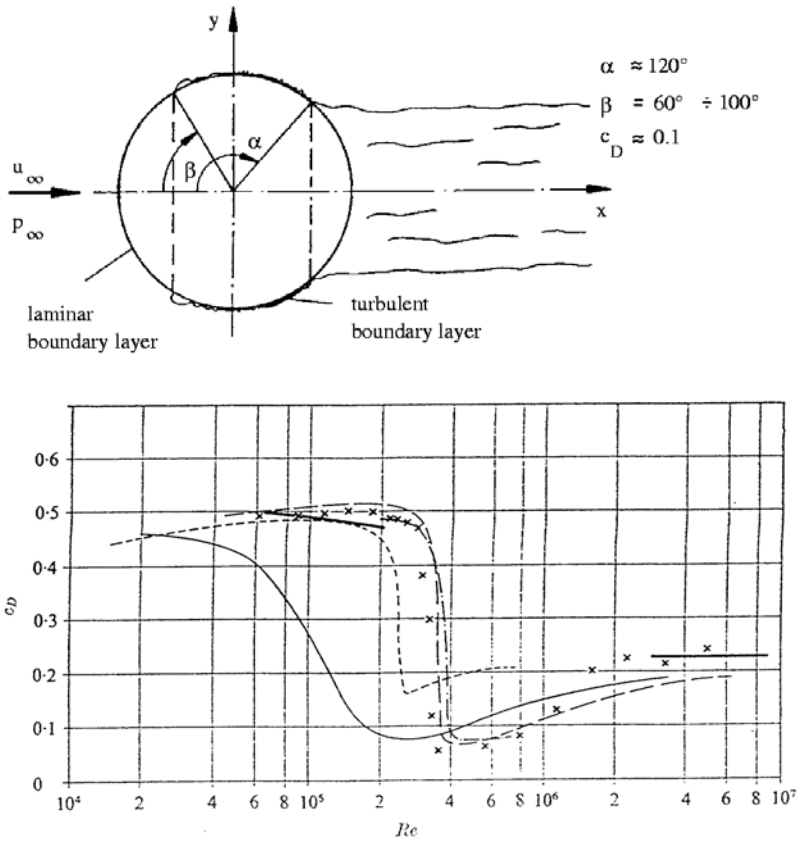


From E. Achenbach [1972] Drag coefficient of the sphere as a function of the Reynolds number; comparison of data of the literature. —, Wieselsberger (1922); —, Bacon & Reid (1924); – · –, Millikan & Klein, free-flight (1933); — , Maxworthy (1969). Achenbach [1974]: – –, with wire strain gauge; x, by integration.

In the so-called *transcritical* regime $Re > 10^6$ a slow increase of the drag coefficient $c_D$ from 0.1 to $c_D \approx 0.2$ is noted. The separation point moves upstream, and periodic vortex shedding is observed downstream from the sphere, similar to the subcritical regime. If the transcritical regime $Re > 10^6$ is not accesssible with the available experimental facility, the flow behavior of this regime can be simulated by mounting a "separation wire"[1] on the rear part of the sphere. Thereby a clearly defined separation line is provided for the turbulent boundary layer.
If the transition of the boundary layer is enforced with a tripping wire on the front part of the sphere, the drag coefficient does not drop to the value $c_D \approx 0.1$, but only to $c_D \approx 0.22$. Obviously the tripping wire does not only influence the laminar-turbulent transition, but also the position of the separation point of the turbulent boundary layer . The details of this behavior of the flow, so far could not be sufficiently clarified and are still subject to ongoing research.

[1] The separation wire is to be distinguished from the tripping wire, which, when mounted on the front part of the sphere in the laminar part of the boundary layer, causes transiton to turbulent flow.

### 6.3.2 Shift of the Critical Reynolds Number by Various Factors of Influence

Since the abrupt drop of the drag coefficient $c_D$ is observed for a certain Reynolds number regime $Re$, the *critical Reynolds number* ($Re_{crit.}$) is defined as the Reynolds number, for which the drag coefficient is $c_D = 0.3$. The first measurements in the transcritical regime were conducted in 1912 and 1914. *Eiffel* determined a drag coefficient of $c_D = 0.176$ in 1912. *Prandtl* repeated the measurements in 1914 and obtained a drag coefficient of $c_D = 0.44$ for the same Reynolds numbers. Only later, more accurate experiments could clarify this apparent discrepancy. It was shown that the drag coefficient depends on the following factors of influence: Reynolds number, intensity of turbulence of the free stream, surface roughness, support of the sphere, and heat transfer.

#### Intensity of Turbulence of the Free Stream

An increase of intensity of turbulence of the free stream shifts the transition of the boundary layer and also the abrupt drop of the drag coefficient to lower Reynolds numbers (see the following diagram).

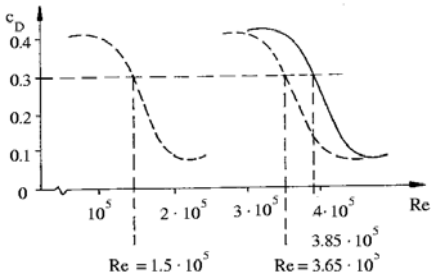


$Re_{crit.} = 1.5 \cdot 10^5$ windtunnel of poor quality (high turbulence intensity)

$Re_{crit.} = 3.65 \cdot 10^5$ windtunnel of good quality (low turbulence intensity)

$Re_{crit.} = 3.85 \cdot 10^5$ max. value reached in free atmosphere (practically zero turbulence intensity)

The highest critical Reynolds number is obtained in measurements in the free atmosphere, it is:

$$Re_{crit.} = 3.85 \cdot 10^5$$

The turbulent fluctuations seem to have little influence on $Re_{crit.}$, since the characteristic length scales of the turbulent eddies are one order of magnitude larger than the boundary-layer tickness of the sphere.

One of the main objectives of wind tunnel testing is to carry out measurements with models of airplanes, the full-scale configurations of which are to be flown in the free atmosphere. Since in many cases the separation of the boundary layer is of greatest interest, it is understandable, that the intensity of turbulence of the wind tunnel is adjusted to that of the free atmosphere. The extreme sensitivy of the critical Reynolds number of the flow around the sphere with regards to the intensity of turbulence of the free stream is used to determine the quality of the wind tunnel with respect to turbulence.

A turbulence factor $TF$ is defined as:

$$TF = \frac{Re_{crit.}(\text{free atmosphere})}{Re_{crit.}(\text{wind tunnel})} > 1 \quad (6.41)$$

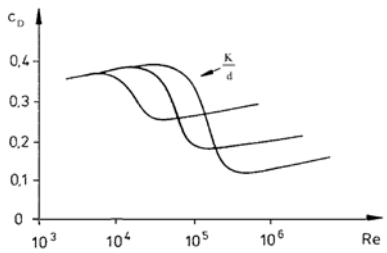


#### Surface Roughness

An increase of roughness of the surface of the sphere affects the flow behavior in a fashion similar to an increase of the intensity of turbulence or the mounting of a tripping wire (see diagram).

$\frac{K}{d}$ = characteristic roughness height, referenced to diameter of the sphere

**Support of the Sphere**

If possible, the support of the sphere should be attached to the sphere in the dead-water region. Otherwise the boundary layer on the sphere could be disturbed (see the following sketch).

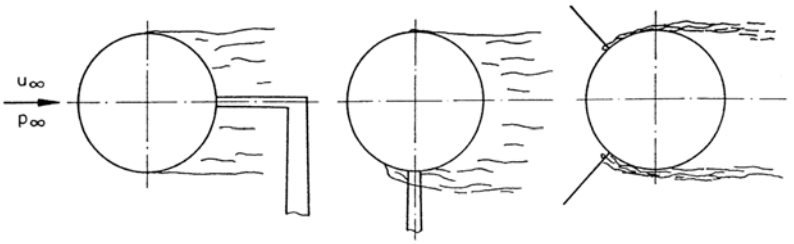


a) Spindle in the dead water b) Suspended crosswise c) Suspended by wires

Bacon and Reid [1924] showed that the drag can be 2.5 times larger if a transverse spindle is used instead of a spindle in the dead-water region.

If the sphere is suspended by wires, turbulent wakes are generated by the wires, which affect the measurement. Special attention has to be paid to mechanical oscillations of the suspension, since they can falsify the measurements markedly.

### 6.3.3 Method of Test

The drag of a sphere is measured for Reynolds numbers $2 \cdot 10^5 < Re < 5 \cdot 10^5$ with the balance in the wind tunnel. The sphere is mounted in the test section with a swordlike support and a spindle, connected to the balance (see sketch). Since in the measurement of the force also the drag of the swordlike support is contained, a second experiment is necessary, in which the drag of the sword is determined. This is done by mounting a mock-up of the sphere upstream of the spindle, so that the same flow is generated around the swordlike support, without connecting the mock-up with the spindle (see sketch). In a third experiment a tripping wire is attached to the front part of the sphere, and the flow is kept at subcritical conditions. In this experiment the abrupt drop of the drag coefficient $c_D$ can be observed.

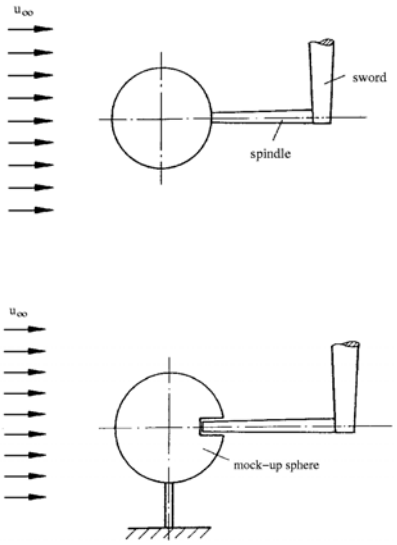


**Selected References**

Achenbach, E.: *Experiments on the flow past spheres at very high Reynoldsnumbers*, J. Fluid Mech., Vol. 54, 1972, Part 3, S. 565-575.

Achenbach, E.: *Vortex shedding from spheres*, J.F.M., 62, 1974, S.209-221.

Bacon, D.L., Reid , E.G.: *The resistance of spheres in wind tunnels and in air*, NACA Rep. 185, 1924.

Bailey, A.B.: *Sphere drag coefficient for subsonic speeds in continuum and free molecular flows*, J.F.M., 65, 1974, S.401-410

Eck, B.: *Technische Strömungslehre, 5. Aufl*, Springer-Verlag, 1957, S. 69, 205, 243, 255.

Fage, A.: *Experiments on a sphere at critical Reynolds numbers*, Aero. Res. Counc. R&M, no. 1766, 1936.

Flachsbart,O.: *Neuere Untersuchungen über den Luftwiderstand von Kugeln*, Phys. Z., 28, 1927, S. 461.

Möller, W.: *Experimentelle Untersuchungen zur Hydrodynamik der Kugel*, Dissertation, Leipzig, 1937, oder Phys. Z., 39, 1938, S. 57-80.

Prandtl, L.: *Über den Luftwiderstand von Kugeln*, Göttinger Nachrichten, 177, 1914.

Schlichting, H. *Grenzschichttheorie, 1. Aufl*, Verlag Braun, Karlsruhe, 1951, S.15-19,33,81.

Tietjens, O.: *Strömungslehre, 1. Band*, Springer-Verlag, 1960, S. 171, 174.

Truckenbrodt, E.: *Strömungsmechanik*, Springer-Verlag, 1968, S. 103, 353, 500-501

### 6.3.4 Evaluation

1. The drag force is to be plotted as function of the dynamic pressure $q_\infty$ of the free stream: $F_{D_s} = f(q_\infty)$
   The dynamic pressure is determined with the pressure in the settling chamber $\Delta p_{sc}$ of the wind tunnels:

$$q_\infty \left[\frac{\mathrm{N}}{\mathrm{m}^2}\right] = \Delta p_{sc}[\text{mm } \mathrm{H_2O}] \cdot g \left[\frac{\mathrm{N}}{\mathrm{m}^2}/\text{mm } \mathrm{H_2O}\right] \cdot \vartheta \tag{6.42}$$

$$\begin{aligned} g &= \text{Gravitaional acceleration} \\ \vartheta &= \text{Nozzle calibration factor } = 0.98[--] \end{aligned}$$

   The drag force is determined with the mass $M$ placed on the balance after the formula:

$$F_D[\mathrm{N}] = M[\mathrm{kg}] \cdot g \left[\frac{\mathrm{m}}{\mathrm{s}^2}\right] \cdot K_c \tag{6.43}$$

$$\begin{aligned} K_c &= \text{Callibration factor of the balance} = 1 \\ g &= \text{Gravitational acceleration} = 9.81 \left[\frac{\mathrm{m}}{\mathrm{s}^2}\right] \end{aligned}$$

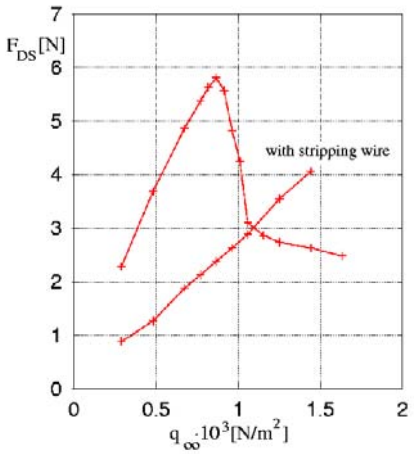


In order to obtain the drag of the sphere, the total drag of the sphere and the support must be reduced by the drag of the support (comp. Sect. 4).

$$F_{D_s} = F_{D_{tot..}} - F_{D_{sup..}} \tag{6.44}$$

The abrupt drop of the drag coefficient $c_D$, caused by the laminar-turbulent transition, depends on several factors of influence: Intensity of turbulence of the free stream; the model support; method of test, (distinguished are the direct and integrated measurement); the measuring probes or the boreholes for the pressure measurements can influence the flow); roughness of the surface of the sphere and possible heat transfer from the sphere to the flow.

2. The drag coefficient $c_D$ is to be plotted as function of the Reynolds number $Re$:
The drag coefficient is defined as

$$c_D = \frac{F_{D_s}}{q_\infty A_s} \tag{6.45}$$

with $A_s$ = projection area of the sphere = $0.0163\,\mathrm{m}^2$

$$Re = \frac{u_\infty\, D_s}{\nu} \tag{6.46}$$

with

$$u_\infty = \sqrt{\frac{2q_\infty}{\rho}}$$

and

$$\rho\left[\frac{\mathrm{kg}}{\mathrm{m}^3}\right] = \frac{Ba[\text{mm Hg}] \cdot 13.6\left[\frac{\text{mm } H_2O}{\text{mm Hg}}\right] \cdot g\left[\frac{\mathrm{N}}{\mathrm{m}^2}/\text{mm } H_2O\right]}{R\left[\frac{\mathrm{Nm}}{\mathrm{kg\ K}}\right] \cdot T[\mathrm{K}]} \tag{6.47}$$

$\rho$ = density

$Ba$ = barometric pressure density ratio
Hg to $H_2$ O = $13.6\left[\frac{\text{mm } H_2O}{\text{mm Hg}}\right]$

$g$ = gravitational acceleration

$R$ = gas constant of air
= $287.14\left[\frac{\mathrm{Nm}}{\mathrm{kg}} \cdot \mathrm{K}\right]$

$T$ = temperature

$D_s$ = diameter of the sphere
= 0.144 [m]

$\nu$ = kinematic viscosity $\left[\frac{\mathrm{m}^2}{\mathrm{s}}\right]$
(from table)

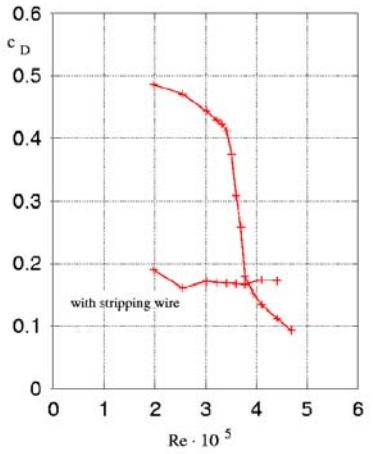


If measurements of different wind tunnels are compared, the test conditions have to be considered. For example, the intensity of the free stream, which depends on the wind tunnel used, can markedly influence the result. In earlier investigations this effect was not taken into account, as the intensity of turbulence was not known yet.

3. Determine the critical Reynolds number with the curve $c_D = f(Re)$ for $c_D = 0.3$.
   $Re_{crit.} = 3.6 \cdot 10^5$ from diagram
   With increasing flow velocity the influence of the compressibility of the air on the flow can be noted. Then the Mach number has to be introduced, so that the drag coefficient does not only depend on the Reynolds number but also on the Mach number of the free stream, i. e. $c_D = f(Ma, Re_\infty)$. This influence can be noted for $Ma_\infty > 0.3$.
4. Determine the intensity of turbulence of the wind tunnel:
   $TF = \frac{3.85 \cdot 10^5}{Re_{crit.\ (c_D=0.3)}} > 1$
   $TF = \frac{3.85 \cdot 10^5}{Re_{crit.}} = 1.07$.

| *Not.* | $\Delta p_{sc}$ | $q_\infty$ | $M_{tot.}$ | $F_{D_{tot.}}$ | $M_{susp.}$ | $F_{D_{susp.}}$ | $F_{D_s}$ | $c_D$ | $u_\infty$ | *Re* |
|---|---|---|---|---|---|---|---|---|---|---|
| *Dim.* | mm $H_2O$ | N/m$^2$ | g | N | g | N | N | – | m/s | $10^5$ |
| 1 | 30 | 288.4 | 245 | 2.403 | 12 | 0.118 | 2.285 | 0.486 | 22.75 | 1.97 |
| 2 | 50 | 480.7 | 400 | 3.924 | 24 | 0.235 | 3.689 | 0.471 | 29.37 | 2.54 |
| 3 | 70 | 673 | 531 | 5.21 | 35 | 0.343 | 4.867 | 0.444 | 34.75 | 3.01 |
| 4 | 80 | 769.1 | 585 | 5.74 | 37 | 0.363 | 5.377 | 0.429 | 37.15 | 3.01 |
| 5 | 85 | 817.2 | 613 | 6.014 | 39 | 0.383 | 5.631 | 0.423 | 38.3 | 3.32 |
| 6 | 90 | 865.2 | 636 | 6.24 | 44 | 0.432 | 5.808 | 0.412 | 39.4 | 3.41 |
| 7 | 95 | 913.3 | 620 | 6.082 | 52 | 0.51 | 5.572 | 0.374 | 40.5 | 3.51 |
| 8 | 100 | 961.4 | 550 | 5.396 | 58 | 0.569 | 4.827 | 0.308 | 41.5 | 3.6 |
| 9 | 105 | 1009.4 | 500 | 4.905 | 67 | 0.657 | 4.248 | 0.258 | 42.5 | 3.69 |
| 10 | 110 | 1057.5 | 385 | 3.777 | 69 | 0.677 | 3.1 | 0.18 | 43.56 | 3.77 |
| 11 | 120 | 1153.6 | 370 | 3.63 | 78 | 0.765 | 2.865 | 0.152 | 45.5 | 3.94 |
| 12 | 130 | 1249.8 | 370 | 3.63 | 91 | 0.893 | 2.737 | 0.134 | 47.35 | 4.10 |
| 13 | 150 | 1442 | 370 | 3.63 | 102 | 1.001 | 2.629 | 0.112 | 50.86 | 4.41 |
| 14 | 170 | 1634.3 | 368 | 3.61 | 115 | 1.128 | 2.482 | 0.093 | 54.15 | 4.69 |

**Measurements with tripping wire:**

| *Not.* | $\Delta p_{sc}$ | $q_\infty$ | $M_{tot.}$ | $F_{D_{tot.}}$ | $M_{susp.}$ | $F_{D_{susp.}}$ | $F_{D_s}$ | $c_w$ | $u_\infty$ | *Re* |
|---|---|---|---|---|---|---|---|---|---|---|
| *Dim.* | mm WS | N/m$^2$ | g | N | g | N | N | – | m/s | $10^5$ |
| 1 | 30 | 288.4 | 110 | 1.079 | 19 | 0.183 | 0.893 | 0.19 | 22.75 | 1.97 |
| 2 | 50 | 480.7 | 160 | 1.569 | 31 | 0.304 | 1.265 | 0.161 | 29.37 | 2.54 |
| 3 | 70 | 673 | 230 | 2.256 | 38 | 0.373 | 1.883 | 0.172 | 34.75 | 3.01 |
| 4 | 80 | 769.1 | 265 | 2.59 | 47 | 0.461 | 1.129 | 0.17 | 37.15 | 3.22 |
| 5 | 90 | 865.2 | 295 | 2.894 | 52 | 0.51 | 2.384 | 0.169 | 39.4 | 3.41 |
| 6 | 100 | 961.4 | 325 | 3.188 | 57 | 0.559 | 2.629 | 0.168 | 41.5 | 3.6 |
| 7 | 110 | 1057.5 | 355 | 3.482 | 61 | 0.598 | 2.884 | 0.167 | 43.56 | 3.77 |
| 8 | 130 | 1249.8 | 430 | 4.218 | 68 | 0.667 | 3.551 | 0.197 | 47.35 | 4.10 |
| 9 | 150 | 1442 | 490 | 4.807 | 76 | 0.746 | 4.061 | 0.173 | 50.86 | 4.41 |

## 6.4 Flat-Plate Boundary Layer

*Abstract*

The laminar and turbulent boundary layer generated by an air stream on a flat plate at zero angle of attack is investigated. The density of the air $\rho$ and the dynamic shear viscosity $\mu$ are assumed to be constant. The change of the flow characteristics caused by the laminar-turbulent transition is discussed, and the critical Reynolds number of transition will be determined. The velocity distributions in the laminar and the turbulent part of the boundary layer will be determined in the experiment and compared with theoretical data, obtained with solutions of the boundary-layer equations.

### 6.4.1 Introductory Remarks

For sufficiently high Reynolds numbers, i. e. when the friction forces are small compared to the inertia forces, the flow over a flat plate can be considered as a potential flow except for the region near the wall. Only in this thin layer of thickness $\delta$, the boundary layer, in which the velocity increases from zero to the value $u_\delta$ of the external flow, are the friction forces of the same order of magnitude as the inertia forces.

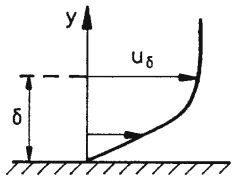


**Characteristic Dimensions of the Boundary Layer**

The boundary-layer thickness $\delta$ is the distance measured from the wall, from where on the velocity $u$ is asymptotically equal to the velocity $u_\delta$ of the outer flow. With experimental accuracy accepted, this requirement is generally satisfied for the distance measured from the wall, where the velocity is about 99% of $u_\delta$.

The displacement thickness $\delta_1$ is a measure for the distance, by which the external flow is displaced from the wall; with $\rho = const.$, the displacement thickness is

$$\delta_1 = \int_0^\infty \left(1 - \frac{u}{u_\delta}\right) dy \tag{6.48}$$

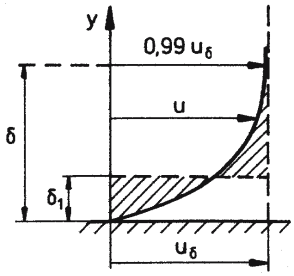


The momentum thickness $\delta_2$ is a measure for the loss of momentum the flow is suffering by the friction forces; for $\rho = const.$, there results

$$\delta_2 = \int_0^\infty \frac{u}{u_\delta}\left(1 - \frac{u}{u_\delta}\right) dy \quad . \tag{6.49}$$

**The Laminar-Turbulent Transition on the Flat Plate**

At relatively low Reynolds numbers the flow is laminar; at high Reynolds numbers the flow in the boundary layer becomes turbulent after a certain laminar starting region. The laminar-turbulent transition sets in at a certain position, designated as $x_{crit.}$. O. Reynolds suggested in 1883 to introduce a thin thread of dye into the flow parallel to the direction of the main flow in order to detect transition (see sketch).

The transition from laminar to turbulent flow in the boundary layer is affected by several quantities, the most important ones being the pressure gradient in the external flow, the roughness of the wall of the plate, and the intensity of turbulence in the flow of the free stream. Small

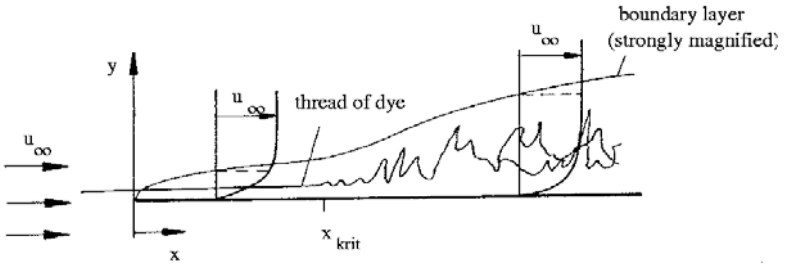


perturbations introduced in the flow in the boundary layer can no longer be damped out anymore by the Stokes stresses, and the flow changes its behavior. First it becomes intermittent, alternating in time between being laminar and turbulent, generating so-called turbulent spots, which appear in irregular intervals of time. They travel downstream. Finally the flow becomes fully turbulent, and velocity fluctuations occur in all three coordinate directions, causing a strong diffusion of the dye, which is then completely spread out in the flow.
While for $x < x_{crit.}$ the thread remains straight in the laminar part of the boundary layer, downstream from $x = x_{crit.}$, the transition point, the thread begins to oscillate irregularly, and for $x > x_{crit.}$ the dye spreads out, caused by the velocity fluctuations in the turbulent part of the boundary layer.
Laminar and turbulent boundary layers are characterized by different boundary-layer thicknesses and velocity distributions. The shear stress at the wall is markedly higher in the turbulent boundary layer. The main quantity influencing the transition of the laminar boundary layer is the Reynolds number $Re_x = u_\infty x/\nu$. The value at which transition occurs, is called $Re_{crit.}$, usually observed between $Re_{crit.} = 10^5$ and $3 \cdot 10^6$. The actual value depends on the

1) shape of the leading edge of the plate,
2) alignment off the plate with respect to the direction of the oncoming flow,
3) technical quality of the surface (roughness, waviness)
4) intensity of turbulence of the free stream.

### 6.4.2 Method of Test

#### Determination of the Critical Reynolds Number of the Plate

The laminar-turbulent transition is first detected with the aid of a hot-wire signal. The hot-wire anemometer is particularly apted for this measurement, since it measures the instantaneous value of the velocity and thereby also the turbulent oscillations of the velocity.

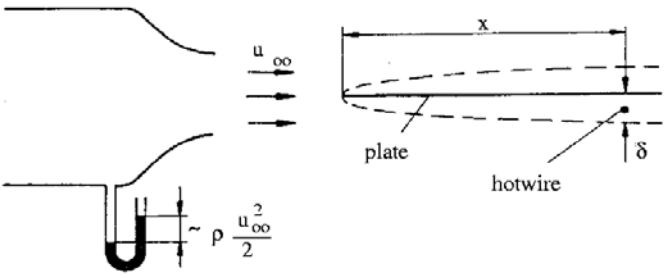

In the experiment the hot wire is positioned shortly upstream of the trailing edge of the plate in the boundary layer. Its signal is recorded with an oscillograph. If the velocity $u_\infty$ is slowly increased, the following signals are observed:

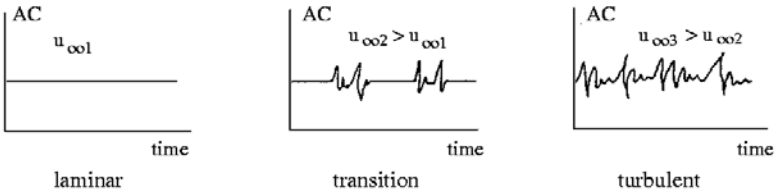


At a certain velocity $u_{\infty\ crit.}$ first fluctuations appear clearly visuable (see the sketch in the middle). The critical Reynolds number is computed with this velocity.

The transition can also be detected by overhearing the boundary layer. A Pitot tube, connected with a stethoscope, is positioned in the boundary layer. The pressure fluctuations, caused by the turbulent velocity fluctuations, can be heard as high-frequency crackling.

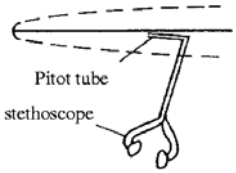


In this experiment the velocity $u_\infty$ is kept constant, and the Pitot tube is held at a constant distance from the wall and moved downstream. The coordinate $x$, where a clear high-frequency crackling is first heard, is used for determining the critical Reynolds number.

**Measurement of the Velocity Distribution**

The velocity distributions are measured with a Pitot tube with a diameter of $0.2\,\mu$m. It is connected with a differential pressure manometer, which measures the following difference:

$$\left(p + \rho\frac{u^2}{2}\right) - p_u \quad ,$$

with $p_u$ being the static pressure outside of the air stream. This difference is approximately equal to

$$\rho\frac{u^2}{2} \quad ,$$

since, in a good approximation, it is

$$p_\infty = p = p_u \quad .$$

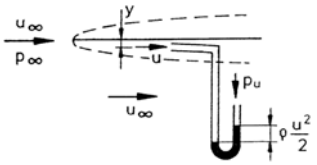


The Pitot tube is held by a support, its distance $y$ from the surface of the plate is varied with a screwed spindle and read on a scale. The diameter of the Pitot tube must be considerably smaller than the thickness of the boundary layer, in order not to falsify the measurements. The dimension sizes of the Pitot tube are given in the sketch in mm.

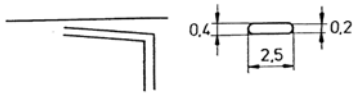

### 6.4.3 Prediction Methods

The differential equations, describing the flow in the boundary layer, are obtained with an order of magnitude estimation of the various term of the Navier-Stokes equations [Schlichting 1982]. For the flat plate at zero incidence they read for steady incompressible flow with constant density and dynamic shear viscosity:

$$\frac{\partial \overline{u}}{\partial x} + \frac{\partial \overline{v}}{\partial y} = 0$$

$$\overline{u}\frac{\partial \overline{u}}{\partial x} + \overline{v}\frac{\partial \overline{u}}{\partial y} = \frac{\mu}{\rho}\frac{\partial^2 \overline{u}}{\partial y^2} - \frac{\partial}{\partial y}\overline{u'v'} \tag{6.50}$$

The quantities $\overline{u}$ and $\overline{v}$ are the time-averaged velocity components in the $x$- and $y$-direction, if the flow is turbulent. The product $\rho\overline{u'v'}$ ist the only term of the Reynolds stress tensor of the turbulent fluctuating motion, that is retained in the boundary-layer formulation. The boundary conditions are:

a) for $y = 0$ : $\overline{u} = 0$ (The Stokes' no-slip condition)
$\overline{v} = 0$ (impermeable wall)

b) for $y \to \infty : u = u_\infty$

#### Similar Solution for the Laminar Boundary Layer

For the laminar boundary layer the velocity components $u$ and $v$ can be determined with a similar solution of (6.50), first obtained by Blasius, [Schlichting 1982]. The validity of the solution is confirmed by experimental data. It is tabulated, for example, in [Walz 1956]. The characteristic quantities are:

$$\begin{aligned}
\frac{\delta}{x} &= \frac{5}{\sqrt{Re_x}} \qquad \left(\text{for } \frac{y}{x}\sqrt{Re_x} = 5 \quad \text{it is} \quad \frac{u}{u_\infty} = 0.99\right) \\
\frac{\delta_1}{x} &= \frac{1.72}{\sqrt{Re_x}} \\
\frac{\tau_o(x)}{\rho u_\infty^2} &= \frac{0.332}{\sqrt{Re_x}} \\
\frac{\delta_2}{x} &= \frac{0.664}{\sqrt{Re_x}}
\end{aligned} \tag{6.51}$$

#### Approximate Solution for the Turbulent Boundary Layer

Following Prandtl the turbulent shear stress in equ. (6.50) can be appproxinated as

$$\overline{u'v'} = -l^2 \frac{\partial \overline{u}}{\partial y} \cdot \left|\frac{\partial \overline{u}}{\partial y}\right|. \tag{6.52}$$

The quantity $l$ is the Prandtl mixing length. In the vicinity of the wall it is assumed to be proportional to $y$, and in the outer part of the boundary layer it is approximately constant. This assumption was experimentally confirmed for turbulent pipe flows, but was also shown to be valid for the turbulent boundary layer on a flat plate . Equation (6.50) can be integrated with this closure, but the solution is not similar. Another possibility to determine the characteristic boundary-layer quantities is given by the approximate integral method of von Kármán and Pohlhausen.

**The von Kármán-Pohlhausen Method**

The simple approximate method of von Kármán and Pohlhausen is based on equs. (6.50), integrated in the $y$-direction for steady, inkompressible flow. For the flow over the flat plate at zero angle of attack the so-called integral condition is (see e. g. [Schlichting 1982]):

$$\frac{\tau_o}{\rho u_\infty^2} = \frac{d}{dx}\int_0^\infty \frac{u}{u_\infty}(1-\frac{u}{u_\infty})dy \tag{6.53}$$

The solution of (6.53) requires an assumption for the unknown velocity distribution $u(x,y)/u_\infty = f(y/\delta(x))$. Pohlhausen replaced $f$ by a fourth-degree polynomial of $\frac{y}{\delta}$.

**Example: Laminar Boundary Layer with Linear Ansatz**

The velocity $u/u_\infty$ is crudely approximated by $u/u_\infty = y/\delta$. With this ansatz there are obtained

$$\tau_o = \mu \cdot \left(\frac{du}{dy}\right)_{y=0} = \mu\frac{u_\infty}{\delta} \qquad \text{and} \qquad \int_0^1 \frac{u}{u_\infty}\left(1-\frac{u}{u_\infty}\right)d\frac{y}{\delta} = \frac{1}{6}$$

After insertion of these values in (6.53), integration yields $\delta/x = 2\sqrt{3}/\sqrt{Re_x}$. The displacement thickness $\delta_1$ results to:

$$\delta_1 = \int_0^\delta \left(1-\frac{u}{u_\infty}\right)dy = \delta\int_0^1 \left(1-\frac{u}{u_\infty}\right)d\frac{y}{\delta} = \frac{\delta}{2}, \qquad \text{and hence} \qquad \frac{\delta_1}{x} = \frac{\sqrt{3}}{\sqrt{Re_x}}.$$

Despite of the crude approximation of for $u/u_\infty$ the displacement thickness $\delta_1$ is rather accurately determined, compared with the similar solution ($\sqrt{3} \approx 1.73$ versus 1.72 in the section "Similar Solution for the Laminar Boundary Layer").

**Example: The Power-Law Ansatz for the Turbulent Boundary Layer**

Prandtl employed the experimental results obtained for the pipe flow and applied them to the flat-plate boundary layer.
With the approximate velocity distribution

$$\frac{\overline{u}}{\overline{U}} = \left(\frac{y}{R}\right)^{1/7} \qquad \text{after Nikuradse}$$

and the drag resistance law

$$\frac{8\tau_o}{\rho\overline{u}^2} = \lambda = \frac{0.316}{\sqrt[4]{\frac{\overline{u}D\rho}{\mu}}} \qquad \text{after Blasius}$$

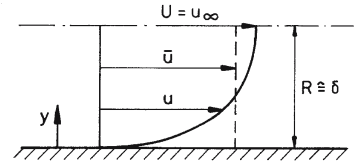


| Pipe | Plate |
|---|---|
| $U$ | $u_\infty$ |
| $R$ | $\delta$ |
| $\frac{\bar{u}}{U} = \left(\frac{y}{R}\right)^{\frac{1}{7}}$ | $\frac{u}{u_\infty} = \left(\frac{y}{\delta}\right)^{\frac{1}{7}}$ |
| $\frac{\tau_0}{\rho U^2}$ | $\frac{\tau_0}{\rho u_\infty^2}$ |

there results for the flat-plate boundary layer

$$\frac{\tau_o}{\rho \overline{u}_\infty^2} = \frac{0.023}{\sqrt[4]{\dfrac{u_\infty \delta \rho}{\mu}}} \qquad \text{and} \qquad \frac{\delta_2}{\delta} = \int_0^1 \frac{u}{u_\infty}\left(1 - \frac{u}{u_\infty}\right) d\frac{y}{\delta} = \frac{7}{72} \quad ,$$

and

$$\frac{\delta_1}{\delta} = \int_0^1 \left(1 - \frac{u}{u_\infty}\right) d\frac{y}{\delta} = \frac{1}{8} \quad .$$

With (6.53) the boundary-layer thickness and the displacement thickness become

$$\frac{\delta}{x} = \frac{0.37}{\sqrt[5]{\dfrac{u_\infty x \rho}{\mu}}} \qquad \text{and} \qquad \frac{\delta_1}{x} = \frac{0.0462}{\sqrt[5]{\dfrac{u_\infty x \rho}{\mu}}} \quad .$$

The results imply that the flow is turbulent from the leading edge on, which is usually not true.

**Selected References**


Kaufmann, W.: *Technische Hydro- und Aeromechanik, 3. Aufl.*, Springer-Verlag Berlin, 1963, S. 232.

Schlichting, H.: *Grenzschichttheorie, 5. Auflage*, Verlag Braun, Karlsruhe, 1965.

Truckenbrodt, E.: *Springer-Verlag*, Berlin, Heidelberg, New-York, 1968, S. 450.

Walz, A.: *Strömungs- und Temperaturgrenzschichten*, Verlag Braun, Karlsruhe, 1966.


### 6.4.4 Evaluation

| | | | |
|---|---|---|---|
| Baromeric pres. | $Ba$ | $= 735.9\,\text{mm Hg}$ | $= 93849.3\,\text{N/m}^2$ |
| Temperature | $\theta$ | $= 21.6°\text{C}$ | $= 294.6\,\text{K}$ |
| Gas ckonstant | $R$ | $= 287\,\text{Nm/kg K}$ | |
| Density | $\rho$ | $= p/RT$ | $= 1.11\,\text{kg/m}^3$ |
| Kinem. viscosity | $\nu$ | $= 15.8 \cdot 10^{-6}\ \text{m}^2/\text{s}$ | |

**Determination of the Critical Reynolds Number**

– **with hot-wire signal**
$x = 1.31$ [m], $q_{\infty_{crit.}} = 41.65$ [mm $H_2O$], $u_{\infty_{crit.}} = 27.13$ [m/s], $Re_{crit.} = 2.25 \cdot 10^6$
– **by "overhearing" the boundary layer**

$q_\infty = 83.3$ [mm $H_2O$], $u_\infty = 38.37$ [m/s], $x_{crit.} = 0.83$ [m], $Re_{crit.} = 2.02 \cdot 10^6$

**Velocity Distribution**

**Laminar Boundary Layer:**
$x = 1.19$ [m],$q_\infty = 27.54$ [mm $H_2O$] = 270.15 [N/m$^2$],$u_\infty = 22.06$ [m/s]

$u/u_\infty = \sqrt{q/q_\infty}$. Diagram: $u/u_\infty = f\left(\frac{y}{x}\sqrt{Re_x}\right)$
**Turbulent Boundary Layer:**
$x = 1.19$ [m],$q_\infty = 117.11$ [mm $H_2O$] = 1148.85 [N/m$^2$],$u_\infty = 45.45$ [m/s]
$u = \sqrt{2q/\rho}$. Diagram: $u = f(y)$ (double-logarithmic).

| Flat-Plate Boundary Layer | | | | | | | |
|---|---|---|---|---|---|---|---|
| laminar | | | | | turbulent | | |
| $x = 1.19$ m, $u_\infty = 22.06\ \frac{\text{m}}{\text{s}}$, $\nu = 15.8 \cdot 10^{-6}\ \frac{\text{m}^2}{\text{s}}$, $Re_x = 1.16 \cdot 10^6$ | | | | | $x = 1.19$ m, $u_\infty = 45.45\ \frac{\text{m}}{\text{s}}$, $\nu = 16 \cdot 10^{-6}\ \frac{\text{m}^2}{\text{s}}$, $Re_x = 3.38 \cdot 10^6$ | | |
| *Not.* | $y$ | $q$ | $\frac{u}{u_\infty}$ | $\frac{y}{x}\sqrt{Re_x}$ | $y$ | $q$ | $u$ |
| *Dim.* | mm | mm $H_2O$ | - | - | mm | mm $H_2O$ | m/s |
| 1 | 0.2 | 1 | 0.191 | 0.22 | 0.2 | 33.0 | 24.15 |
| 2 | 0.4 | 1.4 | 0.225 | 0.43 | 0.7 | 51.8 | 30.26 |
| 3 | 0.7 | 2.5 | 0.301 | 0.76 | 1.2 | 63.4 | 33.48 |
| 4 | 1.2 | 6.3 | 0.478 | 1.3 | 1.7 | 71.7 | 35.60 |
| 5 | 1.7 | 10.8 | 0.626 | 1.84 | 2.2 | 78.8 | 37.32 |
| 6 | 2.2 | 15.1 | 0.740 | 2.38 | 2.7 | 84.8 | 38.72 |
| 7 | 2.7 | 20.1 | 0.854 | 2.92 | 3.7 | 94.9 | 40.96 |
| 8 | 3.2 | 22.6 | 0.906 | 3.47 | 4.7 | 102.4 | 42.54 |
| 9 | 3.7 | 25.2 | 0.957 | 4.01 | 5.7 | 107.9 | 43.67 |
| 10 | 4.2 | 26.6 | 0.983 | 4.55 | 6.7 | 111.9 | 44.47 |
| 11 | 4.7 | 27.2 | 0.994 | 5.09 | 7.7 | 114.4 | 44.97 |
| 12 | 5.2 | 27.5 | 0.999 | 5.63 | 8.7 | 115.9 | 45.29 |
| 13 | 5.7 | 27.7 | 1.003 | 6.17 | 9.7 | 117.2 | 45.51 |
| 14 | 6.2 | 27.8 | 1.005 | 6.72 | 10.7 | 117.5 | 45.57 |
| 15 | 6.7 | 27.8 | 1.005 | 7.26 | 11.7 | 117.7 | 45.61 |
| 16 | | | | | 12.7 | 117.8 | 45.63 |

$$\left(\frac{\delta}{x}\sqrt{Re_x}\right)_{th.} = 5 \qquad \left(\frac{\delta}{x}\sqrt{Re_x}\right)_{exp.} = 4.89$$

$$\left(\frac{\delta_1}{x}\sqrt{Re_x}\right)_{th.} = 1.72 \qquad \left(\frac{\delta_1}{x}\sqrt{Re_x}\right)_{exp.} = 1.36$$

### 6.4.5 Questions

1. State the assumptions for the validity of the boundary-layer theory.
   The characteristic Reynolds number has to be high, $Re_\infty \gg 1$. This requirement implies, that the length of the body and the wall curvature must be much larger than the thickness of the boundary layer.
2. State the reasons for the deviation of the measured velocity profiles from the theoretical predictions and discuss one of them in detail.
   It can be seen in the plot of the measured velocity distribution, that the experimental values at about $\frac{y}{x}\sqrt{Re_x} \approx 0.2$ fall under the curve of the theoretically predicted data, corresponding approximately to $\frac{u}{u_\infty} < 0.25$. Obviously the deviation is caused by a systematic error of measurement. The distance from the wall $\Delta y \approx 0.2\,x\sqrt{Re_x}\ mm$ is of the order of magnitude of the diameter of the Pitot tube. In the vicinity of the wall the Pitot tube influences the flow, so that an accurate measurement of the tangential component of the velocity is not possible.

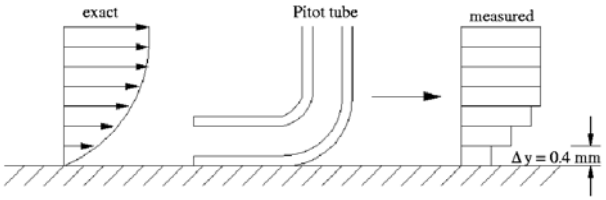


3. Sketch a laminar and a turbulent velocity profile and discuss the differences!

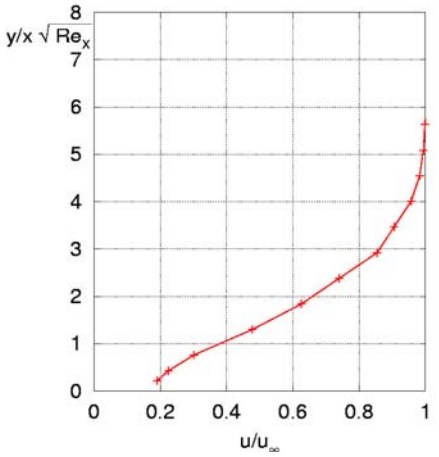


laminar boundary layer on a flat plate

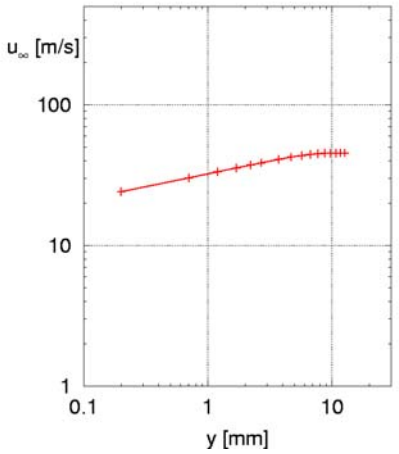


turbulent boundary layer on a flat plate

4. Assume that the boundary layer is turbulent from the leading edge of the plate on and determine the force, exerted by the plate on its the suspension.
(Dimensional sizes of the plate: Length = 1.5 m , width = 0.55 m; Free-stream velocity: see data of experiment)

$$F = 2\, c_D \frac{\rho}{2}\, u_\infty^2\, L\, B \qquad c_D = \frac{\tau_w}{\frac{\rho}{2}\, u_\infty^2}$$

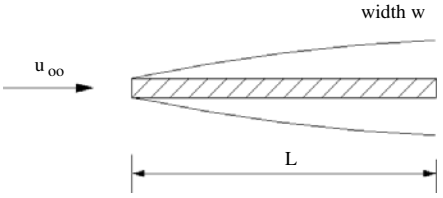


Experiment:

$$\begin{aligned} q_\infty &= 117.11 \text{ mm } H_2O = 1148.85 \text{ Nm}^{-2} \\ u_\infty &= 45.45 \text{ ms}^{-1}; \quad \rho = 1.11 \text{ kgm}^{-3} \\ L &= 1.5 \text{ m}; \qquad B = 0.55 \text{ m} \\ \nu &= 1.6 \cdot 10^{-6}\ \frac{\text{m}^2}{\text{s}} \end{aligned}$$

The von Kármán-Pohlhausen integral method

$$\frac{d\delta_2}{dx} + \frac{1}{u_\infty}\,(2\delta_2 + \delta_1) + \frac{\tau_{(y=0)}}{\rho\, u_\infty^2} = 0 \qquad \left| \frac{du_\infty}{dx} = 0 \right.$$

yields:

$$\begin{aligned} \frac{\tau_0}{\rho\, u_\infty^2} &= \frac{d}{dx}\int_0^\infty \frac{u}{u_\infty}\left(1 - \frac{u}{u_\infty}\right) dy \approx \frac{d\delta_2}{dx} \\ \frac{\delta_2}{\delta} &= \int_0^1 \frac{u}{u_\infty}\left(1 - \frac{u}{u_\infty}\right) d\left(\frac{y}{\delta}\right) \quad . \end{aligned}$$

With

$$\frac{\bar{u}}{u_\infty} = \left(\frac{y}{\delta}\right)^{\frac{1}{7}}$$

there is obtained:

$$\frac{\delta_2}{\delta} = \frac{7}{72}$$

The Blasius approximation:

$$\begin{aligned}
\frac{\tau_0}{\rho\, u_\infty^2} &= 0.023\, \left(\frac{\nu}{u_\infty\, \delta}\right)^{0.25} \\
\Rightarrow \frac{7}{72}\frac{d\delta}{dx} &= 0.023\, \left(\frac{u}{u_\infty}\right)^{0.25}\, \delta^{-0.25} \\
\frac{7}{72}\int_0^\delta \delta^{0.25} d\delta &= 0.023 \left(\frac{\nu}{u_\infty}\right)^{0.25}\, \int_0^x dx \\
\frac{7}{72}\frac{1}{1.25}\delta^{1.25} d\delta &= 0.023 \left(\frac{\nu}{u_\infty}\right)^{0.25}\, \frac{x^{1.25}}{x^{0.25}} \\
\Rightarrow \frac{\delta}{x} &= \frac{0.377}{\sqrt[5]{Re_x}}
\end{aligned}$$

Local skin friction coefficient:

$$\begin{aligned}
c_f &= -\frac{\tau_{(y=0)}}{\frac{\rho}{2}u_\infty^2} \\
-\frac{\tau_{(y=0)}}{\frac{\rho}{2}u_\infty^2} &= 2\frac{d\delta_2}{dx} = \frac{14}{72} = \frac{d\delta}{dx}
\end{aligned}$$

$$\Rightarrow \delta = 0.377\, x\, \left(\frac{\nu}{u_\infty x}\right)^{0.2} \Rightarrow \frac{d\delta}{dx} = 0.377\, 0.8 \left(\frac{\nu}{u_\infty}\right)^{0.2}\, x^{-0.2} = \frac{0.3016}{\sqrt[5]{Re_x}}$$

$$\begin{aligned}
\Rightarrow c_f &= \frac{14}{72}\, \frac{0.3016}{\sqrt[5]{Re_x}} = \frac{14}{72}\, \frac{0.05864}{\sqrt[5]{Re_x}} \\
c_D &= \frac{1}{L}\int_0^L c_f dx = \frac{1}{L}\, \in_0^L 0.05864 \left(\frac{\nu}{u_\infty}\right)^{0.2} x^{-0.2} dx \\
&= \frac{0.05864}{0.8}\frac{1}{L}\left(\frac{\nu}{u_\infty L}\right)^{0.2}\, L
\end{aligned}$$

$$c_D = \frac{0.0733}{\sqrt[5]{Re_L}} \qquad \left(\text{comp. Schlichting:} \quad c_D = \frac{0.455}{(log\ Re_L)^{2.58}} = 3.45 \cdot 10^{-3}\right)$$

$$\begin{aligned}
Re_L &= \frac{u_\infty L}{\nu} = 4.26 \cdot 10^6 \Rightarrow c_D = 3.46 \cdot 10^{-3} \\
\Rightarrow F &= 2\, c_D\, q_\infty\, L\, B = 6.55\ N
\end{aligned}$$

(for turbulent flow and flate plate of zero thickness!)

5. By what experimental measures can the value of the critical Reynolds number of the flat-plate boundary layer be influenced?
The critical Reynolds number $Re_{crit.}$ can be changed by shaping the leading edge of the plate differently and by changing the surface quality of the plate. $Re_{crit.}$ is also affected by the alignment of the plate with the flow direction and by the intensity of turbulence of the free stream.

## 6.5 Pressure Distribution on a Wing

*Abstract*

Pressure distributions are measured in five profile sections on a wing of finite span. The aim of the experiment, carried out in the wind tunnel of the Aerodynamisches Institut for low velocities, is to demonstrate, how lift and pitching moment of the wing can be determined with the pressure measured. Also the dependence of the pressure distributions on the angle of attack is investigated, and flow separation will be demonstrated. The pressure distributions are measured through 25 boreholes in every measuring cross section and recorded with multiple-tubed manometers.

### 6.5.1 Wing of Infinite Span

On a wing of infinite span the velocity does not change in the spanwise direction. The pressure distributions are therefore the same for all wing sections (two-dimensional problem). The lift is determined by decomposing the pressure force $(p - p_\infty)ds \cdot \Delta y$ acting on a surface element of the profile $ds \cdot \Delta y$ into the components tangential ($dT$) and normal ($dN$) to the surface and by subsequent integration over the entire surface area of the wing.

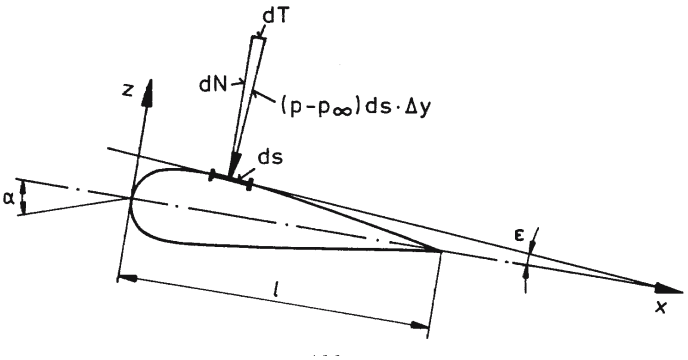


The length element in the spanwise direction $\Delta y$, for example, is chosen to be 1 $m$. The normal component is:

$$\Delta N = (p - p_\infty)\, ds \cos\varepsilon\, \Delta y \quad ,$$

with $ds \cdot \cos\varepsilon = dx$. The resultant $N_{res}$ acting on the profile, is obtained by integrating $dN$ on the upper (subscript $u$) and lower side (subscript $l$) over the wing chord and by taking the difference:

$$\begin{aligned} N_{res} &= \Delta y \int_0^l [(p_l - p_\infty) - (p_u - p_\infty)]\, dx \\ N_{res} &= \Delta y \int_0^l [\Delta p_l - \Delta p_u]\, dx \end{aligned} \tag{6.54}$$

The resulting tangential force can be obtained in similar fashion. However, for small angles $\varepsilon$, i. e. for slender profiles, $T_{res}$ is negligibly small in comparison to $N_{res}$. The dimensionless normal force coefficient $C_N$

$$C_N = \frac{N_{res}}{\frac{\rho_\infty}{2} U_\infty^2 l \Delta y} \tag{6.55}$$

then becomes with the pressure coefficient

$$c_{p_{u,l}} = \frac{\Delta p_{u,l}}{\frac{\rho_\infty}{2} U_\infty^2}$$

$$C_N = \frac{1}{l} \int_0^l (c_{p_l} - c_{p_u}) \cdot dx,$$

with the subscripts $u$ and $l$ designating again the upper and lower side of the profile. If the resulting pressure coefficient

$$c_{pres} = (c_{p_l} - c_{p_u})$$

is plotted versus the wing chord (see the following diagram), it is clear, that the normal force coefficient $C_N$ can be obtained by integration.

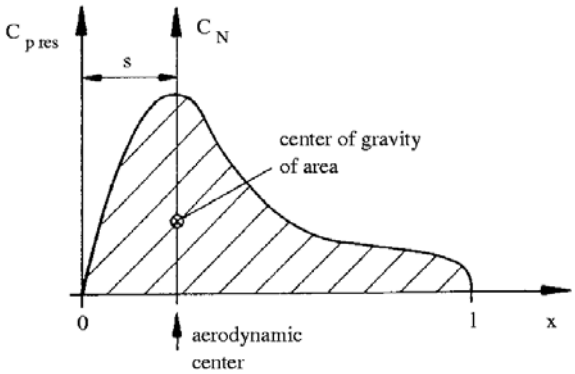


The center of gravity of the shaded area is the location of the aerodynamic center of the profile, i. e. of that point, at which the resulting force acts. The product of the distance of the aerodynamic center from the leading edge of the profile $s$ and the normal force $N$ is the pitching moment $M$ about the leading edge of the profile.

$$M = N \cdot s = C_N \frac{\rho_\infty}{2} U_\infty^2 \, l \, \Delta y \, s \tag{6.56}$$

With the dimensionless moment coefficient $C_M$

$$C_M = \frac{M}{\frac{\rho_\infty}{2} U_\infty^2 \, l^2 \, \Delta y} \tag{6.57}$$

one obtains for $C_M$

$$C_M = C_N \frac{s}{l} \quad .$$

The lift coefficient of the profile

$$C_l = \frac{L}{\frac{\rho_\infty}{2} U_\infty^2 \, l \, \Delta y} \tag{6.58}$$

can for small angles of attack $\alpha$, with the exact relation

$$C_l = C_N \cos\alpha - C_T \sin\alpha$$

approximately be set equal to $C_N$.

### 6.5.2 Wing of Finite Span

#### Determination of the Downwash Distribution

In general the pressure on the lower side of the wing is higher than on the upper side, so that, caused by the pressure difference, a flow about the wing tips is originated.

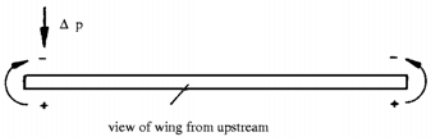


Since the lift vanishes at the wing tips, the circulation has to satisfy the condition $\Gamma(y = \pm b/2) = 0$. For this reason the circulation distribution over the span is assumed to be given by a discontinuous step curve with small increments $\Delta\Gamma$; the vortex elements of strength $\Delta\Gamma$ leave the wing in the downstream direction as free vortices, shown in the following sketch, and form a vortex sheet, which rolls up into the two free tip vortices.

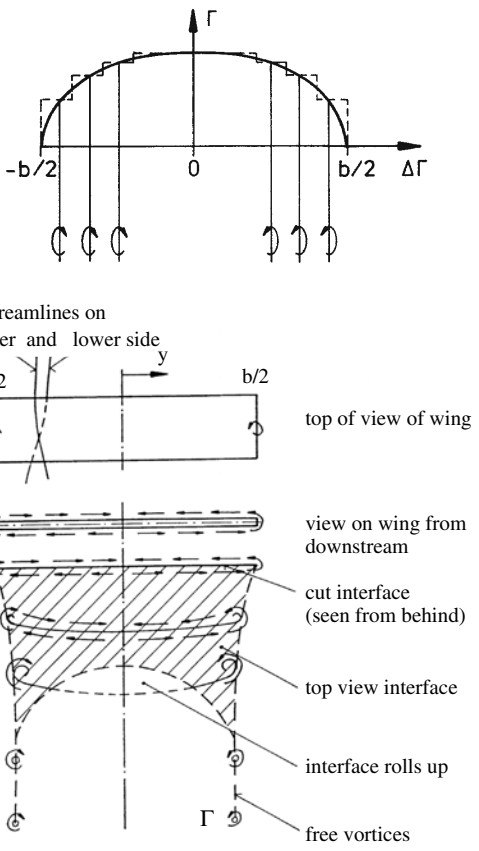


At every positon $y$ on the wing a downwash velocity $w_i(y)$ and thereby an angle of attack $\alpha_i(y)$ is induced; according to the Biot-Savart law they are

$$w_i(y) = \frac{1}{4\pi} \int_{-b/2}^{b/2} \left( \frac{\partial \Gamma(y')}{\partial y'} \right) \frac{dy'}{(y - y')},$$

$$\alpha_i(y) = \frac{w_i(y)}{U_\infty} = \frac{1}{2\pi} \int_{-1}^{+1} \left( \frac{\partial \gamma}{\partial \eta'} \right) \frac{d\eta'}{\eta - \eta'} \quad ; \quad \eta = \frac{2y}{b}, \quad \gamma = \frac{\Gamma}{b \cdot U_\infty}. \tag{6.59}$$

The downwash velocity is superposed on the free-stream velocity, whereby the geometric angle of attack is decreased. If $w_i \ll u_\infty$, then the approximation $w_i/u_\infty = \tan \alpha_i \approx \alpha_i$ can be accepted.
As a consequence of the downwash the resulting aerodynamic force of the wing is no longer normal to the free-stream direction (see the following sketch); the vortices shed from the wing generate an "induced drag" of the magnitude

$$D_i = \frac{1}{U_\infty} \int_{-b/2}^{b/2} \left( \frac{\partial L}{\partial y} \right) w_i(y)\, dy. \tag{6.60}$$

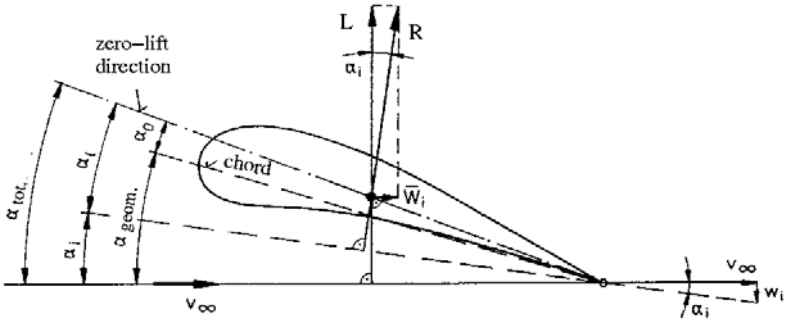


The local lift is now no longer determined by the geometric angle of attack $\alpha_{geom.}$, but by the local "effektive" angle of attack $\alpha_l = \alpha_e$.
The expression for an element of lift $dL$ must now be written as:

$$dL(y) = c_l(y)\, \frac{\rho_\infty}{2} U_\infty^2 l(y) dy \tag{6.61}$$

where

$$c_l(y) = \left( \frac{dc_l}{d\alpha} \right)_\infty \alpha_e(y) = c'_{l\infty}\, \alpha_e(y). \tag{6.62}$$

If it is further assumed, that the local lift is given by the Kutta-Joukowski theorem, one obtains

$$\left( \frac{dc_l}{d\alpha} \right)_\infty \alpha_e(y)\, \frac{\rho_\infty}{2} U_\infty^2 l(y) dy = \rho_\infty U_\infty \Gamma(y) dy \quad . \tag{6.63}$$

The last equation yields $\alpha_e(y)$

$$\alpha_e(y) = \frac{2\Gamma(y)}{U_\infty l(y) c'_{a_\infty}} = \gamma(\eta)\, f(\eta) \tag{6.64}$$

with

$$f(\eta) = \frac{2b}{l(\eta)\, c'_{l_\infty}} \quad . \tag{6.65}$$

With the expression for $\alpha_i$ the local angle of attack can, according to Prandtl, be expressed by the following integro-differential equation:

$$\alpha_g(y) = \frac{2\Gamma(y)}{U_\infty l(y) c'_{a_\infty}} + \frac{1}{4\pi U_\infty} \int_{-b/2}^{b/2} \left(\frac{d\Gamma}{dy'}\right) \frac{dy'}{(y-y')} \tag{6.66}$$

$$\alpha_g(\eta) = f(\eta)\,\gamma(\eta) + \frac{1}{2\pi} \int_{-1}^{+1} \left(\frac{d\gamma}{d\eta'}\right) \frac{d\eta'}{(\eta-\eta')} \tag{6.67}$$

This equation is the starting point of the lifting-line theory, for which two main problems are defined:

| | | | | |
|---|---|---|---|---|
| 1. Main problem: | a) | given: | $\gamma(\eta)$,$f(\eta)$ | |
| | | to be determined: | $\alpha_g(\eta)$ | distribution of the angle of attack (twist) |
| | b) | given: | $\gamma(\eta)$,$\alpha_g(\eta)$ | |
| | | to be determined: | $f(\eta)$ | |
| 2. Main problem: | | given: | $f(\eta)$,$\alpha_g(\eta)$ | |
| | | to be determined: | $\gamma(\eta)$ | |

**Elliptic Circulation Distribution**

The results obtained for the elliptic circulation distribution as obtained in [Trunkenbrodt 1967] are repeated here. If the circulation is given by

$$\Gamma(y) = \Gamma_o \sqrt{1 - \left(\frac{2y}{b}\right)^2}, \tag{6.68}$$

with $\Gamma_o$ being a constant, the lift of the wing is obtained to

$$L = \rho_\infty U_\infty \int_{-b/2}^{b/2} \Gamma(y) \cdot dy = \frac{\pi}{4} \rho_\infty\, U_\infty\, \Gamma_o\, b. \tag{6.69}$$

The downwash velocity is constant

$$w_i(y) = \frac{\Gamma_o}{2b} \quad . \tag{6.70}$$

The induced drag of the elliptic circulation distribution is

$$D_i = \frac{\pi}{8} \cdot \rho_\infty \Gamma_o^2 \quad , \tag{6.71}$$

and the coefficient of the induced drag $C_{D_i}$ can be expressed by the lift coefficient $C_L$ and the aspect ratio of the wing

$$C_{D_i} = \frac{C_L^2}{\pi \Lambda} \quad . \tag{6.72}$$

The aspect ratio is defined as

$$\Lambda = b^2/A \qquad \text{and} \qquad A = \int_{-b/2}^{b/2} l(y) \cdot dy \quad . \tag{6.73}$$

The induced angle of attack is given by

$$\alpha_i = \frac{C_L}{\pi \Lambda} \quad . \tag{6.74}$$

With the last two equations drag coefficients and angles of attack can be determined for different aspect ratios $\Lambda$.

**Solution of the Prandtl Integro-Differential Equation**

Following the ansatz of Glauert and Trefftz (6.63) can be transformed into a system of linear algebraic equations with the aid of a Fourier-series representation for the circulation. The circulation $\gamma$ is represented by a truncated Fourier series

$$\gamma(\vartheta) = 2 \sum_{\mu=1}^{m} a_\mu \sin \mu\vartheta, \tag{6.75}$$

in which $\vartheta$ is obtained from $\eta$ by the transformation

$$\vartheta = \arccos \eta \quad . \tag{6.76}$$

The integration of (6.67) yields (special attention is to be paid to the singularity in the integral)

$$\alpha_g(\vartheta) = 2\, f(\vartheta) \sum_{\mu=1}^{m} a_\mu \sin \mu\vartheta + \sum_{\mu=1}^{m} \mu a_\mu \frac{\sin \mu\vartheta}{\sin \vartheta} \quad . \tag{6.77}$$

The quantities $a_\mu$ are the Fourier coefficients.

$$\alpha_\mu = \frac{1}{\pi} \int_0^\pi \gamma(\vartheta) \sin \mu\vartheta d\vartheta \simeq \frac{1}{m+1} \sum_{n=1}^{m} \gamma_n \sin \mu\vartheta_n \tag{6.78}$$

The trapezoidal rule is used for the solution of the integral. If the coefficients $a_\mu$ are replaced by the approximate expression (6.66), there results

$$\alpha_{g\nu} = f_\nu\, \gamma_\nu + \sum_{n=1}^{m} \gamma_n \sum_{\mu=1}^{m} \frac{\mu}{m+1} \frac{\sin \mu\vartheta_\nu}{\sin \vartheta_\nu} \sin \mu\vartheta_n. \tag{6.79}$$

With (6.78) the Prandtl integro-differential equation is transformed into a system of $m$ linear algebraic equations for $\gamma_\nu(\nu = 1{,}2....m)$.
In matrix formulation (6.5.2) can be written as

$$\underline{\underline{B}} \cdot \underline{\gamma} = \underline{\alpha}_g \tag{6.80}$$

In this equation $\underline{\underline{B}}$ is the coefficient matrix, which depends only on the geometry of the wing, and $\gamma$ is the unknown solution vector.
The model of the wing used in the experiment has a profile NACA 23012; the characteristic quantities are:

$$b = 0.9\, m; \quad l = 0.2\, m; \quad c_l = 5.35; \quad \alpha_g = 6^o; \quad \Lambda = 4.5 \tag{6.81}$$

The results of the calculation with the lifting-line theory are shown by the curve 1 in the following diagram. Also shown are the results of the extended lifting-line theory of [Schlichting, Truckenbrodt 1967] in curve 2.

**The Approximate Method of Schrenk**

Munk could show [Schlichting and Truckenbrodt 1967], that the induced drag attains a minimum, if the circulation distribution on the wing is elliptic. The fact, that the circulation distribution also depends on the shape of the wing (see (6.67), which contains the quantity $l(y)$), offers the possibility to quickly estimate the deviation of the circulation distribution of a given wing from the elliptic distribution; such an estimate is advantageous for design problems. In [Schlichting and Truckenbrodt 1967] it is proposed to assume the local lift to be given by the mean value of the elliptic distribution and a distribution proportional to the local chord:

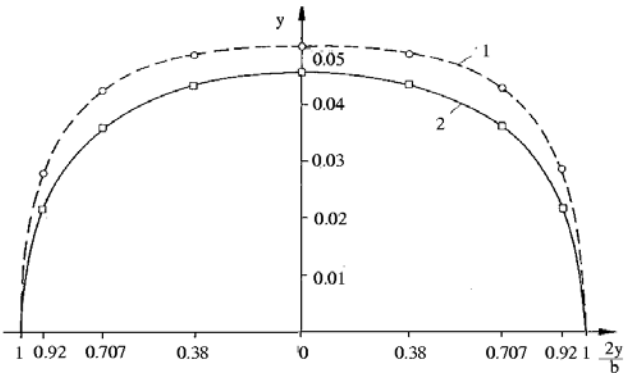


- - - $c_L = 0.39045$ $c_{Di} = 0.01121$ simple lifting-line theory
——— $c_L = 0.3419$ $c_{Di} = 0.0834$ extended lifting-line theory
Lift distribution of the rectangular wing with NACA-profile 23012; $\alpha = 6°$

$$L(y) = \frac{1}{2}\left[a_0 \cdot l(y) + a_1\sqrt{1-\left(\frac{2y}{b}\right)^2}\right] \tag{6.82}$$

The constants $a_0$ and $a_1$ can be obtained by integration in the spanwise direction and requiring that both integrals have to have the same value. One obtains for $c_l(y)$

$$c_l(y) = \frac{C_L}{2}\left[1 + \frac{4l_m}{\pi l(y)} \cdot \sqrt{1-\left(\frac{2y}{b}\right)^2}\right], \tag{6.83}$$

with $l_m$ being the mean chord and $C_L$ the total lift of the wing. The dimensionless circulation distribution then is:

$$\gamma(y) = \gamma_1(y) + \gamma_2(y) = \frac{C_L l(y)}{4b} + \frac{C_L A}{\pi b^2}\sqrt{1-\left(\frac{2y}{b}\right)^2} \tag{6.84}$$

The quantity $\gamma_1(y)$ is the local circulation proportional to the chord, and $\gamma_2(y)$ is the elliptic contribution.
The following distribution is obtained for a rectangular wing:

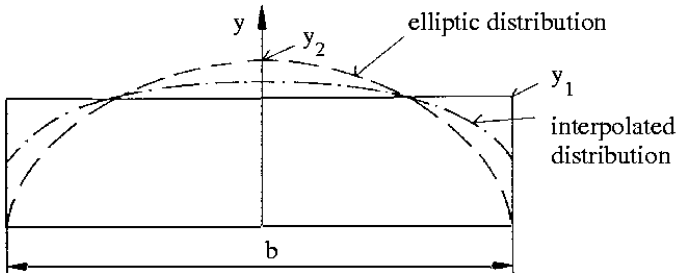


It is to be noted, that the Schrenk approximation does not drop to zero at the end of a rectangular wing. The error is of minor importance, if one remembers the simplicity of the method.

### 6.5.3 Method of Test

In the experiment a model of a wing is used with a span width of 900 mm and a chord of 200 mm. The wing has zero twist and its profile is the NACA 23012 profile with a maximum thickness position of 30% chord, 12% relative thickness, and 1.84% relative camber at 15% chord.
The pressure distribution is measured in five sections at various locations in the spanwise direction (see the following drawing of the model). In each measuring section there are 14 boreholes on the upper side of the wing, and 11 on the lower side. All pressure holes are connected with multiple-tubed manometers via flexible tubes so that 125 connections have to be lead out of the model of the wing. In order to avoid disturbances of the flow by the pressure tubes, they are put inside the sword-like support of the wing, which is mounted at a right angle to it in the wind tunnel (see the following drawing). A comparison of the calculated and the measured lift distribution shows, that there is some disturbance by the sword, but it is small.
The pressure tubes are lead from the sword to five multiple-tubed manometers, which are filled with water as sealing liquid. The entire measuring unit consists of a storage container, filled with water and sealed off against the atmospheric pressure. 27 glas tubes are immerged in the container, and the pressure inside can be raised by letting compressed air in, which causes the water columns in the glas tubes to rise. Since the flexible tubes of every measuring section are connected with 25 glas tubes, the water columns are sucked upward by underpressures and pushed downward by overpressures. The two remaining glas tubes are connected to the surrrounding atmosphere and serve for reference pressure measurements. In this manner the multiple-tubed manomaters are used as differential pressure manometers.
The dimension size of the sword could be reduced and thereby also the error of the measurements, if electric pressure probes were used. The multiple-tubed manometers, however, are prefered here because of their simplicity. Also the pressure distribution can be recorded, when the flow separates and stalls. The position of the boreholes is shown in the following drawing.
The total lift of the wing is obtained by integrating the local lift coefficients in the spanwise direction.
The following page contain a perspective drawing of the model of the wing with the sword and the suspensions. Indicated are the five sections, in which the pressures are measured. Sections $I$ and $II$ are close to the wing tips, sections $III$ and $IV$ further inboard, and section $V$ near the sword.
The table below the drawing gives the positions of the boreholes for the pressure measurements on the upper and lower side of the wing. The corresponding numbering of the holes is shown in the sketch below the table. The drawing on the bottom of the page gives the spanwise positions of the five measuring sections. The various distances are measured in mm.

### Selected References

Multhopp, H.: *Die Berechnung von Auftriebsverteilung von Tragflügeln*, Luftfahrtforschung, Bd. 15, 1938

Schlichting, H., Truckenbrodt, E.: *Aerodynamik des Flugzeugs, 2. Band, 2.Aufl.*, Springer-Verlag, 1967

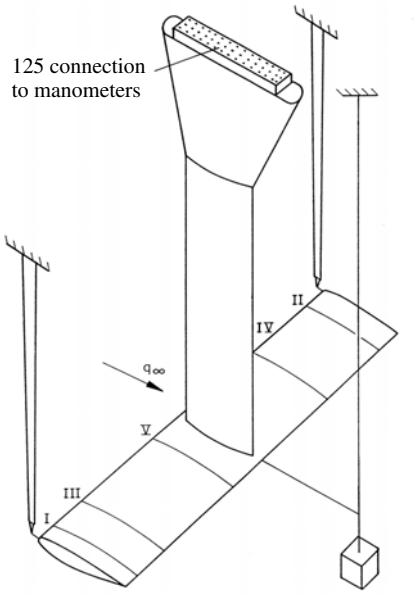


The wing model for measuring the pressure distribution

| Position | Dim. | 1 | 2 | 3 | 4 | 5 | 6 | 7 | 8 | 9 | 10 | 11 | 12 | 13 | 14 |
|---|---|---|---|---|---|---|---|---|---|---|---|---|---|---|---|
| $x_{Upperside}$ | mm | 0 | 6 | 15 | 23 | 32 | 48 | 62 | 77 | 92 | 109 | 122 | 140 | 158 | 175 |
| $x_{Lowerside}$ | mm | 15 | 23 | 32 | 48 | 62 | 77 | 92 | 109 | 122 | 147 | 170 | — | — | — |

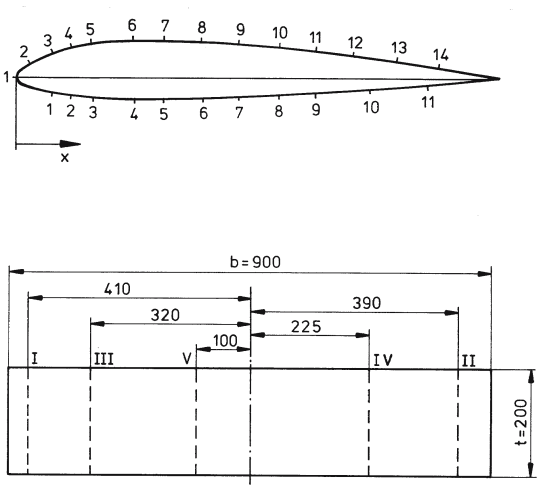


Pressure holes on the NACA profile 23012

### 6.5.4 Evaluation

1. Evaluation of the data:

a) Draw the diagrams $\Delta p = f(x)$ for the five sections I, II, III, IV, V;

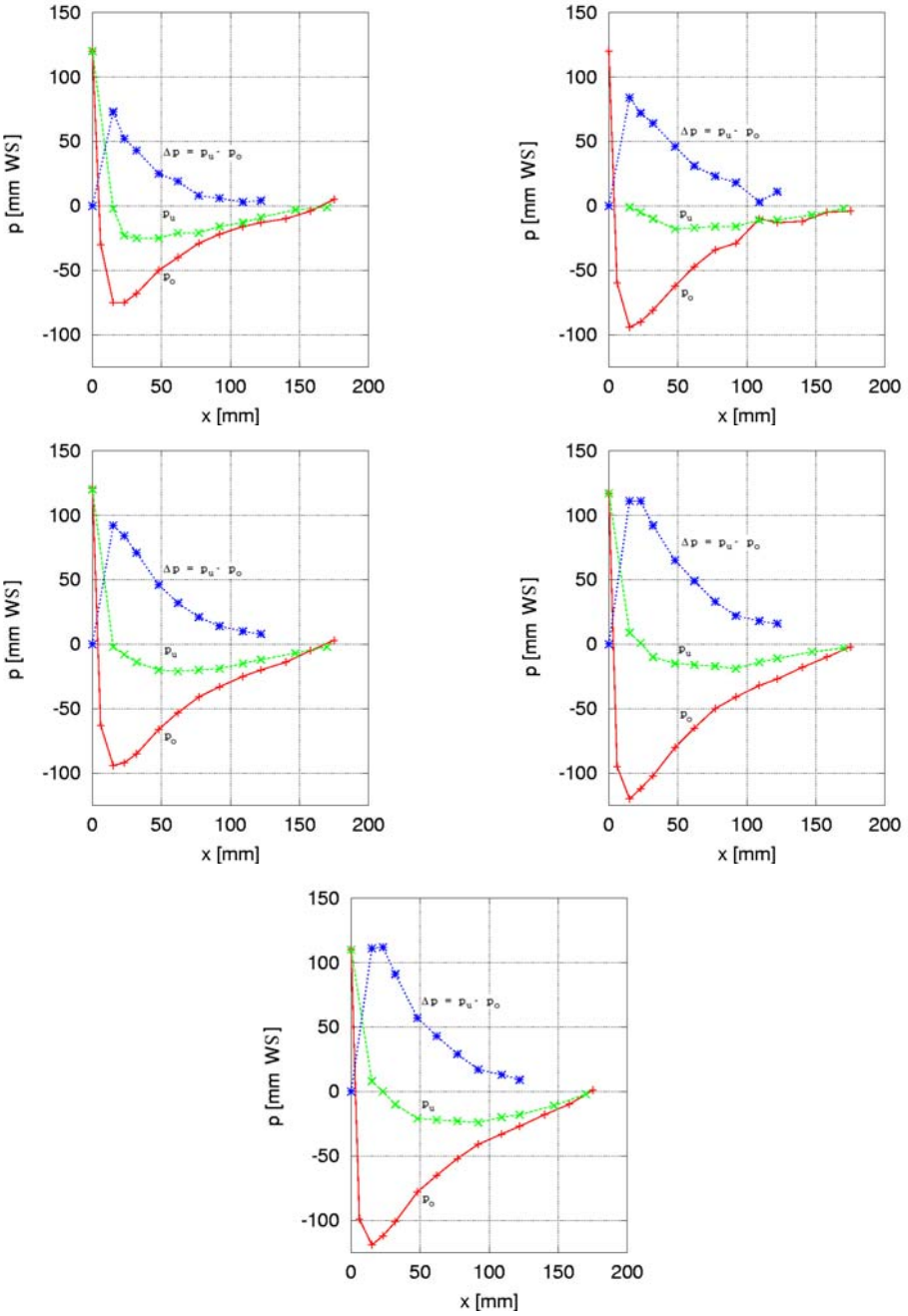

Pressure distribution $p$ [mm $H_2O$]

| | Section I | | Section II | | Section III | | Section IV | | Section V | |
|---|---|---|---|---|---|---|---|---|---|---|
| | $p_u$ | $p_l$ | $p_u$ | $p_l$ | $p_u$ | $p_l$ | $p_u$ | $p_l$ | $p_u$ | $p_l$ |
| 1 | 120 | -2 | 120 | -1 | 121 | -2 | 117 | 9 | 110 | 8 |
| 2 | -30 | -23 | -60 | -5 | -63 | -8 | -95 | 1 | -99 | 0 |
| 3 | -75 | -25 | -94 | -10 | -94 | -14 | -120 | -10 | -119 | -10 |
| 4 | -75 | -25 | -90 | -18 | -92 | -20 | -112 | -15 | -112 | -21 |
| 5 | -68 | -21 | -81 | -17 | -85 | -21 | -102 | -16 | -101 | -22 |
| 6 | -50 | -21 | -62 | -16 | -66 | -20 | -80 | -17 | -78 | -23 |
| 7 | -40 | -16 | -47 | -16 | -53 | -19 | -65 | -19 | -65 | -24 |
| 8 | -29 | -13 | -34 | -11 | -41 | -15 | -50 | -14 | -52 | -20 |
| 9 | -22 | -9 | -29 | -11 | -33 | -12 | -41 | -11 | -41 | -18 |
| 10 | -16 | -3 | -10 | -7 | -25 | -7 | -32 | -6 | -33 | -11 |
| 11 | -13 | -1 | -13 | -2 | -20 | -2 | -27 | -3 | -27 | -2 |
| 12 | -10 | — | -12 | — | -14 | — | -18 | — | -18 | — |
| 13 | -4 | — | -5 | — | -5 | — | -10 | — | -10 | — |
| 14 | 5 | — | -4 | — | 3 | — | -2 | — | 1 | — |

b) Determine the mean pressure for all sections!

$$\begin{aligned}
\Delta p_m &= \frac{1}{l}\int_0^l (\Delta p_u - \Delta p_o)dx \\
\Delta p_m &= \frac{1}{l}\int_0^l \Delta p\ dx \\
\Delta p_m &= \frac{1}{l}\frac{h}{3}\ (\Delta p_0 + 4\ \Delta p_1 + 2\ \Delta p_2 + 4\ \Delta p_3 + ... + 4\ \Delta p_{n-1} + \Delta p_n)
\end{aligned}$$

(Simpson's method)

$$h = \frac{l}{n}; \quad \text{choose:} \quad l = 19.6\ cm \Rightarrow n = 14; \quad h = 1.4\ cm$$

$\Delta p_i$ from diagram (results see following table)

| Section Nr. | 1 | 2 | 3 | 4 | 5 |
|---|---|---|---|---|---|
| $\Delta p_0$ | 0 | 0 | 0 | 0 | 0 |
| $\Delta p_1$ | 627.84 | 941.760 | 922.14 | 1314.54 | 1255.680 |
| $\Delta p_2$ | 451.260 | 706.32 | 725.94 | 961.38 | 961.38 |
| $\Delta p_3$ | 313.920 | 490.5 | 529.74 | 725.94 | 686.7 |
| $\Delta p_4$ | 196.200 | 333.54 | 372.78 | 549.36 | 470.880 |
| $\Delta p_5$ | 117.72 | 176.58 | 255.16 | 392.4 | 333.54 |
| $\Delta p_6$ | 78.48 | 98.1 | 176.58 | 294.3 | 235.44 |
| $\Delta p_7$ | 39.240 | 58.860 | 117.72 | 235.44 | 137.340 |
| $\Delta p_8$ | 19.62 | 39.24 | 78.48 | 176.58 | 98.1 |
| $\Delta p_9$ | 19.620 | 19.620 | 58.86 | 137.34 | 78.480 |
| $\Delta p_10$ | 19.620 | 19.620 | 39.24 | 98.10 | 58.860 |
| $\Delta p_11$ | 9.81 | 9.81 | 19.62 | 78.48 | 39.240 |
| $\Delta p_12$ | 9.81 | 9.81 | 19.62 | 39.240 | 19.620 |
| $\Delta p_13$ | 5.886 | 3.924 | 9.81 | 19.620 | 19.620 |
| $\Delta p_14$ | 0 | 0 | 9.81 | 9.810 | 9.810 |
| $\Delta p_m\ l$ | 28.402 | 43.015 | 50.77 | 74.026 | 64.870 |
| $\Delta p_m$ | 144.908 | 219.464 | 259.03 | 377.685 | 330.971 |
| $c_a$ | 0.126 | 0.190 | 0.225 | 0.327 | 0.287 |
| $\gamma$ | 0.014 | 0.021 | 0.025 | 0.036 | 0.032 |

c) Calculate the local lift coefficient $c_l = \Delta p_m / \Delta p_{sc} \cdot \delta$ for all sections; determine $\gamma = c_a \cdot l/2b$ and plot in diagram (nozzle calibration factor $\delta = 0.98$);

$$c_L = \left(\frac{\Delta p_m}{\Delta p_{sc}}\right) \cdot \delta = \frac{\Delta p_m}{1153.6\ Pa}$$

$$\gamma = c_l\ \frac{l}{2b}$$

d) Determine the location of the aerodynamic center for the section III, measured from the leading edge. $c_{pres.} = c_{pu,l} = \frac{\Delta p}{\frac{\rho_\infty}{2} v_\infty^2} \frac{\Delta p}{q_\infty} = \frac{\Delta p}{1153.6\ Pa}$

See diagram:
Position of center of gravity of the area is approximately at $s = 43\,\text{mm}$

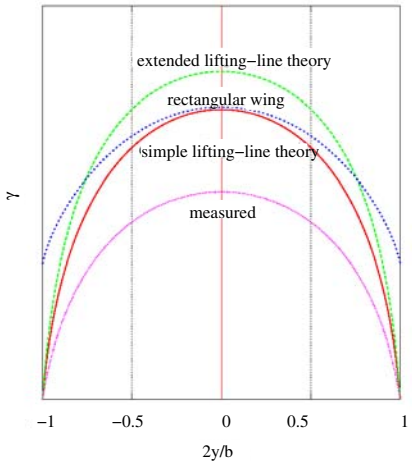


e) Discuss the influence of the Reynolds number $Re$ on the maximum lift of a wing!
At high angles of attack the pressure minimum on the upper side of the wing is located near the leading edge. The pressure rise towards to trailing edge generates a large positive pressure gradient, which either provokes laminar-turbulent transition or separation of the laminar flow. Whether transition or separation is first, mainly depends on the Reynolds number and on the magnitude of the pressure gradient.

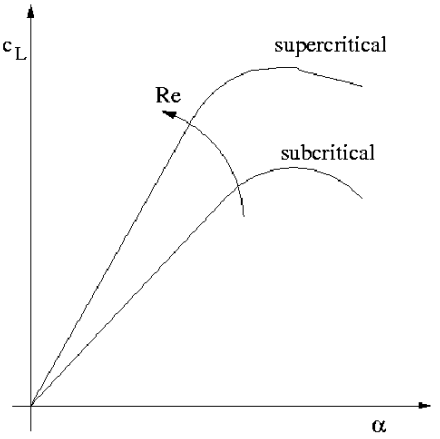


For low Reynolds numbers laminar separation is observed first and leading edge stall may result. The maximum lift coefficient is very low. With increasing Reynolds number transition is posssible, and the flow can reattach. The maximum lift therefore increases with increasing Reynolds number.

## 6.6 Aerodynamic Forces Acting on a Wing

*Abstract*

Lift, drag, and pitching moment of a rectangular wing with the NACA 23012 profile, and the drag of the model suspension are determined by measuring three aerodynamic forces with the balance of the low-speed wind tunnel of the Aerodynamisches Institut. The functioning and the utilization of the balance and the correction of the measured data are explained. Application of the experimental data to full-scale configurations will also be described.

### 6.6.1 Nomenclature of Profiles

Wing profiles for subsonic flight are well rounded at the leading edge and pointed at the trailing edge. The shape of the profile is charcterized by the following parameters:

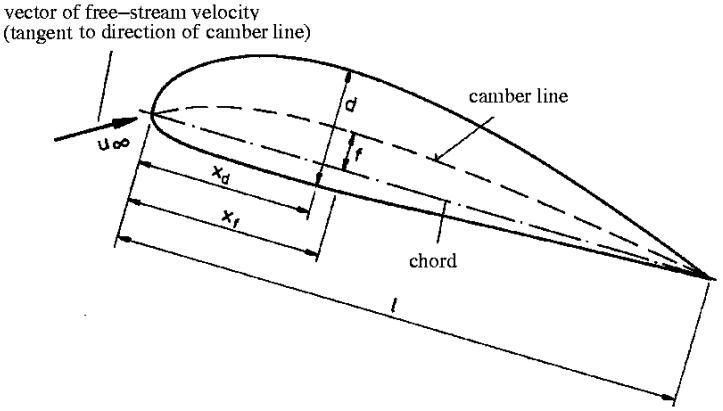


Chord of the profile $l$: The characteristic parameter, to which all dimension sizes are referenced. Maximum relative profile thickness $d/l$; relative thickness position $x_d/l$; maximum relative camber $f/l$; relative camber position $x_f/l$.

The influence of the geometric parameters of a profile on its aerodynamic characteristics has been investigated by numerous authors, see for example [Abbott, v. Doenhoff, Pankhurst, Holder], but especially by NACA Research Laboratories of the United States, see for example [Ann. Reports 193, 1937]. The digits of the profile, used here in the experiment, have the following meaning: For the five-digit series (e. g. NACA 23012), which begins with a 2, $x_d/l$ is $x_d/l = 0.3 = \text{const.}$; for 230....., $f/l = 0.0184$.

The digit 2 indicates 20/3 of the lift coefficient $c_l^*$ (= 0.3) at shockless entrance, i. e. flow direction is tangent to the camber in the point on the leading edge (see sketch above). The 2nd and 3rd digit denote twice the value of $x_f$ in percent of $l$: $x_f/l = 0.15$. The 4th and 5th digit denote $d$ in percent of $l$: $d/l = 0.12$.

### 6.6.2 Measurement of Aerodynamic Forces

The aerodynamic forces acting on a wing of infinite span can be decomposed into lift, drag, and pitching moment about a suitable point. The forces, especially the drag of the profile, cannot be determined from the pressure distribution, since the friction forces are not taken into account. In the flow about a profile the friction forces can become markedly larger than the pressure forces (e. g. the drag of the profile). The accurate determination of the drag alone by integration of the normal forces is only possible for blunt bodies, since the normal forces are considerably larger than the friction forces. It is for this reason that the aerodynamic forces acting on the model are measured directly with a wind-tunnel balance.

**Wind-Tunnel Balances**

For force measurements with multi-components balances the model must be suspended in such a way, that individual forces do not interact with each other, if possible, i. e. a force, which acts in a certain coordinate direction (e. g. the drag) should not generate a component in another direction (e. g. lift). Mechanical and electric balances are used. The working principle of the mechanical lever balances is, that the displacement of the model by the aerodynamic forces is compensated by increasing the weight. The main advantage of this type of balance is, that the model is always brought back to its initial position. The disadvantages are: The space required and their limitation to steady measurements. The electric balances measure the displacement of the model due to the action of the aerodynamic forces indirectly with ohmic, capacitiv, or inductive displacement pickups. The suspension has to be so elastic, that the aerodynamic forces to be expected cause only a small displacement of the model and the suspension. It has to be compromized between the displacement, which generates components in other directions of force and the sensitivity of the reading of the balance. The advantage of the electric balances is mainly to be sought in their possible miniaturization. They can be mounted on models. Because of their short response times measurements of unsteady aerodynamic forces are possible. A large effort is, however, necessary for the design of the suspension of the model, if the interaction of the components of forces, measured with an electric balance, is to be avoided.
The balance used in the test is a mechanical three-components balance with wire suspension and transfer of force via beams of balance, suspended by knife edges.
A model is held in equilibrium position by six wires, with six corresponding forces in the general case, measured with the balances $A'$,$B$,$C$,$D$,$E$, and $F$. The quantities to be measured are specified in the following drawing.
The schematic arrangement of the experimental setup is shown in the sketch on the bottom of the page. Depicted is a model of an airplane with its axes of orientation. Indicated are also the six balances, the wires, and the positions, where the wires are connected with the model. The balances $A'$ and $B$ are fastened at the wing tips, with the wires aligned in the direction of the main flow. The drag is measured with these balances. The wires leading to the balances $C$ and $D$ are fastened at the same positions, but in the direction normal to the main flow. Together with a third balance $E$ they are used for measuring the lift. The side force is measured with the sixth balance $F$, with the wire connected to one of the wing tips, orientated in the spanwise direction. The rolling, yawing, and the pitching moment are obtained as indicated in the sketch from the force measurements.

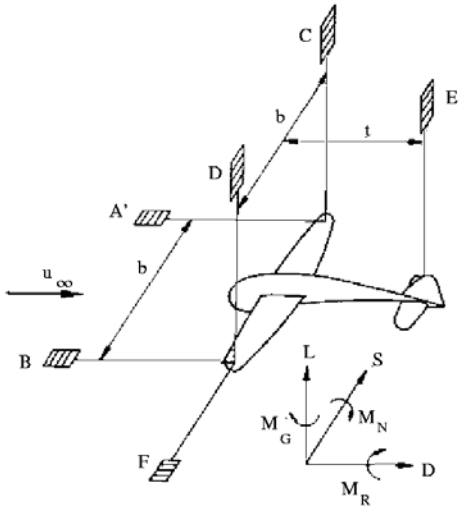


1. Drag $D = A' + B$
2. Lift $L = C + D + E$
3. Side force $S = F$
4. Rolling moment $M_R = (C - D) \cdot b/2$
5. Yawing moment $M_G = (A' - B) \cdot b/2$
6. Pitching moment $M_N = E \cdot t$

The various components to be measured are explained with the aid of the following drawing; a more detailed drawing of the balance is shown on page 296 of the section 6.6.4; the balance for measuring the lift in the rear is displaced horizontally when the model of the wing is positioned at angle of attack, so that the suspension wires in the front and at the rear remain vertical, when the distance between the suspension points is changed.

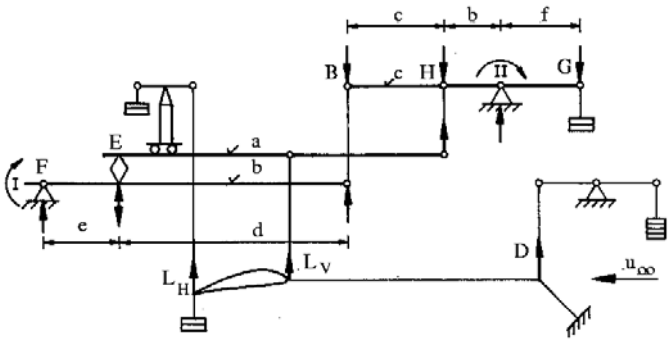


In the diagrammatic sketch the equilibrium condition for the individual systems (beams of balance) is given: The external forces $L_H$ und $L_V$ act on the beam of balance in the middle (a), and the equilibrating forces are $D$ and $H$.

$$\sum K_y = 0 : L_H + L_V = D + H \tag{6.85}$$

The external force $D$ acts on the lower beam of balance (b), and $F$ and $B$ are the balancing forces.

$$\sum M_I = 0 : D \cdot e = B \cdot (e + d) \rightarrow D = B \cdot (e + d)/e \tag{6.86}$$

On the upper beam (c) the equilibrium is given by the bearing forces in point II, $B$, $H$, and $G$ act as external forces.

$$\sum M_{II} = 0 : G \cdot f = H \cdot b + B \cdot (c + b)$$

$$\Rightarrow H = \frac{G \cdot f}{b} - \frac{B \cdot (c + b)}{b} \tag{6.87}$$

$(b)$ and $(c)$ are inserted into $(a)$:

$$L_V + L_H = L_{tot.} = \frac{B \cdot (e + d)}{e} - \frac{B \cdot (c + b)}{b} + \frac{G \cdot f}{b} \tag{6.88}$$

In order to ensure that the lift is proportional to the force $G$ (weight laid on), the following condition has to hold:

$$\frac{B \cdot (e + d)}{e} = \frac{B \cdot (c + d)}{b}, \quad d.h. \frac{d}{e} = \frac{c}{b} \tag{6.89}$$

Finally there is obtained:

$$L_{tot.} = G \cdot \frac{f}{b} = G \cdot Z_{L_{tot.}} \tag{6.90}$$

The balance is constructed according to the condition ($Z_{Ltot.} = 3$). The lever ratios $Z_{LH}$ and $Z_D$ for the lift balance in the rear and also for the drag balance can be read from the diagrammatic sketch on page 296.

**Determination of the Aerodynamic Coefficients from the Measured Data**

The total lift $L_{tot.}$, the rear lift $L_H$, and the total drag of the model, and the suspension $D$ are determined in the measurement with the balance. For a fixed geometry of the profile (i. e. including the angle of attack) it follows from the similarity laws, that the dimensionless

force coefficients depend only on the Reynolds number $Re$: The aerodynamic coefficients are presented in the form $c_L$, $c_D$, $c_m = f(\alpha)$ or as polar diagrams $c_L$, $c_m = f(c_D)$, with the Reynolds number $Re$ as parameter. The drag of the suspension has to be measured separately and be subtracted from the total drag. The mutual interference between model and suspension has to be taken into account.

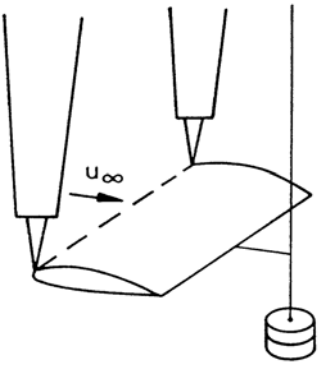


The model is suspended with two swords, fastened at the wing tips and with a wire downstream from the wing, schematically depicted in the sketch. In order to keep the interference between the model and the suspension small, the drag of the swords should be as small as possible. This requirement implies, that the size of the wing should be sufficiently large, so as to guarantee an accurate measurement of the drag.

$$D_{susp.} = D_{swords} + D_{wire}$$

It follows from the above sketch that the drag of the suspension consists of the drag of the two swords and of the drag of the wire. The drag of the swords is measured in a separate experiment without the model and is later on included in the evaluation of the three-components measurements. The drag of the wires is calculated with existing drag formulas for circular cylinders.
The moment coefficient is obtained from the following equilibrium consideration:

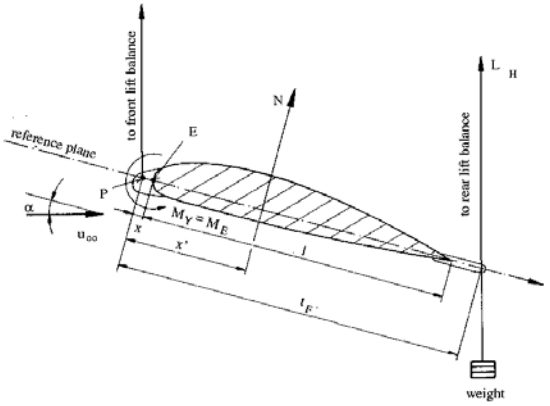


With the suspension included the equilibium of moments is:

$$\sum M_P = 0: \;\; N \cdot x' - L_H \cdot t_F \cdot \cos\alpha = 0 \tag{6.91}$$

The weight of the wing drops out, since the balance is calibrated for $u_\infty = 0$. For the free flight the moment about the point $E$ (again without the weight) is:
$M_E = N(x' - x)$. $N\,x'$ inserted, there results:

$$M_E = M_Y = A_H\, t_F\, \cos\alpha - N\, x \tag{6.92}$$

The diagrammatic sketch shows the aerodynamic forces on page 296; one obtains

$$\begin{aligned} N &= L\cos\alpha + D\sin\alpha \\ T &= D\cos\alpha - L\sin\alpha \quad . \end{aligned} \tag{6.93}$$

The moment coefficient is:

$$c_{m,y} = c_m = \frac{M_y}{\frac{\rho}{2}u_\infty^2 A_{wing}\, l_{wing}} \tag{6.94}$$

For the determination of the moment the change of the rear lift ($\delta L_H$) caused by the static moment for an eccentric location of the center of gravity. The equilibrium of moments about the point $P$ gives (for $\alpha = 0$ with symmetric ($\bullet$) and asymmetric ($\star$) location of the center of gravity (cgl)):

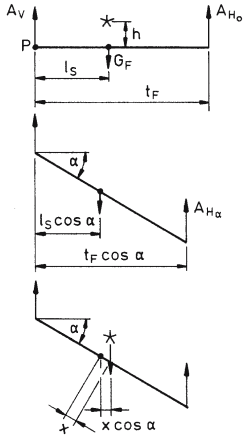


For symmetr. ($\bullet$) and eccentric ($\star$) cgl and $\alpha = 0$
$L_{H_o}\, t_F = G_F\, l_S$

for symmetr. cgl ($\bullet$)
$L_{H_\alpha}\, t_F\, \cos\alpha = G_f\, l_S\, \cos\alpha$

For eccentric cgl ($\star$)
$L_{H_\alpha}\, t_F\, \cos\alpha = G_f\, \cos\alpha\, (l_S + x)$

With $x = h\, \tan\alpha$, there is obtained $\delta L_H = L_{H_\alpha} - L_{H_0}$

For $(\bullet) = 0$ for $(\star) = G_F\, \dfrac{h}{t_F} \tan\alpha$

If the wing is in the normal position the rear lift is measured too small, caused by the change of the static moment. If $h = 0$, (center of gravity on the chord; in general on the line connecting the suspension points), then the correction $\Delta L_H = 0$ is not needed. Estimate for the wing investigated: $G_F \approx 20\, kN; t_F \approx 0.3\, m; h \approx 3.5\, mm; \alpha_{max} \approx 22^o \rightarrow \tan\alpha_{max} \approx 0.4$.

$$\Delta L_{H_{max}} = \frac{2 \cdot 10^4 \cdot 3.5 \cdot 0.4}{300} N \approx 100\ N \tag{6.95}$$

$$\Delta L_H^* = \frac{1}{2}\delta L_H \longrightarrow (\Delta L_H^*)_{max} \approx 50\ N \qquad \text{(Reading round off to 50 } N\text{)} \tag{6.96}$$

Since the maximum error is less than 1%, if $\delta L_H^*$ is neglected, the correction of the rear lift is left out in the evaluation (note that $\Delta L_H$ is larger for strongly cambered profiles).

### 6.6.3 Application of Measured Data to Full-Scale Configurations

#### Influence of the Reynolds number on the Boundary Layer

It the measured data are to be applied to the full-scale configurations, in incompressible flow the Reynolds number has to have the same value for the flight condition and the experiment; this requirement implies large wind-tunnel models. However, only very few profiles have been investigated in full scale in large wind tunnels.

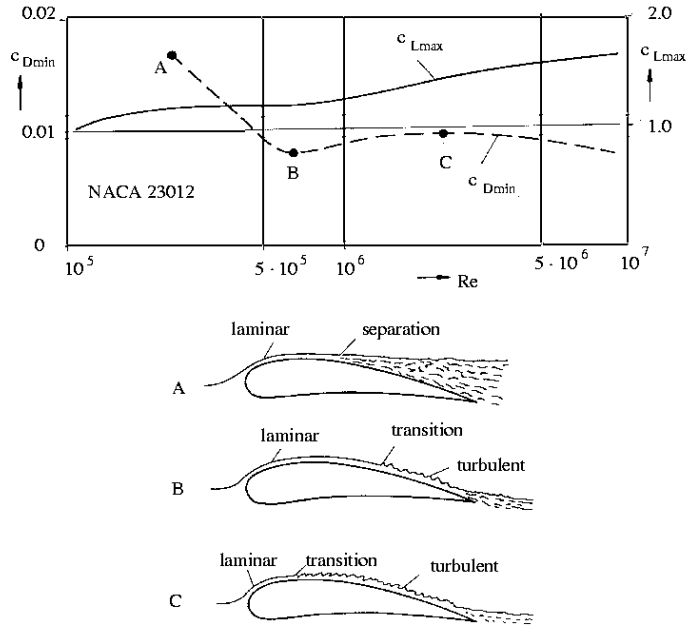


The dependence of the aerodynamic force coefficients (e. g. $c_{Dmin}$ and $c_{L_{max}}$), and of the behavior of the boundary layer on the Reynolds number $Re$ is briefly discussed for the profile NACA 23012 with the following diagrams.

If the laminar boundary layer separates downstream from the location of the maximum thickness (see sketch A), a dead-water region is generated; the drag coefficient $c_D$ is relatively large. If the boundary layer undergoes transition downstream from the location of maximum thickness (see sketch B), because of the large momentum transport in the direction normal to the wall, the turbulent boundary layer separates only shortly upstream of the trailing edge. The drag coefficient $c_D$ drops and attains a minimum value. With increasing Reynolds number $Re$ the transition point moves upstream (see sketch C); the overall flow patterns do not change much in comparison to those shown in sketch B, but the turbulent boundary layer extends over a larger region in the streamwise direction than does the laminar boundary layer; consequently the integral over the Reynolds stresses is larger, and the drag coefficient $c_D$ also rises. If the boundary layer is turbulent from the leading edge on, the drag coefficient decreases with increasing Reynolds number, but the drag increases further.

Since the turbulent boundary layer can withstand a larger pressure increase than the laminar boundary layer, the flow separates only at a larger angle of attack (i. e. high $c_{L_{max}}$); with increasing Reynolds number $c_{L_{max}}$ increases from 1.0 at $Re \approx 10^5$ to 1.7 at $Re \approx 10^7$. The variation of $c_{L_{max}}$ clearly shows the sensitivity of the profile used to changes of the Reynolds number.

### Correction of the Data Due to Finite Diameter of the Test Section

**Boundary conditions in wind tunnels.** Caused by the influence of the edge of the air stream on the flow near the model, a correction of the measured data is necessary prior to applying the data to a full-scale configuration. In order to keep the influence of the edge small, the model must be small in comparison to the diameter of the air stream, while the similarity laws require large models, because of the high Reynolds numbers of the full-scale configurations.

The conditions at the periphery of the test section will first be discussed for the closed and open test section. Consider the following example: The drag coefficient of a circular disk, positioned at a right angle to the oncoming flow, shows the following variation with the Reynolds number $c_D = f(Re)$, indicated schematically in the sketch below.

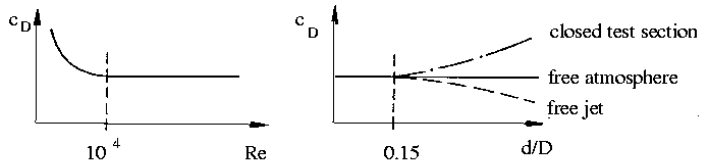


For the range of Reynolds numbers for which $c_D$ = const., one obtains the sketched behavior of wind-tunnel measurements compared to measurements in the atmosphere ($d$ = diameter of the circular disk, and $D$ is the diameter of the air stream in the wind tunnel). As long as the ratio $d/D$ is small (here $d/D < 0.15$), the wind tunnel measurements of the drag coefficient $c_D$ agree with the values measured in the atmosphere.
The comparison of the flow about a blunt body in a closed test section of a wind tunnel (Boundary condition on a rigid wall: $v_n = 0$) with the flow about the same body in the free atmosphere shows, that the wall of the test section squeeses the flow and narrows the stream tube of the actual flow. The walls thereby cause an increase in velocity and higher drag compared to the free atmosphere (see sketch).

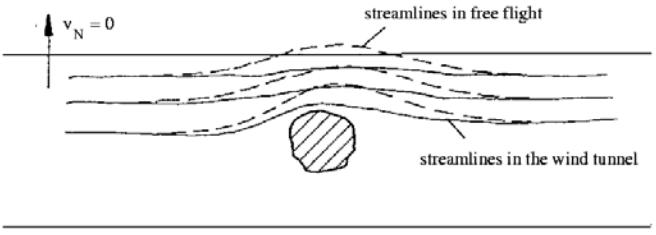


In an open test section the conditions are reversed; the flow can stronger expand in the direction normal to the oncoming flow than in the free atmosphere.
The corrections of the measured data, necessitated by the false lateral boundary conditions in the wind tunnel, can either be obtained from special experiments [NACA Annual Reports 1935, 1937, Pope 1954, Wien and Harms, 1932] or with theoretical estimates [Pope 1954, Prandtl 1961]. The methods of corrections can only briefly be discussed here. The boundary conditions can relatively simply be satisfied in potential flow by superposition of singularities. In order to apply this method, the following assumptions are introduced:

1. The friction forces at the edge of air stream are not considered.
2. The velocity disturbances caused by the body at the edge of the air stream are small compared to $u_\infty$: $f(v_x,v_n,v_t) << u_\infty$ i. e. $h/D << 1$.
3. Incompressibles flow is assumed: $\rho$ = const.
4. The flow is assumed to be steady.

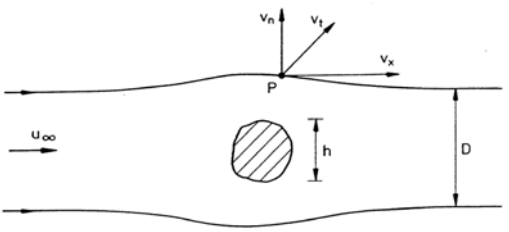


Polar coordinates:
$v_x$ parralel to $u_\infty$
$v_n$ radial
$v_t$ tangential

Boundary conditions at the adge of the air stream with circular cross section: The velocity at the edge is decomposed into $u_\infty$ and the perturbation velocities shown in the sketch above. The Bernoulli equation along the edge streamline yields:

$$p_\infty + \frac{\rho}{2}u_\infty^2 = p + \frac{\rho}{2}\left[(u_\infty + v_x)^2 + v_n^2 + v_t^2\right] \tag{6.97}$$

The static pressure at the edge of the air stream is equal to the atmospheric pressure everywhere: $p = p_\infty$. If quantities of second order are neglected ($v_x$,$v_n$,$v_t$), there is obtained

$$\frac{\rho}{2}u_\infty^2 = \frac{\rho}{2}u_\infty^2 + \rho u_\infty v_x \tag{6.98}$$

$$\rho u_\infty v_x = 0 \rightarrow v_x = 0 \tag{6.99}$$

The perturbation velocity possesses only a normal and a tangential velocity component. The velocity field can be derived from a potential that consists of the potential of the undisturbed free stream and the perturbation potential:

$$\phi = \phi_\infty + \phi_{pert.}; \quad \phi_{pert.} = f(v_n;\ v_t) \tag{6.100}$$

With the assumptions introduced, the lines on the circumference in the $n-t-$plane are equipotential lines, since the Bernoulli equation is valid everywhere.

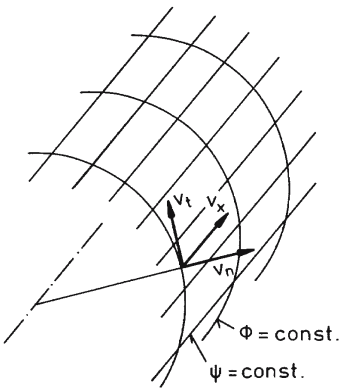


Since the streamlines $\psi$ = const. are normal to the equi-potential lines, it follows that $v_t = 0$. The boundary conditions therefore are: $v_n = 0$ for the closed test section, and $v_x = v_t = 0$ for the open test section.
If the boundary conditions for the corresponding type of wind tunnel can be satisfied a certain distance away from the body to be measured with a suitably chosen potential distribution, then the flow around the body in unrestricted space is similar to the flow in the wind tunnel.

**Mirror Imaging of Singularities.** For plane flows the principle of mirror imaging is a simple method for searching suitable potentials. A few simple examples to illustrate the principle are discussed next:

1. The first question to be discussed is: How does the velocity field (streamlines) of a flow generated by a punctiform source change in infinite two-dimensinal space, if the space is subdivided by a plane wall at the distance $a$ away from the source?
   Obviously the boundary condition $v_n = 0$ cannot be satisfied by the potential of a source alone. By mirror imaging of the source at a wall (with the same strength and the same distance) the velocities add up in such a way, that $v_n$ vanishes along the line of symmetry (see following diagrammatic figure). Two sources generate a flow field, which corresponds to the flow field of a single source in the vicinity of a rigid plane wall (the wall is the mid-vertical to the line connecting the two sources). The second source can also be taken as the mirror image of the first source.

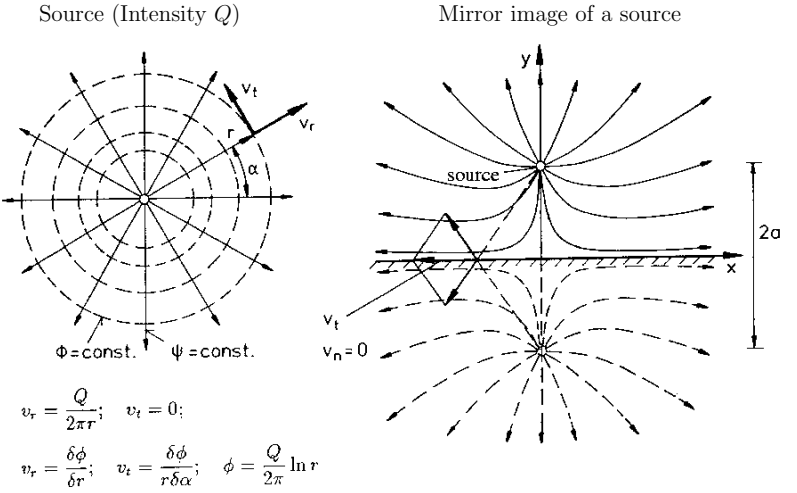


2. The flow field of a vortex in the vicinity of a rigid wall (circulation $\Gamma$) can be generated by mirror imaging of the vortex with the same strength but opposite direction of rotation:

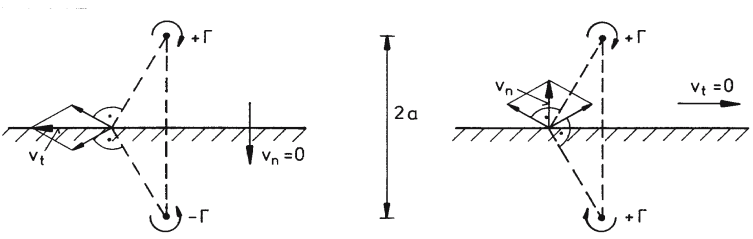


3. A vortex in the vicinity of the edge of a free jet is generated by mirror imaging of a vortex of the same circulation and the same direction of rotation (see afigure above).

**Application of the Principle of Mirror Imaging to the Case of a Wing with Finite Span in an Open Wind Tunnel (Free Jet)**

The cross section of the air stream is assumed to be circular as an approximation to the octagonal cross section of the low-speed wind tunnel of the Aerodynamisches Institut. The wing is represented by a bound vortex and two tip vortices (horseshoe vortex). The lift distribution is assumed to be rectangular.
Since the thickness of the profile is much smaller than the diameter of the air stream, the $x-y$-plane does not have to be considered ($v_x = 0$), (see the following sketch). Since the span is almost as large as the diameter of the air stream, the $y-z$-plane has to be investigated.

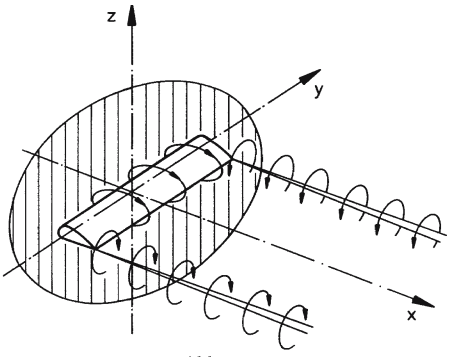


At the location of the bound vortex the cross section of the air stream is represented as depicted in the following sketch:

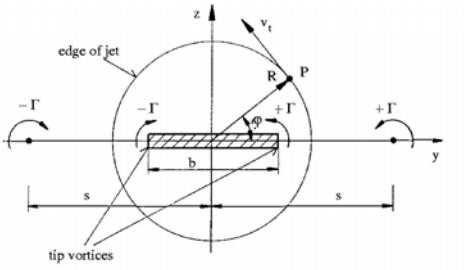


In the $y-z$-plane the boundary condition at the edge of the air stream is $v_t = 0$. This condition is not satisfied by the flow about the wing in the infinite space, since the two tip vortices do not compensate each other to zero (e. g. in the point $P$). The boundary condition mentioned can be satisfied with an additional vortex distribution along the $y$-axis. Since the problem is posed as a two-dimensional one, the position of the mirror-imaged singularities is not immediately evident. For reasons of symmetry at least two potentials with equal distance $s$ measured from the origin of coordinates are needed. The distance $s$ is obtained from the condition, that at an arbitrary point $P$ on the edge of the air stream $v_t$ then vanishes, when the circulation of the mirror-imaged vortices is equal to those of the tip vortices ($\gamma = \text{const}$).

In polar coordinates:
$$v_t = \frac{1}{r}\frac{\partial\phi(r,\varphi)}{\partial\varphi} \tag{6.101}$$

The velocity induced by an infinitely long vortex filament is

$$v_t = \frac{\Gamma}{2\pi r} \tag{6.102}$$

At the location of the bound vortex the free vortices are only half-infinitely long (from 0 to $+\infty$). With the law of Biot-Savart there is obtained:

$$v_t = \frac{\Gamma}{4\pi r} \tag{6.103}$$

Now the four potentials of the vortices shown in the last figure are superposed and the boundary condition on the edge of the air stream $v_t = 0$ is satisfied by a suitable choice of $s$. The following result is obtained:

1. The solution does not depend on $\varphi$; it is valid for all points on the circumference of the edge of the air stream.

2.

$$s = \frac{2\,R^2}{b} \qquad \text{or} \qquad \frac{s}{R} = \frac{2\,R}{b} \tag{6.104}$$

The solution of the equation for $s$ with the boundary condition $v_t = 0$ is tedious. Only the result is reported here. It is seen, that for $b/2 \ll R$ the distance $s$ becomes very large, so that the additional vortices affect the flow near the edge only little.
The corrections of the measured data are now possible since the vortex distribution representing the edge of the air stream is known. First it can be stated, that an additional downwash velocity is induced at the location of the wing, caused by the direction of rotation of the additional vortices. In comparison to the free atmosphere the induced drag and the induced angle of attack measured in the air stream are too large.
In the middle of the wing the downwash velocity induced by the left additional vortex is equal to $\Gamma/4\pi s$, and the one induced by the right is of the same amount $\Gamma/4\pi s$.
The downwash velocity is:

$$\Delta W = 2\,\frac{\Gamma}{4\pi s} = \frac{\Gamma}{2\pi s} = \frac{\Gamma\,b}{4\,\pi\,R^2} \tag{6.105}$$

For an estimate it is assumed that $s \gg b/2$, so that $\Delta W$ can be taken as constant along the span of the wing. Lift and circulation are connected by the Kutta-Joukowsky theorem:

$$\Gamma = \frac{L}{\rho u_\infty b} \quad . \tag{6.106}$$

The downwash velocity then is

$$\Delta W = \frac{L \cdot b/2}{\rho u_\infty b 2\pi R^2} = \frac{L}{4\rho u_\infty A_{freejet}} \quad . \tag{6.107}$$

With the change of the angle of attack

$$\Delta\alpha_i = \frac{\Delta W}{u_\infty} = \frac{2\,L}{8\,\rho\,u_\infty^2 A_n} \tag{6.108}$$

the change of the induced drag is

$$\Delta D_i = L\Delta\alpha_i = \frac{L^2}{4\,\rho\,u_\infty^2 A_n} \quad . \tag{6.109}$$

These values have to be subtracted from the measured values of $\alpha$ and $D$, if the data are to be applied to a full-scale configuration in free flight in the atmosphere. An exact correction should take into account the actual lift distribution at the location of the bound vortex; the additional

vortices then have a corresponding distribtion. Prandtl [1961] carried out this computation for the elliptic lift distribution.

$$\Delta D_i = \frac{L^2}{8\frac{\rho}{2}u_\infty^2 A_n}\left[1 + \frac{3}{16}\left(\frac{b}{D}\right)^4 + \frac{5}{64}\left(\frac{b}{D}\right)^8 + ...\right] \tag{6.110}$$

with $D = 2R$; and $A$ = cross-section area of the air stream.

$$\Delta\alpha_i = \frac{L}{8\frac{\rho}{2}u_\infty^2 A_n}\left[1 + \frac{3}{16}\left(\frac{b}{D}\right)^4 + \frac{5}{64}\left(\frac{b}{D}\right)^8 + ...\right] \tag{6.111}$$

The first term agrees with the rough estimate presented here; the second contributes only an additional amount of about 1 % of the first term for $b/D = 1/2$.
The correction formulas are listed on the evaluation sheet.

**Selected References**

Abbott, J.H., v. Doenhoff, A.E. *Theory of Wing Sections*, Dover Publications, Inc., New York, 1959.

Ergebnisse der AVA Göttingen: III Lieferung, 1927.

NACA Annual Reports: *e. g. for profile NACA 23012:*, Tech. Rep. Nr. 530, $21^{st}$ Ann. Rep. 1935 Tech. Rep. Nr. 586, $23^{rd}$ Ann. Rep. 1937.

Pankhurst, R.C., Holder, D.W.: *Wind-Tunnel Technique* Pitmann & Sons, Ltd. London.

Pope, A *Wind-Tunnel Testing*, Wiley & Sons, Inc., New York, 1954.

Prandtl, L.: *Gesammelte Abhandlungen zur angewandten Mechanik, Hydro- und Aerodynamik, 1. Teil,* Springer-Verlag 1961.

Riegels, W. *Aerodynamische Profile*, Oldenburg, München 1958,

Wien - Harms: *Handbuch der Experimentalphysik, Bd. IV, 2. Teil*, Akad. Verlagsges., Leipzig, 1932.

### 6.6.4 Evaluation

1. Draw the curves of the following functions in a diagram!
   a) $c_L$, $c_D$, $c_m = f(\alpha)$ b) $c_L$, $c_m = f(c_D)$

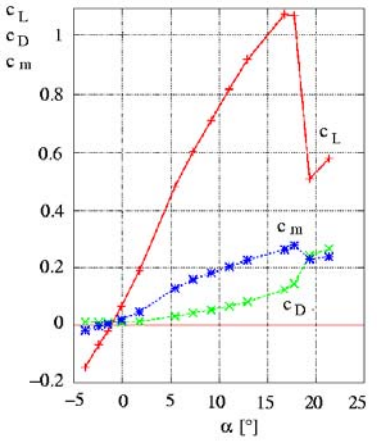


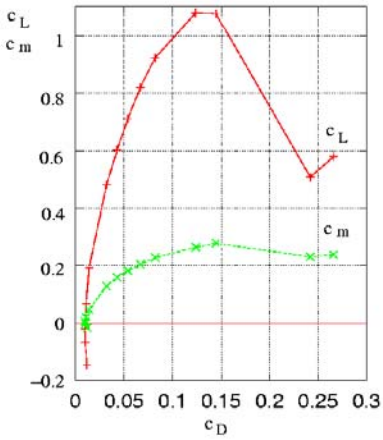


**Evaluation of a three-components measurement $L_{tot.}$,$D_{tot.}$,$M_y$ for a rectangular wing, profile NACA 23012**

| | | |
|---|---|---|
| Geometric data of the wing: | Span width | $b_f = 0.9\,\text{m}$ |
| | Wing chord | $l = l_\mu = 0.2\,\text{m}$ |
| | ⇒Wing area | $A = [\text{m}^2]$ |
| Wind tunnel data: | Diameter of air stream | $D_n = 1.22\,\text{m}$ |
| | Cross section of air stream | $A_n = 1.165\,\text{m}^2$ |
| | Nozzle calibration factor | $\vartheta = 0.98$ |
| Suspension: | | $t_F = 0.2965\,\text{m}$ |
| | | $x = 0.0075\,\text{m}$ |
| | Diameter of wire | $\varnothing = 0.6\,\text{mm}$ |
| | Total area | $f_{D_{susp.tot.}} = 2.868 \cdot 10^{-3}\,\text{m}^2$ |
| Geometry of balance: | | $z_{L_{tot.}} = \frac{d}{e} = \frac{c}{b} = 3$ |
| | | $z_{L_H} = \frac{h}{g} = 2$ |
| | | $z_D = \frac{k}{i} = 1$ |

| | | |
|---|---|---|
| Data of air: | Atmospheric pressure | $Ba =$ [mm Hg] |
| | Kinematic viscosity | $\nu =$ [m$^2$/s] |
| | Gas constant | $R = 287\,\text{J/kgK} = 287\,\text{m}^2/\text{s}^2\,\text{K}$ |
| | Temperature | $t_{Str} =$ [°C] |
| | | ⇒ $T_{Str} =$ [K] |

The pressure in the settling chamber during the test was 81.6 mm $H_2O$. The dynamic pressure in the test section with this value is

$$q'_\infty = \Delta p_{sc} \cdot \vartheta \qquad [\text{mm } H_2O]$$

$$q_\infty = \rho_W \cdot g \cdot q'_\infty \quad [\text{Nm}^2]$$

Determine the free-stream velocity $u_\infty$ and the Reynolds number.
Three-components measurement: Model and aerodynamic forces see sketch on page 286 and balance see the following sketch

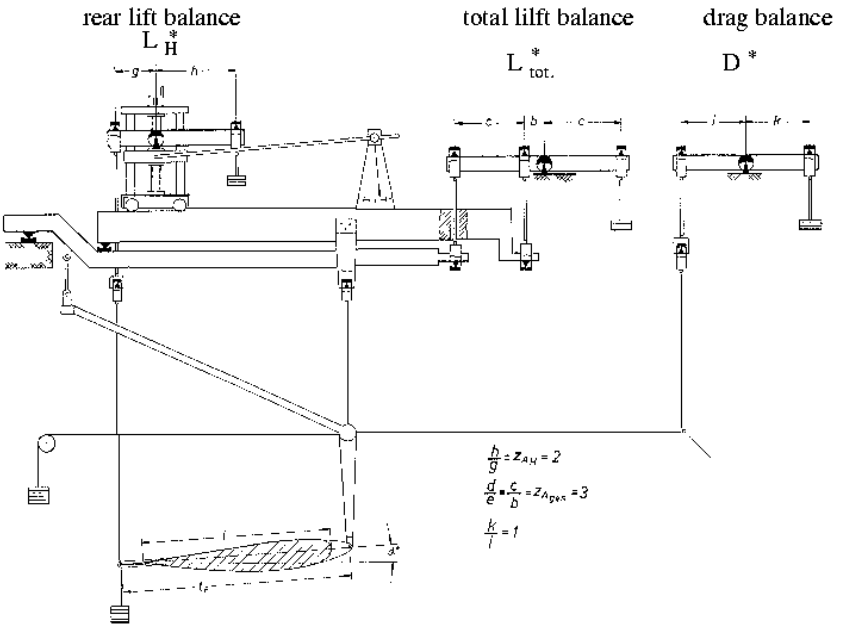

| 1 | 2 | 3 | 4 | 5 | 6 | 7 | 8 | 9 | 10 | 11 | 12 | 13 | 14 | 15 | 16 | 17 |
|---|---|---|---|---|---|---|---|---|---|---|---|---|---|---|---|---|
| $\alpha^*$ | $D^*$ | $L^*_{tot}$ | $L^*_H$ | $L_{tot}$ | $c_L$ | $W'$ | $\Delta D_i$ | $W$ | $c_D$ | $\Delta\alpha_i$ | $\alpha$ | $N$ | $M_H$ | $M_N$ | $M_y$ | $c_m$ |
| [°] | [N] | [N] | [N] | [N] | - | [N] | [N] | [N] | - | [°] | [°] | [N] | [Nm] | [Nm] | [Nm] | - |
| -4 | 4.200 | -6.916 | -1.030 | -20.748 | -0.147 | 1.94 | 0.06 | 1.88 | 0.013 | -0.17 | -3.83 | -20.83 | -0.609 | -0.156 | -0.453 | -0.0160 |
| -2.5 | 3.700 | -3.300 | -0.206 | -9.800 | -0.069 | 1.43 | 0.01 | 1.41 | 0.010 | -0.08 | -2.42 | -9.85 | -0.122 | -0.074 | -0.048 | -0.0017 |
| -1.5 | 3.600 | -0.883 | 0.294 | -2.649 | -0.019 | 1.35 | 0.00 | 1.35 | 0.010 | -0.02 | -1.48 | -2.68 | 0.174 | -0.020 | 0.195 | 0.0069 |
| 0 | 3.730 | 3.100 | 1.148 | 9.300 | 0.066 | 1.48 | 0.01 | 1.46 | 0.010 | 0.08 | -0.08 | 9.30 | 0.681 | 0.070 | 0.611 | 0.0216 |
| 2 | | | | | | | | | | | | | | | | |
| 4 | 5.500 | 15.412 | 4.611 | 46.235 | 0.327 | 3.19 | 0.39 | 2.89 | 0.020 | 0.38 | 3.62 | 46.32 | 2.729 | 0.347 | 2.381 | 0.0843 |
| 6 | 7.152 | 22.180 | 6.798 | 66.541 | 0.471 | 4.90 | 0.64 | 4.26 | 0.030 | 0.55 | 5.45 | 66.65 | 4.013 | 0.500 | 3.513 | 0.1244 |
| 8 | 9.133 | 28.174 | 8.623 | 84.523 | 0.598 | 6.88 | 1.03 | 5.85 | 0.041 | 0.70 | 7.30 | 84.58 | 5.072 | 0.634 | 4.438 | 0.1571 |
| 10 | 11.203 | 33.334 | 9.996 | 100.003 | 0.708 | 8.95 | 1.44 | 7.51 | 0.053 | 0.83 | 9.17 | 99.92 | 5.852 | 0.749 | 5.103 | 0.1806 |
| 12 | 13.096 | 38.249 | 11.311 | 114.748 | 0.812 | 10.85 | 1.90 | 8.95 | 0.063 | 0.95 | 11.05 | 114.33 | 6.583 | 0.858 | 5.725 | 0.2027 |
| 14 | | | | | | | | | | | | | | | | |
| 16 | 19.400 | 47.549 | 13.901 | 142.647 | 1.010 | 17.11 | 2.94 | 14.18 | 0.100 | 1.18 | 14.82 | 141.53 | 7.969 | 1.061 | 6.907 | 0.2445 |
| 18 | 22.632 | 50.796 | 15.107 | 152.400 | 1.079 | 20.38 | 3.35 | 17.03 | 0.121 | 1.26 | 16.74 | 150.84 | 8.579 | 1.131 | 7.448 | 0.2636 |
| 19 | 25.400 | 50.747 | 15.892 | 152.242 | 1.078 | 23.12 | 3.34 | 19.77 | 0.140 | 1.26 | 17.74 | 151.03 | 8.976 | 1.133 | 8.035 | 0.2844 |
| 20 | 27.654 | 50.914 | 16.334 | 152.742 | 1.081 | 25.40 | 3.37 | 22.04 | 0.156 | 1.26 | 18.74 | 151.73 | 9.173 | 1.138 | 8.035 | 0.2844 |
| 21 | 39.240 | 27.420 | 13.057 | 82.300 | 0.582 | 36.99 | 0.98 | 36.01 | 0.255 | 0.68 | 20.32 | 89.64 | 7.261 | 0.672 | 6.589 | 0.2332 |
| 22 | 40.340 | 27.184 | 13.312 | 81.550 | 0.577 | 38.09 | 0.96 | 37.13 | 0.263 | 0.67 | 21.33 | 89.47 | 7.354 | 0.671 | 6.683 | 0.2365 |

**(Numbers in () give the numbers of the columns in the test report)**

**Measured Data:**
(1) geometric angle of attack $\alpha^*[^o]$ (3) Total lift $L^*_{tot.}[N]$

(2) Drag $D^*[N]$ (4) Rear lift $L^*_h[N]$

**Determination of the Lift Coefficient:**
(5) $L_{tot.} = z_{L_{tot.}} \cdot L^*_{tot.}$ (6) $c_L = \dfrac{L_{tot.}}{q_\infty \cdot A}$

**Determination of the Corrected Drag Coefficient:**
a) Correction of the influence of the suspension:
(7) $D' = z_D(D^* - D_{susp.})$
with $D_{susp.} = c_D \cdot q_\infty \cdot f_{D_{susp.}}$
$c_D = 1$

b) Correction of the influence of the induced drag
(8) $\Delta D_i = \dfrac{L^2_{tot.}}{8 q_\infty A_n}\left(1 + \dfrac{3}{16}\left(\dfrac{b_w}{D_n}\right)^4\right)$
(9) $D = D' - \Delta D_i$
(10) $c_D = \dfrac{D}{q_\infty A}$

**Determination of the Effective Angle of Attack:**
Induced angle of attack $\Delta\alpha_i$ in the air stream
(11) $\Delta\alpha_i = \dfrac{L_{tot.}}{8 q_\infty A_n}\left(1 + \dfrac{3}{16}\left(\dfrac{b_w}{D_n}\right)^4\right)\dfrac{180}{\pi}$
(12) $\alpha = \alpha^* - \Delta\alpha_i$

**Determination of the Normal Force: (comp. page 296)**
(13) $N = L_{tot.}\cos\alpha + D\sin\alpha$

**Determination of the Pitching Moment Coefficient Referenced to Point E:**
(14) $M_H = L_H \cdot t_F \cdot \cos\alpha$
with $L_H = L^*_H \cdot z_{LH}$
(15) $M_N = N \cdot x$
(16) $M_E = M_y = L_H \cdot t_F \cdot \cos\alpha - N \cdot x$
(17) $c_{my} = c_m = \dfrac{M_y}{q_\infty \cdot A \cdot l_\mu}$

## 6.7 Water Analogy – Propagation of Surface Waves in Shallow Water and of Pressure Waves in Gases

*Abstract*

The analogy between the flow proccesses in shallow water and the flow of compressible gases is called "water analogy". The analogy is demonstrated here for the propagation of a surface wave in a shallow open channel flow and the propagation of a pressure wave in a gas-filled pipe.

### 6.7.1 Introduction

Different physical processes are called analogous, if they can be described by the same mathematical relations. In a flow field the local changes of state are in general described by partial differential equations with prescribed boundary and initial conditions. If another physical proccess can be found, which can be described by the same differential equations, boundary and initial conditions, then the field in which this process takes place is anlogous to the flow field. It is clear that only those analogies are meaningful, which make it possible to describe the flow field in a simpler manner by transferring results of observations and measurements obtained for the analogous field than by a direct flow experiment. Two known examples of such analogies are:

a) The electric analogy of the incompressible potential flow

The potential $u$ of the electric current in a homogeneous three-dimensional conductor satisfies the Laplace differential equation in the same way as does the flow potential $\Phi$

$$\Delta u = 0 \quad ; \quad \Delta \Phi = 0 \tag{6.112}$$

b) The Hele-Shaw flow

If in an incompressible flow the inertia forces can be neglected in comparison to the friction forces, the flow is described by the Laplace equation for the pressure $p$:

$$\Delta p = 0 \tag{6.113}$$

The pressure $p$ is therefore the quantity that is analogous to the flow potential $\Phi$ of the incompressible potential flow. This analogy is employed in the experiment on the pressure distribution on a half body for simulating potential flows about blunt bodies.

### 6.7.2 The Water Analogy of Compressible Flow

The flow analogous to the gas flow is the shallow-water flow. This analogy is valid for steady and unsteady flows.

#### Observation

In shallow, supercritical steady water flow in open channels surface waves are observed, which are caused by roughness elements of the walls, similar to the Mach lines in supersonic nozzle flow:

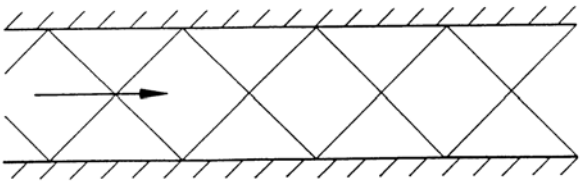

Upstream of an obstacle the water rises in an almost discontinuous "jump", which is similar in shape to the bow shock in front of a blunt body in supersonic flow:

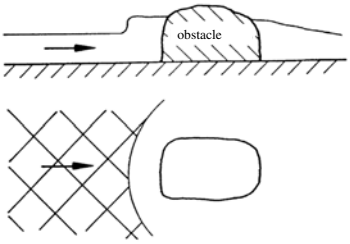


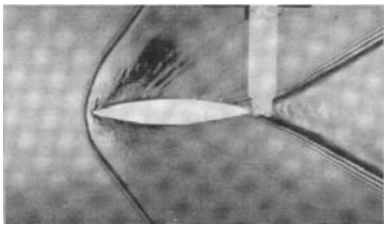

An analogy between the supersonic flow of gases and the supercritical flow of water can therefore be infered by such an obersvation alone. This analogy also exists for subsonic gas flows, as an exact analysis of [Preiswerk 1938] shows.

**Surface Waves**

Waves observed on the boundary of two media are called surface waves [Prandtl 1965]. The waves on free surfaces of liquids are classified, according to the nature of their restoring force, in gravity and capillary waves.

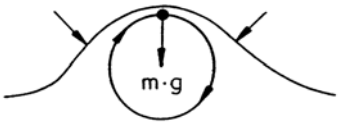


**Gravity Waves**

Caused by inertia and gravitational forces the individual fluid particles move along approximately circular paths in planes normal to the water surface, the diameter of which strongly decreases with the depth below the surface of the water. With the aid of the potential theory the propagation velocity of a wave crest, also called phase velocity can be determined [Truckenbrodt 1968] to

$$c = \sqrt{\frac{\lambda\, g}{2\,\pi} \tan h \left(\frac{2\,\pi h}{\lambda}\right)} \quad . \tag{6.114}$$

The dependence of the propagation velocity on the wave length is called dispersion. If the water depth is large in comparison to the wave length ($h \ll \lambda$), the last equation reduces to

$$c = \sqrt{\frac{\lambda\, g}{2\,\pi}} \quad . \tag{6.115}$$

Vice versa, if the water depth is much smaller than the wave length ($h << \lambda$), the propagation velocity is simply

$$c = \sqrt{g\, h} \quad . \tag{6.116}$$

In the following the analogy between the propagation velocity $c = \sqrt{g\, h}$ of a shallow-water wave and the propagation velocity of waves in perfect gases with constant specific heats will be derived.

**Capillary Waves**

In waves with very short wave length the restoring forces, which tend to smoothen the wave motion, are not due to gravity but primarily to surface tension. The propagation velocity is then:

$$c = \sqrt{\frac{2\,\pi\,\sigma}{\rho\,\lambda}} \tag{6.117}$$

The quantity $\sigma$ is the capillary constant, which for water is $\sigma = 72{\cdot}10^{-3} N/m$. If both, gravitation and capillarity have to be taken into account, the propagation velocity of surface waves of deep water is

$$c = \sqrt{\frac{\lambda\,g}{2\,\pi} + \frac{2\,\pi\,\sigma}{\rho\,\lambda}} \quad . \tag{6.118}$$

The propagation velocity attains a minimum for the wave length $\lambda = 2\,\pi\sqrt{\sigma/g\,\rho}$. The values for water are $\lambda = 1.7\ cm$ and $c_{min} = 23.3\ cm/s$.
In the following the analogous laws will be derived for the special case of the propagation of a pressure disturbance in a gas-filled pipe with constant cross section and in the shallow-water flow in an open channel. The laws for the gas flow will be considered on the left-hand side of the page, and those for the shallow-water flow on the right. This form is chosen, in order to demonstrate the completely analogous forms of the laws to be derived.
The derivation begins with the statements of the assumptions to be introduced for the derivation of the analogies.

**Derivation of the Analogous Laws**

With the assumptions for

| Gas | Water |
|---|---|
| - perfect gas with constant specific heats | -shallow water $z_0 \ll \lambda$ (which means: The vertical components of the velocity and acceleration can be neglected) |
| -isentropic flow | -inviscid flow |

it can be shown, that a plane unsteady gas flow and the shallow-water flow can be described by analogous differential equations [Niehus 1968].
The analogy between the propagation of a pressure disturbance in a gas-filled pipe with constant cross section and in a shallow open channel with constant width is considered as a special case.

| Gas | Water |
|---|---|
| 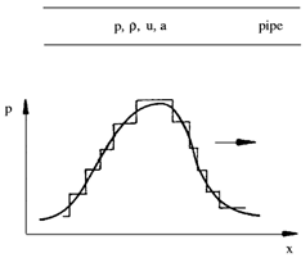  | 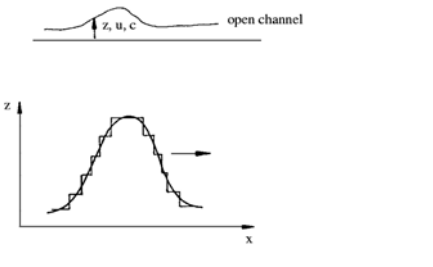  |

Consider a continuous solitary wave of finite amplitude in the sketch. It is approximated by a sequence of a finite number of wave elements, in which the flow conditions are changing discontinuously.
Such a wave element which changes the flow conditions only slightly, for example the velocity $u$ to $u + du$, propagates with the speed of sound in the gas and with the phase velocity in the water. Its absolute velocity is therefore $u + a$ and $u + c$, respectively. It is assumed that the control surface sketched below also moves with the absolute velocity.

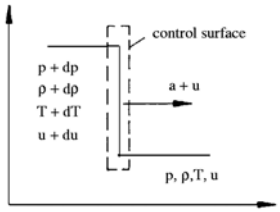


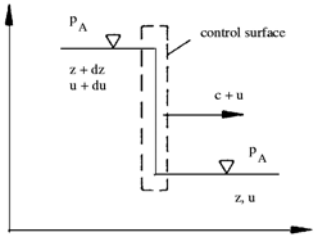


The changes of conditions generated by the wave element appear to be steady to an observer moving with the control surface. For this frame of reference the fundamental equations can be formulated for steady flow:

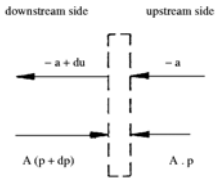


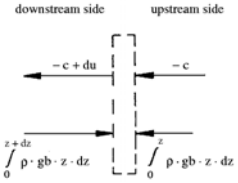


$u-(u+a)=-a$ Upstream velocity $u-(u+c)=-c$

$u+du-(u+a)=-a+du$ Downstream velocity $u+du-(u+c)=-c+du$

The continuity equation then reads:

$$-a\rho\cdot A=(-a+du)(\rho+d\rho)\cdot A \;\big|\; -c\rho bz=(-c+du)\rho\cdot b(z+dz)$$

If higher-order terms are neglected, there is obtained

$$\rho\,du=a\,d\rho \qquad\qquad z\,du=c\,dz$$

The momentum theorem yields:

$$-(\rho+d\rho)\,(-a+du)^2\,A+\rho a^2\,A = (p+dp)\,A-p\,A$$

$$-\rho b(z+dz)(-c+du)^2+\rho bzc^2 = \int_0^{z+dz}\rho gb\cdot z\,dz-\int_0^{z}\rho gb\cdot z\,dz$$

Again, neglecting higher-order terms gives

$$dp=a\rho\,du \qquad\qquad d\left(\frac{gz^2}{2}\right)=cz\,du$$

The relative speed of propagation follows from the simplified continuity and momentum equation to

$$a^2 = \frac{dp}{d\rho} \qquad c^2 = \frac{d}{dz}\left(\frac{gz^2}{2}\right)$$

respectively

$$a^2 = \gamma\frac{p}{\rho} \qquad c^2 = 2\frac{\frac{g}{2}z^2}{z} = gz$$

(Corresponding assumption:
Isentropic change of state)

Other analogous quantities can be found. From the above relations it follows:

$$\frac{a_2^2}{a_1^2} = \frac{\gamma_2 R}{\gamma_1 R}\frac{T_2}{T_1} \qquad \frac{c_2^2}{c_1^2} = \frac{2\frac{g}{2}z_2}{2\frac{g}{2}z_1}$$

and for $\gamma = \text{const.}$

$$\frac{a_2^2}{a_1^2} = \frac{T_2}{T_1} \qquad \frac{c_2^2}{c_1^2} = \frac{z_2}{z_1}$$

For a perfect gas with constant specific heats it follows with $h = c_p T = \frac{a^2}{\gamma - 1}$ and $dh - \frac{1}{\rho}dp = 0$ (isentropic relation) from the simplified momentum equation

$$du = \frac{2}{\gamma - 1}da$$

Directly from the continuity and momentum equation with the propagation velocity

$$du = 2d(\sqrt{gz})$$

It is seen, how for both flows from mass-flow and momentum considerations relations are obtained, which in their form are completely equivalent, if only the variable in question in one system is replaced by the corresponding variable or a group of variables in the other system. The analogies can be extended, if additional assumptions are introduced, as for example the extension to two media, as shown by the relations for the speed of sound of the gas flow and for the propagation velocity of the wave in the shallow-water flow.

**Analogous Quantities and Conclusions**

The following analogous quantities can be identified from these considerations:

| *Gas* | *Water* |
|---|---|
| compressible | incompressible |
| velocity $u$ | velocity $u$ |
| speed of sound $a$ | phase velocity c |
| density $\rho$ | water depth $z$ |
| pressure $p$ | product $\frac{1}{2}gz^2$ |
| ratio of the spec. heats $\gamma$ | constant 2 |
| temperature $T$ | water depth z |
| gas constant $R$ | costant $\frac{g}{2}$ |
| specific heat $c_p$ | constant g |
| specifice heat $c_v$ | constant $\frac{g}{2}$ |
| Mach number $Ma = \frac{u}{a}$ | Froude number $Fr = \frac{u}{c}$ |
| subsonic flow $Ma < 1$ | subcritical flow $Fr < 1$ |
| supersonic flow $Ma > 1$ | supercritical flow $Fr > 1$ |

The last equations show, how pressure, particle velocity, speed of sound, and phase velocity change in the wave: The front of the wave moves faster than the tail. Wave fronts in which pressure or water hight, respectively, increase, become steeper, and fronts, in which these quantities decrease, are flatened. In gases the steepening of the front results in a non-isentropic compression shock; the steepening of a surface wave leads to the hydraulic jump, also causing losses in the flow.
The water analogy derived here for the example of a solitary wave for a gas with isentropic exponent $\gamma = 2$ is generally valid for the shallow-water flow. A gas with $\gamma = 2$ does not exist, as $\gamma = \frac{f+2}{f}$ corresponds to a gas with only two degrees of freedom, while a monatomig gas ($\gamma = 1.66$) possesses already three degrees of freedom. If an open channel is used with a cross section different from a rectangular one, gases with different isentropic exponents $\gamma$ can be included in the analogy. A triangular cross section would lead to an analogy with a gas with $\gamma = 1.5$.
The water analogy can be used to clarify qualitatively complex flow processes, which are theoretically and experimentally difficult to analyze. For example the propagation of a pressure wave in an exhaust system, which is difficult to follow because of the high propagation velocity, can conveniently be studied in the analogous proccess in an open channel.

**Selected References**

Niehaus, G.: *Die Anwendbarkeit der Gas-Flachwasser-Analogie in quantitativer Form auf Strömungen um stumpfe Körper*, DLR, FB 68-21, 1968.

Prandtl, L: *Führer durch die Strömungslehre*, Vieweg-Verlag, 1965

Preiswerk, E.: *Anwendung gasdynamischer Methoden auf Wasserströmungen mit freier Oberfläche*, ETH-Bericht Nr. 7, 1938.

Truckenbrodt, E: *Strömungsmechanik*, Springer-Verlag, 1968, S.355 ff.

*Lexikon der Physik*, Francksche Verlagsbuchhandlung Stuttgart

### 6.7.3 The Experiment

A simple unsteady flow process is considered, namely the propagation of a surface wave in a shallow-water open channel with constant width as analogy to the propagation of a pressure wave in a gas-filled pipe with constant cross section.

In the experiment the dependence of the phase velocity $c$ on the depth of the water $z_0$ is measured first. It is analogous to the dependence of the speed of sound of a gas on the temperature. In the second part of the experiment the change of the profile of a surface wave is investigated during the propagation of the wave in the open channel, which is analogous to the change of the profile of a pressure wave in a pipe.

### 6.7.4 Evaluation

1. Measurement of the propagation velocity of a small disturbance as a function of the water depth and comparison of the measured velocity values $c = \frac{\Delta x}{\Delta t}$ with data obtained from theory $c = \sqrt{g \cdot z_0}$.

| $\Delta x$ | $z_0$ | $\Delta t$ | $c = \frac{\Delta x}{t}$ | $c = \sqrt{g \cdot z_0}$ |
|---|---|---|---|---|
| mm | mm | s | $\frac{m}{s}$ | $\frac{m}{s}$ |
| 2000 | 25 | 3.6 | 0.55 | 0.495 |
| | | 3.8 | 0.526 | |
| | | 3.8 | 0.526 | |
| | 35 | 3.3 | 0.61 | 0.586 |
| | | 3.3 | 0.61 | |
| | | 3.25 | 0.615 | |
| | 46 | 2.8 | 0.714 | 0.672 |
| | | 2.8 | 0.714 | |
| | | | | |

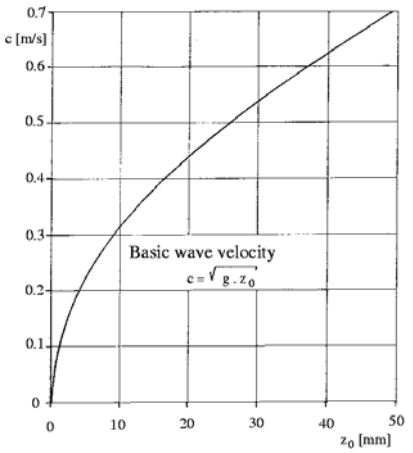


2. Comparison of measured (upper curve) with computed change of shape (lower curve) of a surface wave moving in the open channel.

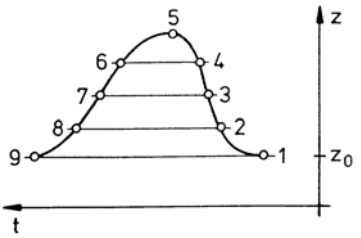


The initial wave (measuring position I) is to be subdivided into at least 8 sections, for which the theoretical propagation velocity is to be determined. The change of the shape of the wave, which would result from the propagation of the wave through the open channel is to be compared with the measured values.

As shown before, the absolute propagation velocity of a wave element is

$\frac{dx}{dt} = c(z) + u(z)$ with $c(z) = \sqrt{g \cdot z}$

$u(z) = 2(\sqrt{g \cdot z} - \sqrt{g \cdot z_0})$

$\frac{dx}{dt} = 3\sqrt{g \cdot z} - 2\sqrt{g \cdot z_0}$

| Point | $z$[mm] | $3\sqrt{g \cdot z}$[m/s] | $2\sqrt{g \cdot z_0}$[m/s] | $dx/dt$[m/s] | $\Delta x$[m] | $\Delta t$[s] |
|---|---|---|---|---|---|---|
| 1;9 | 40.3 | 1.886 | | 0.634 | | 1.18 |
| 2;8 | 42.3 | 1.933 | | 0.683 | | 1.10 |
| 3;7 | 44.3 | 1.977 | 1.25 | 0.727 | 0.75 | 1.03 |
| 4;6 | 46.3 | 2.022 | | 0.772 | | 0.97 |
| 5 | 47.7 | 2.052 | | 0.802 | | 0.935 |

The form of the wave computed for the measuring point II is to be plotted.

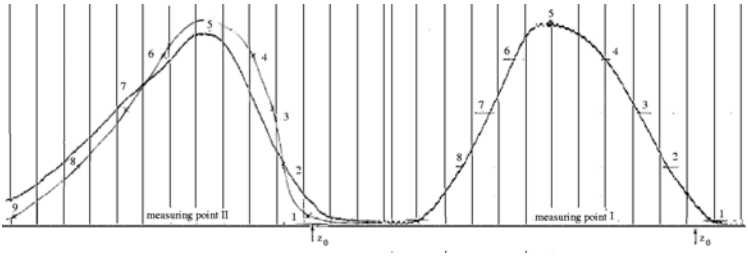


Propagation of a surface wave in an open channel of constant cross section

Discuss the deviation of the computed form of the wave from the measured form.
The amplitude of the measured wave is smaller than that of the computed. On the whole, the experimentally determined wave is somewhat flatter. The flow was assumed to be inviscid for the computation. In the experiment the action of the friction forces results in a damping of the wave. Additionally, the vertical components of the velocity and of the acceleration are neglected in the computation, i. e. it was assumed that $z_0 \ll \lambda$. In the experiment $z_0 = 4\ cm$, and $\lambda \approx 11\ cm$.
3. Discuss the change of the shape of a sinosoidal pressure wave, which is moving in a pipe with constant cross section, filled with a compressible gas.
In the initial phase the sinosoidal wave propagates with the speed of sound relative to the flowing gas; the change of state can be assumed to be isentropic, and the pressure wave steepens according to the water analogy, until the density gradient becomes large.
4. Discuss the advantages and disadvantages of the investigation of gas flows with the aid of the shallow-water analogy.
The advantages are, that complex flow processes, which are difficult to analyze either experimentally or theoretically, can be simualted in a simple manner, as for example pressure waves with high propagation velocities, which barely can directly be followed visually.
The disadvantages are, that the simulated analogous results can only qualitatively be applied to the actual flow to be investigated. The formulation of the analogy may also contain simplifying assumptions, which cannot always be realized in the experiment.

## 6.8 Resistance and Losses in Compressible Pipe Flow

*Abstract*

The resistance coefficient of a standard orifice and its gasdynamic losses are measured in a smooth cylindrical pipe as a function of the free-stream Mach number $Ma_1$ for values of $0.1 < Ma_1 < 0.3$. The experimental data are obtained by measuring the pressure distribution along the wall of the pipe and by measuring the volume rate of flow with a standard nozzle connected in series with the pipe.

### 6.8.1 Flow Resistance of a Pipe with Inserted Throttle (Orificee, Nozzle, Valve etc.)

The total resistance $R_{1,2}$ of a pipe of length $l_{1,2}$ with a device inserted consists of the friction and pressure resistance

$$R_{1,2} = R_F + R_P \tag{6.119}$$

The momentum theorem yields

$$R_{1.2} = A[(p_1 + \rho_1 u_1^2) - (p_2 + \rho_2 u_2^2)] \tag{6.120}$$

with $A = \pi D^2/4$, the velocity $u$, and the density $\rho$ averaged over the cross section. In incompressible flow it is $\rho_1 u_1^2 = \rho_2 u_2^2 = \rho u^2$, and the total resistance coefficient is defined as

$$\zeta_{1,2inc.} = \frac{R_{1,2}}{\frac{\rho}{2} u^2 A} = \frac{p_1 - p_2}{\frac{\rho}{2} u^2} \tag{6.121}$$

Since in compressible pipe flow the dynamic pressure $\rho u^2/2$ is changing in the flow direction with the other flow quantities, (6.121) cannot be used for the determination of the resistance coefficient. The method of test for compressible flow will be described later.

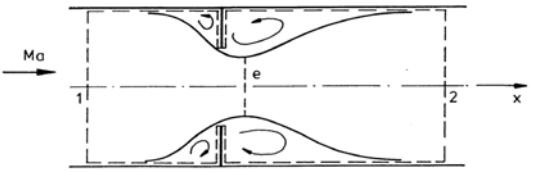


### 6.8.2 Friction Resistance of a Pipe Without a Throttle

#### Friction Coefficient $\lambda$ of Fully Developed Pipe Flow

The friction coefficient

$$\lambda = \frac{4\tau_w}{\frac{\rho u^2}{2}} \tag{6.122}$$

is defined by the local wall shear stress $\tau_w$, non-dimensionalized with the local dynamic pressure. For the fully developed compressible flow in rough pipes $\lambda$ depends on the Reynolds number $Re$, on the equivalent sand roughness $r/k$, and also on the Mach number $Ma$. Early experiments [Frössel 1936, Naumann 1956, Jaeneke 1975] showed, that in supersonic flows ($Ma > 1$) the friction coefficient $\lambda$ varies strongly with $Ma$, while in subsonic flows $\lambda$ is almost independent of $Ma$, so that the data measured in incompressible flow remain also valid for subsonic compressible flow for $Ma < 1$. The following formula is valid for smooth pipes for Reynolds numbers $2 \cdot 10^4 < Re < 2 \cdot 10^6$:

$$\lambda = 0.0054 + 0.396 \cdot Re^{-0.3} \tag{6.123}$$

**The Change of the State Variables by Skin Friction**

For steady, one-dimensional, adiabatic flow of a perfect gas the conservation equations for mass, momentum, and energy have the following differential form:

Continuity equation $$\frac{d\rho}{\rho} + \frac{du}{u} = 0$$

Momentum equation $$dp + \rho u du + \frac{\lambda dx}{D}\frac{\rho u^2}{2} = 0$$

Energy equation $$c_p dT + u du = 0$$

and further

Equation of state $$\frac{dp}{p} = \frac{d\rho}{\rho} + \frac{dT}{T}$$

and for constant specific heats $$\frac{dMa^2}{Ma^2} = \frac{du^2}{u^2} - \frac{dT}{T}$$

The relation between the increase of entropy and the decrease of stagnation pressure is obtained from the second law of thermodynamics:

$$T ds = c_p dT - \frac{dp}{\rho} \tag{6.124}$$

$$ds = c_p \frac{dT}{T} - R\frac{dp}{p} \tag{6.125}$$

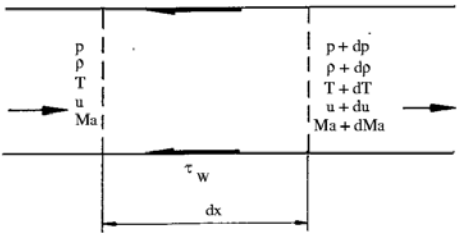


The stagnation conditions ($T_0$,$p_0$) of a flowing gas are defined by the assumption, that they are generated by an isentropic deceleration to zero velocity u = 0. The following relations are then valid:

$$s = s_0, \quad ds = ds_0 \text{ and } ds_0 = c_p \frac{dT_0}{T_0} - R\frac{dp_0}{p_0} \tag{6.126}$$

With the adiabatic change of state assumed, i. e. ($dT_0 = 0$), there results

$$s_{02} - s_{01} = s_2 - s_1 = R \ln\left(\frac{p_{01}}{p_{02}}\right) \quad . \tag{6.127}$$

The changes of the state variables are obtained with the above equations [Shapiro 1953, Emmons 1958]:

| | | | $Ma < 1$ | $Ma > 1$ |
|---|---|---|---|---|
| $\frac{du}{u}$ | $=$ | $\frac{\gamma Ma^2}{2\,(1-Ma^2)} \cdot \frac{\lambda}{D} dx$ | $> 0$ | $< 0$ |
| $\frac{dT}{T}$ | $=$ | $-\frac{\gamma Ma^2}{2\,(1-Ma^2)}(\gamma - 1) \cdot \frac{\lambda}{D} dx$ | $< 0$ | $> 0$ |
| $\frac{dp}{p}$ | $=$ | $-\frac{\gamma Ma^2}{2\,(1-Ma^2)}[1 + (\gamma - 1)Ma^2] \cdot \frac{\lambda}{D} dx$ | $< 0$ | $> 0$ |
| $\frac{d\rho}{\rho}$ | $=$ | $-\frac{\gamma Ma^2}{2\,(1-Ma^2)} \cdot \frac{\lambda}{D} dx$ | $< 0$ | $> 0$ |
| $\frac{dMa^2}{Ma^2}$ | $=$ | $\frac{\gamma Ma^2}{1-Ma^2} \cdot \left(1 + \frac{\gamma - 1}{2} Ma^2\right) \frac{\lambda}{D} dx$ | $> 0$ | $< 0$ |
| $\frac{ds}{R}$ | $=$ | $\frac{\gamma Ma^2}{2} \cdot \frac{\lambda}{D} dx$ | $> 0$ | $> 0$ |
| $\frac{dp_0}{p_0}$ | $=$ | $-\frac{\gamma Ma^2}{2} \cdot \frac{\lambda}{D} dx$ | $< 0$ | $< 0$ |

For constant mass flow $\rho u = \dot{m}/A$ the adiabatic change of state can be plotted in the $T - s$-diagram.

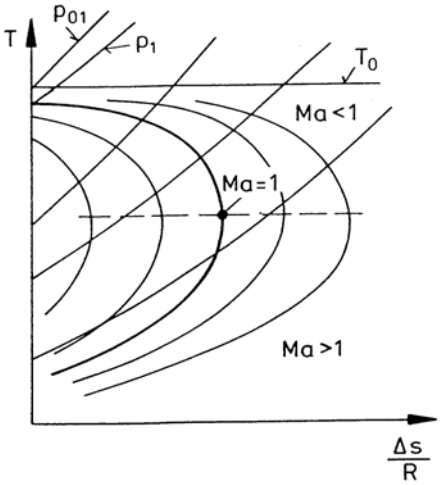


The diagram mainly serves the purpose to trace the flow process in a pipe during a change of state. The curves are easier to follow than the equations stated above. The ordinate $T$ can be taken as a distorted scale of the velocity, and for a perfect gas, also of the speed of sound and the Mach number. As other physical processes the pipe flow proceeds in the direction of increasing entropy. The curves for constant mass flow attain an extreme at $Ma = 1$. They can be made to coincide by shifting them in the direction of increasing entropy. The line $Ma = 1$ is parallel to the abscissa, separating the diagram into the subsonic region (upper part) and supersonic region (lower part):

The considerations are not necessarily restricted to pipe flows with circular cross sections. The relations also hold true for ducts with constant cross sections.
The resulting curves are called Fanno curves. They are obtained from the above equations:

$$\frac{s-s_1}{R} = ln\left[\left(\frac{T}{T_0}\right)^{\frac{1}{\gamma-1}}\sqrt{1-\frac{T}{T_0}}\right] - ln\left[\left(\frac{T_1}{T_0}\right)^{\frac{1}{\gamma-1}}\sqrt{1-\frac{T_1}{T_0}}\right] \tag{6.128}$$

According to the second law of thermodynamics the entropy increases in the flow direction and attains a maximum for $Ma = 1$. In subsonic and also in supersonic flow through a pipe with constant cross section, the Mach number tends to unity, $Ma = 1$. For prescribed inflow conditions the flow will either be accelerated or decelerated to sonic speed at a maximum pipe length $L_{max}$.

**The Resistance Coefficient $\zeta_{max}$**

The maximum pipe length at which $Ma = 1$ is reached, is obtained by integration of the equation for $\frac{dMa^2}{Ma^2}$, within the limits given by the Mach number at inflow conditions $Ma_1(x = 0)$ and $Ma(x = L_{max}) = 1$:

$$\int_0^2 L_{max}\lambda\frac{dx}{D} = \int_{Ma_1^2}^{Ma^2=1}\frac{1-Ma^2}{\kappa Ma^4\left(1+\frac{\gamma-1}{2}Ma^2\right)}dMa^2 \tag{6.129}$$

Since $\lambda = \lambda(Re)$, and since the Reynolds number and the Mach number are changing, the following simplification is introduced:

$$\bar{\lambda} = \frac{1}{L_{max}}\cdot\int_0^{L_{max}}\lambda\, dx \tag{6.130}$$

With the definition

$$\zeta_{max} = \bar{\lambda}\frac{L_{max}}{D} \quad , \tag{6.131}$$

there is obtained

$$\zeta_{max} = \frac{(1-Ma_1^2)}{\gamma Ma_1^2} + \frac{(\gamma+1)}{2\gamma}\ln\left[\frac{(\gamma+1)Ma_1^2}{2+(\gamma-1)Ma_1^2}\right] \quad . \tag{6.132}$$

The following diagram shows the plot of $\zeta_{max} = \zeta(Ma)$, determined with (6.132) for $\gamma = 1.4$.

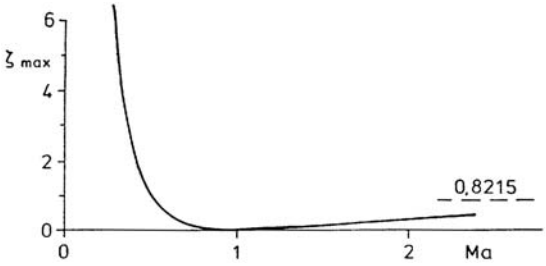


For a given perfect gas with constant specific heats the resistance coefficient $\zeta_{max}$ depends only on the Mach number, and is - as the Mach number - therefore a state variable of the adiabatic pipe flow.
It follows, that if the Mach numbers $Ma_1$ and $Ma_2$ are known for two points, with the distance $l_{1,2}$ between them, the resistance coefficient $\zeta_{1,2}$ of this part of the pipe is

$$\zeta_{1,2} = \zeta_{max}(Ma_1) - \zeta_{Ma_2} \quad , \tag{6.133}$$

and it follows with (6.131) that

$$\zeta_{1,2} = \frac{\bar{\lambda}}{D}[L_{max}(Ma_1) - L_{max}(Ma_2)] = \bar{\lambda}\frac{l_{1,2}}{D} \quad . \tag{6.134}$$

### 6.8.3 Resistance of an Orifice

Since $\zeta_{max}(Ma)$ is a state variable, $\zeta_{1,2} = \zeta(Ma_1,Ma_2)$ in adiabatic pipe flow depends only on the conditions at the positions "1" and "2", but not on the change of state from "1" to "2". It is therefore irrelevant, whether the change of state is caused by the action of friction or pressure forces or both. The total resistance coefficient $\zeta_{1,2}$ of a piece of pipe with an orifice can therefore be determined with (6.133), if only the position "2" is located far enough downstream from the orifice, so that the process of entropy increase equivalent to the work done by the resistance force has come to an end.
For the design of a pipe system it is important to know the additional resistance, which is caused by the insertion of an orifice, or in general by a throttle. The resistance consists of the pressure resistance caused by the throttle and of the change of the frictional resistance caused by the insertion of the throttle in comparison to that of the fully developed pipe flow. The additional resistance is then given by the difference between the resistance of the pipe measured with the insertion and without, such that

$$\zeta_O = \zeta_{1,2} - \bar{\lambda}\frac{l_{1,2}}{D} \quad . \tag{6.135}$$

The following diagram shows the rsistance coefficient of an orifice $\zeta_O$ of a standard orifice ($m = (D_O/D)^2 = 0.5$) as a function of the Mach number $Ma_1$. The Reynolds number of the flow was $Re \approx 3 \cdot 10^5$ .

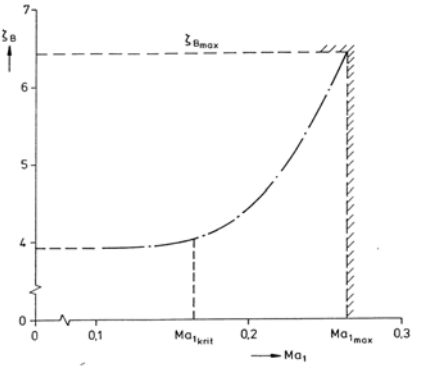


The variation of $\zeta_O(Ma_1)$ is discussed with the aid of the following sketches of the flow through the orifice, which changes with the Mach number $Ma_1$.

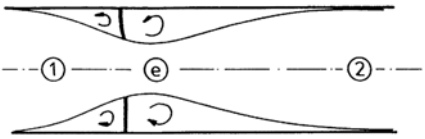


For low Mach numbers $Ma_1$ the friction coefficient depends only on the Reynolds number, i. e. $\zeta_O = \zeta_O(Re)$. It is almost constant. With increasing Mach number $Ma_1$ the friction coefficient also depends on the Mach number, i. e. $\zeta_O = \zeta_B(Re,Ma)$, increasing only slightly until the speed of sound is reached in the narrowest cross section near the orifice ($Ma_e = 1$) for the so-called critical inflow Mach number $Ma_{1crit.}$.

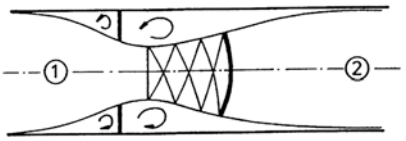


If then $p_2/p_{01}$ is further increased, $\zeta_O$ increases rapidly, and downstream from the orifice the flow expands to supersonic speed, subsequently being decelerated again to subsonic speed by a compression shock. The narrowest cross section of the stream, where $Ma_e = 1$, is enlarged. As a consequence the mass flow is increased, and $Ma_1$ exceeds $Ma_{1crit.}$.

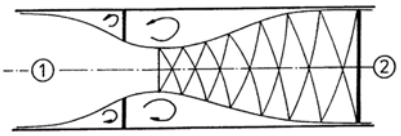


The resistance coefficient of the orifice attains its maximum value $\zeta_{Omax}$, if the supersonic flow extends to the wall of the pipe. A further increase of the Mach number beyond $Ma_{1max}$ is not possible.

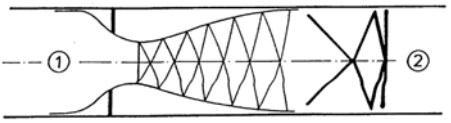


An additional decrease of the pressure ratio $p_2/p_{01}$ causes a downstream motion of the compression shock, and the flow downstream from the orifice is supersonic, intersected by a system of oblique shocks: The resistance coefficient of the orifice now remains almost constant.

**Losses**

The losses due to flow resistance can be classified in the following manner.

**Mechanical Losses (Loss of Momentum)**

The loss of momentum, which the fluid or gas is experiencing by the resistance (friction and pressure resistance) of the pipe with or without a throttle, is determined by the momentum theorem independent of the choice of the control surface. It is advantageous to choose it in such a way, that the experimental effort for measuring the resistance is as small as possible, i. e. a cross section should be chosen, in which the radial pressure and velocity variations have decayed.
For geometrically similar insertions in pipes with the same relative roughness the dimensionless resistance coefficient $\zeta_{1,2}$, computed from the losss of momentum, depends only on the Reynolds number $Re$ and on the Mach number $Ma$.

**Thermodynamic and Gasdynamic Losses in Adiabatic Flow**

The irreversible processes caused by the friction and the pressure resistance result in an increase of entropy and a decrease of the stagnation pressure. In general these processes are not felt at

the same location, where the resistance force acts. The control surface must therefore be chosen in such a way, that it includes the region, in which the entropy generation equivalent to the mechanical losses has taken place. This is in particular true for the thermodynamic losses caused by the pressure resistance. The axial extent of this region can be estimated from the pressure distribution on the body (here the orifice). In the experiment reported here the entropy is increased and the stagnation pressure is decreased by the mixing process refered to as Carnot's shock. For $Ma_1 > Ma_{crit.}$, the increase of entropy and the decrease of the stagnation pressure are not only caused by the mixing process but also by the compression shock at the downstream end of the supersonic region. For $Ma_1 = Ma_{max}$ the entropy increase and also the decrease in stagnation pressure are solely due to the terminating compression shock, since the flow in front of the shock is almost isentropic.

### Selected References


Emmons, H.W.: *High Speed Aerodynamics and Jet Propulsion, Vol. II: Fundamentals of Gas Dynamics, Princeton* New Jersey, 1958, S. 228 ff..

Frössel, W.: *Strömung in glatten, geraden Rohren mit Überschall- und Unterschallgeschwindigkeit*, Forsch. Ing.-Wesen, 1936, Bd. 7,S.75.

Jaeneke, Ch.: *Untersuchungen zur Überschallströmung in einem Rechteckkanal*, Dissertation RWTH Aachen, 1975

Naumann, A.: *Druckverlust in Rohren nicht kreisförmigen Querschnitts bei hohen Geschwindigkeiten* Allgem. Wärmetechnik, 1956, Bd. 7, S.32

Prandtl, L.: *Strömungslehre*, Vieweg-Verlag, 1669, S. 229.

Shapiro, A.: *The Dynamics and Thermodynamics of Compressible Fluid Flow, Part I*, New York, 1953, S.114, 155-160.


## 6.8.4 Evaluation

### Method of Test

The pressure distribution on the wall of the pipe is measured in the vicinity of the orifice with a multiple-tubed manometer for a prescribed Mach number $Ma_1$.

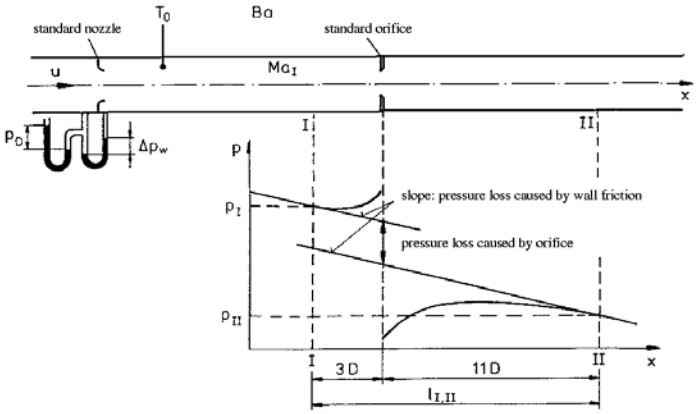

The following quantities are measured: $p_D$, $\Delta p_w$, $T_0$, $Ba$,$p(x)$

| n | 1 | 2 | 3 | 4 | 5 | 6 | 7 | 8 | 9 | 10 | 11 | 12 |
|---|---|---|---|---|---|---|---|---|---|---|---|---|
| $x/D$ | -5 | -4 | -3 | -2 | 0 | 0.1 | 1.8 | 2.2 | 2.6 | 3.0 | 3.4 | 3.8 |
| $p(x) - Ba$ [mm Hg] | 491 | 490 | 489 | 490 | 500 | 73 | 195 | 217 | 234 | 244 | 251 | 259 |
| $p(x)$[N/m$^2$] $\cdot 10^3$ | 165 | 165 | 165.2 | 165 | 166.6 | 109.8 | 126.1 | 129 | 131.3 | 132.6 | 133.5 | 134.6 |
| n | 13 | 14 | 15 | 16 | 17 | 18 | 19 | 20 | 21 | 22 | 23 | 24 |
| $x/D$ | 4.2 | 4.6 | 5.0 | 5.4 | 5.8 | 6.2 | 6.6 | 7.6 | 8.6 | 9.6 | 10.6 | 11.6 |
| $p(x) - Ba$ [mm Hg] | 260 | 261 | 260 | 261 | 261 | 260 | 260 | 259 | 257 | 257 | 255 | 254 |
| $p(x)$[N/m$^2$] | 134.7 | 134.8 | 134.7 | 134.8 | 134.8 | 134.7 | 134.7 | 134.6 | 134.3 | 134.3 | 134.1 | 133.9 |

**Data Evaluation**

The mass flow $\rho u$ can be determined with the data $p_D$, $\Delta p_w$, $T_0$ and the dimension sizes of the nozzle according to standard specifications (NORM DIN 1952 in Germany).

$$\rho u = m_D \, \alpha \, \epsilon \sqrt{2 \rho_D \, \Delta p_w} \tag{6.136}$$

Inserting the quantities $\rho u$, $p$, and $T_0$ into the gasdynamic relations the state variables in the cross sections I and II can be computed, and the resistance coefficient of the orifice $\zeta_O$ is obtained as a function of $Ma_I$ and $Re_I$.
If the static pressure $p$ is known at a certain location, the Mach number can be determined with the following relations

$$\frac{\dot{m}}{Ap}\sqrt{\frac{RT_0}{\gamma}} = \frac{\rho u}{\rho T}\sqrt{\frac{RT_0}{\gamma}} = Ma\sqrt{\frac{T_0}{T}} \tag{6.137}$$

and

$$\frac{T_0}{T} = 1 + \frac{\gamma - 1}{2} Ma^2 \quad . \tag{6.138}$$

If the abbreviation $Ma\sqrt{\frac{T_0}{T}} = K$ is used, there is obtained

$$Ma^2 = \frac{1}{\gamma - 1}\left[\sqrt{1 + 2K^2(\gamma - 2)} - 1\right] \quad . \tag{6.139}$$

If $Ma$ is known, the temperature ratio $T/T_0$ can be computed from (6.138) and

$$\frac{p_0}{p} = \left(\frac{T_0}{T}\right)^{\frac{\gamma}{\gamma - 1}} \quad . \tag{6.140}$$

For the temperature of the experiment the viscosity of air is approximated by the relation

$$\frac{\mu}{\mu_{0°\mathrm{C}}} = \left(\frac{T}{T_{0°\mathrm{C}}}\right)^{0.76} \quad . \tag{6.141}$$

The Reynolds number can be expressed as

$$Re = \frac{\rho u D}{\mu(T)} = \frac{\rho u D}{\mu(T_0)} \left(\frac{T_0}{T}\right)^{0.76} = Re_0 \left(\frac{T_0}{T}\right)^{0.76} \quad . \tag{6.142}$$

*Resistance and losses of a compressible pipe flow with a standard orifice (details of evaluation)*

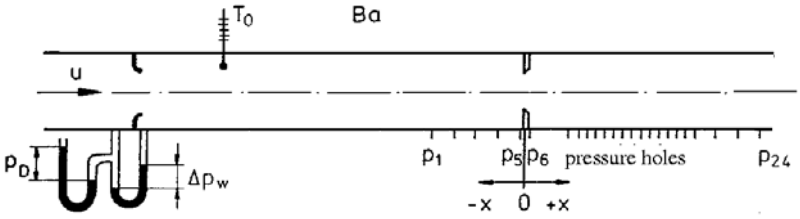

| Nr. | | Symbol | Numerical value | Unit | Equation |
|---|---|---|---|---|---|
| 1 | Diameter of pipe | D | 0.05 | m | |
| 2 | Diamter of nozzle | $d_n$ | 0.04 | m | |
| 3 | Opening ratio of nozzle | $m_D$ | 0.64 | | $m_n = (d_n/D)^2$ |
| 4 | Diameter of orifice | d | 0.0353 | m | |
| 5 | Opening ratio | m | 0.5 | | $m = (d/D)^2$ |
| 6 | Gas constant | R | 287.3 | Nm/kgK | |
| 7 | Viscosity at $0^oC$ | $\mu_{0^oC}$ | $1.71 \cdot 10^{-5}$ | Ns/m$^2$ | |
| 8 | Barometer reading | Ba | 753 | mm Hg | |
| 9 | Stagnation temperature | $T_0$ | 293 | K | |
| 10 | Nozzle excess pressure | $h_n$ | 555 | mm Hg | |
| 11 | Differential pressure | $\Delta p_w$ | 1085 | mm $H_2O$ | 1 mm $H_2O$ = 9.81 N/m$^2$ |
| | | | 10643.85 | N/m$^2$ | |
| 12 | Pressure ahead of nozzle | $p_n$ | 1308 | mm Hg | $p_n = Ba + h_n$ |
| | | | 173964 | N/m$^2$ | 1 mm Hg = 133 N/m$^2$ |
| 13 | Density ahead of nozzle | $\rho_n$ | 2.066 | kg/m$^3$ | $\rho_n = p_n/R\ T_0$ |
| 14 | Viscosity at $T_0$ | $\mu_0$ | $1.8044 \cdot 10^{-5}$ | Ns/m$^2$ | (6.141) |
| 15 | Pressure ratio | $p_2/p_1$ | 0.9388 | | $p_2/p_1 = 1 - \Delta p_w/p_n$ |
| 16 | Expansion coefficient | $\epsilon$ | 0.9389 | | from table |
| 17 | Estim. discharge coefficient | $\alpha_0$ | 1.1732 | | from table<br>$\alpha_0 = \alpha(Re = 10^5, m_n)$ |
| 18 | Mass flow | $\rho\ u(a_0)$ | 147 | kg/s m$^2$ | (6.136) |
| 19 | Reynolds number | $Re_0$ | $4.096 \cdot 10^5$ | | $Re_0 = \rho\ u(a_0)\ D/\mu_0$ |
| 20 | Discharge coefficient | $\alpha$ | 1.1707 | | from table |
| 21 | Mass flow [1] | $\rho\ u$ | 147.523 | kg/s m$^2$ | $\rho u = \rho u(a_0)\ a/a_0$ |
| 22 | Total mass flow | $\dot{m}$ | 0.2896 | kg/s | $\dot{m} = \rho u D^2\pi/4$ |
| 23 | Pressure at I | $p_I$ | $165.2 \cdot 10^3$ | N/m$^2$ | $p(x)$ |
| 24 | Combination | $K_I$ | 0.2189 | | (6.137) |
| 25 | Mach number | $M_I$ | 0.2178 | | (6.139) |
| 26 | $\zeta_{max}(M_I)$ | $\zeta_{maxI}$ | 13 | | diagram |
| 27 | Temperature ratio | $T_0/T_I$ | 1.0095 | | (6.138) |
| 28 | Stagnation pressure | $p_{0I}$ | $1.707 \cdot 10^5$ | N/m$^2$ | (6.140) |
| 29 | Reynolds number | $Re_I$ | $4.125 \cdot 10^5$ | | (6.142) |
| 30 | Friction coefficient | $\lambda_I$ | 0.01358 | | (6.123) |
| 31 | Pressure at II | $p_{II}$ | $134.1 \cdot 10^3$ | N/m$^2$ | $p(x)$ |
| 32 | Combination | $K_{II}$ | 0.2697 | | (6.137) |
| 33 | Mach number | $M_{II}$ | 0.2678 | | (6.139) |
| 34 | $\zeta_{max}(M_{II})$ | $\zeta_{maxII}$ | 8 | | diagram |
| 35 | Temperature ratio | $T_0/T_{II}$ | 1.01434 | | (6.138) |
| 36 | Stagnation pressure | $p_{oII}$ | $1.409 \cdot 10^5$ | N/m$^2$ | (6.140) |
| 37 | Reynolds numberl | $Re_{II}$ | $4.14 \cdot 10^5$ | N/m$^2$ | (6.142) |
| 38 | Friction coefficient | $\lambda_{II}$ | 0.01357 | | (6.123) |
| 39 | Total friction coefficient | $\zeta_{I,II}$ | 5 | | (6.133) |
| 40 | $\zeta_{Friction}$ | $\bar{\lambda} l_{I,II}/D$ | 0.19005 | | $\bar{\lambda} = 1/2(\lambda_I + \lambda_{II})$ |
| 41 | Resistance coefficient of orifice | $\zeta_B$ | 4.81 | | (6.135) |
| 42 | Ratio of stagnation pressures | $p_{0I}/p_{0II}$ | 1.2115 | | |
| 43 | Increase of entropy | $\Delta s/R$ | 0.192 | | (6.127) |

[1] additional iterations do not improve the result

### 6.8.5 Problems

1. The pressure distribution measured on the wall of the pipe is to be plotted in the diagram $p = f(x)$.

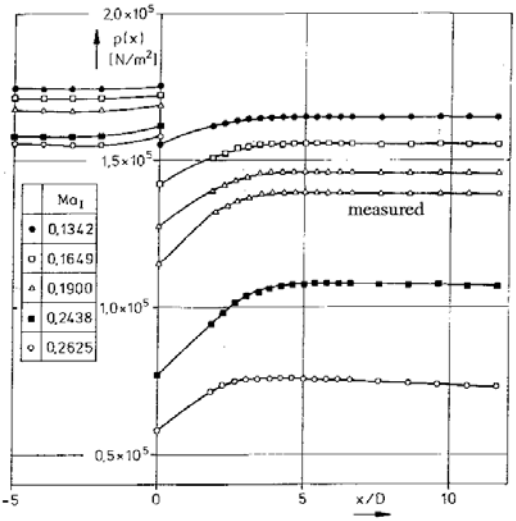


2. The resistance coefficient of the orifice, the ratio of the stagnation pressures $p_{0II}/p_{0I}$, and the increase of entropy $\Delta S_{I,II}/R$ are to be plotted in the corresponding diagrams.

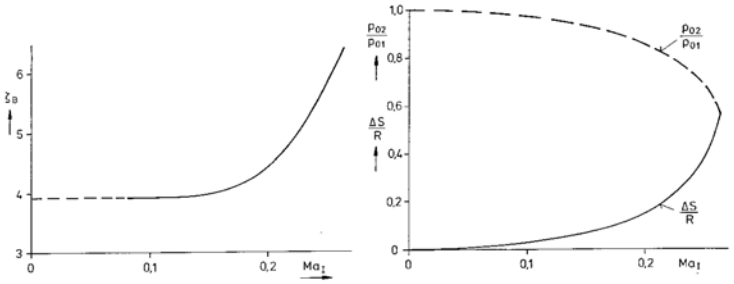


Resistance coefficient $\zeta_B$, increase of entropy, and loss of stagnation pressure of a standard orifice with $m = 0.5$ as a function of the free-stream Mach number $Ma_1$

3. What quantities must be measured for the determination of the Mach number $Ma_I$?
The quantities $h_n$, $p_w$, $T$, $Ba$, and $p_I$ must be measured, if the Mach number $Ma_I$ is to be determined.
4. Which flow is described by the Fanno curve in the T-s diagram? Do the flow conditions upstream of and downstream from a normal compression shock also lie on the Fanno curve?
The Fanno curve describebs the dependence of the temperature $T$ on the entropy difference $\Delta S/R$ for an one-dimensional, compressible flow with constant mass flow $\rho\ u = const.$ for an adiabatic change of state. The conditions upstream of and downstream from a normal compression shock lie on the Fanno curve, since $\rho\, u$ and $T_0$ remain constant.
Gasdynamic quantities as a function of the pressure ratio:

$$\frac{u\rho}{a_0\rho_0}\left(\frac{T_0}{T}\right)^{0.76} = \frac{Re}{\frac{a_0\,\rho_0\cdot l}{\mu_0}} = f\left(\frac{p}{p_0}\right)$$

$$Ma\,\frac{a_0}{a} = \frac{\dot{m}}{p\,A}\sqrt{\frac{RT_0}{\gamma}} = f\left(\frac{p}{p_0}\right)$$

$$Ma = f\left(\frac{p}{p_0}\right); \quad \frac{u}{a_0} = f\left(\frac{p}{p_0}\right)$$

with the assumptions

$$s = s_0; \qquad \gamma = 1.4$$

$$\mu = \mu_0\left(\frac{T_0}{T}\right)^{0.76}$$

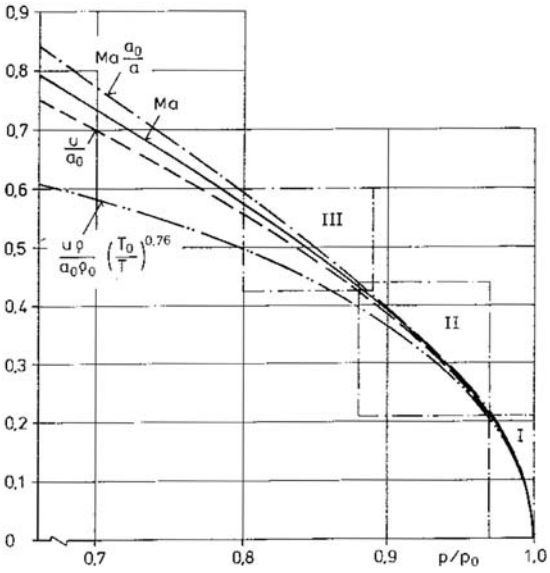


The quantities to be determined from the pressure measurements are summarized above and plotted in the diagram.

Resistance of adiabatic pipe flow ($\gamma = 1.4$)

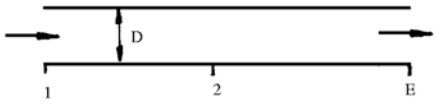


$\xi_{max} = (\bar{\lambda}\frac{l}{D})_{max} = \xi_{max}(Ma_1)$

$D$ = diameter of pipe

$Ma_1$ = Mach number at pipe entrance

$\xi_{max}$ = max. resistance coefficient at $Ma_g = 1$

$$\lambda = \frac{2\,d\,(p + \rho\,u^2)}{\rho\,u^2\,d\,\frac{x}{D}}$$

= pipe friction coefficient

$\xi_{max1} - \xi_{max2} = \frac{\lambda\, l_{1,2}}{D}$ = resistance coefficient of a pipe (without installations) of length $l_{1,2}$, the diameter D, and the friction coefficient $\bar{\lambda}$.

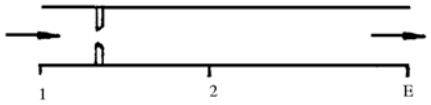


$$\xi_{max1} - \xi_{max2} = \xi_B + \frac{\bar{\lambda}\, l_{1,2}}{D} =$$

resistance coefficient with installations.

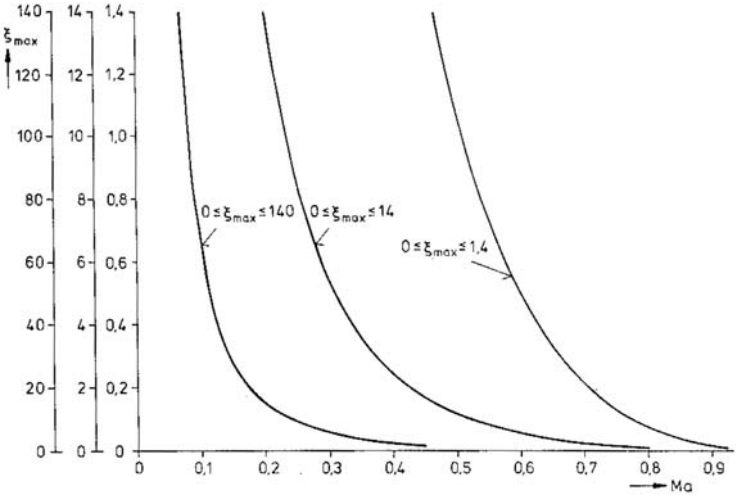


| $Re$ | | $2 \cdot 10^4$ | $2.5 \cdot 10^4$ | $3 \cdot 10^4$ | $4 \cdot 10^4$ | $6 \cdot 10^4$ | $7 \cdot 10^4$ | $10^5$ | $2 \cdot 10^5$ | $10^4$ - $2 \cdot 10^5$ |
|---|---|---|---|---|---|---|---|---|---|---|
| $m$ | $m^2$ | $\alpha_0$ | | | | | | | | |
| 0.1000 | 0.01 | | | | | | 0.9892 | 0.9895 | 0.9895 | 0.9896 |
| 0.1414 | 0.02 | | | | | | 0.9917 | 0.9924 | 0.9927 | 0.9928 |
| 0.1732 | 0.03 | | | | | | 0.9946 | 0.9954 | 0.9959 | 0.9960 |
| 0.2000 | 0.04 | 0.9768 | 0.9849 | 0.9883 | 0.9926 | 0.9951 | 0.9973 | 0.9984 | 0.9992 | 0.9994 |
| 0.2236 | 0.05 | 0.9822 | 0.9871 | 0.9906 | 0.9951 | 0.9977 | 1.0002 | 1.0015 | 1.0026 | 1.0027 |
| 0.2449 | 0.06 | 0.9849 | 0.9895 | 0.9930 | 0.9976 | 1.0005 | 1.0033 | 1.0047 | 1.0059 | 1.0061 |
| 0.2646 | 0.07 | 0.9876 | 0.9921 | 0.9956 | 1.0002 | 1.0033 | 1.0064 | 1.0080 | 1.0093 | 1.0095 |
| 0.2828 | 0.08 | 0.9907 | 0.9951 | 0.9984 | 1.0031 | 1.0063 | 1.0096 | 1.0113 | 1.0128 | 1.0130 |
| 0.3000 | 0.09 | 0.9939 | 0.9982 | 1.0014 | 1.0060 | 1.0093 | 1.0128 | 1.0147 | 1.0163 | 1.0166 |
| 0.3162 | 0.10 | 0.9973 | 1.0015 | 1.0046 | 1.0092 | 1.0125 | 1.0162 | 1.0182 | 1.0199 | 1.0202 |
| 0.3317 | 0.11 | 1.0009 | 1.0050 | 1.0080 | 1.0126 | 1.0159 | 1.0196 | 1.0217 | 1.0235 | 1.0238 |
| 0.3464 | 0.12 | 1.0048 | 1.0086 | 1.0116 | 1.0160 | 1.0194 | 1.0230 | 1.0263 | 1.0272 | 1.0275 |
| 0.3606 | 0.13 | 1.0088 | 1.0123 | 1.0153 | 1.0197 | 1.0230 | 1.0266 | 1.0290 | 1.0309 | 1.0312 |
| 0.3742 | 0.14 | 1.0129 | 1.0163 | 1.0192 | 1.0235 | 1.0267 | 1.0303 | 1.0328 | 1.0347 | 1.0350 |
| 0.3873 | 0.15 | 1.0173 | 1.0206 | 1.0234 | 1.0274 | 1.0305 | 1.0341 | 1.0366 | 1.0385 | 1.0388 |
| 0.4000 | 0.16 | 1.0219 | 1.0251 | 1.0276 | 1.0316 | 1.0345 | 1.0380 | 1.0405 | 1.0424 | 1.0427 |
| 0.4123 | 0.17 | 1.0266 | 1.0297 | 1.0321 | 1.0358 | 1.0386 | 1.0420 | 1.0445 | 1.0463 | 1.0467 |
| 0.4243 | 0.18 | 1.0315 | 1.0344 | 1.0367 | 1.0402 | 1.0428 | 1.0461 | 1.0486 | 1.0504 | 1.0507 |
| 0.4359 | 0.19 | 1.0366 | 1.0393 | 1.0415 | 1.0447 | 1.0472 | 1.0503 | 1.0527 | 1.0545 | 1.0547 |
| 0.4472 | 0.20 | 1.0418 | 1.0444 | 1.0464 | 1.0494 | 1.0517 | 1.0546 | 1.0569 | 1.0586 | 1.0589 |
| 0.4583 | 0.21 | 1.0472 | 1.0496 | 1.0515 | 1.0543 | 1.0563 | 1.0590 | 1.0612 | 1.0628 | 1.0631 |
| 0.4690 | 0.22 | 1.0528 | 1.0550 | 1.0567 | 1.0593 | 1.0611 | 1.0636 | 1.0656 | 1.0671 | 1.0674 |
| 0.4796 | 0.23 | 1.0586 | 1.0606 | 1.0621 | 1.0644 | 1.0660 | 1.0682 | 1.0701 | 1.0715 | 1.0718 |
| 0.4899 | 0.24 | 1.0645 | 1.0662 | 1.0677 | 1.0697 | 1.0710 | 1.0730 | 1.0746 | 1.0760 | 1.0762 |
| 0.5000 | 0.25 | 1.0706 | 1.0721 | 1.0734 | 1.0751 | 1.0763 | 1.0779 | 1.0793 | 1.0805 | 1.0807 |
| 0.5099 | 0.26 | 1.0769 | 1.0782 | 1.0792 | 1.0806 | 1.0816 | 1.0830 | 1.0841 | 1.0852 | 1.0854 |
| 0.5196 | 0.27 | 1.0833 | 1.0844 | 1.0853 | 1.0864 | 1.0871 | 1.0881 | 1.0890 | 1.0899 | 1..0901 |
| 0.5292 | 0.28 | 1.0899 | 1.0908 | 1.0914 | 1.0923 | 1.0928 | 1.0934 | 1.0941 | 1.0948 | 1.0949 |
| 0.5385 | 0.29 | 1.0966 | 1.0972 | 1.0976 | 1.0982 | 1.0985 | 1.0989 | 1.0993 | 1.0998 | 1.0999 |
| 0.5477 | 0.30 | 1.1035 | 1.1037 | 1.1039 | 1.1042 | 1.1043 | 1.1045 | 1.1046 | 1.1049 | 1.1049 |
| 0.5568 | 0.31 | 1.1106 | 1.1106 | 1.1105 | 1.1104 | 1.1102 | 1.1101 | 1.1101 | 1.1101 | 1.1101 |
| 0.5657 | 0.32 | 1.1179 | 1.1176 | 1.1173 | 1.1168 | 1.1164 | 1.1159 | 1.1156 | 1.1155 | 1.1154 |
| 0.5745 | 0.33 | 1.1253 | 1.1246 | 1.1241 | 1.1233 | 1.1225 | 1.1218 | 1.1214 | 1.1209 | 1.1208 |
| 0.5831 | 0.34 | 1.1329 | 1.1320 | 1.1312 | 1.1300 | 1.1290 | 1.1279 | 1.1272 | 1.1266 | 1.1264 |
| 0.5916 | 0.35 | 1.1407 | 1.1394 | 1.1384 | 1.1368 | 1.1355 | 1.1341 | 1.1332 | 1.1324 | 1.1321 |
| 0.6000 | 0.36 | 1.1486 | 1.1470 | 1.1457 | 1.1438 | 1.1423 | 1.1406 | 1.1394 | 1.1383 | 1.1379 |
| 0.6083 | 0.37 | 1.1567 | 1.1548 | 1.1532 | 1.1510 | 1.1493 | 1.1472 | 1.1457 | 1.1445 | 1.1439 |
| 0.6164 | 0.38 | 1.1650 | 1.1627 | 1.1609 | 1.1583 | 1.1564 | 1.1540 | 1.1523 | 1.1508 | 1.1501 |
| 0.6245 | 0.39 | 1.1734 | 1.1709 | 1.1668 | 1.1658 | 1.1636 | 1.1609 | 1.1590 | 1.1573 | 1.1565 |
| 0.6325 | 0.40 | 1.1821 | 1.1793 | 1.1768 | 1.1735 | 1.1711 | 1.1680 | 1.1660 | 1.1641 | 1.1630 |
| 0.6403 | 0.41 | 1.1909 | 1.1877 | 1.1861 | 1.1813 | 1.1788 | 1.1754 | 1.1732 | 1.1710 | 1.1698 |

**Discharge coefficients** $a_0 = f(m^2,Re)$ for standard nozzles in smooth pipes, valid for pipe diameters $D$ between 50 tos 500 mm. The values of $m^2$ listed (not of $m$) can be interpolated linearly.

| $p_2/p_1$ | | 1.0 | 0.98 | 0.96 | 0.94 | 0.92 | 0.90 | 0.85 | 0.80 | 0.75 |
|---|---|---|---|---|---|---|---|---|---|---|
| $m$ | $m^2$ | $\epsilon$ for $\gamma = 1.2$ | | | | | | | | |
| 0 | 0 | 1.0 | 0.9874 | 0.9748 | 0.9620 | 0.9491 | 0.9361 | 0.9029 | 0.8089 | 0.8340 |
| 0.3162 | 0.1 | 1.0 | 0.9856 | 0.9712 | 0.9568 | 0.9423 | 0.9278 | 0.8913 | 0.8543 | 0.8169 |
| 0.4472 | 0.2 | 1.0 | 0.9834 | 0.9669 | 0.9504 | 0.9341 | 0.9178 | 0.8773 | 0.8371 | 0.7970 |
| 0.5477 | 0.3 | 1.0 | 0.9805 | 0.9613 | 0.9424 | 0.9238 | 0.9053 | 0.8602 | 0.8163 | 0.7733 |
| 0.6325 | 0.4 | 1.0 | 0.9767 | 0.9541 | 0.9320 | 0.9105 | 0.8895 | 0.8390 | 0.7909 | 0.7448 |
| 0.6403 | 0.41 | 1.0 | 0.9763 | 0.9532 | 0.9308 | 0.9090 | 0.8877 | 0.8366 | 0.7881 | 0.7416 |
| | | $\epsilon$ for $\gamma = 1.3$ | | | | | | | | |
| 0 | 0 | 1.0 | 0.9884 | 0.9767 | 0.9649 | 0.9529 | 0.9408 | 0.9100 | 0.8783 | 0.8457 |
| 0.3162 | 0.1 | 1.0 | 0.9867 | 0.9734 | 0.9600 | 0.9466 | 0.9331 | 0.8990 | 0.8645 | 0.8294 |
| 0.4472 | 0.2 | 1.0 | 0.9846 | 0.9693 | 0.9541 | 0.9389 | 0.9237 | 0.8859 | 0.8481 | 0.8102 |
| 0.5477 | 0.3 | 1.0 | 0.9820 | 0.9642 | 0.9466 | 0.9292 | 0.9120 | 0.8697 | 0.8283 | 0.7875 |
| 0.6325 | 0.4 | 1.0 | 0.9785 | 0.9575 | 0.9369 | 0.9168 | 0.8971 | 0.8495 | 0.8039 | 0.7599 |
| 0.6403 | 0.41 | 1.0 | 0.9781 | 0.9567 | 0.9358 | 0.9154 | 0.8954 | 0.8472 | 0.8012 | 0.7569 |
| | | $\epsilon$ for $\gamma = 1.4$ | | | | | | | | |
| 0 | 0 | 1.0 | 0.9892 | 0.9783 | 0.9673 | 0.9563 | 0.9449 | 0.9162 | 0.8865 | 0.8558 |
| 0.3162 | 0.1 | 1.0 | 0.9877 | 0.9753 | 0.9628 | 0.9503 | 0.9377 | 0.9058 | 0.8733 | 0.8402 |
| 0.4472 | 0.2 | 1.0 | 0.9857 | 0.9715 | 0.9573 | 0.9430 | 0.9288 | 0.8933 | 0.8577 | 0.8219 |
| 0.5477 | 0.3 | 1.0 | 0.9833 | 0.9667 | 0.9503 | 0.9340 | 0.9178 | 0.8780 | 0.8388 | 0.8000 |
| 0.6325 | 0.4 | 1.0 | 0.9800 | 0.9604 | 0.9412 | 0.9223 | 0.9038 | 0.8588 | 0.8154 | 0.7733 |
| 0.6403 | 0.41 | 1.0 | 0.9796 | 0.9596 | 0.9401 | 0.9209 | 0.9021 | 0.8566 | 0.8127 | 0.7704 |
| | | $\epsilon$ for $\gamma = 1.66$ | | | | | | | | |
| 0 | 0 | 1.0 | 0.9909 | 0.9817 | 0.9724 | 0.9629 | 0.9533 | 0.9288 | 0.9033 | 0.8768 |
| 0.3162 | 0.1 | 1.0 | 0.9896 | 0.9791 | 0.9685 | 0.9578 | 0.9471 | 0.9197 | 0.8917 | 0.8629 |
| 0.4472 | 0.2 | 1.0 | 0.9879 | 0.9759 | 0.9637 | 0.9516 | 0.9394 | 0.9088 | 0.8778 | 0.8464 |
| 0.5477 | 0.3 | 1.0 | 0.9858 | 0.9718 | 0.9577 | 0.9438 | 0.9299 | 0.8953 | 0.8609 | 0.8265 |
| 0.6325 | 0.4 | 1.0 | 0.9831 | 0.9664 | 0.9499 | 0.9336 | 0.9176 | 0.8782 | 0.8397 | 0.8020 |
| 0.6403 | 0.41 | 1.0 | 0.9827 | 0.9657 | 0.9490 | 0.9324 | 0.9161 | 0.8762 | 0.8373 | 0.7993 |

**Expansion** coefficient $\epsilon$ for standard nozzles for arbitrary gases and vapors, for different pressure ratios $p_2/p_1$. Listed are also the squares of the opening ratios $m$ and Isentropic exponent $\gamma$.
The numerical values $m = m^2 = 0$ and $p_2/p_1 = 1$ are listed only to enable the interpolation of values of $\epsilon$ for $m^2 < 0.1$ and $p_2/p_1 > 0.98$.

## 6.9 Measuring Methods for Compressible Flows

*Abstract*

Optical methods for measuring density fields of gas flows are introduced: The shadow method, the Mach-Zehnder interferometer , the differential interferometer, and the working principle of the holographic interferometer. For measuring the local velocity the hot-wire anemometer and the Laser-Doppler anemometer are briefly described.

### 6.9.1 Tabular Summary of Measuring Methods

1. Optical methods for measuring the density
2. Hot-wire and Laser-Doppler anemometry for measurements of velocities and turbulent fluctuation velocities
3. Pressure measurement
4. Measurement of forces and moments
5. Temperature measurement
6. Skin friction measurement
7. Visualization of streamlines
8. Concentration measurement
9. Film thermometer for measuring heat transfer

### 6.9.2 Optical Methods for Density Measurements

The propagation velocity of light $c$ in gases depends on the gas itself and on its density $\rho$. It is smaller than in vacuum. The index of refraction $n_1$ of a gas "1" is defined as the ratio of the velocity of light in vacuum $c_0$ to its value in the gas

$$n_1 = \frac{c_0}{c_1} \quad . \tag{6.143}$$

The optical path length $S$ is defined as the distance, which a light ray would cover in vacuum in the time $t$, in which the ray would cover the geometric distance $l_1$ in the gas with index of refraction $n_1$

$$S = n_1 \, l_1 \quad . \tag{6.144}$$

If a light ray crosses the boundary between two gases of different index of refraction, it is deflected. If two rays travel different optical paths, a phase difference between the two results.

#### Methods Based on the Deflection of the Light

If a light ray enters a transparent wedge with index of refraction $n_2$ and wedge angle $\alpha_2$, the ray is deflected by the angle $\varepsilon$, when it leaves the wedge.

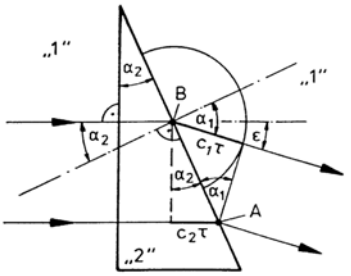


$$\begin{aligned}
c_1 &> c_2 \quad , \quad n_1 < n_2 \\
\varepsilon &= \alpha_1 - \alpha_2 \\
\sin\alpha_1 &= c_1\tau/\overline{AB} \\
\sin\alpha_2 &= c_2\tau/\overline{AB} \\
\frac{\sin\alpha_1}{\sin\alpha_2} &= \frac{c_1\tau/\overline{AB}}{c_2\tau/\overline{AB}} = \frac{c_1}{c_2} = \frac{n_2}{n_1} \\
\sin\alpha_1 &= \sin\alpha_2 \frac{n_2}{n_1}
\end{aligned}$$

From the sketch it follows for small angles $\alpha$

$$\varepsilon \approx \alpha_2 \left( \frac{n_2}{n_1} - 1 \right) \quad . \tag{6.145}$$

The index of refraction $n$ of a gas or vapor can approximately be expressed in terms of the density $\rho$ by the following relation:

$$n - 1 = K\,\rho \qquad \text{Gladstone-Dale} \tag{6.146}$$

The Gladstone-Dale constant $K$ depends on the gas and on the wave length of the light, for example:

$$\begin{aligned} \text{Air at}15^\circ\text{C}, \quad \lambda &= 644\,\text{nm} \rightarrow K = 0.2255 \cdot 10^{-3}\,\text{m}^3/\text{kg} \\ \lambda &= 447\,\text{nm} \rightarrow K = 0.2290 \cdot 10^{-3}\,\text{m}^3/\text{kg} \end{aligned}$$

Other examples are listed below:

Gladstone - Dale constant $K$

| $K$ [ $\text{m}^3/\text{kg}$ ] | $\lambda$ [nm] | Gas |
|---|---|---|
| $0.2239 \cdot 10^{-3}$ | 912.5 | |
| $0.2274 \cdot 10^{-3}$ | 509.7 | Air ($T = 288\,\text{K}$) |
| $0.2330 \cdot 10^{-3}$ | 356.2 | |
| $0.190 \cdot 10^{-3}$ | 589 | $O_2$ ($T = 273\,\text{K}$) |
| $0.229 \cdot 10^{-3}$ | 589 | $CO_2$ ($T = 273\,\text{K}$) |
| $0.238 \cdot 10^{-3}$ | 589 | $N_2$ ($T = 273\,\text{K}$) |

Index of refraction ($\lambda = 589$ nm, $T = 293\,\text{K}$)

| | |
|---|---|
| Air: | $n = 1.00027$ ($p = 1\,\text{bar}$) |
| Water: | $n = 1.333$ |
| Crown glass (BK 7) | $n = 1.519$ |
| Flint glass (SF 10) | $n = 1.734$ |

Coherence length of light rays

| | | |
|---|---|---|
| Sun | $\sim$ | $10^{-7}\,\text{m}$ |
| Spectroscopic lamp | $\sim$ | $10^{-1}\,\text{m}$ |
| Ar - Laser | $\sim$ | $10^{2}\,\text{m}$ |
| He - Ne - Laser | $\sim$ | $10^{4}\,\text{m}$ |

The continuous increase of the geometric path in the medium "2" in the wedge with constant index of refraction $n_2$ causes a deflection of the incident ray. It can also be concluded that an increase of the index of refraction causes a deflection of the light if the geometric path 1 is constant.
An object, which causes the product $n \cdot l$ to change in an arbitrary direction, is called schlieren. If the index of refraction $n$ remains constant in the direction of the incident ray ($x$) and if the geometrical path does not change in the $y$-direction, then the schlieren is called two-dimensional. The following approximation is valid for a weak deflection in the schlieren

$$\varepsilon \approx \frac{l}{n} \frac{dn}{dy} \tag{6.147}$$

With (6.146) the following proportionality holds for the two-dimensional schlieren:

$$\varepsilon \sim l \frac{d\rho}{dy} \tag{6.148}$$

**The Shadow Method**

The angles $\varepsilon$ occuring in applications are very small ($\epsilon < 1/10^o$). Two methods are used to make them visible. A very simple method is the shadow method. If the light after passing through a schlieren is captured on a film, the part of the field, from which the light is deflected, generates an image which is not as dark as the image of the area, which is additionally lightened by the deflected light rays.

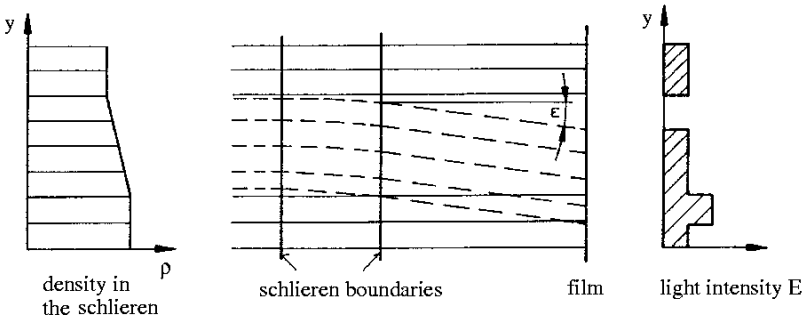


It is clear from the sketch above, that a constant density gradient in the phase object deflects the entire incident light, but does not change the distribution of the light intensity on the film. Only a change of the density gradient leads to a brightening and darkening of parts of the image. The light intensity is approximately given by

$$\Delta E \sim \frac{d^2\rho}{dy^2} \tag{6.149}$$

Jumps in the distribution of the density gradient, as they occur in compression shocks, are extremely well detected.

### The Schlieren Method

In order to build up a schlieren optic a focus (focal spot) must be generated between the object and the image screen. The focal spot serves to focus the non-deflected rays (regular bundle of rays). A knife edge, positioned close to the focus, captures the light, deflected by the schlieren to it, so that the corresponding areas on the film are not illuminated.

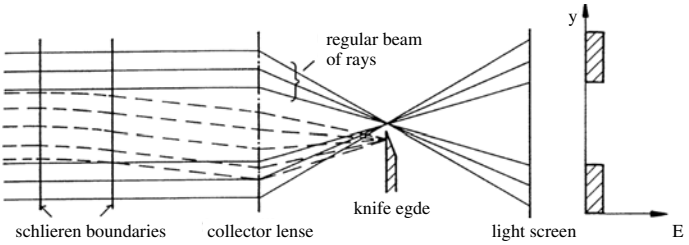


Because of the finite size of the focal spot, about half of it is covered with the knife edge, so that the optical sytem is sufficiently sensitive. The schlieren then appear in different grey tints, depending on their direction and intensity, which is approximately given by

$$\Delta E \sim \frac{d\rho}{dy}. \tag{6.150}$$

The schlieren method is more sensitive than the shadow method and provides very clear pictures of the flow field.

### Methods Based on the Measurement of Phase Differences (Interferometric Methods)

If two equal light rays travel along different optical paths, the light waves of the two rays are shifted relative to each other.

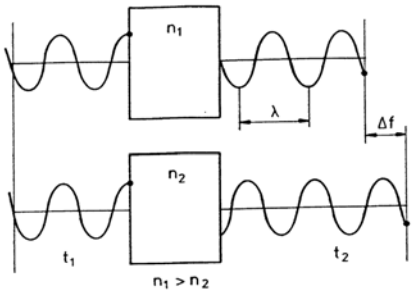


The shift $\Delta f$ is called phase difference. If the two light rays are superposed, they cancel each other, if $\Delta f$ is an uneven, integral multiple of one half of the wave length. If $\Delta f$ is an integral multiple of the wave length, then they amplify each other.
Two light rays, which are identical in all aspects except for their phases, are called coherent. They are not coherent, if they are generated by different light sources; they therfore have to be generated by the same light source and split into two rays, if they are to be coherent. After they have travelled different optical paths, their phase difference can be determiend by superposition of the two rays.

**Mach-Zehnder Interferometer**

In a Mach-Zehnder interferometer the splitting and superposition of the light rays is done with semitransparent mirrors.
If the mirrors 1 to 4 are positioned parallel to each other, then all geometric paths of both rays are equal. If there is a density field in the test section, constant in the direction of the ray, then the interference fringes represent lines of constant density.

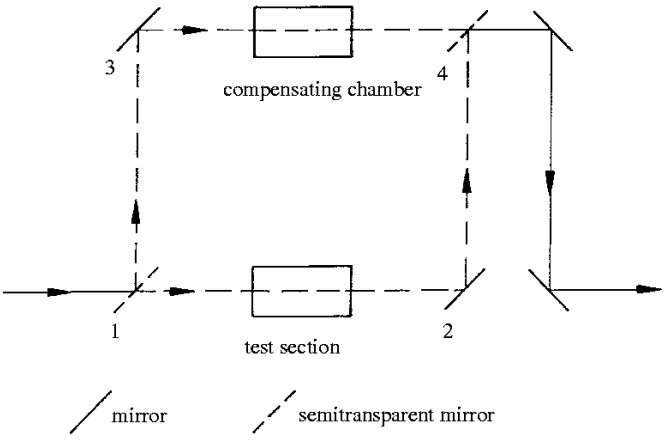


This condition is very well suited for a qualitative evaluation of a flow process. For quantitative evaluation so-called finite-fringe spacing is used. By turning the corresponding mirror a linearly increasing density field, also called wedge field is simulated, such that a field of parallel equidistant interference fringes, generated without a flow process, appears. If a real flow is investigated, the known wedge field has to be subtracted from the field obtained with the flow. This is done by measuring the shift of the fringes in the picture of the flow process in comparison to its position in the wedge field. This method of evaluation makes it possible to catch optical errors,

resulting from the glass panes of the wind tunnel or from the mirrors and from those that are contained in the wedge field.

### Differential Interferometer

In the differential interferometer the light ray is split with doubly refracting crystals, for example wollaston prisms, the action principle of which is explained in the following sketch. The distance $d$ between both rays is so samll, that both can travel through the test section (The distance is of the order of magnitude of 1 mm).

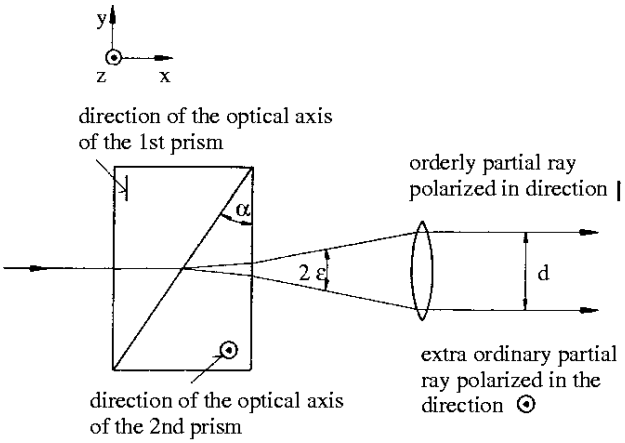


Both rays are superposed after they have passed the test section, and the superposition yields density gradients in two-dimensional and axially symmetric flows. If the wollaston prism is positioned in such a way, that with constant density in the test section interference fringes do not appear (infinite fringe), then the interference fringes which appear after generating a two-dimensional density field, are lines of constant density gradients. A suitable polarisation is necessary for generating interference fringes.

A field of equidistant interference fringes can be generated by shifting the wollaston prism. The fringe shift $\Delta W$ is then a measure for the density gradient. It is [Merzkirch 1974]:

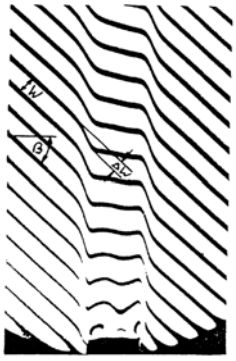


$$\frac{\Delta W}{W} = \frac{d}{\lambda} \cdot \left[ \sin\beta \int \frac{\partial n}{\partial x} dl + \cos\beta \int \frac{\partial n}{\partial y} dl \right] \tag{6.151}$$

$n$ = Index of refractionx
$d$ = Distance between the rays
$l$ = geometrical path

For the analysis of axially symmetric density fields, Abel's integral equation has to be solved.

### 6.9.3 Optical Setup

So far only the physical principles of some of the optical measuring methods were briefly explained. In order to apply them, an optical setup must be arranged, which has to depict the object to be measured and also the signal, for example the fringes of the interferometer on the film. In addition the setup should also provide the possibility of passing parallel light through the test section. An example of an optical setup is shown below for the so-called Z-arrangement of the differential interferometer, which is often used to keep the defects of the images small.

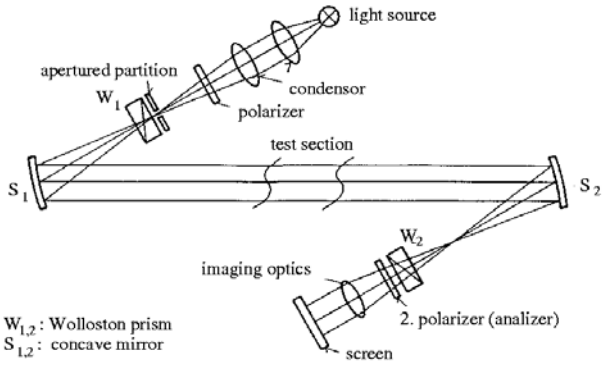


The light of the source is focussed by a condenser in a point, which is so chosen that it coincides with the focus of a concave reflector. The light rays leaving the reflector are parallel to each other. They pass the test section and are focussed again by a second reflector. Special imaging optics are required to depict the test section in a suitable size on the film.

#### Holographic Interferometry

The methods discussed so far can only be used for the analysis of two-dimensional density fields. With the development of the Laser it became possible to use the holgraphy as a measuring technique and record the wave fronts generated by a body. A typical setup is shown below. A parallel light beam, generated by a Laser, is split with a splitter plate; one part of it, the reference beam, after being deflected by a mirror, is directly led to a photographically sensible layer H (Hologram). The second beam is diffusedly scatteerd on a ground-glass plate.

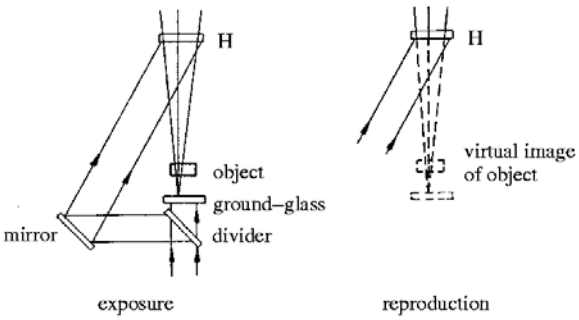


The object is behind the ground-glass plate in the diffused light. The wave fronts, passing through the object, interfere with the reference beam and are recorded on the photographically sensible layer.

For reconstruction of the image the hologram H is again exposed to the reference beam. In this manner a three-dimensional picture of the phase relationship of the light penetrating the flow is generated. The method of double exposure of the hologram is preferably used, i. e., the

photographically sensible layer is exposed without the flow and a second time with the flow. In this manner the change of density caused by the flow can be determined.

### 6.9.4 Measurements of Velocities and Turbulent Fluctuation Velocities

The optical methods just discussed, in general provide data which represent values averaged over the width of the test section. Hot-wire and Laser-Doppler anemometer enable the measurement of the velocity at a point with a resolution of about $1\,\mathrm{mm}^3$.

#### Hot-Wire Anemometer

The hot-wire and the hot-film anemomter are measuring devices which are heated with an electric current, so that a temperature difference is generated between the device and the flowing medium (Temperature differences in gases are about 200 to 300 K).
The measuring devices consist of hot wires (ø $10^{-6}$ to $10^{-4}$ m) which are fixed to two pins, hot films (thickness $10^{-8}$ to $10^{-6}$ m) are fastened to glass or ceramic supporting bodies.
Two methods are used to construct a relation between the heat transfer from the measuring device to the flowing medium and its local velocity: Either the heating current is kept constant and temperature or electric resistance are measured (constant-current method) or the temperature or the electric resistance are kept constant and the current is readjusted (constant-temperature method). The adjustment of the heating current can be achieved in a simple manner by combining the measuring device with a Wheatstone's bridge. The limit of the methods are given by the spatial, temporal, and amplitude resolution. It must also be remembered that the heat transfer of the anemometer is affected by a change of density or temperature of the flowing medium.

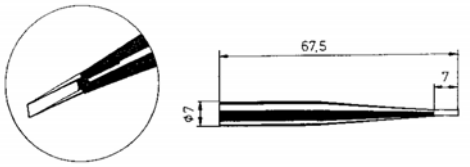


A single hot-wire probe is shown above. The wire has a diameter of the order of $5\,\mu$m. Modern hot-wire anemometers measure all three velocity components with three wires, orthogonally arranged to each other in a measuring volume of about $1\,\mathrm{mm}^3$, gold-soldered to six prongs, which lead the electric current to the bridge.

#### Laser-Doppler Anemometer (LDA)

The Laser-Doppler anemometer is an opto-elektronic measuring method. The position of the measurement is given by the volume of intersection of two intersecting Laser beams (typical size: $\approx .1\,\mathrm{mm}^3$). The velocity of small particles, travelling with the flow (ø $10^{-7}$ to $10^{-5}$ m) is determined with the aid of the light scattered by the particles and is assumed to be approximately equal to the velocity of the flow.
Since the particles move relative to the light source, the frequencies of the stray light of the two Laser beams is distorted as a consequence of the Doppler effect, by different amounts, resulting from the different directions of the beams. The difference in the frequencies of the Doppler shifts is called Doppler frequency $f$. It can be determined from the beat frequency of the two parts of the stray light with the aid of photodetectors.
Of the many possible setups the "two-beam method" is shown here. With this method the frequency $f$ can also be explained with the interference of the two Laser beams.

#### Selecte References

Durst, F., Melling, A, Whitelaw, J.H.: *Principles and practice of laser-doppler-anemometrie,* Academic Press, 1976.

FRANCON, M.: *Holographie*, Springer-Verlag, 1972.

MERZKIRCH, W.: *Flow visualition*, Academic Press, 1976.

SCHARDIN, H.: *Die Schlierenverfahren und ihre Anwendung,* Ergebnisse der exakten Naturwissenschaften, Bd.20, 1942.

STRICKERT, H.: *Hitzdraht- und Hitzfilmanemometrie*, VEB Verlag Technik, Berlin, 1974.

WUEST, W.: *Strömungsmeßtechnik,* Vieweg-Verlag, 1969.

### 6.9.5 Evaluation

Determination of the Mach number by measuring the pressure:

$$\begin{aligned} \text{Measured data:} \quad p_0 - p &= 696 \text{ mm Hg} \\ p_0 &= 747.5 \text{ mm Hg} \\ \Rightarrow \frac{p}{p_0} &= 1 - \frac{p_0 - p}{p_0} = 0.068; \quad \frac{p_0}{p} = 14.51 \\ Ma &= \sqrt{\frac{2}{\gamma - 1}\left(\left(\frac{p_0}{p}\right)^{\frac{\gamma-1}{\gamma}} - 1\right)} = 2.39 \end{aligned}$$

1. Pitot-pressure measurement at supersonic speeds

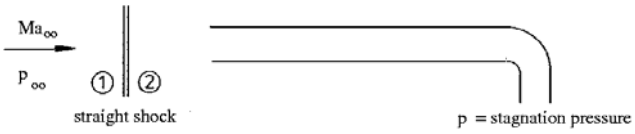


Given:

$$\frac{p_{02}}{p_{01}} = g(Ma_\infty, \gamma)$$

To be determined:

$$\frac{p_g}{p_\infty} = f(Ma_\infty, \kappa) \qquad \text{(Give derivation!)}$$

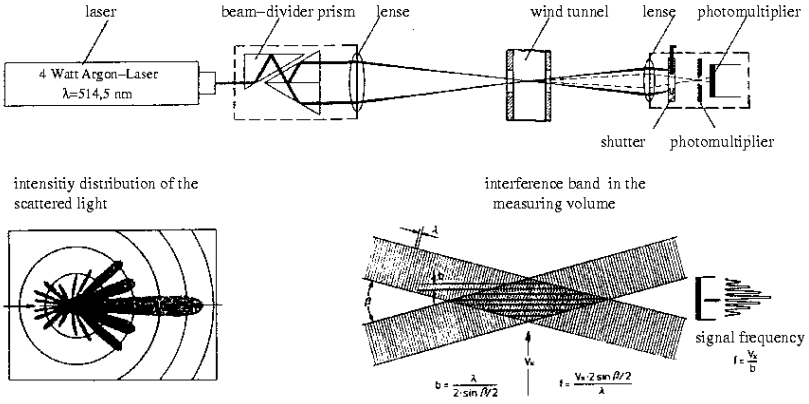

$$g(Ma_\infty,\gamma) = \frac{p_{02}}{p_{01}} = \left[1 + \frac{2\,\gamma}{\gamma+1}\left(Ma_\infty^2 - 1\right)\right]^{\frac{\gamma}{\gamma+1}} \cdot \left[\frac{\gamma+1}{\gamma - 1 + \frac{2}{Ma_\infty^2}}\right]^{\frac{\gamma}{\gamma-1}}$$

$$p_{02} = p_g \quad ; \qquad p_\infty = p_1$$

$$\frac{p_g}{p_\infty} = \frac{p_{02}}{p_1} = \frac{p_{02}}{p_{01}} \cdot \frac{p_{01}}{p_1} = g(Ma_\infty,\gamma)\,\frac{p_{01}}{p_1} = g(Ma_\infty,\gamma) \cdot \left(1 + \frac{\gamma-1}{2} Ma_\infty^2\right)^{\frac{1}{\gamma-1}} = f(Ma_\infty,\gamma)$$

2. State the difference between the shadow and the schlieren method! (optical setup, measured quantities, advantages and disadvantages)
The shadow method: Changes of the density gradient cause brightening or darkening in the picture, $\Delta E \sim \frac{d^2\,\rho}{d\,y^2}$.
The schlieren method: The density gradients visualize themselves, $\Delta E \sim \frac{d\,\rho}{dy}$.

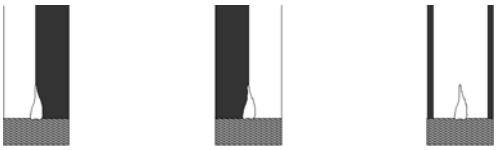

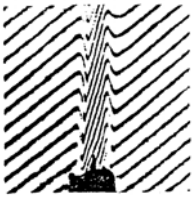

3. The picture shows a photograph of a candle light, obtained with a differential interferometer as finite fringe interferogram.
a) How can the density profile be determined from these data?
b) Sketch the picture for infinite fringe spacing. Explain the interference fringes generated!
c) Sketch the setup of a Mach-Zehnder interferometer for finite fringe spacing, if the interference fringes in the reference field without the flame run diagonally.

a) The fringe shift is the measure for the density ⇒ density profile.

from equ: $\frac{\Delta w}{w} = \frac{d}{\lambda}\left[\sin\beta \int \frac{\partial u}{\partial x}\,dl + \cos\beta \int \frac{\partial u}{\partial y}\,dl\right] \quad \Rightarrow \frac{\partial u}{\partial x}\,,\,\frac{\partial u}{\partial y}\;;\; n = (K\cdot\rho) + 1 \;\Rightarrow \frac{\partial \rho}{\partial x}$

b)

The interference fringes are lines of constant density gradients.

c)

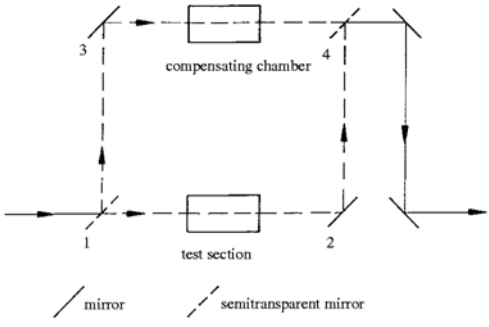


If the reflectors 2 and 4 are not turned, the light rays pass through. A phase difference is generated and thereby an interference field.

## 6.10 Supersonic Wind Tunnel and Compression Shock at the Wedge

*Abstract*

Several types of wind tunnels are reviewed. The working principle of supersonic wind tunnels is explained. The straight oblique compression shock in steady two-dimensional flow of a perfect gas with constant specific heats is experimentally investigated. Friction forces and addition and removal of heat are neglected. The pressure ratio across the shock $p_2/p_1$ and the shock angle $\sigma$ of an oblique shock generated with a wedge are measured for a certain Mach number and compared with theoretical values.

### 6.10.1 Introduction

The objective of wind-tunnel testing is to generate spacially and temporally constant flows for the investigation of fluid-mechanical problems. Studies of problems in fluid mechanics often have to rely on experiments, since theoretical analyses of complex flow processes are not always possible.

Since experimental investigations of flows about full-scale models can be realized only in rare cases, wind-tunnel testing has to resort to reduced-scale models and the similarity laws have to be observed. In addition to geometric similarity the following similarity parameters are of importance:

Reynolds number $Re = \frac{\rho\, u\, l}{\mu}$

Mach number $Ma = \frac{u}{a} = \frac{\text{Flow velocity}}{\text{Speed of sound}}$

Knudsen number $Kn = \frac{l_m}{l} = \frac{\text{Mean free ath}}{\text{Characteristic length}}$

Prandtl number $Pr = \frac{\mu\, c_p}{\lambda}$

Strouhal number $Str = \frac{\omega\ l}{u} = \frac{f\ l}{u}$

Schmidt number $Sc = \frac{\nu}{D_{12}} = \frac{\text{Kinematic viscosity}}{\text{Diffusion coefficient}}$

Lewis number $Le = \frac{Pr}{Sc}$ ,

The regimes of the flow characteristics to be simulated in wind tunnels can be obtained from the missions of the air- or spaceplanes to be built. It is generally not possible to cover all flight conditions with a single wind tunnel (see the following Re-Ma-number diagram), and to abey all similarity laws. In particular the Reynolds similarity law is difficult to implement since either very high stagnation pressures or very large wind tunnels would be required ($Re \sim p_0 \cdot l_{\text{model}}$). The following diagram shows the working areas of several wind tunnels.

### 6.10.2 Classification of Wind Tunnels

**Classification According to Mach Number**

| | | |
|---|---|---|
| Subsonic tunnel (incompressible) | 0 | $< Ma < 0.25$ |
| Subsonic tunnel (compressible) | 0.25 | $< Ma < 0.8$ |
| Transonic tunnel | 0.8 | $< Ma < 1.2$ |
| Supersonic tunnel | 1.2 | $< Ma < 5$ |
| Hypersonic tunnel | 5 | $< Ma$ |

The hypersonic tunnels are designed as either cold and hot tunnels. In the former only the Mach number is simulated, in the latter also the stagnation temperature. Hot wind tunnels are also used to study real-gas effects.

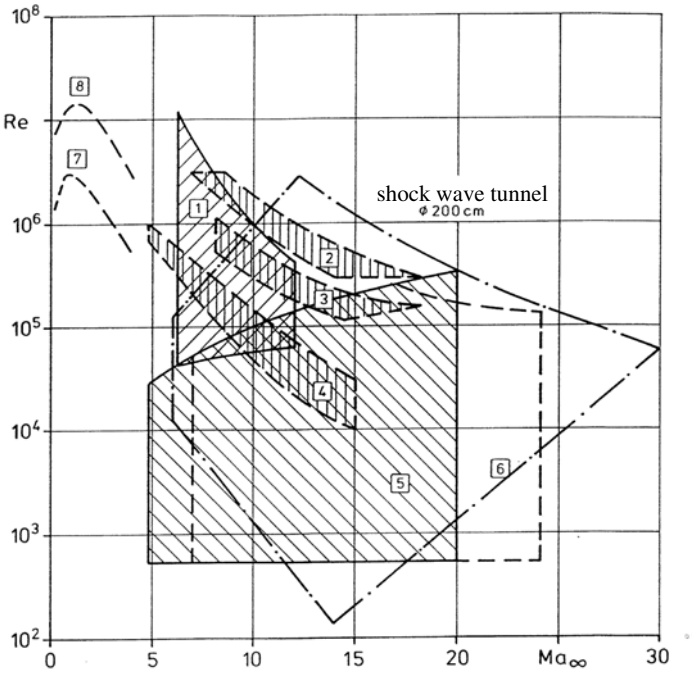


| | | | |
|---|---|---|---|
| 1 | DLR Hypersonic tunnel | 5 | DLR Plasma tunnel PK1 |
| 2 | DLR Gun tunnel | 6 | DLR Vacuum tunnel |
| 3 | DFL Gun tunnel | 7 | AIA Vacuum tunnel 15 x 15 $cm^2$ |
| 4 | Shock-wave tunnels (RWTH Aachen u. ISL Saint Louis) | 8 | AIA Vacuum tunnel 40 x 40 $cm^2$ |

DLR - Deutsches Zentrum für Luft- und Raumfahrt
RWTH - Rheinisch Westfälische Technische Hochschule
ISL - Insitute Saint Louis

**Classification According to Type of Construction**

Closed-circuit, continuously operating wind tunnels (Göttingen Type)
Open wind tunnels (Eiffel Type)

**Classification According to Time of Operation**

| Continuously operating tunnels | intermittently operating tunnels |
|---|---|
| Wind tunnels with closed circuit and returning of the air | Vacuum storage tunnel |
| (Transonic tunnel Göttingen) | Pressure storage tunnel |
| Plasma tunnel | Shock-wave tunnel |
| MHD tunnel (Magneto-hydrodynamic tunnel) | Injector tunnel, pipe wind tunnel |
| | Kryo-shock-wave tunnel, gun tunnel |

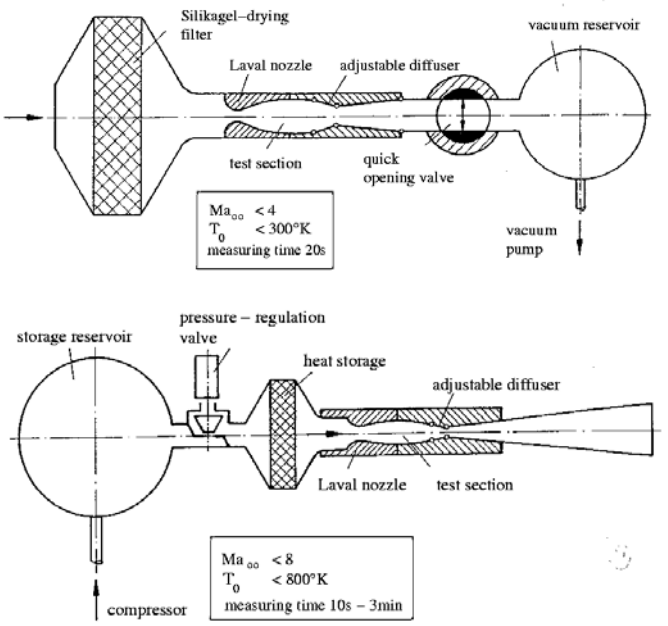


Vacuum-storage tunnel of the AIA (above)
Pressure-storage tunnel (below)

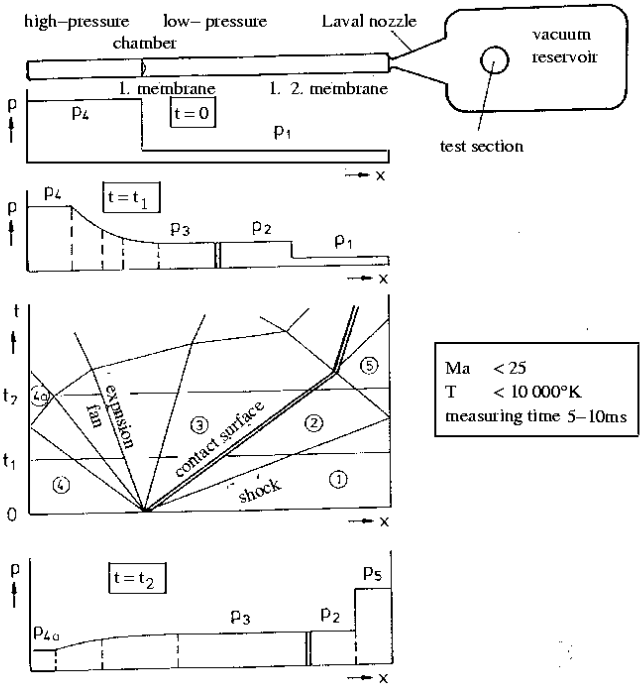


Shock-wave tannel

### 6.10.3 Elements of a Supersonic Tunnel

#### Supersonic Nozzle with Test Section

The nozzle of a supersonic wind tunnel is designed with the method of characteristics [Shapiro 1953]. The purpose of the nozzle is to accelerate the flow from sonic speed ($Ma = 1$) in the throat of the nozzle to a prescribed supersonic speed in the test section (See the following sketch and diagram). The nozzle consists of the subsonic part, the transonic part, the expansion part, and the part for correction of the flow to uniform conditions in the test section.
The flow expands in the area (7-5-3), with several reflections along the wall of the nozzle. The expansion waves hitting the wall of the nozzle in the correction part (3-1) are cancelled there by generating equally strong compression waves with the concave curvature of the contour of the wall. If the nozzle geometry is correctly designed, the flow in the measuring rhombus is parallel and its Mach number is constant. A change of the Mach number can only be achieved by changing the entire nozzle geometry. This can be realized with
a) exchangeable nozzles
b) nozzles with variable contours
c) combinations of a) and b).

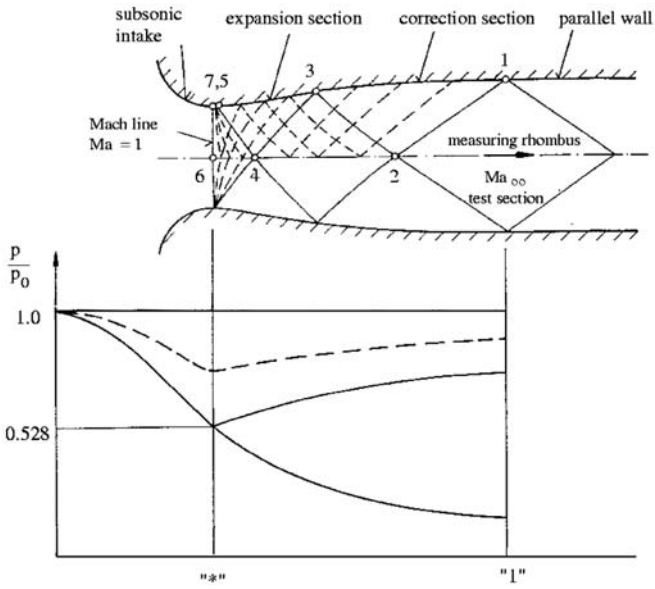


Data of air: $\gamma = 1.4$, $T_0 = 288\,\mathrm{K}$

| $Ma_\infty$ | 1 | 1.5 | 2 | 3 | 5 | 10 | 20 |
|---|---|---|---|---|---|---|---|
| $A_1/A^*$ | 1.0 | 1.17 | 1.68 | 4.19 | 24.4 | 533 | 15300 |
| $p_1/p_0$ | 0.527 | 0.279 | 0.1277 | 0.0273 | 0.0019 | $+2.4 \cdot 10^{-5}$ | $2.1 \cdot 10^{-7}$ |
| $u$ [m/s] | 310 | 424 | 507 | 610 | 694 | 742 | 755 |
| $T$ [K] | 240 | 198 | 157 | 102 | 47.5 | 13 | |

#### Diffuser

Analogously to the generation of the supersonic flow in the Laval nozzle, the deceleration of the velocity with pressure recovery is facilitated in a convergent-divergent diffuser. The pressure

recovery should be as large as possible in order to keep the required compressor power as small as possible for continuously operating tunnels or to achieve optimum measuring times for intermittently operating tunnels.
The largest pressure recovery is obtained, if critical flow conditions prevail in the throat of the diffuser and if the deceleration of the flow to subsonic conditions is facilitated by a weak normal compression shock in the divergent part of the diffuser, immediately downstream from the throat of the diffuser $A^* = A^{*'}$. Since the shock is weak, the losses caused by the shock are small. The start of the supersonic tunnel , however, requires a different cross section of the throat of the diffuser, as is clear from the following consideration [Pope and Goin 1960, Voigt 1960].
During the initial phase of the start of the tunnel subsonic flow prevails in the entire tunnel. The speed of sound is first attained in the throat of the Laval nozzle. The flow expands to supersonic speeds in the divergent part of the nozzle, with a normal shock terminating the supersonic part. With increasing velocity the shock moves downstream. The shock intensity and the losses in the flow reach their maximum, when the shock is located in the test section. In order to guarantee that the mass flow can pass the diffuser, the cross section of the throat of the diffuser must then be sufficiently large.
The continuity equation yields

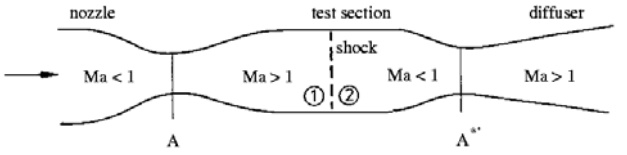


$$\begin{aligned} \rho^* A^* a^* &= \rho^{*'} A^{*'} a^{*'} \\ T_{01} &= T_{02} \quad \rightarrow \quad a^* = a^{*'} \quad \rightarrow \quad T^* = T^{*'} \\ \frac{A^{*'}}{A^*} &= \frac{\rho^*}{\rho^{*'}} = \frac{p^*}{p^{*'}} \cdot \frac{T^{*'}}{T^*} = \frac{p_{01}}{p_{02}} > 1 \end{aligned}$$

Several tunnels were built with an adjustable cross section of the throat of the diffuser, which immediately after the start of the tunnel is reduced from $A^{*'}$ to $A^*$, in order to garantee a maximum pressure recovery.

### 6.10.4 The Oblique Compression Shock

#### Introduction

The flow in a concave corner is continuously turned, if the velocity is subsonic, but discontinuously by a compression shock, if the velocity is supersonic.
It is justified to consider the compression shock as a discontinuity here, since the thickness of the layer, in which pressure, density, temperature, velocity and other quatities change, is of the order of magnitude of several free mean paths only.

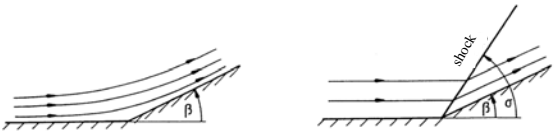


If the turning angle does not exceed a certain angle and if the Mach number in front of the shock is sufficiently large, in two-dimensional flow the shock is straight.

If the turning angle is large, the shock is detached from the contour and curved, normal at the wall (see sketch), so that the flow is subsonic in its immediate vicinity. Further away from the wall the curvature of the shock is decreased, and the flow velocity downstream from it is supersonic. A sonic line $w = a$ separates the supersonic flow from the subsonic flow near the wall.

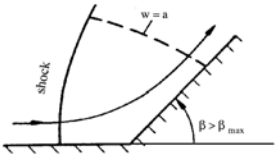


**Computation of the Change of State Across the Oblique Compression Shock**

**Assumptions**

1. The flow is steady and two-dimensional.
2. Gravitational and friction forces can be neglected.
3. Heat transfer with the surroundings can be neglected.
4. The flowing medium is a perfect gas with constant specific heats.

**Basic Equations**

With a small change in notation the jump conditions for the oblique shock are listed again in the following. They were already derived in section 4.5, but are needed here for comparison of the theoretical results with the measured data.

With the assumptions listed, the conservation equations for the control surface indicated in the sketch are the following:

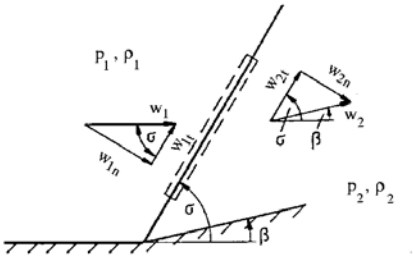


Continuity equation:

$$\rho_1 w_{1n} = \rho_2 w_{2n} \qquad (6.152)$$

Momentum equation normal to the shock:

$$p_1 - p_2 = \rho_2 w_{2n} w_{2n} - \rho_1 w_{1n} w_{1n} \quad (6.153)$$

Momentum equation tangential to the shock:

$$0 = \rho_2 w_{2n} w_{2t} - \rho_1 w_{1n} w_{1t} \qquad (6.154)$$

Energy equation:

$$\frac{1}{2}(w_{1t}^2 + w_{1n}^2) + \frac{\gamma}{\gamma - 1}\frac{p_1}{\rho_1} = \frac{1}{2}(w_{2t}^2 + w_{2n}^2) + \frac{\gamma}{\gamma - 1}\frac{p_2}{\rho_2} \qquad (6.155)$$

The following relations can be derived from the sketch:

$$\sin\sigma = w_{1n}/w_1 \qquad (6.156)$$

$$\tan\sigma = w_{1n}/w_{1t} \qquad (6.157)$$

$$\tan(\sigma - \beta) = w_{2n}/w_{2t} \qquad (6.158)$$

$$\sin(\sigma - \beta) = w_{2n}/w_2 \qquad (6.159)$$

After introducing the Mach number in front of the shock,

$$Ma_1 = \frac{w_1}{a_1} = w_1 / \sqrt{\gamma \frac{p_1}{\rho_1}} \quad , \qquad (6.160)$$

with $a$ being the local speed of sound, (6.156) can be rewritten in the following form:

$$Ma_1^2 \sin^2\sigma = w_{1n}^2 / \left(\gamma \frac{p_1}{\rho_1}\right) \qquad (6.161)$$

**Solution**

It follows from (6.152) to (6.155) and (6.161):

$$w_{1t} = w_{2t} \tag{6.162}$$

$$\frac{w_{2n}}{w_{1n}} = \frac{\rho_1}{\rho_2} = \frac{1+\frac{\gamma-1}{2}\frac{w_{1n}^2}{\gamma p_1/\rho_1}}{\frac{\gamma+1}{2}\frac{w_{1n}^2}{\gamma p_1/\rho_1}} = \frac{1+\frac{\gamma-1}{2}Ma_1^2\sin^2\sigma}{\frac{\gamma+1}{2}Ma_1^2\sin^2\sigma} = \frac{w_{2n}}{w_{1n}}(\gamma,Ma,\sigma) \tag{6.163}$$

$$\frac{p_2}{p_1} = 1+\frac{2\gamma}{\gamma+1}\left(\frac{{w_1}_n^2}{\gamma p_1/\rho_1}-1\right) = 1+\frac{2\gamma}{\gamma+1}(Ma_1^2\sin^2\sigma-1) = \frac{p_2}{p_1}(\gamma,Ma,\sigma) \tag{6.164}$$

With (6.162) there is obtained from (6.157) and (6.158):

$$\frac{w_{2n}}{w_{1n}} = \frac{\tan(\sigma-\beta)}{\tan\sigma} \quad , \tag{6.165}$$

and further

$$\cot\beta = \tan\sigma\left(\frac{\frac{\gamma+1}{2}Ma^2}{Ma^2\sin^2\sigma-1}-1\right) \quad ; \quad \sigma=\sigma(\gamma,Ma,\beta) \quad . \tag{6.166}$$

Equations (6.164) and (6.166) yield a relation for the construction of the heart-curve diagram, after elimination of $\sigma$

$$\tan^2\beta = \left[\frac{Ma_1^2}{1+\frac{\gamma+1}{2\gamma}\left(\frac{p_2}{p_1}-1\right)}-1\right]\cdot\left[\frac{\frac{p_2}{p_1}-1}{\gamma Ma_1^2-\left(\frac{p_2}{p_1}-1\right)}\right]^2 \quad . \tag{6.167}$$

It follows from (6.156) and (6.159) that

$$\frac{w_2}{w_1} = \frac{w_{2n}}{w_{1n}}\cdot\frac{\sin\sigma}{\sin(\sigma-\beta)} \quad . \tag{6.168}$$

This equation together with (6.166) and the critical speed of sound $a^*$,

$$a^{*2} = \frac{2\gamma}{\gamma+1}R\cdot T_0,$$

after elimination of $\sigma$, with $R$ being the gas constant, and $T_0$ the stagnation temperature, leads to the expression for the shock polar:

$$(w_2\sin\beta)^2 = (w_1-w_2\cos\beta)^2\frac{w_1w_2\cos\beta-a^{*2}}{\frac{2}{\gamma+1}w_1^2-w_1w_2\cos\beta+a^{*2}}. \tag{6.169}$$

**Heart-Curve Diagram and Shock Polar**

The heart-curve diagram and the shock polar are sketched for constant $\gamma$ for a given free-stream Mach number.

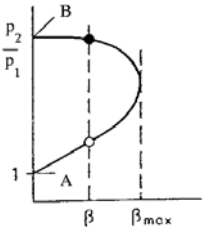


heart-curve diagram

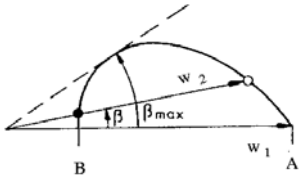


shock polar

Only the physically meaningful regions are shown ($p_2/p_1 \geq 1$ and $w_2/w_1 \leq 1$). Two solutions exist for a prescribed value of $\beta$ indicated by the symbols $\circ$ and $\bullet$). In the actual flow the weak solution ($\circ$) with the smaller $p_2$ and the larger $w_2$ is observed in straigth oblique shocks. For the case that$\beta = 0$ the heart-curve diagram and the shock polar contain the solution for the normal compression shock ($B$) and the trivial solution for the unperturbed flow ($A$). Closed-form solutions for the straight shock do not exist for turning angles $\beta > \beta_{max}$; the turning of the flow takes place in a curved shock.

**Supplementary Remarks**

The Hugoniot relation: With (6.152) to (6.155) the energy equation is cast into the following form, named after Hugoniot

$$\frac{\rho_2}{\rho_1} = \frac{(\gamma+1)\frac{p_2}{p_1} + (\gamma-1)}{(\gamma-1)\frac{p_2}{p_1} + (\gamma+1)}, \tag{6.170}$$

or in the form given by von Kármán

$$\frac{p_2 - p_1}{\rho_2 - \rho_1} = \gamma \, \frac{p_2 + p_1}{\rho_2 + \rho_1}. \tag{6.171}$$

It follows from (6.170) for the very strong shock ($p_2/p_1 \to \infty$), that the maximum compression ratio of an perfect gas with constant specific heats is

$$\left(\frac{\rho_2}{\rho_1}\right)_{p_2/p_1 \to \infty} = \frac{\gamma+1}{\gamma-1} \tag{6.172}$$

Vice versa, it follows from (6.171) for the weak shock ($p_2/p_1 \to 1$)

$$\left(\frac{\Delta p}{\Delta \rho}\right)_{\hat{p}/p \to 1} = \gamma \, \frac{p}{\rho} = \left(\frac{dp}{d\rho}\right)_{isentrop.} \tag{6.173}$$

Very weak shocks can in a first approximation be considered as isentropic compression waves.
The maximum turning angle:
For $\gamma = 1.4$ the maximum turning angle $\beta_{max.}$ has the following values:

| $\beta_{max.}$ | $0^o$ | $23^o$ | $34^o$ | $42^o$ | $44^o$ | $45^o$ |
|---|---|---|---|---|---|---|
| $Ma$ | 1 | 2 | 3 | 5 | 8 | $\infty$ |

*Construction of the Shock Polar*

All velocity components are non-dimensionalized with the critical speed of sound $a^*$,the speed of sound in the throat of the Laval nozzle, in which the flow expands in the divergent part to supersonic conditions corresponding to the Mach number $Ma$. The relation connecting the velocity non-dimensionalized with $a^*$ and $Ma$ is

$$\frac{w}{a^*} \equiv Ma^* = \frac{w}{a} \cdot \frac{a}{a^*} = Ma \sqrt{\frac{\frac{\gamma+1}{2}}{1 + \frac{\gamma-1}{2} Ma^2}} \quad . \tag{6.174}$$

The shock polar was explained in Sect. 4.5.3, where it was introduced in conjunction with the transformation of the flow quantities from the physical plane into the hodograph plane. The shock polar offers a convenient means of determining the velocity immediately downstream from an oblique shock.

If the velocity components in front and downstream from the shock are plotted as indicated in the sketch, it is seen that for given values of $Ma$,$\gamma$,$\beta$ und $w_1$ the quantities $w_2$,$w_{n2}$,$w_{t2}$, and $\sigma$ can be determined from the shock polar.

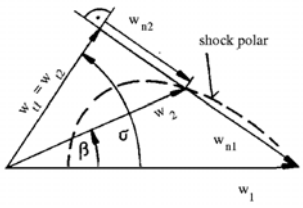


### 6.10.5 Description of the Experiment

The experiment is carried out in the intermittently operating supersonic wind tunnel of the Aerodynamisches Institut. The air is sucked from the surroundings ($p_0$, $T_0$) through the Laval nozzle and the test section into the vacuum storage.

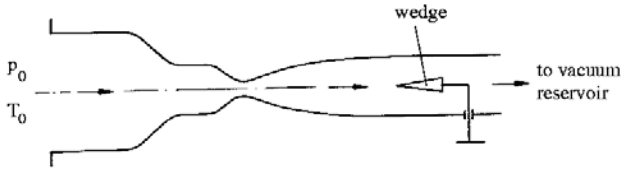


A supersonic flow with a Mach number of $Ma \approx .2.0$ in the test section is generated by expansion of the air in the Laval nozzle.
The Laval nozzle is a continuously adjustable nozzle and admits a variation of the test Mach number from about $Ma = 1$ to $Ma = 5$. The contour of the nozzle is generated with flexible steel sheets, which are fastened at one end of the nozzle frame. The sheets are held in position by six supporting jacks. The jacks are adjusted in such a way, that the metal sheets take on the form of the nozzle contour required for the test Mach number.
The model support enables a change of the angle of attack of the model. It can be varied in steps of one half, one, and two degrees. The maximum angle of attack the model can be held at is 39.5°.
In order to obtain a symmetric flow about the wedge, it is turned with the aid of its support until the pressure difference $p_{22} - p_{23}$ measured at the two symmetrically positioned pressure holes vanishes. After this directional adjustment of the wedge, the pressure differences $p_0 - p$, $p_0 - p_2$, and $p_0 - p_{exp}$ are measured with U-tubes. The shock angle $\sigma$ and the Mach angle $\alpha$ of a Mach line of the free stream are visualized with a schlieren picture:

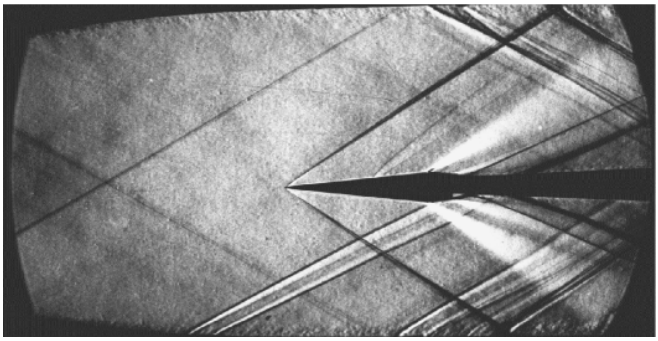

The Mach line, inclined by the angle $\alpha$, can be recognized in the photograph. In the actual flow it is a very weak oblique compression shock, generated by a small perturbation of the flow, caused by a piece of Scotch tape, pasted to the wall.

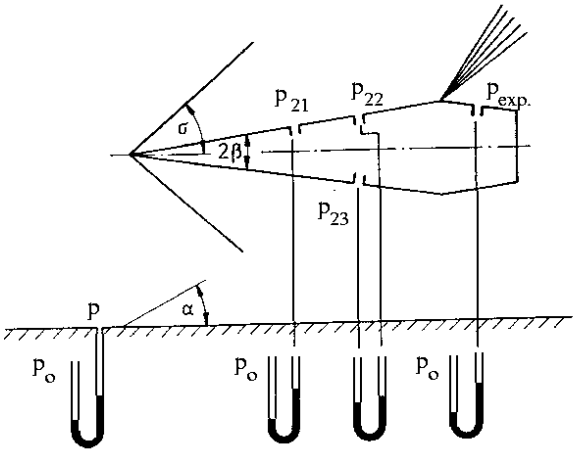


The sketch shown above depicts the arrangement of the pressure measurement on the wedge. The U-tube on the left measures the pressure ratio $p_\infty/p_0$. The U-tube in the middle of the sketch measures the pressure ratio $p_{21}/p_0$, i. e. the ratio of the static pressure on the wedge to the stagnation pressure. The third U-tube measures the pressures $p_{22}$ and $p_{23}$, which serve to align the model with the direction of the free stream. The angle of attack of the wedge is changed until $p_{22} = p_{23}$. The U-tube on the right measures the pressure downstream from the shoulder, after the expansion, $p_{\text{exp.}}$, referenced to the stagnation pressure $p_0$.
Also indicated is the Mach angle a of the free stream, as made visible by a roughness element of the wall of the wind tunnel. The lines at the nose of the wedge indicate the shock angle $\sigma$ for the weak solution.

**Selected References**

Wuest, W.: *Strömungsmeßtechnik,* Vieweg-Verlag, 1969.

Pope, A., Goin, K.L. *High-Speed Wind Tunnel Testing*, Jihn Wiley, 1965.

Oertel, H.: *Stoßrohre*, Springer-Verlag, 1966.

Naumann, A.: *Moderne Entwicklung bei Windkanälen, Die Umschau in Wissenschaft und Technik*, Heft 20, 1964, S. 613.

Naumann, A.: *Aerodynamische Gesichtspunkte der Windkanalentwicklung*, Jahrbuch WGL, 1954.

Heyser, A.: *Vorlesung: Versuchsanlagen der Strömungstechnik für Unter-, Über- und Hyperschallgeschwindigkeiten*, RWTH Aachen, 1972.

Shapiro, A.H.: *The Dynamics and Thermodynamics of Compressible Fluid Flow*, Ronald Press, Vol. I, 1953, S. 507-512.

Cummings, J.C.: *Development of a high-performance cryogenic shock tube*, Journal of Fluid Mechanics, Vol. 66, Part 1, 1874, S. 177-187.

Voigt, F.: *Vorgänge beim Start einer Überschallströmung, Dissertation*, RWTH Aachen, 1960

Prandtl, L. *Führer durch die Strömungslehre*, Vieweg-Verlag, 1965, S.302.

Flügge, S.: *Handbuch der Physik: Strömungsmechanik,* Springer-Verlag, Band IX, 1959.

### 6.10.6 Evaluation

**Measured Data**

$$p_0 = 747\ mm\ Hg$$
$$p_0 - p_1 = 690\ mm\ Hg$$
$$p_0 - p_2 = 632\ mm\ Hg$$
$$\beta = 5.75^o$$
$$\gamma = 1.4$$
$$p_0 - p_{exp} = 700\ mm\ Hg$$

$$\frac{p_0}{p} = \frac{1}{1-(p_0-p_1)/p_0} = 13.1$$

$$\frac{p_2}{p_1} = \frac{1-(p_0-p_2)/p_0}{1-(p_0-p_1)/p_0} = 2.017$$

**Determination of the Mach Number**

1. $Ma = \dfrac{1}{sin\alpha} = 2.13$ $\alpha$ is determined from photograph

2. $$Ma = \sqrt{\frac{2}{\gamma-1}\left[\left(\frac{p_0}{p_1}\right)^{\frac{\gamma-1}{\kappa}} - 1\right]} = 2.33$$

**Determination of $\sigma$**

1. $\sigma = 33.0^\circ$ from photograph
2. $\sigma = 39.9^\circ$ from $\sin\sigma = \sin\alpha \cdot \sqrt{\dfrac{\gamma+1}{2\gamma}\left(\dfrac{p_2}{p_1}-1\right)+1}$
3. $\sigma = 32.5^\circ$ from shock polar $\left(Ma^* = Ma\sqrt{\dfrac{\frac{\gamma+1}{2}}{1+\frac{\gamma-1}{2}Ma^2}} = 1.767\right)$

**Determination of the Pressure Ratio $p_2/p_1$**

1. $\dfrac{p_2}{p_1} = 2.017$ from measurement
2. $\dfrac{p_2}{p_1} = 1.4$ from heart-curve diagram

**Questions**

1. Sketch the contour of the shock in the sections (1, 2, 3) parallel to the side walls of the tunnel.

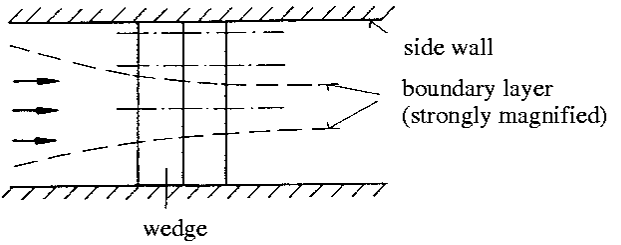

The sketch shown above depicts the top view of the wedge in the test section of the wind tunnel. The model extends to both side walls of the tunnel. As indicated in the sketch by the dashed curved lines a turbulent boundary layer develops on the side walls. The thickness of the boundary layer is strongly magnified. Also indicated in the sketch are 3 sections, one in the middle of the tunnel (section 1), one closer to the side wall (section 2), and the third near the wall (section 3).

Case 1:

$$Ma = 2.13$$

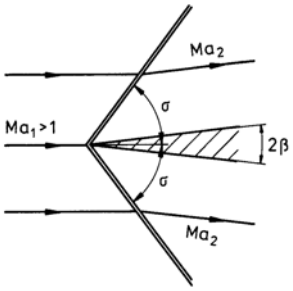


Case 2:

$$\begin{aligned} Ma &> 1 \\ \sigma &> 33^\circ \end{aligned}$$

or detached shock for $\beta > \beta_{max}$

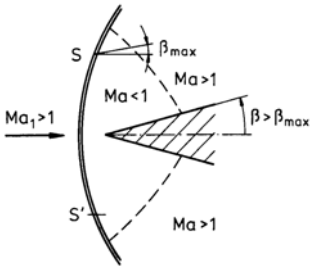


Case 3:
$Ma < 1$, no shock,
flow decelerated by wall friction
or $M > 1 \Rightarrow$ detached shock

2. The pressures in front of and downstream from a normal compression shock are measured with two Pitot tubes. What pressures are measured and how do the readings differ from each other? (It is assumed that the shock is not affected by the Pitot tube positioned in front.)
The total pressure downstream from a normal compression shock is measured. The reading is the same in both cases.

3. Given is a wedge at an angle of attack with $\beta = 20^o$ at a free-stream Mach number $Ma_\infty = 2.91$.

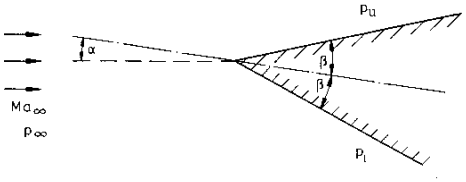


How large can the angle of attack $\alpha$ become, without having the compression shock detach from the wedge?
$\beta_{max} = 33.8^\circ$ from heart-curve diagram
here $\beta_{max} = \beta + \alpha_{max}$ for lower side
$\Rightarrow \alpha_{max} = 13.8^\circ$

How large is then the pressure difference $\dfrac{p_l - p_u}{p_\infty}$?

$\frac{p_l - p_u}{p_\infty} = 6.43$

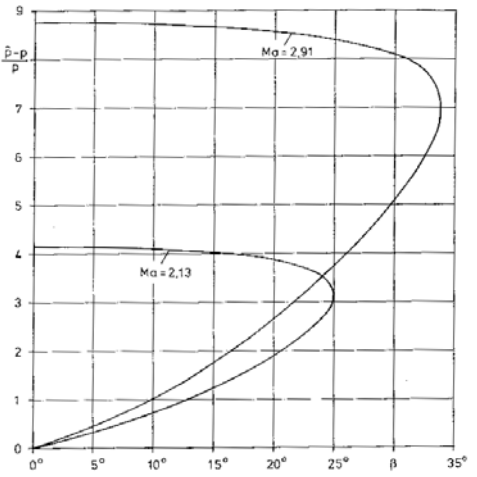


Heart-curve diagram for $\gamma = 1.4$

## 6.11 Sphere in Compressible Flow

*Abstract*

The drag of a sphere is investigated experimentally in compressible subsonic flow. The drag coefficient $c_D$ depends on the Reynolds number $Re$ and on the Mach number $Ma$. The influence of the critical Mach number on the separation of the boundary layer is studied with two spheres of different diameter. The drag of the spheres is measured for several free-stream velocities. The different flow patterns of sub- and supercritical Mach numbers $Ma$ are visualized with the schlieren method.

### 6.11.1 Introduction

In this experiment the influence of the compressibility of the air on the flow field about a sphere is studied in an experiment. The compressibility has to be taken into account in steady flows, if the density changes are larger than about one percent. The drag coefficient $c_d$ then also depends on the Mach number in addition to the similarity parameters mentioned already in the experiment sphere in incompressible flow.
The drag coefficient of the sphere measured in the wind tunnel

$$c_D = \frac{D}{q_\infty \frac{\pi}{4} D_S^2} \tag{6.175}$$

with

$$\begin{array}{cl} \mathrm{D} & \text{drag,} \\ q_\infty = \frac{\rho}{2} w_\infty^2 & \text{dynamic pressure of the free stream,} \\ D_S & \text{diameter of the sphere,} \end{array}$$

depends on the following similarity and other parameters:

$$c_D = f(Re, Ma_\infty, \gamma, \frac{k_s}{D_S}, Tu, \frac{A_{WT}}{A_S}, \text{support}, Kn, ...) \tag{6.176}$$

The quantities mentioned in the above equation are defined as follows:

| | |
|---|---|
| $Re_\infty$ | Reynolds number $\left(\frac{\rho_\infty u_\infty D_S}{\mu_\infty}\right)$ |
| $Ma_\infty$ | Mach number $\left(\frac{w_\infty}{a_\infty}\right)$ |
| $\gamma$ | ratio of the specific heats |
| $\frac{k_s}{D_S}$ | relative roughness of the surface |
| Tu | Turbulence intensity of the free stream |
| $\frac{A_{WT}}{A_S}$ | ratio of the cross-sections tunnel-sphere |
| $Kn$ | Knudsen number $\frac{\lambda_\infty}{D_S}$ with $\lambda_\infty$ = mean free path. |

In (6.179) the function $f$ is unknown. In the experiment only the Reynolds number $Re_\infty$ and the Mach number $Ma_\infty$ are varied; the other parameters, which are given by the experimental facility, are kept constant.

### 6.11.2 The Experiment

#### Experimental Facility

The experiment is carried out in the intermittently operating vaccum-storage tunnel of the Aerodynamisches Institut, with a test section of $15 \cdot 15\,\mathrm{cm}^2$. Air is sucked out of the atmosphere through a well-rounded intake and the test section into the vacumm tank. A convergent-divergent diffuser with an adjustable throat is positioned between the test section and the tank. If the ratio of the pressures in the tank and in the atmosphere is sufficiently small, the velocity

of the air in the throat of the diffuser is equal to the speed of sound. With this arrangement it is guaranteed, that despite of the increasing pressure in the tank the flow conditions in the test section remain constant for a certain time. The similarity parameters $Re$ and $Ma$ are coupled by the following relation, if it is assumed, that the viscosity $\mu = \mu(T)$ is konwn:

$$Re = \frac{\rho\, u\, D_S}{\mu} = \frac{\rho}{\rho_0} \cdot \rho_0 \cdot \frac{u}{a_\infty} \cdot \frac{a_\infty}{a_0} \cdot a_0 \cdot \frac{\mu_0}{\mu} \cdot \frac{1}{\mu_0} \cdot D_S = f(Ma_\infty) \cdot \frac{\rho_0 \cdot a_0}{\mu_0} \cdot D_S \qquad (6.177)$$

$\rho_0$ Stagnation density of the air
$a_0$ Speed of sound at stagnation conditions
$\mu_0$ viscosity

In a vacuum-storage tunnel with constant $\rho_0$,$a_0$, and $\mu_0$, with the Mach number $Ma$ held constant, the Reynolds number $Re_\infty$ can only be changed by changing the diameter of the sphere.
Two spheres with diameters of 25 mm and 50 mm were used in the experiments. The spheres were mounted on the model support, which was positioned in the dead-water region of the spheres. The drag was measured with a strain-gauge balance mounted in the support.

**Balance for Measuring the Drag**

The balance mounted in the support measures the drag of the sphere by recording the change of the electric resistance, caused by the elongation of an electric conductor (strain gauge). The installation of the support and the balance are sketched below.

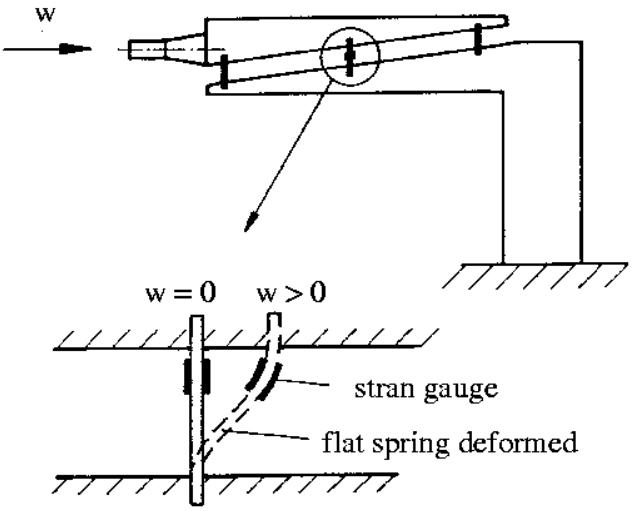


The spring elements of the balance are deformed when they are exposed to strain. The deformation is measured with two strain gauges connected to a bridge circuit. The strain gauges are arranged in such a way that sufficient temperature compensation is guaranteed. The balance was calibrated in an extra experiment prior to the drag measurement by taking the balance out of the support and loading it with weights. The influence of the support on the drag of the sphere could not be taken into account.

**Description of the Measurement**

The drag of two spheres with 25 mm and 50 mm diameters is measured for several free-stream velocities $w$. The free-stream velocity is varied by varying the cross section of the throat of the diffuser, where sonic conditions prevail.
The unperturbed free-stream conditions are determined with a measurement of the pressure. A sketch of the pressure measurements is given on the data sheet.
The flow field about the sphere is visualized with the schlieren method.

### 6.11.3 Fundamentals of the Compressible Flow About a Sphere

**Potential Flow**

According to potential theory, the flow of an incompressible medium about a sphere is obtained by superposing a spacial dipole with a parallel flow. Some of the streamlines are shown below.

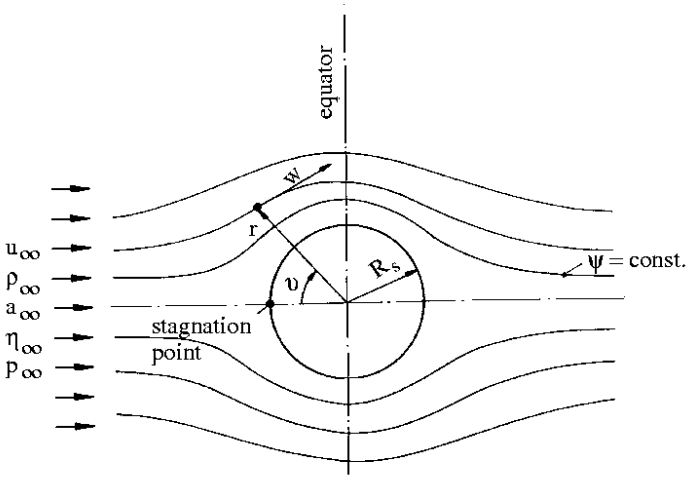


The velocity and the pressure on the surface of the sphere in incompressible flow are described by the following relations:

$$\frac{w}{w_\infty} = \frac{3}{2}\sin\theta \tag{6.178}$$

$$\frac{p_s - p_\infty}{\rho\frac{u_\infty^2}{2}} = 1 - \frac{9}{4}\sin^2\theta \text{ on } r = R_s \tag{6.179}$$

Lamla [1939] investigated the potential flow of a compressible gas about a sphere. The following diagram shows the ratio of the velocities $w_{compr.}/w_{incompr.}$ for the surface of the sphere. In the vicinity of the upstream stagnation point the deceleration of the compressible flow is more pronounced, and near the equator the acceleration is stronger than in the incompressible flow. According to Lamla [1939] the critical Mach number of the free stream $Ma$ is given by the condition, that the velocity at the equator becomes sonic, which with $\gamma = 1.4$ yields a value of

$$Ma_{crit.} = 0.57 \quad Ma^*_{crit.} = 0.6 \tag{6.180}$$

The velocity $w_{compr.}$ at the equator for $Ma_{crit.}$ is about ten percent higher than the velocity computed for incompressible flow.

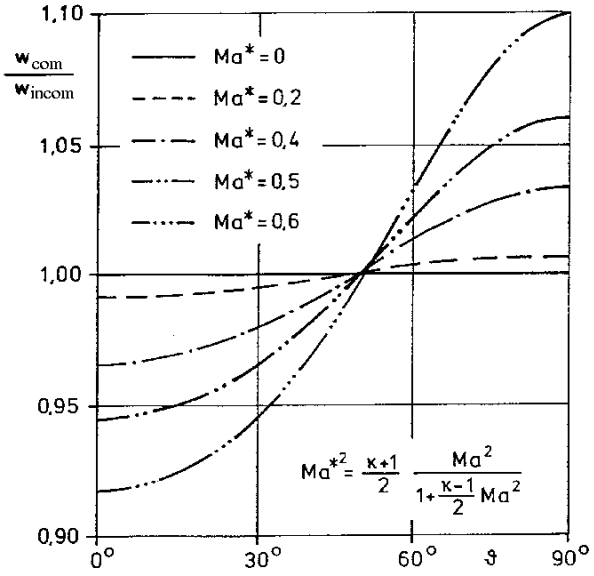


**Definition of the Critical Reynolds Number**

The location of the separation line and the size of the dead-water region are strongly influenced by the nature of the flow in the boundary layer, which can either be laminar or turbulent. If the laminar-turbulent transition occurs upstream of the separation line, it is shifted from the upstream to the downstream side of the equator and reduces the dead-water region. The Reynolds number $Re$, at which the transition occurs, is called critical Reynolds number.

**Definition of the Critical Mach Number**

An increase of the Mach number $Ma$ in subsonic flow leads to an increase of the velocity in the vicinity of the equator, and, aided by the displacement effect of the sphere, eventually to the formation of a local supersonic pocket, which is terminated by a shock. The lowest free-stream Mach number, at which the local velocity is equal to the local speed of sound, is called critical Mach number.

**The Dependence of the Flow Field on Reynolds and Mach Number**

As previously mentioned, the magnitude of the drag coefficient depends on the location of the separation line, which in turn is influenced by the nature of the flow in the boundary layer. It was, however, shown in experiments, that for supercritical Mach numbers separation in the vicinity of the equator is also influenced by the shock, terminating the supersonic pocket. The following diagrams and sketches on the left show the flow patterns, if the critical Reynolds number $Re_{crit.}$ is attained prior to the critical Mach number $Ma_{crit.}$. When the critical Reynolds number $Re_{crit.}$ is reached, the drag coefficient $c_D$ decreases abruptly. The flow separates downstream from the equator.
When the critical Mach number is reached, a shock is generated at the equator, which causes the boundary layer to separate. The drag coefficient $c_D$ rises again. If $Ma_{crit.}$ is reached prior to $Re_{crit.}$ (diagram and sketches on the right below), the shock prevents the drag coefficient

$c_d$ from dropping abruptly at the critical Reynolds number, since the separation line, usually observed to move downstream, when $Re_{crit.}$ is reached, is now fixed by the shock at the equator. The different $c_D$-distributions can be explained by using spheres with different diameters; the results for the sphere with the larger diameter are shown on the left, those for the sphere with the smaller on the right.

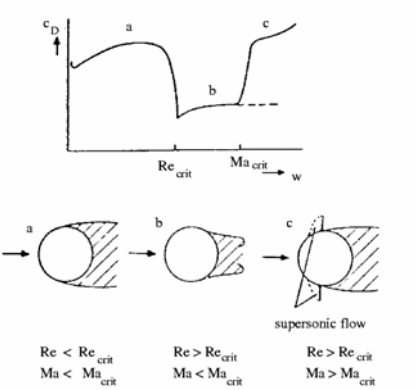


Schematic diagram of the drag coefficient and the flow patterns as a function of the free-stream velocity for large diameters of the sphere.

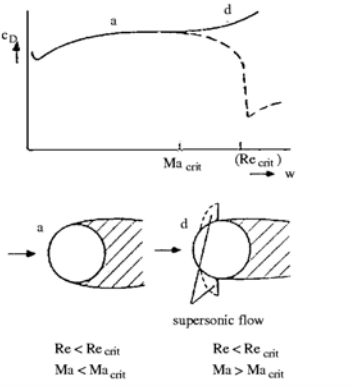


Schematic diagram of the drag coefficient and the flow patterns as a function of the free-stream velocity for small diameters of the sphere.

The free-stream velocities, at which $Re_{crit.}$ and $Ma_{crit.}$ are observed, are

$$w_{Re,crit.} = \frac{Re_{crit.}\,\mu_\infty}{\rho_\infty D_S} \tag{6.181}$$

$$w_{Ma,crit.} = Ma_{crit.}\,a_\infty. \tag{6.182}$$

If the free-stream conditions are kept constant, then $w_{Macrit.} = \text{const.}$, and $w_{Recrit.} \approx 1/D_S$. Therefore for large diameters $w_{Recrit.} < w_{Macrit.}$ (see diagram on the left), and for smaller diameters $w_{Recrit.} > w_{Macrit.}$ (see diagram on the right). In the limiting case $w_{Recrit.} = w_{Macrit.}$ the critical Reynolds number and the critical Mach number are reached at the same free-stream velocity. The diameter of the sphere, correponding to this condition is somwhere between 30 and 50 mm.

**Experimental Results**

The experimental results $c_D = f(Re,Ma)$ of Naumann and Walchner, shown in the following two diagram confirm these considerations, [Naumann 1953].
The curves in the first of the following diagrams show the influence of the free-stream Mach number on the drag coefficient $c_D$ for different diameters of the sphere. It can be seen, that for small diameters up to approximately 30 $mm$ $Ma_{crit.}$ is reached before $Re_{crit.}$. After $Ma_{crit.}$ is exceeded, the drag coefficient increases slightly, as the shock intensity and also the fluid mechanical losses are increased.
For spheres with diameters larger than 50 $mm$, $Re_{crit.}$ is reached before $Ma_{crit.}$. The abrupt drop of the drag coefficient $c_d$ is observed as in incompressible flow. If the critical Mach number is exceeded, the drag coefficient $c_D$ increases sharply.
In the second diagram the drag coefficients measured by Naumann [1953] are shown as a function of the Reynolds number $Re$ and of the Mach number $Ma$.

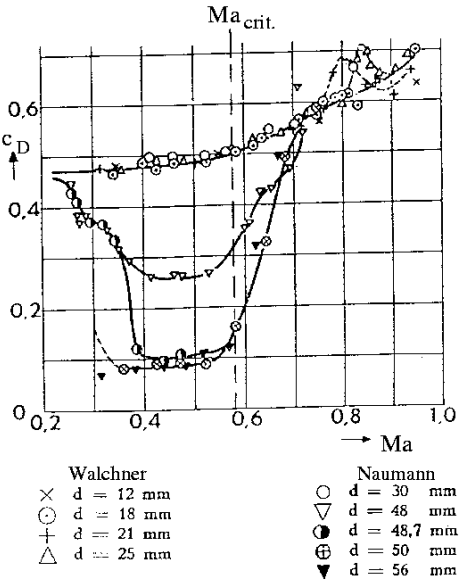
Ma crit.
0,6
$c_D$
0,4
0,2
0
0,2
0,4
0,6
0,8
1,0
Ma
Walchner
× d = 12 mm
⊙ d = 18 mm
+ d = 21 mm
△ d = 25 mm
Naumann
○ d = 30 mm
▽ d = 48 mm
◑ d = 48,7 mm
⊕ d = 50 mm
▼ d = 56 mm

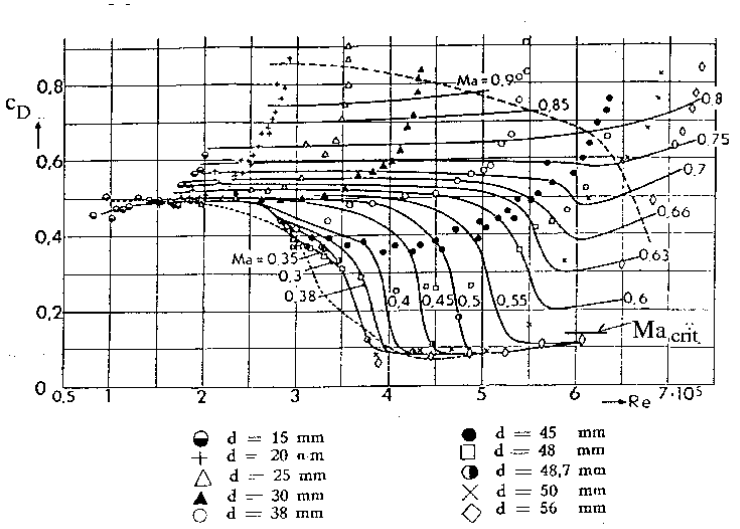
$c_D$
0,8
0,6
0,4
0,2
0
0,5
1
2
3
4
5
6
Re 7·10⁵
Ma = 0,9
0,85
0,8
0,75
0,7
0,66
0,63
0,6
Ma = 0,35
0,3
0,38
0,4
0,45
0,5
0,55
Ma crit.
◒ d = 15 mm
+ d = 20 mm
△ d = 25 mm
▲ d = 30 mm
○ d = 38 mm
● d = 45 mm
□ d = 48 mm
◑ d = 48,7 mm
× d = 50 mm
◇ d = 56 mm

**Selected References**

BAILEY: *Sphere drag coefficient for subsonic speeds in continuum and free molecular flows*, J. Fluid Mech., Vol. 65, 1974, pp. 401-410.

LAMLA, E.: *Symmetrische Potentialströmung eines kompressiblen Gases Kreiszylinder und Kugel im unterkritischen Gebiet*, F.B. 1014, DVl, 1939.

NAUMANN, A.: *Luftwiderstand der Kugel bei hohen Unterschallgeschwindigkeiten*, Allgemeine Wärmetechnick 4/10, 1953.

### 6.11.4 Evaluation

The drag coefficients $c_D = f(Re,Ma)$ are to be computed from the measured data given on page 350:
All equations, needed for the computation are listed on the data sheet.
The drag coefficients $c_D = f(Ma,D_s)$ and $c_D = f(Re,D_s)$ are to be plotted and to be discussed.
The experiment and the results of the measurements are to be commented critically.

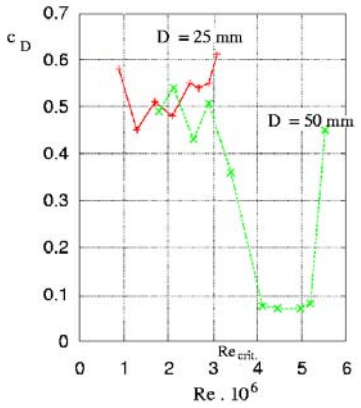


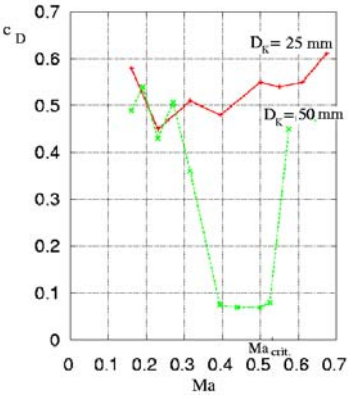


For $D_s = 50\,\text{mm}$ the drag coefficient $c_D$ drops abruptly at $Re \approx 3.5{\cdot}10^5 \approx Re_{crit.}$ and $Ma = 0.3$, caused by the sudden shift of the separation line further downstream from the equator, reducing the dead-water region and also the drag coefficient. At $Ma = Ma_{crit.} \approx 0.55$ the drag coefficient $c_D$ increases sharply, since the flow velocity exceeds the local speed of sound just upstream of the equator and becomes supersonic, with a shock terminating the supersonic pocket near the equator. The sudden pressure rise enforces flow separation just downstream from the shock, and the dead-water region is immediately increased.
The drop of the drag coefficient $c_D$ is not observed in the experiment with the sphere with a diameter of 25 mm, as in this case $Ma_{crit.}$ is reached before $Re_{crit.}$ and the shock prevents the shift of the separation line. In principle, measurements of the drag are rather inaccurate, which explains the deviation of the data from each other.

### 6.11.5 Questions

1. Sketch the flow field about a sphere for the following free-stream conditins:
   a.) $Ma = 0, \quad Re > Re_{crit.}$
   b.) $Ma > Ma_{crit.}, \quad Re > Re_{crit.}$

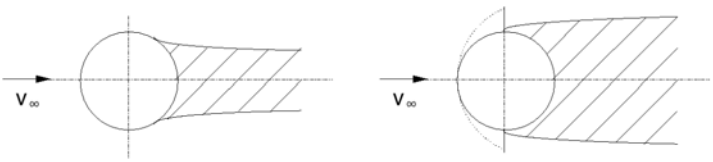


2. Why does the drag coefficient $c_D$ increase with increasing Ma for $Ma_{crit.} < Ma < 1$?
The shock moves upstream, which causes an enlargement of the dead-water region.
3. How large is the density change at the equator in a potential flow about the sphere $(\rho_\infty - \rho)/\rho_\infty$, if the free-stream Mach number $Ma_\infty = Ma_{crit.}$? Assume isentropic change of state ($\gamma = 1.4$,air).

$$M_\infty = 0.57 \rightarrow \left(\frac{\rho_0}{\rho_\infty}\right) = 1.17$$

$$\frac{\rho_\infty - \rho}{\rho_\infty} = 1 - \frac{\rho}{\rho_\infty} \cdot \frac{\rho_0}{\rho_0} = 1 - \left(\frac{\rho}{\rho_0}\right)\left(\frac{\rho_0}{\rho_\infty}\right) = 1 - 0.634 \cdot 1.17 = 0.258$$

4. Up to what flow velocity can the influence of the compressibility of dry air on the flow be neglected ($T_0 = 293K$)?

$$\frac{\rho_\infty - \rho}{\rho_\infty} > 0.01 \quad \Rightarrow \text{compressible flow}$$

$$\Rightarrow \frac{\rho}{\rho_0} < 0.99 \Rightarrow Ma > 0.14$$

$$u_\infty = Ma\sqrt{\gamma\ R\ T_0} \Rightarrow u_\infty \geq 48\frac{m}{s}$$

The influence of the compressibility can be neglected up to a flow velocity of about $48\frac{m}{s}$, since then the relative density changes are below 1%.

Calibration values of the strain gauge balance

| loading F | [N] | 0 | 0.71 | 2.71 | 4.71 | 6.71 | 8.71 | 10.71 | 15.71 | 20.71 |
|---|---|---|---|---|---|---|---|---|---|---|
| Reading loading | [Units] | 0 | 1.4 | 4.7 | 8.1 | 11.6 | 15.0 | 18.5 | 27.1 | 35.7 |
| Reading unloading | [Units] | 0.2 | 1.5 | 4.9 | 8.4 | 11.8 | 15.1 | 18.5 | 27.1 | 35.7 |

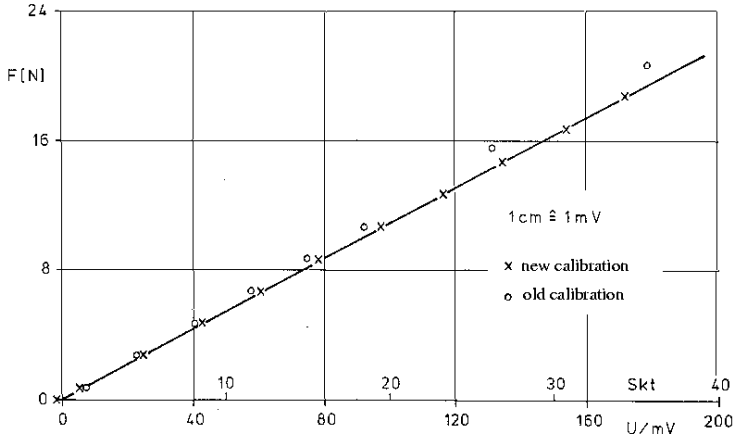


Calibration curve

| 1 | 2 | 3 | 4 | 5 | 6 | 7 | 8 | 9 | 10 | 11 | 12 | 13 | 14 | 15 | 16 | 17 | 18 | 19 | 20 | 21 |
|---|---|---|---|---|---|---|---|---|---|---|---|---|---|---|---|---|---|---|---|---|
| $D_K$ | $\Delta p_0$ | $p_0$ | $\Delta p_1'$ | $\Delta p_1$ | $p_1$ | $\frac{p_1}{p_0}$ | Ma | $\frac{u}{a_0}$ | R | $a_0$ | $u_1$ | $\rho_0$ | $\frac{\rho_1}{\rho_0}$ | $\rho_1$ | $q_1$ | W | W | $c_D$ | $\frac{a_0\,\rho_0\,D_K}{\mu_0}$ | $Re \cdot 10^{-5}$ |
| [mm] | [mmH$_2$O] | [Nm$^{-2}$] | [mmHg] | [Nm$^{-2}$] | [Nm$^{-2}$] | | | | | [ms$^{-1}$] | [ms$^{-1}$] | [kgm$^{-3}$] | | [kgm$^{-3}$] | [Nm$^{-2}$] | [Skt] | [N] | | | |
| Me | Me | | Me | | | | DIA | DIA | DIA | | | | | | | Me | Calibr. | | | |
| 25 | | | 12 | 1601 | 98194 | 0.984 | 0.160 | 0.160 | 0.160 | | 54.9 | | 0.987 | 1.17 | 1763 | 1.1 | 0.5 | 0.58 | | 0.89 |
| | | | 27 | 3602 | 96193 | 0.964 | 0.230 | 0.230 | 0.230 | | 79.0 | | 0.974 | 1.15 | 3589 | 1.5 | 0.8 | 0.45 | | 1.29 |
| | | | 49 | 6537 | 93258 | 0.934 | 0.315 | 0.310 | 0.305 | | 106.5 | | 0.952 | 1.13 | 6408 | 2.9 | 1.6 | 0.51 | | 1.70 |
| | | | 77 | 10273 | 89522 | 0.897 | 0.395 | 0.390 | 0.370 | | 133.9 | | 0.926 | 1.10 | 9861 | 4.2 | 2.3 | 0.48 | | 2.09 |
| | | | 117 | 15610 | 84185 | 0.844 | 0.500 | 0.485 | 0.445 | | 166.6 | | 0.885 | 1.05 | 14572 | 7.0 | 3.9 | 0.55 | | 2.49 |
| | | | 140 | 18678 | 81117 | 0.813 | 0.550 | 0.535 | 0.480 | | 183.7 | | 0.863 | 1.02 | 17210 | 8.2 | 4.6 | 0.54 | | 2.68 |
| | | | 167 | 22280 | 77515 | 0.777 | 0.610 | 0.590 | 0.520 | | 202.6 | | 0.836 | 0.99 | 20318 | 9.7 | 5.5 | 0.55 | | 2.91 |
| | | | 197 | 26283 | 73512 | 0.737 | 0.675 | 0.645 | 0.555 | | 221.5 | | 0.804 | 0.95 | 23305 | 12.4 | 7.0 | 0.61 | | 3.10 |
| | | | | | | | | | | | | | | | | | | | | |
| 50 | | | 12 | 1601 | 98194 | 0.984 | 0.160 | 0.160 | 0.160 | | 54.9 | | 0.987 | 1.17 | 1763 | 3.0 | 1.7 | 0.49 | | 1.79 |
| | | | 19 | 2535 | 97260 | 0.975 | 0.190 | 0.190 | 0.190 | | 65.2 | | 0.982 | 1.16 | 2466 | 4.7 | 2.6 | 0.54 | | 2.12 |
| | | | 27 | 3602 | 96163 | 0.964 | 0.230 | 0.230 | 0.230 | | 79.0 | | 0.974 | 1.15 | 3589 | 5.5 | 3.1 | 0.43 | | 2.57 |
| | | | 37 | 4936 | 94859 | 0.951 | 0.270 | 0.265 | 0.260 | | 91.0 | | 0.964 | 1.14 | 4720 | 8.4 | 4.7 | 0.51 | | 2.91 |
| | | | 49 | 6537 | 93258 | 0.934 | 0.315 | 0.310 | 0.305 | | 106.5 | | 0.952 | 1.13 | 6408 | 8.0 | 4.5 | 0.36 | | 3.41 |
| | | | 77 | | | | | | | | | | | | | 2.5 | | | | |
| | | | 94 | | | | | | | | | | | | | 3.1 | | | | |
| | | | 117 | 15610 | 84185 | 0.844 | 0.500 | 0.485 | 0.445 | | 166.6 | | 0.885 | 1.05 | 14572 | 3.8 | 2.1 | 0.07 | | 4.98 |
| | | | 128 | 17077 | 82718 | 0.829 | 0.525 | 0.510 | 0.465 | | 175.1 | | 0.874 | 1.04 | 15943 | 5.0 | 2.8 | 0.08 | | 5.20 |
| | | | 149 | 19878 | 79917 | 0.801 | 0.575 | 0.555 | 0.495 | | 190.6 | | 0.852 | 1.01 | 18346 | 28.3 | 16.1 | 0.45 | | 5.53 |

$Ba = 748$ [mmHg]
$p_a =$ [Nm$^{-2}$]
$t_a = 20.5$ [°C]
$T_a =$ [K]
$R = 287$ [m$^2$s$^{-2}$K$^{-1}$]
$\gamma = 1.4$
$\mu_0 = 1.82 \cdot 10^{-5}$ [Nsm$^{-2}$]

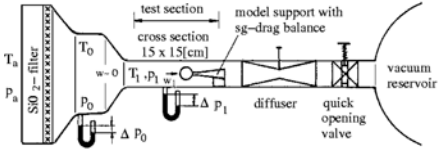


(3) $p_0 = p_a - \Delta p_0$

(5) $\Delta p_1 = \Delta p_1' \cdot 133.3$

(6) $p_1 = p_a - \Delta p_1$

(11) $a_0 = \sqrt{\gamma \cdot R \cdot T_0}$

(12) $u_1 = \frac{u_1}{a_0}$

(13) $\rho_0 = \rho_a \cdot \frac{p_0}{p_a}$

(14) $\frac{\rho_1}{\rho_0} = \frac{1}{\left(1+\frac{\gamma-1}{2}\,Ma_1^2\right)^{\frac{1}{\gamma-1}}}$

(15) $\rho_1 = \frac{\rho_1}{\rho_0}\,\rho_0$

(16) $q_1 = \frac{1}{2}\,\rho_1\,u_1^2$

(19) $c_D = \frac{D}{q_1\,\frac{\pi\,D_S^2}{4}}$

(21) $Re = \kappa\,\frac{a_0\,\rho_0\,D_S}{\mu_0}$

# Index